# *In vivo* and *in vitro* studies of adipogenesis with particular reference to adipocyte development in rodent skin.

## (Vol. I and Vol. II)

### Volume I of two volumes

by
Kamila Wojciechowicz-Grzadka

**Thesis submitted for the degree of Doctor of Philosophy.**
**School of Biological and Biomedical Sciences**
**Durham University**

2012

## Abstract

Skin comprises an epidermis, dermis, skin appendages including hair follicles, and a fat layer. There is a growing interest in the biology of specific fat depots, and skin fat is relatively poorly studied. Importantly, most knowledge about the molecular control of adipocyte differentiation comes from *in vitro* studies on cell lines. This thesis aimed to provide new insights into adipogenesis in vivo by directly studying development of the skin fat layer and its relationship to the surrounding skin and hair follicles.

Work, presented in Chapter 2, investigated the timing and localisation of developing fat cells in back skin of rodent embryos. Analysis of the adipogenic transcription factor C/EBPalpha and lipid accumulation revealed preadipocytes in the lower dermis of embryonic mouse skin at e17 and the start of lipid accumulation by e19. The dermal fat cells then created an adipose layer between and beneath hair follicles apparently independently of subcutaneous fat tissue. In Chapter 3, a combined laser capture microdissection and microarray approach generated gene expression profiles of cells from upper and lower dermis over three time points. Verification of the microarray data by qPCR and immunohistochemistry, and bioinformatics analysis confirmed a subdivision of the lower dermis with enriched fat-related pathways. Comparison of this microarray data with published information on adipogenesis of 3T3-cells *in vitro* showed important early differences with regard to transcription factor, cell cycle, cytoskeletal and extracellular matrix gene expression. Later time points revealed greater similarities between *in vivo* and *in vitro* data involving genes characteristic of mature adipocytes. In Chapter 4, the involvement of the *Egfr* gene (selected from generated microarray lists) in dermal fat development was investigated functionally using a skin organ culture model. In Chapter 5, a marker gene selected from the arrays (*Cd36*) was successfully used to develop a method of isolating dermal preadipocytes by fluorescence activated cell sorting. Specialised organ culture techniques, presented in Chapters 4 and 5, allowed the adipogenic capabilities of cells from different mouse embryonic skin compartments to be investigated. This revealed a high plasticity of dermal cells at earlier embryonic time points (e15 - 15.5) and their specialisation into either non-fatty cells (upper dermis) or adipocytes (lower dermis) later (e18.5 - 19).

As summarised in Chapter 6, this thesis confirmed that the fat layer that develops from cells of the lower dermis should have a distinct nomenclature (dermal adipose tissue) from the subcutaneous fat depot and could be under different regulatory mechanisms. The work has established a new in situ model of *in vivo* adipogenesis and the microarray data obtained has provided novel information on molecular control of adipogenesis in general, as well as pointers as to why the lower, but not the upper compartment of the late embryonic dermis turns into fat.

This thesis is entirely a result of my work. It has not been accepted for any other degree and is not being submitted for any other degree.

Kamila Wojciechowicz-Grzadka

2012

## Table of contents

**VOLUME I** **page**

## List of Tables

**VOLUME I** **page**

### Chapter 1



### Chapter 3:

**VOLUME II**

**Chapter 4:**



**Chapter 5:**

## List of Figures

**VOLUME I** **page**

**Chapter 1:**



**Chapter 2:**

**Chapter 3:**

**VOLUME II** **page**

**Chapter 4:**

**Chapter 5:**

## List of Appendices

**Volume II** **page**

## Abbreviations

| | |
|---|---|
| ADIP | adipogenic medium |
| BT | bottom part of the back skin |
| C | control medium |
| cDNA | complementary deoxyribonucleic acid |
| d | day |
| DAPI | 4',6-diamidino-2-phenylindole |
| DAT | dermal adipose tissue |
| DEPC | diethylpyrocarbonate |
| DMD | dermis microarray data |
| D-MEM | Dulbecco's Modified Eagle's Medium |
| DNA | deoxyribonucleic acid |
| dNTP | deoxynucleoside triphosphate |
| DP | dermal papilla |
| DS | dermal sheath |
| e | embryo |
| EDTA | ethylenediaminetetraacetic acid |
| EGF | Epidermal Growth Factor |
| EGFR | Epidermal Growth Factor Receptor |
| FBS | foetal bovine serum |
| FLs | fat layers |
| Fu | funigzone |
| Ge | gentamicyn |
| H&E | Haematoxylin and Eosin |
| LCM | laser capture microdissection |
| LD | lower dermis |
| mRNA | messenger ribonucleic acid |
| M | muscle layer |
| MEM | Minimal Essential Medium |
| N | newborn |
| NCBI | National Centre for Biotechnology Information |
| NCS | newborn calf serum |
| PBS | phosphate buffered saline |
| PCR | polymerase chain reaction |
| PF | posterior fat |
| qRT-PCR | quantitative reverse transcription-polymerase chain reaction |
| RNA | ribonucleic acid |
| RT | room temperature |
| SAT | subcutaneous adipose tissue |
| S-d | skin from the dermis site |
| S-e | skin from the epidermis site |
| TP | top part of the back skin |
| 2D | two dimensional |
| 3D | three dimensional |

# Acknowledgments

First of all, I would like to thank Professor Colin Jahoda for giving me the opportunity to work on this project which has become a crucial part of my scientific carrier. During my four years at Durham University I definitely learned how to be an efficient and successful scientist.

I want to thank all my previous colleagues from Prof Jahoda's research group; Amy Fearn, Heather Crawford, Gavin Richardson and James Waters, for being very helpful on each step of my study. Especially, Amy Fearn was very supportive as a colleague but also as a very good friend. I would like to thank to Dr Ewa Markiewicz for her scientific advice. I also want to acknowledge people that I met at Durham University and who became my friends: Kasia, Yoko, Iris and Rebecca, Gavin, Simon, Craig and Andy.

I would like to acknowledge Professor Angela Christiano from Columbia University in New York that agreed for me to stay in her lab in order to continue several major experiments of my study. Without her support I would not have been able to perform my core microarray-based study. In addition, I would like to mention Dr Claire Higgins, a former member of Prof Jahoda's group and a researcher in Prof Christiano's laboratory, as without her help I would not have been able to finish my microarray work. In addition, I want to thank Claire for helping me with all organizational and social aspects of my stay in New York.

I would like to acknowledge the LSSU facility at Durham University for providing the animals for my work and the FACS facility at the Centre of Live in Newcastle that helped me with my flow-based cell sorting analysis.

Last but not the least, I would like to acknowledge my beloved family, my mother, brother and my husband. I want to thank them for a huge support and their faith in me. Dziękuję mamo i bracie za wsparcie i wiarę we mnie podczas mojego doktoratu. Dziękuję, mój Rzepku, ze wierzyłeś we mnie podczas tej naukowej drogi. Dziękuję Wam, za podtrzymywanie mnie na duchu.

# Chapter 1:

# Introduction.

## 1.1. Skin.

Skin creates the most outer organ in the body crucial for protection and thermoregulation. It allows contact with the outside environment and takes part in sensation or immune response. It consists of epidermis and dermis layers (see sections 1.1.1 and 1.1.2). The proper function of skin is also associated with fat tissue adjacent to dermis (for more details see section 1.2). The very basic, general view of skin compartments and fat cells related with skin dermis is shown in Figure 1.1A. Among structures seen in skin are hairs (see section 1.1.3).

Skin is a complicated organ, created by different cell types where niches for stem cells have been observed (see section 1.1.4).

### 1.1.1. Epidermis.

Epidermis, stratified epithelium, is the most outer part of skin. Epidermis is crucial for the protection against water loss and creates a barrier against infections (Elias and Feingold, 1992; Schröder, 2010). During epidermal differentiation changes in lipid content take place which are related with a barrier function of this skin compartment. For example, both cholesterol and fatty acids are shown to be synthesized straight after the disruption of skin barrier.

Epidermis can be divided into several cell layers, such as stratum basale (stratum germinativum) and stratum spinosum, stratum granulosum and stratum corneum (reviewed by McGrath *et al*, 2008; see also Figure 1.1B). The outermost layer is the stratum corneum, created by flattened cells without both nuclei and cytoplasmic organelles. These cells are called corneocytes. The stratum basale, the innermost layer of epidermis, is created by two to three layers of small cells which are dividing constantly. The basement membrane, beneath the stratum basale layer, separates epidermis from dermis.

The main cells of this skin part are keratinocytes. Keratinocytes are formed from dividing cells in the basal layer of epidermis and they are constantly moving from the innermost to the outermost part of epidermis, creating finally the stratum corneum. Keratin is a protein produced by keratinocytes and it creates a cytoskeleton of keratinocytes. Keratinocytes are connected with each other by desmosomes (protein bridges). Among other epidermal cells are Merkel cells, Langerhans cells and melanocytes. Merkel cells, localised in the basal layer of the epidermis, are suggested to have a mechanoreceptive role related with a detection of deformations along the tissue (reviewed by Lucarz and Brand, 2007). Langerhans cells are specialized dendritic cells (reviewed by Merad *et al*, 2008). Melanocytes, originated from neural crest, are in close contact with kerationcytes. These cells

produce melanin which is transported to keratinocytes and they are involved in skin pigmentation (reviewed by Tsatmali *et al*, 2002).

### 1.1.2. Dermis.

Dermis has mesenchymal origin and is localised beneath the epidermis layer (reviewed by Sorrell and Caplan, 2004 and McGrath *et al*, 2008). The heterogeneity along dermis seems to be crucial for proper functions of skin. It is consisted of a papillary layer and a reticular layer (Figure 1.1B). The thinner papillary layer lies below epidermis and has loose fibers of collagen. This dermis layer is responsible for a supply of nutrients to the avascular epidermis. Then, there is a bigger reticular layer which consists of dense, organized collagen fibers.

Fibroblasts are the main components of dermis and they produce elastin (crucial for skin elasticity), proteoglycans (related with hydration) and collagen (dermis strength). The papillary dermis has more type III collagen, when compared with the reticular dermis. Next, types XII or XVI collagen are specific for the papillary dermis and type IV collagen is seen in the reticular dermis (reviewed by Sorrell and Caplan, 2004). Among other cells seen in dermis are mast cells or histiocytes. Dermal mast cells are suggested to have immunological functions in skin as well as their relation in skin cancer development have been investigated (Grimbaldeston *et al*, 2004; Byrne *et al*, 2008).

In this skin compartment, the blood supply is very well developed (Braverman and Keh-Yen, 1981). The rete subpapillare (vascular plexus) is localised between two dermis layers and is connected with rete cutaneum (Figure 1.1B). The rete cutaneum is also a vascular plexus, presented at the base of the reticular layer (reviewed by reviewed by Sorrell and Caplan, 2004). Also interactions between elements of the nervous system and skin are crucial for the proper function of skin (Ansel *et al*, 1997).

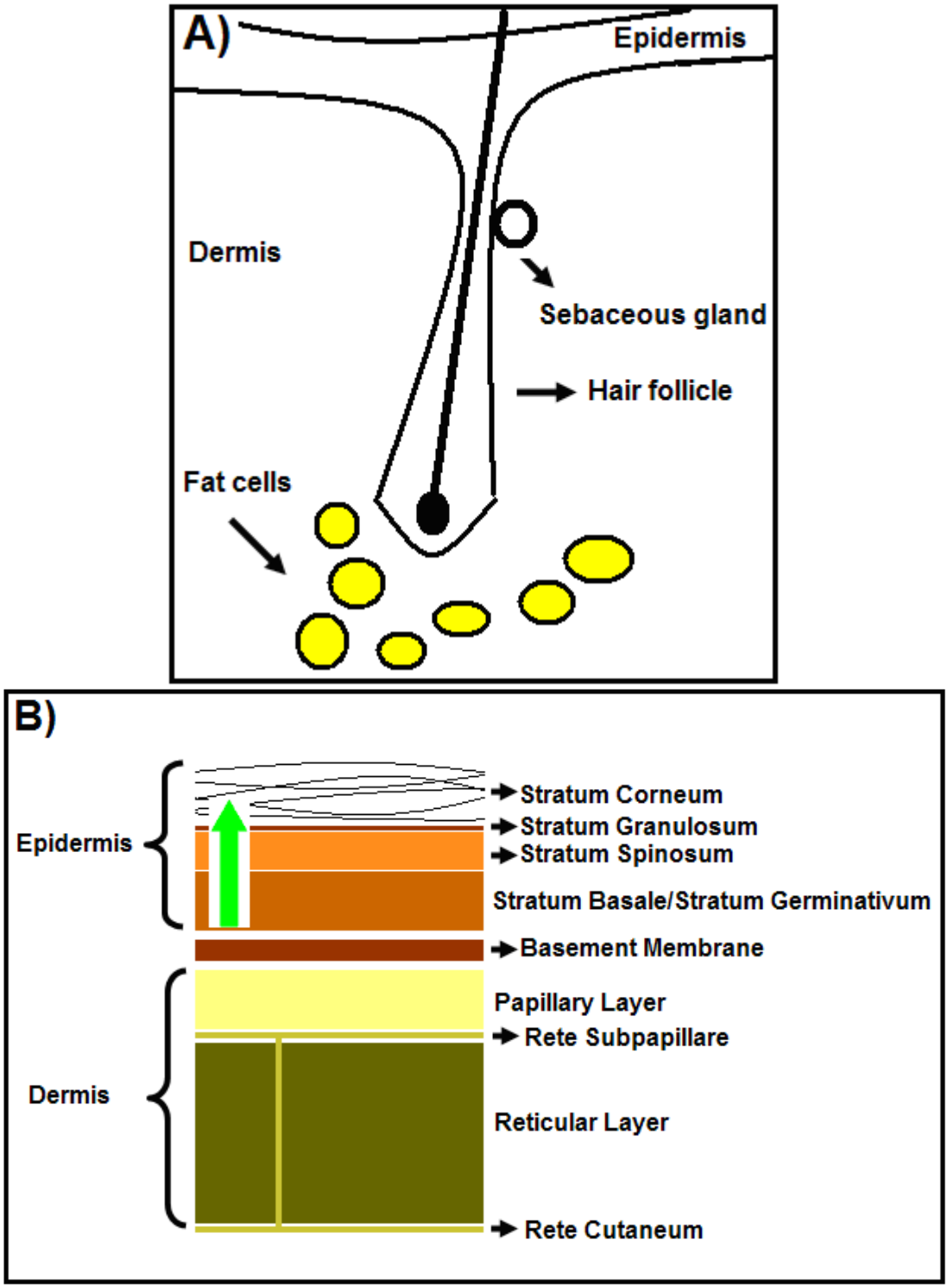


Figure 1.1. A schematic description of skin compartments. (A) Epidermis, dermis and hair follicle with fat cells. (B) Layers creating epidermis and dermis with basement membrane. Direction of keratinocyte movement along the dermis is shown by green arrow. Adapted from Sorrell and Caplan, 2004 and McGrath *et al*, 2008.

### 1.1.3. Hairs.

#### 1.1.3.1. The hair follicle development.

The hair follicle is a complex structure formed from the ectoderm (that gives the epidermis) and the mesoderm (that forms the dermis) (reviewed by Hardy, 1992; Millar, 2002; Schmidt-Ullrich and Paus, 2005). In general, the hair follicle development is divided into three steps (induction, organogenesis and cytodifferentiation) and consists in total of eight stages (Figure 1.2). The formation of the hair follicle is observed during embryogenesis and is connected with the epithelial-mesenchymal interactions. The dermal mesenchyme activates (first dermal signal) agglomeration of cells from epidermis which leads to the development of a placode. The thickening from the epidermis (placode) and its growth into the deeper parts of the skin is observed. When the epithelial signal occurs, at the germ stage, the dermal papilla (DP) is formed. Then, second dermal signal is directed to the epithelium to grow down to the dermis. Next, at the bulbous peg stage the hair follicle bulb occurs and development of both inner root sheath (IRS) and hair shaft takes place.

In mice, the primary hair follicle development starts in about 14.5 day old embryos. The placode can be seen in 14.5 day old embryos, peg at day 15.5 and bulbous peg at day 18.5. The secondary intermediate hairs (awl and auchene) start to develop in about 16.5 - 17 day old embryos, whereas downy (zigzag) hairs occur after the animal's birth.

Different factors and signalling pathways are involved in the regulation of hair follicle development. For example, WNT-signalling and beta-catenin are involved in the induction step. Other key regulatory molecules that control the hair follicle development are members of the TGF/BMP, FGF or TNF families (reviewed by Hardy, 1992; Millar, 2002; Schmidt-Ullrich and Paus, 2005; Schneider *et al*, 2009).

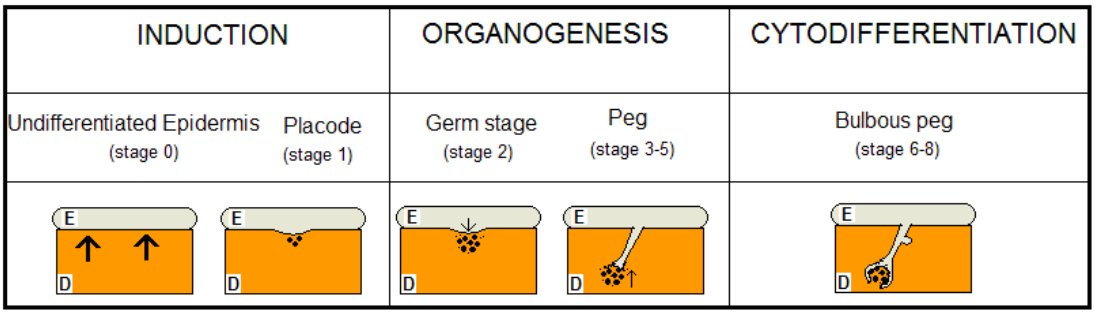


Figure 1.2. A schematic presentation of primary hair follicle development in mouse skin. Arrows show epithelial-mesenchymal interactions during hair follicle development. E - epidermis; D - dermis. Based on Millar, 2002 and Schneider *et al*, 2009.

### 1.1.3.2. The structure of hairs and the hair follicle cycle.

A fully developed (in anagen phase, see below) hair follicle can be divided into two parts: the upper, less dynamic part and the lower part which undergoes changes during hair follicle cycle (reviewed by Schneider *et al*, 2009). The upper part consists of the outermost infundibulum and the isthmus, whereas the lower part is divided into suprabulbar region and the bulb part (Figure 1.3A).

Sebaceous glands are seen in the upper part of hair follicles and they produce sebum, which consists of lipids (Picardo *et al*, 2009). Small smooth muscles, called arrector pili muscles, are also in the upper part of hair follicle and they connect hairs to the dermis (reviewed by Schneider *et al*, 2009). A bulge region is in the isthmus part and is treated as a stem cell niche (see section 1.1.4 for details).

The progenitor cells from the bulge can move to the upper part of skin and populate sebaceous glands as well as epidermis between hair follicles (inter-follicular epidermis). Other progenitor cells move down along the skin and take part in forming hair follicles. Progenitor cells in hair matrix divide, move from dermal papilla (DP) and then stop their division and differentiate into layers of growing hair follicle. The growth of hair continues during the anagen phase of the so-called hair follicle cycle (see above). The anagen bulb has matrix stem cells where keratinocytes move to the adjacent area undergoing proliferation or create layers of hair shaft and inner root sheath (IRS). Matrix surrounds DP which is a key signalling center for maintaining the hair growth and which control the hair follicle life cycle. Hair shaft consists of medulla, cortex and hair cuticle, whereas IRS is created by four parts (companion, Henle's and Huxley's layers and IRS cuticle; see Figure 1.3B). The outermost layer of hair follicle is called outer root sheath (ORS). Finally the hair follicle is surrounded by a dermal sheath (DS) which is believed to have an important function in the process of reparation of the injured skin (Jahoda and Reynolds, 2001).

The upper part of hair follicle, the bulge and matrix of the hair bulb have ectodermal origin. Both dermal papilla and dermal sheath have mesodermal origin (reviewed by Schneider *et al*, 2009).

Hair follicles undergo the cyclic growth that consists of four phases: anagen (an active phase), catagen (a regression and shortening phase), telogen (a resting phase) and exogen phase (a shedding stage) (reviewed by Schneider *et al*, 2009). In the anagen, as it was mentioned above, keratinocytes of the hair matrix cells give rise to hair follicle layers and development of the hair takes place. In mouse, the first

anagen phase starts at embryonic level and continues to about 12 days after the animal's birth. In the next phase (the catagen phase), the follicle stops producing hair and cell death (apoptosis) occurs. It is also observed that the dermal papilla shrinks and is released from the bulb. In a resting telogen phase, the papilla is localised very close to the bugle which is believed to be related with interaction between cells from these two areas. The telogen hair (club hair) is a dead hair. Next, the activation of anagen takes part and new hair is created.

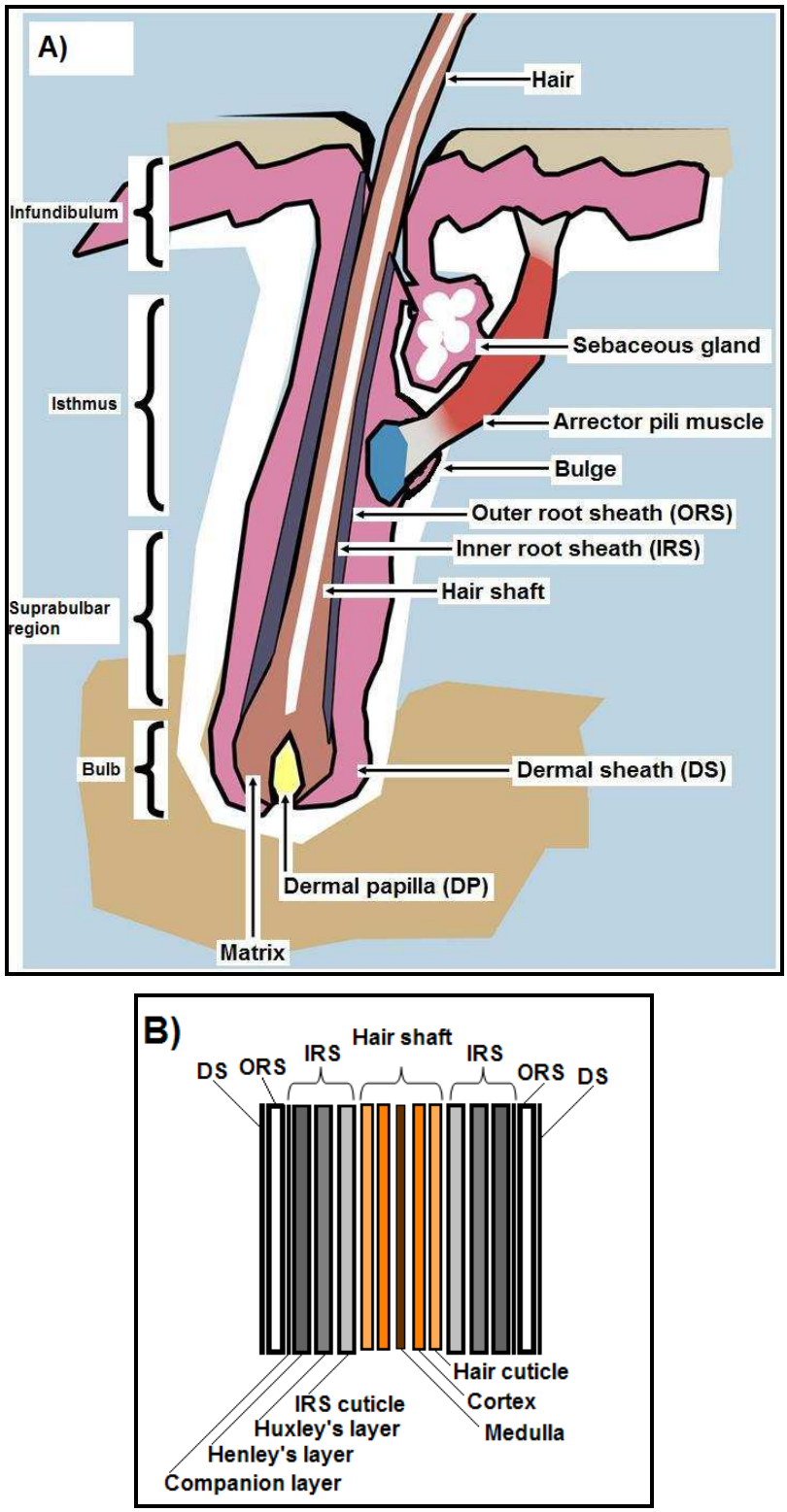


Figure 1.3. A schematic representation of the hair follicle structure. (A) Elements of the hair follicle. (B) Parts that create hair shaft and inner root sheath - IRS, surrounded by outer root sheath - ORS and dermal sheath - DS. Adapted from Schneider *et al*, 2009. Drawing of hair (A) by Paweł Wojciechowicz.

### 1.1.4. Skin and hair follicles as a source of adult stem cells.

Recently, the attention has been focused on so-called adult stem cells, that are undifferentiated cells found in different tissues, and which are able to renew themselves and differentiate into some specialized cell types of tissues/organs (reviewed by Wagers and Wiessman, 2004). These kinds of cells are responsible for maintaining and repairing tissues in which they are localised. It is suggested that these cells are quiescent for most of the time and are activated after the injury of tissue/organ or the onset of disease.

Adult stem cells have been investigated in the skin. The stratum basale layer of epidermis is treated as a source of epidermal stem cells, which are crucial for the proper regenerative processes of skin (reviewed by Kamstrup *et al*, 2008). Stem cells isolated from the rodent and human skin dermis and called “skin-derived precursors” (SKPs) were shown to produce adipocytes, smooth muscle cells or neurons and glia (Toma *et al*, 2001; Fernandes *et al*, 2004). Stem cell niches have been found along hair follicles. The bulge region of hair follicles has been characterised by the presence of epithelial stem cells. These cells are a source of hair follicle cells and are crucial for replacement of stem cells in epidermis (Taylor *et al*, 2000). In addition, it is said that the whisker follicle dermal papilla can be a niche for SKP cells (Fernandes *et al*, 2004). In the context of stem cell capability, it was observed that when dermal papilla (DP) and dermal sheath (DS) cells were cultured, they expressed different types of blood cell markers and had interesting haematopoietic potential (Lako *et al*, 2002). It was also published that follicle dermal cells can express some osteogenic markers (for example osteopontin or alkaline phosphatase) or can accumulate lipids (Jahoda *et al*, 2003). It is suggested that DP and DS cells are able to differentiate into different lineages (such as adipogenic or osteogenic) *in vitro* and this process can occur spontaneously or can be induced (by adipogenic medium, for details see section 1.3.2.2).

Adult stem cells are thought to be a good source of cells used in cell therapies, for transplantations in different diseases (Wagers and Wiessman, 2004). Thus, it is important to enlarge the knowledge about adult stem cells, analyse their features and check their potential implications in different fields of medicine.

## 1.2. Adipose organ.

### 1.2.1. General division of adipose depots.

Adipose organ is created by two tissues: brown adipose tissue (BAT) and white adipose tissue (WAT) (Cinti, 2001). These two depots have different fat cells (adipocytes) morphology and function in relation to energy expenditure and accumulation. In addition, they differ because of the colour appearance (brown cells in BAT and yellowish in WAT depot) (Avram *et al*, 2005). Because of the localisation in the body, fat depots can be subcutaneous - SAT (subcutaneous adipose tissue) and visceral - VAT (visceral adipose tissue) (Cinti, 2001). White adipose tissue in subcutaneous and visceral localisation can contain brown adipocytes, whereas BAT tissue can be characterised by a presence of white fat cells (section 1.2.2.3).

The human subcutaneous depots are these observed beneath the skin (abdomen, thighs or buttocks areas as well as under the head/face skin), whereas adipose depots that surrounds internal organs can have omental, retroperitoneal or visceral localisation; see Figure 1.4a) (reviewed by Gesta *et al*, 2007). In human skin, fat cells localised between hairs (dermal adipose tissue) are not separated from subcutaneous adipose tissue (Cinti, 2007) (Figure 1.4b). In addition, human BAT has especially interscapular localisation and was found in cervical, supraclavicular or paravertebral areas. It is abundant in humans at birth and its level decreases in adults. In rodents, the brown adipose tissue has mainly the interscapular localisation and is seen throughout the whole animal's life (Figure 1.5. Part A). The visceral tissue, in mice and rats, can be mesenteric and mediastinic, retroperitoneal, perirenal or perigonadal and epididymal (Figure 1.5. Part A) (Cinti, 2001; Cinti, 2007; Gesta *et al*, 2007; Tran and Kahn 2010). In relation to fat cells associated with mouse back skin, two fat compartments are seen: subcutaneous adipose tissue (SAT) and dermal adipose tissue (DAT) (Figure 1.5. Part A and Part B). The subcutaneous adipose tissue is localised below the skin, whereas the dermal adipose tissue develops in lower dermal compartment and is localised between hair follicles. These two adipose depots are divided from each other by a muscle layer (panniculus carnosus). DAT is observed along the whole length of mouse back skin lower dermis, whereas SAT is can be divided into anterior and posterior depots (Figure 1.5. Part B). The study presented in this thesis was focused on the dermal adipose tissue - DAT.

Except main fat depots, adipocytes were observed in many organs and tissues (bone marrow, pancreas, synovial, skin) and have for example intramuscular or pericardial localisation (Cinti, 2001, Gesta *et al*, 2007). In addition, the word "infiltrate" has been used for the description of fat cells in these organs (Cinti, 2001).

a)

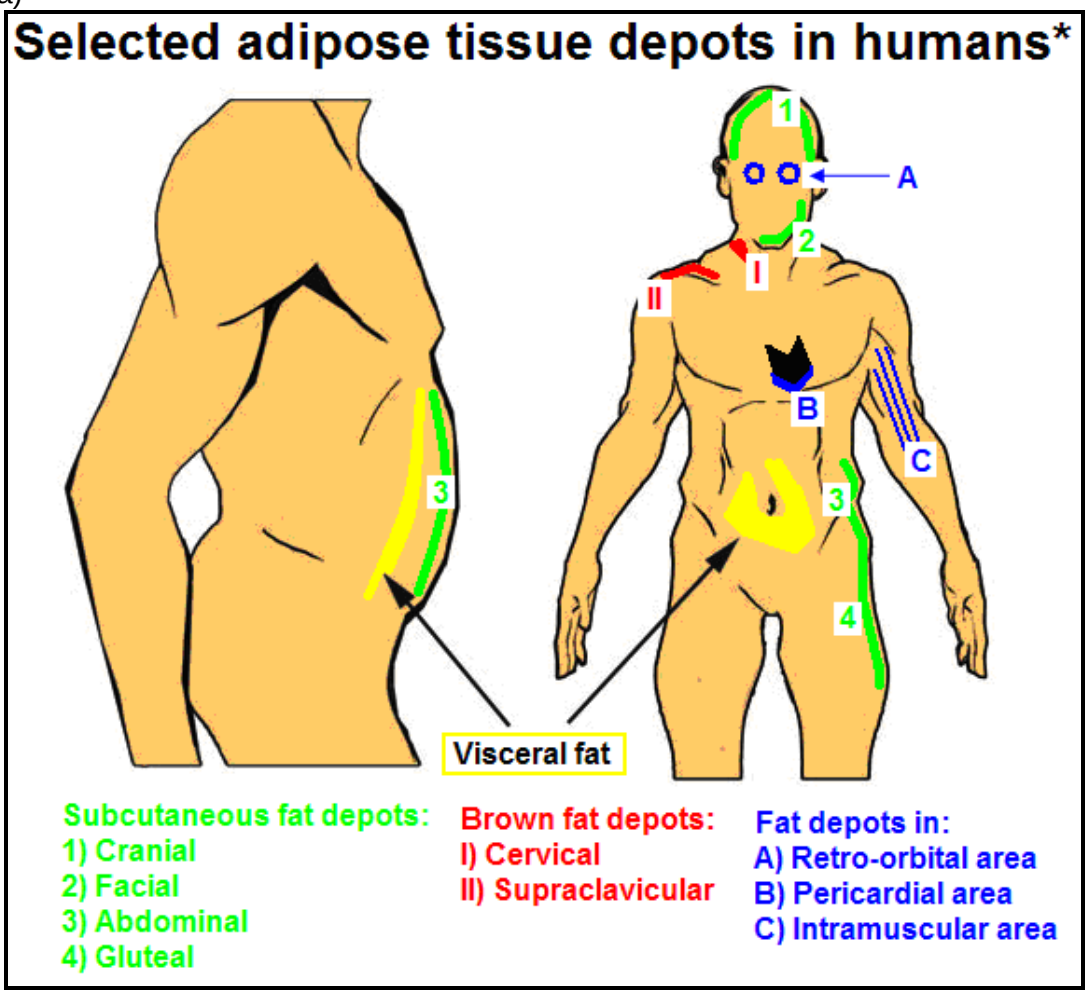


b)

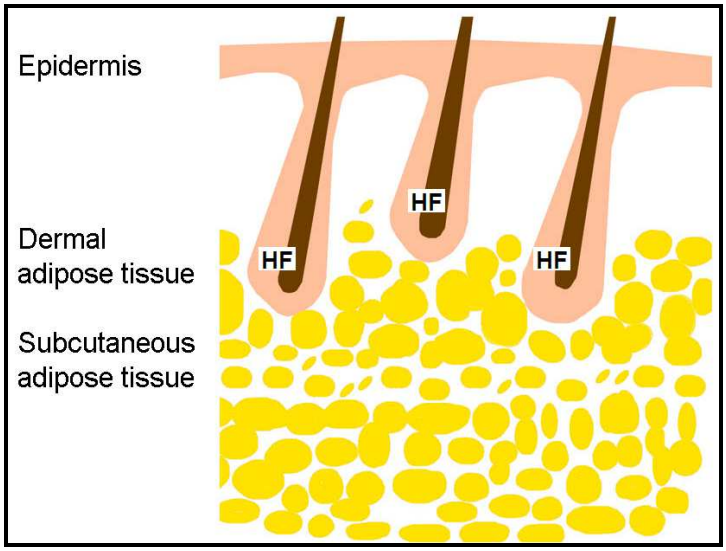


Figure 1.4. A schematic presentation of selected fat depots in human body. (a) The main known fat depots are subcutaneous (shown in green) and visceral (shown in yellow). Small amounts of brown fat depots can be seen in adults (shown in red). In addition, fat cells are present in other tissues and organs (shown in blue). *Information based on Gesta *et al*, 2007. (b) Dermal adipose tissue is connected with subcutaneous adipose tissue in human body (based on Cinti, 2007). HF – hair follicle. Drawings by Paweł Wojciechowicz.

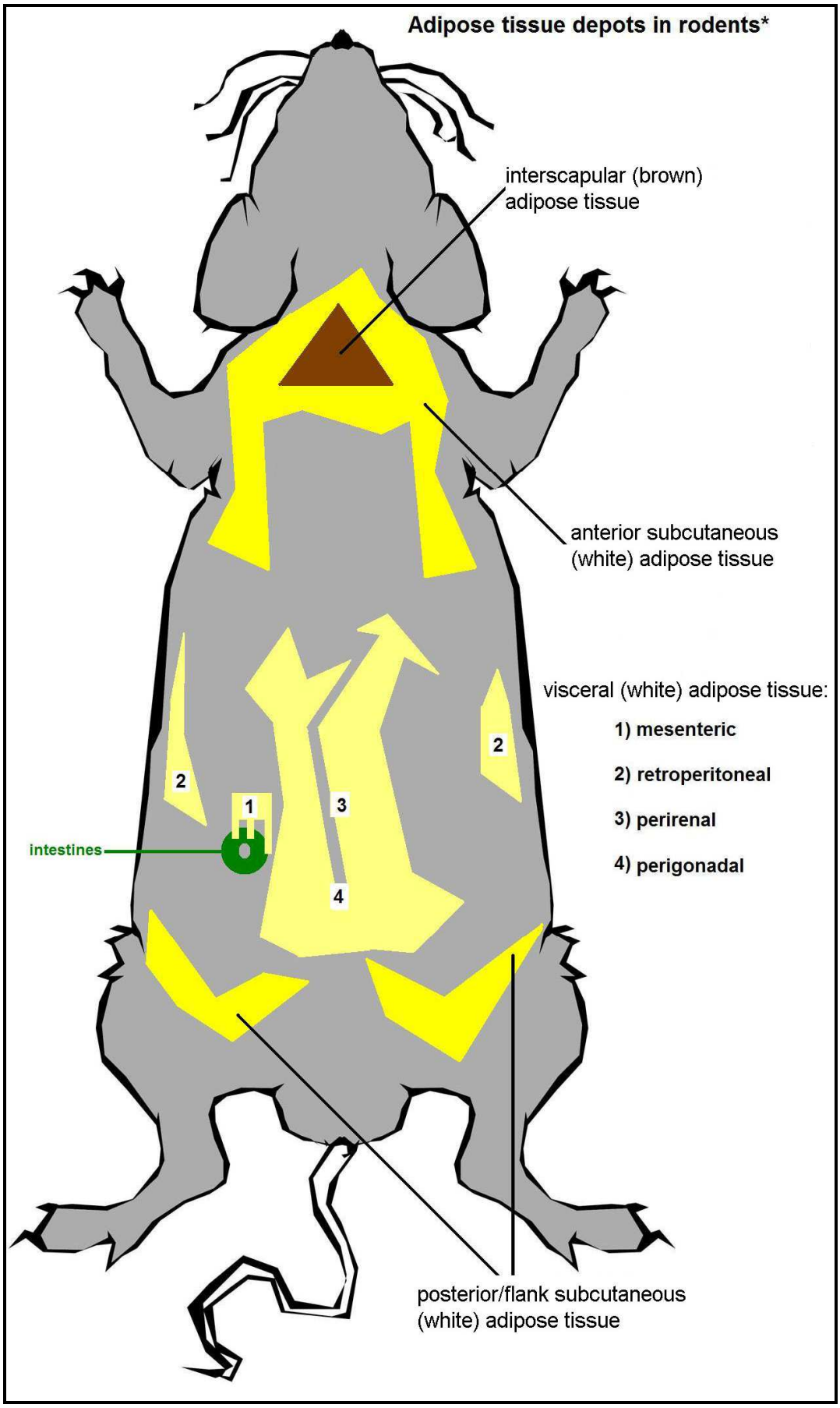


Figure 1.5. Part A. For description see Figure 1.5. Part B.

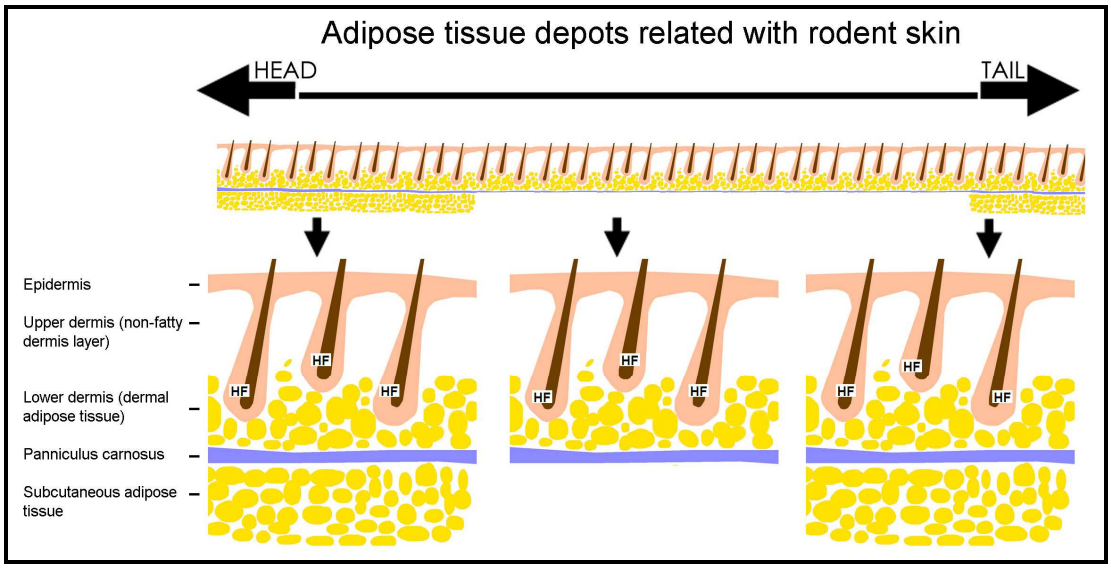


Figure 1.5. Part B. A schematic presentation of main fat depots in rodents.
(Part A) The brown adipose tissue (shown in brown) is seen in the anterior part of the rodent body. Subcutaneous adipose tissue, just beneath the skin, develops in anterior and posterior areas (shown in darker yellow colour). Selected visceral depots are shown in a lighter yellow colour. *Information based on Cinti, 2001; Cinti, 2007; Gesta *et al*, 2007 and Tran and Kahn, 2010. Drawing by Paweł Wojciechowicz.
(Part B) The localisation of adipose depots associated with rodent back skin. Adipocytes create dermal adipose tissue along the whole back skin. Subcutaneous fat depot is seen below the skin in anterior (near head and upper limbs) and posterior (near lower limbs) localisation (see Chapter 2, for more details). HF – hair follicle. Based on Cinti, 2007. Drawing by Paweł Wojciechowicz.

### 1.2.2. Morphology and function of adipose tissue.

Development of fat depots starts in foetuses, continues after the birth and subcutaneous depots can occur before visceral ones (Cinti, 2001).

Adipose organs consist of fibroblasts and fibroblast-like cells, histiocytes and mast cells, blood vessels and nerves, preadipocytes and mature fat cells, called adipocytes (Cinti, 2001; Cinti, 2007). Elongated fibroblasts, elements of the connective tissue, produce a connective matrix and are characterised by the presence of the rough endoplasmic reticulum (that comprises most of the cytoplasmic space). Histiocytes, with many lysosomes and well developed Golgi complexes, are suggested to take part in adipose tissue modifications, depending on the amounts of stored lipids. Some adipose organs (anterior and posterior subcutaneous depots in rodents) can have their own, specific vascular and nerve elements. Whereas white visceral fat depots can be connected to the vascular and nervous systems of other organs, such as the kidneys or intestines.

Preadipocytes undergo a specific differentiation process that leads to a development of mature fat cells. Adipocytes are capable of accumulating lipids and are crucial for the specific functions of this organ (Avram *et al*, 2005). Detailed description of adipocyte differentiation (adipogenesis), analysed mainly by *in vitro* studies, is presented in section 1.3.

#### 1.2.2.1. Brown adipose tissue (BAT).

##### 1.2.2.1.1. Brown adipocytes.

Brown fat cells in brown tissue can have an ellipsoid shape with sizes, depending on the literature source, between 10 - 15 and 25 - 50 μm (Cinti, 2001; Cinti, 2007). Lipids are accumulated in small vacuoles (multilocular cells) of these brown adipocytes that have round-shaped nuclei (usually in central areas of cells) and high number of large mitochondria. On the surface of these small lipid droplets, perilipin protein has been characterised. Both, Golgi apparatus and rough endoplasmic reticulum are not well-developed, whereas smooth endoplasmic reticulum is easy to detect in these cells. Also, external lamina can be easily detectable outside of the plasma membrane.

#### 1.2.2.1.2. Main function of BAT.

The unique feature for brown cells is related with the presence of so-called uncoupling protein-1 (UCP-1) in the inner mitochondrial membrane. This protein is responsible for main function of BAT, as an organ important for energy expenditure. Uncoupling proteins are related with dissipation of the proton electrochemical gradient and releasing of energy as heat (thermogenesis) (reviewed by Wajchenberg, 2000). For example, in adult rodents kept for several hours in low temperatures (4 - 8$^{o}$C), most lipids disappear from BAT (Cinti, 2001).

#### 1.2.2.1.3. BAT in humans.

In human the amount of BAT significantly decreases after birth (Gesta el at, 2007). For quite a long time BAT was thought not to have an important function in adult humans. However, this view underwent changes when BAT was investigated in adults. In one study, the PET-CT (Positron Emission Tomography - Computed Tomography) technique was used that allowed the identification of potential brown adipose depots that had a high rate of uptake of 18F-fluorodeoxyglucose (18F-FDG) (Cypess *et al*, 2009). Brown tissue (with large depots seen in area from anterior neck to the thorax) was analysed in patients that differ in age or sex. The mass of BAT was higher in women (than in men) and the inverse correlation was noticed between BAT amount and BMI index (people with lower BMI tend to have higher activity of BAT) and this was mainly related with older people.

Interestingly, the presence of brown depots (mainly around the neck) was also observed in a group of people that were working outside (in Finland) (Huttunen *et al*, 1981).

To sum up, brown adipose tissue has become an interesting depot for researchers because of its suggested role in metabolism in adults and as a potential tool that could be used in controlling the energy expenditure in humans and maybe developing treatments for obesity (Celi, 2009; Seale and Lazar, 2009).

#### 1.2.2.1.4. Development of BAT in rodents.

The electron microscope allowed the investigation of BAT development during the perinatal period in rats (Cinti, 2001). BAT in rat could be detected in the dorsal area (in the trunk), near the spinal cord. In young, 15 day old embryos, this part of rat body was filled only with mesenchymal tissue, whereas in 19 day old embryo, brown adipocytes were observed together with UCP-1 expression. During rat development, progressive accumulation of mitochondria was spotted in these

cells. At the early step of development (so-called adipoblast stage 1) cells had high number of mitochondria. Then, during differentiation process the number of mitochondria increased which became more similar to these seen in mature brown fat cells and lipid accumulation was observed. At so-called adipoblast stage 2, unilocular lipids were seen. Then, at next differentiation stage (adipocyte precursors) multilocular lipids were spotted. In general, at 19 - 21 day old rat embryos, cells at all mentioned above stages were observed.

### 1.2.2.2. White adipose tissue (WAT).

#### 1.2.2.2.1. White fat cells and their development.

Cells of white adipose depot are characterised by small, elongated mitochondria, an easy to observe smooth endoplasmic reticulum and lamina on the outside area of plasma membrane (reviewed by Cinti, 2001). In addition, these fat cells can differ from each other because of the size, which can be between 20 and 150 μm and such big difference depends on the amount of accumulated lipids (Cinti, 2007). Developed white adipocytes, have spherical shape with one big vacuole (unilocular) that takes central place in the cell and leads to a creation of a thin cytoplasm and elongated nuclei localised at the edge of the cell.

First signs of rat white fat cells were observed in perinatal period and were related with the inguinal region (Cinti, 2001). Preadipocytes differ from other surrounding cells because of the presence of external lamina. Differentiating cells are characterised by small lipid droplets and granules of glycogen. Then, an increase in accumulating lipids leads to the development of unilocular (mature) white fat cells.

During the development of white adipocytes, the increase in cell size (hypertrophy) is followed by the increase in cell number (hyperplasia). It is suggested that a fat cell has a maximum volume for the lipids accumulation and this differs depending on type of fat depot (Cinti, 2007). For example, in adult male rats (Wistar) hypertrophy was mainly observed in mesenteric and epididymal fat depots, whereas hyperplasia dominated during development of the retroperitoneal depot (DiGirolamo *et al*, 1998).

Among characteristic proteins produced by white fat cells, are S-100 protein and leptin (reviewed by Cinti, 2001). S-100 protein is suggested to be an example of carrier protein for fatty acids in adipocytes (Haimoto *et al*, 1985). Leptin is described in section 1.2.2.2.2.3.

#### 1.2.2.2.2. WAT functions.

White adipose tissue is the largest energy storage organ that controls synthesis and accumulation of triacylglycerols and functions as an endocrine organ (reviewed by Gregoire *et al*, 1998). In addition, subcutaneous fat depots function as a thermo-insulator (reviewed by Cinti, 2007).

##### 1.2.2.2.2.1. Lipid metabolism.

Lipid metabolism in fat cells is related with the uptake of fatty acid, lipogenesis and lipolysis (Large *et al*, 2004; Avram *et al*, 2005). After food consumption, accumulation of lipids increases in WAT and free fatty acids (FFAs) are stored in a form of triacylglycerol (TG/TAG) in adipocytes. The term lipogenesis is used for the description of fatty acid and TG synthesis.

When a fasting period occurs, lipolysis takes place. In this process, TG is hydrolyzed into fatty acids (FAs) and glycerol. Then, fatty acids leave adipocytes, in the form of free fatty acids (FFAs), which can be processed in muscles and liver and used as a source of energy for different organs.

In addition, lipid storage and lipid release are controlled by hormonal signals (for example insulin), exercise and the food intake. Dysregulation of processes that control lipid metabolism in adipocytes is thought to lead to obesity and fat-related disorders (diabetes, insulin resistance) and is discussed in section 1.2.7.

###### 1.2.2.2.2.1.1. Fatty acid (FA) transport.

Two main processes are suggested to be responsible for fatty acid (FA) transport: a passive diffusion through a flip-flop process and transport by protein transporters (for example integral membrane protein called FAT/CD36, which is discussed in Chapter 3 and Chapter 5) (reviewed by Kampf and Kleinfeld, 2007).

Inside the fat cell, transport of FA has a membrane to membrane feature or can be carried by cytoplasmic LBPs (lipid-binding proteins also known as fatty acid binding proteins - FABPs). Among well-known LBPs is adipocyte lipid binding protein (FABP4/ALBP/A-FABP/aP2), seen in fat cells. In addition, KLBP (keratinocyte lipid binding protein) is seen in adipocytes and other cell types (Simpson *et al*, 1999).

Also present in adipocytes are caveolae which take part in the transport of fatty acids and their conversion into TG (Öst *et al*, 2005). A subclass of caveolae responsible for this process is characterised by the presence of perilipin protein. Perilipins are encoded by a Plin gene and create a family of phosphoproteins and

their expression goes up during adipogenesis. They were found on the lipid droplet surfaces in fat cells (white and brown adipocytes).

#### 1.2.2.2.2.1.2. Synthesis of triacylglycerol.

After the transportation of fatty acids into the fat cell, they are quickly changed into triacylglycerol (TG/TAG), which is accumulated in central fat droplets in adipocytes. Adipocytes synthesize triacylglycerol mainly from fatty acids bound to plasma albumin or from TAG-rich lipoproteins (such as very low density lipoprotein VLDL-TG). Adipocytes have VLDL-receptors that seem to control uptake of TG-fatty acids and these cells express lipoprotein lipase (LPL) responsible for the release process of TG-fatty acids from lipoproteins (Large *et al*, 2004). Non lipid substrates can also be involved in the fatty acid synthesis (for example carbohydrates) and this process is called “de novo lipogenesis” (DNL). DNL process takes place in liver and can be present in adipocytes. However, DNL process in human adipose organ has not been fully characterised (Large *et al*, 2004).

#### 1.2.2.2.2.1.3. Lipolysis.

In white adipocytes, during the lipolysis process TAGs are changed into diacylglycerols (DAG) and monoacylglycerols (MAG). Finally, free fatty acids (FFA) and glycerol are released (Large *et al*, 2004). In the lypolysis process, the hormone-sensitive lipase (HSL) is one of the crucial enzymes, sensitive to insulin and which controls modification of TAG into DAG and MAG. In addition, perilipins (see also section 1.2.2.2.2.1.1) are thought to be involved in regulation of lipolysis in adipocytes (Holm, 2003). The protein kinase A–mediated phosporylation of HSL and perilipins can result in enhanced lipolysis.

### 1.2.2.2.2.2. Glucose metabolism.

Fat cells are involved in glucose metabolism (Avram *et al*, 2005). Glucose is a sugar used by the body to store energy. Adipocytes are characterised by the presence of insulin-dependent glucose transporter 4 (Glut4) which allows the transport of glucose into these cells. In addition, adipose tissue can influence glucose metabolism in other organs, such as liver (Wajchenberg, 2000). By releasing FFAs (from fat cells) into the circulation, skeletal muscles can be influenced in relation to promotion of insulin resistance (Avram *et al*, 2005). Insulin resistance is discussed in section 1.2.7.

### 1.2.2.2.2.3. Adipose tissue as an endocrine organ.

The endocrine function of WAT was suggested with a discovery that this adipose organ is capable of producing a hormone related with food intake or activation of energy dispersion, called leptin (Cinti, 2007).

Leptin, encoded by the obesity (*ob*) gene, is expressed mainly in adipocytes (Margetic *et al*, 2002). It functions through the leptin receptor. Leptin expression starts at embryonic level and leptin is thought to be a signalling factor that influences the nervous system and controls proper food intake and weight in rodents and humans (reviewed by Wajchenberg, 2000). Abnormalities in leptin levels and their function are known to lead to obesity and metabolic abnormalities (commented by Ahima, 2008). Increased levels of leptin were observed in obese individuals in whom an energy expenditure and appetite seemed to be disturbed (Münzberg and Myers, 2005). In rodents and humans, plasma leptin was correlated with body mass index. Food restrictions that leaded to weight loss were associated with lower levels of leptin (Maffei *et al*, 1995).

Secreted by adipocytes factors control function of many organs as well as they control adipose tissue. In general, their action can have autocrine, paracrine and endocrine roles (Kim and Moustaid-Moussa, 2000). Several factors, secreted by adipose tissue have been summarised in Table 1.1. In addition, several proteins related with mature adipocytes are presented and discussed in Chapter 3 (sections 3.3 and 3.4).

Table 1.1. Examples of factors that are produced and secreted by adipose tissue. Information based on Kim and Moustaid-Moussa, 2000.

| **Examples of factors secreted by adipose tissue*:** | |
|---|---|
| **1) Obesity genes:** | **Leptin**<br>**Agouti** |
| **2) Sex steroids** | |
| **3) Cytokines:** | **Tumor necrosis factor (TNFalpha)**<br>**Interleukin-6 (IL-6)** |
| **4) Free fatty acids (FFAs)** | |
| **5) Complement components:** | **Acylation stimulating protein (ASP)**<br>**Adipsin** |
| **6) Proteins of lipoprotein metabolism:** | **Lipoprotein lipase (LPL)**<br>**Apoprotein E (ApoE)** |
| **7) Proteins related to cardiovascular function:** | **Plasminogen activator inhibitor-1 (PAI-1)**<br>**Angiotensinogen (AGT)** |
| **8) Eicosanoids:** | **Prostaglandin E2 (PGE2)**<br>**Prostaglandin I2 (PGI2)** |
| **9) Growth factors:** | **Transforming growth factor beta (TGFbeta)**<br>**Insulin-like growth factor-1 (IGF-1)** |

*Reference for each presented factor is included in Kim and Moustaid-Moussa, 2000.

### 1.2.2.3. The presence of white and brown cells in the same fat depot.

Brown and white adipose cells can occur along the same adipose tissue depot (Cinti, 2007). In obese animals, presence of white adipocytes was observed along brown fat depots. In addition, so-called Sv129 mice had enhanced resistance to obesity and diabetes and higher number of brown adipocytes was observed in their adipose depots (Almind and Kahn, 2004; Cinti, 2007). Moreover, as an effect of cold-exposure, brown adipocytes were present in white adipose organs in rodents (Cinti, 2001).

A general suggestion has been made, that so-called reversible transdifferentiation process occurs along some fat cells and allows the transfer of white adipocytes into brown cells (Cinti, 2007). Moreover, all fat depots can consist of two types of adipocytes and their differentiation might be dependent on such factors as age or changes in outside temperatures.

## 1.2.3. Developmental origin of fat cells.

Still little is known about the exact steps of fat cell origin (Cinti, 2007; Gesta *et al*, 2007; Billon *et al*, 2007; Billon *et al*, 2008). It is accepted that adipocytes might develop from mesenchymal stem cells (MSCs). Embryonic stem cells give a rise to MSCs which were observed for example in human bone marrow and are capable to differentiate into several cell types, such as myoblasts, osteoblast or adipocytes.

MSCs were suggested to develop from mesoderm. In addition, it was suggested that there might be another source of mesenchymal cells, related with the neural crest (NC). Neural crest, derived from neuroectoderm, leads to the development of facial bones. In addition, the neural crest cells (NCCs) are capable of an epithelial-to-mesenchyme transition and develop into different cells, depending on their localisation along the body (for example neurons or endocrine cells) (reviewed by Billon *et al*, 2008).

Adipocytes could develop from so-called adipoblast (early precursor of fat cells) which differentiate from mesenchymal stem cells, however the exact mechanism of such process has not been yet confirmed (Gesta *et al*, 2007). Questions arise in relation to pathways that control embryonic stem cells, differentiation of MSC into adipocytes or number and types of precursors for fat cells (one or several precursors for white and brown fat cells, for visceral and subcutaneous fat preadipocytes, see Figure 1.6).

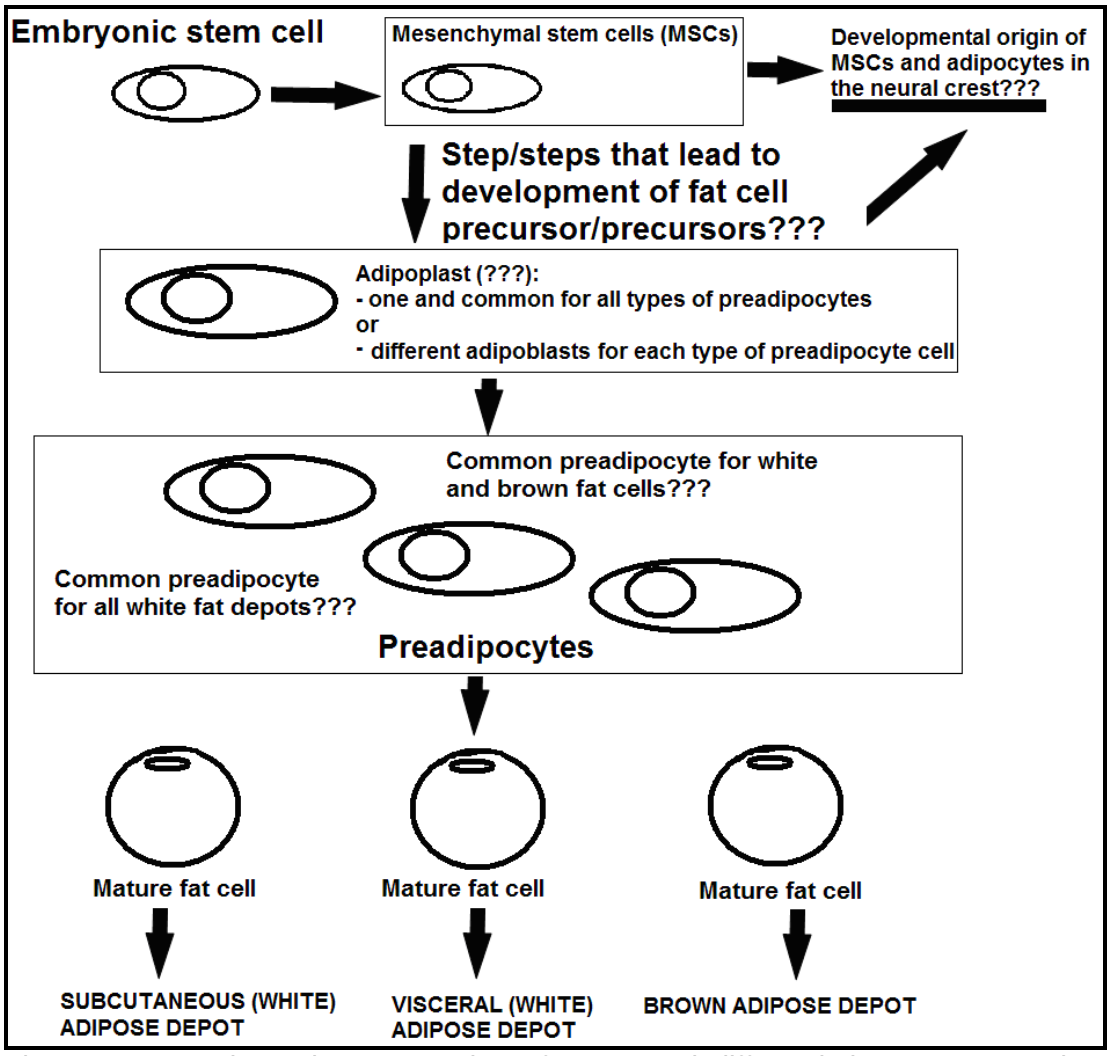


Figure 1.6. A schematic presentation of suggested differentiation processes that lead to development of mature fat cells and different fat depots. The origin of fat cells remains elucid, however it is believed that these cells develop from mesenchymal stem cells (MSCs). Some differentiation stages have yet to be clarified. Adapted from Gesta *et al*, 2007 and Billon *et al*, 2007.

The suggested origin of fat cells was related with several studies where a capability to undergo adipogenesis was analysed in different embryonic cell lines (reviewed by Billon *et al*, 2008). Mouse embryonic stem cells (mESCs), isolated from mouse blastocyst, after the integration into the embryo take part in development of all cell lineages. It was shown that mESCs can differentiate into adipocytes, when treated with retinoid acid (RA) or insulin (Dani *et al*, 1997). Also, human embryonic stem (hES) cells were capable of undergoing adipogenesis after the exposure on adipogenic factors (Xiong *et al*, 2005; for adipogenic factors see section 1.3.2.2).

In addition, in mESCs treated with RA, reduction of mesodermal markers was observed and high concentrations of RA were able to activate neural differentiation (Bain *et al*, 1995). Billon *et al* (2007) designed experiment where mouse embryonic stem cells, expressing Sox2 (that is specific for neuroepithelial cells), were treated with retinoid acid in order to activate neural differentiation. Then, neuroepithelial cells (purified by fluorescence activated cell sorting - FACS method) were treated with adipogenic factors (for example insulin) and differentiated into adipocytes. The neural crest stem cells were shown to differentiate into adipocytes. Finally, it was shown that during mouse development *in vivo,* adipocytes can develop from neural crest (NS) cells (Billon *et al*, 2007). In this work, transgenic animals with Sox10-Cre/Rosa26R-YFP were used where Cre recombinase was under control of the Sox10 promotor. The Sox10 is believed to be efficient marker of NC cells and is not expressed in mesoderm. The immunofluorescence staining was performed where antibody against perilipin (adipocyte marker seen on the surface of lipid droplets) was used. This study showed the co-expression of perilipin with YFP (yellow fluorescent protein) in the area of salivary gland. It suggested that YFP-positive and perilipin-positive (YFP+/perilipin+) adipocytes developed from NC and not from mesoderm. Then, subcutaneous fat depots, positive for perilipin, were not expressing YFP (Billon *et al*, 2007). Thus, different fat depots along animal body seemed to differ because of the origin.

To sum up, it is suggested that white adipocytes in the cephalic region develop from the neural crest (NC) and adipocytes from the trunk area might arise from the mesoderm (Billon *et al*, 2008). This hypothesis remains to be elucidated by more detailed studies.

### 1.2.4. Human adipose tissue.

In humans, first signs of adipose tissue were observed in the second trimester of gestation (Poissonnet *et al*, 1984). The term “mesenchymal lobules” was used to describe structures without lipids, which developed into a “primitive fat lobules” (first signs of lipids) and then to “definitive fat lobules” (Poissonnet *et al*, 1984). In this study, adipose organ was observed to develop first in the head and neck (for example chin fat developed between 14.5 and 17 week of foetal life), then trunk area (for abdominal wall between 14.5 and 20.5 week), whereas the fat organ in limbs developed as the latest depot (from 15 untill 23.5 week for shoulder fat).

General morphological features of human (white and brown) fat cells and localisation of SAT and WAT fat depots is in agreement with rodent-related work (Cinti, 2007). Because of the sex, amount of intra-abdominal WAT in men is higher when compared with women. In women there are more subcutaneous fat depots (hips and thighs) (Gesta *et al*; 2007).

### 1.2.5. Adipose tissues in animals: subcutaneous depots and fat cells around hairs.

Because of the importance of fat production from meat animals, detailed studies on adipose depots were performed, mainly on pigs and developed in XIX century (Flemming, 1871). In addition, the association between fat cells and hair follicles in pigs and rats was elucidated (sections 1.2.5.1 and 1.2.5.2).

Studies on such animals as pigs, lambs or calves allowed to systematize developmental steps of subcutaneous adipose fat depots (Hausman, 1978; Hausman and Kauffman, 1986). The area lacking lipids and filled with short, not organized collagen fibers and cells with different sizes and shapes was named as “presumptive adipose tissue”. Next, during development of adipose organ, fibers became more organized and were capable of creating so-called “connective tissue” (CT) between clusters of fat cells. First lipids were observed before the CT was fully formed. During the gradual occurrence of adipocytes, the connective tissue became thicker. Next, after reaching maximum thickness, the size of CT decreased during progressive hypertrophy of fat cells.

The fat cell clusters were suggested to derive from so-called “presumptive adipose lobules”, which can be a source of both adipocytes and capillaries. Lipids

were first accumulated in a form of many small droplets. Then, multilocular fat cells became unilocular (when small droplets were modified into one big lipid droplet).

Because of the morphological similarities between very early preadipocytes and endothelial cells, a suggestion was made that fat cells, creating subcutaneous depots in pigs have endothelial origin (Hausman, 1978). In addition, the occurrence of both adipocytes and capillaries at the same time during fat depot development was treated as a confirmation of suggested hypothesis about fat cells origin. For more recent and detailed studies on fat cell origin see section 1.2.3.

The association between blood vessels and adipocytes was noticed during foetal development of pigs and blood vessels seemed to be crucial for the proper features of fat cells in subcutaneous swine depots (Hausman *et al*, 1981b).

#### 1.2.5.1. Pigs.

##### 1.2.5.1.1. General features of pig subcutaneous tissue.

The major fat depot in pigs is a subcutaneous tissue. During animal growth, increase in size of adipocytes and amount of accumulated lipids were observed in some basic studies on pig fat tissue (Mersmann *et al*, 1975). In Mersmann *et al* (1975) study, the subcutaneous depot in dorsal area was observed in lower skin dermis and reached muscle layer. The connective tissue, that divided fat depot into upper and lower layers, was observed in newborn animals. Just after birth, multilocular cells with many lipid droplets were observed. Next, adipocytes were becoming (very fast) bigger and at day 3 fat cells were characterised by large (central) lipid droplets and some additional smaller fat droplets on the periphery of the cells. In addition, presence of collagen was spotted in all analysed time-points (day 0, 3, 9, 23, 40, 60, 110 and 160).

##### 1.2.5.1.2. Association between fat depots and skin compartments during foetal pig development.

Detailed analysis of fat cells features was performed on decapitated (*in utero*) pig foetuses (at 45 day of pregnancy) (Hausman *et al*, 1981b). The analysis was related with dorsal depot of subcutaneous tissue (with skin layer) at 110 days of gestation (when laparotomy was performed). Decapitation resulted in not fully developed epidermis and dermis, decreased number of hair follicles or blood vessels. Moreover, the outer layer of adipose tissue was thin and there was reduced

amount of fat cells around hair follicles in decapitated animals. Interestingly, adipocytes seen in decapitated animals (in outer fat layer) were characterised by bigger diameter of fat cells when compared with adipocytes from control animals.

Hausman *et al* (1981b) suggested that normal development of subcutaneous depots in pigs might be related with developmental processes of skin compartments. Next, abnormal development of subcutaneous fat depot might lead to an enhanced hypertrophy of fat cells that are still seen in decapitated animals.

### 1.2.5.1.3. Development of subcutaneous fat depot in foetal and newborn pigs.

Detailed analysis of subcutaneous fat development was carried out on pig foetuses (Hausman and Kauffman, 1986). Pig foetuses (at age: 45, 60, 75 and 105) were obtained for the analysis of dorsal subcutaneous depot. In addition, newborn pigs were included in this analysis.

Hausman and Kauffman (1986) suggested an age-dependent development of subcutaneous fat depot that started in pig foetuses between day 45 and 60. This depot developed into two distinguishable layers: the outer and the inner and this division was strongly marked in the caudal (posterior) body part and much less obvious in the cranial (anterior part). From 60 day old foetus a clear connective tissue border was seen between the outer and inner layers. At day 60, the outer subcutaneous layer was thinner when compared with inner layer. However, after day 75, the thickness of both layer become similar and did not change significantly after the onset of fat deposition and during next steps of foetal development.

Short strands of collagen fibers were observed between cells in subcutaneous area. Blood vessels with different size were mainly related with subcutaneous layer localised near the skin. Whereas, the inner layer was “almost avascular” and only bottom part of this layer contained of large vessels (Hausman and Kauffman, 1986).

First fat cell clusters were observed in the bottom part of the inner subcutaneous layer in pig foetuses at day 60. Then at day 75, fat cell clusters were seen in the outer layer and near the hair follicles. Progressive development of clusters was observed with lipid deposition at similar level in caudal and cranial samples. Vascular and stromal occurrence, together with differentiation of fat cell clusters was suggested to have a gradient from the muscle to the skin.

#### 1.2.5.1.4. Adipocytes related with hair follicles in pigs.

Fat cells between hair follicles were suggested to be different from other adipocytes of subcutaneous fat depot in pigs (Hausman and Kauffman, 1986).

The hair follicle-related fat cells were analysed in 45, 65, 85 and 112 day old foetal pigs (Hausman and Martin, 1982). First, the general features of skin dermis were investigated, such as presence of so-called papillary dermis (with horizontally organized elastic fibers and collagen) just below epidermis layer and dense reticular dermis in the lower skin area. The term “hypodermis” was used by Hausman and Martin (1982) to describe layer filled with adipose tissue and into which developing hair follicles extends. Areas localised in close proximity to hair follicles and contained lipids were called “hair follicle adipose lobules”. The developing hair follicle was growing through two layers of dermis (mentioned above) and both collagen and fibroblast from the reticular dermis seemed to be localised very close to the outer parts of hair follicles. While hair follicles were growing inside the hypodermis, cells closely attached to these follicles were thought to “unravel” to the hypodermis. The connective tissue, localised around follicles in the hypodermis, was characterised by different (frizzled, unorganized) morphology when compared with connective tissue (flattened) from the reticular dermis. Small hair follicle lobules were related with bottom part of hair follicles, whereas bigger lobules (with more spaces lacking fat cells around areas with adipocytes) were seen in middle part of follicles (Hausman and Martin, 1982).

Hausman and Martin (1982) suggested that in pigs interactions between growing hair follicles and connective tissue close to hairs could lead to a creation of “undifferentiated cells” from which fat cells (and other types of cells seen in fat lobules) developed and surrounded hair follicles. Moreover the translocation of hairs along skin into the hypodermis could be crucial for development of these fat cells.

Interestingly, adipose clusters around hairs developed earlier in obese foetuses (for example at day 90 and 110) and were characterised by the bigger size, when compared with lean animals (Hausman, 1985). A suggestion was made that some metabolic factors might have a capability to influence fat cells near hair follicles, whereas other subcutaneous adipocytes are more resistant to these factors (Hausman and Kauffman, 1986).

### 1.2.5.2. Rats.

The light microscopy technique was applied for the analysis of newborn rat skin with developing fat cells (Hausman *et al*, 1981a). The correlation between hair follicles and adipocytes in rat hypodermis (filled with fat cells) was studied. In whole body section, from one day old rat, more hair follicles were seen along the dorsal (back) part of the body. The hypodermis was separated from subcutaneous tissues by a muscle layer. Thinner hypodermis was seen in ventral (abdominal) area, whereas thicker layer of hypodermis existed in dorsal (back) part of rat body. The hypodermis consisted of different cells: macrophages, mast cells, cells of blood vessel walls, immature adipocytes and adipocytes. Immature adipocytes were though to have the largest nuclei.

The hair follicles were observed to grow along the skin, inside the hypodermis layer. So-called “precursor cells” (with big nuclei and low amount of cytoplasm) could be localised very close to the external root sheath and were developing into adipocytes. In small rats, first lipid droplets were observed in cell aggregates in close proximity to lower part of hair follicles. Unilocular fat cells were seen in bigger animals. Increase in body weight was related with higher diameter of fat droplets, however changes in number of litters influenced this correlation.

When developed hair follicles were presented along the hypodermis, adipocytes around lower areas of hairs were seen. Then, areas where hairs were characterised by a non-finished development were lacking fat cells. It was suggested that fat cells from hypodermis and from other subcutaneous fat depots were characterised by similar size.

A suggestion was made that the growing hairs (in rat skin) influenced dermis cells and this lead to adipocyte development (Hausman *et al*, 1981a). Hair follicles were thought to grow into “reaction areas” and this resulted in the translocation of dermis cells into the hypodermis layer (“star-shaped” cells, observed after the activation of hair development, were next presented in the hypodermis, close to growing hairs). After the movement of hairs down to the skin compartment, concentrated cells close to hairs were able to develop into adipocytes. It was suggested that pathways which controlled hairs growth might be also involved in the regulation of rat hypodermis development.

### 1.2.6. Comparison of hair follicle-related adipocytes in different species: man, pig and rat.

As was shown in section 1.2.5.1, subcutaneous tissue is the major fat organ in pigs and is suggested to develop in a form of several distinguishable layers (Mersmann *et al*, 1975). Fat cells, localised between developing hairs, are thought to create the outer subcutaneous layer in pigs (Mersmann *et al*, 1975). In rodents, fat cells that create dermal adipose tissue are thought to be divided from subcutaneous depots (beneath the skin) by a muscle layer (Cinti, 2007). Next, in humans subcutaneous depots and fat cells in skin dermis (skin adipose tissue) are not separated (as it is suggested in rodents) and create together a distinguishable structure (Cinti, 2007).

It was suggested that rat hypodermis share anatomical similarities with fat cells around hairs in humans and pigs (Hausman *et al*, 1981a). In addition, a similarity in development of such hair follicle-related fat cells was suggested between rats, pigs and man.

Because of the number of fat cells around hairs, more adipocytes were seen in man and pig specimens when compared with rat samples (reviewed by Hausman *et al*, 1981a). Then, more hairs (hair coat) were spotted in rats. Thus, Hausman *et al* (1981a) commented that increase of fat cells might compensate decreased insulating function of hairs.

Hair follicle adipose lobules were seen in human scalp, where the hair cycle is characterised by long growing time (reviewed by Hausman and Martin, 1982). Then hair follicles from other parts of the body seemed to have longer resting periods. Thus, a suggestion was made that adipocyte lobules in the scalp help to enhance activity of growing hairs. In humans, each hair follicle was though to have own growth cycles, whereas in mouse skin hair follicles undergo the same growth phase. Moreover, in adult mice hair follicles were observed in close proximity to adipocytes, but these fat cells were not considered as a part of distinct lobules (as it is observed for human scalp follicles). The presence of lobules around hairs was suggested to be related with cycles of hair growth (Hausman and Martin, 1982).

To summarise, morphological-based studies on several animals suggested the correlation between growing hair follicles and development of fat cells adjacent to follicles (see above). Moreover, developing hair follicles might be responsible for the features of adipose lobules (Hausman and Martin, 1982). However, to best of my knowledge, no more specific *in vivo* studies have been performed that would verify this hypothesis and analyse, on molecular level, events which take part along the skin dermis cells and lead to gradual differentiation of fat cells between hair follicles.

Thus, in this thesis, after the basic analysis of the onset and development of fat cells in mouse embryonic skin dermis (Chapter 2), a microarray approach was applied in order to obtain information about gene expression profiles in dermis cells (in both adipocytes and non-fatty dermis cells) from mouse embryos (Chapter 3).

### 1.2.7. Brief description of obesity and fat-related disorders.

The imbalance between food intake and energy expenditure develops abnormal accumulation of fat in organs that are crucial for metabolism (such as pancreatic muscle, liver or adipose tissue) and leads to obesity (reviewed by Wajchenberg, 2000; reviewed by Ahima, 2008; reviewed by Puhl and Heuer, 2009).

Obesity occurs in adults as well as in children and is an issue during pregnancy. In relation to the size of developing subcutaneous fat organ in humans, the correlation between obese mothers and fatter newborn babies was suggested by Whitelaw (1976). Maternal excess in fat depots has been related with high risk of diabetes development in mothers (Tsoi *et al*, 2010). North America, Great Britain and countries in south-western Europe were characterised by the highest number of overweight and obese kids (Janssen *et al*, 2005) and because of the growing number of obese people, the better understanding of development and features of fat cells is crucial for creating treatments for abnormal lipid accumulation.

Among known obesity-related disorders are insulin resistance, type 2 diabetes mellitus, atherosclerosis or cardiovascular disease (Reaven *et al*, 2004; Sydow *et al*, 2005; de Paula *et al*, 2010). Obesity was related with changes in secretory capability of fat cells (dramatic increase in production of factors secreted from adipocytes) which can lead to the development of insulin resistance and diabetes type 2 (Hajer *et al*, 2008).

Insulin is a hormone produced by the pancreas and responsible for the control of glucose levels (De Meyts, 2004). After meals, high levels of glucose in blood lead to increase in insulin levels (in blood) and glucose can be used immediately by cells or stored in the form of glycogen (in muscles and liver) or as triglycerides (in adipose tissue, see section 1.2.2.2.2.1). Insulin is also capable of preventing the excessive release of glucose from organs.

In general, the term “diabetes mellitus” is used to describe a group of metabolic abnormalities related with high levels of blood glucose (hyperglycemia) as an effect of absence or abnormal function of insulin (reviewed by Raslova, 2010). Type 1 diabetes is related with destruction of pancreatic beta-cells producing insulin, whereas type 2 diabetes is associated with lower levels of produced insulin and reduced sensitivity of different cells in the body (insulin resistance). The insulin resistance syndrome (IRS), observed in individuals with insulin resistance can be associated with metabolic abnormalities: high plasma triglyceride or low concentration of high-density lipoprotein cholesterol: HDL-C. Insulin resistance syndrome is also called as the metabolic syndrome (Sydow *et al*, 2005).

Treatments of diabetic patients are related with monitoring of glucose levels in blood, with healthy diet and lifestyle that will help to keep proper weight and finally with injections of insulin and/or implication of oral anti-diabetic agents (Keating, 2010). The untreated diabetes can result in cardiovascular problems, development of chronic dental diseases, blindness or so-called diabetic foot alternation (Neely *et al*, 1998; Ship, 2003; Wajchenberg *et al*, 2008; Vuorisalo *et al*, 2009).

## 1.3. Adipogenesis.

The differentiation process during which preadipocytes develop into mature fat cells (adipocytes) and accumulate lipid droplets is called adipogenesis (reviewed by: Gregoire *et al*, 1998; Rosen, 2005; Poulos *et al*, 2010).

Detailed analysis of adipocyte differentiation steps and investigation of genes involved in this process were obtained from *in vitro* work, where different cells lines were used (see section 1.3.1.1). These cells, influenced by so-called adipogenic medium, were capable of progressive differentiation which leaded to accumulation of lipids and development of mature fat cells (see section 1.3.2). In addition, the use of transgenic animals allowed the verification of fat-related functions of genes, whose role in adipogenesis in different cell lines was studied (section 1.3.1.2).

Development of a microarray approach has lead to detailed studies of cell features on a molecular level and made it possible to analyse gene expression pathways and investigate mechanisms involved in the control of cell fate and development of different tissues and organs (Heller, 2002; Shergill *et al*, 2004; Chen and Tzeng, 2006). Microarray-based studies, in relation to adipocyte differentiation in different cell lines, are presented in Chapter 3, section 3.1. In addition, in Chapter 3, microarray work has been presented for the investigation of adipocyte differentiation of skin dermis cells located around hair follicle end bulbs.

### 1.3.1. Investigation of adipocyte differentiation process: *in vitro* and *in vivo* studies.

#### 1.3.1.1. Cell lines.

The most popular cell lines, used for the analysis of adipogenesis, were clonally isolated from Swiss 3T3 cells. First, whole embryos from Swiss mice (at age between 17 and 19 days) were used for the establishment of cell line (Todaro and Green, 1963). Embryos were minced and trypsinised and grown in monolayers. It was observed that this 3T3 fibroblast cell line, when reaching their confluency, seemed not to grow anymore and be alive for a while (Todaro and Green, 1963). In addition, some cells from resting cultures were showed to accumulate lipid droplets and be organized in clusters (Green and Kehinde, 1974). In very first experiments, after the trypsiniation of confluent 3T3 cells, lipid-accumulated cells disappeared. When this cell line reached once again its confluency and resting phase, the fatty cells developed. Next, two clones, called 3T3-L1 and 3T3-L2 were isolated that were

able to accumulate high amounts of lipids. The established 3T3-L1 line has become a widely used pre-adipose cell line that has the capability of undergoing adipogenesis and differentiates into mature fat cells (Green and Meuth, 1974; Green and Kehinde, 1975; Green and Kehinde, 1976).

In addition, the 3T3-F442A cells have also been derived from the same source as 3T3-L1 cells and are widely used for adipocyte-related studies (Kuri-Harcuch *et al*, 1984; Moustaïd *et al*, 1988). These two cell lines can be influenced by so-called inducing agents (see section 1.3.2.2) in order to activate/enhance adipogenesis process.

Because of the increase in obesity and diabetes epidemic, a need for better understanding of the mechanisms that control fat cell differentiation led to the establishment of many other cell lines and primary cultures capable of undergoing adipogenesis and some of them are summarised in Table 1.2.

Despite, all knowledge that was gained from preadipocyte/adipocyte cell lines, several disadvantages and problems can be pointed in relation to *in vitro* studies which are discussed in Chapters 3, 4 and 5 of this thesis. Experimental work presented in these three Chapters aimed to develop an *in vivo*-like technique for the investigation of very early steps of adipogenesis in mouse embryonic skin dermis.

Table 1.2. Selected cell lines and primary cultures used for the analysis of adipogenesis process. Based on table from Gregoire *et al*, 1998.

| Organism: | Cell lines; Primary cultures: | Reference: |
|---|---|---|
| **Human** | **LS14 cell line** from human metastatic liposarcoma. | Hugo *et al*, 2004 |
| **Pig** | **Pig culture** from stromal-vascular (SV) subcutaneous adipose tissue cells. | Hausman and Richardson, 1998 |
| **Mouse** | **3T3-L1 cells** and **3T3-F442A cells** from mouse embryos (from 17 to 19 days) | Green and Meuth, 1974<br>Moustaïd *et al*, 1988 |
| | **mES cells** from mouse blastocyst. | Dani *et al*, 1997 |
| | **Ob17 cells** from epididymal fat pads of Ob/Ob (obese) mouse*. | Négrel *et al*, 1978;<br>Grimaldi *et al*, 1982 |
| | **Preadipocyte cell line, AP-18** from subepidermal layer of ear skin from an adult mouse. | Doi *et al*, 2005 |
| | **Mouse culture** from inguinal fat pads. | Litthauer and Serrero, 1992 |
| **Rat** | **Rat culture** from stromal-vascular cells from the epididymal fat pad. | Deslex *et al*, 1987 |

*For more details about ob/ob mouse see section 1.3.1.2.

### 1.3.1.2. Mouse models.

Mouse models have been widely used for analysis of fat depot development *in vivo* (reviewed by Valet *et al*, 2002). Mice have been used for such studies because of their small size, easier breeding and maintaining requirements (in comparison to other animals), beneficial effects of mating process and relatively high number of pups. Finally, because of the availability of sufficient and well established techniques for gene manipulation in these animals.

Functions of a particular gene can be analysed by the specific expression of this gene in adipose fat depot and examples of such animals for adipogenesis related studies are presented in Table 1.3. The preparation of such animals is related with the expression of different genes under promoter regions specific for adipose fat depots, such as UCP-1 (uncoupling protein-1) that is specific for brown adipose tissue (for more details see section 1.2.2.1.2) or ALBP (adipocyte lipid binding protein, also known as aP2 or FABP4, for more details see sections 3.3 and 3.4 of Chapter 3) which targets white and brown adipose tissue. In addition, some promoters can target adipose depots and other organs (for example GLUT4 - insulin-dependent glucose transporter 4).

Table 1.3. Examples of promoters used for the specific (over-) expression of selected genes in mouse models. Such study allowed to investigate fat-related features in these animals. Based on Valet *et al*, 2002.

| Promoter: | Targeted tissue: | Gene: | Analysis of transgenic animals: | Reference: |
|---|---|---|---|---|
| **UCP-1** | brown adipose tissue | Beta3-adrengeric receptor ($\beta_3$-AR) | $\beta_3$-AR needed to rescue effect of $\beta_3$-AR agonists on insulin secretion or food intake | Grujic *et al*, 1997 |
| **ALBP (FABP4)** | brown and white adipose tissues | GLUT4 | increased adipose tissue | Shepherd *et al*, 1993 |
| | | UCP-1 | reduced subcutaneous adipose tissue | Kopecky *et al*, 1995 |
| | | Leptin | changes in adipose tissue weight, dependent on age | Qiu *et al*, 2001 |
| **GLUT4** | adipose tissue and muscles | Glutamine: fructose-6-phosphate amidotransferase | development of insulin resistance | Hebert *et al*, 1996 |

In addition, mice with silenced (invalidated) gene or with specific mutations incorporated into the gene have been used for the fat-related studies (reviewed by Valet *et al*, 2002; Table 1.4). Such mouse models allowed the investigation of features of many adipogenic transcriptional factors, such as C/EBPalpha or PPARgamma (described in section 1.3.3), genes involved in lipid and glucose metabolism or factors secreted by adipose tissue (Table 1.4).

Interestingly, some of these transgenic animals die just before or after birth, thus the analysis of fat depots development is difficult in them. For example, the knockout animal for C/EBPalpha gene (C/EBPα-/- mice) died within 8 hours after birth as a result of hypoglycemia (low levels of blood glucose) (Wang *et al*, 1995). This work showed that C/EBPalpha factor has a crucial role in controlling the proper energy homeostasis. Next, in order to keep C/EBPα-/- mice alive for longer, these animals were crossed with transgenic mice which expressed C/EBPalpha in liver (because of the albumin enhancer/promoter) (Linhart *et al*, 2001). Normally, the C/EBPalpha is expressed by both adipose tissue and liver. Expression of C/EBPalpha in liver enhanced survival of these transgenic animals which at day 7 were lacking white adipose tissue (perirenal, epididymal or subcutaneous fat depots). Brown adipose tissue (BAT) was still detected, however it was characterised by higher accumulation of lipids, when compared with wild type BAT. This work showed that C/EBPalpha is needed for the development of white adipose fat depots *in vivo* (Linhart *et al*, 2001).

Similar complications were related with PPARgamma gene in transgenic mice (Barak *et al*, 1999). Barak *et al* (1999) performed a mutation on the PPARgamma gene related with the elimination of DNA-binding and ligand-binding functions of this factor. PPARgamma null mice were characterised by severe lethality at embryonic level (in utero). These embryos were characterised by disrupted function of placenta and abnormal cardiac development (which occurred at about 10 day of embryonic development). Next, the chimeric embryos were created which allowed the supplementation of PPARgama null embryos with wild type tertraploid cells (they contributed to placenta but not embryo development). Such animal survived several days after birth, and PPARgamma null tetraploid-rescued mice were characterised by the lack of fat depots, thus it was suggested that PPARgamma is crucial for adipogenesis *in vivo*. Barak *et al* (1999) mentioned that "…white fat pads and subcutaneous fat started to emerge in the heterozygote pup, while completely absent in the mutant (data not shown)..." (citation from Barak *et al*, 1999). Next, in analysed pups, brown adipose fat (BAT) depot was seen in

heterozygote, whereas it was not present in null animal. In addition, the observation was made that similar pattern of an establishment of PPARgamma-positive-brown adipose lineage seemed to take place at E15.5 in both heterozygote and homozygote. Thus, PPARgamma was suggested not be crucial for the onset of BAT but for further modifications of BAT (Barak *et al*, 1999).

Moreover, the brown adipose tissue is suggested to be the first fat depot with high PPARgamma (together with PPARalpha and PPARbeta) expression in rats (Braissant and Wahli, 1998).

Table 1.4. Examples of knockout animals used for the analysis of genes function in relation to adipogenesis *in vivo*. Based on Valet *et al*, 2002. C/EBPalpha, PPARgama are discussed in Chapters 2 and 3, angiotensinogen in Chapter 3, whereas CD36 in Chapters 3 and 5.

| **Target:** | | **Analysis of transgenic animals:** | **Reference:** |
|---|---|---|---|
| **Transcription factors** | C/EBPalpha knockout | hypoglycaemia; newborns died within 8 hours after the birth | Wang *et al*, 1995 |
| | C/EBPalpha expressed only in the liver but not in other tissues | absence of white adipose fat depots (visceral and subcutaneous); enhanced accumulation of lipids in brown adipose tissue | Linhart *et al*, 2001 |
| | PPARgama mutation | utero lethality | Barak *et al*, 1999 |
| | PPARgamma mutation with rescued placental defect | lack of adipose tissue | Barak *et al*, 1999 |
| **Lipid and glucose metabolism** | CD36/FAT | defective fatty acid uptake | Febbraio *et al*, 1999 |
| | Perilipin | reduced adipose tissue; aberrant adipocyte lipolysis | Martinez-Botas *et al*, 2000<br>Tansey *et al*, 2001 |
| **Secreted (by adipose tissue) factors** | Interleukin-6 | mature-onset obesity | Wallenius *et al*, 2002 |
| | Angiotensinogen | alteration in development of adipose tissue | Massiera *et al*, 2001 |

It is worth mentioning the animal models used for the investigation of obesity and diabetes. A mouse with spontaneously developing obesity was observed in the Jackson laboratory (Ingalls *et al*, 1950). These animals started to gain weight between four to six weeks of their life and could become four times bigger than normal mice. In 1994, the nonsense mutation of *ob* gene (which codes leptin, for more details about leptin see section 1.2.2.2.2.3) has been related with the development of these obese animals (for example in C57BL/6J ob/ob mouse strain) and mouse *ob* gene and its human homologue was successfully cloned and sequenced (Zhang *et al*, 1994). Briefly, the occurring point mutation changes C to T and arginine codon is changed for a stop codon (at position 105) (Zhang *et al*, 1994). As an effect of such change, no 16kDa leptin is present in homozygous mice.

In addition, obese animals can develop diabetes (Coleman, 1982), thus the ob/ob mouse model became very popular in the analysis of fat-related disorders (Drel *et al*, 2006). Moreover, mutations in the *ob* gene were combined with other mutations in order to further investigate adipose tissue features, metabolic processes and obesity. For example, mice were created that were lacking leptin and neuropeptide Y (NPY) gene and this work confirmed a role of NPY in energy homeostasis (reviewed by Butler and Cone, 2001).

### 1.3.2. Adipocyte differentiation *in vitro*.

Adipogenesis process, analysed in different cell lines and primary cultures (section 1.3.1.1), is related with such terms as the growth arrest, clonal expansion or adipogenic medium and inducing agents (Figure 1.7A and Figure 1.7B).

#### 1.3.2.1. Growth arrest and clonal expansion.

The growth arrest, together with the occurrence of confluence, is observed as a first step of the activation of adipogenesis *in vitro* and the contact inhibition leads to the growth arrest (Rosen and Spiegelman, 2000). In relation to confluence, this feature is dependent on the type of cell line and primary culture and for example it was shown that primary preadipocytes established from rat and kept at low density, are capable of differentiation without the cell-cell contact (reviewed by Gregoire *et al*, 1998).

It is suggested that the growth arrest (the G1/S boundary) can be activated by a hormonal “regimen” and seems to be related with adipogenic transcriptional factors (such as C/EBPs and PPARgamma, which are also discussed in section 1.3.2.2). The growth arrest is followed by the clonal expansion process (Ailhaud *et al*, 1989; Rosen and Spiegelman, 2000). C/EBPalpha, antimitotic agent, inhibits cell proliferation and is involved in activation of a cell cycle component p21/SDI-1 (Timchenko *et al*, 1996). Also, p18 (cyclin-dependent kinase inhibitor) can be influenced by adipogenic factors and its level was induced by expression of PPARgamma in NIH-3T3 fibroblasts (Morrison and Farmer, 1999). After the growth arrest, cells require factors (see section 1.3.2.2 for more details) which activate the next steps of differentiation and then, during the clonal expansion one or two rounds of cell division take place (Ailhaud *et al*, 1989). Depending on the type of cells, DNA synthesis seems to be important for adipocyte conversion (for example in 3T3-F442A cells: shown by Kuri-Harcuch and Marsch-Moreno, 1983) or the cell division is not needed for further steps of *in vitro* differentiation (precursor cells from human adipose tissue, shown by Entenmann and Hauner, 1996).

Retinoblastoma proteins have been related with adipogenesis *in vitro* (Richon et at, 1997; Ross *et al*, 2008). Such proteins as pRb, p107 (retinoblastoma like-1) and p130 (retinoblastoma like-2) bind and regulate the activity of E2F transcription factors and control the cell cycle progression. At the G1 phase of the cell cycle, complex pRB-E2F (with underphosphorylated pRb) inhibits the E2F-dependent transcription. The p130 is related with GO/G1 phase, whereas the

complex p107-E2F occurs during S-phase. Both, p107 and p130 were analysed in relation to adipogenesis and the re-entry step into the cell cycle (clonal expansion) from the growth arrested step (Richon *et al*, 1997; Ross *et al*, 2008).

Richon *et al* (1997) showed that confluent 3T3-L1 preadipocytes at day 0 (non-treated cells, before the addition of adipogenic medium) were in the growth arrested phase (low number of BrdUrd positive cells), whereas at day 1 (approximately one day after the addition of adipogenic medium with insulin, dexamethasone and isobutylmethylxanthine which are discussed later in this Chapter) cells were proliferating, while at day 3 they become “quiescent” (Richon *et al*, 1997). On the protein level, it was shown that in 3T3-L1 cells at day 0, both p130 and the p130-E2F complex were observed, whereas no free E2F or p107 were seen. At day 1, complex p107-E2F together with p107 and free E2F were detected, whereas the level of p130 dramatically decreased. During next days of adipogenic induction, p130 protein level was gradually increasing, whereas the p107 protein was decreasing. In addition, on mRNA levels, only p107 was changed (but not p130) during the adipocyte differentiation and it was related first with a dramatic up-regulation at day 1 and then its dramatic down-regulation during days 2 - 4. This suggested the specific regulation of p107 at a transcriptional level during adipogenesis *in vitro*. Because p130 mRNA levels did not change during analysed time-points, it was suggested that its regulation occurs at post-transcriptional level (Richon *et al*, 1997).

A study performed on human adipose derived stem cells (hASC) aimed to analyse changes in p107 and p130 levels (Ross *et al*, 2008). These multipotential stem cells (not already committed cells to adipogenesis as 3T3-L1 preadipocytes) required longer treatment with adipogenic medium (10 days) for terminal differentiation and occurrence of fat cells with lipids. During these ten days, hASC cells did not undero the clonal expansion and levels of p130 gradually decreased during the adipogenesis process (Ross *et al*, 2008). In addition, p107 protein was up-regulated in hASC cells at day 4 and then gradually its level decreased, suggesting a similar expression pattern of p107 in both 3T3-L1 and hASC during adipocyte differentiation (Ross *et al*, 2008).

In general, it is not clear if the clonal expansion is always needed during adipogenesis. A suggestion was made that clonal expansion can be a form of an “artifact” of cell culture environment or that some isolated cells are already after this step (Rosen and Spiegelman, 2000).

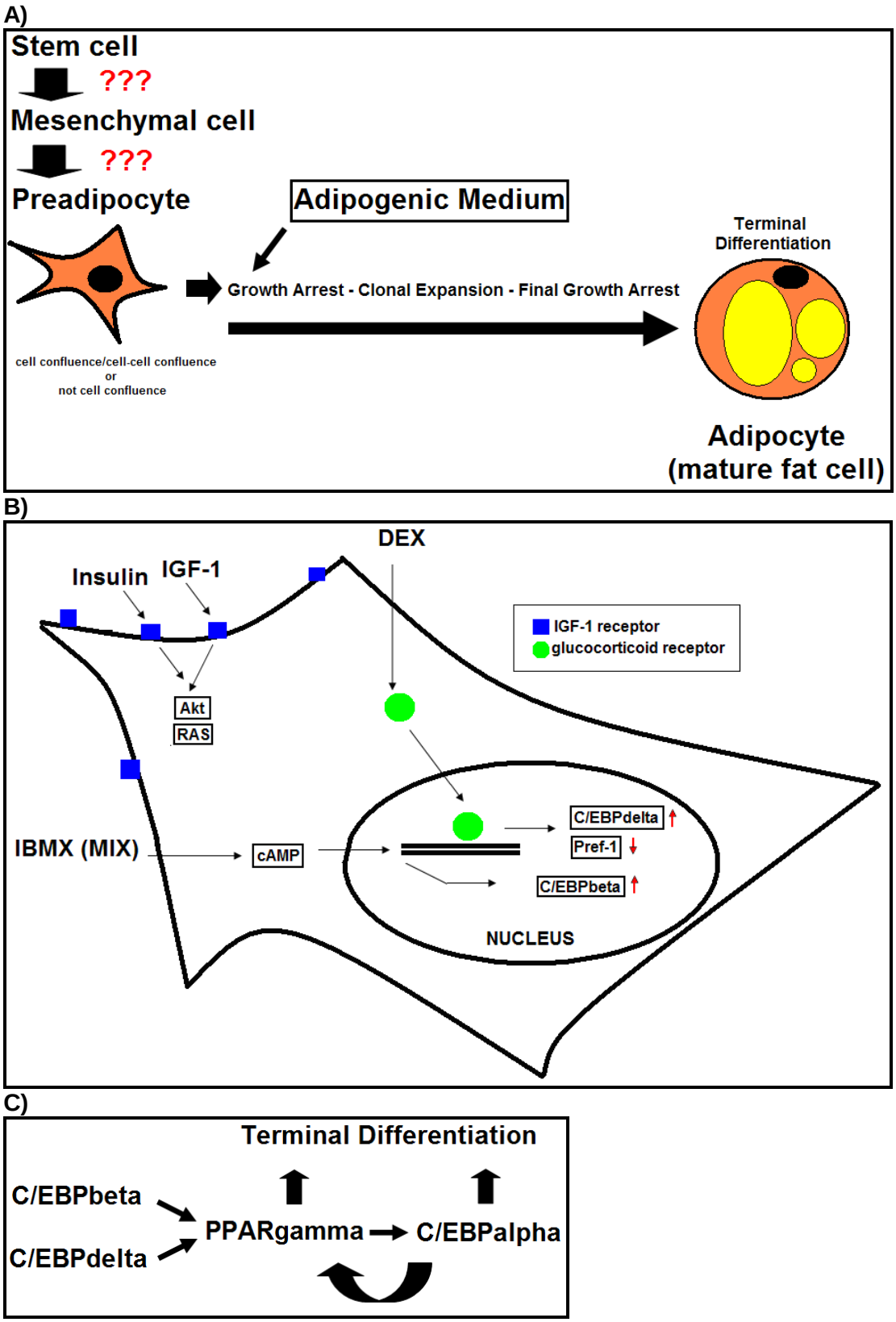


Figure 1.7. A schematic presentation of adipogenic differentiation *in vitro*. (A) Stages of preadipocyte differentiation. (B) Components of adipogenic medium and suggested pathways of adipogenesis activation. (C) Chronology of adipogenic transcription factor activation progress to terminal differentiation of the fat cell. Information derived in part from: Richon *et al*, 1997; Gregoire *et al*, 1998; Morrison and Farmer, 1999; Rosen and Spiegelman, 2000; Rosen *et al*, 2002.

### 1.3.2.2. Adipogenic medium and steps of adipogenesis *in vitro*.

Adipogenic medium, with specific agents, is used for the activation and enhancement of adipogenesis *in vitro* (reviewed by Gregoire *et al*, 1998). Such agents as insulin, dexamethasone (DEX) and isobutylmethylxanthine (IBMX, MIX: methylisobutylxanthine) are widely used for the induction of adipogenesis in 3T3 cells and were applied in experiments shown in Chapter 4 and 5 of this thesis (see also Figure 1.7B). In addition, insulin is the main ingredient of adipogenic medium used on both cell lines and primary cultures (reviewed by Gregoire *et al*, 1998).

It is worth mentioning that, depending on the exact type of cells, other factors (for example together with insulin) were observed which activated adipogenesis. The influence of both insulin and lipolytic hormones (epinephrine and corticotrophin which induce lipolysis) or 3,3',5-triiodothyronine was analysed on Ob17 cells (Négrel *et al*, 1978; Grimaldi *et al*, 1982). Insulin-like growth factor 1 (IGF-1), similarly as insulin, was shown to be important for the activation of adipogenesis in 3T3-L1 preadipocytes (Smith *et al*, 1988).

Insulin was suggested to react with insulin-like growth factor 1 receptor (similarly as IGF-1) and stimulate ras and protein kinase B (Akt). Both ras and Akt were shown to influence adipogenic differentiation (Benito *et al*, 1991; Magun *et al*, 1996). Dexamethasone (DEX) might interact with the glucocorticoid receptor (nuclear hormone receptor) and was shown to induce C/EBPδ (C/EBPdelta) mRNA and reduce mRNA and protein levels of Pref-1 (Cao *et al*, 1991; Smas and Sul, 1993). Isobutylmethylxanthine (IBMX, MIX: methylisobutylxanthine), a phosphodiesterase inhibitor, was shown to activate C/EBPβ (C/EBPbeta) probably by the increase of cAMP (cyclic AMP) levels and this was shown to influence adipogenesis in 3T3 cells (Cao *et al*, 1991; Yarwood *et al*, 1995; Rosen and Spiegelman, 2000). It is important to mention here that the exact role of suggested adipogenic factors and detailed description of pathways involved in adipogenesis activation, especially in relation to *in vivo* process, are not fully understood or defined and still have to be examined (Rosen and Spiegelman, 2000).

After the activation of both C/EBPdelta and C/EBPbeta, expression of PPARγ (PPARgamma) occurs, which is suggested to influence the activation of C/EBPα (C/EBPalpha) (Figure 1.7C). In mice fibroblasts, null for PPARgamma ($PPAR\gamma^{-/-}$ cells), C/EBPalpha was not capable of promoting adipogenesis on its own (Rosen *et al*, 2002). In addition, it is believed that activated C/EBPalpha influences PPARgamma in order to remain adipocyte differentiation (positive feedback loop).

C/EBPalpha null fibroblasts were capable of adipogenesis, however these cells had lower amount of lipids and were characterised by low levels of PPARgamma (Wu *et al*, 1999). Then, the application of C/EBPalpha to these cells (by the retroviral vector) allowed the activation of PPARgamma expression.

Among other factors involved in regulation of adipogenesis are GATA-binding transcription factors or cAMP response element binding protein (CREB) (reviewed by: Gregoire *et al*, 1998; Rosen, 2005; Poulos *et al*, 2010).

Mature fat cells (adipocytes) accumulate lipids and produce proteins which are next secreted by these cells (for example resistin and leptin, adipsin or adiponectin; see Table 1.1 in this Chapter and Chapter 3, section 3.3.2).

When adipogenesis is activated, the cell shape is changed and fibroblast-like cells acquire a spherical structure (reviewed by Gregoire *et al*, 1998). Some interesting changes in cell morphology and the level of extracellular matrix (ECM) and cytoskeletal elements are also observed. For example, it was shown that when adipogenesis was activated in 3T3 cells, decreases in beta and gamma actin, alpha and beta tubulin and vimentin were observed (Spiegelman and Farmer, 1982). It was suggested that these changes are very early processes that occur during differentiation. They can be responsible for the development of the specific morphology of adipocytes and they may activate expression of C/EBP factors and PPARgamma.

### 1.3.3. Adipogenic transcription factors - crucial regulators of early stages of adipogenesis.

#### 1.3.3.1. CCAAT/enhancer binding protein family.

One of the most important transcription factors, involved in the adipogenesis activation, belong to the CCAAT/enhancer binding protein family (C/EBP). The C/EBPs include several nuclear transcription factors: C/EBP α, β, γ, δ, ε (Landschulz *et al*, 1988).

It was observed that the sequence of different C/EBPs are identical in the C-terminal part (55 - 65 amino acid residue), in which bZIP domain is present (Hurst, 1994; Gregoire *et al*, 1998; Ramji and Foka, 2002). The highly conserved bZIP domain has a basic amino-acid rich DNA-binding part and a dimerization motif called the “leucine zipper”. The leucine zipper has heptad repeat of four or five leucine residues. These residues give α-helical configuration, which then leads to the formation of a coiled-coil structure. Dimerization is needed for the DNA binding, which is controlled by the basic region. It was shown that the DNA binding depends on the amino acid sequence within the basic region (Hurst, 1994). The dimer structure has Y-shaped architecture and each arm of this structure is made from the basic region and binds to one-half of a sequence in the DNA major groove (Hurst, 1994). The different C/EBP proteins can form interfamilial heterodimers because of the fact that the bZIP domain is highly conserved. The N-terminal of C/EBPs contains three short parts conserved in most C/EBPs, which represent the activation domain that can stimulate transcription. The activation domain does not occur in C/EBPgamma factor, which therefore can form inactivated heterodimers with other C/EBPs. The general sequence preferences, specific for these factors is related with: RTTGCGYAAY element, where R is A or G and Y is C or T (Osada *et al*, 1996).

It was noticed that C/EBP proteins are expressed at different levels in various tissues. The high expression of C/EBPalpha was observed in the adipose tissue, placenta, intestine, liver, and lung, whereas the C/EBPbeta level is quite high in the lung, spleen, kidney, adipose tissue, and lung (Ramji and Foka, 2002).

Among functions of C/EBPs are control of metabolism, cell differentiation or proliferation and these factors play crucial role in adipogenesis, as was mentioned earlier.

### 1.3.3.2. Peroxisome proliferator-activated receptors (PPARs).

PPARs are transcription factors, which belong to type II nuclear hormone receptor family and form heterodimers with retinoid X receptors (RXRs) (Schoonjans *et al*, 1996). They have two conserved domains: the centrally located DNA-binding domain and the C-terminal region, which has the ligand-binding domain (LBD) (Uppenberg *et al*, 1998; Lee *et al*, 2003). Prostaglandins are specific ligands for PPARgamma (Nosjean and Boutin, 2002). Among other known ligands for PPARgamma are thiazolidinedione (TZD) class of anti-diabetic drugs (Lehmann *et al*, 1995). PPAR with RXRs binds to so-called PPAR response elements (PPREs) and regulate transcription of genes.

PPAR factors, such as PPARα (NR1C1), PPARδ/β (NR1C2), and PPARγ occur in different tissues and have different biological activities. PPARalpha, for example is expressed in the heart, muscles or kidney and controls lipid homeostasis (Lee *et al*, 2003; Rosen, 2003).

PPARgamma, as was mentioned earlier in this Chapter, is up-regulated in cells treated with adipogenic medium and is responsible for adipocyte differentiation (see section 1.3.2). There are two isoforms of PPARgamma: gamma 1 and gamma 2 (Zhu *et al*, 1995). Mouse PPARgamma gene was observed to give two mRNAs, which differ at 5' ends and PPARgamma 2 isoform was characterised by the additional 30 N-terminal amino acids. These two mRNAs were related with different promoters and tissue-specificity. PPARgamma 2 is treated as an adipocyte-specific nuclear hormone receptor (Tontonoz *et al*, 1994).

## 1.3.4. Examples of factors and pathways involved in regulation of adipogenesis.

Adipogenesis is controlled by a variety of proteins and pathways that can activate or inhibit this differentiation process. One of the suggested adipogenesis inhibitors is Pref-1, synthesized as a plasma membrane protein (reviewed by Gregoire *et al*, 1998). The high level of Pref-1 is observed in preadipocytes and its downregulation is needed for adipose conversion. This molecule can have two forms (50 kDa and 25 kDa) and the bigger one is thought to be responsible for the inhibition of adipogenesis (Mei *et al*, 2002). Pref-1 is also discussed in Chapter 2 (sections 2.2.5.1 and 2.4.5).

Adipogenesis is also controlled by the Wnt pathway and beta-catenin (Kennell and MacDougald, 2005). In general, the Wnt signalling is related with

differentiation processes of cells and organogenesis in mammals. The family of Wnt genes encodes secreted factors (glycoproteins), called “Wnts” and Wnts are responsible for different structures created during organogenesis (Dale, 1998; Smalley and Dale, 1999). The Wnt-10b ligand is responsible for the regulation of adipogenesis and its high level was observed in preadipocytes (Katoh and Katoh, 2005). It is suggested that Wnt-10b may govern adipogenesis by inhibiting the activity of C/EBPalpha and PPARgamma (Ross *et al*, 2000). It was also noticed that adipogenic factors (for example PPARgamma) can inhibit Wnt signalling (Moldes *et al*, 2003).

The multifunctional protein, beta-catenin, plays an important role in the Wnt pathway. In general, the Wnt system regulates both the amount and localisation of beta-catenin (Eberhart and Argani, 2001). Briefly, the secreted Wnts bind to the “frizzled” membrane receptors, which transfer the signal inside the cell and the activity of GSK kinase is inhibited (Figure 1.8). Because of this, beta-catenin can not be phosphorylated and can not be degraded in the proteasome. Thus its level increases and beta-catenin is translocated into the nucleus. In the nucleus, active beta-catenin forms a complex with Tcf/Lef factors and expression of different genes is activated (Dale, 1998). When active beta-catenin is accumulated in the nucleus, the inhibition of adipogenesis is observed. When the Wnt signalling is turned off, adipocyte differentiation is activated.

The WNT signalling pathway is also discussed in Chapter 3 (section 3.4.1).

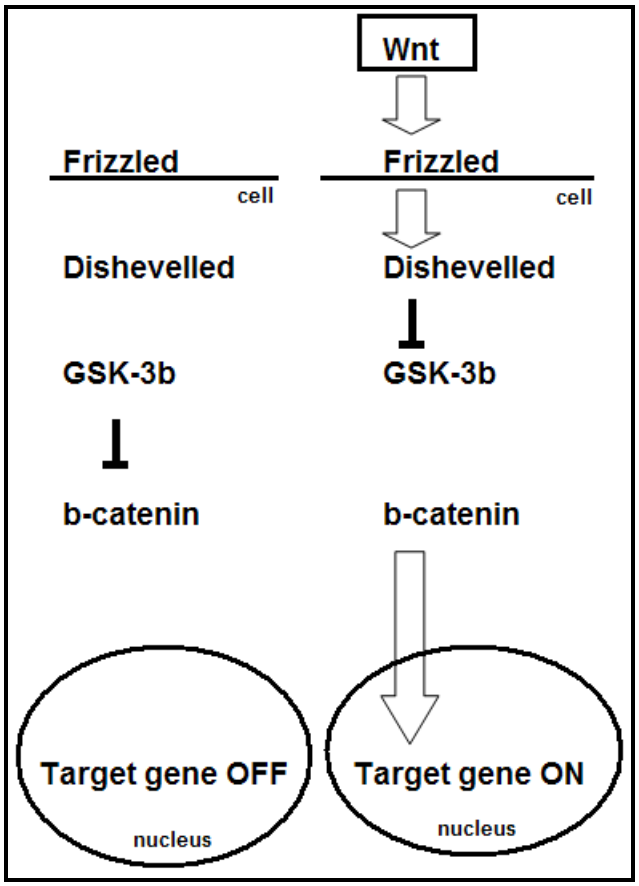


Figure 1.8. A schematic presentation of the canonical Wnt signalling pathway. Adapted from Dale, 1998.

## 1.4. Thesis aims.

Work presented in this thesis aimed to increase knowledge about the process of adipogenic differentiation *in vivo*, leading to development of the fat depot in rodent back skin.

The first hypothesis tested in this study was that precursors of fat cells, localised in lower back skin dermis, undergo adipogenic differentiation during late stages of rodent embryonic development and create the dermal adipose tissue after the animal birth. The work in Chapter 2 investigated the timing and location of the onset of adipogenesis and the subsequent development of a fat depot in skin dermis. This was achieved by dissection and staining of the whole skin and subcutaneous fat layer; tracking the accumulation of lipid droplets (Oil Red O analysis) and by following the expression of an adipogenic transcription factor C/EBPalpha (immunofluorescence technique) at different time points in late embryonic/foetal development.

The aim of the work from Chapter 3 was to clarify the hypothesis that dynamic changes at molecular level take place between e17 and e19 time points in two dermal compartments which are crucial for the development a non-fatty area (upper dermis) and the dermal adipose tissue (lower dermis). In addition, the adipogenesis process observed in lower dermis was hypothesised to differ in some extent from adipogenic differentiation widely investigated using *in vitro* approaches (3T3-L1 cells). Chapter 3 describes a microarray-based study using laser capture microdissected cells from embryonic back skin dermis, based on the timing and location of the events of adipogenesis established in Chapter 2.

The work in Chapter 4 was directed at developing tools for functionally assessing the activities of genes associated with adipogenesis. It involved modifying techniques for culturing pieces of embryonic/foetal skin, or growing dermal cell populations, and then examining the effects of an exemplar *Egfr* gene chosen from the microarray lists from Chapter 3. The hypothesis presented in Chapter 4 was that the EGF-EGFR signalling pathway is involved in the regulation of adipogenic differentiation *in vivo* in lower dermis between e17 and e19 time points.

Chapter 5 aimed to establish a protocol for the fluorescence activated cell sorting (FACS), in order to dissect a preadipocyte population from embryonic skin dermis. Once again this approach was underpinned by the microarray data in

Chapter 3, from which the cell surface markers (CD36, Fzd4) were obtained. It was hypothesised that FACS sorted CD36-positive cells, represent a lower dermal cell population that undergo adipogenesis and create dermal adipose tissue in mouse back skin.

Chapter 6 intended to bring together some of the main ideas and themes of this thesis; to suggest some answers to more general questions raised from these studies about the control of adipogenesis in skin; and to suggest some ideas for future studies.

# Chapter 2 :
# The investigation of dermal adipose tissue development and an effective marker for preadipocyte/adipocyte cells in rodent skin dermis.

## 2.1. Introduction.

Nowadays, interest in adipocytes (their development and functions) has enlarged because of the obesity and high number of fat-related disorders. Widely available knowledge about adipogenesis process comes mainly from *in vitro* studies, where a number of cell lines have been used (for example 3T3 cells, for more details see Chapter 1, section 1.3.1.1). In addition, the investigation of adipose organ development is being investigated in mouse models (Valet *et al*, 2002).

White adipose tissue is divided into two depots: visceral adipose tissue - VAT and subcutaneous adipose tissue - SAT (Cinti, 2001). Subcutaneous fat depots beneath mouse skin have either anterior (under the head, near the neck and upper limb area) or posterior localisation (near the lower limbs). The VAT has been associated with insulin resistance or type 2 diabetes and its removal in humans can lead to a decrease of both glucose and insulin levels (Porter *et al*, 2009). Subcutaneous adipose tissue was suggested to have a beneficial effect on the metabolism (in relation to its transplantation into visceral fat depots) (Tran *et al*, 2008). These few results clearly show how important it is to carry out fat-related studies and develop *in vivo* techniques where more features of adipocytes can be investigated.

Fat depots in close proximity and beneath the skin are treated as a subcutaneous adipose tissue that seems to develop at foetal level in the form of several distinguishable layers that are divided by a connective tissue (Poulos *et al*, 2010). During the detailed analysis of subcutaneous fat in pigs and rats, the outer layer was observed to differ from other fat layers, because of the presence of fat cells around hair follicles (Hausman *et al*, 1981a; Mersmann *et al*, 1975). Hausman and his colleagues analysed the rat hypodermis layer, where adipogenesis had been suggested to be linked with the development of hair follicles (Hausman *et al*, 1981a). In addition, some basic analysis of fat depots occurrence in human foetuses was carried out (Poissonnet *et al*, 1984). A suggestion was made that the rat hypodermis is anatomically similar to the outer layer of subcutaneous fat in both pigs and humans (Hausman *et al*, 1981a). In rodents fat depot in dermis was named the dermal adipose tissue and was observed to be separated from subcutaneous adipose tissue by a muscle layer (Cinti, 2007).

The main experiments presented in Chapter 2 were performed on mouse back skin specimens in order to test the hypothesis that a population of

preadipocytes resides in lower skin dermis of mouse embryos and is being activated to undergo adipoenesis at late stages of embryonic development which leads to a creation of a dermal adipose tissue in back skin of newborn animals.

In general, available knowledge about fat cells in and beneath the skin was performed on different skin sections stained with dyes that bound to lipids. Next, the light microscopy allowed information to be obtained about the morphology of fat cells and features of accumulated lipids (Hausman *et al*, 1981a). This *in vivo* analysis however is lacking more advanced study of very early signals of adipogenesis, when no fat is yet accumulated in so-called preadipocytes that gradually differentiate into mature fat cells. Development of cell culture techniques and establishment of preadipocyte cell lines gave insight into the molecular mechanisms of adipogenesis and allowed to gain knowledge about genes involved in differentiation of fat cells *in vitro* (for more details see Chapter 1, section 1.3.1.1). Next, the use of mouse models helped to study the function of different adipocyte-related genes (see Chapter 1, section 1.3.1.2). However, there are still questions related with the “real” *in vivo* features of very early steps of adipogenesis. Thus, in the second part of Chapter 2, results form the investigation of an *in vivo* marker for preadipocytes and adipocytes in lower rodent skin dermis were shown. The cross-sections from back skin samples were incubated with antibodies against several factors known to be involved in early stages of adipogenesis, mainly based on *in vitro* work. Finally, the antibody, against adipogenic transcription factor C/EBPalpha allowed the investigation of the timing and location of cells that undergo adipocyte differentiation in lower skin dermis of rats and mice.

To sum up, the first part of the study presented in Chapter 2 is related with the analysis of the onset and development of rodent fat cells in lower skin dermis (with the main focus on mouse skin) and investigation of the correlation of these adipocytes with other subcutaneous fat depots. Next, the marker for preadipocyte and adipocyte cells in lower dermis was successfully established which enhanced knowledge about general features of early stages of fat cell differentiation. Work presented in this Chapter has been published (Wojciechowicz *et al*, 2008).

In addition, study presented in Chapter 2 helped to set up a more detailed experiment where the gene expression pattern of differentiating preadipocytes in lower embryonic mouse dermis was obtained during rodent development. This work is described in Chapter 3.

## 2.2. Methods.

### 2.2.1. Housing, breeding and feeding conditions of rodents.

Mice (CD1) and rats (PVG), from the Durham University Life Sciences Support Unit, were bred and maintained at a temperature of 21$^{o}$C, with 55% humidity and kept on a 12 hour light/dark cycle. All animals were on Harlan Teklad 2014 Rodent Maintenance diet, and watered and fed ad libitum.

Analysis of vaginal plugs was used to establish the baseline age of embryos used for experiments. Breeding pairs were kept together overnight and the presence of a vaginal plug in the morning indicated a successful mating, at which point embryos were considered to have undergone 0.5 days of gestation.

Rodents were sacrificed using carbon dioxide and/or cervical dislocation, as under Schedule 1 of the Animal (Scientific Procedures) Act 1986.

### 2.2.2. Preparation of whole mouse skin samples for the global analysis of fat accumulation.

Animals from multiple developmental time points (few hours, 2 and 6 day old mouse newborns) were used in order to collect the skin from their whole bodies for global analysis of fat accumulation in mouse skin. First, an incision was made in the abdomen of the mouse body from the caudal to dorsal direction. Then, incisions were made in the other skin areas of the abdomen part (such as along the limbs, neck and tail). Skin was carefully pulled off from the mouse body by cutting off the muscle connection between the skin and the body. Skin was not collected from the extremities of the animal limbs. Skin from the head and ears was taken from most samples, but not from vibrissae pads (because of the tight connection of the skin and hair follicles to the mouse body). While the whole skin was removed from the mouse body, the biggest anterior fat depots under the skin were not collected. The skin area of main interest was related to dermis from the mouse back. The whole skin samples underwent the Oil Red O analysis according to the protocol presented in section 2.2.4.

### 2.2.3. Preparation of skin sections from rodent back skin.

Skin samples were taken from 15 (e15; 15dE time point), 16.5 - 17 (e17; 17dE time point), 18 (e18; 18dE time point), 18.5 - 19 (e18.5 - 19; 18.5 - 19dE time point) and about 19 (e19; 19dE time point) day old mouse (CD1) embryos. In addition, samples were taken from 18 (e18; 18dE time point) and 20/21 (e20/21; 20/21dE time point) day old rat (PVG) embryos.

Samples were also prepared from mouse (CD1) newborns (0.5, 1, 2, 4, 5, 8, 10, 12, 15, 17 and 19 days, named respectively as 0.5dN, 1dN, 2dN, 4dN, 5dN, 8dN, 10dN, 12dN, 15dN, 17dN and 19dN time points) and rat (PVG) neonates (at 1, 2 and 6 days: 1dN, 2dN and 6dN time points).

Skin specimens were collected from the animal back (Figure 2.1 and Figure 2.2, for detailed analysis of both figures see also section 2.3.2). First, incisions along both sites of the rodent back were made from the caudal to dorsal (head to tail) direction. Then, skin was cut along the neck and below the tail and a square-like piece of back skin was obtained that was carefully removed from rodents by cutting the muscle connection between skin and the rest of the body. Fat layers, beneath the back skin in anterior and posterior localisations, were collected with the back skin specimen for the Oil Red O analysis. Back skin samples, used for immunohistochemical analysis and lipid detection in skin dermis, were rolled up. Rolled samples were put into the Tissue-Tek® O.C.T.$^{TM}$ Compound (Sakura), then snap frozen in liquid nitrogen and kept at -80$^{o}$C. For lipid detection in skin dermis and fat layers seen beneath the skin, back skin samples were not rolled but cut in half (Figure 2.2c) and then put into the Tissue-Tek and frozen (in liquid nitrogen). All back skin sections (7 μm for embryonic mouse samples and all rat samples and 10 - 14 μm from mouse newborns), were cut on a cryostat (LEICA CM 3050S) and attached to SuperFrost®Plus slides (Menzel-Glaser), air dried for up to 90 min at room temperature, and then used immediately for lipid detection, immunofluorescence or immunohistochemical analysis. The Oil Red O study allowed the investigation of lipid depots along the skin and beneath the skin. The immunofluorescence and immunohistochemical analysis were related with the analysis of skin epidermis and dermis.

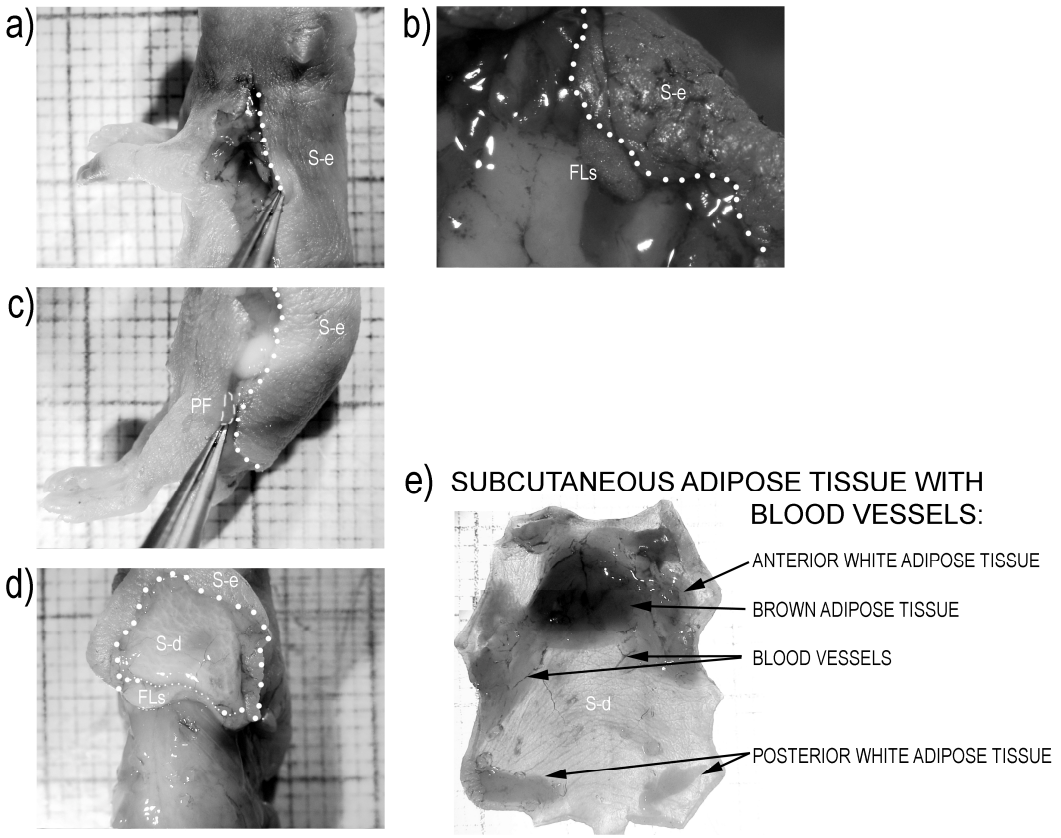


Figure 2.1. Stages of the back skin removal procedure performed on a one day old newborn mouse. a) Incisions were made in the top part of the back skin (near the neck area) on both sides of the body. b) Fat depots were observed under the top part of back skin. c) Fat depots were observed in the bottom part of mouse body, near the limbs. d) The back skin was carefully removed from mouse body. e) A back skin sample with fat depots under the skin. S-e: skin from the epidermis site. S-d: skin from the dermis site. FLs: fat layers. PF: posterior fat. Specimens were placed on a 1 $mm^2$ grid paper. Images were captured using a Ziess StemiSVII microscope.

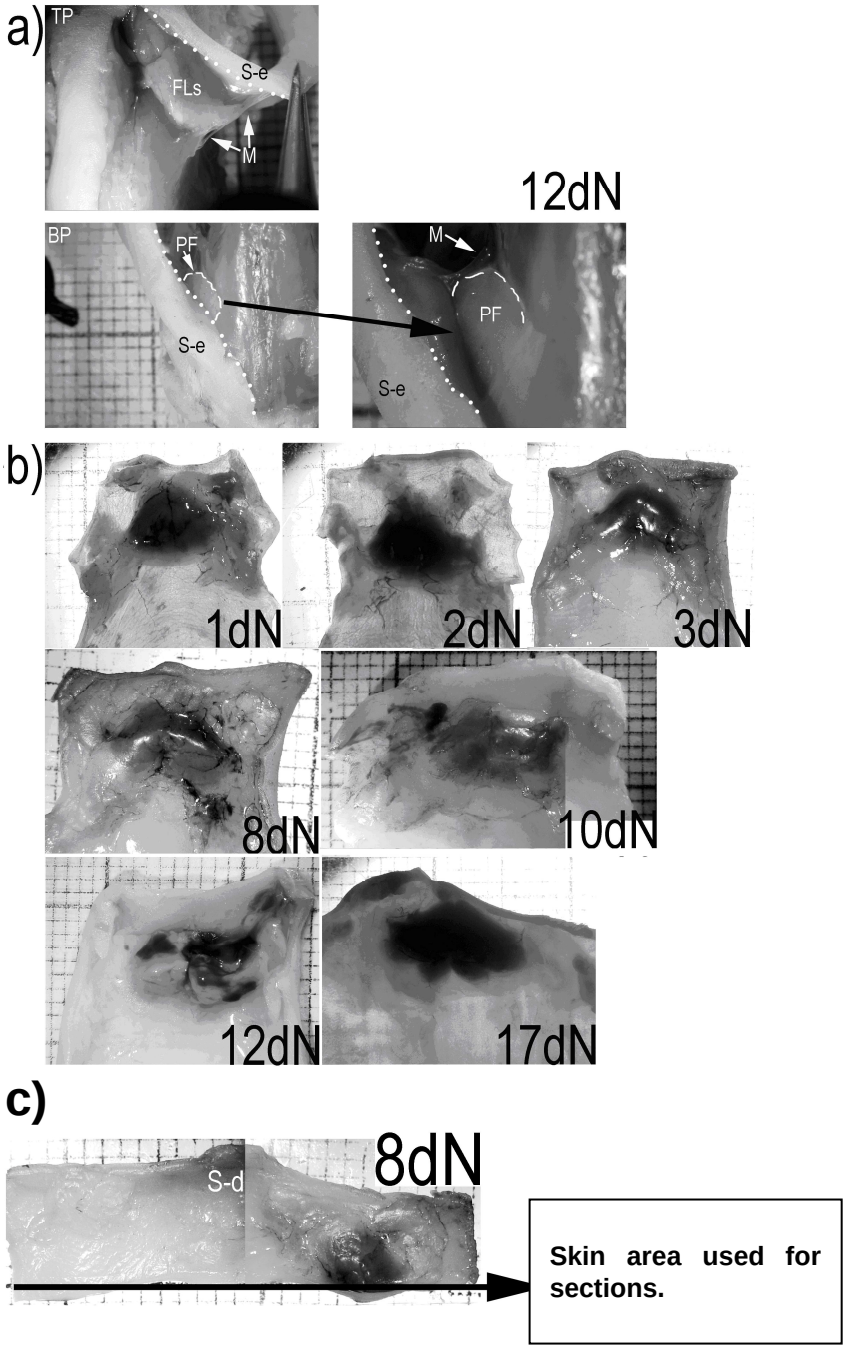


Figure 2.2. Features of fat depots localised beneath the mouse back skin. a) Fat depots attached by thin layers of muscle to the skin. b) Fat depots in the top part of the back skin from newborn mice at different stages of development (d - day; N - newborn). c) The skin sections were obtained from approximately the central part of the back skin specimen. TP: top part of the back skin. BT: bottom part of the back skin. S-e: skin from the epidermis site. FLs: fat layers. M: muscle layer. PF: posterior fat. Specimens were placed on a 1 $mm^2$ grid paper. Images were captured using a Ziess StemiSVII microscope.

### 2.2.4. Oil Red O staining and modified H&E staining.

Skin samples were stained with the Oil Red O dye (Sigma) to detect lipids presence along and beneath the skin. In addition, the analysis of fat in rodent skin was performed only on the frozen sections. The wax method was not applied for this study, because it removes lipids.

The Oil Red O staining protocol was used previously by Richardson *et al* (2005). Prepared on the cryostat back skin sections were washed three times in PBS (Phosphate buffered saline; Appendix I) (each wash lasted 5 min) and fixed in calcium formal: 4% formaldehyde (Sigma) and 1% calcium chloride (Sigma) for one hour at room temperature (RT). Next, samples were incubated for 15 min in 60% isopropanol (Sigma) and then stained for 15 min with a filtered solution of three parts of Oil Red O (saturated in isopropanol) and two parts of water. For the next step skin samples were briefly rinsed in 60% isopropanol, washed thoroughly in distilled or double distilled water ($dH_2O$, $ddH_2O$). Cells were counterstained in Mayer's Hematoxylin solution (Fluka) and mounted in Glycergel (DakoCytomation) or mowiol (Appendix I).

When whole mouse skin samples were stained with the red dye, they underwent the protocol described above, however the incubation step with the Oil Red O dye was related with the thickness of skin (thicker skin - longer incubation, up to 30 - 60 min). In addition, whole mouse skin samples were not counterstained in Mayer's Hematoxylin solution and were not mounted in Glycergel. Stained samples were kept in PBS at $4^oC$.

### 2.2.5. Immunofluorescence analysis.

#### 2.2.5.1. Pref-1 staining.

The unfixed skin sections were first washed three times in PBS (each wash lasted 5 min) and blocked with 20% goat serum (Sigma) in PBS for 30 min at RT. Sections were then incubated with a polyclonal rabbit antibody Pref-1/DKL-1 (PTG) overnight at $4^oC$ or 1 hour at room temperature (1:10, 1:50 or 1:100 dilutions in 1% goat serum/PBS). Skin sections were washed three times in PBS as described above and incubated with goat anti-rabbit antibody (AlexaFluor, for details see Chapter 3, Table 3.3B), diluted 1:500 in 1% goat serum/PBS for 1 hour at room temperature or overnight at $4^oC$. Normally DAPI (Insight Biotechnology) was added to this secondary antibody solution at a dilution of 1:5000. Sections were then washed three times in PBS as before and mounted in anti-fade Immu-mount

(Thermo Electron Corporation) or mowiol (Appendix I) and covered by the coverslips. Incubations with antibodies were performed in the dark. Slides were kept in 4$^{o}$C, in the dark.

### 2.2.5.2. PPARgamma staining.

Skin samples were incubated in 4% paraformaldehyde (Sigma)/PBS for 15 min at room temperature (RT), next in 0.5% TritonX-100 (Sigma)/PBS for 5 min in 4$^{o}$C. Then samples were washed three times in PBS (each wash lasted 5 min) and blocked with 20% donkey serum (Sigma) in PBS for 30 min at RT. Sections were incubated with a polyclonal rabbit antibody PPARgamma (Abcam) for one hour at RT (1:50 dilution in 1% donkey serum/PBS). Skin sections were washed three times in PBS as described above and incubated with donkey anti-rabbit antibody (AlexaFluor, for more details see Chapter 3, Table 3.3B) diluted 1:500 in 1% donkey serum/PBS for one hour at RT. Normally DAPI (Insight Biotechnology) was added to this secondary antibody solution at a dilution of 1:5000. Sections were then washed three times in PBS as before and mounted with mowiol (Appendix I) and covered by the coverslips. Incubations with antibodies were performed in the dark. Slides were kept in 4$^{o}$C, in the dark.

### 2.2.5.3. C/EBPalpha staining.

The unfixed skin sections were first washed three times in PBS (each wash lasted 5 min) and blocked with 20% goat serum (Sigma) in PBS for 30 min at RT. Sections were then incubated with a polyclonal rabbit antibody (C/EBPalpha, Santa Cruz Biotechnology) overnight at 4$^{o}$C (1:50 or 1:300 - 350 dilutions in 1% goat serum/PBS). Skin sections were washed three times in PBS as described above and incubated with goat anti-rabbit antibody (AlexaFluor, for details see Chapter 3, Table 3.3B) diluted 1:500 in 1% goat serum/PBS for one hour at RT. Normally DAPI (Insight Biotechnology) was added to this secondary antibody solution at a dilution of 1:5000. Sections were then washed three times in PBS as before and mounted in anti-fade Immu-mount (Thermo Electron Corporation) or mowiol (see Appendix I) and covered by the coverslips. Incubations with antibodies were performed in the dark. Slides were kept in 4$^{o}$C, in the dark.

### 2.2.6. Double staining: Oil Red O and immunohistochemical detection.

Skin sections were cut and stained with the Oil Red O stain (for details see section 2.2.4), but not counterstained. Sections were then processed for immunohistochemical detection using the StrepABComplex/HRP Duet, Mouse/Rabbit kit from DakoCytomation. Samples were rinsed in water, in TBS buffer (Tris buffered saline; Appendix I) for 5 min and incubated with the primary antibody (C/EBPalpha, Santa Cruz Biotechnology) diluted (1:50) in TBS/1% bovine serum albumin (FLUKA) for 20 min. They were then rinsed with water, placed in TBS (5 min) and incubated with the biotinylated goat antibody working solution for 20 min. Next, samples were rinsed with water, placed in TBS (5 min) and incubated with the strepABComplex/HRP working solution for 20 min, then rinsed with water and placed in TBS (5 min). They were then incubated with a 3,3'-diaminobenzidine tetrahydrochloride-prepared chromogenic substrate solution for peroxidase (DakoCytomation) for 6 or 10 min, rinsed in water and mounted in Glycergel (DakoCytomation).

### 2.2.7. The microscopic analysis of skin samples from rodents.

#### 2.2.7.1. Whole mouse skin samples.

The analysis of the Oil Red O staining on whole mouse skin samples was performed on the Ziess StemiSVII microscope (with the digital camera KY-FI030 JVC and with the KyLink software). Figures from taken photographs were prepared on the Adobe Photoshop CS2 v 9.0.

#### 2.2.7.2. Rodent back skin samples.

The back skin samples, removed from mice were analysed on the Ziess StemiSVII microscope (with the digital camera KY-FI030 JVC and with the KyLink software).

Next, rodent back skin sections (obtained from specimens frozen in tissue tek - for details see section 2.2.3.) that underwent the Oil Red O and immuno-based study, were analysed on a Zeiss Axio Imager.M1 microscope and OpenLab software (Improvision). Figures from taken photographs were prepared on the Adobe Photoshop CS2 v 9.0.

#### 2.2.7.2.1. The calculation of average size of lipid droplets (in relation to Figure 2.9).

Photos of skin sections with accumulated lipids in lower dermis were used in order to count the average size of selected lipid droplets (see Figure 2.9), the diameter was presented by a yellow line who's length, given in pixels, was transferred into μmeters (according to the scale bar on each analysed image). The length of the scale bar was 30 μm which equates to 93 pixels. Based on the simple mathematical calculation, a diameter of each selected droplet was obtained in μmeters and this counting is presented in Appendix II. The values presented on the Figure 2.9 were rounded to the second place after the comma.

#### 2.2.7.2.2. The thickness of the non-fatty skin layer (in relation to Figure 2.10).

The thickness of the non-fatty skin layer in skin specimens was shown by the vertical yellow lines on photos from mouse back skin samples at different time points (see Figure 2.10).

#### 2.2.7.2.3. The "control staining" for the PPARgamma antibody (in relation to Figure 2.14).

The "control staining" was performed on cross-skin sections from back skin sample, where incubation in primary antibody was replaced by the incubation in 1% donkey or 1% goat serum (in PBS). This allowed the testing of any potential background (unspecific staining) from secondary antibody. The control staining for PPARgamma antibody was analysed in relation to the overexposure of experimental staining (skin samples were incubated with PPARgamma antibody). First, a photo was taken from the experimental staining with exposure set up for a bright epidermal staining (Figure 2.14 - all left panels). Next, the over-exposure was set up in order to analyse the presence of signal along the dermis (Figure 2.14 - all middle panels). Finally, the over-exposure time set up for experimental samples was used on the control staining (Figure 2.14 - all right panels). The results of this analysis are described in section 2.3.4.2.

## 2.3. Results.

### 2.3.1. Lipid accumulation in the whole mouse skin.

In order to analyse the capability to accumulate lipids by mouse skin, the Oil Red O staining was performed on the skin removed from the whole rodent body (for details see section 2.2.2). Skin was compared in few hours, 2 and 6 day old newborn mice. The biggest anterior fat depots beneath the skin were removed from these specimens. This aimed to analyse lipid accumulation in skin and not the presence of lipids in depots beneath the skin.

In skin from younger animals, the Oil Red O staining was weaker than that of older animals (Figure 2.3a, b and c). In skin from the middle back area, staining was easily detectable at day 6. Furthermore, in 6 day old mouse specimen, the top edge of the whole skin (skin removed from the head/neck) was darker due to the high accumulation of red dye in areas seen between hair follicles (Figure 2.3c - top panels). These areas stained by the Oil Red O dye were representing droplets of lipids.

The amount of accumulated lipids in the whole mouse skin seemed to increase during mouse development after birth.

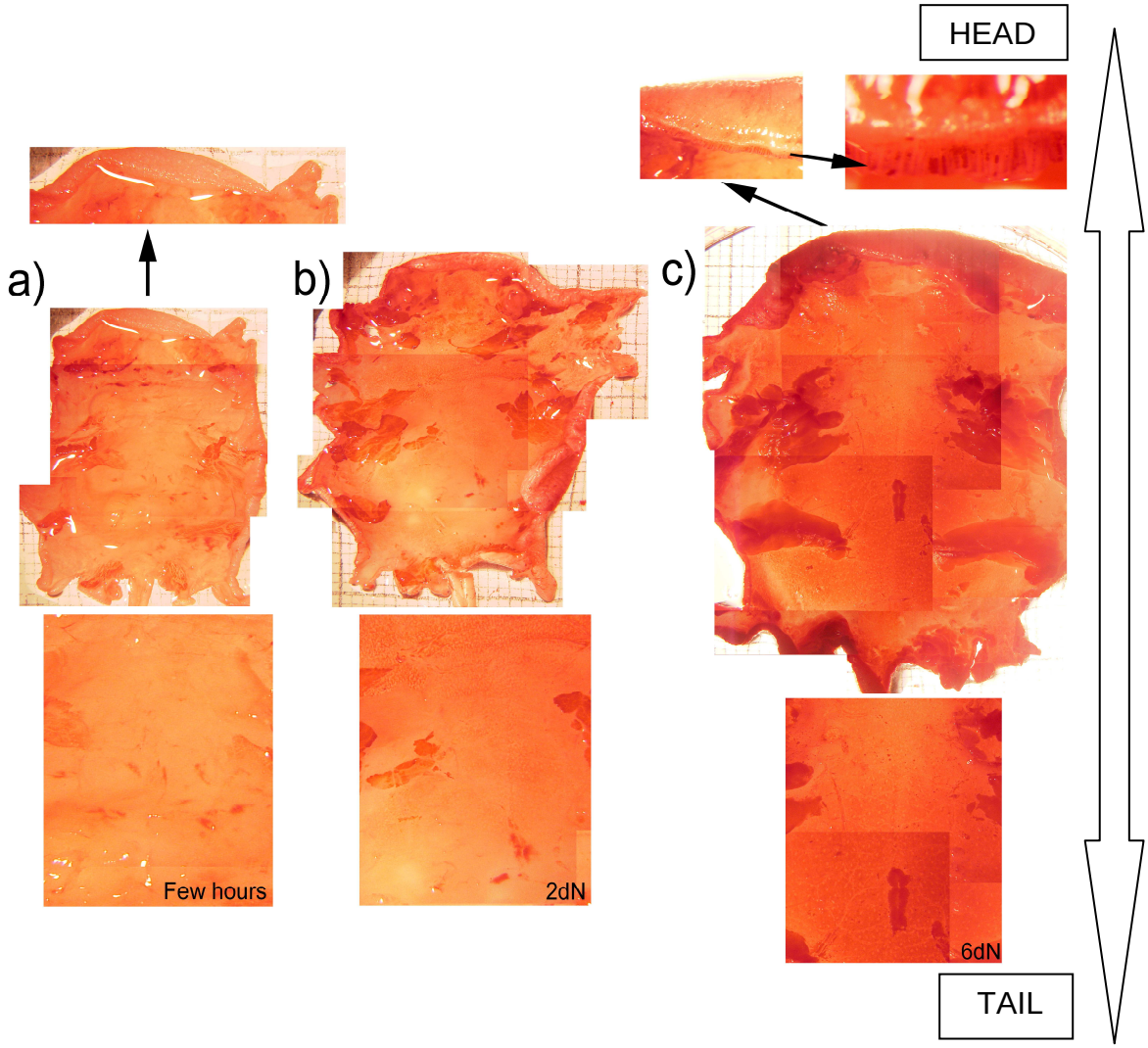


Figure 2.3. Whole mouse skin samples stained with red dye (Oil Red O) and analysed from the dermis site. Red dye gradually accumulates as mouse skin ages and thickens. Darker areas are clearly seen in the middle part of the back skin taken from a 6 day old newborn mouse (c - bottom panel). In addition, at day 6 the red dye can be easily observed in dermis, between hair follicles (c - top panels). a) A newborn mouse just a few hours after birth. b) A 2 day old newborn mouse. c) A 6 day old newborn mouse. Specimens were placed on a 1 $mm^2$ grid paper. Images were captured using a Ziess StemiSVII microscope. The Oil Red O staining on whole skin specimens was performed one time.

### 2.3.2. General features of fat depots under the mouse back skin.

Mouse newborns at different stage of the development were used to obtain back skin samples with depots beneath the skin, in close proximity to the neck/head (top part of the skin sample) and near the lower limbs (bottom part of the skin sample). The localisation of these depots, the general morphology (Figure 2.1 and 2.2) and the Oil Red O analysis confirmed that they are adipose tissues (Figure 2.6 and Figure 2.10).

First, incisions along the right and left side of mouse back were made and skin was cut from the caudal to dorsal (head to tail) direction (Figure 2.1a and 2.1c). Fat layers, were seen under the mouse skin, both in anterior and posterior localisation (Figure 2.1a - c). These adipose depots were bounded with both the skin layer and the rest of mouse body by thin muscle layers (Figure 2.2a). The connection between fat depots and skin seemed to be very fragile and quite loose. Thus, it was crucial to carefully cut the connection between the fat depot and the rest of the body, otherwise the fat depot would stay on the mouse body and will not be lifted with the skin.

The adipose depots presented near the mouse neck and head could be divided into two types: the middle darker part with the triangle-like shape (a possible brown fat) and the lighter depot localised around darker depot as well as between this brown fat and skin layer (an expected white fat depot) (Figure 2.1e). In the posterior area, the fat depots were treated as a white adipose tissue. All these adipose depots observed below the skin were referred in this thesis as subcutaneous adipose tissue – SAT (see Figure 1.5. Part B in Chapter 1; Figure 2.1e and section 2.3.3.1 in Chapter 2). Analysed fat depots were presented under all analysed mouse specimens (Figure 2.2b). In addition, all fat layers were tightly related with the presence of blood vessels (Figure 2.1e).

### 2.3.3. Detailed analysis of the progressive accumulation of fat cells in rodent back skin.

The features of cells that accumulate lipids (adipocytes) in rodent back skin (at different stage if their development) were analysed in cross-sections by the Oil Red O staining technique. In this analysis, fat depots beneath the back skin were included.

#### 2.3.3.1. The general terminology for analysed mouse skin areas and fat depots.

Several terms were used for the description of analysed skin elements and fat depots beneath the skin (Figure 2.4).

The subcutaneous adipose tissue (SAT) was observed beneath the top (near the mouse neck/head) and bottom (near lower limbs) part of the back skin specimen (Figure 2.4; see also Figure 1.5. Part B). This fat depot consisted of anterior and posterior white adipose tissue, and interscapular brown adipose tissue.

The dermal adipose tissue (DAT) term was related with the dermis fat layer seen in lower skin dermis (Figure 2.4; see also Figure 1.5. Part B). This layer was created from cells undergoing adipogenesis that were localised around hair follicle end bulbs and between developing hairs. In contrast, the upper dermis (non-fatty dermis layer) was devoid of cells that accumulate lipids (no red dye seen). In the upper dermis, the Oil Red O staining was positive only in sebaceous glands (Figure 2.4 - see black arrows).

In addition, subcutaneous adipose tissue was separated from dermal adipose tissue by a non-fatty, muscle skin layer, called the panniculus carnosus (Figure 2.4). The panniculus carnosus was present along the whole length of rodent back skin below the dermal adipose tissue (see Figure 1.5. Part B).

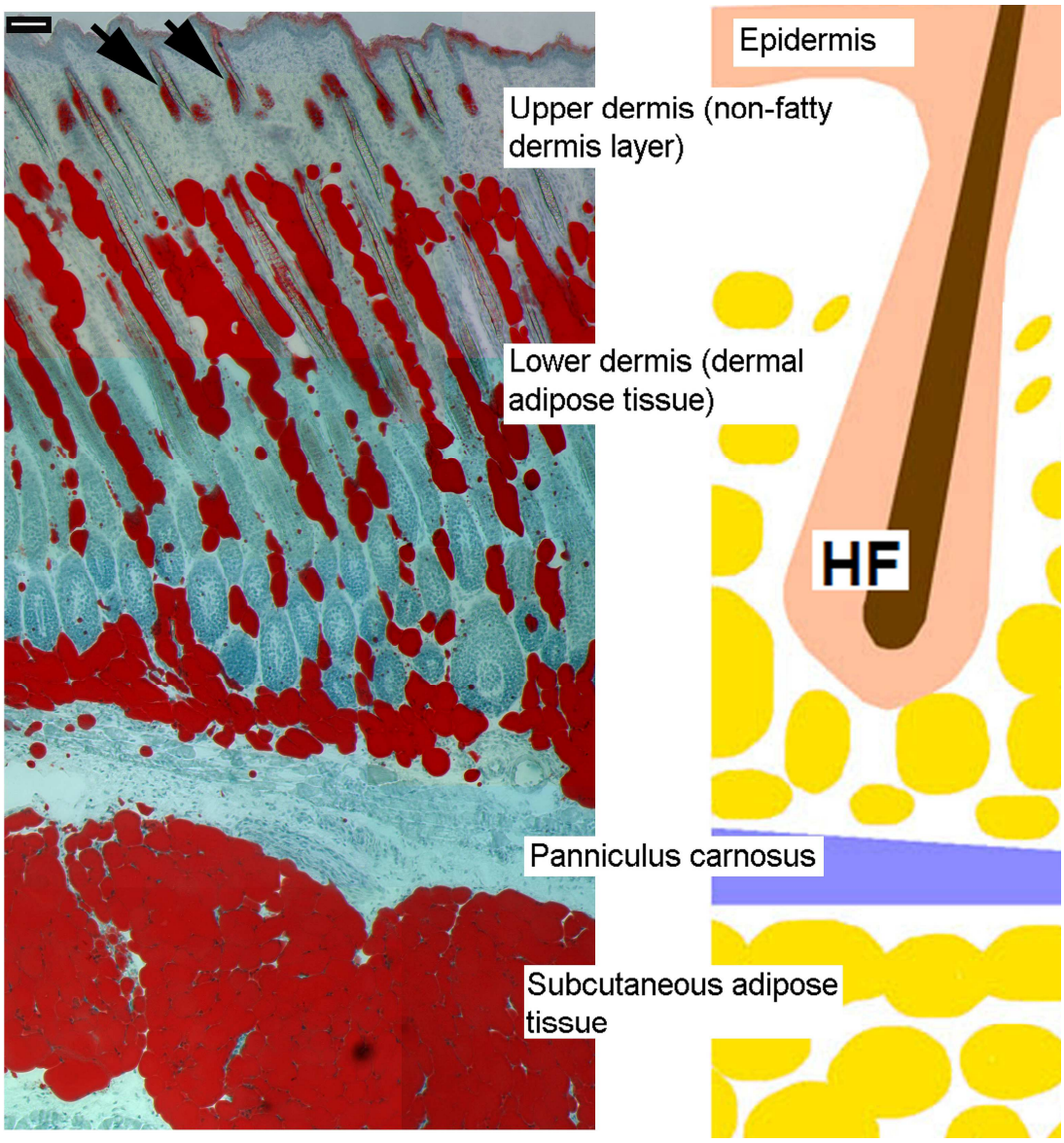


Figure 2.4. A section of back skin from a 10 day old mouse with lipids accumulated in the dermis and under the skin layer. Skin section was stained with Oil Red O to detect lipids. The dermis layer in lower dermis area, localized between hair follicles, was called dermal adipose tissue. The subcutaneous adipose tissue is localised below the skin layer and divided from lower dermis by a muscle layer (panniculus carnosus). Sebaceous glands, filled with lipids, are shown by black arrows. Scale bar = 65 μm. Images were captured using a Zeiss Axio Imager.M1. microscope. A schematic division of presented back skin section is shown by drawing on the right. Drawing by Pawel Wojciechowicz.

### 2.3.3.2. Lipid droplets in mouse embryonic skin.

According to preliminary work on the onset of fat cells in mouse skin dermis, carried out in Prof. Jahoda's research group, an observation was made that the accumulation of lipids in lower mouse skin dermis takes place at late stages of embryonic development. This observation was confirmed by some additional work on embryonic back skin samples (Figure 2.5).

Mouse embryos younger than 18 days, had back skin dermis free from fat droplets (Figure 2.5a and b). Then, among analysed sections from 18 day old skin, only a few cells in the lower dermis seemed to have tiny lipid droplets (Figure 2.5d). The accumulation of first easily detectable fat droplets could be observed in animals older than e18 time point (Figure 2.5f and g; Appendix III). These lipids were in close proximity to hair follicle end bulbs. The multilocular cells, with several small lipid droplets localised around round nuclei, were organized in clusters (Figure 2.5g). Lipids were not present in all areas of lower skin dermis and many cells free of lipids could be observed at e19 time point (Figure 2.5e).

In mouse hair follicles, sebaceous glands were stained positively for the Oil Red O after e18 time point (Figure 2.5g).

Subcutaneous adipose tissue (SAT), analysed in 18.5 - 19 day old embryonic sample, was easy to detect beneath skin and was intensively stained by the red dye (Appendix III).

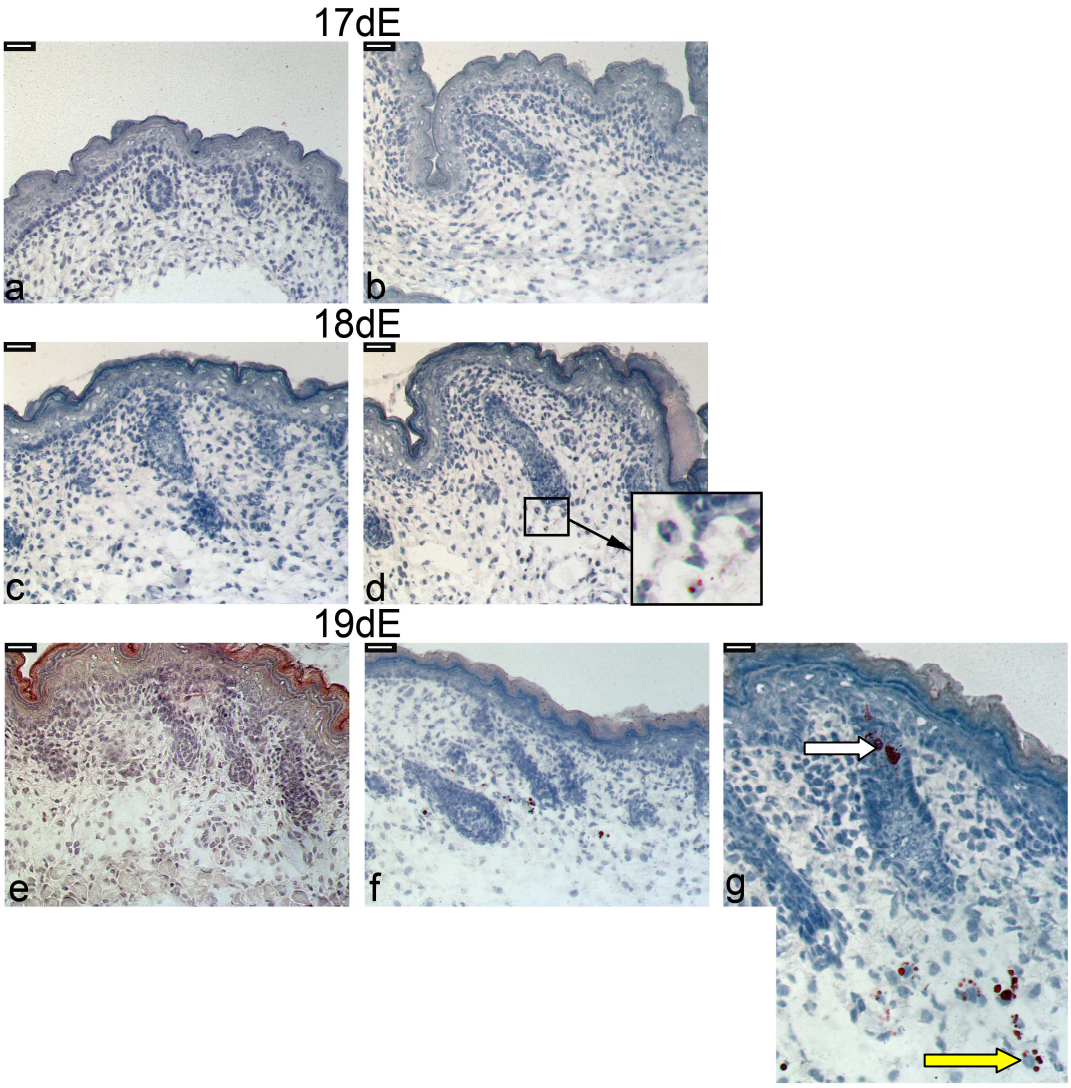


Figure 2.5. Progressive accumulation of lipids in inter-follicular back skin dermis during mouse embryonic development. Skin sections were stained with Oil Red O to detect lipids. (a, b) e17 time point (c, d) e18 time point. (e, f, g) e19 time point. Sebaceous gland is shown by white arrow. Lipid droplets around cell nuclei are shown by yellow arrow. (a - f) Scale bar = 30 μm. (g) Scale bar = 15 μm. Images were captured using a Zeiss Axio Imager.M1. microscope. The Oil Red O staining on embryonic back skin specimens was performed multiple times. Photos in Figure 2.5 were taken at random areas along back skin with no focus on a specific side of a specimen. For the whole embryonic back skin view - see Appendix III.

### 2.3.3.3. Features of back skin and skin-related fat cells during newborn mice development.

The cross-sections from back skin samples (with fat depots beneath the skin) were performed from 0.5, 1, 2, 4, 5, 8, 10, 12, 15, 17 and 19 day old newborn mice and the Oil Red O staining technique allowed the investigation of features of fat cells in skin dermis and beneath skin during mouse development after the animals birth (Figure 2.6A - K).

The subcutaneous adipose tissue (SAT), from the anterior part of a mouse body, was observed beneath skin at all analysed time points and was tightly packed by fat cells as the red dye stained all areas of the SAT in skin cross-sections (Figure 2.6A - K). SAT was separated from the back skin by a non-fatty skin layer (panniculus carnosus) in all analysed time points (for more details see section 2.3.3.4).

Fat cells, noticed in lower dermis of mouse embryonic skin (at late stages of the development), were seen in skin from half a day old mouse newborn (Figure 2.7a). The gradual increase of red staining in lower dermis was observed from half a day old newborn, while hair follicles were growing along the skin (Figure 2.6 and Figure 2.7). A layer of dermal adipose tissue was already easy distinguishable from upper dermis in skin samples from 1 and 2 day old animals (Figure 2.6B and C).

The skin thickness varied at analysed time points and these changes were related mainly with the size of dermal adipose tissue (Figure 2.6A - K). From day 5 to day 12 back skin was getting thicker because of growing hairs and the dermal adipose tissue took approximately 80% of the dermis thickness (Figure 2.7f). Next, in animals older than 12 days, the skin gradually became thinner and the fat layer in lower dermis got smaller (50% of dermis thickness at day 19; see Figure 2.6K and Figure 2.7i).

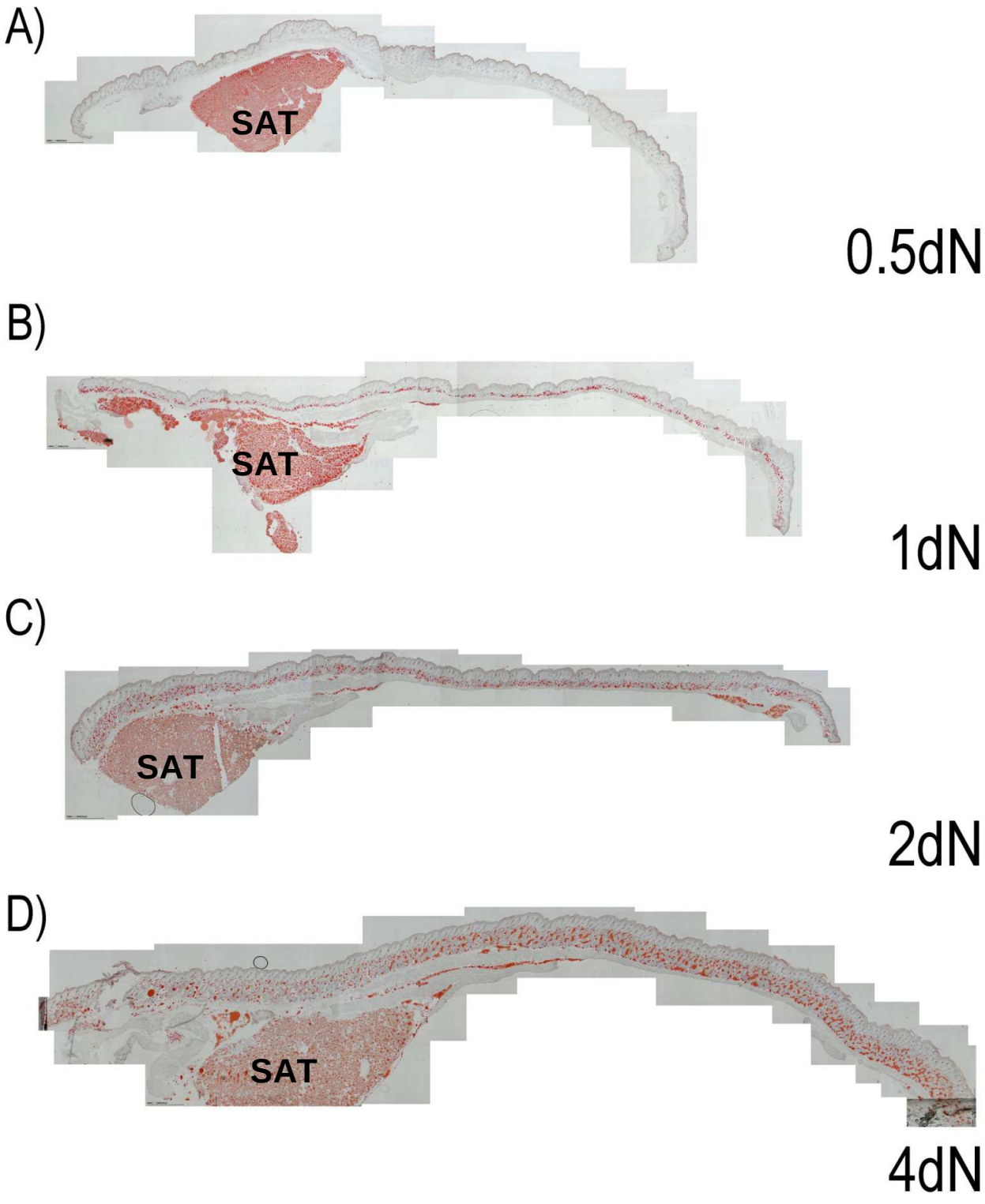


Figure 2.6. Part A. For description see Figure 2.6. Part C.

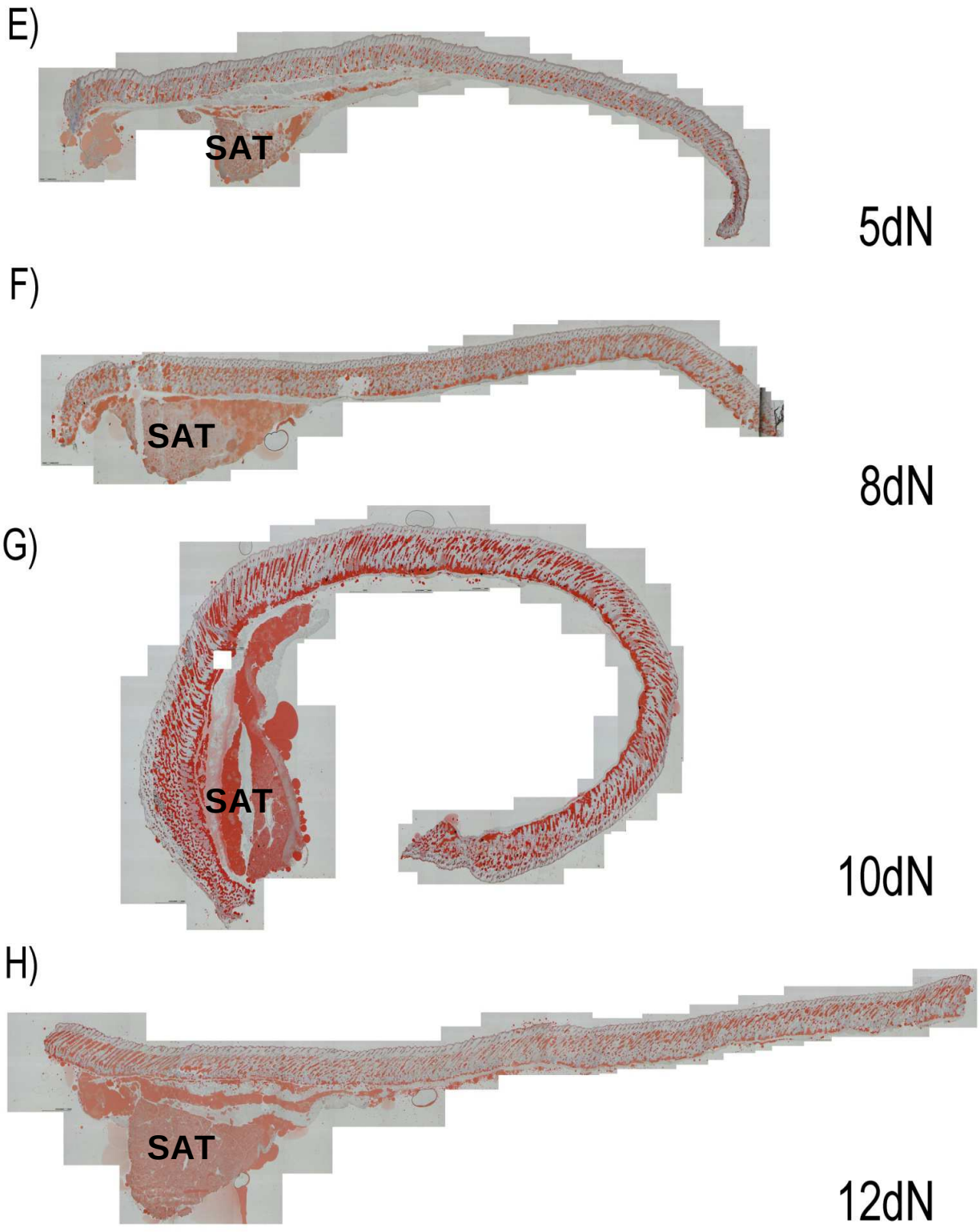


Figure 2.6. Part B. For description see Figure 2.6. Part C.

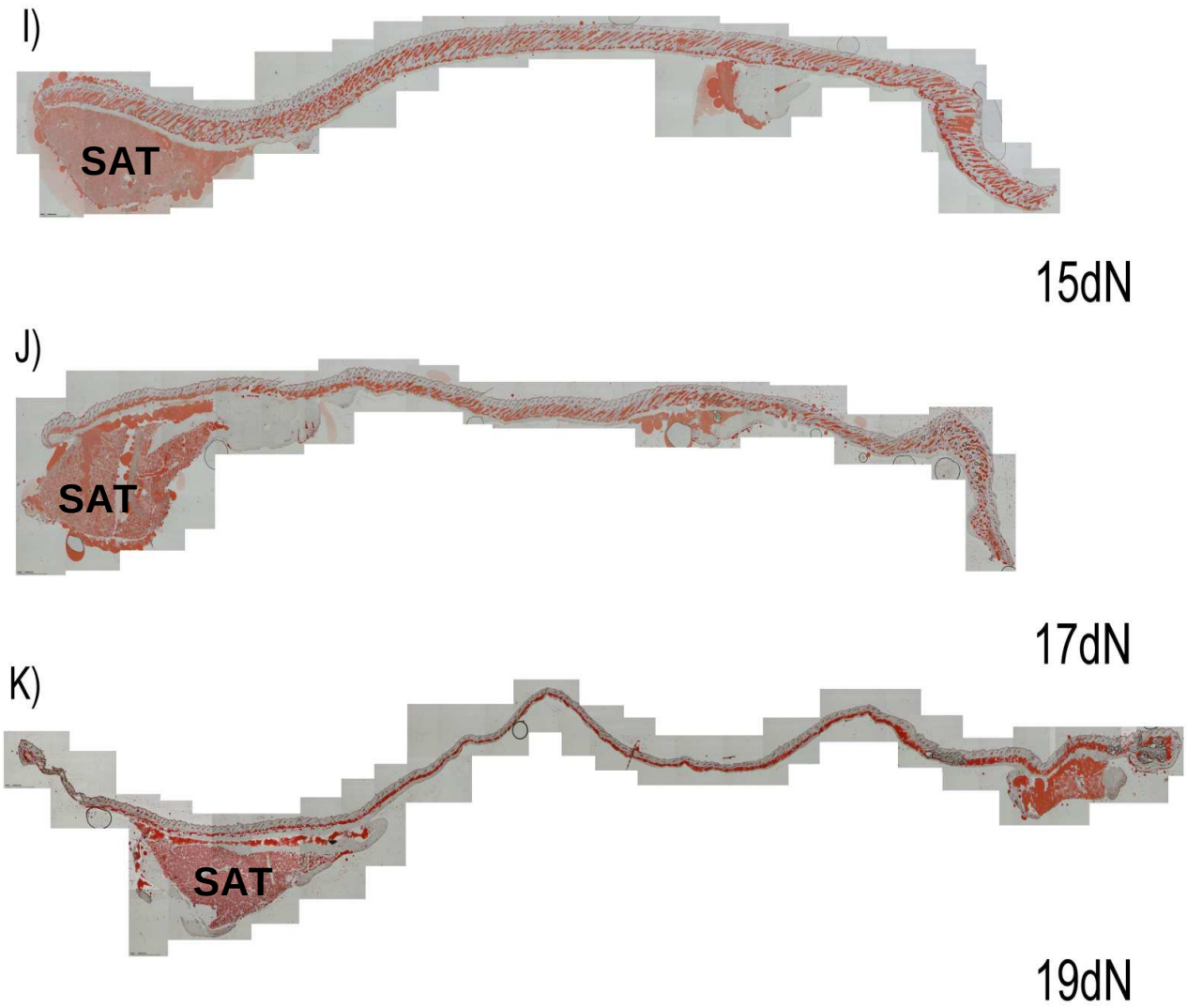


Figure 2.6. Part C. Lipid accumulation in back skin specimens with fat depots beneath the skin. Skin sections were stained with Oil Red O to detect lipids. Samples were prepared from newborn mice at different stages of the development. A) 0.5 day old newborn mouse. B) 1 day old newborn mouse. C) 2 day old newborn mouse. D) 4 day old newborn mouse. E) 5 day old newborn mouse. F) 8 day old newborn mouse. G) 10 day old newborn mouse. H) 12 day old newborn mouse. I) 15 day old newborn mouse. J) 17 day old newborn mouse. K) 19 day old newborn mouse. SAT - subcutaneous adipose tissue seen in anterior part of skin specimens. (A - K) Scale bar = 300 μm. Images were captured by a Laser Capture Microdissection Microscope (PALM MicroBeam Zeiss Microscope). The Oil Red O staining on whole newborn back skin specimens (Figures 2.6 - 2.10) was performed between one (8dN, 15dN, 17dN), two (0.5dN, 2dN, 12dN, 19dN) and three (1dN, 5dN) times.

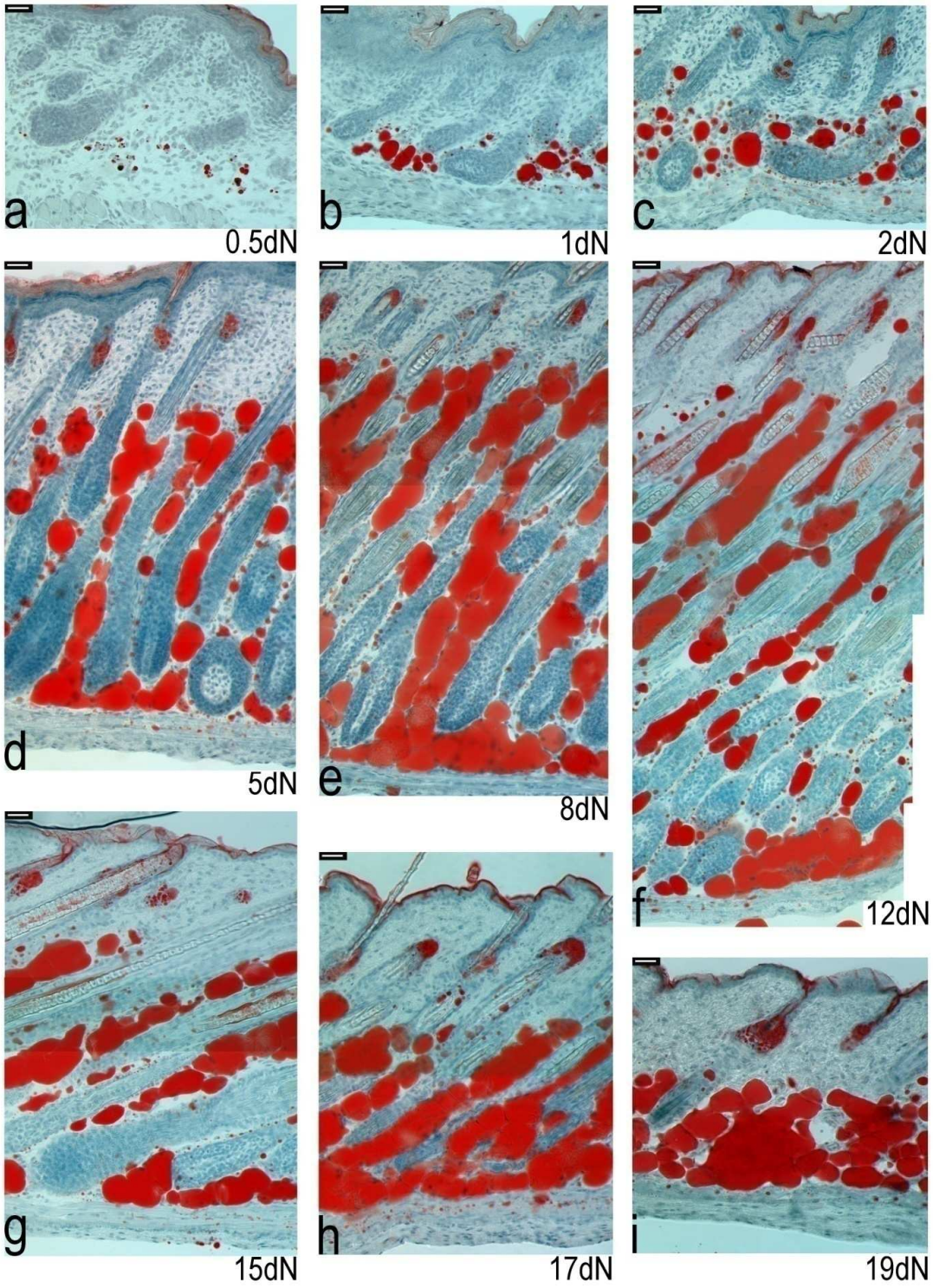


Figure 2.7. The analysis of skin thickness and dermal adipose tissue development in lower skin dermis from newborn mouse. Skin sections were stained with Oil Red O to detect lipids. The gradual increase in lipid accumulation is observed from 0.5dN time point. Dermal adipose tissue layer became thicker from day 0.5 till day 12. After day 12, skin became thinner. a) 0.5 day old newborn mouse. b) 1 day old newborn mouse. c) 2 day old newborn mouse. d) 5 day old newborn mouse. e) 8 day old newborn mouse. f) 12 day old newborn mouse. g) 15 day old newborn mouse. h) 17 day old newborn mouse. i) 19 day old newborn mouse. (a - i) Scale bar = 30 μm. Images were captured using a Zeiss Axio Imager.M1. microscope.

During mouse development, the amount and size of fat droplets in lower dermis were increasing between hair follicles from 0.5 day old mice (Figure 2.7a - d). In addition, at day 0.5, observed lipid droplets varied in their size (Figure 2.8b - right panel and Figure 2.8c - bottom left panel). In this half a day old mouse skin, dermis areas of cells filled with lipids were surrounded by cells where no fat accumulation was seen (Figure 2.8c - all three panels). However, less lipid-free cells in lower dermis were present in 0.5 day old newborn skin, when compared with 18.5 - 19 day old embryonic back skin (compare Appendix III with Appendix IV).

In general, at 0.5 day, many multilocular-like cells were seen with very small lipid droplets (Figure 2.9a). Then, at day one many bigger fat droplets developed around small lipids (Figure 2.9b). Observed droplets had a mainly round shape, because of the available space between hairs. In skin older than 2 days, dermal adipose tissue layer was created from mainly unilocular cells with big fat droplets (Figure 2.9c). Droplets had either a round shape or were elongated, as growing hair follicles reduced available dermis space and seemed to “squeeze” fat cells against each other. The growing tendency of lipid droplets was observed till day 5 and accumulated droplets seemed to keep similar (or only slightly different) diameter in older mice (Figure 2.7d - i). However, in some skin specimens the clear boundary between fat droplets was difficult to identify (Figure 2.9c).

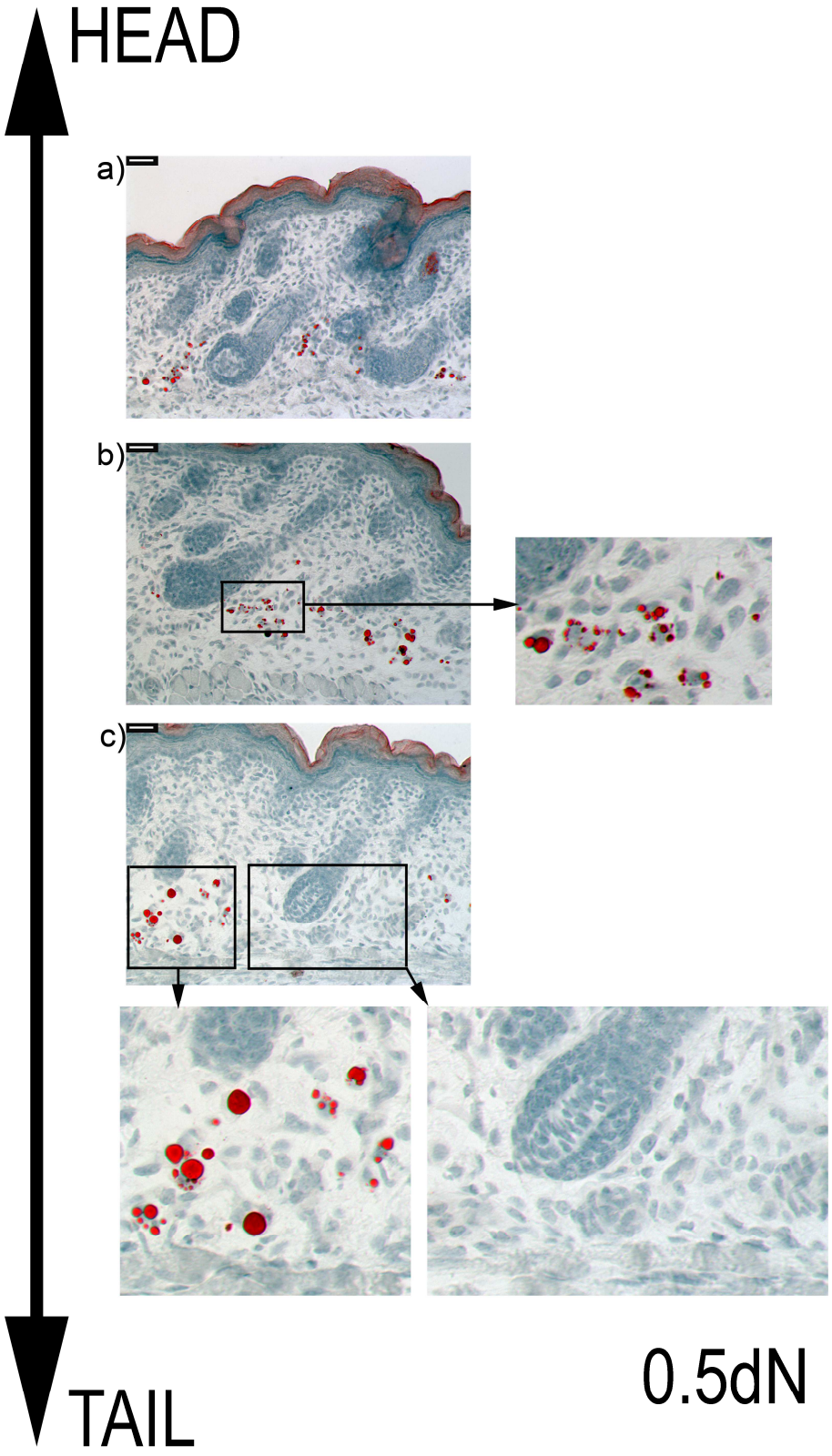


Figure 2.8. Lipid accumulation in lower skin dermis from 0.5 day old newborn mouse. Skin sections were stained with Oil Red O to detect lipids. a) Section from the skin area above fat depots. b) Section from the middle area of back skin specimen. c) Section close to the end of back skin specimen. (a - c) Scale bar = 30 μm. Images were captured by the Zeiss Axio Imager.M1. microscope.

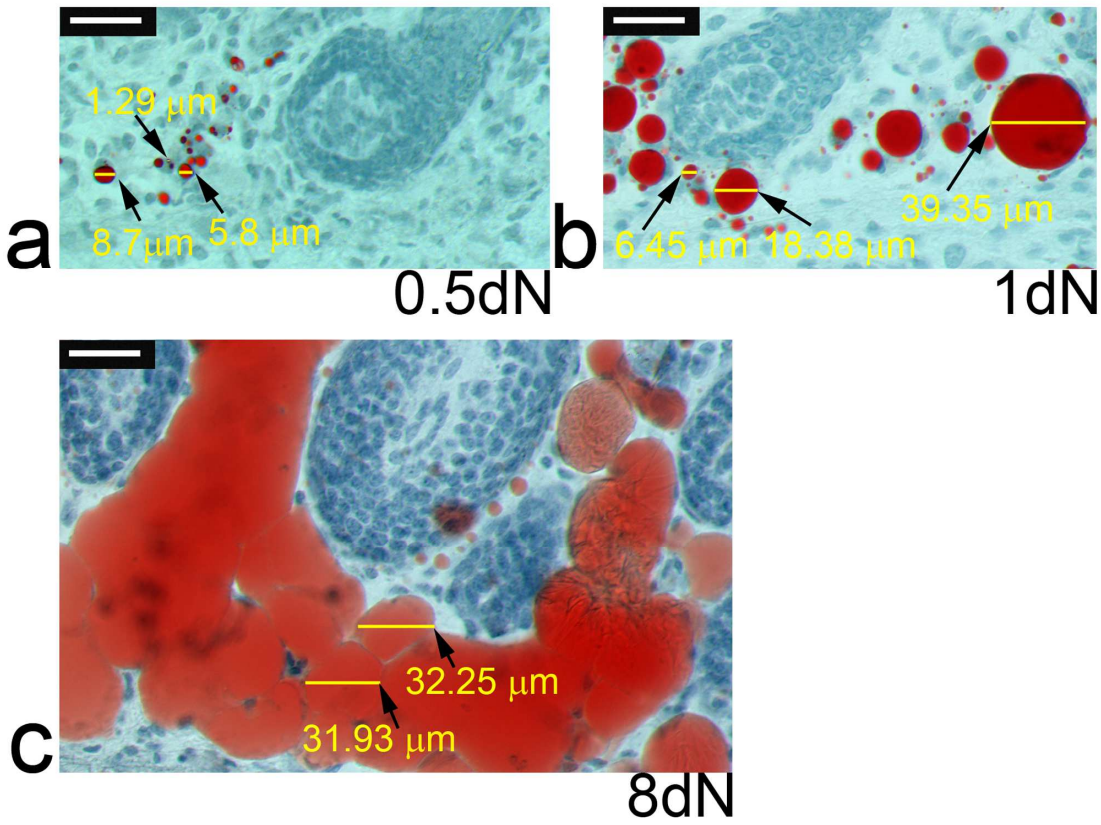


Figure 2.9. An analysis of fat droplet diameter in lower dermis at selected time points. Skin sections were stained with Oil Red O to detect lipids. The gradual increase in lipid accumulation and size of lipid droplets is observed from 0.5dN time point. a) 0.5 day old mouse skin. b) 1 day old mouse skin. c) 8 day old mouse skin. Images were taken from the skin sections above the fat organs in the top part (near the head) of specimens. (a - c) Scale bar = 30 µm. Images were captured using a Zeiss Axio Imager.M1. microscope. The mathematical calculation of fat droplet diameter is presented in Appendix II.

### 2.3.3.4. The non-fatty skin layer (panniculus carnosus) under the mouse skin.

The non-fatty skin layer (panniculus carnosus), without lipids, was seen along the whole length of back skin specimens under dermal adipose tissue (see Figure 2.4; Figure 2.6 and Figure 2.7). It continuously separated fat cells in lower dermis from subcutaneous adipose tissue (SAT) and these two areas filled with lipids did not merge at any of analysed time points.

The panniculus carnosus in area where no subcutaneous adipose tissue was seen under the skin (middle part of a mouse body), had similar thickness in specimens from animals older than 1 day (Figure 2.6B - K and 2.7b - i). In the anterior area of back skin, where SAT was seen, thickness of the panniculus carnosus seemed to vary in analysed time points. At days 0.5 and 1, the non-fatty skin layer was bigger than in other time points (Figure 2.10a and Figure 2.10b). It gradually decreased its size from day 5 to 19 (Figure 2.10d - i).

Interestingly, in some analysed specimens, additional, thin fat cell layers (2 - 3 layers of cells with lipids) were infiltrating the non-fatty skin layer (at day 5; see Figure 2.10d). Some of these lipids were close to dermal adipose tissue (Figure 2.10d).

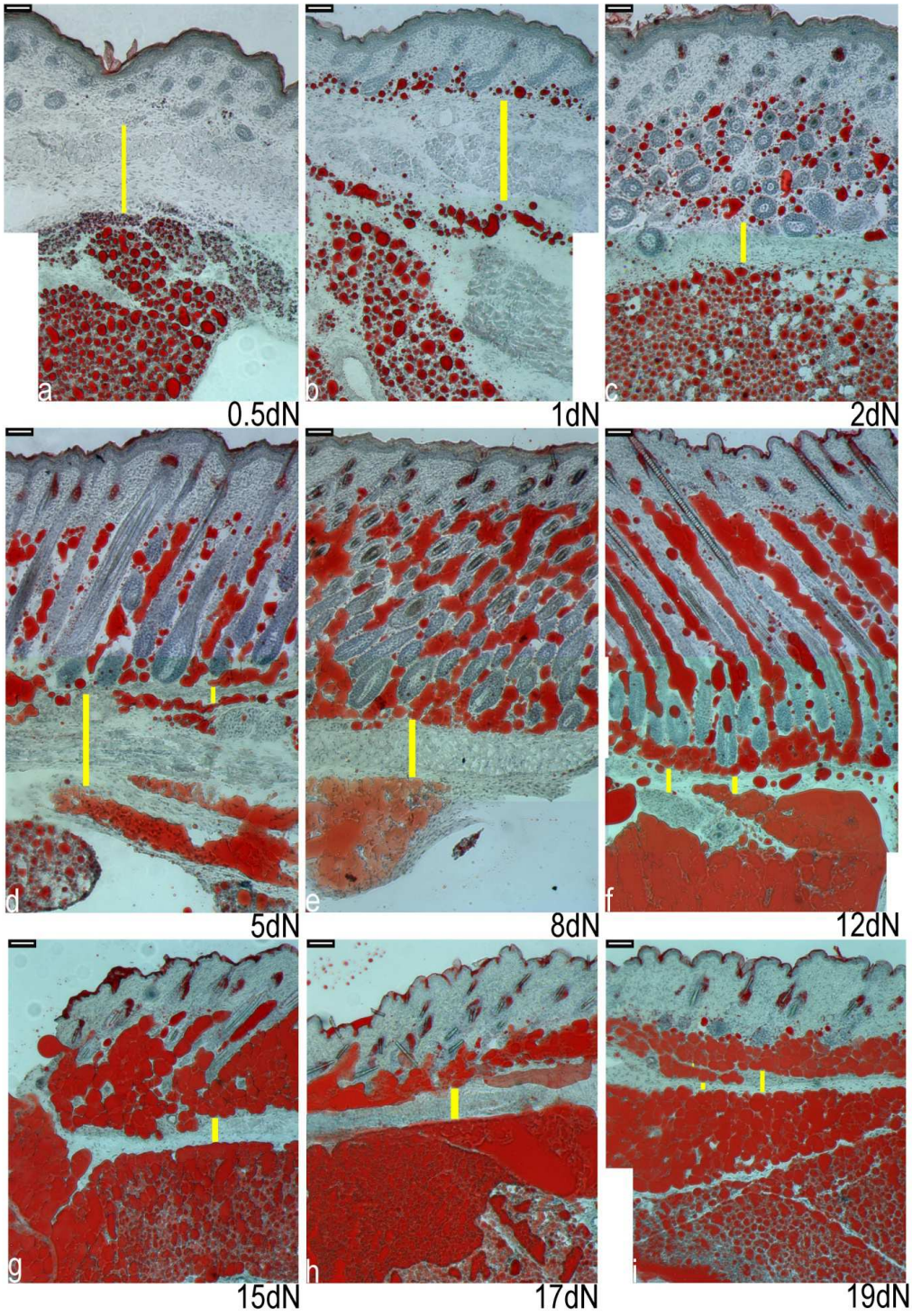


Figure 2.10. Mouse skin sections in close proximity to the anterior white adipose tissue and brown adipose tissue (the top part of the back skin specimen) at different age. Skin sections were stained with Oil Red O to detect lipids. The thickness (marked by yellow lines) of the "non-fatty" skin layer area differs in the top part of analysed specimens. The additional thin layers of lipid droplets can be seen under the fat dermis layer (dermal adipose tissue), for example at day 5 (d - see area close to smaller yellow line). a) 0.5 day old newborn mouse. b) 1 day old newborn mouse. c) 2 day old newborn mouse. d) 5 day old newborn mouse. e) 8 day old newborn mouse. f) 12 day old newborn mouse g) 15 day old newborn mouse. h) 17 day old newborn mouse. i) 19 day old newborn mouse. (a - i) Scale bar = 65 μm. Images were captured by a Zeiss Axio Imager.M1. microscope.

### 2.3.3.5. Lipid accumulation in rat skin.

The pattern of lipid accumulation in rat back skin dermis was similar to that seen in mice. However, the first appearance of fat droplets was observed later than in mouse specimens (compare Figure 2.5 and Figure 2.11). The Oil Red O dye did not stain any structures in back skin sections from e18 rat embryos (Fig. 2.11a - c), but in e20/e21 rat embryonic skin, just before birth, small droplets of lipids were visible in the lower dermis (Figure 2.11e). The fat droplets localisation was maintained in lower dermis trough all analysed time points. In samples from newborn rats, increasing amounts of lipid staining was detectable (Figure 2.11g - o). In 1 and 2 day old newborn rat skin, droplets of fat were predominantly clustered around follicles in the lower dermis. Subsequently, both the amount of lipid and size of droplets increased, and over time more fat droplets were observed between adjacent follicles as they became more tightly clustered, so that by 6 days after birth, the most prominent staining was seen in the gaps between the follicles. This pattern of staining is maintained for at least 3 more days, since in 9 day old newborn rat skin, the spaces between hair follicles were almost entirely filled with lipid (based on previous work done in Prof. Jahoda's research group). The Oil Red O staining was seen in sebaceous glands of follicles from 1 day old newborn rats (Figure 2.11g) and increased progressively.

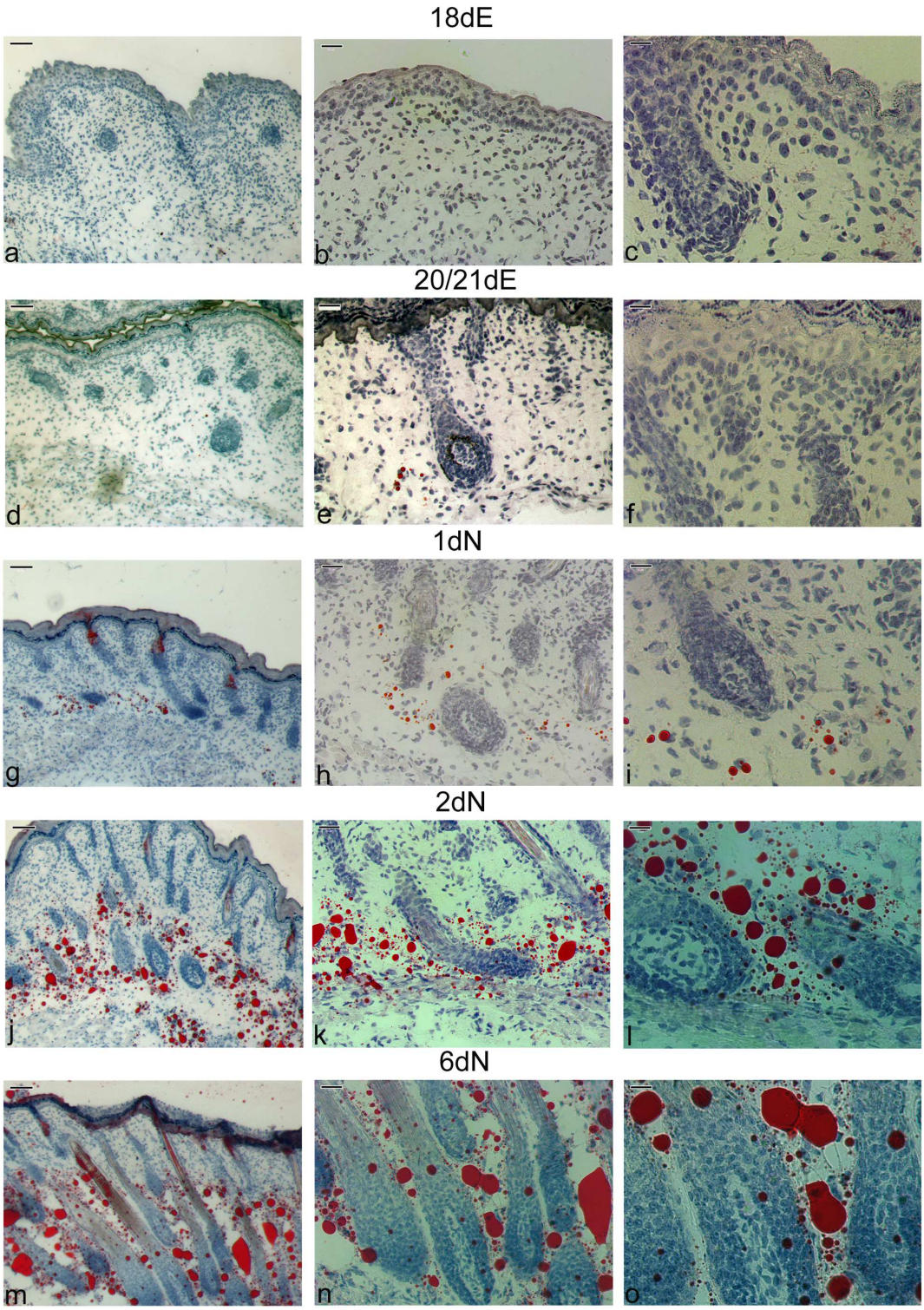


Figure 2.11. Progressive accumulation of lipids in inter-follicular dermis during rat skin development. Skin sections were stained with Oil Red O to detect lipids. (a, b, c) 18 day old rat embryo (18dE). (d, e, f) 20/21 day old rat embryo (20/21dE). (g, h, i) 1 day old newborn (1dN). (j, k, l) 2 day old newborn rat (2dN). (m, n, o) 6 day old newborn rat (6dN). (a, d, g, j, m) Scale bar = 65 µm. (b, e, h, k, n) Scale bar = 30 µm. (c, f, i, l, o) Scale bar = 15 µm. Images were captured using a Zeiss Axio Imager.M1. microscope. The Oil Red O staining on rat back skin was performed minimum two times.

### 2.3.4. The investigation of an *in vivo* maker for fat-like cells developing in rodent dermis skin.

Because the first, easy to detect Oil Red O staining in lower dermis was seen in approximately 18.5 - 19 day old mouse embryo, embryonic skin from late stages of the development was used to find an *in vivo* marker for fat-like cells. This work aimed to find a marker for dermis cells just before they start accumulating lipids (preadipocytes) and after they undergo adipocyte differentiation (adipocytes).

Several antibodies were chosen for three proteins suspected to be a useful marker for preadipocyte/adipocyte cell population in skin: Pref-1, C/EBPalpha and PPARgamma. These candidates are known to be involved in early stages of adipogenesis, based on *in vitro* work on for example 3T3 cell lines (for more details see Chapter 1, section 1.3).

The immunofluorescence and immunohistochemical analysis was performed on skin sections from both rodent embryos and newborns. In addition, photos presented in Figures 2.12 - 2.20 were taken randomly from the whole length of analysed skin cross-sections.

#### 2.3.4.1. The expression of Pref-1 in embryonic skin.

Preadipocyte factor 1 (Pref-1) is a transmembrane glycoprotein, highly expressed in 3T3-L1 preadipocytes, before they undergo adipogenesis. Pref-1 is suggested to inhibit adipogenesis (Smas and Sul, 1993).

When the immunofluorescence analysis, with the antibody against Pref-1, was performed on the 18 day old embryonic rat skin (Figure 2.12), the staining was random through the dermis. The antibody signal was seen in the top dermis as well as in the lower areas of skin.

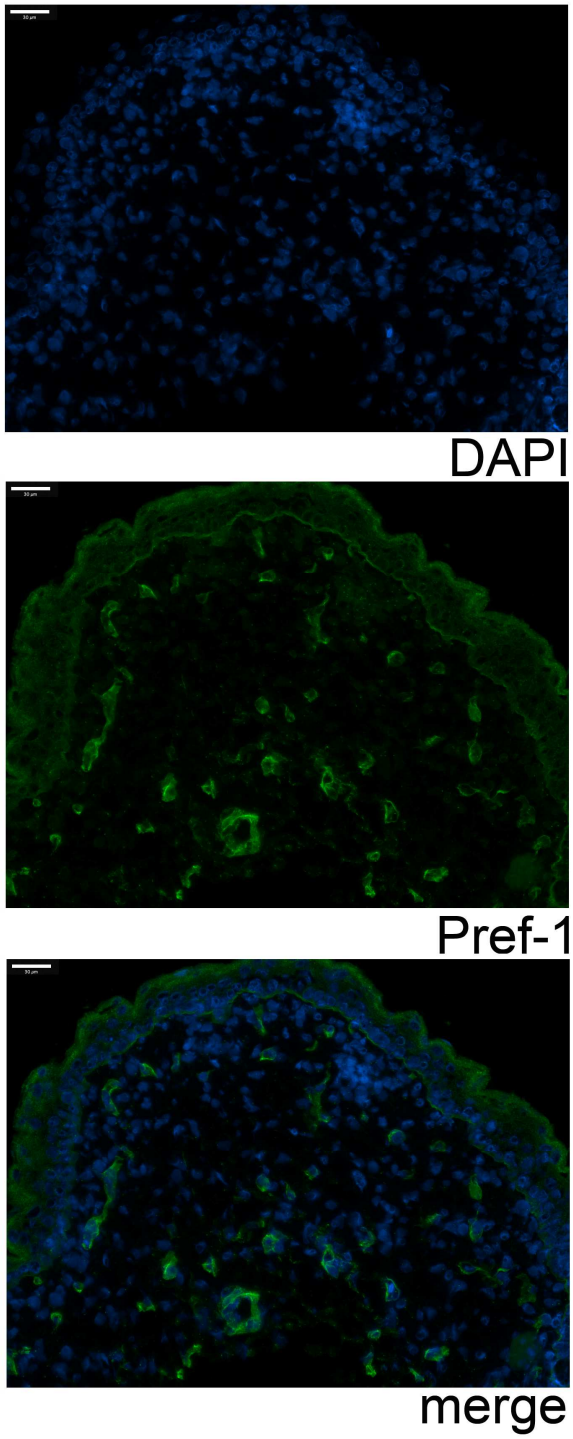


Figure 2.12. Pref-1 expression in 18 day old rat embryo skin. Back skin sections were probed with an antibody against Pref-1. DNA was counterstained with DAPI. Scale bar = 30 μm. Fluorescent images were visualised using a Zeiss Axio Imager.M1. microscope. The Pref-1 staining was performed four times.

### 2.3.4.2. The antibody against early adipogenic transcription factor: PPARgamma.

PPAR gamma is expressed at early stages of adipocyte differentiation (see Chapter 1, section 1.3.2.2).

It was expected that the expression of PPARgamma could be seen in the lower dermis at late embryonic developmental stages, thus the antibody staining was performed on several time points (Figure 2.13). Surprisingly, the very strong PPARgamma staining was seen along the epidermis and through the developing hair follicles at e17, e18 and e19 time points (Figure 2.13a - c). However, the whole skin dermis was lacking an easy to observe signal. This tendency was continued in skin after the mouse birth (Figure 2.13d). Because the intensity of green signal from the epidermis was very strong, a suggestion was made that this may hide the signal from dermis. Thus, the over-exposure for the green channel was performed for each analysed sample and the dermis staining was analysed (Figure 2.14). Some weak signal was seen in dermis that might have a nuclear character. However it was equal along the whole length of the dermis (Figure 2.14 - middle panels). In addition, photos for the “antibody control” samples were taken (no primary antibody incubation with only secondary antibody incubation to check the “non-specific binding” of the secondary antibody). The pattern of green signal in dermis from these control sections resembled the dermis signal observed in over-exposed experimental samples (Figure 2.14a - d: compare middle panels with right panels).

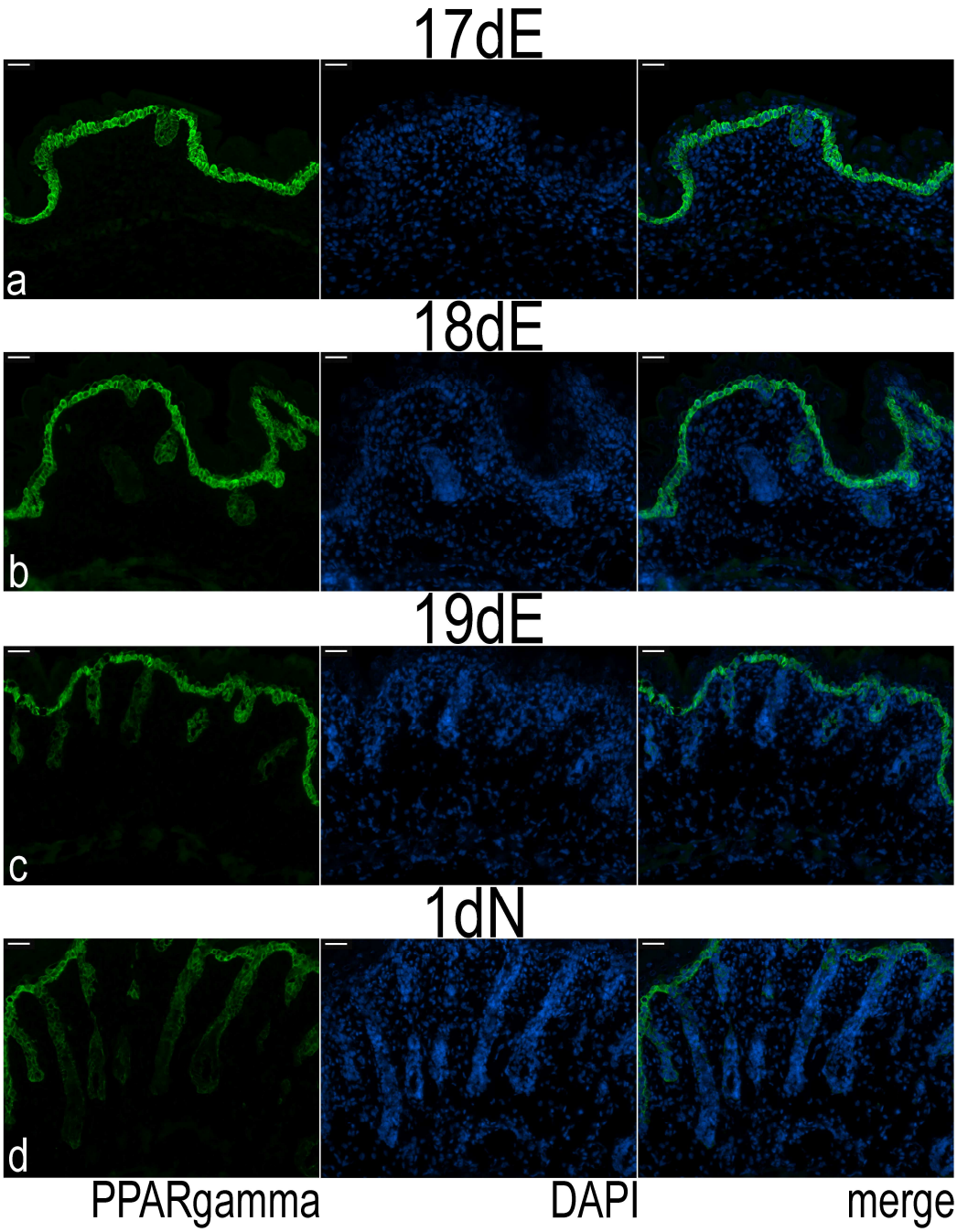


Figure 2.13. Dynamic changes in expression and localisation of adipogenic transcription factor PPARgamma in different stages of mouse skin development. Back skin sections (7 μm) were prepared from embryos at e17 (17dE), e18 (18dE) and e19 (19dE) time points and from 1 day newborn (1dN) mouse, and then probed with antibody against PPARgamma. DNA was counterstained with DAPI. (a - d) Scale bar = 30 μm. Fluorescent images were visualised using a Zeiss Axio Imager.M1. microscope. The PPARgamma staining was performed multiple times.

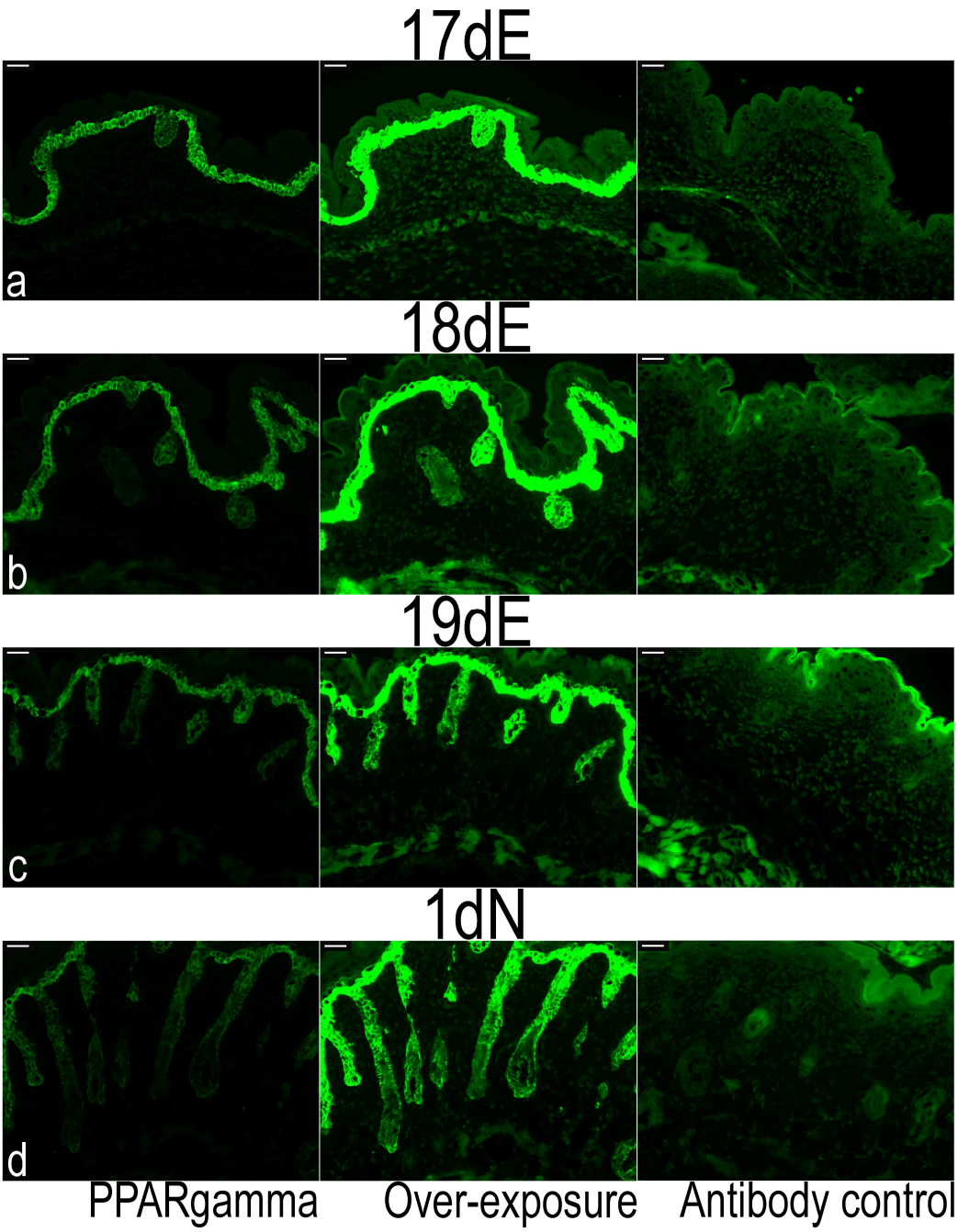


Figure 2.14. Preliminary PPARgamma antibody staining during different stages of mouse skin development with the analysis of a control antibody staining. Back skin sections (7 μm) were prepared from embryos at e17 (17dE), e18 (18dE) and e19 (19dE) time points and from 1 day newborn (1dN) mouse. (a, b, c, d - left and middle panels): Skin sections were probed with antibody against PPARgamma. (a, b, c, d - right panels): Skin sections were incubated with 1% donkey serum/PBS instead of the primary antibody against PPARgamma. (a - d) Scale bar = 30 μm. Fluorescent images were visualised using a Zeiss Axio Imager.M1. microscope.

### 2.3.4.3. C/EBPalpha (C/EBPα) identifies differentiating preadipocytes around hair follicles in foetal and neonatal rat and mouse skin.

Expression of C/EBPalpha (C/EBPα) in back skin was analyzed in both rats and mice. In rat embryos at e18, strong labelling was visible in the suprabasal layers of the epidermis (Figure 2.15). By comparison, in developing hair follicles the epithelium was very weakly labelled or unstained. In the skin dermis, at the same developmental stage there was no positive labelling for C/EBPalpha. At e20 in rat skin, the suprabasal layers of the epidermis were still strongly fluorescent (Figure 2.15c and d). In the rat dermis at e20, however, a small number of cells now displayed strong nuclear staining. These cells were all clustered around or close to the lower regions of hair follicles (Figure 2.15c and d). In postnatal rat skin at 1 and 2 days, the epidermis remained strongly stained for C/EBPalpha, while expression in the follicle epithelium remained weak. Within some well-developed follicles, strong nuclear staining was also seen in the region of developing sebaceous glands. The number of labelled dermal cells had also increased, but staining was still nuclear and distributed around the bottom half of hair follicles. By 6 days, C/EBPalpha expression in all epithelial compartments was largely unchanged (Figure 2.15i and j). Labelled cells in the dermis were now visible between follicles, but were still restricted to the lower two thirds of the dermis and few marked cells were seen deeper in the dermis than the follicle bases.

Mouse embryos followed an almost identical pattern of C/EBPalpha staining, however the timing of events was earlier than in the rat embryos (compare Figure 2.15 with Figures 2.16 and 2.17). As in the rat, the suprabasal layers of the mouse epidermis were strongly stained and the follicle epithelium to a lesser extent (Figures 2.16 and 2.17). At e18 time point, clear and strong nuclear staining could be identified in skin dermis especially around hair follicle end bulbs (compare Figure 2.17a with b). Subsequently, the location and pattern of dermal cell labelling mirrored that of rat skin, with strongly fluorescent cells visible primarily around the follicles initially and then principally between follicles.

By arbitrarily splitting skin into three layers (specifically: epidermis with upper follicle containing dermis; middle layer with hair follicle end bulbs; lower part of back skin below hairs) it was observed that the stained cells resided predominantly in the middle layer, between hair follicle end bulbs (Figure 2.18a and 2.18b).

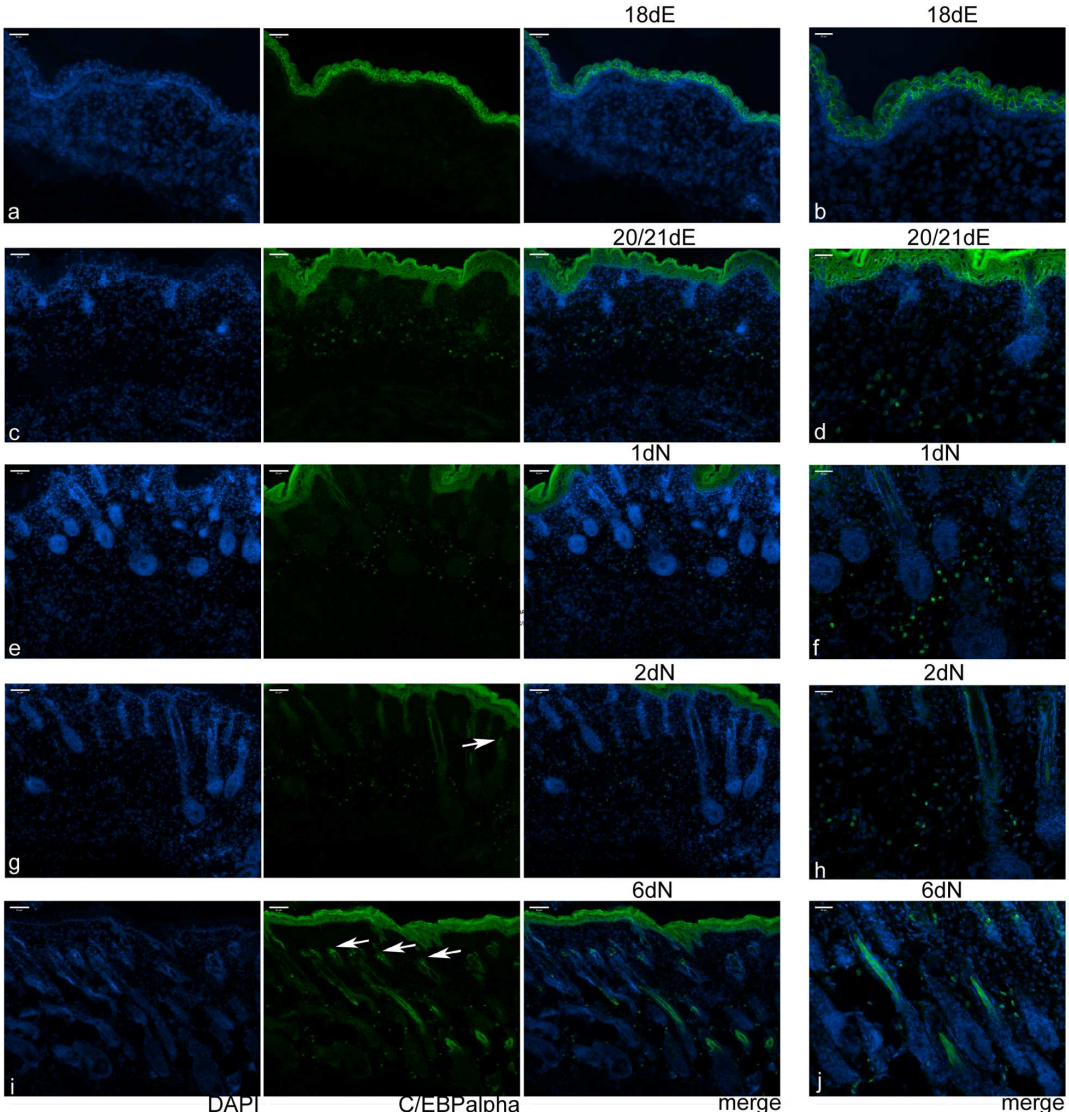


Figure 2.15. Dynamic changes in expression and localisation of adipogenic marker C/EBPalpha (C/EBPα) during different stages of rat skin development. Back skin sections (7 μm) were prepared from embryos at e18 (18dE) and e20/21 (20/21dE) time points and 1 day newborn (1dN), 2 days newborn (2dN) and 6 days newborn (6dN) and then probed with an antibody against C/EBPα. Nuclear expression of the protein is evident in inter-follicular dermal cells in e20/21 embryos and 1 and 2 day old newborn mice, preceding the hair-specific epidermal expression in later stages. DNA was counterstained with DAPI. Sebaceous glands are shown by arrows. (a, c, e, g, i) Scale bar = 65 μm. (b, d, f, h, j) Scale bar = 30 μm. Fluorescent images were visualised using a Zeiss Axio Imager.M1. microscope. The C/EBPalpha staining on rat back skin was performed minimum two times.

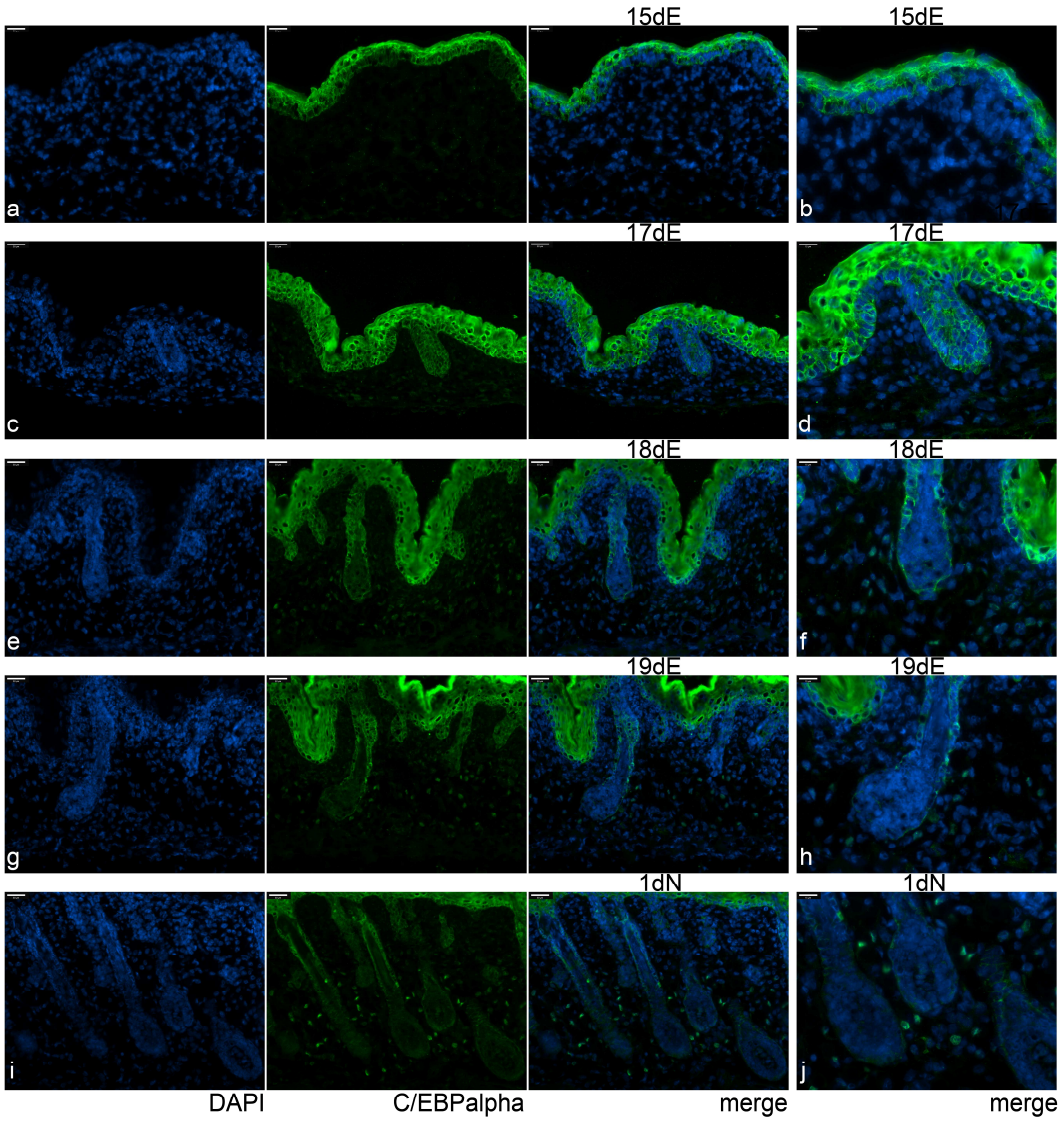


Figure 2.16. Dynamic changes in expression and localisation of adipogenic marker C/EBPalpha (C/EBPα) during different stages of mouse skin development. Part A. Back skin sections (7 μm) were prepared from embryos at e15 (15dE), e17 (17dE), e18 (18dE) and e19 (19dE) time points and from 1 day newborn (1dN) mouse and then probed with an antibody against C/EBPα. Strong, nuclear expression of the protein is evident in inter-follicular dermal cells from about 18 day old mouse embryos. DNA was counterstained with DAPI. (a, c, e, g, i) Scale bar = 65 μm. (b, d, f, h, j) Scale bar = 30 μm. Fluorescent images were visualised using a Zeiss Axio Imager.M1. microscope. The C/EBPalpha staining on mouse back skin (Figures 2.16 – 2.19) was performed multiple times.

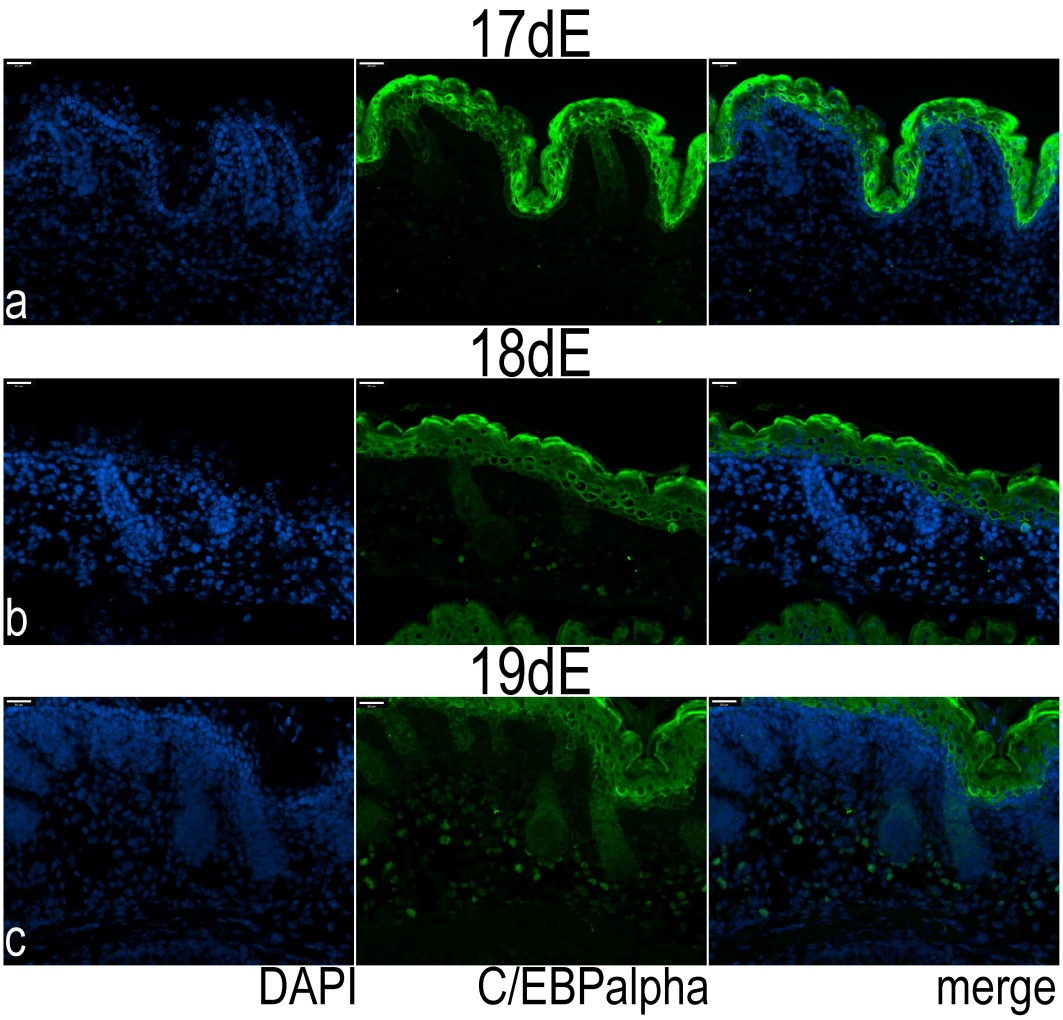


Figure 2.17. Dynamic changes in expression and localisation of adipogenic marker C/EBPalpha (C/EBPα) during different stages of mouse skin development. Part B. Back skin sections (7 μm) were prepared from embryos at e17 (17dE), e18 (18dE) and e19 (19dE) time points and probed with antibody against C/EBPα. Nuclear expression of the protein is evident in inter-follicular dermal cells in 18 day old mouse embryos. (a - c) Scale bar = 30 μm. DNA was counterstained with DAPI. Fluorescent images were visualised using a Zeiss Axio Imager.M1. microscope.

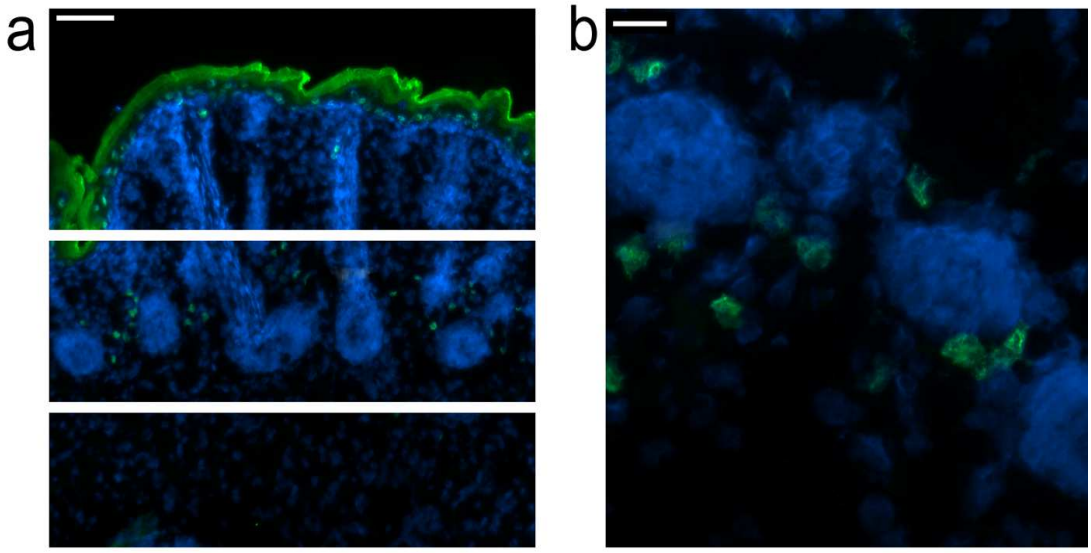


Figure 2.18. Cell type-specific expression of C/EBPalpha (C/EBPα) in different layers of 1 day newborn mouse skin. a) Upper, middle and lower parts of the back skin were visualised after co-staining with C/EBPalpha antibody together with DAPI. C/EBPalpha is detected in skin epithelium (upper panel) and in the cells of inter-follicular dermis (middle panel) but not below the hair follicle end bulbs (lower panel). Scale bar = 65 μm. (b) Expression of C/EBPα is restricted to the dermal cells around the bases of hair follicles. Scale bar = 15 μm. Fluorescent images were visualised using a Zeiss Axio Imager.M1. microscope.

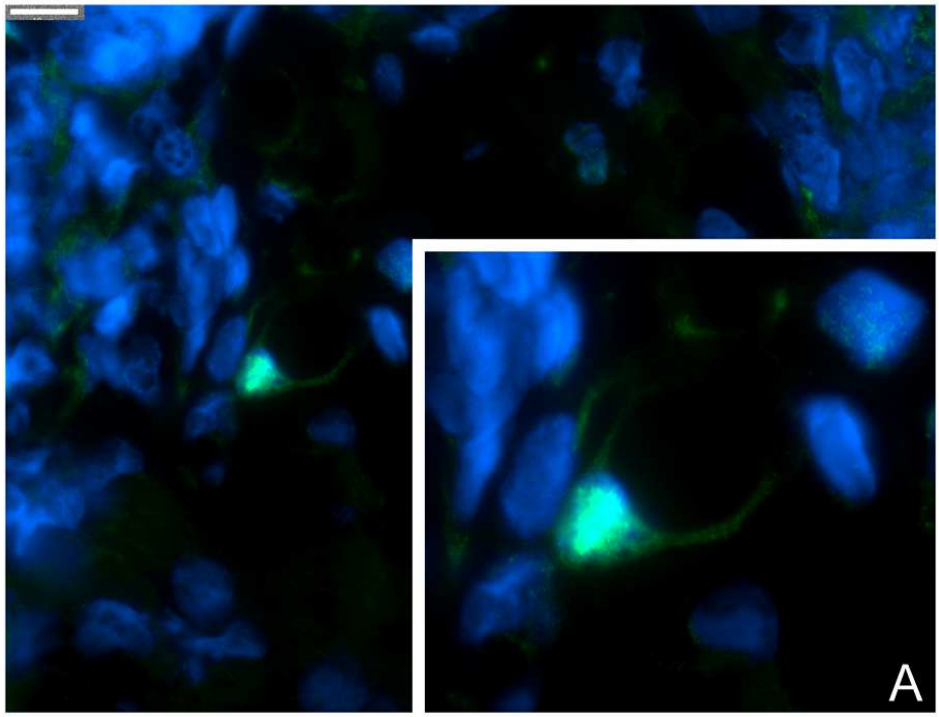


Figure 2.19. Accumulation of fat droplets in C/EBPalpha (C/EBPα) positive cells. Sections of back skin taken from a 2 day old newborn rat were stained with C/EBPalpha antibody and counterstained with DAPI. Magnified region showing C/EBPalpha nuclear staining and typical adipocyte morphology and fat accumulation is shown in box A. Scale bar = 10 μm. Cells were visualised using a Zeiss Axio Imager.M1. microscope.

### 2.3.4.3.1. Features of C/EBPalpha-positive cells in mouse skin.

To verify that the cells expressing C/EBPalpha were in fact the same cells that gave rise to adipocytes, the labelled cells were scrutinized microscopically and it showed that their nuclei became elongated and crescent shaped, with large round cytoplasmic vacuoles, typical of lipid accumulation in adipocytes (Figure 2.19).

Double labelling with C/EBPalpha and the Oil Red O dye, showed that C/EBPalpha strongly labelled the nuclei of dermal cells at embryonic day 18 that were lacking easy to detect lipid droplets (Figure 2.20a). In skin sections from 1 day old newborn rodents, C/EBPalpha staining occurred between and around hair follicles in nuclei of dermal cells, most of which contained droplets of fat of varying size (Figure 2.20b - d). Older newborn skin showed cells with the same pattern of double labelling but with more fat inclusions (Figure 2.20e).

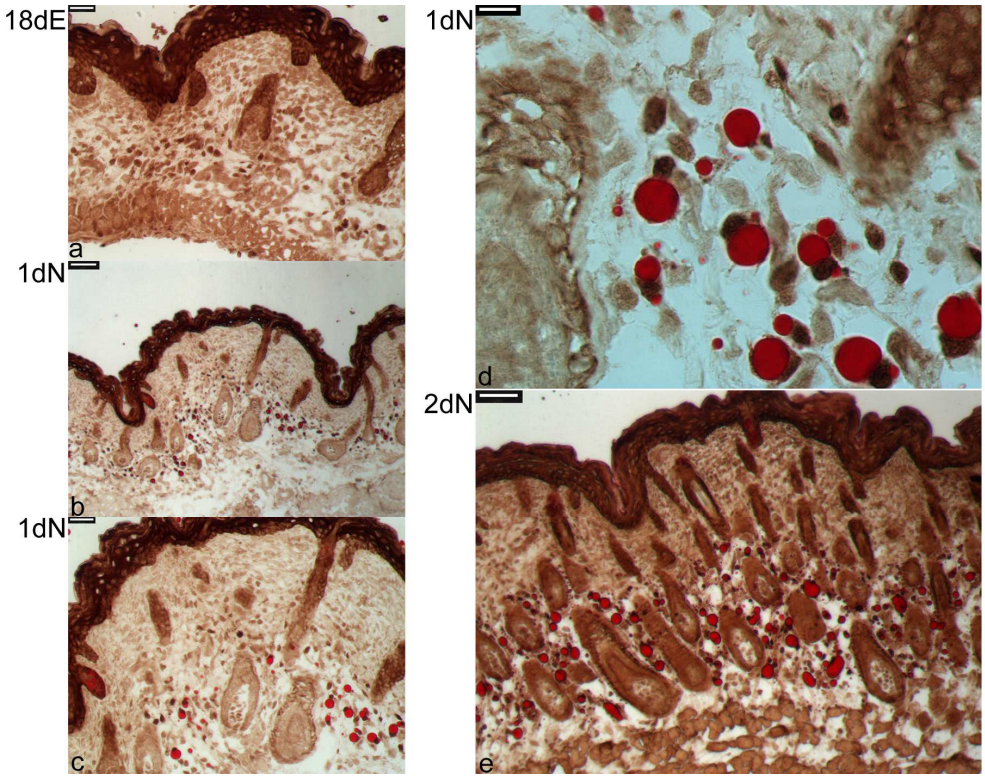


Figure 2.20. Analysis of the co-localisation of C/EBPalpha (C/EBPα) and lipid accumulation in dermal cells from mouse back skin. (a) A section taken from an 18 day old embryo (18dE) showed cells whose nuclei expressed C/EBPα however, these were not positive for Oil Red O staining. (b, c, d) In 1 day newborn (1dN) skin most dermal cells with nuclei expressing C/EBPalpha now have lipid droplets. (e) Newborn skin at 2 days (2dN) shows widespread and increased accumulation of Oil Red O in dermal cells that expressed C/EBPalpha around the bottom half of the hair follicles. (b, e) Scale bar = 65 μm. (a, c) Scale bar = 30 μm. (d) Scale bar = 10 μm. Images were visualised using a Zeiss Axio Imager.M1. microscope. The analysis was performed twice on 18dE and 2dN time points and one time on 1dN time point.

## 2.4. Discussion.

The rodent back skin sample underwent detailed analysis in relation to the onset and development of cells accumulating lipids in lower dermis. The main focus was on mouse specimens. In addition, other subcutaneous fat depots beneath the skin were briefly analysed.

Hausman described fat cells around hair follicles as the outer subcutaneous fat layer that is separated from other subcutaneous layer by a connective tissue (for more details see Chapter 1, section 1.2.5). Despite he suggested different developmental pattern of this outer layer from other fat depots beneath the skin, it seems that this fat layer is treated as a part of the whole subcutaneous adipose tissue. Interestingly, it seems that after the basic analysis of fat cells present in lower dermis in rats and pigs (Hausman's or Mersmann's study, discussed in Chapter 1, section 1.2.5), this subject has not been developed into a more specific and detailed study. In addition, in the literature a term "infiltrate" is used to describe the presence of fat cells in skin (Cinti, 2001), which may suggests that these fat cells are not functionally or developmentally interesting study material for scientists (as they only "infiltrate" skin).

### 2.4.1. Lipid accumulation by mouse skin and development of fat cells in lower dermis.

In work presented in Chapter 2, the Oil Red O technique allowed analysis of the capability of lipid accumulation by whole mouse skin during a newborns development. For this study, the main (biggest) fat depots, presented under the top area of back skin, were not included. The older skin was characterised by the darker red staining seen under the microscope (Figure 2.3). It appeared the red dye was "able" to infiltrate the skin. The darker staining, seen along the analysed back skin samples, could be treated as a staining of fat depots inside the skin (if we assume that the red dye, after binding to lipids, can be seen under the microscope). In addition, a question can be asked if the thickness of the skin influenced the view under the microscope (older skin is thicker, thus less light may pass through the specimen which could lead to the "illusion" of darker skin). However, this seemed not to be an issue, as when the top edge of stained skin was checked under the microscope it was clear that the red dye was observed inside the skin dermis, between hair follicles, where it bound to the lipid lobules (Figure 2.3c - two top panels).

Next, the cross-sections from mouse back skin (with fat depots beneath the skin) were stained with the Oil Red O dye (section 2.3.3). In general, the first lipids were seen in lower dermis from embryos at late stages of their development (Figure 2.5). The gradual increase of lipid accumulation was seen in skin from newborns that lead to a formation of a distinguishable fat layer between developed hair follicles, named dermal adipose tissue (Figure 2.6). The similar pattern of fat cells development in lower dermis was seen in rat skin, however this lipid accumulation process seemed to be activated a couple days later than in mouse skin (Figure 2.11)

In mouse skin dermis, the localisation of developing fat cells in lower dermis is in a general agreement with studies on rat or pig skin (Mershman *et al*, 1975; Hausman *et al*, 1981a; Hausman *et al*, 1981b). In general, subcutaneous fat development starts in foetuses and continues postnatally (Poulos *et al*, 2010). Hausman and his colleagues noticed that in newborn rat skin the localisation of lipids in lower dermis (hypodermis) was strictly related with the presence of hair follicles. In one day old rat skin, the fat cells were not seen in the lower dermis if the hair follicles were not present there ("incomplete" hair follicle development: Hausman *et al*, 1981a).

In work, presented in this thesis, mouse skin dermis from half a day old animal had lipid droplets in close proximity to hair follicle end bulbs (Figure 2.8c - left panel). Interestingly, there were areas in lower dermis that consisted of developed hair follicles, but did not have lipid droplets (Figure 2.8c - right panel). In addition, the heterogeneity in lipid occurrence was seen along the whole length of back skin in lower dermis at 18.5 - 19 day old mouse embryo and this feature was maintained a couple of hours after the birth. However in older animal less "lipid-free" areas were present in lower dermis. These features of lipid occurrence show that precursors of fat cells are present in mouse lower skin dermis and they are activated for adipogenic differentiation at late embryonic stages of development. This activation is not equal in all areas of lower skin dermis.

The morphological features of fat cells in animal skin were similar to these observed by other researchers (for example in Hausman's work: Hausman *et al*, 1981a). First multilocular cells were seen with many small lipids around round nuclei (Figure 2.8b). Next, the gradual development of unilocular fat cells with big central fat droplets were seen, with the "squeezed" nuclei on the peripheral part of the cell (Figure 2.9b). In some areas of lower dermis the boundary between fat droplets was difficult to observe (Figure 2.9c). The question can be raised, was this difficulty

related with the high number of adipocytes filled with lipids in one area of skin dermis (and because of the small space between hairs, these fat droplets were “squeezed”) or because this area presented one very big mature adipocyte with a high number of lipids accumulated in it.

### 2.4.2. The correlation between skin thickness and hair follicle cell cycle.

Changes in mouse skin thickness were observed during the newborn development and skin became gradually thicker from day 0.5 till day 10 - 12 (Figure 2.6A - G and H). Then, skin got thinner till day 19 (Figure 2.6I - K).

A connection between the skin thickness with the fat layer size and the hair follicle cycle was analysed in adult mice (Borodach and Montagna, 1956). The study, presented in this Chapter confirmed this correlation and showed that it takes place during the first couple of weeks of newborn mouse life. To sum up, during the anagen stage (the hair follicle growing stage) fat layer got bigger, and when hairs moved to the catagen and then telogen phase (resting phase) the fat layer was thinner (Figure 2.6A - K). The skin thickness underwent modifications along the whole length of skin specimens at each of the analysed time points.

It appears that not only are the very early stages of adipogenesis in lower dermis related with developed hair follicles but also the fully developed dermal adipose tissue layer is dependent on the hair follicle cell cycles in mouse skin.

### 2.4.3. Two distinguishable adipose tissue depots in mice separated by the non-fatty skin layer (panniculus carnosus).

It was observed that dermal adipose tissue developed later than subcutaneous adipose tissue (SAT) seen beneath the skin. When, for example first clear lipid droplets were seen in lower dermis at e18.5 - 19, the SAT organ beneath the skin was already developed at this time point (Appendix III). These two fat depots were separated by a non-fatty skin layer (panniculus carnosus) that was seen along the whole length of back skin samples at each analysed time points (Figure 2.6 and Figure 2.10). There was no area that could suggest a connection between dermal adipose tissue and SAT. Moreover, during the removal of back skin, it was difficult to lift subcutaneous fat depots with the skin and they seemed to be slightly better connected with the mouse body than back skin. The fat depots were surrounded by thin layers of possible muscle tissue and it was crucial to be delicate when back skin was lifted with these fat depots. In addition, stages of hair follicles had an influence on dermal adipose tissue, whereas no obvious, dramatic changes were seen in SAT beneath the skin, when hairs went from anagen to catagen and telogen. Thus, it could be suggested that the mouse dermal adipose tissue layer is a developmentally different fat depot from subcutaneous adipose tissues.

When the non-fatty skin layer (panniculus carnousus) was analysed during the mouse newborn development, changes in its thickness were mainly related with the back skin area where SAT were localised beneath the skin (Figure 2.10). The additional, thin fat layers were seen along the non-fatty skin layer, either in close proximity to dermal adipose tissue or near SAT beneath the skin. The question can be raised, to which fat depot do these additional layers belong, and if their occurrence is related with specific features of skin at the particular time point or maybe they are just random structures with no apparent importance for the whole skin and fat organ function.

### 2.4.4. The differences between upper and lower rodent skin dermis.

The majority of cells in lower dermis seemed to turn into fat cells and create the fat layer, whereas no lipid accumulation was seen in upper dermis at any of the analysed time points. This easy to identify difference between two areas of dermis may suggest two opposite mechanisms that control differentiation of skin cells and their fate depending on the localisation along the dermis. In upper dermis, either progenitor fat cells are absent or some inhibitory mechanisms of adipogenesis are activated that do not allow cells to accumulate lipids in this area of skin. This hypothesis has been discussed in more detail in Chapter 3.

### 2.4.5. The investigation of an effective *in vivo* marker of developing fat cells in rodent lower dermis.

Based on the Oil Red O analysis, the first lipids in the lower dermis close to hair follicles were seen between e18 - e19 time points, whereas this area of dermis was free from red dye in younger skin (Figure 2.5). The occurrence of lipids was heterogeneous and cells stained by Oil Red O dye were surrounded by not stained areas in lower dermis after e18 time point. Such observation suggested that preadipocyte cells (cells committed to undergo adipogenesis, before the lipid accumulation) may be seen in embryonic skin between e17 and e19. The next step of the study aimed to investigate a marker for fat cells in mouse embryonic skin.

Detailed analysis of adipogenesis *in vitro*, mainly by using the 3T3 cells, identified several proteins crucial for the early stages of adipocyte differentiation, such as members of CCAAT-enhancer binding protein family (C/EBPs) or PPARgamma (reviewed by Rosen and Spiegelman, 2000). In addition, several proteins (for example Pref-1) were identified to be highly up-regulated in preadipocytes and their level gradually decreased when cells underwent adipocyte differentiation (see Chapter 1, section 1.3.4). Antibodies against Pref-1, PPARgamma and C/EBPalpha were used on the rodent back skin samples, in order to analyse their expression pattern in *in vivo* conditions. In addition, an effective marker for early fat cells in skin could help to track the occurrence of cells before they accumulate lipids.

Despite that Pref-1 expression is abundant in preadipocytes and decreases dramatically in differentiated fat cells, it is a questionable marker for preadipocytes *in vitro* (Boney *et al*, 1996). Moreover, the staining for Pref-1, performed on the

embryonic skin, seemed to be quite random along the dermis and was seen not only in bottom dermis (where lipid accumulating cells developed) but also in top dermis, close to the epidermis (Figure 2.12). Because of this observation a suggestion can be made that Pref-1 is not a reliable marker for dermis cells that give a beginning of the dermal adipose tissue *in vivo*.

Next, the antibody against PPARgamma was tested on rodent cross-sections (Figure 2.13 and Figure 2.14). This antibody stained epidermis whereas the dermis seemed to lack the signal. A suggestion can be made that the antibodies used are against epitopes for PPARgamma protein that may be somehow hidden in skin dermis. The second suggestion may be that at the protein level PPARgamma is not seen in lower dermis where cells committed to lipid accumulation are present, however this suggestion may be controversial (as it may negate the role of PPARgamma in fat cell differentiation both *in vitro* and *in vivo*; see Chapter 1, sections 1.3.1 and 1.3.2). On the other hand, the clear differences between metabolic features of different fat depots have been recently discussed mainly in relation to the fat transplantation (for details see Chapter 1, section 1.2.8), thus maybe these differences are also related with the regulation of fat cell development and maybe dermal adipose tissue is controlled in a slightly different way from other known (and widely studied) fat depots. Finally, as the third explanation is that used antibodies were not sufficient for back skin sample analysis and gave “fake” staining across skin section.

In order to verify the working efficiency of used antibodies for the detection of Pref-1 and PPARgamma, an experiment should be performed on 3T3-L1 preadipocytes and differentiated 3T3-L1 fat cells. As said previously, Pref-1 protein is abundantly expressed in preadipocytes (Wang *et al*, 2006a), whereas expression of PPARgamma protein occurs in 3T3-L1 cells between 42 and 60 hours after the induction of adipogenic differentiation (Morrison and Farmer, 1999). Therefore samples from both undifferentiated and differentiated 3T3-L1 cells could undergo analysis for the expression of Pref-1 and PPARgamma with antibodies used in study from Chapter 2 (sections 2.3.4.1 and 2.3.4.2). In addition, both the immunofluorescence staining and the western blot analysis of samples from 3T3-L1 cells could give a better view on the working capabilities of used antibodies.

Then, the antibody against C/EBPalpha worked nicely on rodent dermis skin (Figures 2.15 - 2.20). It seems very likely that most cells of the rodent dermis that have nuclei labelled with C/EBPalpha at late gestation represent preadipocytes at

an advanced stage of adipocyte differentiation and are the same ones that go on to make lipids. This idea was supported initially by the independent C/EBPalpha immunofluorescence and Oil Red O labelling work that showed close anatomical co-localisation between the groups of labelled cells, and the observation that increasing numbers of C/EBPalpha labelled dermal cells became vacuolated and their nuclei took on an elongated moon-shape typical of adipocytes over time. Double staining of C/EBPalpha with the Oil Red O dye confirmed this relationship directly and showed clearly that lipid accumulation appeared in cells with C/EBPalpha expression during development. As C/EBPalpha was seen in dermal cells before the start of fat formation, the fact that expression was maintained after lipid accumulation suggested that C/EBPalpha may be needed both for the activation of adipogenesis, and possibly later to promote the lipid accumulation and maintenance of fat cells *in vivo* in back skin dermis. This work has been published (Wojciechowicz *et al*, 2008).

Because of the localisation of C/EBPalpha positive cells in close proximity to hair follicle end bulbs, there might be a correlation between differentiating fat cells and developing hair follicles in mouse back skin. Such relation was discussed in pigs and rats skin (Chapter 1, section 1.2.5). However, no detailed study seems to be available that would verify this suggestion.

Finally, the analysis of rodent dermis cells and the discovery of an *in vivo* marker for preadipocytes and adipocytes in skin helped to design an experiment where more details of dermis cells were analysed. This new study gave the possibility to investigate *in vivo* gene expression pattern in differentiating fat cells during embryonic mouse development and is presented in Chapter 3.

In addition, work presented in the next Chapters of this thesis aims to discuss the potential correlation between lower dermis cells that are undergoing adipogenesis and other skin compartments that are gradually developing in mouse back skin dermis.

# Chapter 3:

# The laser capture microdissection (LCM) technique and microarray approach for the analysis of differentiation processes in skin dermis at late stages of mouse embryonic development. Implications for (better) understanding adipogenesis *in vivo*.

## 3.1. Introduction.

Knowledge of how mature fat cells develop is crucial for our understanding of adipose biology and pathology so it is perhaps surprising that most of what is known about adipogenesis comes from work on cultured cells. In Chapter 2, foetal and newborn mice were investigated to establish where and when adipocyte formation takes place in developing skin. This work showed that differentiation of cells in the lower dermis during late foetal development leads exclusively to the development of the dermal layer of fat cells, with no apparent input from the subcutaneous depots present beneath the skin. It also confirmed that the initiation of adipogenesis occurs close to the lower region of hair follicles as described previously in other species (Hausman and Martin, 1982). Up to now, however, there has been no detailed analysis of the molecular changes that occur when adipocytes are formed *in situ*. Having established a location for preadipocytes, and knowing the timing of their appearance, we have a platform from which to address this question for the first time.

Detailed information about adipogenesis comes from *in vitro* work, involving the use of cell culture models, both established cell lines and primary cultures (for details see Chapter 1, part 1.3.1.1). Despite the knowledge, gained from this work, there is still a need to understand the differentiation process of preadipocytes *in vivo*. Cell culture models have several limitations. In the first place they are in a 2D environment and growing on an artificial surface. Thus they lack the third dimension and many of the proper contacts with other cells and extracellular elements that would normally take place in the body. Indeed recent work has highlighted that three dimensional culture systems are more realistic for studying biological processes than conventional 2D models (Higgins *et al*, 2010). In addition, 3T3 cells widely used for *in vitro* adipogenic studies were derived from whole mouse embryos, and not adipocyte-like cells. Such cells have to be “pushed” by adipogenic medium in order to obtain full adipogenic characteristics. Also, recently there is increasing evidence to suggest that different fat deposits have different functions and perhaps even developmental origins (Gesta *et al*, 2007; Porter *et al*, 2009). Thus, a general model like the 3T3 cells may not be representative of all fat depots so detailed investigation of the developmental features of different fat depots may eventually be required. Keeping in mind the limitations of the above systems, the following section discusses studies that have used such culture models for the investigation of adipogenesis on molecular level *in vitro* by microarray approach.

The development of microarray technologies has opened a new direction in analysis of different processes in cells, tissues and organs at the molecular level (Heller, 2002; Chen and Tzeng, 2006). In fat-related studies, cell lines treated with adipogenic medium and differentiated into mature adipocytes, have been subjected to detailed analysis by microarray technology. Guo and Liao (2000) used the cDNA/expressed sequence tag (EST) microarray approach for the analysis of gene expression profiles in 3T3-L1 cells (Guo and Liao, 2000). In general ESTs are small fragments of cDNA sequence obtained from sequencing pieces of expressed genes (Hatey *et al*, 1998). ESTs have been successfully used for the design of probes for microarray analysis. The Gene Discovery cDNA/EST array (Genome Systems) allowed researchers to investigate the gene expression profile from undifferentiated (day 0) and differentiated (day 6 after the adipogenic treatment) 3T3-L1 cells (Guo and Liao, 2000). In total, 83 genes were seen to be up-regulated (with at least 10 fold difference) in adipocytes, when compared with preadipocytes. This work confirmed up-regulation of specific fat-related genes in differentiated cells, such as PPARgamma, as well as revealing unknown ESTs seen only in preadipocytes or only in adipocytes.

A microarray approach was also used for the detailed analysis of 3T3-L1 cells during first 24 hours of incubation with adipogenic medium (Burton *et al*, 2002). In this study, RNA was collected from cells at day 0 (just before treatment with adipogenic medium) and at 2, 4, 16 and 24 hours after addition of adipogenic medium. In this work, the analysis was performed on microarray gene chips from Affymetrix with 13,179 cDNA/ESTs (Affymetrix murine Mu11K Array Set). This analysis revealed 285 mRNAs with fold changes equal or higher than 5, that were differently regulated (up or down) during the first 24 hours of adipogenic differentiation *in vitro.* These genes were known to play a role in cell cycle processes (p107) or regulation of transcription (C/EBPbeta). The use of bioinformatic self-organizing map (SOM) clustering allowed the authors organize 285 genes in five clusters, depending on their expression profiles.

A further microarray study analysed 3T3-L1 cells treated with adipogenic medium or adipogenic medium with an adipogenic inhibitor (trichostatin A - TsA), at time points: 0, 2, 8, 16, 24, 48 and 96 hours (Burton *et al*, 2004). Prepared cRNA was hybridized on Affymetrix MG_U74Av2 microarray gene chips (Affymetrix) that have 12,488 cDNA/Expressed Sequence Tags (ESTs) probe sets. The microarray data was analysed only for genes with at least a 2 fold-change. After discarding

genes common to stimulated or inhibited cells, a total number of 1016 transcripts specific to differentiated 3T3-L1 cells were analysed by SOM clustering. The data showed the up-regulation of mRNA levels for PPARgamma and C/EBPalpha in 3T3-L1 cells after 48 hours of treatment with adipogenic medium, not seen in cells treated with TsA. In addition, several genes with specific expression profiles (for example latexin) were suggested to have potential role in relation to adipogenesis (Burton *et al*, 2004).

Another comprehensive microarray-based study of adipogenesis was performed by Soukas *et al* (2001). Pre-confluent and confluent (day 0) 3T3-L1 cells, together with cells treated with adipogenic medium (6 hours, 12 hours and 1, 2, 3, 4, 7 and 28 days) were hybridized to 11K GeneChip microarrays (Affymetrix). In addition, this study included investigation of gene expression profiles in preadipocytes and adipocytes isolated from 8-weeks old C57Bl/6J mice, both wild-type and ob/ob (obese) animals. These cells were isolated from fresh, peri-uterine fat pads (white adipose tissue). Analysis of the 3T3-L1 cells, where the κ-means clustering algorithm was applied, highlighted 1259 genes differently expressed during induced adipogenesis with an increase of at least 3 fold. These genes were grouped into 27 clusters, among which 15 had a general up-regulated tendency while 12 clusters had genes whose expression was decreased. Overall, this analysis showed the complexity of adipogenesis at the mRNA expression level. Many genes considered to be involved in adipogenesis (from other types of investigation) were observed in this microarray based-study, appearing to confirm their role in the adipocyte differentiation process. For example, up-regulation of the PPARgamma 2 isoform (see Chapter 1, part 1.3.3.2) and of C/EBPalpha was noted during differentiation of 3T3-L1 cells (Soukas *et al*, 2001). The same study included a comparison between *in vitro* and *in vivo* preadipocytes and mature fat cells. In a group of genes common for both *in vitro* and *in vivo* preadipocytes was C/EBPdelta, whereas among genes enriched *in vitro* and *in vivo* in mature adipocytes were adiponectin (AdipoQ), C/EBPalpha and PPARgamma 2. As well as similarities between *in vitro* and *in vivo* cells, some interesting differences were also observed. For example, within a group of genes specific to 3T3-L1 preadipocytes was Pref-1, a recognised preadipocyte cell marker (Smas and Sul, 1993) and C/EBPbeta which has been suggested to play a crucial role in the early stages of adipogenesis in cell lines (Cao *et al*, 1993). In addition, a group of genes with enriched expression specific to *in vivo* adipocytes was created including the Frizzled 4 gene.

The global analysis of genes regulated during adipogenesis in 3T3-L1 cells was also performed by Hackl *et al* (2005) where RNA isolated from cells at eight time points (0, 6, 12, 24, 48, 72 hours and 7, 14 days) during differentiation was used for the microarray-based analysis. This study gave an additional view on genes regulated *in vitro* during adipocyte maturation and biological processes activated in such cells.

The microarray data generated from 3T3 cells helped to investigate function of selected genes in relation to adipogenic differentiation. Ross *et al* (2002) investigated a potential role of liver X receptor alpha (LXRalpha) in adipogenesis, as this gene was specifically expressed in adipocytes when compared with 3T3-L1 preadipocytes in microarray study.

Microarray techniques have been also applied for the analysis of other types of cells that undergo adipogenic differentiation. Such analysis was performed on human bone marrow mesenchymal stem cells (hMSCs), which are capable of fat cell differentiation when treated with adipogenic medium (Nakamura *et al*, 2003). In this work, genes differently expressed during hMSCs differentiation were organized in nine clusters and compared with genes expressed in 3T3-L1 cells. Among genes up-regulated in cells treated with adipogenic medium, were known adipogenic transcriptional factors, such as C/EBPalpha and PPARgamma 2. In addition, some of the up-regulated genes in the early stages of hMSCs cell differentiation, such as the transcription factor SLUG, were found to be down-regulated in differentiated 3T3-L1 cells. This work shows that between different mammals, differences can occur in relation to stages/mode of adipocyte differentiation.

It has also become increasingly common to use microarray approaches for the global analysis of genes from different adipose tissue depots - white and brown fat cells, visceral versus subcutaneous fat depots in different animals, or in relation to obese individuals. Features of white and brown hamster preadipocytes were analysed by microarray technology by Boeuf *et al* (2001). Microarray analysis was also applied to the investigation of adipocytes in chickens as a means of better understanding obesity development in these organisms (Wang *et al*, 2006b). Wang *et al* (2006b) have identified genes whose expression levels in adipose tissue differed between fat line broilers and so-called Bai'er layers at 10 weeks of age (for example lipoprotein lipase level was higher in broilers). Urs *et al* (2004) performed a study, where gene expression profiles were analysed in both adipocytes and

preadipocytes (from stromal-vascular fraction) of subcutaneous abdominal fat depot from women (Urs *et al*, 2004). This work revealed an enrichment of genes related with lipid metabolism (fatty acid binding protein, lipoprotein lipase or perilipin) in human adipocytes and high expression of genes associated with extracellular matrix components (for example fibronectin) in a preadipocyte fraction from analysed fat depot.

In addition, Affymetrix HG-U95 GeneChip arrays were used for analysis of adipocytes from non-obese and obese humans (Lee *et al*, 2005). Adipocytes were isolated from abdominal subcutaneous fat of non-diabetic Pima Indians. This work revealed that many inflammation-related genes were up-regulated in obese individuals including many chemokines, for example the monocyte chemoattractant protein-1 MCP-1.

Microarray analysis, on both subcutaneous and visceral fat cells from morbidly obese humans allowed researchers to track differences in gene expression profiles between these two fat depots (Ramis *et al*, 2002). They constructed a cDNA microarray that consisted of 154 selected and named genes and 286 human adipose tissue-derived cDNA clones. Two genes, carboxypeptidase E and thrombospondin-1 were found to be up-regulated in the visceral depot when compared with subcutaneous fat cells.

To sum up, adipogenesis process has been intensively investigated *in vitro* in several types of cell lines, among which the most popular are 3T3-L1 cells (see section 1.3.1.1. and Table 1.2 in Chapter 1). It is suggested that activation of crucial adipogenic factors *in vitro* takes place during the first 24 - 48 hours of adipogenic induction by differentiation medium and the first lipid droplets can be identified in differentiating cells by day 3 (Richon *et al*, 1997; Soukas *et al*, 2001). The microarray approach enhanced knowledge about steps of adipogenic differentiation in these cells between day 0 (confluent cells before addition of adipogenic medium) and day 28 after the induction of adipogenesis (by adipogenic medium). Such studies confirmed the specific expression patterns of adipogenic transcription factors (C/EBPs and PPARgamma) or genes involved in cell cycle regulation (p107) during first 24 - 48 hours of adipogenesis or the over-expression of genes specific for mature fat cells (adiponectin) after several days of differentiation. However, microarray approaches revealed some differences in expression profiles between different cell lines used for adipogeneic studies as well as suggesting the presence

of differences at molecular level between *in vitro* cell lines and cells isolated from adipose deposits and treated as a representative of *in vivo* conditions.

In addition, different *in vivo* mouse models have been widely used, to study the functions of particular genes relating to adipogenesis, based on over-expression, silencing or mutation (see Chapter 1, part 1.3.1.2). Many mouse model-related studies have aimed to analyse adipose tissue development processes mainly after the birth of animals (reviewed by Valet *et al*, 2002). Genetically abnormal animals are recognised to be important for functional studies. However, in the current work the aim was to produce a new global analysis of the events of adipogenesis *in vivo*, at the embryonic stage, and focused on fat cells in lower skin dermis, a population not previously analysed at the transcriptional level.

The hypothesis tested in Chapter 3 is that transcriptional changes take place in mouse embryonic back skin dermis *in vivo* between e17 and e19 time points which lead to differentiation of lower dermal cells into fat cells and development of non-fatty cells in upper dermis. In addition, it was hypothesised that early steps of fat cell differentiation observed *in vivo* in mouse back skin differ in some extent from these observed during *in vitro* adipogenesis in 3T3 cell lines. This work was achieved by combining the laser capture microdissection technology with microarray analysis in mouse. This investigation revealed interesting differences in gene expression profiles between upper dermis, where no lipid accumulation is observed, and lower dermis, where dermal adipose tissue develops. The detailed analysis of lower dermis cells targeted molecular profile of cells differentiating into adipocytes. Such data from lower dermis was compared to available expression data from fat cell differentiation in 3T3-based cells (*in vitro* studies). To best of my knowledge such work represents the first global analysis of dynamic processes taking place in mouse back skin dermis during the late stages of embryonic development *in vivo*.

## 3.2. Methods.

Microarray related work was carried under the RNase free conditions where RNase ZAP (Sigma) and 0.1% DEPC water (Appendix I) were used. All surgical tools were baked at 150$^{o}$C for 2 hours and washed in DEPC water before using. Filter tips were free of detectable RNase, DNase and DNA.

### 3.2.1. Housing, breeding and feeding conditions of rodents.

For details on mouse age determination, housing, breeding and feeding conditions see Chapter 2, section 2.2.1.

### 3.2.2. Back skin preparation.

Back skin samples were collected in RNAse free conditions from mouse (CD1) embryos between 16.5 and 17 (designated e17 time point), 18 (designated e18 time point) and about 19 (designated e19 time point) day old. Embryos were transferred into sterile Petri dishes containing MEM - Minimal Essential Medium (Sigma) and antibiotics (2 μl/ml Fu - fungizone from Sigma and 1 μl/ml Ge - gentamicin from Gibco). Back skin was removed from mouse body, and snap frozen in a water-based embedding compound (Tissue Tek) in liquid nitrogen according to a protocol described in Chapter 2 (section 2.2.3).

### 3.2.3. Dermal cell collection and microarray sample preparation.

#### 3.2.3.1. Back skin sample preparation and H&E staining.

Back skin samples, frozen in Tissue Tek, were cut on a cryostat (LEICA CM 3050S) and 10 μm skin sections were placed on PALM Membrane Slides (Nuclease and human nucleic acid free PEN/NF (D), Carl Ziess Microscopy). A schematic description of the back section preparation is presented in Figure 3.1. In addition, the cryostat was wiped with chloroform and slides were kept under UV for 30 min before use.

Slides with skin sections were air-dried for 6 - 10 min, and underwent a shortened version of haematoxylin and eosin (H&E) staining. Samples were incubated in cold 70% ethanol for 2 min and washed in DEPC water. They were then stained for 1 min in haematoxylin (Hematoxylin solution prepared according to Mayer, Fluka by Sigma), put into Bluing Solution (Thermo Electron Group) for 1 minute, stained for 10 sec in EosinY solution (Sigma), and washed in 70% ethanol (1 min), 96% ethanol (1 min) and 100% ethanol (Sigma) (1 min). Finally, skin sections were dried for 3 - 5 min at room temperature (RT), and used for cell

collection on the Laser Capture Microdissection Microscope (PALM MicroBeam Zeiss Microscope, CryLaS, FTSS 355-50 with PALM Robo v3.2 software).

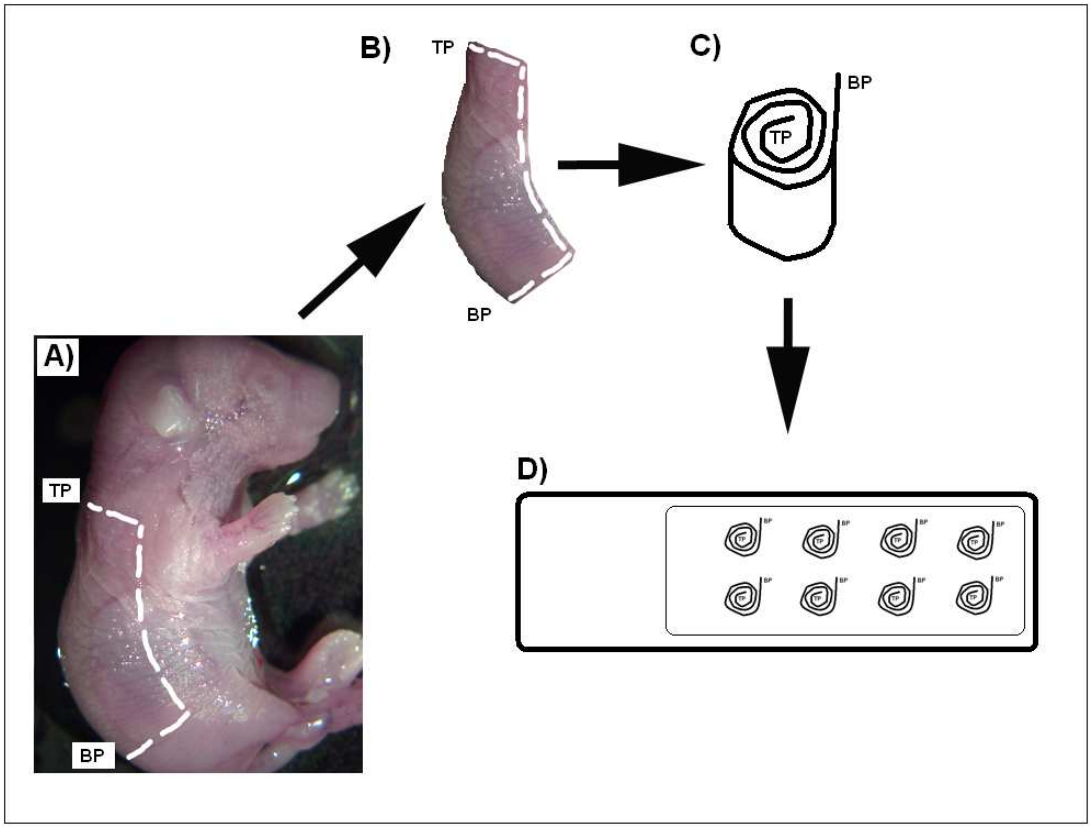


Figure 3.1. A schematic presentation of back skin sample preparation for the laser capture microdissection work. (A, B) Back skin sample cut out from mouse. C) Back skin rolled up and frozen in Tissue Tek. D) 10 μm sections cut on the cryostat, then placed on PALM Membrane slides and used for the laser capture microdissection work. TP - top part of the back skin. BP - bottom part of the back skin.

### 3.2.3.2. Laser capture microdissection (LCM) technique.

Slides with skin sections were examined under the Laser Capture Microdissection (LCM) Microscope and two areas of dermis were selected for the subsequent collection of material (Figure 3.2). Area “1” (upper dermis) was characterised by cells localised in the upper dermis, close to the epidermal layer, whereas Area “2” (lower dermis) was represented by cells from the lower dermis, between and around hair follicle end bulbs. Both areas were cut out and catapulted by the laser into the lids of PALM Adhesive Caps (Carl Ziess Microscopy). The presence of captured skin on the lids was verified on the LCM microscope (Figure 3.3B and C).

In order to collect a sufficient amount of material for microarray analysis, from each embryonic back skin sample, between six and seven sets of laser-captured cells were prepared. From each set, two areas of dermis (Area “1” and Area “2”) were collected separately using the laser capture apparatus. For each set, approximately three slides were prepared with back skin sections. Each set represented around 100 pieces of skin for each dermis area, and each piece contained between 5 and 15 cells. The specimens from the two areas of dermis were collected in two separate PALM Adhesive Caps, then a maximum of 50 μl of the lysis buffer RLT (Qiagen) with β-mercaptoethanol (b-ME; Sigma) was added and the sample was incubated for 10 min on ice and stored at -80$^{o}$C.

Before RNA isolation, six (or seven) sets of cells collected from Area “1” of the back skin dermis of one animal were transferred from PALM Adhesive caps into one 1.5 ml centrifuge tube (Eppendorf). Then, six (or seven) sets of cells collected from Area “2” (in back skin dermis) were combined in another centrifuge tube. To sum up, from a single embryonic sample, the minimum number of collected cells was around 3000 - 9000 cells per 300 - 350 μl of typical lysis buffer that was used for RNA isolation and microarray work.

In addition, three mouse embryos (from the same mother) were used for each analysed time point therefore the whole microarray work was performed in triplicate with three biological samples.

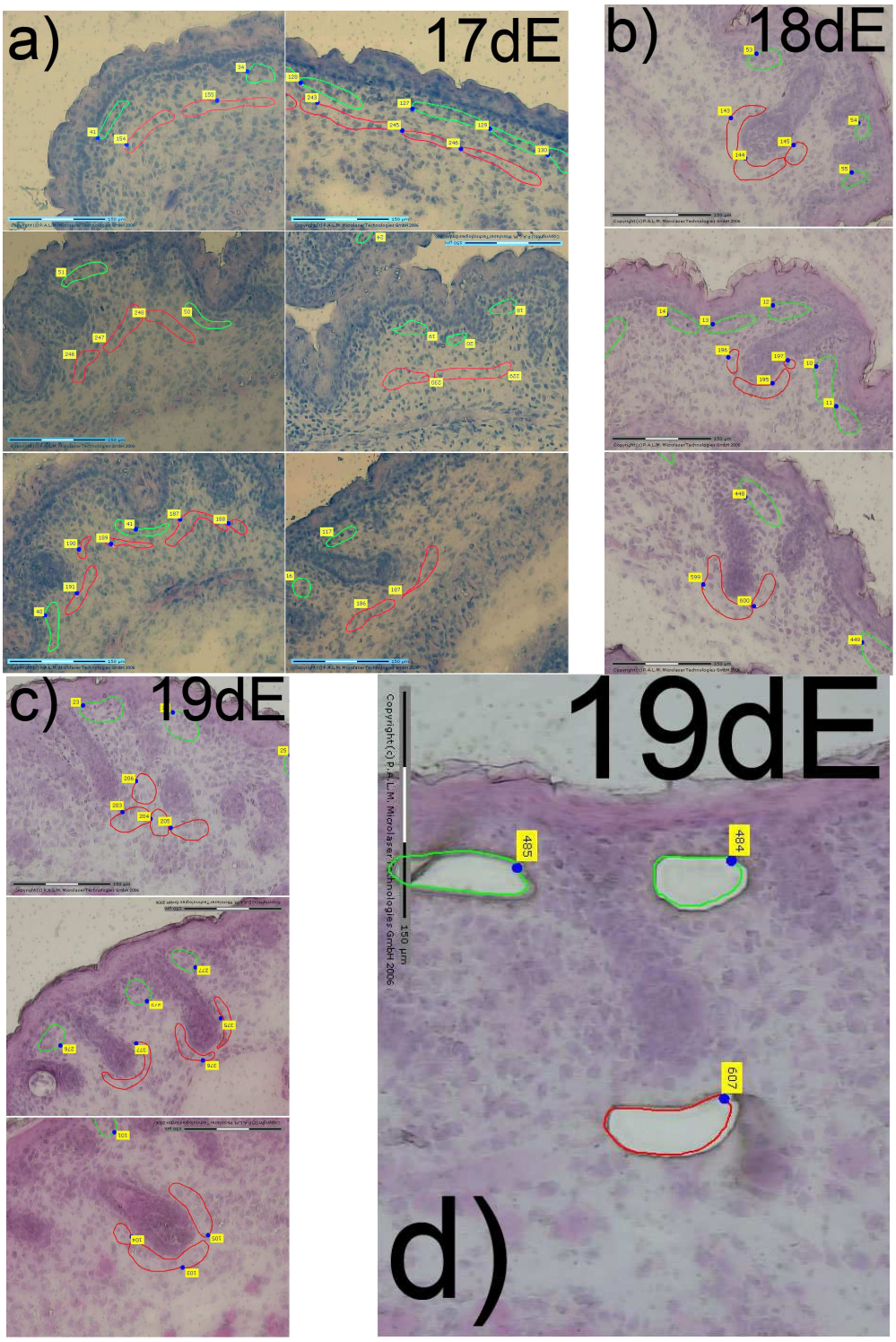


Figure 3.2. A schematic presentation of dermis areas collected on the Laser Capture Microdissection microscope and used for RNA isolation. (a - d) Cells were collected from upper dermis (Area “1” - shown in green) and lower dermis (Area “2” - shown in red) cross-sections cut from back skin of embryos at e17 (17dE), e18 (18dE) and e19 (19dE) time points. (d) Back skin section after the cut off cells from dermis areas. Scale bar = 150 µm. Images were captured using a Laser Capture Microdissection Microscope (PALM MicroBeam Zeiss Microscope).

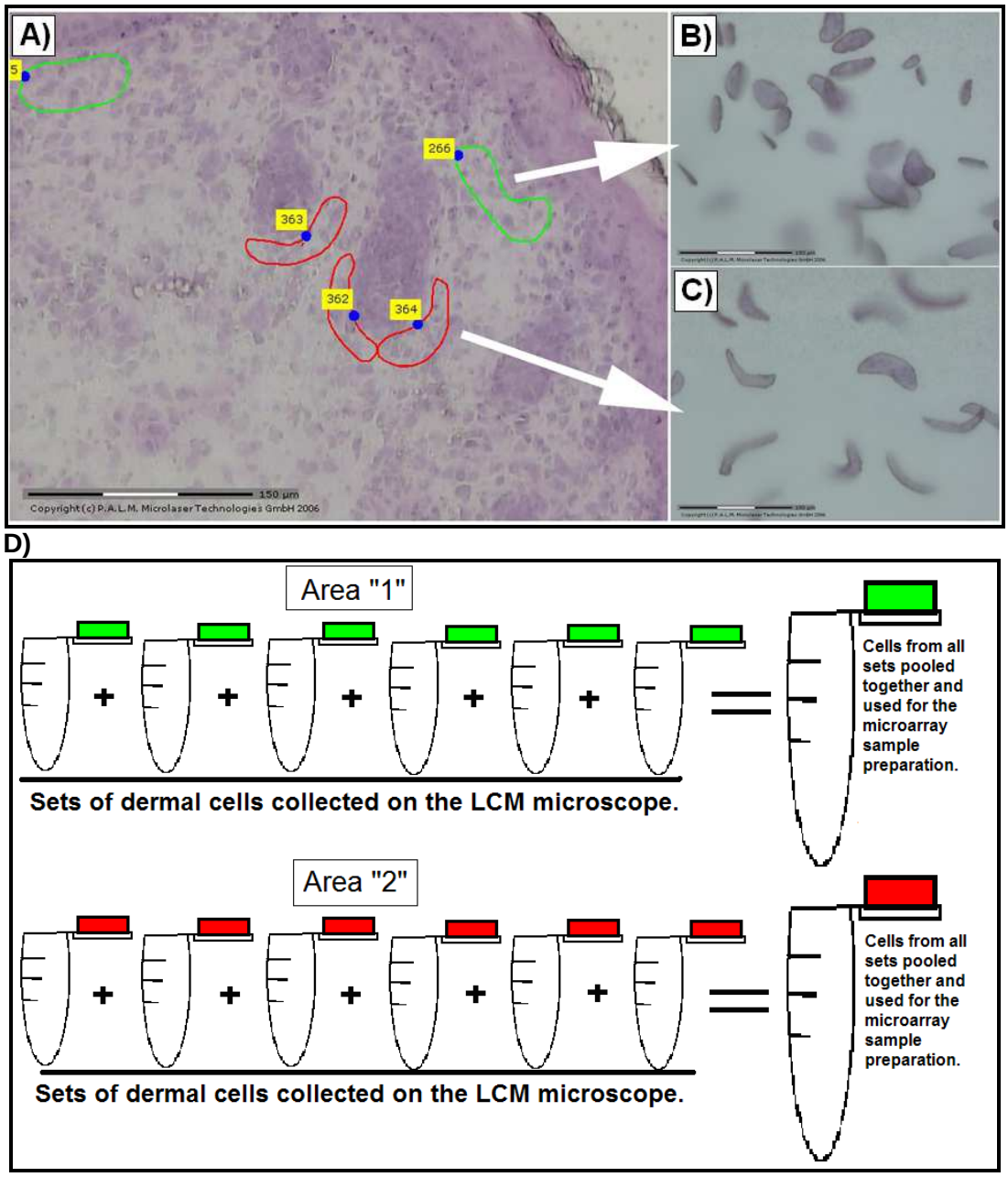


Figure 3.3. Collection of dermal cells on the LCM microscope. (A) Two areas of dermis selected for microdissection: upper Area “1” (green) and lowerd Area “2” (red). (B, C) Cells from dermis areas collected on the lids of small Eppendorf. (D) Up to 6 - 7 sets of dermis cells (from each area) were collected from a single embryo (at e17, e18 or e19 time point) and pooled together for RNA isolation and microarray sample preparation. Scale bar = 150 µm. Images were captured using a Laser Capture Microdissection (LCM) microscope (PALM MicroBeam Zeiss Microscope).

### 3.2.3.3. Microarray sample preparation - molecular biology techniques.

#### 3.2.3.3.1. Purification of RNA.

Total RNA was extracted using the RNeasy® Micro kit from Qiagen. Cell samples from the dermis (Area "1" and "2") of 16.5 - 17, 18 and 19 day old mouse were adjusted to the final volume of 350 μl with the Lysis Buffer RLT (Qiagen) with β-ME. Then 5 μl of a 4 ng/μl carrier RNA solution (Qiagen) was added to each lysate. Next, 1 volume (350 μl) of 70% ethanol was added to each lysate and the whole sample was transferred to an RNeasy MinElute spin column (Qiagen) in a 2 ml collection tube and centrifuged for 15 seconds at 10 000 rpm. The whole flow-through sample was placed once again on the spin column and centrifuged a second time under the same conditions. After the flow-through was discarded, 700 μl of the supplied buffer RW1 was added to the sample and centrifuged for 15 seconds at 10 000 rpm. The spin column was placed into a new 2 ml collection tube and 500 μl of supplied buffer PRE (with ethanol) was added to the sample and centrifuged for 15 seconds at 10 000 rpm. Next, 500 μl of 80% ethanol was added to the spin column and centrifuged for 2 min at 10 000 rpm. The spin column was then placed into a new collection tube and centrifuged with the lid open at full speed for 5 minutes. Finally, the spin column was placed into 1.5 ml collection tube and 14 μl of RNase-free water (at 65$^{o}$C) was added to the centre. The column was incubated for 3 - 5 min at room temperature with the RNase-free water and centrifuged for 1 minute at full speed to elute RNA. All extraction steps were performed at room temperature and the isolated RNA was stored at -80$^{o}$C.

#### 3.2.3.3.2. RNA quantification and its assessment.

The quantity of total isolated RNA (and cRNA from section 3.2.3.3.3) was determined on either the BioPhotometer (Eppendorf) or on a NanoDrop® Spectophotometer (ND-1000 with V3.5.2. software, Labtech International). Diluted RNA (1:50, for BioPhotometer) or 1 μl of undiluted RNA (for NanoDrop) was used.

Additionally, the quality of cRNA (from step 3.2.3.3.3.) could be checked by electrophoresis. Between 1 and 2 μl of RNA was loaded on the 1 - 2.0% agarose gel (Severn Biotech Ltd), containing Ethidium Bromide (0.1 μl/ml, Fluka) in 1 x Tris Acetate-EDTA (TAE) (Appendix I). In addition, between 1 and 2 μl of glycerol loading buffer (Appendix I) were added to each sample, before electrophoresis.

The techniques, presented above, were also used for the analysis of cRNA.

### 3.2.3.3.3. Synthesis and cleanup of Double-Stranded cDNA from Total RNA.

All steps of cDNA synthesis were prepared under RNase free conditions. The "GeneChip® Expression 3'-Amplification Reagents Two-Cycle cDNA Synthesis Kit" (Figure 3.4) from Affymetrix and MEGAscript® T7 Kit from Ambion were used for this work. Incubations were performed in a BiometraR thermocycler and after each incubation and addition of new reagents, samples were briefly centrifuged in order to collect samples at the bottom of tubes. The "GeneChip Sample Cleanup" Module (Affymetrix) was used for the cleanup steps.

#### 3.2.3.3.3.1. First-Cycle cDNA Synthesis.

##### 3.2.3.3.3.1.1. First-Cycle, First-Strand cDNA Synthesis.

Reagents for this step were provided in the Affymetrix kit. The T7-Oligo(dT) Primer/Poly-A control mix was prepared, which contained 4 μl of 50 μM T7-Oligo(dT) Primer and 16 μl of RNase-free water. Between 50 and 150 ng of total isolated RNA from each sample was placed in a 0.2 ml PCR tube with 1 μl of T7-Oligo(dT) Primer/Poly-A control mix and RNase-free water to a total volume of 5 μl. Tubes were incubated for 6 minutes at 70$^{o}$C and 2 minutes at 4$^{o}$C. Next, 5 μl of First-Cycle, First-Strand master mix was added to each sample. This master mix contained 2 μl of 5X 1$^{st}$ Strand Reaction Mix, 1 μl of 0.1M DTT, 0.5 μl of RNase inhibitor, 0.5 μl of 10mM dNTP and 1 μl of SuperScript II per each sample. Samples were incubated for 1 hour at 42$^{o}$C, 10 minutes at 70$^{o}$C and at least 2 minutes at 4$^{o}$C and immediately used for the next step of First-Strand cDNA Synthesis (see above).

##### 3.2.3.3.3.1.2. First-Cycle, Second-Strand cDNA Synthesis.

To each sample, prepared in the First-Cycle, First-Strand cDNA Synthesis Step, 10 μl of First-Cycle, Second-Strand master mix were added. This master mix contained 4.8 μl of RNase-free water, 4 μl of freshly diluted 17.5 mM $MgCl_2$, 0.4 μl of 10mM dNTP, 0.6 μl of *E. coli* DNA Polymerase I and 0.2 μl of RNase H per sample. Samples were incubated for 2 hours at 16$^{o}$C, 10 minutes at 75$^{o}$C and at least 2 minutes at 4$^{o}$C. For the 16$^{o}$C incubation, the lid of the thermocycler was left open.

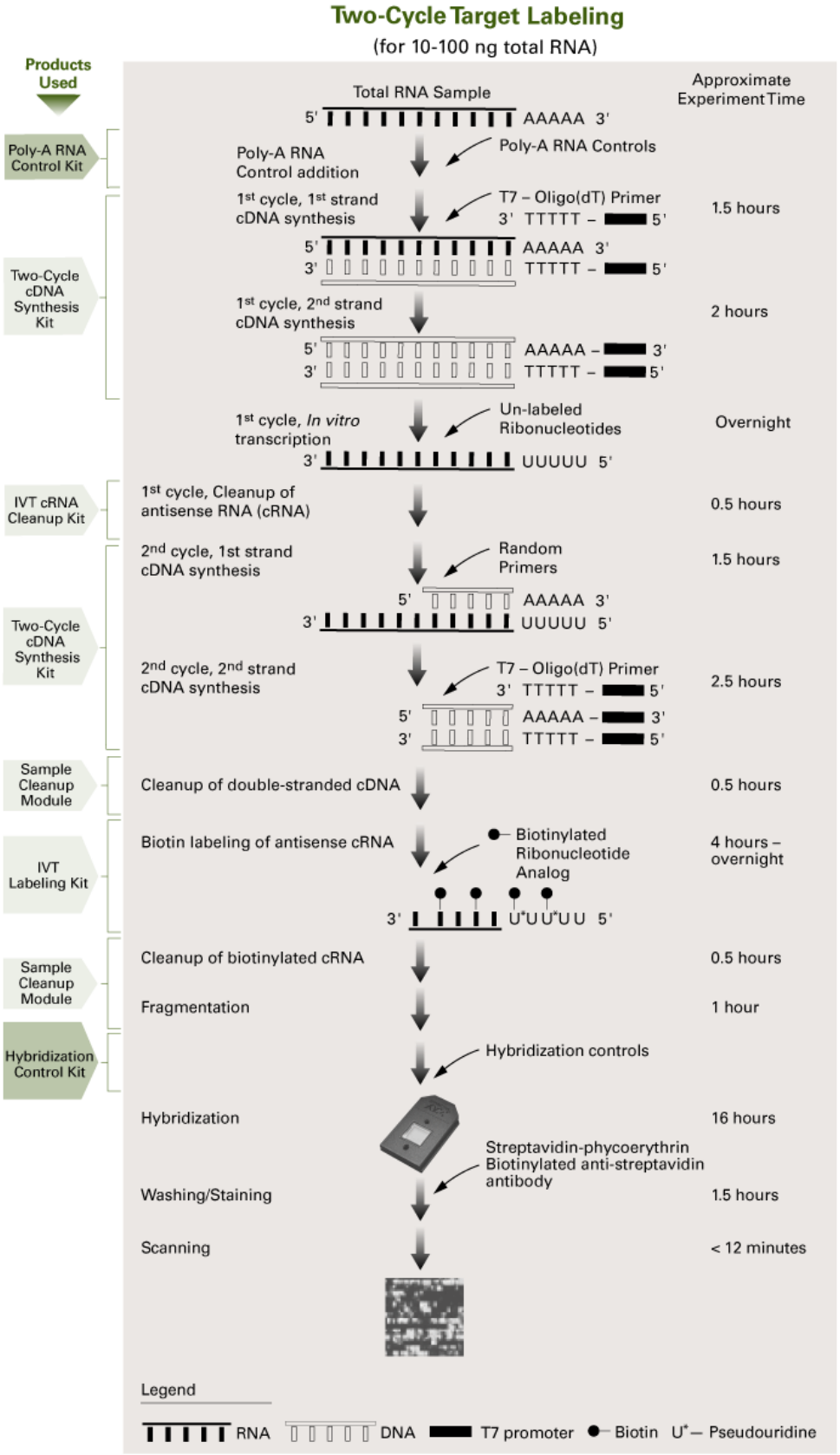


Figure 3.4. A schematic presentation of experimental steps for microarray samples preparation. Samples were prepared according to the two-cycle target labeling assay (The “GeneChip® Expression 3’-Amplification Reagents Two-Cycle cDNA Synthesis Kit”). Source: http://www.biomics.nl/images/two_cycle_target_labeling.gif

#### 3.2.3.3.3.1.3. First-Cycle, IVT Amplification of cRNA.

The First-Cycle, IVT master mix was prepared for this step (all reagents were provided in MEGAscript® T7 Kit) and contained 5 μl of 10X reaction buffer, 5 μl of ATP solution, 5 μl of CTP solution, 5 μl of UTP solution, 5 μl of GTP solution and 5 μl of enzyme mix for a single reaction. 30 μl of prepared First-Cycle, IVT master mix were transferred to each reaction sample and samples were incubated for 16 hours at 37$^{o}$C and cooled down to 4$^{o}$C.

#### 3.2.3.3.3.1.4. First-Cycle, Cleanup of cRNA.

All steps of the cleanup of amplified cRNA were carried at room temperature. Samples were transferred into 1.5 ml tube and 50 μl of RNase-free water, 350 μl of IVT cRNA Binding Buffer and 250 μl of 100% ethanol were added to each sample. Next, samples (700 μl) were added to the IVT cRNA Cleanup Spin Columns in 2 ml collection tubes and centrifuged for 15 seconds at 10 000 rpm. The whole flow-through was placed once again on the spin columns and centrifuged for a second time in the same conditions. Next, spin columns were transferred into a new 2 ml collection tubes and 500 μl of IVT cRNA Wash Buffer was added to each spin column that was then centrifuged for 15 seconds at 10 000 rpm. The flow-through was discarded, 500 μl of 80% ethanol was put into each column that was centrifuged for 15 seconds at 10 000 rpm. After the flow-through was discarded, all spin columns were centrifuged for 5 minutes at maximum speed (13 000 rpm) with their caps opened. Next, columns were placed into 1.5 ml collection tubes and 13 μl of RNase-free water (pre-warmed to 65$^{o}$C) was put directly onto each spin column membrane. All samples were incubated at room temperature for 3 - 5 minutes and centrifuged for 1 minute at maximum speed (13 000 rpm) in order to elute cleaned cRNA. Each sample was quantified and assessed (for details see section 3.2.3.3.2) and used for Second-Cycle cDNA Synthesis (section 3.2.3.3.3.2).

### 3.2.3.3.3.2. Second-Cycle cDNA Synthesis.

#### 3.2.3.3.3.2.1. Second-Cycle, First-Strand cDNA Synthesis.

A fresh dilution of 0.2 μg/μl random primers was prepared by mixing 2 μl of 3 μg/μl random primers with 28 μl of RNase-free water. Next, 550 - 650 ng of each purified cRNA sample was placed in a 0.2 ml PCR tube with 2 μl of freshly diluted random primers and RNase-free water to a final volume of 11 μl. All tubes were incubated for 10 minutes at 70$^{o}$C and cooled for at least 2 minutes at 4$^{o}$C. Then, 9 μl

of Second-Cycle, First-Strand master mix were added to each sample. This master mix contained 4 µl of 5X 1st Strand Reaction Mix, 2 µl of 0.1M DTT, 1 µl of RNase inhibitor, 1 µl of 10 mM dNTP and 1 µl of SuperScript II per each sample. Samples were incubated for 1 hour at 42°C and cooled for 2 minutes at 4°C. 1 µl of RNase H was added to each sample and incubation for 20 minutes at 37°C was performed. Next, samples were incubated for 5 minutes at 95°C and cooled for at least 2 minutes at 4°C.

### 3.2.3.3.3.2.2. Second-Cycle, Second-Strand cDNA Synthesis.

A fresh dilution of 5 µM T7-Oligo(dT) Primer was made by adding 2 µl of 50 µM T7-Oligo(dT) to 18 µl of RNase-free water. 4 µl of freshly diluted T7-Oligo(dT) Primer was added to each sample prepared as in the Second-Cycle, First-Strand cDNA Synthesis Step (section 3.2.3.3.3.2.1). Then, samples were incubated for 6 minutes at 70°C and cooled for at least 2 minutes. The Second-Cycle, Second-Strand master mix was prepared that consisted of 88 µl RNase-free water, 30 µl 5X 2nd Strand Reaction Mix, 3 µl 10 mM dNTP and 4 µl *E. coli* DNA Polymerase I per sample. 125 µl of this Master Mix was added to each sample that was then incubated for 2 hours at 16°C and cooled down to 4°C. Next, 2 µl of T4 DNA Polymerase was added to each sample which was incubated for 10 minutes at 16°C and at least 2 minutes at 4°C. For the 16°C incubation, the lid of a thermal cycle was left open.

Prepared samples were either purified straight after the Second-Cycle, Second-Strand cDNA Synthesis or immediately frozen at -20°C and cleaned next day.

### 3.2.3.3.3.2.3. Cleanup of double-stranded cDNA.

All steps were performed at room temperature. Samples were transferred into 1.5 ml tubes and 600 µl of cDNA Binding Buffer was added to each of them. Next, samples were added to the cDNA Cleanup Spin Columns in 2 ml Collection Tubes and centrifuged for 2 minutes at 10 000 rpm. The whole flow-through was placed once again on the spin columns and centrifuged for a second time under the same conditions. Then, spin columns were placed into new collection tubes, 750 µl of cDNA Wash Buffer was added to each column and the columns centrifuged for 1 minute at 10 000 rpm. The flow-through was discarded and the spin columns were centrifuged with opened caps for 5 minutes at maximum speed (13 000 rpm). Next,

they were transferred into 1.5 ml collection tubes and 14 μl of cDNA Elution Buffer (pre-warmed to 60$^{o}$C) was added to each spin column membrane. All samples were incubated at room temperature on the bench for approximately 3 - 5 minutes and centrifuged for 1 minute at maximum speed (13 000 rpm) in order to elute cDNA. Eluted samples were stored at -20$^{o}$C.

### 3.2.3.3.4. Biotin-Labeled cRNA - final steps of microarray sample preparation.

#### 3.2.3.3.4.1. Synthesis of Biotin-Labeled cRNA.

Cleaned double-stranded cDNA (dsDNA) (section 3.2.3.3.3.2.3) was used for a synthesis of biotin-labelled cRNA, using the "GeneChip IVT Labeling Kit" (Affymetrix). IVT reaction mix was prepared that contained of 12μl dsDNA template, 4 μl 10X IVT Labeling Buffer, 12 μl IVT Labeling NTP Mix, 4 μl IVT Labeling Enzyme Mix, and 8μl of RNase free water giving a total volume of 40μl. This reaction was incubated for 16 hours at 37$^{o}$C in a thermal cycler (Peltier Thermal Cycler).

#### 3.2.3.3.4.2. Cleanup and quantitation of Biotin-Labeled cRNA.

Each IVT reaction sample was mixed with 60 μl of RNase-free water, 350 μl of IVT cRNA Binding Buffer and 250 μl of 100% ethanol. Next, each sample was added to an IVT cRNA Cleanup Spin Column in a 2 ml Collection Tube and centrifuged for 15 seconds at ≥ 10 000 rpm. Spin columns were transformed into new collection tubes and 500 μl of IVT cRNA Wash Buffer was added to columns that were centrifuged for 15 seconds at 10 000 rpm. Next, the spin columns were centrifuged with 500 μl of 80% ethanol for 15 seconds at 10 000 rpm. The flow-through was discarded and columns were centrifuged for 5 minutes at maximum speed with opened caps. Spin columns were placed on the 1.5 ml Collection Tubes and RNase-free water was applied on the membranes to elute samples that were centrifuged for 1 minute at maximum speed. The concentration of Biotin-Labeled cRNA was checked by spectrophotometry on a Biomate spectrophotometer (Thermo Electron Corporation).

#### 3.2.3.3.4.3. Fragmentation and hybridization of cRNA.

The Sample Fragmentation Reaction Mix was prepared with 15 μg of cRNA (at a final concentration of 0.5 μg/μl), 5X Fragmentation Buffer and RNase-free water up to a final volume of 30 μl. Samples were incubated for 35 minutes at 94$^{o}$C, then transferred to new RNase-free 1.5 ml tubes and used for the hybridization step

on the genechip. Samples were hybridized on the Mouse Genechip 430 2.0 from Array (Affymetrix). The synthesis and cleanup and fragmentation of biotin labeled RNA was performed by Dr Claire Higgins in the Department of Dermatology, Columbia University, and the hybridization of cRNA onto the genechip was performed by Vladan Miljkovic in the GeneChip Analysis facility at Columbia University.

### 3.2.4. The generation of dermis microarray data (DMD) by the GeneSpring® GX11.0 software.

The microarray data from dermal cells (named as the dermis microarray data – DMD) was generated on the GeneSpring® GX11.0 software (Silicon Genetics, USA) by Dr Claire Higgins at Columbia University (New York). Genechips contained 100 normalised probe-sets, and GeneSpring was able to use these to normalise samples so that they were comparable. Next, the filtration was done on expression-genes that had to be present in at least one sample. A statistical analysis was performed to filter for significant genes based on their p-value ($p<0.05$). Next, genes that were both significantly and differentially regulated were detected by filtering the statistically significant genes on a fold change cut off of 2. Three microarray lists were generated that contained genes regulated in lower versus upper dermis at e17 (E17 list), e18 (E18 list) or e19 (E19 list) time points. In addition, microarray data were generated with specific gene expression profiles only in lower dermis during mouse embryo development (e17 to e18 and from e17 to e19 time points), which was called the lower dermis - LD microarray data (the LD microarray list). This LD list, contained of genes with fold change equal or higher than 2 in at least one of analysed time point (e18 versus e17 or e19 versus e17). For the generation of E17, E18 and E19 lists the statistical test used was an unpaired t-test, whereas the One Way Analysis of Variance (ANOVA) was used comparing both e18 and e19 back to e17 time points (the LD microarray list).

### 3.2.5. The bioinformatics analysis of microarray data.

Two bioinformatics tools (described in section 3.2.5.1 and section 3.2.5.2) were included in the analysis of the generated microarray data from embryonic skin dermis (section 3.2.4), in order to get familiar with different bioinformatics softwares.

#### 3.2.5.1. The DAVID v6.7 programme.

The Database for Annotation, Visualization and Integrated Discovery - DAVID v6.7 is a web-available programme that permits analysis of the gene lists in order to investigate biological features of transcripts. First, a gene list with specific ID for the analysed genes (for example by Affymetrix IDs) is uploaded on the DAVID web site and then the detailed analysis is performed by using one of the available tools (for example “Functional Annotation Clustering” or “Functional Annotation Chart”).

For the work presented in this Chapter the “AFFYMETRIX_3PRIME_IVT_ID” was used as identifier, the Mus Musculus as species and the “Gene list” as a list type, when the gene lists were uploaded. The Affymetrix IDs are verified by DAVID and transformed into known DAVID IDs. In the analysed microarray list, several IDs could represent the same gene, and DAVID verifies this information and connects all IDs with specific genes (so in the end the total number of DAVID IDs is lower that the total number of Affymetrix IDs). Next, “Functional Annotation Clustering” analysis was performed. For this, the DAVID v6.7 tool associates each gene with different terms, for example the term “secreted” is associated with genes known to code for secreted proteins, and so on. For each term, the number of relevant genes from the analysed gene list is given as well as their percentage in relation to the total number of analysed genes. In addition, category information is provided and this gives the possibility of checking which data base/source the presented term comes from - for example the term “secreted” belongs to category “SP_PIR_KEYWORDS”. Each analysed gene can be associated with several different terms. The “Count threshold”, as the minimum number of genes related with each term, was set to 2. Depending on how many analysed genes (from all genes of the microarray list) are related with one term and how many genes are known to be related with this term (from all genes based on DAVID v6.7 database), such term is characterised by a p-value. The smaller the value, the more enriched the group is. In general, the p-value equal or smaller than 0.05 is treated as highly enriched. In the DAVID analysis presented in this Chapter, all created terms (with all given p-values) were taken under consideration and analysed. The main aim of the analysis is to investigate the developmental processes that occur in mouse embryonic skin dermis. During the developmental

and differentiation processes, genes can be activated progressively and we can assume that not all crucial genes for a specific pathway will be activated at the same time. At the embryonic level, it can be predicted that some genes will not be activated whereas other will be. Finally, after a certain time, when the tissue/organ is properly developed, all genes related with its function will be present. To illustrate this an artificial example can be given for a differentiation process called “process A” that is related with the maxumum gene number 70. For example at the e17 time point in lower dermis only one gene relating to the “the process A” is up-regulated. Then at e18 a further 20 genes are up-regulated and finally 55 genes are regulated in e19 (and p-values are smaller - more significant at e18 and e19, when compared with p-value at e17). This could indicate that up-regulation of the 1 gene at e17 is not random, (even though its upregulation is not statistically significant), and just illustrates that the beginning of the process “A” is occuring at e17.

#### 3.2.5.2. The GeneCoDis 2.0 tool.

The lower dermis (LD) microarray list was analysed by the GeneCoDis 2.0 tool in order to investigate biological features of genes from lower skin dermis. The GO_CC (cellular component) analysis was performed. After an elimination, by the GeneCoDis 2.0, genes not showing any annotations, genes were organized in groups depending on their known cellular localisation. A minimum number of genes associated with each created group was three. The “affy_mouse430_2” was selected as a microarray reference list, due to the fact that analysed microarray data was generated on the Mouse Genechip 430 2.0 from Affymetrix. Alternatively, the “Ensembl” option was used as a reference list.

### 3.2.6. The verification of dermis microarray data (DMD).

In total, eighteen genes, selected from the dermis microarray data, underwent the verification work. Seventeen genes were analysed on mRNA level by qRT-PCR (see Table 3.2 for details). In addition, antibodies against six genes (section 2.2.5.3 in Chapter 2 and Table 3.3A) tracked their expression profile at the protein level in embryonic back skin samples (the immunofluorescence analysis). In total, five genes (*Cebpa*, *Fabp4*, *Adipoq*, *Trps* and *Egfr*) were analysed on both mRNA and protein levels. The PDGFRa was analysed only on the protein level. Results from the immunofluorescence analysis of C/EBPalpha were presented in Chapter 2. The investigation of EGFR expression was described in Chapter 4. Finally, results from the rest of staining were included in Chapter 3, section 3.3.

Among selected eighteen genes, three (Gremlin 2, trichorhinophalangeal syndrome I - Trps and PDGFRa) were characterised by the over-expression in upper dermis of mouse embryonic back skin. The other fifteen genes had increased expression in lower dermis and majority of these genes were up-regulated during embryonic development of lower dermis (for more details see section 3.3). Genes up-regulated in lower dermis were selected for this analysis because of their known (or suggested) role in adipogenesis *in vitro* (for example C/EBPalpha) or their high up-regulation in fat-related disorders (for example MUPs).

### 3.2.6.1. Relative mRNA expression.

The verification analysis of the microarray lists was carried out on RNA that was either used earlier for the microarray work from e17 and e18 time points or was prepared from another three 19 day old mouse embryos ("additional 19 day samples") from the same litter as the original 19 day old embryos used for the microarray samples. These "additional 19 day samples" had to be prepared as the original samples from e19 time point were used for the microarray work. In addition, one sample from the "additional 19 day samples" was incorporated into the microarray work. This gave three samples for e19 time point which were sufficient quality to perform microarray analysis in triplicates. For the verification work, RNA samples were used before the fragmentation and hybridization steps (section 3.2.3.3.4.3.).

#### 3.2.6.1.1. First-Strand cDNA Synthesis.

Reagents for this step were sourced from Invitrogen. First, the experimental sample was prepared, which contained 1 μl of random primers/Oligo(dT) Mix (2:1), 1 μl of 10 mM dNTP mix, RNA (1 μg) and water (up to 11 μl). The mixture was incubated for 5 minutes at 65$^{o}$C and immediately cooled on ice for at least 1 minute. Next, 7μl of Master Mix was added to each experimental sample. This Master Mix contained 4 μl of 5X First-Strand Buffer, 1 μl of 0.1 M DTT, 1 μl of RNAseOU$^{TM}$ Recombinant Ribonuclease Inhibitor and 1 μl of SuperSctipt $^{TM}$ III per sample. Samples were next incubated for 5 minutes at 25$^{o}$C, 60 minutes in 50$^{o}$C, 15 minutes at 70$^{o}$C and cooled on ice. Then, 1 μl of RNase H was added to each sample, and samples were then incubated 20 minutes at 37$^{o}$C. Samples were stored at -20 $^{o}$C.

### 3.2.6.1.2. The quantitative reverse transcriptase-polymerase chain reaction (qRT-PCR).

The qRT-PCR was performed on a 7300 or 7500 Fast Real-Time System with compatible 7300 or 7500 Fast System software (SDS version 1.4 Applied Biosystems), The “ddCt Relative Quantitation” assay was used for this work.

Each individual PCR reaction contained 1 μl of diluted (1:5 or 1:10) cDNA, 1 μl of primer mix (2.5 μM Forward primer and 2.5 μM Reverse primer), 10 μl of Power SYBR Green PCR Master MIX (Applied Biosystems) and 8 μl of sterile water. For each cDNA used, four identical reactions were prepared for each set of primers. Reactions were performed in 96-well reaction plates (for example: in MicroAmp® Fast Optical 96-Well Reaction Plate with Barcode, 0.1 ml, Applied Biosystems). The general conditions of the qRT-PCR reaction and the primer sequences are shown in Table 3.1 and Table 3.2 respectively.

Table 3.1. The protocol for qRT-PCR reactions used for the verification of microarray data.

| **Steps:** | **Temperature and time of each step:** |
|---|---|
| Step 1 | 95$^{o}$C; 10 minutes |
| Step 2 | 95$^{o}$C; 15 seconds |
| Step 3 | 60$^{o}$C; 1 minute |
| Step 5 | Back to Step 2, then Step 3 (39 times). |
| (Alternative) Step 4 | 60$^{o}$C; 5 minutes |

Table 3.2. The characterisation of primer pairs designed and used for qRT-PCR reaction. The verification work of microarray data.

| Targeted gene (whole name; gene symbol) | Forward primer (FP) and reverse (RP) primer sequences: | Primer length (bp) | Melting temp.** ($^{o}$C) | Product length (bp) |
|---|---|---|---|---|
| Ribosomal protein, large, P0 (*Rplp0*) Housekeeping gene | FP: 5'CACTTACTGAAAAGGTCAAGGC<br>RP: 5'AGACCGAATCCCATATCCTCA | 22<br>21 | 61.6<br>64.4 | 166 |
| CCAAT/enhancer binding protein, alpha (*Cebpa*) | FP: 5'CGGTGCGTCTAAGATGAGG*<br>RP: 5'ATTTTTGCTCCCCCTACTCG* | 19<br>20 | 63.4<br>64.0 | 169 |
| Peroxisome proliferator activated receptor gamma (*Pparg*) | FP: 5'AACAGGCCTCATGAAGAACC*<br>RP: 5'CCGGCAGTTAAGATCACACC*<br>(transcript variants 1 and 2) | 20<br>20 | 63.0<br>64.4 | 174 |
| Glycerol-3-phosphate dehydrogenase 1 (soluble) (*Gpd1*) | FP: 5'GAAGAATATAGTGGCCGTTGG*<br>RP: 5'AGGTCGTGATGAGGTCTGC* | 21<br>19 | 62.2<br>63.1 | 185 |
| Fatty acid binding protein 4, adipocyte (*Fabp4*) | FP: 5'GATGAAATCACCGCAGACG*<br>RP: 5'GCCCTTTCATAAACTCTTGTGG* | 19<br>22 | 64.4<br>63.5 | 182 |
| CD36 antigen (*Cd36*; CD36/FAT ) | FP: 5'GTGCAAAACCCAGATGACG*<br>RP: 5'CAGTGAAGGCTCAAAGATGG*<br>(transcript variants 1, 2, 3, 4 and 5) | 19<br>20 | 64.2<br>62.4 | 171 |
| Adiponectin, C1Q and collagen domain containing (*Adipoq*) | FP: 5'ACTTGTGCAGGTTGGATGG*<br>RP: 5'CCTTCAGCTCCTGTCATTCC* | 19<br>20 | 63.7<br>63.8 | 167 |
| Angiotensinogen (serpin peptidase inhibitor, clade A member 8)(*Agt*) | FP: 5'GCACCCTACTTTTCAACACC*<br>RP: 5'TCACGGAGAAGTTGTTCTGG* | 20<br>20 | 61.0<br>62.9 | 174 |
| Complement factor D (adipsin) (Cfd; *Adn*) | FP: 5'TGAACCCTACAAGCGATGG*<br>RP: 5'GTTCCACTTCTTTGTCCTCG* | 19<br>20 | 63.7<br>61.3 | 167 |
| Resistin (*Retn*) | FP: 5'CTTGTCCCTGAACTGCTGG*<br>RP: 5'AAGACTGCTGTGCCTTCTGG* | 19<br>20 | 63.6<br>64.6 | 182 |
| Carbonic anhydrase 3 (*Car3*) | FP: 5'TCCTGAACAATGGGAAGACC*<br>RP: 5'TCAGCAGCGTATTTTACTCCG* | 20<br>21 | 63.9<br>64.0 | 175 |
| Major Urinary Proteins (*Mups*) *** | FP: 5'GACCTATCCAATGCCAATCG*<br>RP: 5'CAGTGAGACAGGATGGAATGC* | 20<br>21 | 64.1<br>64.7 | 165 |
| Haptoglobin (*Hp*) | FP: 5'GGTCAGCTTTTTGCTGTGG*<br>RP: 5'TGTACACCCCATCTCCTTCG* | 19<br>20 | 63.5<br>64.9 | 160 |
| Retinol binding protein 4, plasma (*Rbp4*) | FP: 5'CCTTTGTGTTTTCTCGTGACC*<br>RP: 5'GATGAAGACCGGATGAAAGC*<br>(transcript variants 1 and 2) | 21<br>20 | 63.4<br>63.5 | 209 |
| G0/G1 switch gene 2 (*G0s2*) | FP: 5'AGTGTCCCTCCCAAAGAGC*<br>RP: 5'CAGCTCCTGCACACTTTCC* | 19<br>19 | 63.3<br>63.7 | 162 |
| Gremlin 2 homolog, cysteine knot superfamily (Xenopus laevis) (*Grem2*) **** | FP: 5'CTCTGTCATCGTAGAGCTCGAAT<br>RP:5'GGAGTCACTCAGGTTCACTGACAT | 23<br>24 | 63.6<br>64.9 | 109 |
| trichorhinophalangeal syndrome I (human) (*Trps*) | FP: 5'TCTCTCTGGCGAAAGAATGC*<br>RP: 5'CCCTCTGCTGTTTGTTGAGC*<br>(TRPS gene and predicted similar to TRPS transcript variants 1, 2, 3 and 4) | 20<br>20 | 64.5<br>64.9 | 193 |
| Epidermal growth factor receptor (*Egfr*) ***** | FP: 5'GAGGACAACATAGATGACGC*<br>RP: 5'CACTACTGAGACAGGTAGGC*<br>(transcript variant 1) | 20<br>20 | 59.7<br>56.5 | 214 |
| Frizzled homolog 4 (Drosophila) (*Fzd4*) ****** | FP: 5'CTCGGCTACAACGTGACC*<br>RP: 5'GCACATAAACCGAACAAAGG* | 18<br>20 | 62.0<br>61.9 | 145 |

| | | | | |
|---|---|---|---|---|
| Kruppel-like factor 10 (*Klf10*) ****** | 5'TCCTGGATTCTCTCCTTCAGC*<br>5'CCTCCTTTCACAGCCTTTCC* | 21<br>20 | 64.7<br>64.9 | 187 |
| estrogen receptor 1 (alpha) (*Esr1*) ****** | 5'CAGCACCTTGAAGTCTCTGG*<br>5'TGTTGTAGAGATGCTCCATGC* | 20<br>21 | 62.7<br>62.9 | 194 |

**In reference to Table 3.2. on the previous page:**

* Primers were specifically designed to Mus Musculus genes (using the primer designing tool available from NCBI website and based on the website: http://www.basic.northwestern.edu/biotools/oligocalc.html).
** Showed Tm values were obtained together with desalted primers synthesised by Sigma-Aldrich.
*** Proteins from MUPs family, for which primers were designed: Mup1, (variant 2), Mup2 (variant 1), Mup LOC100048885, Mup10, Mup11, Mup17.
**** Sequences for gremlin 2 primers were taken from Sudo *et al*; 2004, they were designed within one exon, whereas other primers aimed to span exon-exon junction.
***** Results from qRT-PCR with primers for EGFR gene were presented in Chapter 4.
****** Examples of primers sets which occurred to be not efficient for the qRT-PCR analysis (no signal, very low/weak signal, not clear results, high variations in Ct values between four reactions performed on one cDNA sample, high differences in signal intensity between triplicates), due to poor design or low mRNA levels of genes of interest in analysed samples.

### 3.2.6.1.3. The relative mRNA expression based on the qRT-PCR reaction.

To sum up, the qRT-PCR analysis was performed on back skin samples from 17, 18 and 19 day old mouse embryos. For each time point three animals were analysed (triplicate biological replicates). From each animal cDNA samples from upper dermis (Area "1") and lower dermis (Area "2") were used. For each cDNA sample, four identical reactions were prepared and analysed. After, the reaction (on FAST Real Time Machine), the obtained Ct values were used in order to calculate the relative gene expression. The Delta-Delta-Ct (ddCT) method (reviewed by Yuan *et al*, 2006) was applied for this purpose. The Ct (cycle threshold) is a number of cycles at which the detected fluorescence signal crosses the established (on the 7300/7500 Fast System software) threshold. For a single cDNA sample a signal was obtained from two, three or four reactions, then Ct values were selected (minimum of two and maximum of three Ct values) that were lower or equal to 36 and these were used for further analysis. Other cDNA samples with only one Ct value (one signal from all four reactions) and/or with any Ct values higher than 36, were treated as samples with a very low amount of analysed gene, or undetectable up-regulation of analysed gene and their fold-change was treated as "0". In addition, some Ct values higher than 36-38 could be related to a signal obtained by primer-dimerization, thus it was crucial to take this under consideration and eliminate these Cts from further analysis.

### 3.2.6.2. Immunofluorescence analysis.

The immunofluorescence analysis was performed on back skin samples taken from the same animals as used for both microarray analysis and the verification work. Skin sections were also prepared from mice derived from other mothers than animals used for microarray analysis and verification work.

#### 3.2.6.2.1. Preparation of skin sections and the staining protocol.

Back skin samples and skin sections were prepared according to methods in section 2.2.3.

The unfixed and fixed (see section 3.2.6.2.2) skin sections were first washed two or three times in PBS (each wash 5 minutes) and blocked with 20% serum (Sigma; for more details see Table 3.3A) in PBS for 30 minutes at RT. Sections were then incubated with a diluted primary antibody (overnight at 4$^{o}$C or 1 hour at RT), in 1% serum/PBS. Skin sections were washed three times in PBS as described above and incubated with secondary antibody (AlexaFluor; for more details see Table 3.3B) diluted 1:500 in 1% serum/PBS for one hour at RT. Normally, DAPI (Insight Biotechnology) was added to this secondary antibody solution at a final dilution of 1:5000. Sections were then washed three times in PBS as before, mounted in mowiol (Appendix I) and covered by coverslips. Incubations with antibodies were performed in covered trays. After staining slides were stored at 4$^{o}$C, in the dark.

#### 3.2.6.2.2. Fixation methods using acetone and methanol.

Three different methods were used that involved these fixatives.

**Acetone/Methanol fixation (A/M).**

Skin sections were incubated in 100% acetone (Sigma) for 10 minutes at -20$^{o}$C, then in 100% methanol (Sigma) for 10 minutes in -20$^{o}$C.

**Methanol/Acetone no. 1 (M/A no. 1).**

Skin sections were incubated in 100% methanol (Sigma) for 15 minutes at -20$^{o}$C, then in 100% acetone (Sigma) for 2 minutes in -20$^{o}$C.

**Methanol/Acetone no. 2 (M/A no. 2).**

Skin sections were incubated in 100% methanol (Sigma) for 15 minutes at -20$^{o}$C,
Then in 100% acetone (Sigma) for 5 minutes in -20$^{o}$C.

### 3.2.6.2.3. Primary and secondary antibodies.

A summary of the conditions used for different primary antibodies is shown in Table 3.3A. Secondary antibodies used are shown in table 3.3B.

Table 3.3.A. Summary of primary antibodies and conditions used for the verification of dermis microarray data by immunofluorescence.

| **Primary antibody:** | | **Details of immunofluorescent staining:** | | | | |
|---|---|---|---|---|---|---|
| **Antibody/ Manufacturer** | **Raised in/ P or M*** | **Fixation (Fix.)** | **Blocking** | **Dilution** | **Incub.**** | **Sec. ant.***** |
| FABP4/ R&D Systems | Goat/ P | A/M | 20% donkey serum | 1:50 in 1% donkey serum | overnight at 4$^{o}$C | DantiG (FITC) |
| AdipoQ (Acrp30)/ Santa Cruz Biotechnology | Rabbit/ P | No Fix. | 20% donkey serum | 1:50, 1:100 | overnight at 4$^{o}$C or 1 h at RT | DantiR (FITC) |
| TRPS**** | Rabbit/ P | M/A no. 1 | 20% donkey serum | 1:5000 in 1% donkey serum | overnight at 4$^{o}$C | DantiR (FITC) |
| PDGFRa/ Santa Cruz Biotechnology | Rabbit/ P | M/A no. 2 | 20% donkey serum | 1:200 in 1% donkey serum | overnight at 4$^{o}$C | DantiR (FITC) |
| EGFR*****/ Santa Cruz Biotechnology | Rabbit/ P | No Fix. | 20% donkey or goat serum | 1:50 or 1:100 | overnight at 4$^{o}$C or 1 h at RT | DantiR (FITC) |

* P - polyclonal; M - monoclonal
** Time and temperature of skin sections incubation with primary antibodies
*** Type of secondary antibodies used for staining.
**** A gift from Prof A .Christiano's laboratory (Columbia University; New York; USA)
***** Results from EGFR staining have been presented in Chapter 4
h - hour
RT - room temperature

Table 3.3.B. Summary of secondary antibodies used for the verification work of dermis microarray data by immunofluorescence.

| **Secondary antibody:** | | **Company:** | **Used/tested dilutions:** |
|---|---|---|---|
| DantiG (FITC) | AlexaFluor$^{R}$ 488 donkey anti-goat IgG(H+L) 2ml/ml | Invitrogen/Molecular probes | 1:500 |
| DantiR (FITC) | AlexaFluor$^{R}$ 488 donkey anti-rabbit IgG(H+L) 2ml/ml | Invitrogen/Molecular probes | 1:500 |

## 3.3. Results.

### 3.3.1. Investigation of genes from E17, E18 and E19 microarray lists.

A brief schematic description of steps used for the analysis of the microarray data is presented in Figure 3.5. The three initial microarray lists, obtained using the GeneSpring® GX11.0 software, were termed: “E17”, “E18”, and “E19” corresponding to the gestational age of the samples (e17, e18 and e19 time points respectively). Each list contained genes with 2 fold or greater increase in expression either in upper dermis or in lower dermis of mouse embryonic back skin. Unique Affymetrix IDs (probe set) were associated with both known and unknown genes. Moreover, a single gene could be represented by several IDs.

Using the Venn function in GeneSpring software, genes common for two or three time points (overlapping expression), as well as genes unique for single time points were identified (Figure 3.6). The Venn diagram gave a preliminary view on the differences and similarities between genes expressed in two areas of skin dermis at e17, e18 and e19 time points. IDs that represented genes unique only for one list were spotted in each analysed time point (516 IDs in E17 list, 247 IDs in E18 list and 1416 IDs in E19 list). In addition, genes common for two out of three lists were seen in the Venn diagram and the highest number if IDs (663) common for two list was observed for e18 and e19 time points, whereas the lowest number of common IDs was observed between E17 and E19 lists. Finally, almost 300 IDs were spotted to be common for all three lists.

In addition, hierarchical clustering analysis gave a view on the correlations between expression intensity of genes in upper (Area “1”) and lower (Area “2”) dermis areas at three time points (e17, e18 and e19) (Figure 3.7). Each analysed gene (line on a hierarchical combined tree with the gene name shown on the right) is characterised by a specific expression intensity (presented by a colour from blue – lowest intensity to red – highest intensity) in analysed samples (rows on a hierarchical combined tree: upper area “1” or lower area “2” of dermis at three time points “17”, “18” and “19”). Rows representing genes from area “1” (upper dermis) and area “2” (lower dermis) from E17 list were clustered most closely together (see first two rows in Figure 3.7). Genes from area “1” of E18 list were clustered most closely with area “1” from E19, list (see two middle rows in Figure 3.7). Then area “2” from E18 list shared most similarity with area “2” from E19 list (see last two rows in Figure 3.7).

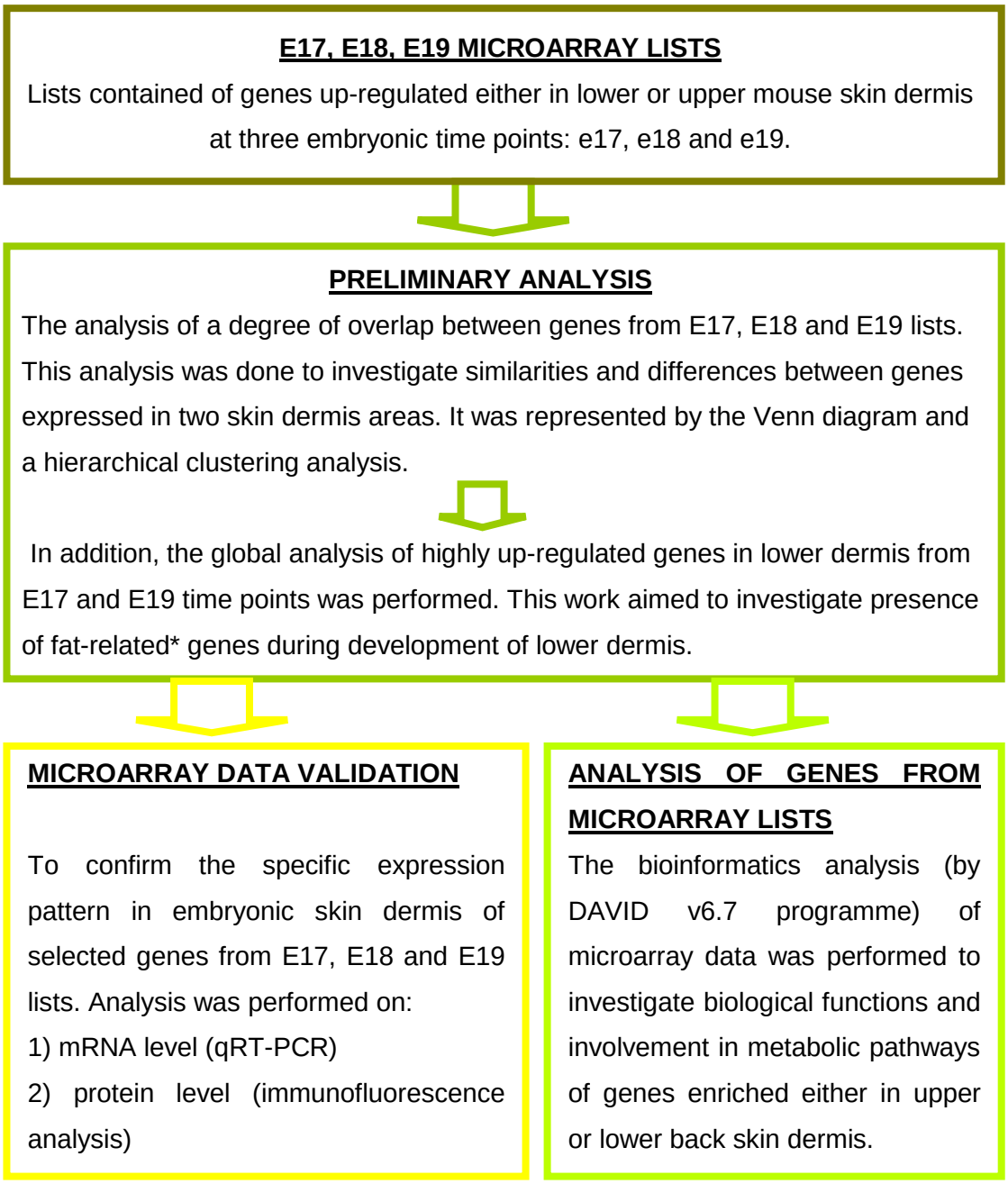


Figure 3.5. A schematic presentation of analysis following E17, E18 and E19 microarray lists generation by GeneSpring® GX11.0 software. *Genes related to adipocytes/adipose tissue/adipogenesis studies, diabetes/obesity/insulin/nutrition-related work, and genes associated with metabolic syndrome/lipid metabolism/lipodystrophy terms.

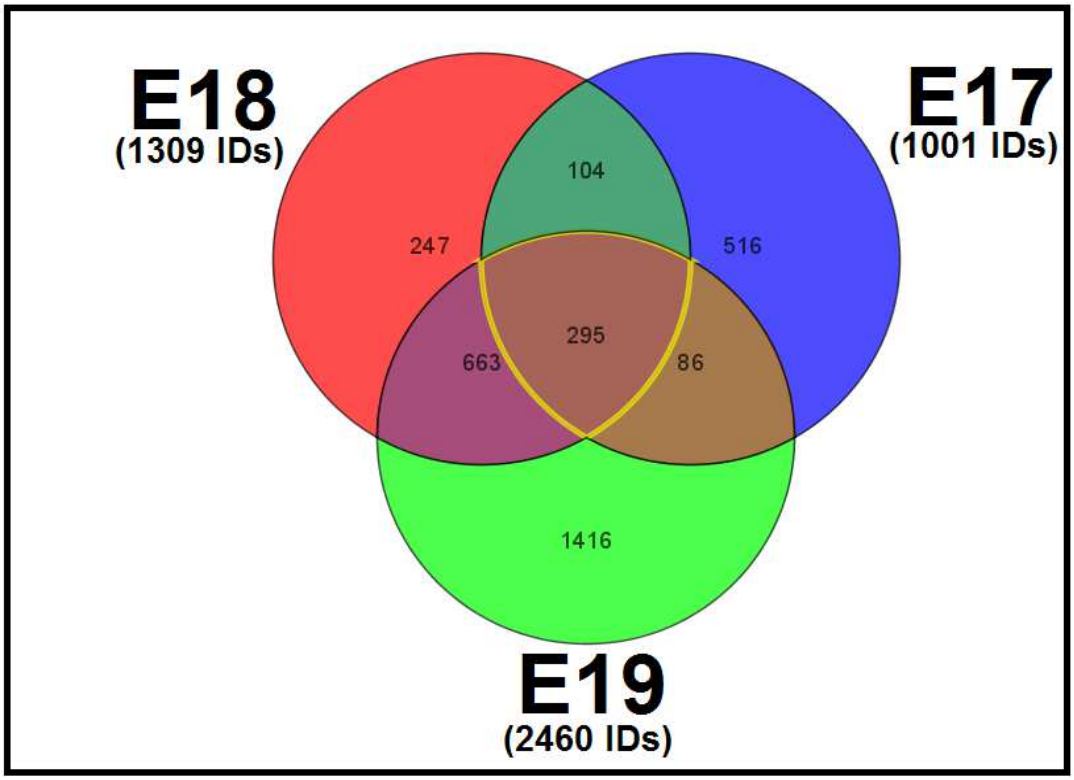


Figure 3.6. Analysis of microarray data generated by using GeneSpring® GX11.0 software. The Venn diagram represents genes (both up-regulated and down-regulated) common to two or three time points or to the individual time points analysed: e17, e18 and e19. The total number of IDs generated for each microarray list is shown in brackets.

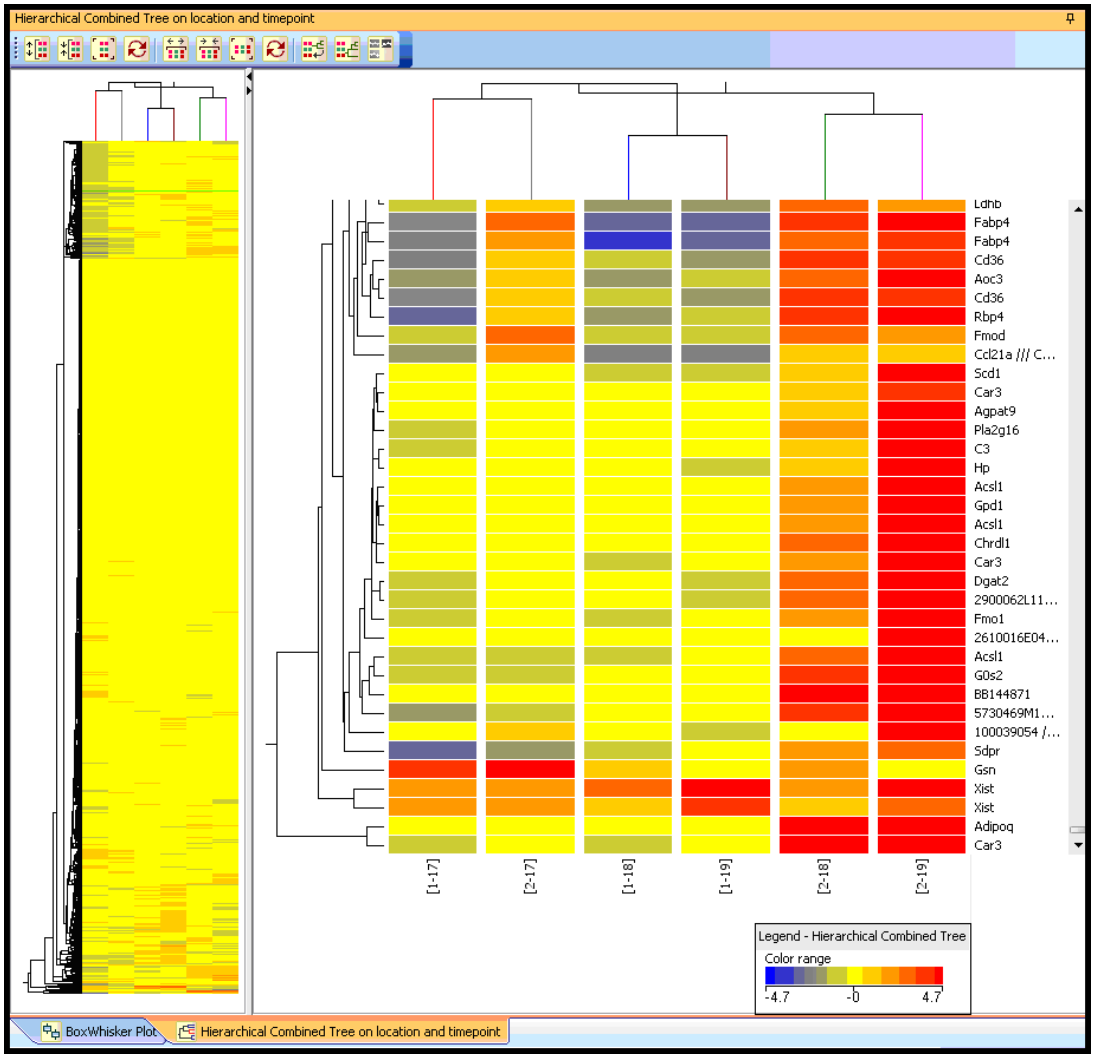


Figure 3.7. Hierarchical combined tree generated by GeneSpring® GX11.0 software. Samples are grouped according to the degree of similarity of their expression profiles over the selected probes. Samples with more similar expression profiles are grouped closer to each other in the tree. Rows represent analysed embryonic skin samples: [1-17] - upper dermis at e17 time point; [2-17] - lower dermis at e17 time point; [1-18] - upper dermis at e18 time point; [2-18] - lower dermis at e18 time point; [1-19] - upper dermis at e19 time point; [2-19] - lower dermis at e19 time point. Each line represents an analysed gene with its name shown on the right. The colour range: blue - the lowest (expression) intensity, red - the highest (expression) intensity.

Lists generated from each time point analysed, were used for the detailed investigation of genes either up-regulated in the upper dermis (control samples; Area “1”) or up-regulated in lower dermis (experimental area; Area “2”) (Figure 3.8A, B and C). Each list contained of IDs representing genes ether up-regulated in upper dermis (Area “1”) or up-regulated in lower dermis (Area “2”) (Figure 3.8D). Interestingly, upper dermis from the e17 time point was characterised by the lowest number of enriched genes in this skin area (90), when compared with number of genes enriched in upper dermis at e18 (557) and e19 (1534) time points. In comparison, the number of IDs for genes up-regulated in the lower dermis at all three time points was quite similar.

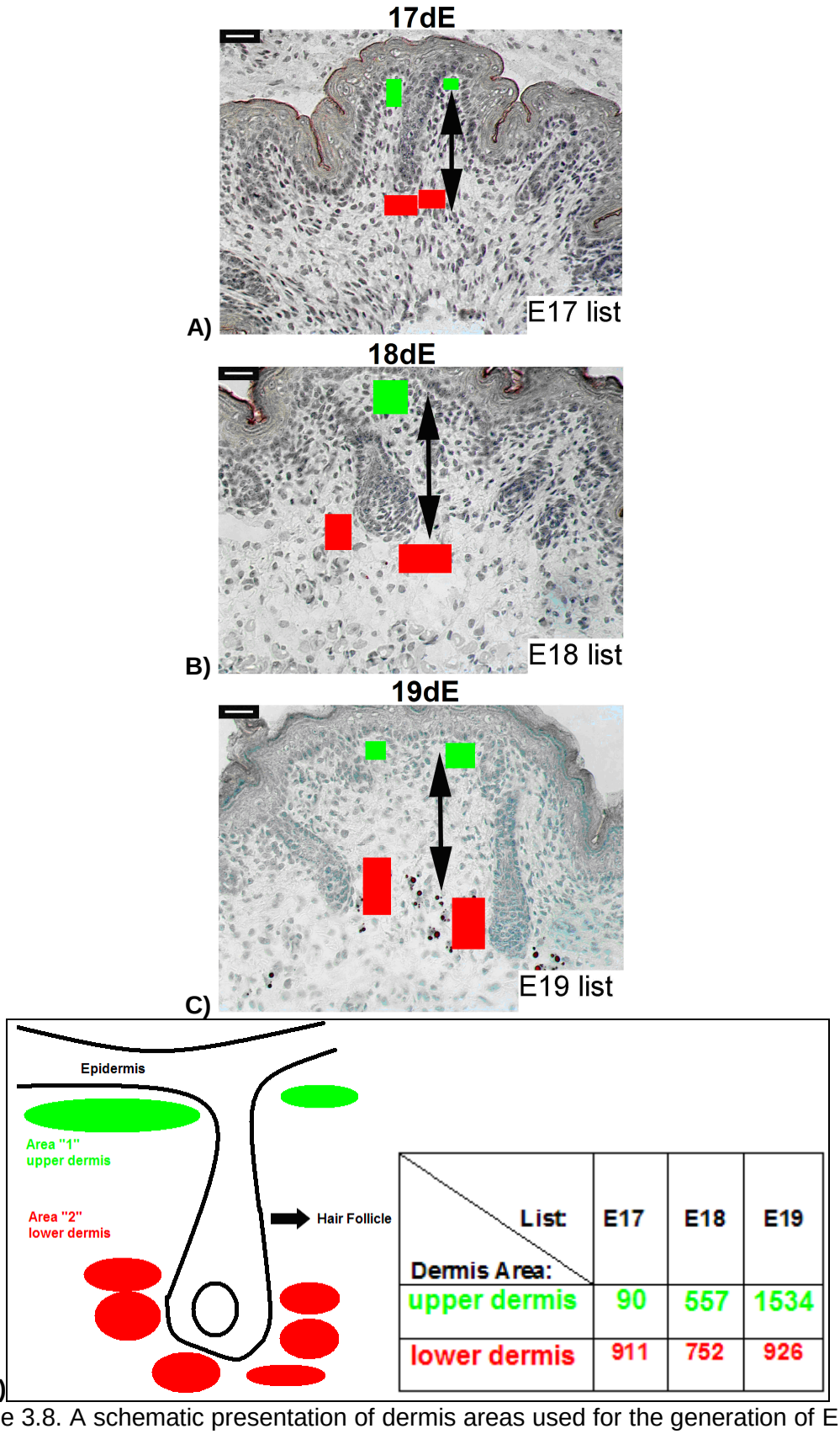


Figure 3.8. A schematic presentation of dermis areas used for the generation of E17, E18 and E19 microarray lists at three time points. (A) e17 time point. (B) e18 time point. (C) e19 time point. (D) Numbers of Affymetrix IDs (from three microarray lists) for genes up-regulated in upper dermis (shown in green) or in lower dermis (shown in red).

**Global changes in fat-related gene expression over time.**

The Oil Red O staining, performed on embryonic back skin sections, allowed the observation of lipid droplets in differentiating fat cells localised in lower skin dermis between e18 and e19 time points (Figure 2.5 in Chapter 2). Therefore, the microarray work performed on embryonic skin dermis from e17, e18 and e19 time points was expected to provide valuable information on adipogenesis *in vivo* at the molecular level.

Two generated microarray lists, E17 and E19, underwent so-called initial global analysis. One aim of this work was to gauge whether, at the stage of the first time point (e17), there were indications from the lower dermis that adipogenesis or a future transition to the adipocyte phenotype had been initiated. Another was to demonstrate that by the final time point (e19), the overall trend towards adipogenesis had increased. None of the features of the bioinformatics packages that were available to me at the time of the analysis had a specific function or classification for very detailed analysis of adipogenesis or fat-related genes. Therefore for the preliminary analysis of the microarray data, from the E17 list and E18 list, the function of the 100 genes with the highest up-regulation in the lower dermis versus the upper dermis was examined by searching databases. All these genes from E17 list were characterised by a fold change equal or higher than 4. Selected genes from E19 list had a fold change equal and higher than 7. These genes were investigated principally through published literature, including using the PUBMED website with such main keywords as: adipocytes or adipogenesis, diabetes and obesity, insulin or metabolic syndrome. Genes, associated with at least one of these terms, were treated as “fat-related genes”, those with functions not encompassed by one of these terms were designated as “other genes” (Figure 3.9) and genes with as yet no discovered function were classified as “unknown” genes.

Among analysed 100 genes from E17 list, 42% of the genes were reported in studies as “fat-related genes”. The majority of genes (57%) were in the “other” category, while a very small number (1%) of genes were “unknown” (Figure 3.9A).

When the same type of analysis was performed on the E19 microarray lists the percentage of fat-related genes had increased to become the majority (60%) with half of this number having other functions (Figure 3.9B). Interestingly, the group of unknown genes had increased to 10% of the total.

To sum up, the increasing tendency was seen with numbers of genes specific for fat-related terms that were up-regulated in lower dermis during mouse embryonic development (from e17 to e19 time points).

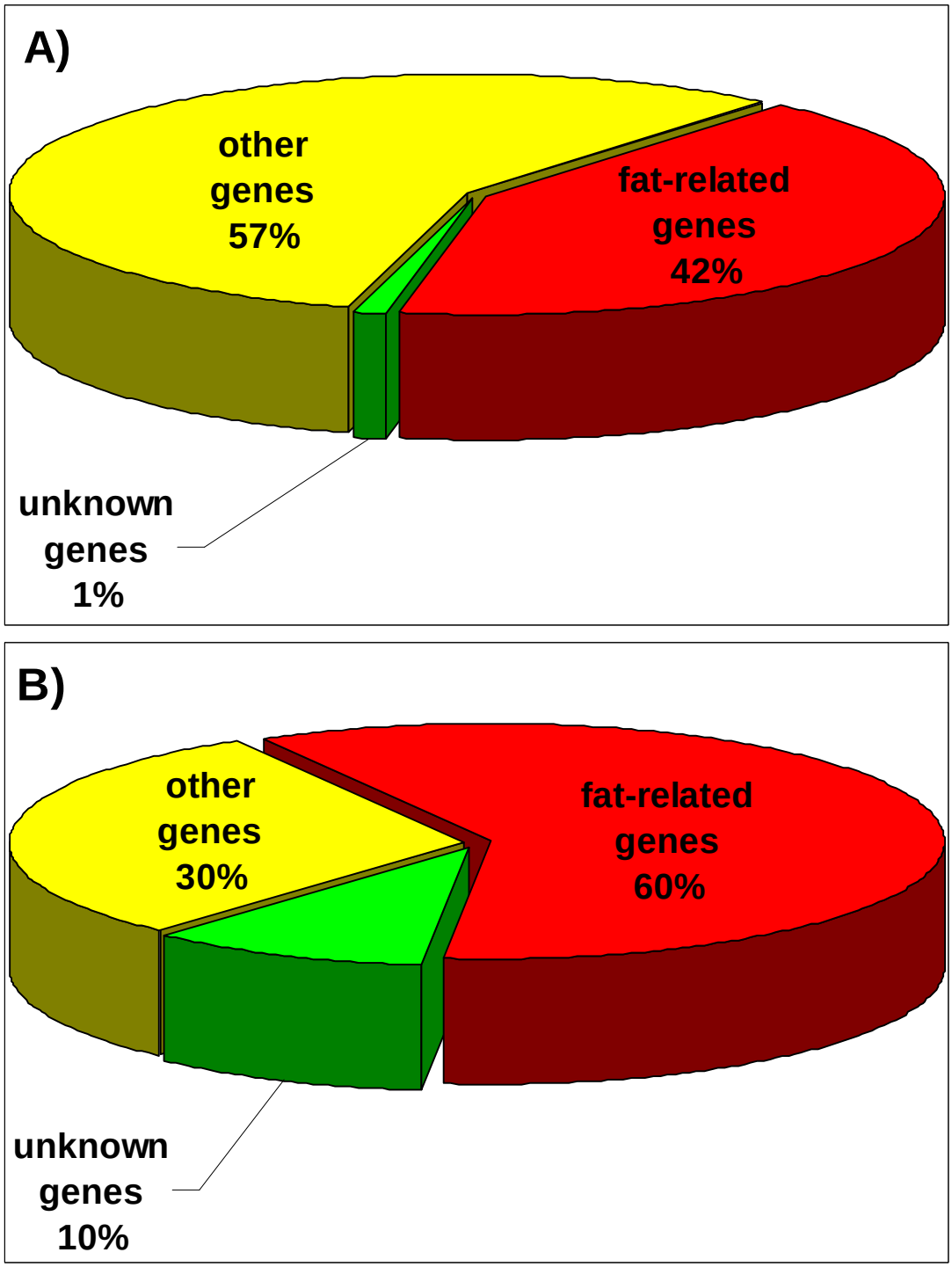


Figure 3.9. Global characterisation of 100 genes from the E17 (A) and E19 (B) microarray lists, displayed as pie charts. Selected genes had the highest fold change among all up-regulated genes in the lower dermis versus upper dermis. Genes presented in adipocytes/adipose tissue/adipogenesis based studies, or in diabetes/obesity/insulin/nutrition-related work or finally, genes associated with metabolic syndrome/lipid metabolism/lipodystrophy, were classified into the group of fat-related genes.

**Changing patterns of gene expression and selection of genes for array validation.**

In addition to the trend showing greater numbers of up-regulated fat-related genes over the three time points, fold change values also increased. Thus in the E18 list, the range of fold change values was bigger overall than at E17 (see Table 3.4 with selected genes from microarray data). At E18 the highest fold change was about 242 for carbonic anhydrase 3 (*Car3*) (Table 3.4). In the E19 list, the *Car3* gene had the second highest fold change value, of 489 (gene up-regulated in lower dermis). Another gene, with a similar expression pattern to *Car3*, was adiponectin (*Adipoq*). Again this gene was not present in the E17 list, but then became up-regulated in the lower dermis at e18 (fold change: 57) and even more strikingly at e19 (fold change: 721) where it topped the list of genes up-regulated in the lower dermis (Table 3.4). Another cohort of genes showed a marked up-regulation in the lower dermis only at day e19. Included in the group were the major urinary proteins, adipsin and resistin (Table 3.4). Yet another pattern of expression was revealed by genes such as retinol binding protein 4 (*Rbp4*) or fatty acid binding protein 4 (*Fabp4*), that showed consistent up-regulated gene expression in the lower dermis at all time points (Table 3.4). Other features of these genes are discussed later in this Chapter, but the initial analysis showed that a) fat-related genes, observed in E17 microarray list, are also present in E18 and E19 lists; b) The number, and relative expression levels of fat-related genes in the lower dermis increases during development from E17 to E19 and c) a number of genes not previously associated with the development of fat are prominent in the gene lists.

All the above mentioned genes were chosen to be verified by qRT-PCR analysis. They were selected to cover the different patterns of developmental expression and their presence in the general category of “fat-related genes”. Major urinary protein-1 had previously been associated with diabetic individuals and not adipocyte differentiation (Hui *et al*, 2009). Others, including fatty acid binding protein 4 and adiponectin were validated by qRT-PCR and at the protein level by immunohistochemistry, since although they have been previously associated with adipocytes in mature fat tissues, their developmental involvement in embryonic rodent skin dermis has not been yet clearly defined (see section 3.4) Other genes chosen for the verification process included three that were up-regulated in upper dermis (Table 3.4).

Table 3.4. Selected genes from microarray lists: E17, E18 and E19 with specific gene expression patterns and fold changes in analysed skin dermis areas.

| **Gene symbol; Whole name; Affymetrix ID:** | **The regulation and fold change of selected genes from three microarray lists. Gene expression profile in lower dermis area ("2") versus upper dermis area ("1") at three time points: e17 e18 e19** | | |
|---|---|---|---|
| | **2 17 vs 1 17** | **2 18 vs 1 18** | **2 19 vs 1 19** |
| ***Fabp4***; fatty acid binding protein 4, adipocyte; 1417023_a_at | + 25.73805 | + 91.76061 | + 170.3202 |
| ***Rbp4***; retinol binding protein 4, plasma; 1426225_at | + 15.71429 | + 75.41824 | + 60.66678 |
| ***G0s2***; G0/G1 switch gene 2; 1448700_at | NP | + 19.24273 | + 72.4153 |
| ***Adipoq***; adiponectin, C1Q and collagen domain containing; 1422651_at | NP | + 57.37421 | + 721.3733 |
| ***Hp***; Haptoglobin; 1448881_at | NP | + 2.511893 | + 79.72434 |
| ***Car3***; carbonic anhydrase 3; 1449434_at | NP | + 241.5143 | + 489.1857 |
| ***Mups***; predicted gene, 100039054 /// RIKEN cDNA 2610016E04 gene /// major urinary protein LOC100048885 /// novel member of the major urinary protein (Mup) gene family /// major urinary protein 1 /// major urinary protein 2 /// predicted gene, OTTMUSG00000007428 /// predicted gene, OTTMUSG00000007431 /// predicted gene, OTTMUSG00000007486 /// predicted gene, OTTMUSG00000008509 /// predicted gene, OTTMUSG00000012492 /// predicted gene, OTTMUSG00000012493 /// predicted gene, OTTMUSG00000015595; 1420465_s_at | NP | NP | + 421.3903 |
| ***Cfd***; complement factor D (adipsin; ***Adn***); 1417867_at | NP | NP | + 12.97235 |
| ***Retn***; resistin; 1449182_at | NP | NP | + 7.096386 |
| ***Trps***; trichorhinophalangeal syndrome I (human); 1457445_at | - 5.823731 | - 13.77049 | - 53.56554 |
| ***Grem2***; gremlin 2 homolog, cysteine knot superfamily (Xenopus laevis); 1418492_at | NP | - 18.70761 | - 44.30882 |
| ***Pdgfra***; platelet-derived growth factor receptor, alpha polypeptide; 1438946_at | NP | NP | - 4.353716 |

"+": gene was up-regulated in lower dermis (versus upper dermis)

"-": gene was down-regulated in lower dermis (versus upper dermis)

"NP: gene was not present in the microarray list with a fold change cut off 2

### 3.3.2. Microarray data validation.

#### 3.3.2.1. Highly up-regulated genes in lower dermis of mouse embryonic back skin.

In order to verify microarray data, several genes were selected from microarray lists that were characterised by high up-regulation in lower dermis (versus upper dermis) in one, two or three analysed time points (Table 3.4).

Retinol binding protein 4 (*Rbp4*), associated with diabetes and fatty acid binding protein 4 (*Fabp4*) observed in adipose tissue (Janke *et al*, 2006; Samulin *et al*, 2008) stood out in the microarray lists because at all analysed time points they were up-regulated in the lower dermis (Table 3.4). When their expression profiles were verified by qRT-PCR reaction (Figure 3.10A and B) this pattern of expression was confirmed, showing an increase in the lower dermis from e17 to e19 time points, whereas their expression in the upper dermis remained at relatively low levels. The highest expression of both genes was seen in lower dermis of e19 time point sample (called “19 2”) and the expression levels of lower dermis samples (called “17 1”, “18 1” and “19 1”) were significantly low when compared with “19 2” samples, based on the t-test results (Figure 3.10A and B).

When antibodies against fatty acid binding protein 4 (FABP4) were used to investigate distribution of the protein in back skin, immunofluorescence analysis confirmed its localisation as being in the lower skin dermis, at all time points (Figure 3.11). Labelling was visible in the lower dermis at e17 time point (Figure 3.11a), all be it with a somewhat patchy distribution, with regions of stronger expression alongside areas where staining was clearly weaker. Overall, staining became more widespread and increased in intensity at e18 and e19 time points (Figure 3.11b, c) but labelling was still predominantly restricted to the lower inter-follicular dermis. Magnification of the photo from 19 day old skin section revealed cytoplasmic localisation of FABP4 in the cells of the lower dermis (Figure 3.11d). There was little or no labelling of the hair follicles or inter-follicular epidermis apart from a line of immunofluorescence in the outermost layer, that was apparently non-specific as it was also apparent in otherwise blank negative control sections (Figure 3.12).

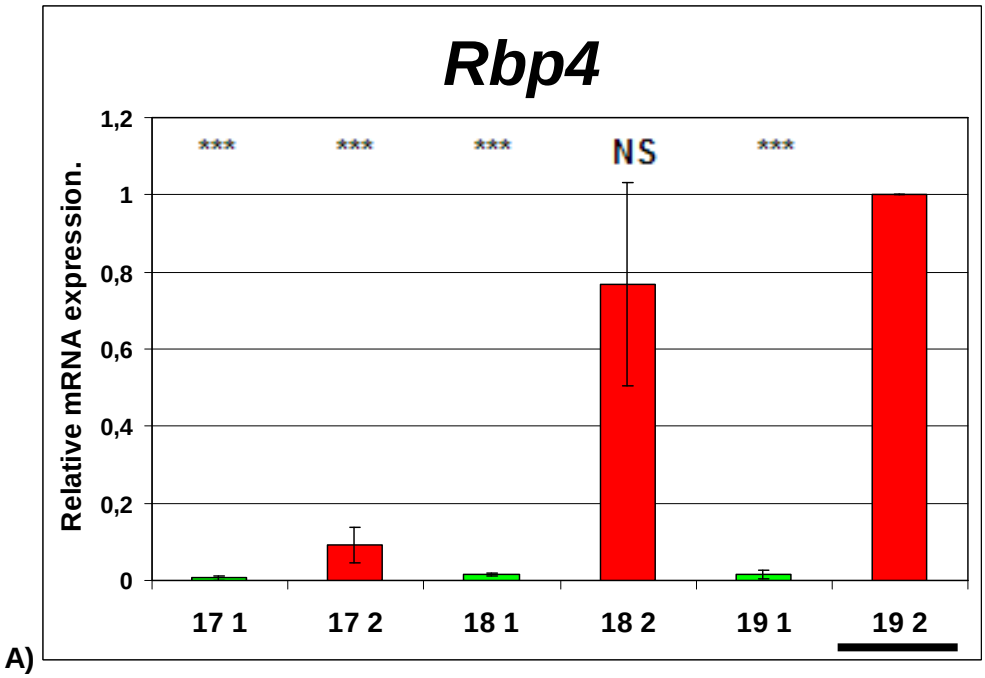


A)

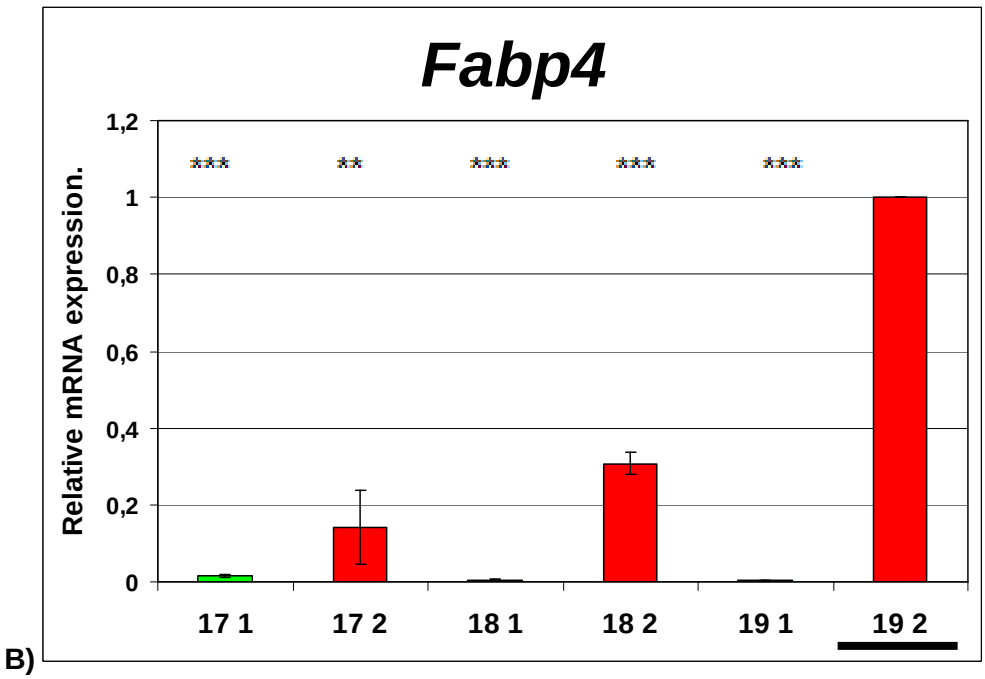


B)

Figure 3.10. Verification of microarray data by qRT-PCR for two genes: *Rbp4* and *Fabp4*. The relative mRNA expression for both genes was analysed on samples from dermis at: e17 (17), e18 (18) and e19 (19) time points, from upper (Area "1", green) and lower (Area "2", red) dermis. Data were obtained from triplicate biological replicates. The baseline (1-fold change) was established for the e19 lower dermis sample (underlined on the figure) and the mRNA levels of the other samples are shown relative to this. Both genes are up-regulated in lower dermis (Area "2") when compared with upper area (Area "1") in all analysed time points. This observation is in agreement with *in vivo* microarray data generated from dermal cells (Table 3.4). The mRNA level of *Rbp4* increases in lower dermis from e17 to e18 time point and then remains at a constant level in lower dermis between e18 and e19 time points (Figure 3.10A - red columns). *Fabp4* expression gradually increased in lower dermis from e17 to e19 time point (Figure 3.10B - red columns). P value refers to the comparison with "19 2" sample (* P <0.05, ** P <0.01, *** P <0.001). The "NS" indicates not significant differences in the mRNA gene expression.

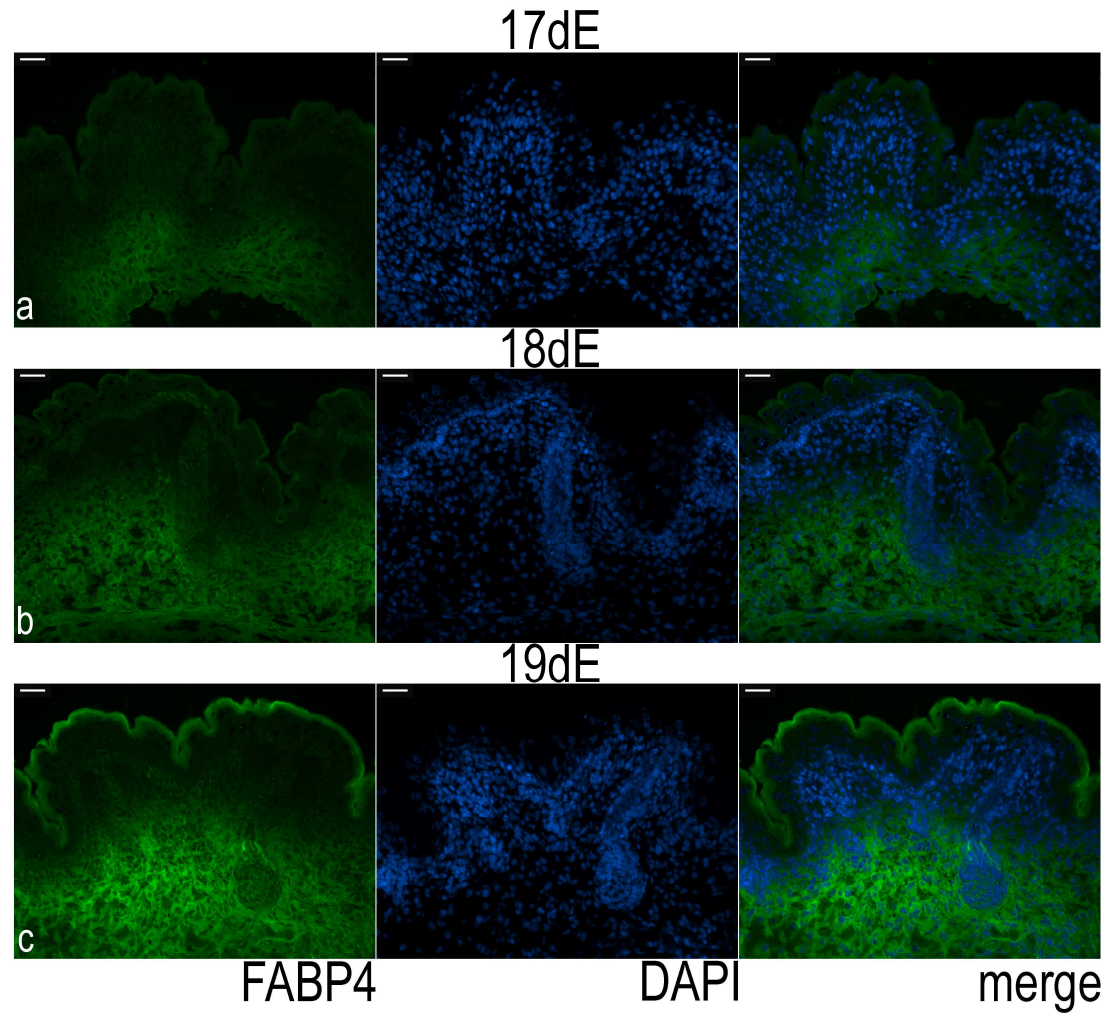


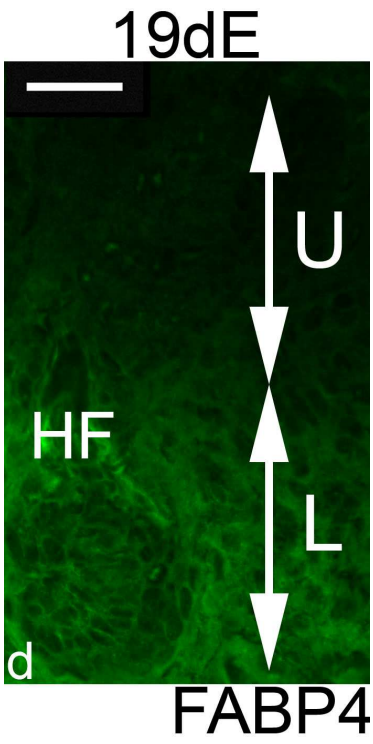


Figure 3.11. Localisation of fatty acid binding protein 4 (FABP4) in mouse embryonic skin. Back skin sections (7 μm) were prepared from embryos at e17 (17dE), e18 (18dE) and e19 (19dE) time points and probed with antibody against FABP4. Expression of the protein is evident in lower part of dermis and in inter-follicular dermal cells. Scale bar = 30 μm. U - upper dermis, L - lower dermis, HF - hair follicle. DNA was counterstained with DAPI. Fluorescent images were visualised using a Zeiss Axio Imager M1. microscope.

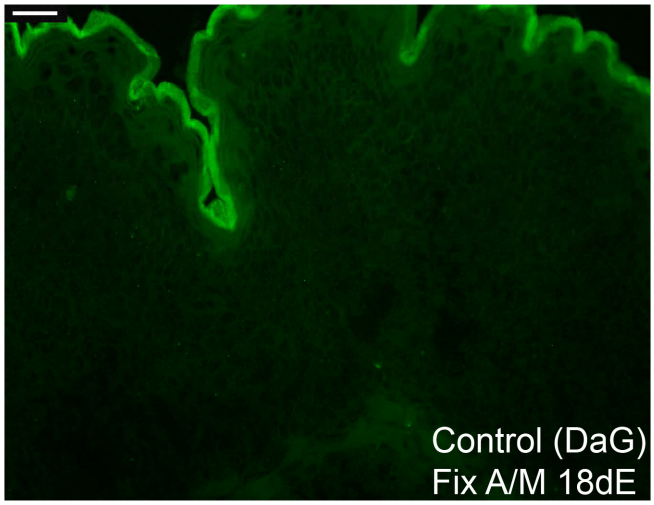


Figure 3.12. Control staining performed together with the investigation of FABP4 expression in mouse embryonic back skin samples. Control staining for secondary antibody (DaG - donkey anti-goat), where primary antibody (for experimental samples) was replaced with 1% donkey serum. Control skin sections underwent the same fixation method as experimental samples: the Acetone/Methanol fixation (A/M). Scale bar = 30 μm. Fluorescent images were visualised using a Zeiss Axio Imager M1. microscope.

Verification by qRT-PCR was performed for the G0/G1 switch gene (*G0s2*) that is suggested to interact with adipogenic transcriptional factor PPARgamma and regulates lipolysis (Zandbergen *et al*, 2005; Yang *et al*, 2010b). The results showed clear up-regulation of this gene in the lower dermis versus upper dermis in 18 and 19 day old mouse embryos (Figure 3.13A), a finding consistent with the pattern seen in the microarray data (Table 3.4). Interestingly, the qRT-PCR analysis showed that this gene was present in upper dermis in all analysed time points, and its levels at e17 and e18 time points (samples “17 1” and “18 1”) were at a significantly low level when compared with lower dermis sample from e19 time point (sample “19 2”; see Figure 3.13A).

Among other genes which up-regulation in lower dermis was observed at e18 and was continued at e19 time point was adiponectin (*Adipoq*; Table 3.4), known to be involved in the regulation of adipogenesis process (Fu *et al*, 2005). Its mRNA level was verified by qRT-PCR which confirmed the specific expression pattern in lower skin dermis (Figure 3.13B). The expression of *Adipoq* was significantly enriched (based on the t-test analysis) in lower dermis from 19 day old skin dermis (sample “19 2”) when compared with upper dermis sample at the same time point (“19 1”) and with samples from both dermis areas at e17 and e18 time points (“17 1”, “17 2”, 18 1” and “18 2”, see Figure 3.13B).

In addition, expression of adiponectin was analysed at the protein level by immunofluorescence which revealed presence of this protein in back skin sections from all analysed time points (Figure 3.14a - d). The positive staining could be spotted in cells from lower dermis area, localised between hair follicle end bulbs (Figure 3.14d - see white arrow). However, the antibody against AdipoQ stained also the upper dermis area, along the epidermis-dermis border as well as dermal cells localised very close to hair follicles (Figure 3.14a - d). It could also be suggested that the antibodies against AdipoQ stained the very outer areas of hairs (dermal sheath). When compared to the negative control the staining with adiponectin can be seen to be specific in embryonic back skin (compare Figure 3.14 with Figure 3.15).

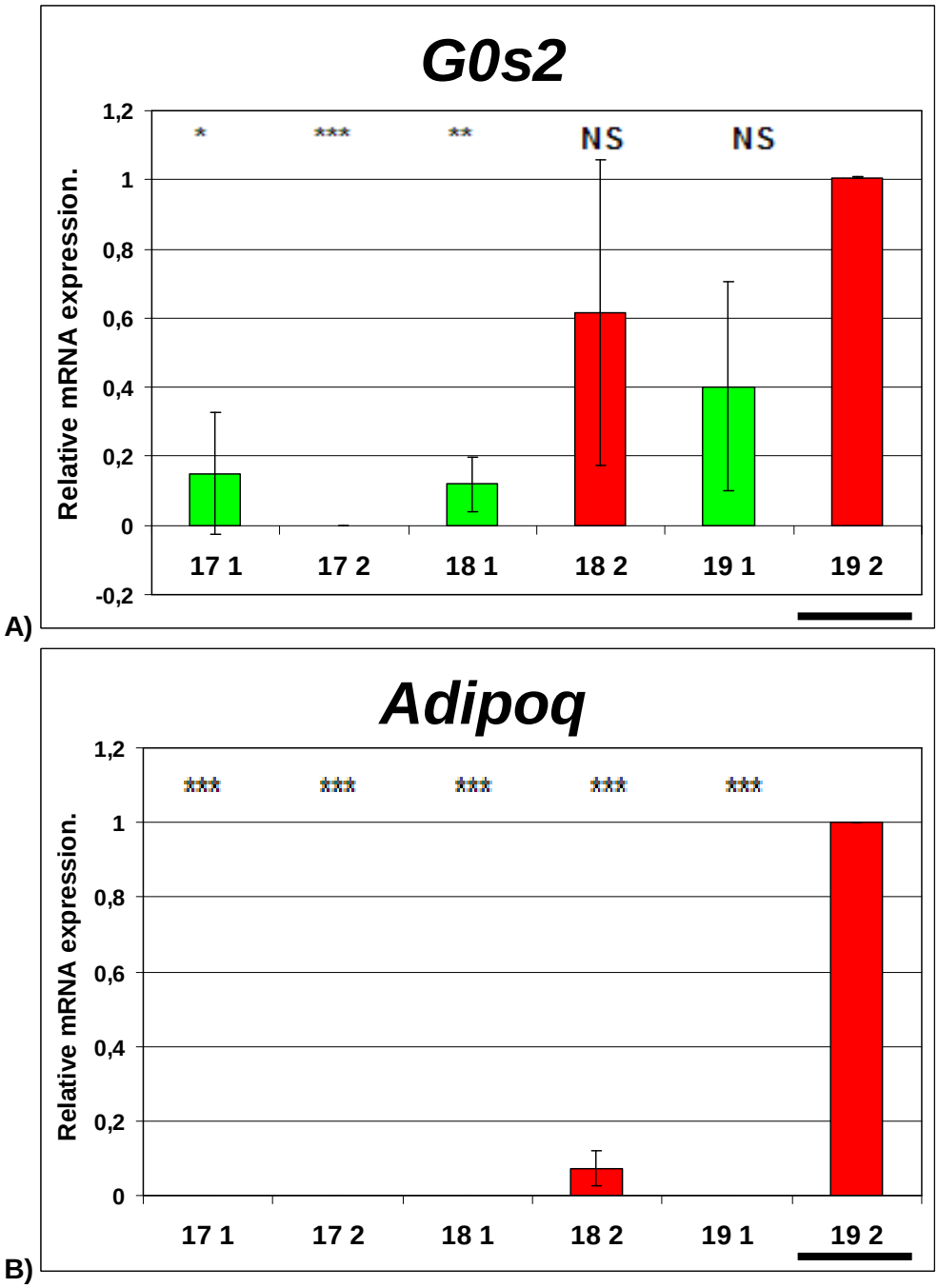


Figure 3.13. Verification of microarray data by qRT-PCR for two genes: *G0s2* and *Adipoq*. The relative mRNA expression for both genes was analysed on samples from dermis at: e17 (17), e18 (18) and e19 (19) time points, from upper (Area "1", green) and lower (Area "2", red) dermis. Data were obtained from triplicate biological replicates. The baseline (1-fold change) was established for the e19 lower dermis samples (underlined on the figure) and the mRNA levels of the other samples are shown relative to this. Both genes are up-regulated in lower dermis (Area "2"), compared with upper area (Area "1") in e18 and e19 time points. This observation is in agreement with *in vivo* microarray data generated from dermal cells (Table 3.4). *G0s2* gene is detected in both lower and upper dermis (Figure 3.13A - green and red columns), whereas *Adipoq* is observed only in lower dermis (Figure 3.13B - red columns). P value refers to the comparison with "19 2" sample (* P <0.05, ** P <0.01, *** P <0.001). The "NS" indicates no significant differences in the mRNA gene expression.

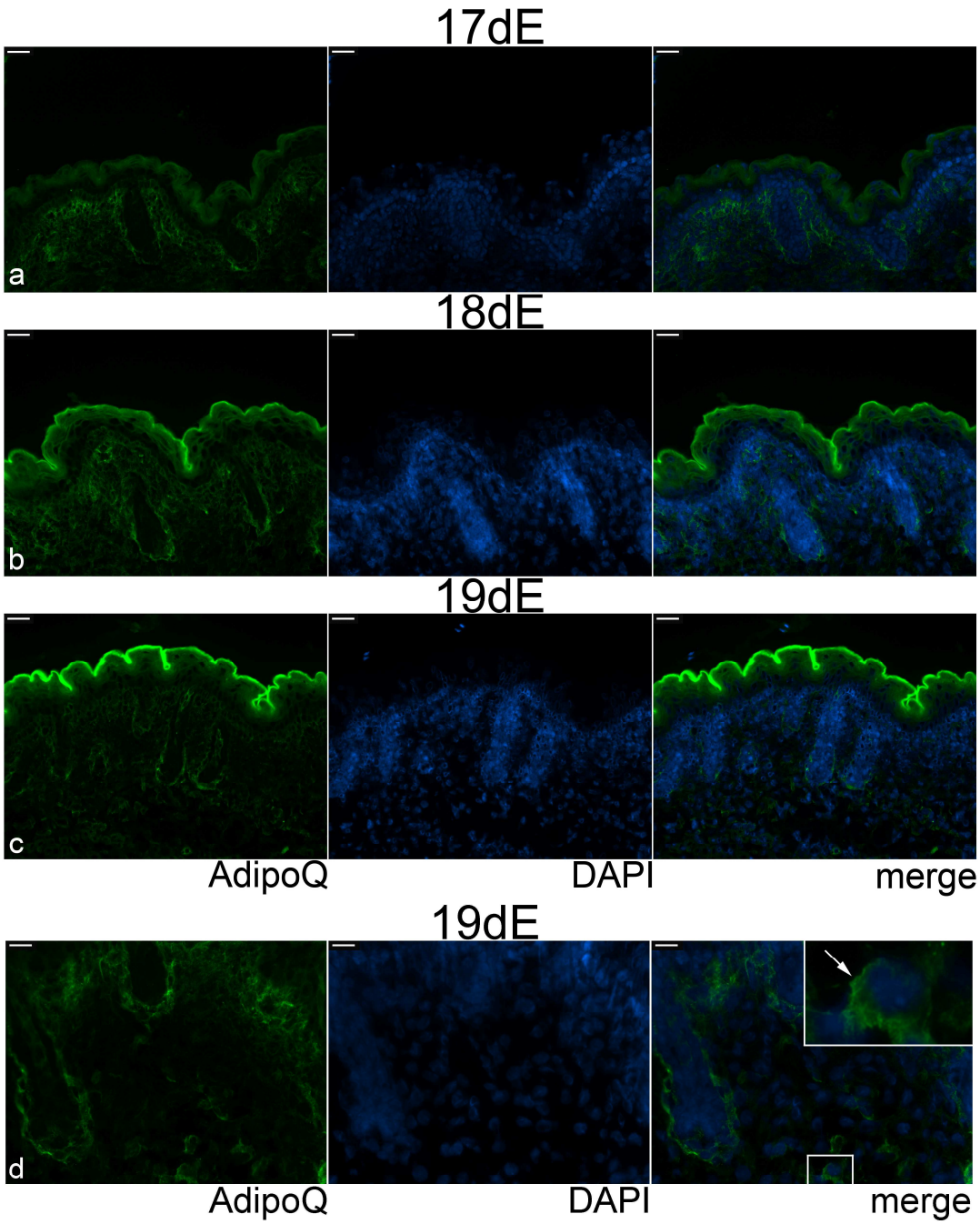


Figure 3.14. Localisation of Adiponectin (AdipoQ) in mouse embryonic skin. Back skin sections (7 μm) were prepared from embryos at e17 (17dE), e18 (18dE) and e19 (19dE) time points and probed with an antibody against AdipoQ. Strong staining is observed in areas adjacent to hair follicle end bulbs and in dermal sheath. Cells close to the epidermis layer are also stained. Weak expression of AdipoQ can be seen in cells from the lower dermis (d - see white arrow). (a, b, c) Scale bar = 30 μm. (d) Scale bar = 15 μm. HF - hair follicle. DNA was counterstained with DAPI. Fluorescent images were visualised using a Zeiss Axio Imager M1. microscope.

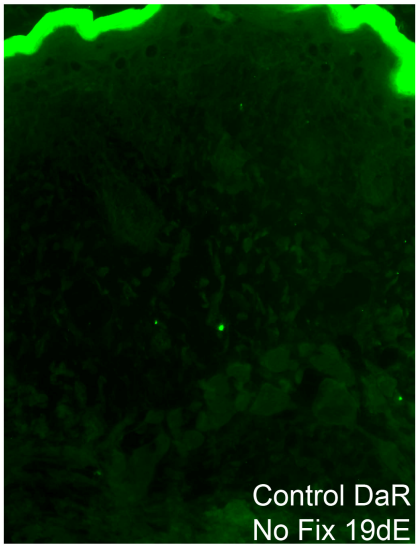


Figure 3.15. Control staining performed together with the investigation of AdipoQ expression in mouse embryonic back skin samples. Control staining for secondary antibody (DaR – donkey anti-rabbit), where primary antibody (for experimental samples) was replaced with 1% donkey serum. No fixation was used. Fluorescent images were visualised using a Zeiss Axio Imager M1. microscope.

Examples of other genes, highly up-regulated in the lower dermis from the array data, were haptoglobin (*Hp*), carbonic anhydrase 3 (*Car3*) or major urinary proteins family (*Mups*) (Table 3.4). These genes have been investigated in obese and diabetic individuals (Lynch *et al*, 1993a; Chiellini *et al*, 2002; Hui *et al*, 2009). Expression of carbonic anhydrase 3 was also detected in differentiated 3T3 adipocytes (Lynch *et al*, 1993b). The qRT-PCR analysis confirmed dramatic up-regulation of these genes in lower dermis cells from 19 day old mouse embryo (Figure 3.16A - C). In addition, low mRNA signal for *Hp* and *Car3* genes was spotted in 18 day old skin, in lower dermis (Figure 3.16A and B). Based on the PCR analysis, over-expression of *Hp* gene in lower dermis occurred as the earliest one (very weak signal detected from sample "17 2"), and the up-regulation of *Car3* took place approximately 24 hours later (compare Figure 3.16A and B). The dramatic over-expression of *Hp*, *Car3* and *Mups* took place in e19 time point sample from lower dermis (Area "2"). No expression of all three genes on mRNA level was seen in upper dermis at any of analysed time points (compare Figure 3.16A with 3.16B and with 3.16C). The t-test analysis showed highly significant up-regulation of these three genes in lower dermis from 19 day old embryonic skin (sample "19 2"), when compared with other analysed samples ("17 1", "17 2", "18 1", "18 2" and "19 1", see Figure 3.16A - C).

Based on the microarray data (Table 3.4), among genes up-regulated in lower dermis from the oldest skin sample (e19 time point), were adipsin (*Adn*) and resistin (*Retn*), known to be produced and secreted by mature fat cells and analysed in obesity related studies (Lu *et al*, 2006). This up-regulation was also confirmed by the qRT-PCR analysis, where mRNA signal was detected in lower dermis of 19 day old skin (Figure 3.17A and B). Therefore, this expression was significantly enriched in lower dermis when compared in upper dermis, based on the t-test analysis at analysed e19 time point

To sum up, the qRT-PCR work allowed to confirm expression patterns for several selected genes from generated microarray data and clearly show either their gradual (for example for *Fabp4*) or very dramatic (for example *Hp*) up-regulation in lower dermis versus upper dermis at all analysed time points.

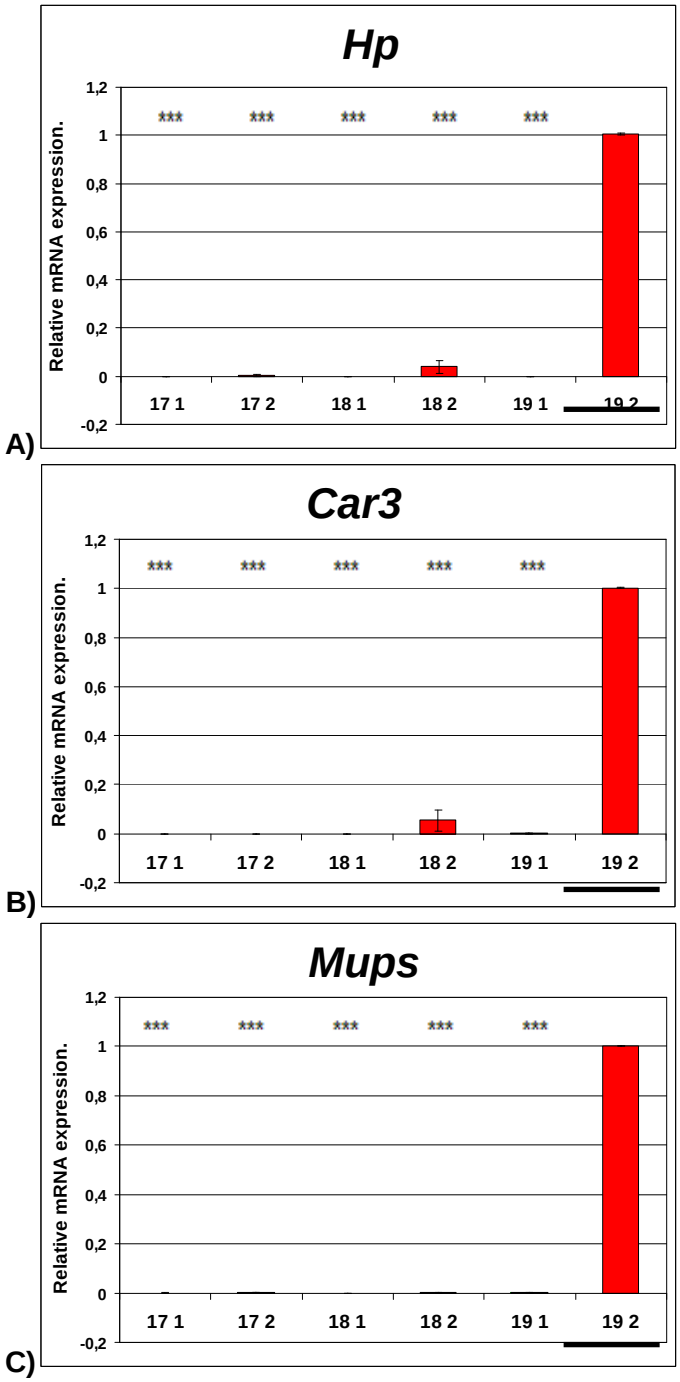


Figure 3.16. Verification of microarray data by qRT-PCR for three genes: *Hp*, *Car3* and *Mups*. The relative mRNA expression for genes was analysed on samples from dermis at: e17 (17), e18 (18) and e19 (19) time points, from upper (Area "1", green) and lower (Area "2", red) dermis. Data were obtained from triplicate biological replicates. The baseline (1-fold change) was established for the e19 lower dermis sample (underlined on the figure) and the mRNA levels of the other samples are shown relative to this. Expression of analysed genes is significantly up-regulated in lower dermis (Area "2") when compared with upper area (Area "1") for the e19 time point. This observation is in agreement with *in vivo* microarray data generated from dermal cells (Table 3.4). At e18 time point, both *Hp* and *Car3* genes are detectable at low level in lower dermis (Figure 3.16A and Figure 3.16B - red columns). P value refers to the comparison with "19 2" sample (* P <0.05, ** P <0.01, *** P <0.001). The "NS" indicates no significant differences in mRNA gene expression.

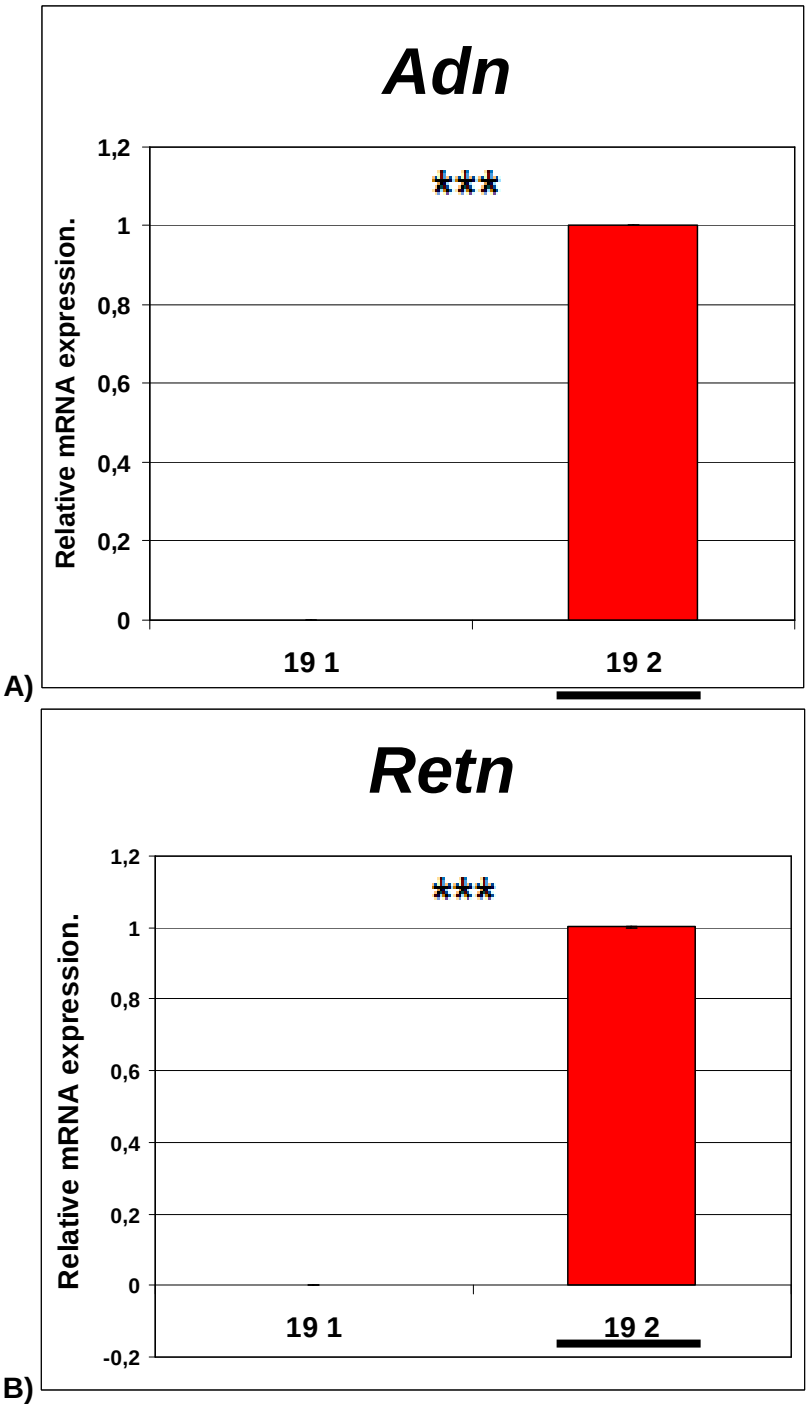


Figure 3.17. Verification of microarray data by qRT-PCR for two genes: *Adn* and *Retn*. The relative mRNA expression for both genes was analysed on samples from dermis at e19 (19) time point, from upper (Area "1") and lower (Area "2", red) dermis. Data were obtained from triplicate biological replicates. The baseline (1-fold change) was established from the e19 lower dermis sample (underlined on the figure) and the mRNA levels of the other samples (19 1) are shown relative to this. Based on *in vivo* microarray data, the up-regulation of adipsin and resistin in lower dermis (versus upper dermis) could be detected at e19 time point (Table 3.4). Therefore qRT-PCR reaction was only performed for this time point confirming the expression profile of these genes in 19 day old embryonic back skin. *Adn* and *Retn* genes were up-regulated in lower dermis (Figure 3.17A and Figure 3.17B - red columns). P value refers to the comparison with "19 2" sample (*** P <0.001).

### 3.3.2.2. Genes down-regulated in lower dermis versus upper dermis (higher expression in Area "1" of mouse skin dermis).

As well as genes up-regulated in lower dermis, the microarray work allowed to investigate genes specifically expressed in the upper dermis. Three genes, observed to be up-regulated in upper dermis, were chosen for the verification work, such as gremlin 2 (*Grem2*), trichorhinophalangeal syndrome I (*Trps*) and platelet-derived growth factor receptor alpha (*Pdgfra*) (Table 3.4).

The up-regulation of *Grem2* gene in upper dermis (Area "1") was observed in microarray lists generated from the analysis of 18 and 19 day old back skin samples and this expression pathway was confirmed by the PCR work (Figure 3.18). The mRNA of *Grem2* gene was not detected in both areas of e17 time point skin (samples "17 1" and "17 2") and in lower dermis from 19 day old skin (sample "19 2"). In addition, only one out of two biological samples used for qRT-PCR analysis, showed the presence of *Grem2* gene in lower dermis at e18 time point.

Next, the up-regulation of *Trps* gene in upper dermis was seen when comparing to lower dermis at all analysed time points (Table 3.4), this was seen at both the mRNA and protein level (Figure 3.19 and Figure 3.20). The high expression of *Trps* gene was observed in upper dermis samples at all analysed time points (Figure 3.19 - green columns), whereas levels of this gene were very low in lower dermis areas (Figure 3.19 - red columns). The highest up-regulation of *Trps* gene in sample "19 1" was significantly enriched when compared with expression of this gene in lower dermis samples from e17, e18 and e19 time points (compare sample "19 1" with samples "17 2", "18 2" and "19 2" on Figure 3.19). In addition, the immunofluorescence analysis showed a positive nuclear staining for TRPS in dermal cells close to epidermal layer and in the hair follicles, whereas no signal was detected in lower dermis area, between hair follicle end bulbs (Figure 3.20). This expression pattern was seen in all three analysed time points. The specificity of the primary antibody was also confirmed by the negative control staining (compare Figure 3.20 with Figure 3.21).

Finally, the platelet-derived growth factor receptor alpha expression was up-regulated on the mRNA level (based on microarray data) in upper dermis versus lower dermis at e19 time point (with fold change 4.35; see Table 3.4). When platelet-derived growth factor receptor alpha was analysed on the protein level by immunofluorescence, staining was seen in upper area of skin dermis (Figure 3.22).

In addition, antibody against PDGFRa seemed to stain the hair follicles. The negative control staining was performed in parallel (compare Figure 3.22 with Figure 3.23).

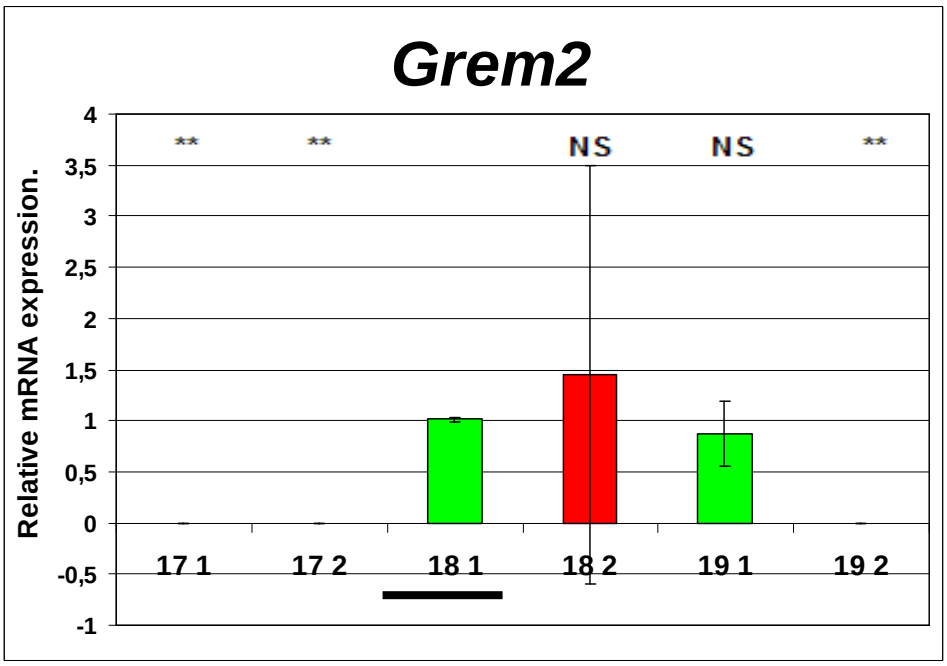


Figure 3.18. Verification of microarray data by qRT-PCR for *Grem2* gene. The relative mRNA expression for gene was analysed on samples from dermis at: e17 (17), e18 (18) and e19 (19) time points, from upper (Area "1", green) and lower (Area "2", red) dermis. Presented data were obtained from duplicate. The third biological sample was omitted because of observed water contamination. The baseline (1-fold change) was established for the e18 upper dermis sample (underlined on the figure) and the mRNA levels of the other samples are shown relative to this. Based on E17, E18 and E19 microarray lists, the up-regulation of *Grem2* gene was observed in upper dermis (Area "1") at e18 and e19 time points (Table 3.4). The qRT-PCR reaction confirmed the presence of this gene in upper dermis of e18 and e19 time points (green columns). Among two "18 2" samples only one gave a signal during qRT-PCR and this situation can explain the high standard deviation for analysed e18 time point from lower dermis (see Figure 3.18 - red column). P value refers to the comparison with "18 1" sample (* P <0.05, ** P <0.01, *** P <0.001). The "NS" indicates no significant differences in the mRNA gene expression.

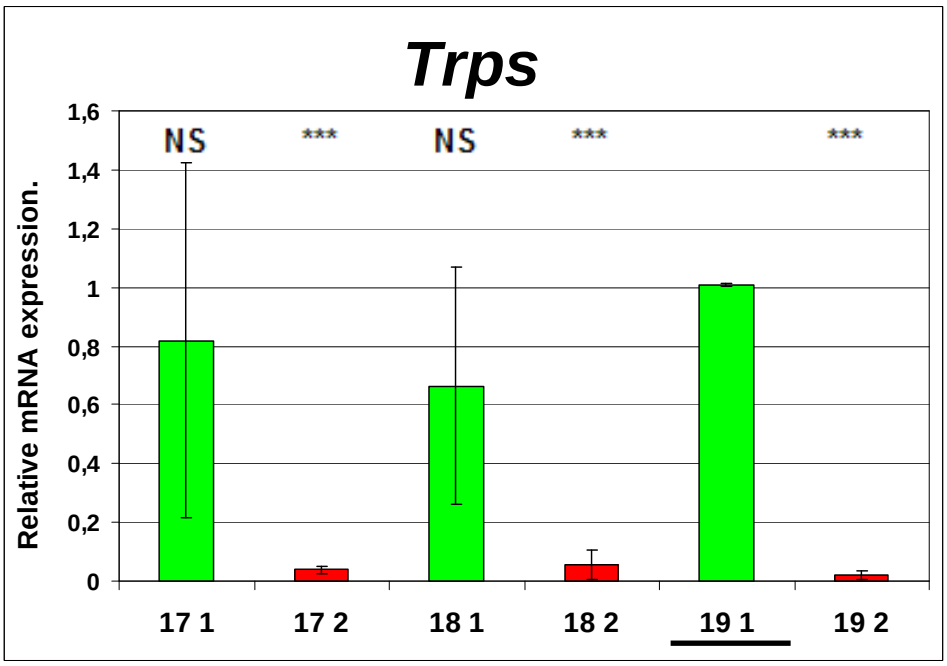


Figure 3.19. Verification of microarray data by qRT-PCR for *Trps* gene. The relative mRNA expression for *Trps* was analysed on samples from dermis at: e17 (17), e18 (18) and e19 (19) time points, from upper (Area "1", green) and lower (Area "2", red) dermis. Data were obtained from triplicate biological replicates. The baseline (1-fold change) was established for the e19 upper dermis sample (underlined on the figure) and the mRNA levels of the other samples are shown relative to this. Expression of *Trps* is significantly up-regulated in upper dermis (Area "1") when compared with lower area (Area "2") for all time points. This observation is in agreement with E17, E18 and E19 microarray lists (Table 3.4). P value refers to a comparison with "19 1" sample (* P <0.05, ** P <0.01, *** P <0.001). The "NS" indicates no significant differences in the mRNA gene expression.

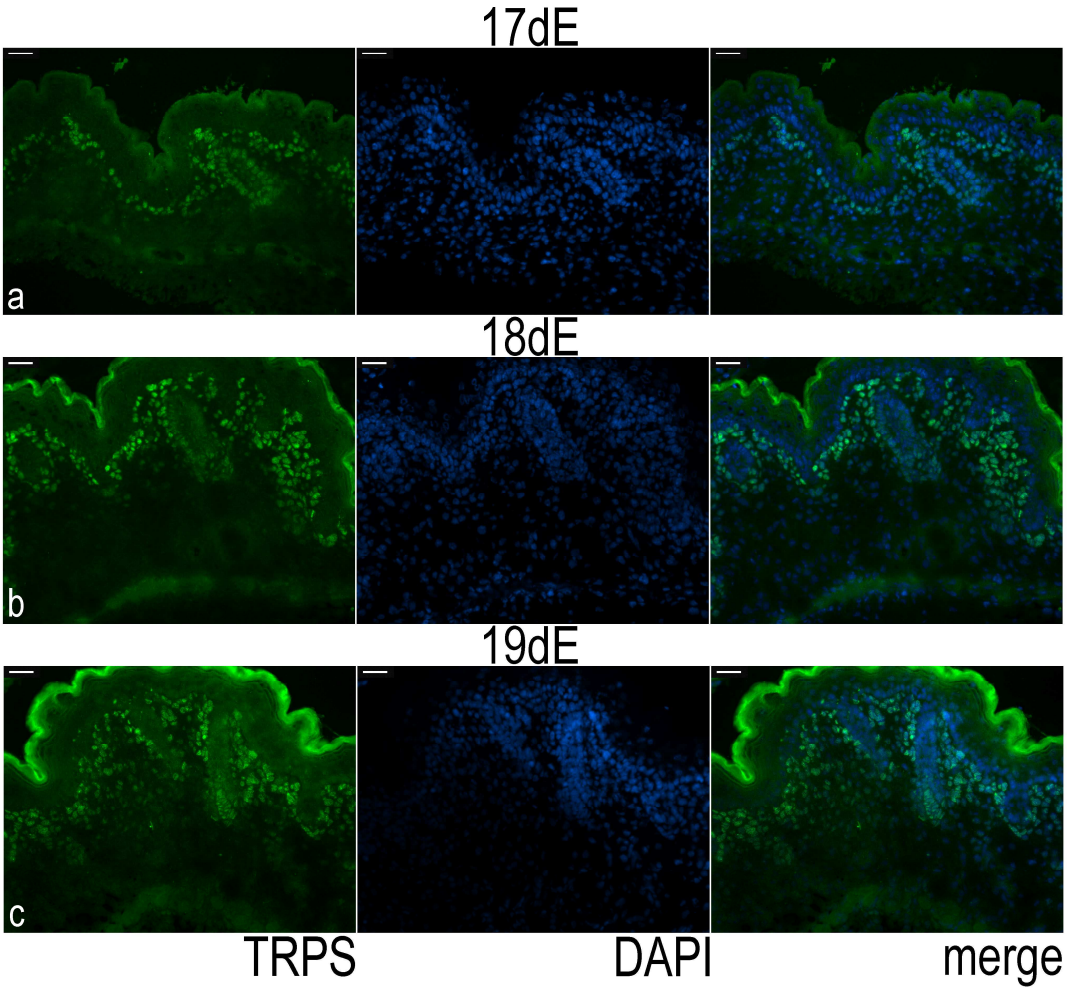


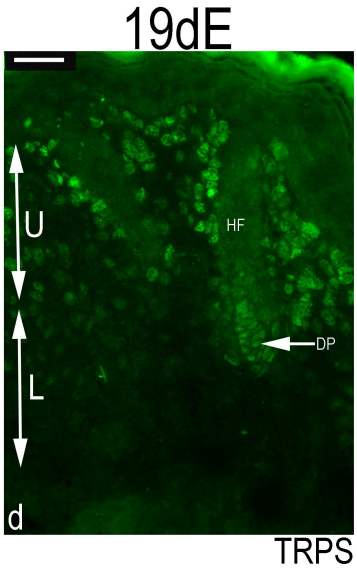


Figure 3.20. Localisation of trichorhinophalangeal syndrome I (TRPS) in mouse embryonic skin. Back skin sections (7 μm) were prepared from embryos at e17 (17dE), e18 (18dE) and e19 (19dE) time points and probed with an antibody against TRPS. The nuclear staining of TRPS is observed at all analysed time points, beneath the epidermis layer, in cells close to the top part of hair follicles (upper dermis) and along hair follicles structures (for example in dermal papilla). Scale bar = 30 μm. U - upper dermis, L - lower dermis, HF - hair follicle, DP - dermal papilla. DNA was counterstained with DAPI. Fluorescent images were visualised using the Zeiss Axio Imager M1. microscope.

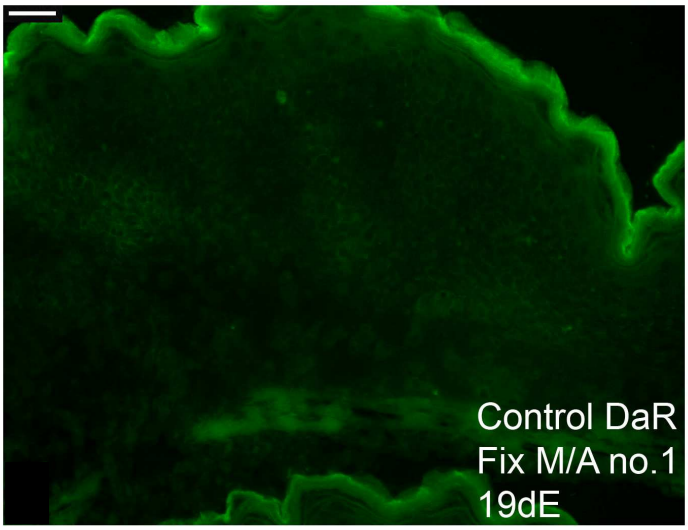


Figure 3.21. Control staining performed together with the investigation of TRPS expression in mouse embryonic back skin samples. Control staining for secondary antibody (DaR – donkey anti-rabbit), where primary antibody (for experimental samples) was replaced with 1% donkey serum. Control skin sections underwent the same fixation method as experimental samples: the Methanol/Acetone (M/A) no.1 method. Scale bar = 30 μm. Fluorescent images were visualised using a Zeiss Axio Imager M1. microscope.

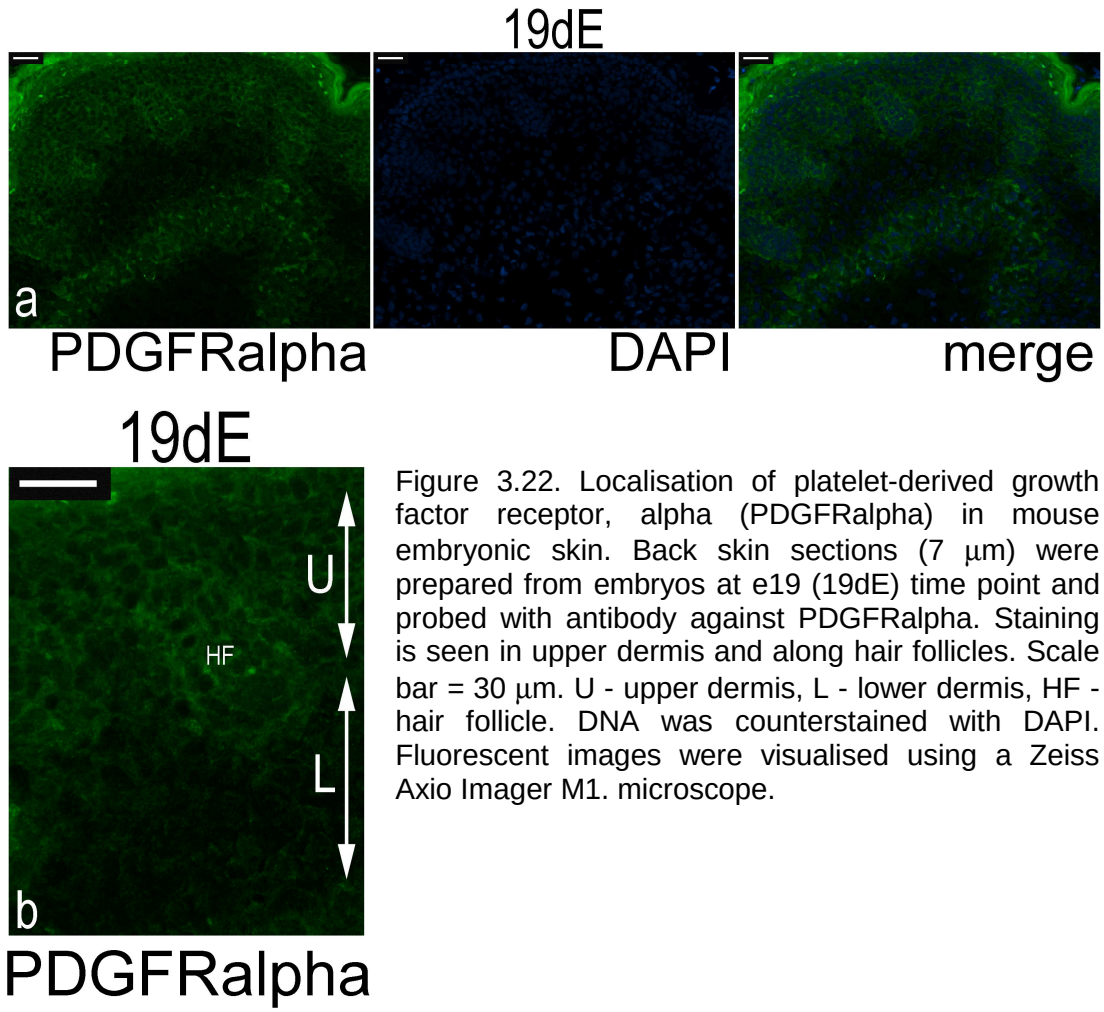


Figure 3.22. Localisation of platelet-derived growth factor receptor, alpha (PDGFRalpha) in mouse embryonic skin. Back skin sections (7 μm) were prepared from embryos at e19 (19dE) time point and probed with antibody against PDGFRalpha. Staining is seen in upper dermis and along hair follicles. Scale bar = 30 μm. U - upper dermis, L - lower dermis, HF - hair follicle. DNA was counterstained with DAPI. Fluorescent images were visualised using a Zeiss Axio Imager M1. microscope.

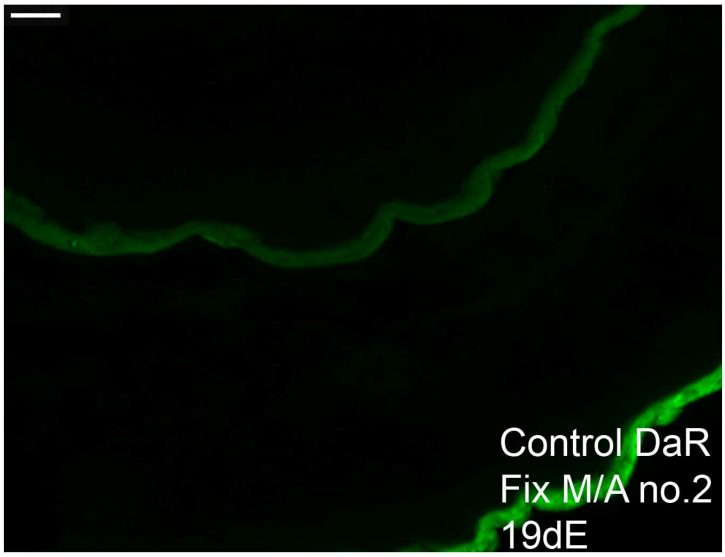


Figure 3.23. Control staining performed together with the investigation of PGDFRalpha expression in mouse embryonic back skin samples. Control staining for secondary antibody (DaR – donkey anti-rabbit), where primary antibody (for experimental samples) was replaced with 1% donkey serum. Control skin sections underwent the same fixation method as experimental samples: the Methanol/Acetone (M/A) no. 2 method. Scale bar = 30 μm. Fluorescent images were visualised using a Zeiss Axio Imager M1. microscope.

### 3.3.3. Analysis of E17, E18 and E19 microarray lists by The Database for Annotation, Visualization and Integrated Discovery - DAVID v6.7 programme.

The verification work carried out on selected genes from three microarray lists (section 3.3.2) confirmed the unique expression profiles of these genes in embryonic skin dermis. It also showed that the generated microarray data can be treated as a reliable and useful source of information about molecular processes taking place during mouse embryonic development in back skin dermis. Moreover, selected genes (such as *Fabp4*, *Adipoq*, *Adn* and *Retn* or *Rbp4*, *Hp*, *Car3* and *Mups*) that were highly up-regulated in lower skin dermis from e17, e18 and e19 time points, have been observed in differentiating adipogenic cell lines and mature fat cells or they have been investigated in obese and diabetes related studies (section 3.3.2).

As the preliminary analysis of E17, E18 and E18 microarray lists (sections 3.3.1 and 3.3.2) showed that cells from lower skin dermis are characterised by a presence of genes specific for fat cells, the next aim was to obtain a broader view on changes taking places in this dermis area of mouse embryonic skin between e17 and e19 time points. In addition, it seemed interesting to perform analysis on all genes up-regulated in upper dermis that could confirm the lack of fat-related genes (or a very low level of these genes) in dermal cells localised below the epidermis layer.

Therefore, genes from E17, E18 and E19 lists underwent further analysis by using the DAVID v6.7 programme. This work permitted features of up-regulated genes in lower or upper dermis of mouse embryos at three time points to be investigated in relation to biological processes (Gene ontology - Biological Process terms: GO_BP terms). The DAVID v6.7 programme also correlated genes with known metabolic pathways (KEGG pathway database).

First, each of three microarray lists (E17, E18 and E19) was divided into two sub-lists: a list comprising only those genes up-regulated in the upper dermis versus lower dermis and a list with genes up-regulated in lower dermis versus upper dermis. In total, six sub-lists were created, named as E17 UPPER, E18 UPPER, E19 UPPER sub-lists and E17 LOWER, E18 LOWER and E19 LOWER sub-lists. These gene sub-lists underwent DAVID analysis. This work allowed association of genes, based on their known functions and suggested involvement in different molecular

pathways, with both Gene Ontology Biological Process (GO_BP) terms and KEGG pathways terms (Table 3.5).

Table 3.5. Number of gene ontology biological terms (GO_BP) and KEGG pathways terms associated with genes from six microarray sub-lists. The analysis was performed by the DAVID v6.7 tool.

| **Sub-lists:** | **Number of terms associated with genes from sub-lists:** | |
|---|---|---|
| | **GO_BP terms** | **KEGG pathways terms** |
| **E17 UPPER** | 106 | - |
| **E18 UPPER** | 208 | 12 |
| **E19 UPPER** | 419 | 25 |
| **E17 LOWER** | 386 | 28* |
| **E18 LOWER** | 347 | 20 |
| **E19 LOWER** | 349 | 32 |

* two groups of genes were created from E17 LOWER sub-list that shared the same KEGG pathway term: “Glycosphingolipid biosynthesis”.

**The analysis of Gene Ontology - Biological Process (GO_BP) terms for dermis genes.**

Genes from all analysed six microarray sub-lists were related with biological terms by the DAVID v6.7 (Table 3.5). The E17 UPPER list was characterised by the lowest number of these terms (106). The E18 UPPER and E19 UPPER list had 208 and 419 terms respectively. All three sub-lists with genes up-regulated in lower dermis were associated with similar number of GO_BP terms namely 386, 347 and 349 (Table 3.5).

The GO_BP terms with the highest percentage of involved genes were “cellular process”, common for five analysed gene lists and “metabolic process” for three lists (Figure 3.24A). There were three GO_BP terms common for all six lists: “cell differentiation”, “developmental process” and “organ development” and the E17 UPPER sub-list had the highest percentage of genes associated with these three terms.

There were several GO_BP terms created only for genes from upper dermis, such as “regulation of gene expression”, “regulation of RNA metabolic process” or “transcription” (Figure 3.24B). In addition, the “Wnt receptor signalling pathway” and “neurogenesis” terms were also associated with genes from upper dermis. The percentage of genes from upper dermis involved in these terms decreased from e17 to e19 time points.

Many GO_BP terms were associated only with genes from the lower dermis (Figure 3.24C). For example, the “response to stimulus” term was associated with a high percentage of lower genes with the trend decreasing from e17 to e19 time points. Among other terms associated with lower dermis were: “lipid metabolic process”, “cellular lipid metabolic process” or “fatty acid metabolic process”, “fat cell differentiation” or “brown fat cell differentiation” and the percentage of genes from lower dermis that were involved in these categories increased from e17 to e19 time points .

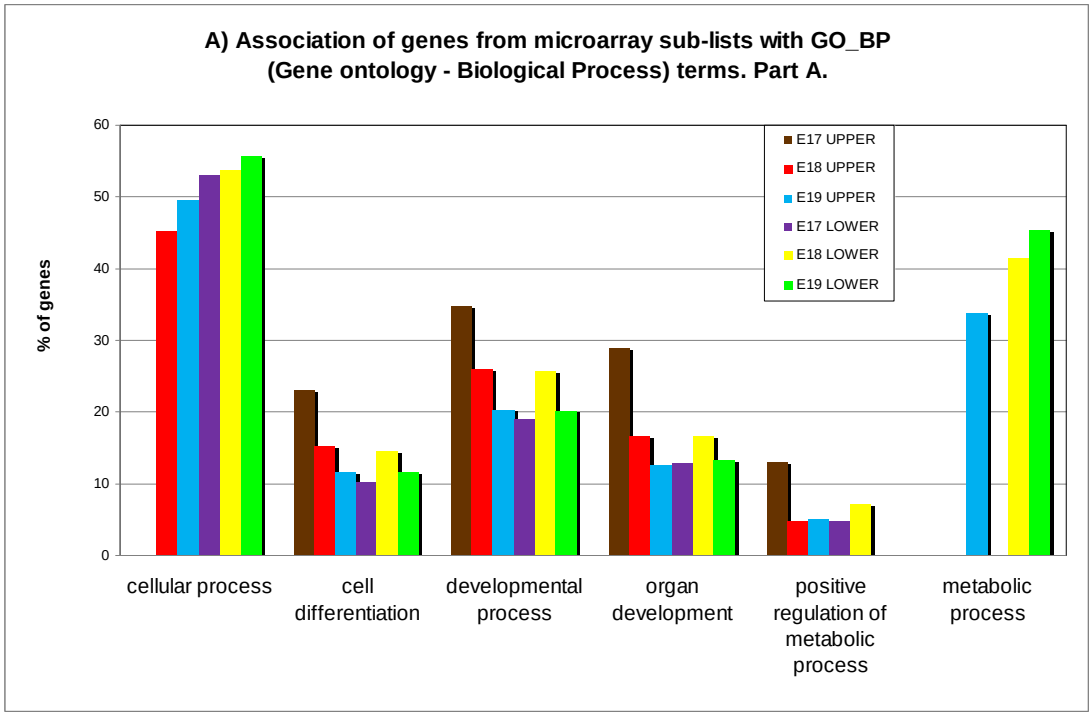


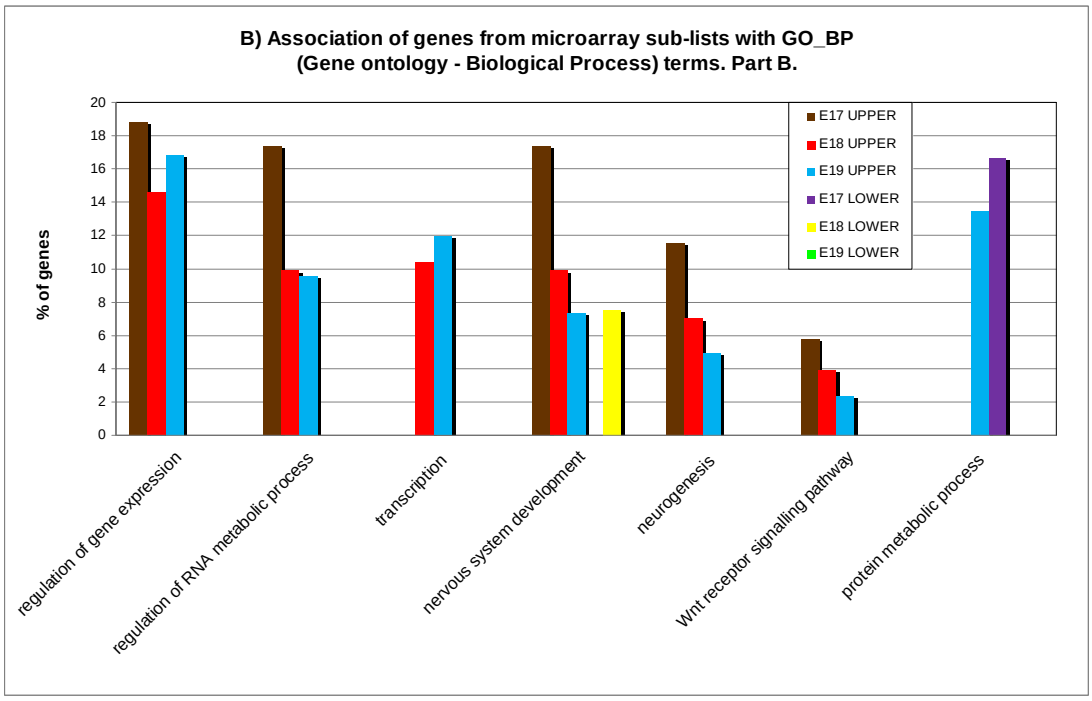


Figure 3.24. Part A and B. For description see Figure 3.24. Part C.

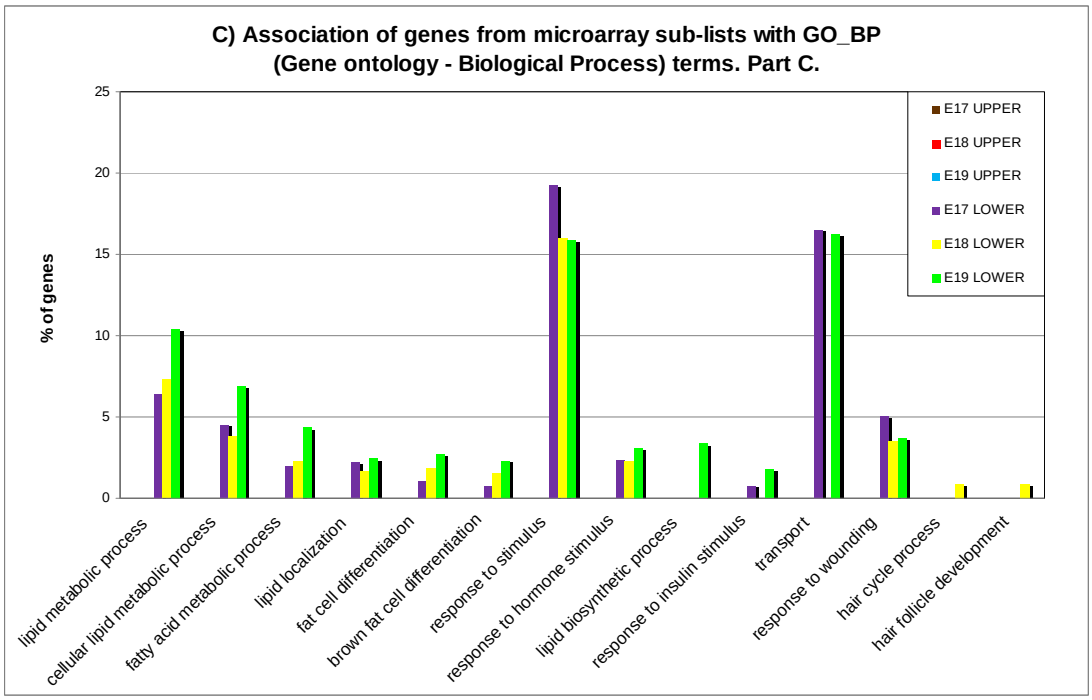


Figure 3.24. Part C. The association of genes from microarray sub-lists with gene ontology - biological terms (GO_BP). The analysis was performed by DAVID v6.7 programme. Single gene can be involved in several terms.

**KEGG pathways associated with genes from skin dermis.**

The DAVID v6.7 allowed the association of genes (from microarray sub-lists) with the online available KEGG (Kyoto Encyclopedia of Genes and Genomes) pathways that present known interactions between different genes. Only genes from the E17 UPPER sub-list were not associated with pathways which suggests that at this time point in the upper dermis, the number of activated genes was not sufficient to create a significant KEGG pathway term by DAVID6.7 programme (Table 3.5).

Therefore the KEGG analysis showed that in the lower dermis the activation of genes involved in different pathways and known processes takes place earlier than in upper dermis. At e17 time point in lower dermis, 28 KEGG pathway terms were obtained for the gene sub-list (Table 3.5). At e18 and e19 time points, genes were also associated with KEGG pathways. Genes from E18 UPPER sub-list were associated with 12 pathways, whereas from the E18 LOWER sub-list with 20 pathways. There were 25 KEGG pathways associated with the E19 UPPER gene sub-list and 32 pathways with the E19 LOWER sub-list.

When the generated KEGG pathways for sub-lists were compared, a clear difference between pathways relating to the upper and lower dermis was seen (Table 3.6). Among the 12 pathways at e18 in the upper dermis, only three were present in the lower dermis (Table 3.6). From 32 pathways at e19 from the lower dermis, only two were present in upper dermis at the same time point (Table 3.6). More similarities were seen between diferent time points in the upper or lower dermis. For example, ten KEGG pathway terms were common for genes from the upper dermis at e18 and e19. In the lower dermis, 15 pathways were common between the e18 and e19 time points. In addtion, there were six terms related with genes up-regulated in lower dermis at each analysed time point (Table 3.6).

Table 3.6. The analysis of genes up-regulated in upper and lower dermis at three time points (e17, e18 and e19) performed by DAVID v6.7 programme. Genes were associated with KEGG pathway terms. "+" - the KEGG term associated with sub-list; "-" - the KEGG term not associated with sub-list. Single gene can be involved in several terms.

| KEGG PATHWAY / SUB-LIST: | E17 UPPER | E18 UPPER | E19UPPER | E17 LOWER | E18 LOWER | E19 LOWER |
|---|---|---|---|---|---|---|
| MAPK signalling pathway | - | + | + | - | + | - |
| Tight junction | - | + | + | - | + | - |
| Colorectal cancer | - | + | + | + | - | - |
| Cell adhesion molecules (CAMs) | - | + | - | - | + | - |
| Wnt signalling pathway | - | + | + | - | - | - |
| Melanogenesis | - | + | + | - | - | - |
| Axon guidance | - | + | + | - | - | - |
| Arrhythmogenic right ventricular cardiomyopathy (ARVC) | - | + | + | - | - | - |
| Vascular smooth muscle contraction | - | + | + | - | - | - |
| Dilated cardiomyopathy | - | + | + | - | - | - |
| Basal cell carcinoma | - | + | + | - | - | - |
| Acute myeloid leukemia | - | + | - | - | - | - |
| Focal adhesion | - | - | + | + | + | + |
| ECM-receptor interaction | - | - | + | + | + | + |
| Pathways in cancer | - | - | + | + | + | - |
| Regulation of actin cytoskeleton | - | - | + | + | - | - |
| Pancreatic cancer | - | - | + | + | - | - |
| Small cell lung cancer | - | - | + | - | + | - |
| Endocytosis | - | - | + | - | - | - |
| Ubiquitin mediated proteolysis | - | - | + | - | - | - |
| Prostate cancer | - | - | + | - | - | - |
| Hypertrophic cardiomyopathy (HCM) | - | - | + | - | - | - |
| Hedgehog signalling pathway | - | - | + | - | - | - |
| Adherens junction | - | - | + | - | - | - |
| Gap junction | - | - | + | - | - | - |
| TGF-beta signalling pathway | - | - | + | - | - | - |
| Lysine degradation | - | - | + | - | - | - |
| Leukocyte transendothelial migration | - | - | - | + | + | + |
| Glutathione metabolism | - | - | - | + | + | + |
| Adipocytokine signalling pathway | - | - | - | + | + | + |
| PPAR signalling pathway | - | - | - | + | + | + |
| Glycolysis / Gluconeogenesis | - | - | - | + | - | + |
| Pentose phosphate pathway | - | - | - | + | - | + |
| Porphyrin and chlorophyll metabolism | - | - | - | + | - | + |
| Lysosome | - | - | - | + | - | - |
| Cytokine-cytokine receptor interaction | - | - | - | + | - | - |
| Fc gamma R-mediated phagocytosis | - | - | - | + | - | - |
| Natural killer cell mediated cytotoxicity | - | - | - | + | - | - |
| Antigen processing and presentation | - | - | - | + | - | - |
| Fc epsilon RI signalling pathway | - | - | - | + | - | - |
| Complement and coagulation cascades | - | - | - | + | - | - |
| B cell receptor signalling pathway | - | - | - | + | - | - |
| Renal cell carcinoma | - | - | - | + | - | - |
| Aldosterone-regulated sodium reabsorption | - | - | - | + | - | - |
| Glycosaminoglycan degradation | - | - | - | + | - | - |
| Other glycan degradation | - | - | - | + | - | - |
| Prion diseases | - | - | - | + | - | - |
| Glycosphingolipid biosynthesis * | - | - | - | + | - | - |
| Huntington's disease | - | - | - | - | + | + |
| Alzheimer's disease | - | - | - | - | + | + |
| Glycerolipid metabolism | - | - | - | - | + | + |
| Metabolism of xenobiotics by cytochrome P450 | - | - | - | - | + | + |
| Drug metabolism | - | - | - | - | + | + |
| Citrate cycle (TCA cycle) | - | - | - | - | + | + |
| Pyruvate metabolism | - | - | - | - | + | + |
| Fatty acid metabolism | - | - | - | - | + | + |
| Valine, leucine and isoleucine degradation | - | - | - | - | + | + |
| Parkinson's disease | - | - | - | - | - | + |
| Oxidative phosphorylation | - | - | - | - | - | + |
| Insulin signalling pathway | - | - | - | - | - | + |
| Cardiac muscle contraction | - | - | - | - | - | + |
| Propanoate metabolism | - | - | - | - | - | + |
| Nitrogen metabolism | - | - | - | - | - | + |
| Glycine, serine and threonine metabolism | - | - | - | - | - | + |
| Biosynthesis of unsaturated fatty acids | - | - | - | - | - | + |
| Starch and sucrose metabolism | - | - | - | - | - | + |
| Tyrosine metabolism | - | - | - | - | - | + |
| Cysteine and methionine metabolism | - | - | - | - | - | + |
| Fatty acid elongation in mitochondria | - | - | - | - | - | + |
| Glyoxylate and dicarboxylate metabolism | - | - | - | - | - | + |
| Renin-angiotensin system | - | - | - | - | - | + |

* The DAVID v6.7 programme created for E17 LOWER sub-list two groups of genes that shared the same KEGG pathway term ("Glycosphingolipid biosynthesis"). These genes were treated as they belong to one term, therefore 27 terms instead of originally created 28 terms (Table 3.5) are shown in Table 3.6 which are associated with E17 LOWER sub-list genes.

Such KEGG pathway term as “adipocytokine signalling pathway” was associated with genes from lower dermis at all analysed time points (Figures 3.25). The adipocytokine signalling pathway is associated with the activity of cytokines which are secreted by adipose tissue (Guerre-Millo, 2004). Among known adipocytokines are adiponectin (AdipoQ), leptin or TNF-α (tumor necrosis factor alpha). These take part in lipid and glucose metabolism and inflammatory processes. The enrichment of adiponectin gene (*Adipoq*) in the lower dermis was confirmed by the qRT-PCR work (section 3.3.2.1; Figure 3.13B). Both leptin and adiponectin acts via receptors (Lepr, Adipor1 and Adipor2) and up-regulation of these receptors in lower dermis (versus upper dermis) was observed at all analysed time points on mRNA level (Table 3.7).

The next interesting pathway associated with genes only from LOWER sub-lists was the “PPAR signalling pathway” (Figure 3.25). PPARgamma gene, involved in this pathway, was enriched in lower dermis area from e17 till e19 time points and its expression was confirmed by the qRT-PCR reaction (section 3.3.5.1; Figure 3.41B). The number of genes up-regulated in the lower dermis that were associated with the “PPAR signalling pathway” term increased from e17 (9) to e19 (18).

Among other KEEG terms specific only to lower gene sub-lists, “fatty acid metabolism” term was associated with genes from e18 and e19 time points (Figure 3.25). In addition, the “fatty acid elongation in mitochondria”, the “biosynthesis of unsaturated fatty acids” and the “insulin signalling pathway” terms were created for genes from the lower dermis at e19 time point (Figure 3.25). It is known that modifications of fatty acids are observed in fat cells, whereas insulin influences lipolysis process in such cells (Pearce, 1983; Duncan *et al*, 2007).

Interestingly, several terms were associated, by DAVID v6.7 programme, with genes from UPPER sub-lists, such as the “MAPK signalling pathway”, the “TGF beta signalling pathway” or the “WNT signalling pathway” term (Figure 3.25). The “WNT signalling pathway” is known to be invovled in the regulation of adipogenesis (Bennett *et al*, 2002). In general, the Wnt pathway is responsible for the control of adipocyte differentiation through both b-catenin-dependent and b-catenin-independent cascades (Kennell and MacDougald, 2005; Bennett el at, 2002). The WNT/B-catenin (canonical) pathway had been related with the inhibiton of adipogensis, whereas the non-canonical WNT cascade may activate adipocyte differentiation (Kennell and MacDougald, 2005; Nishizuka *et al*, 2008). Interestingly,

the b-catenin gene was not presented in microarray sub-lists that contained of genes with equal or greater than 2 fold expression change. In addition, genes related with a complex that is responsible for b-catenin degradation (*Axin2* and *Gsk3b*) were associated (by DAVID v6.7 programme) with E18 UPPER and/or E19 UPPER sub-lists (Table 3.8A; Appendix V). Among other genes related with this pathway and enriched in upper embryonic skin dermis (versus lower skin dermis) were at e18 time point *Wnt4* (2-fold change) and Wnt inhibitory factor 1 (*Wif1*) (3.71-fold change) genes (Table 3.8A). At the e19 time point, the up-regulation of Wif1 had a 28 fold increase in upper dermis versus lower dermis. The Wnt4 was related with non-canonical WNT pathway and its role may be associated with the activation of adipogenesis, whereas Wif1 binds to Wnt proteins and inhibits their activity (Nishizuka *et al*, 2008). The full role Wif1 is still not fully understood and the work of Cho *et al* (2009) has shown that it can in some cases increase adipocyte differentiation.

In addition to the analysis of sub-lists by DAVID programme, a bioinformatics independent analysis was performed on microarray data and presence of several genes, related with the WNT signalling pathway (based on available literature and online sources) was investigated in LOWER sub-lists. This analysis revealed an enrichment of genes specific for the WNT pathway in lower dermal cells that were not associated with the “WNT signalling pathway” term by DAVID programme. For example *Fzd4* (frizzled-4/frizzled homolog 4/Fz-4) gene was up-regulated in all analysed time points in lower dermis versus upper dermis (Table 3.8B). In addition, this up-regulation in lower dermis versus upper dermis was higher in older (e19) skin when compared with younger samples, such as e17 or e18. Frizzled4 gene was shown to be enriched in adipocytes from adult mice (Soukas *et al*, 2001). The presence of Fzd4 in lower dermal cells is discussed in Chapter 5, in relation to the fluorescence activated cell sorting (FACS) work.

The DAVID v6.7 programme was a useful tool for a global analysis of microarray data, however it was important to analyse microarray data also independently to such programs to get a better view of gene expression pattern based on microarray data. Therefore, in the section below (3.3.4) a combination of bioinformatics and non-bioinformatisc analysis was applied for the further investigation of presented here microarray data.

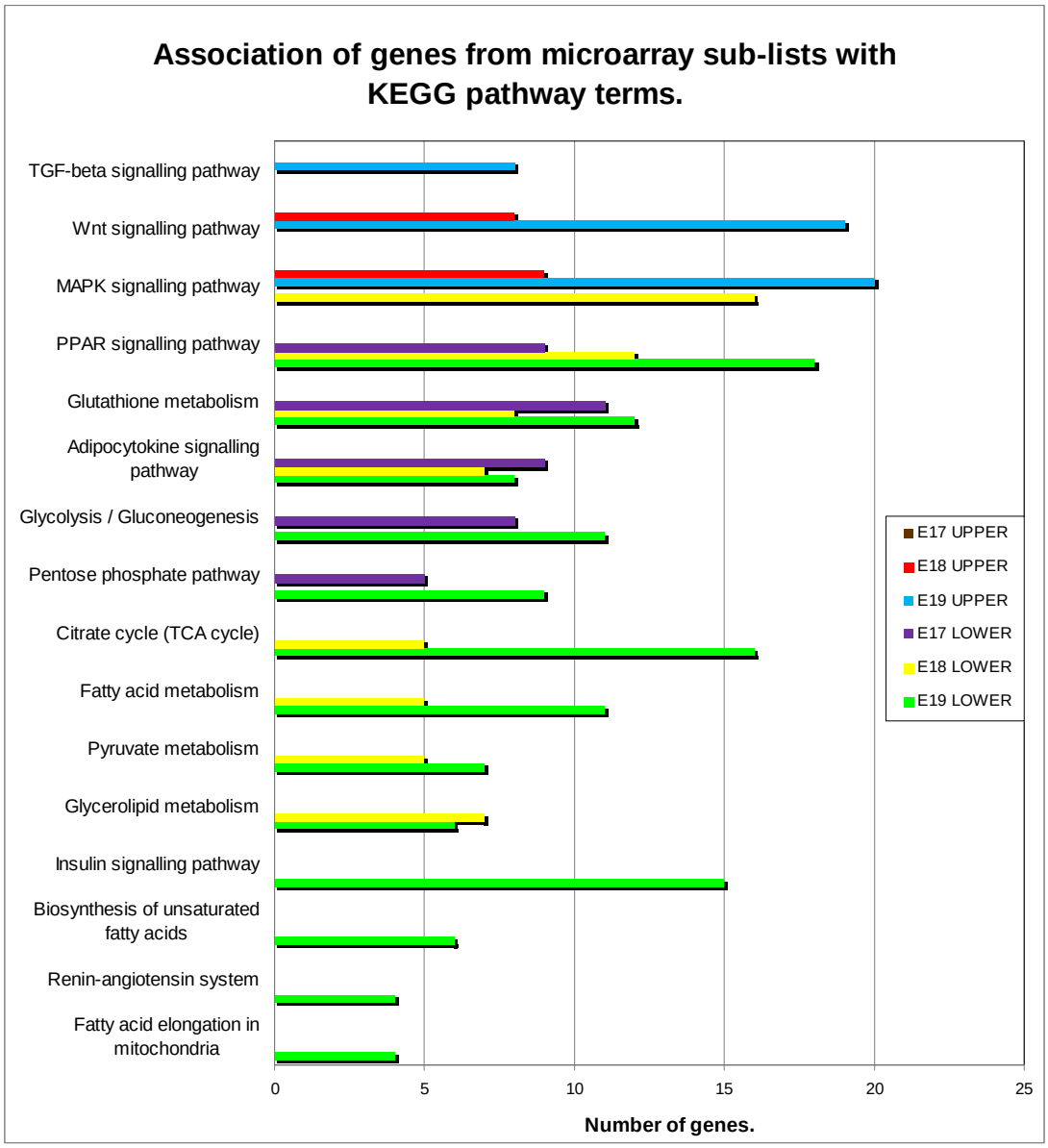


Figure 3.25. The association of genes from microarray sub-lists with KEGG pathway terms. The analysis was performed by DAVID v6.7 programme. Note that DAVID v6.7 programme did not associate genes from E17 UPPER sub-list with KEGG pathway terms. Single gene can be involved in several terms.

Table 3.7. The expression profiles of selected microarray genes associated with the "adipocytokine signalling pathway" term. Presented genes were associated with the analysed term by DAVID v6.7 programme.

| Whole name; gene symbol; gene Affymetrix ID: | Sub-list: | Fold change*: |
|---|---|---|
| leptin receptor; *Lepr*; 1456156_at | E17 LOWER | + 5.31194 |
| | E18 LOWER | + 12.64453 |
| | E19 LOWER | + 7.111806 |
| adiponectin receptor 1; *Adipor1*; 1439017_x_at | E17 LOWER | + 2.266466 |
| | E18 LOWER | NP** |
| | E19 LOWER | NP** |
| adiponectin receptor 2; *Adipor2*; 1434329_s_at | E17 LOWER | NP** |
| | E18 LOWER | + 2.485648 |
| | E19 LOWER | + 6.915786 |

* regulation (enrichment) in **lower dermis versus upper dermis**
** gene was not present in the microarray sub-list with a fold change cut off 2

Table 3.8. The expression profiles of selected microarray genes associated with the "WNT signalling pathway" term. (A) Presented genes were associated with the analysed term by DAVID v6.7 programme. (B) The additional gene associated with the WNT signalling pathway was pointed in the microarray sub-lists during the non-bioinformatics analysis.

**A)**

| Whole name; gene symbol; gene Affymetrix ID: | Sub-list: | Fold change*: |
|---|---|---|
| axin2; *Axin2*; 1436845_at | E18 UPPER | + 7.553152 |
| | E19 UPPER | + 13.53982 |
| glycogen synthase kinase 3 beta; *Gsk3b*; 1439949_at | E18 UPPER | NP** |
| | E19 UPPER | + 2.071018 |
| wingless-related MMTV integration site 4; *Wnt4*; 1450782_at | E18 UPPER | + 2.021527 |
| | E19 UPPER | NP** |
| Wnt inhibitory factor 1; *Wif1*; 1425425_a_at | E18 UPPER | + 3.718775 |
| | E19 UPPER | + 28.04123 |

* regulation (enrichment) in **upper dermis versus lower dermis**
** gene was not present in the microarray sub-list with a fold change cut off 2

**B)**

| Whole name; gene symbol; gene Affymetrix ID: | Sub-list: | Fold change*: |
|---|---|---|
| frizzled homolog 4 (Drosophila); *Fzd4*; 1419301_at | E17 LOWER | + 2.65587 |
| | E18 LOWER | + 7.128446 |
| | E19 LOWER | + 9.34063 |

* regulation (enrichment) in **lower dermis versus upper dermis**
** gene was not present in the microarray sub-list with a fold change cut off 2

### 3.3.4. A global comparison study between *in vitro* (3T3-L1 cells) and *in vivo* (lower dermal cells) adipocyte differentiation.

**Strategy:**

Previous analysis in section 3.3.3 where the microarray sub-lists were analysed by a DAVID v6.7 programme, showed an enrichment of fat-related genes up-regulated in the lower dermis area during mouse embryonic development. The next aim was to use this data to compare this "naturally" occurring adipogenic differentiation with adipogenesis analysed intensively in *in vitro* cell lines, especially in 3T3-L1 cells (Green and Kehinde, 1974; reviewed by Gregoire *et al*, 1998).

Initially the aim was to compare the lower dermis (LD) microarray data with the microarray data from 3T3-L1 cells lines (Figure 3.26) to investigate qualitative and quantitative differences between the two data sets directly. However, in practice this proved to be impractical for two reasons. First, much of the key microarray data was produced over a much longer time scale, for example 0 to 28 days (Soukas *et al*, 2001). Secondly there were differences in array platforms used and these would certainly complicate or annul any attempts to compare the intensity of analysed signals for individual genes from both experiments.

Nevertheless, a broad general microarray analysis/comparison was possible with a specific publication in which the expression profile of 3T3-L1 cells undergoing adipocyte differentiation from day 0 till up to 96 hours of incubation was investigated. (Burton *et al*, 2004). In this study microarray data was analysed by so-called hierarchical clustering which allowed the researchers to organize groups of genes, expressed in the differentiating 3T3-L1 cells into clusters depending on their expression profiles and whether they were enriched (induced) or repressed over the time period. To make the comparison with work in this thesis, genes in lower dermis microarray lists were cross referenced directly with genes in the clusters in relation to both their presence or absence and as to whether they were enriched or repressed in a pattern between the e17 and e19 time points *in vivo*, as in 3T3-L1 cells (Figures 3.27 - 3.35). When a gene from an *in vitro* cluster was also seen in the *in vivo* lower dermis (LD) list it was classified as "present". Genes from the clusters not present in the LD list were treated as "absent". As a further comparative indicator, the expression levels of those *in vivo* genes in the "present" category were drawn graphically over the e17 to s19 time points to see whether their patterns of expression mirrored those seen *in vitro*.

**The lower dermis (LD) microarray data.**

Expression profiles of genes regulated in lower dermis area during mouse embryonic development.

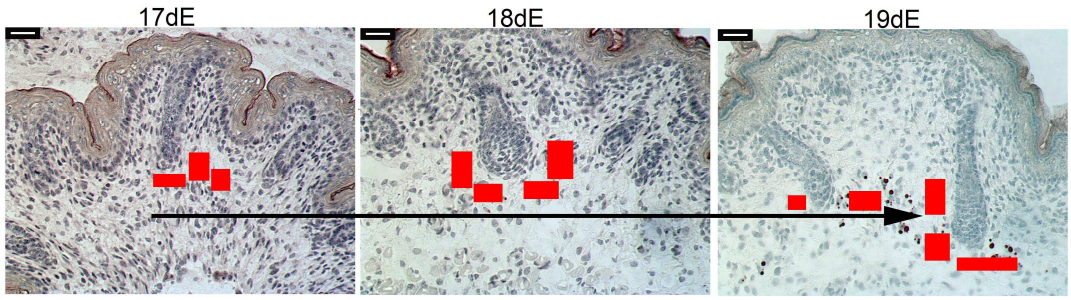


***In vivo* versus *in vitro* adipogenesis.**

A comparison study aimed to reveal similarities and differences between genes involved in fat cell differentiation *in vitro* (cell lines) and genes detected in cells from lower dermis that differentiate into adipocytes *in vivo* (the LD microarray data).

Figure 3.26. A schematic presentation of analysis carried after the lower dermis (LD) microarray data generation by GeneSpring® GX11.0 software. Cells from lower dermis area (marked by red rectangles) were collected from embryonic mouse back skin at three time points and used for microarray analysis.

**Observations:**

The first two enriched clusters contained genes whose expression in 3T3-L1 cells underwent major changes in the hours immediately after the addition of adipogenic medium (Figure 3.27A and Figure 3.28A). Of the genes highly up-regulated 2 hours after adipogenic treatment in the 3T3-L1 cells (enriched Cluster 1) only 12% of them were present in the LD data, whereas almost 70% were absent *in vivo* microarray list (Figure 3.27B). All present genes from this cluster were up-regulated *in vivo* from e17 to e18 (Figure 3.27C). Similarly only 14% of the genes in Cluster 2 whose genes had a peak of expression around 8 hours after adipogenic treatment *in vitro* were present in the LD array lists from foetal skin (Figure 3.28B). However, among this cohort some of the *in vivo* genes followed a different pattern and were down-regulated between e17 and e18 (Figure 3.28C).

A slightly higher percentage (19%) of genes present in *in vivo* LD microarray list was observed in Cluster 3 which contained genes enriched between 16 and 24 hours of incubation in adipogenic medium (Figure 3.29A and B). A similar percentage of genes (21%) was found for Cluster 4, which represented genes whose expression peaked around 48 hours after incubation in adipogenic medium (Figure 3.30A and B). Most of the genes from Clusters 3 and 4 found *in vivo* followed a similar expression pattern to their counterparts *in vitro* and only one (stem-loop binding protein; *Slbp*) was down-regulated *in vivo* between e17 and e19 (see Figure 3.29C and Figure 3.30C).

Finally, when the analysis was performed on genes from Clusters 5 and 6, representing genes most highly expressed in 3T3-L1 cells after 96 hours in adipogenic medium the percentages of genes present in the *in vivo* microarray data were 64% and 39% respectively (Figure 3.31B and Figure 3.32B). Moreover, all these genes were up-regulated *in vivo* from e17 to e19 as *in vitro*, albeit to differing degrees. Therefore it could be said that they were following the same trend if not the same pattern as their *in vitro* counterparts (Figure 3.31C and Figure 3.32C).

In addition to the analysis of up-regulated cluster profiles, the *in vivo* LD array data was also compared to several repressed clusters from the Burton *et al* (2004) work that contained genes down-regulated during the 3T3-L1 adipogenesis. For all the three *in vitro* clusters examined, only 14 - 18% of the genes were also present *in vivo* (Figures 3.33B, 3.34B and 3.35B). Moreover, about 56% of these genes showed different trends *in vivo*, being increased in expression at some points between e17 to e19 (compare Figure 3.33A with 3.33C; Figure 3.34A with 3.34C; Figure 3.35A with 3.35C).

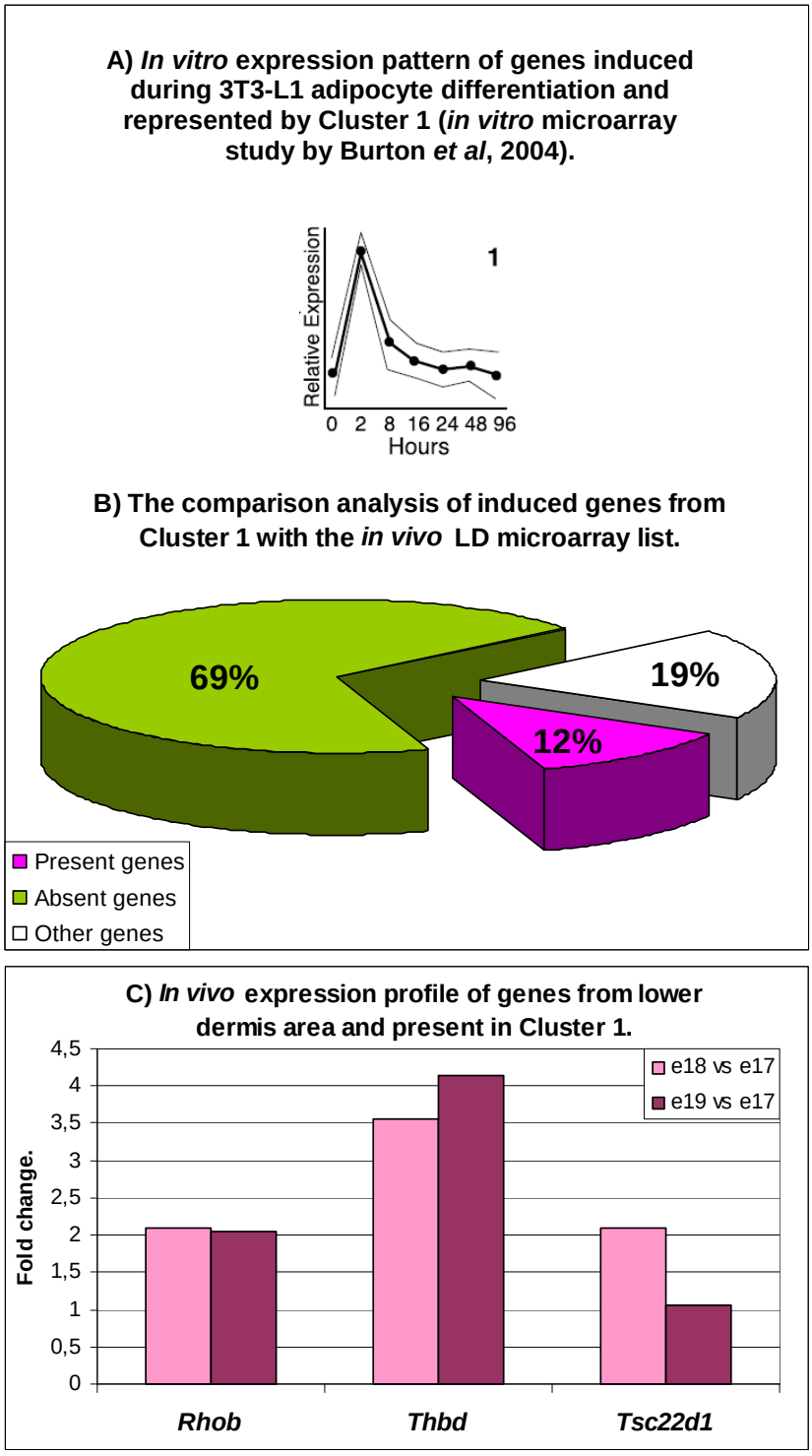


Figure 3.27. The global comparison analysis of genes regulated during *in vitro* and *in vivo* adipogenesis, part A. (A) Expression pattern of genes up-regulated (induced) in 3T3-L1 cells during their adipogenic differentiation shown by Cluster 1 (adapted from Burton *et al*, 2004). (B) The presence of genes associated with Cluster 1 was investigated in the *in vivo* lower dermis (LD) microarray list. Pink - *in vitro* genes present in the LD list. Green - *in vitro* genes absent in the LD list. White - *in vitro* genes with unclear names and with unrecognized presence in the LD list. (C) *In vivo* expression profile of genes expressed in the lower dermis (from e17 until e19) that were also induced in differentiating 3T3-L1 cells *in vitro* (Cluster 1). The full names of genes are included in Appendix VI.

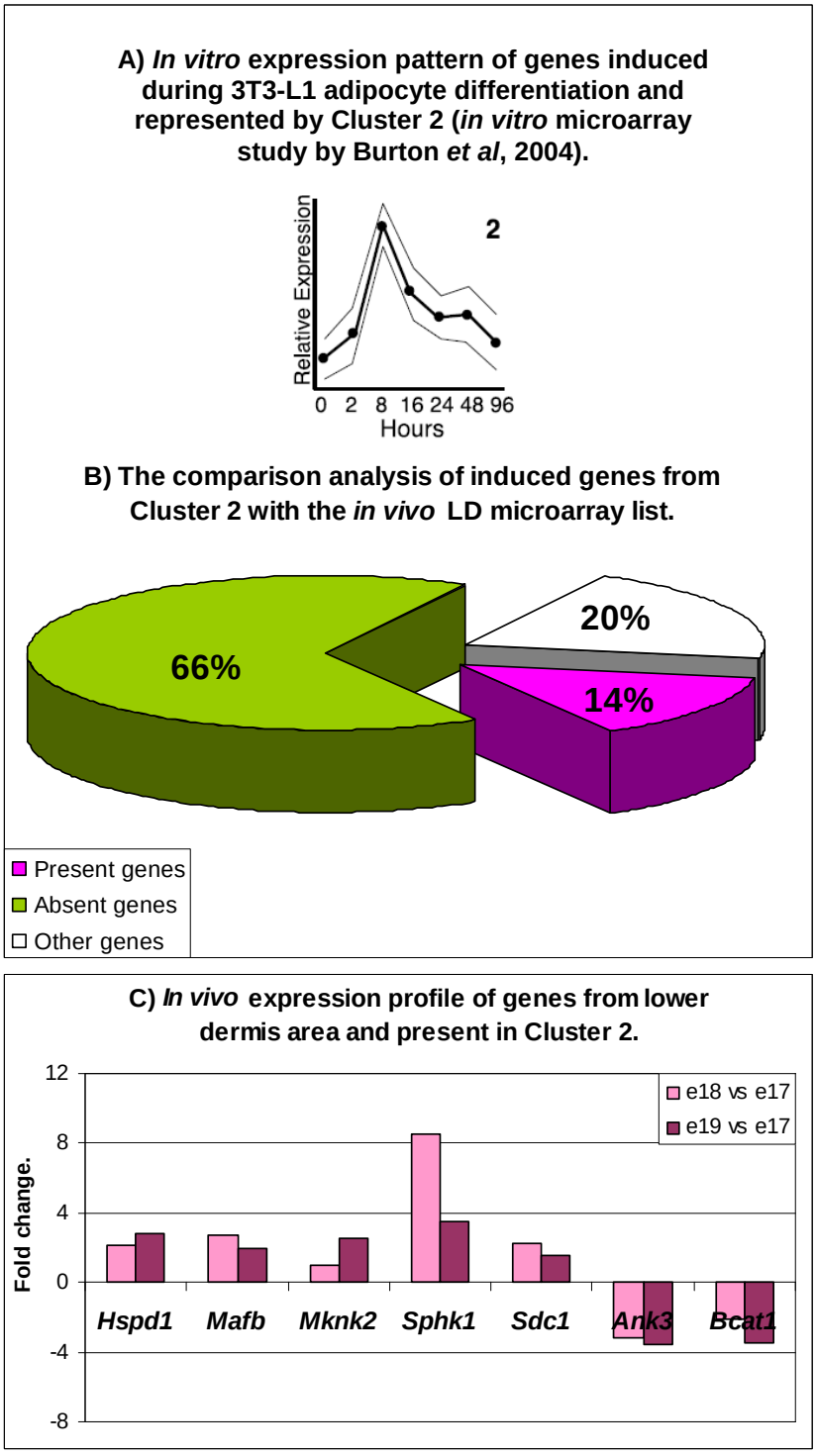


Figure 3.28. The global comparison analysis of genes regulated during *in vitro* and *in vivo* adipogenesis, part B. (A) Expression pattern of genes up-regulated (induced) in 3T3-L1 cells during their adipogenic differentiation shown by Cluster 2 (adapted from Burton *et al*, 2004). (B) The presence of genes associated with Cluster 2 was investigated in the *in vivo* lower dermis (LD) microarray list. Pink - *in vitro* genes present in the LD list. Green - *in vitro* genes absent in the LD list. White - *in vitro* genes with unclear names and with unrecognized presence in the LD list. (C) *In vivo* expression profile of genes expressed in the lower dermis (from e17 until e19) that were also induced in differentiating 3T3-L1 cells *in vitro* (Cluster 2). The full names of genes are included in Appendix VI.

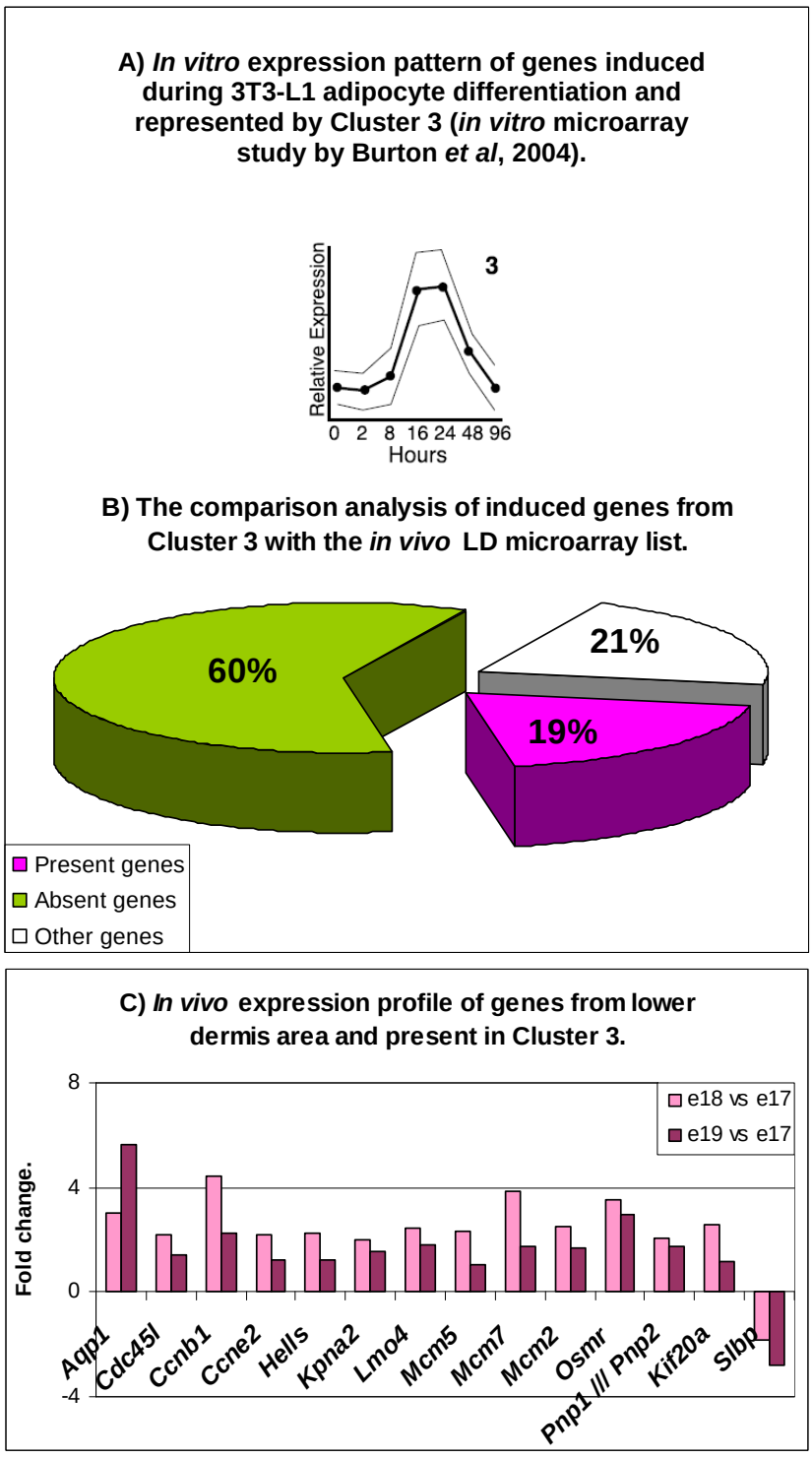


Figure 3.29. The global comparison analysis of genes regulated during *in vitro* and *in vivo* adipogenesis, part C. (A) Expression pattern of genes up-regulated (induced) in 3T3-L1 cells during their adipogenic differentiation shown by Cluster 3 (adapted from Burton *et al*, 2004). (B) The presence of genes associated with Cluster 3 was investigated in the *in vivo* lower dermis (LD) microarray list. Pink - *in vitro* genes present in the LD list. Green - *in vitro* genes absent in the LD list. White - *in vitro* genes with unclear names and with unrecognized presence in the LD list. (C) *In vivo* expression profile of genes expressed in the lower dermis (from e17 until e19) that were also induced in differentiating 3T3-L1 cells *in vitro* (Cluster 3). The full names of genes are included in Appendix VI.

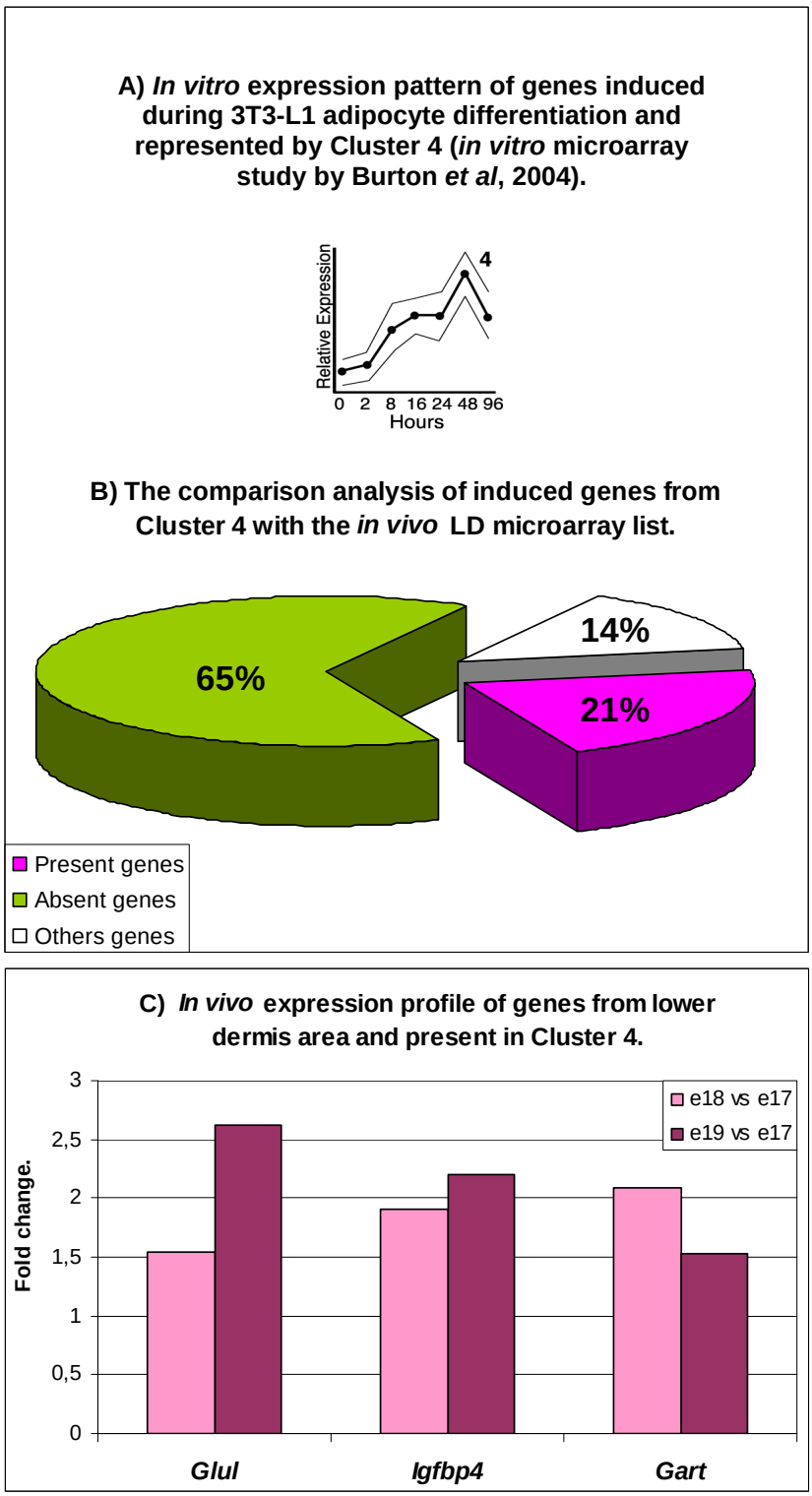


Figure 3.30. The global comparison analysis of genes regulated during *in vitro* and *in vivo* adipogenesis, part D. (A) Expression pattern of genes up-regulated (induced) in 3T3-L1 cells during their adipogenic differentiation shown by Cluster 4 (adapted from Burton *et al*, 2004). (B) The presence of genes associated with Cluster 4 was investigated in the *in vivo* lower dermis (LD) microarray list. Pink - *in vitro* genes present in the LD list. Green - *in vitro* genes absent in the LD list. White - *in vitro* genes with unclear names and with unrecognized presence in the LD list. (C) *In vivo* expression profile of genes expressed in the lower dermis (from e17 until e19) that were also induced in differentiating 3T3-L1 cells *in vitro* (Cluster 4). The full names of genes are included in Appendix VI.

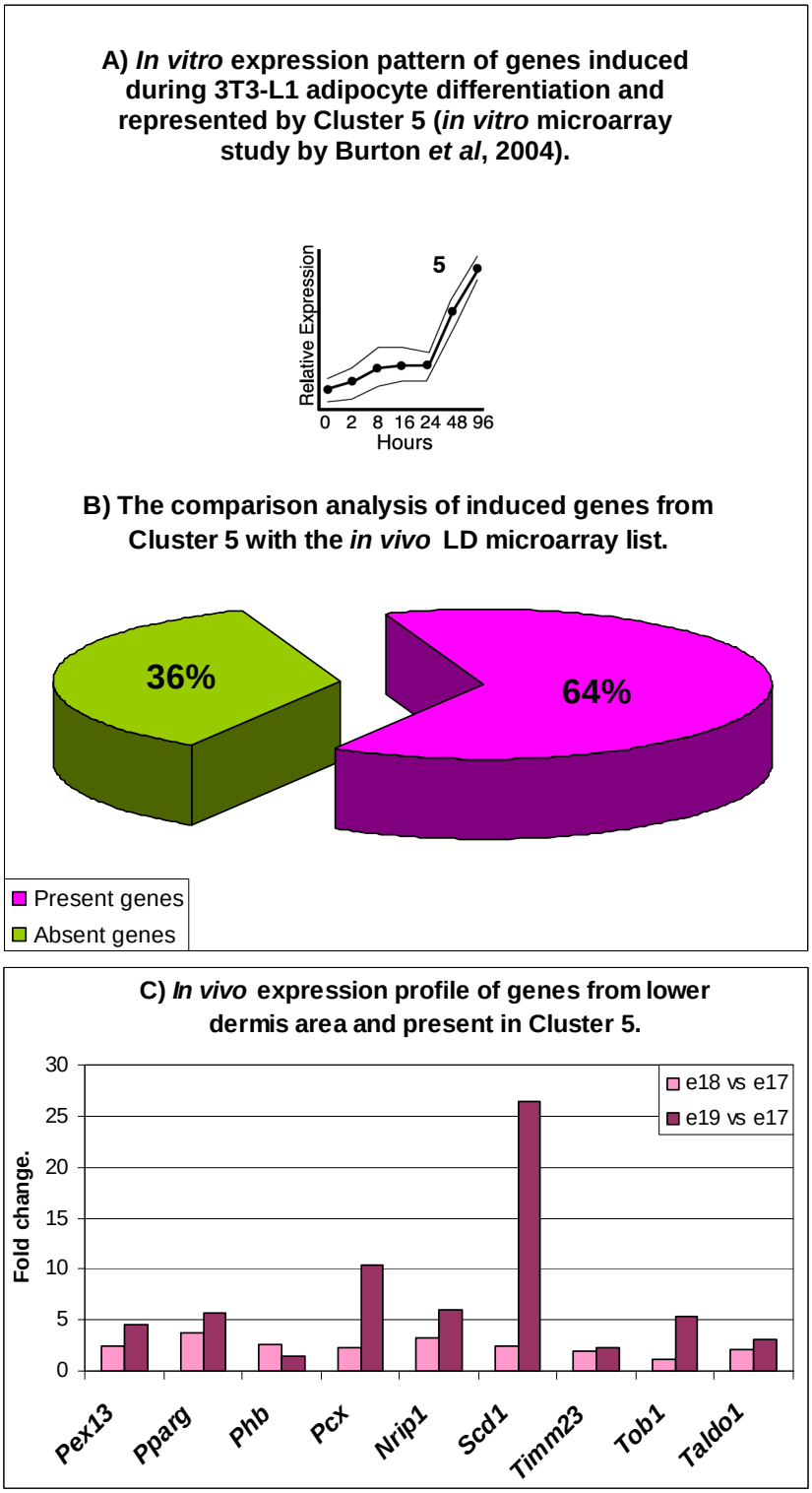


Figure 3.31. The global comparison analysis of genes regulated during *in vitro* and *in vivo* adipogenesis, part E. (A) Expression pattern of genes up-regulated (induced) in 3T3-L1 cells during their adipogenic differentiation shown by Cluster 5 (adapted from Burton *et al*, 2004). (B) The presence of genes associated with Cluster 5 was investigated in the *in vivo* lower dermis (LD) microarray list. Pink - *in vitro* genes present in the LD list. Green - *in vitro* genes absent in the LD list. (C) *In vivo* expression profile of genes expressed in the lower dermis (from e17 until e19) that were also induced in differentiating 3T3-L1 cells *in vitro* (Cluster 5). The full names of genes are included in Appendix VI.

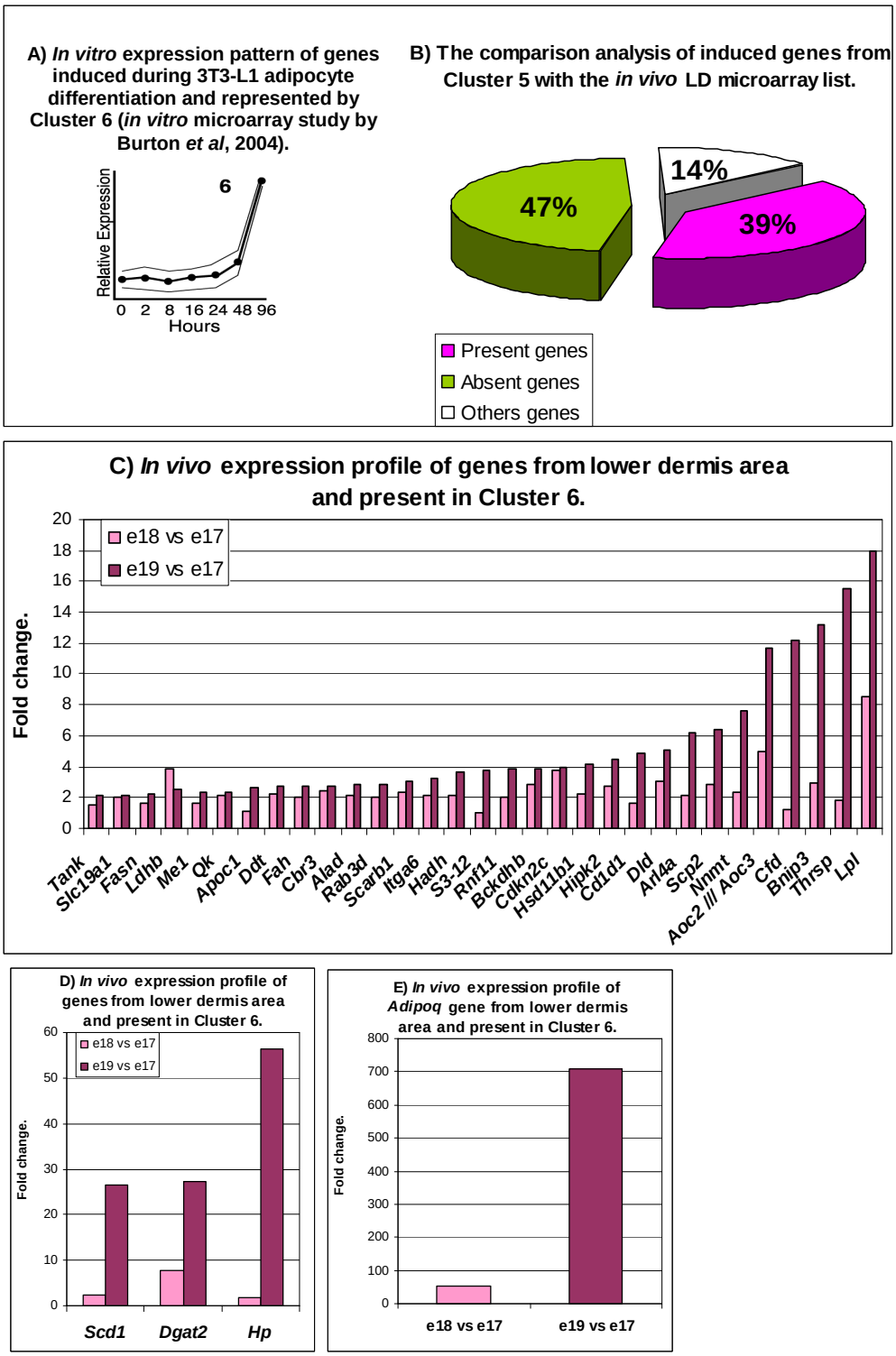


Figure 3.32. The global comparison analysis of genes regulated during *in vitro* and *in vivo* adipogenesis, part F. (A) Expression pattern of genes up-regulated (induced) in 3T3-L1 cells during their adipogenic differentiation shown by Cluster 6 (adapted from Burton *et al*, 2004). (B) The presence of genes associated with Cluster 6 was investigated in the *in vivo* lower dermis (LD) microarray list. Pink - *in vitro* genes present in the LD list. Green - *in vitro* genes absent in the LD list. White - *in vitro* genes with unclear names and with unrecognized presence in the LD list. (C, D, E) *In vivo* expression profile of genes expressed in the lower dermis (from e17 until e19) that were also induced in differentiating 3T3-L1 cells *in vitro* (Cluster 6). The full names of genes are included in Appendix VI.

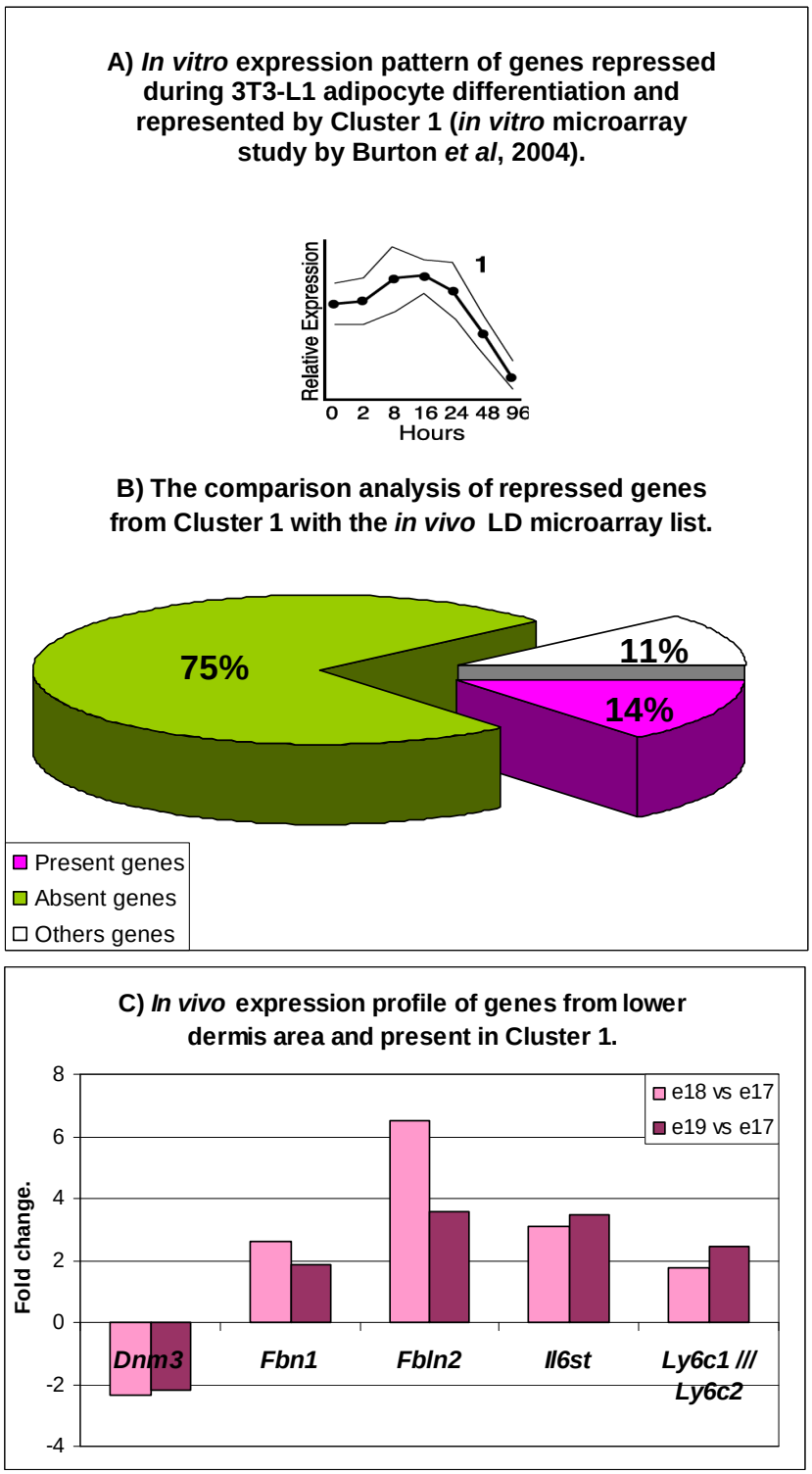


Figure 3.33. The global comparison analysis of genes regulated during *in vitro* and *in vivo* adipogenesis, part G. (A) Expression pattern of genes down-regulated (repressed) in 3T3-L1 cells during their adipogenic differentiation shown by Cluster 1 (adapted from Burton *et al*, 2004). (B) The presence of genes associated with Cluster 1 was investigated in the *in vivo* lower dermis (LD) microarray list. Pink - *in vitro* genes present in the LD list. Green - *in vitro* genes absent in the LD list. White - *in vitro* genes with unclear names and with unrecognized presence in the LD list. (C) *In vivo* expression profile of genes expressed in the lower dermis (from e17 until e19) that were also repressed in differentiating 3T3-L1 cells *in vitro* (Cluster 1). The full names of genes are included in Appendix VI.

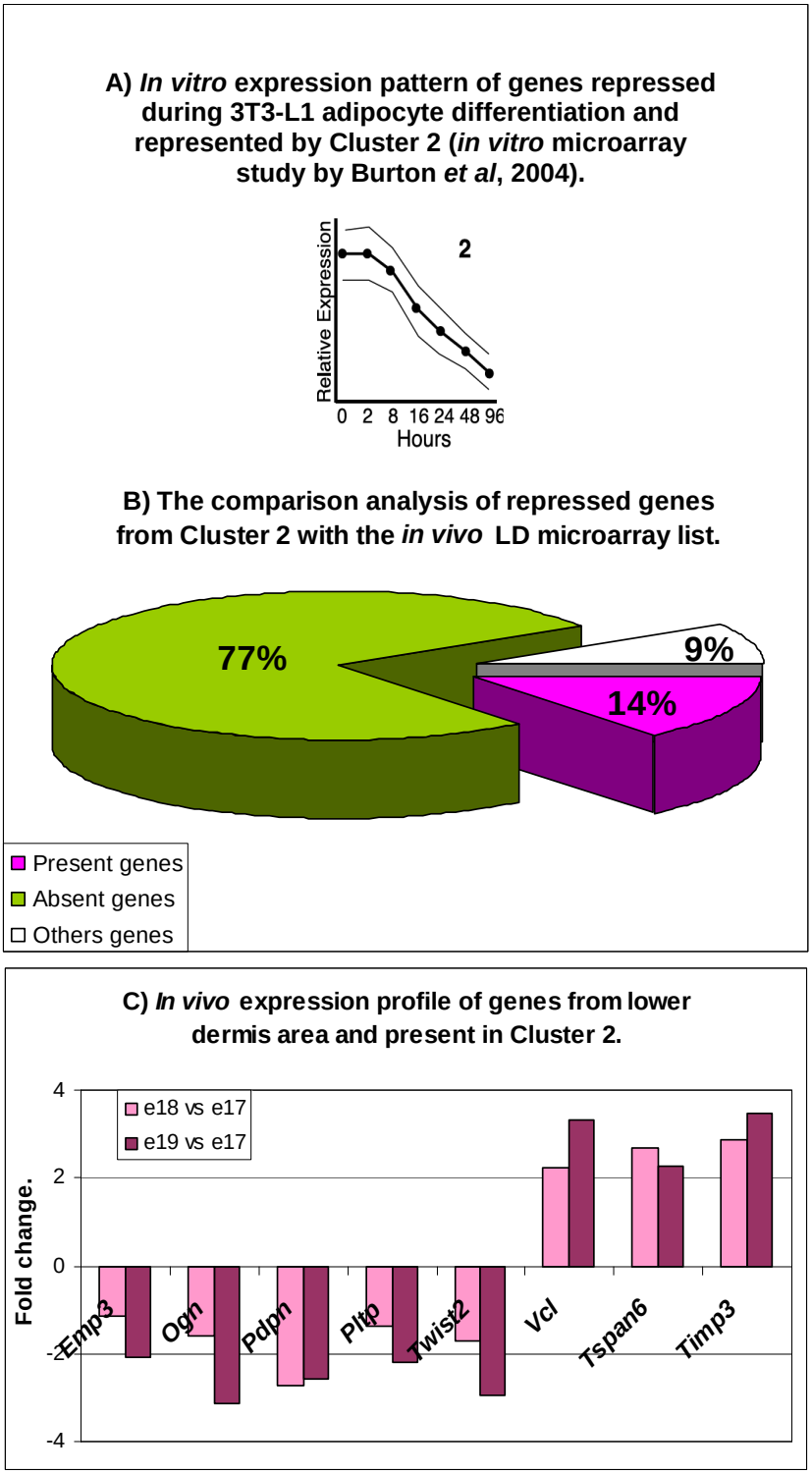


Figure 3.34. The global comparison analysis of genes regulated during *in vitro* and *in vivo* adipogenesis, part H. (A) Expression pattern of genes down-regulated (repressed) in 3T3-L1 cells during their adipogenic differentiation shown by Cluster 2 (adapted from Burton *et al*, 2004). (B) The presence of genes associated with Cluster 2 was investigated in the *in vivo* lower dermis (LD) microarray list. Pink - *in vitro* genes present in the LD list. Green - *in vitro* genes absent in the LD list. White - *in vitro* genes with unclear names and with unrecognized presence in the LD list. (C) *In vivo* expression profile of genes expressed in the lower dermis (from e17 until e19) that were also repressed in differentiating 3T3-L1 cells *in vitro* (Cluster 2). The full names of genes are included in Appendix VI.

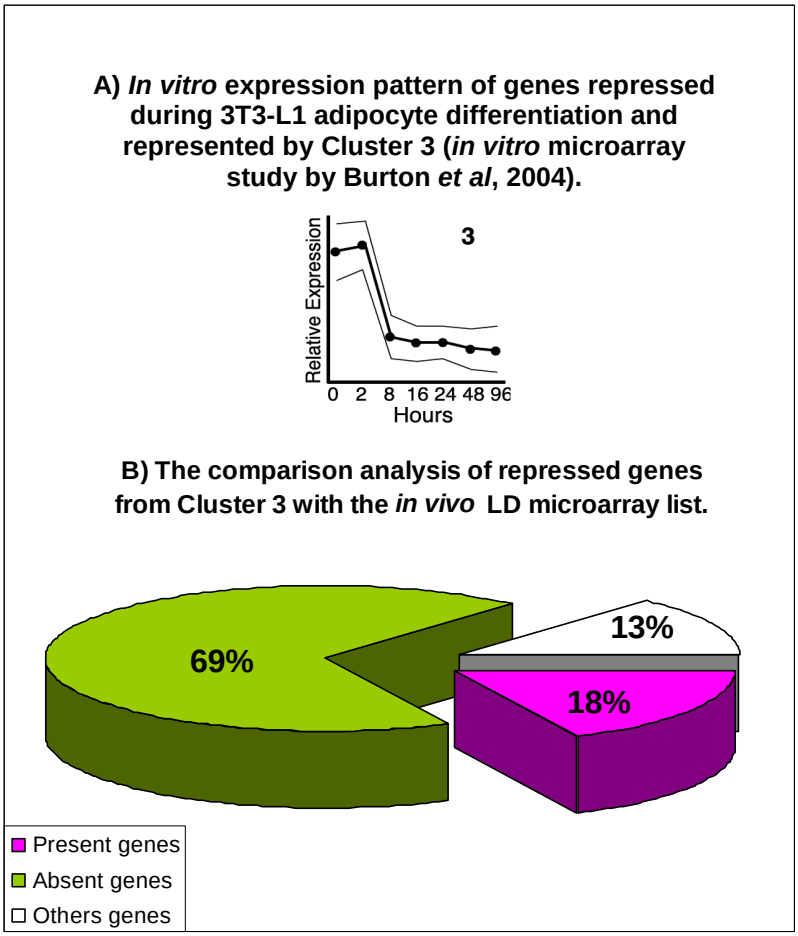


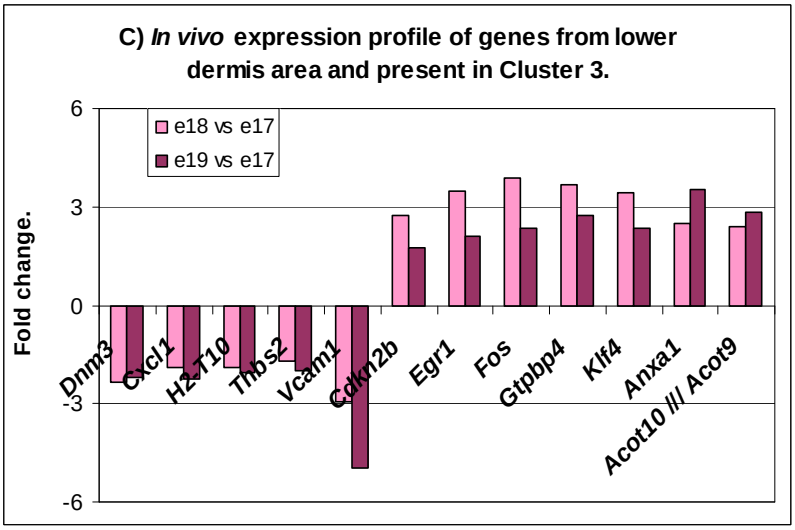


Figure 3.35. The global comparison analysis of genes regulated during *in vitro* and *in vivo* adipogenesis, part I. (A) Expression pattern of genes down-regulated (repressed) in 3T3-L1 cells during their adipogenic differentiation shown by Cluster 3 (adapted from Burton *et al*, 2004). (B) The presence of genes associated with Cluster 3 was investigated in the *in vivo* lower dermis (LD) microarray list. Pink - *in vitro* genes present in the LD list. Green - *in vitro* genes absent in the LD list. White - *in vitro* genes with unclear names and with unrecognized presence in the LD list. (C) *In vivo* expression profile of genes expressed in the lower dermis (from e17 until e19) that were also repressed in differentiating 3T3-L1 cells *in vitro* (Cluster 3). The full names of genes are included in Appendix VI.

### 3.3.5. The investigation of similarities and differences at early steps of adipogenesis between *in vitro* and *in vivo* fat cells.

The above analysis, although limited, provided initial evidence for clear differences between *in vitro* and *in vivo* adipocyte differentiation, particularly for genes up-regulated in the early stages of the process (8 - 24 hours *in vitro*). However, the caveat remains that these early time points in particular might not be comparable with the *in vivo* ones. Interestingly a similar disparity was seen when down-regulation of genes was compared, although here the level of discrepancy remained high for all analysed groups of genes. The overall observation that gene expression is much more comparable at later time points in adipogenesis provided further tentative indications that while final more differentiated profiles might be similar *in vitro* and *in vivo*, early events/processes might be very different. These pointers formed part of the basis for further analysis.

**Further analysis:**

As a strategy for further comparing *in vivo* adipogenesis with known *in vitro* events, it was considered appropriate to break up the lists into specific cellular activities. By this means it was hoped that a broad picture would emerge of the similarities between *in vivo* and *in vitro* differentiation, but that also it would be possible to investigate specific questions pertaining to individual genes or gene families or pathways and their role in these processes. Given the size of the array lists, the many cellular functions/activities contained within them, a limited number of categories were analysed, namely: transcription factors; growth/signalling factors; the cell cycle; cytoskeleton; extracellular matrix and adipocyte related enzyme activity. Most of the analysis was performed through direct examination of the gene lists, and investigation of literature and online resources, however for some of the groupings (cytoskeleton and extracellular matrix) bioinformatics tools were also used. As the final category relates more to lipogenesis and the late stages of adipocyte formation, it was anticipated this would provide further clues as to the overall validity of the *in vivo* analysis in that it would be predicted that the most similarities would be seen here.

### 3.3.5.1. Adipogenic transcription factors (TFs).

Several transcription factors and transcription factor families have been identified as being associated with the regulation of adipogenesis, with a good deal of this data coming from *in vitro* analyses (Figure 3.36). As there is evidence that many of these TFs are crucial for the proper differentiation process, it was important to investigate their presence in the lower dermal cells during *in vivo* adipogenesis using the *in vivo* lower dermis (LD) microarray data. Importantly, transcription factors have been shown to be activated in a specific order or cascade. Therefore an additional element of the current analysis, apart for asking whether specific TFs were present or absent, was to use it to investigate whether the pattern and timing of TF activity in the lower dermis was similar to that published elsewhere. This in turn could provide information about the validity of the data as a whole. So, for example, a haphazard pattern of TF expression would indicate that the data could not be trusted in terms of adipogenic processes having a clear link with sample timings. Alternatively, if the main pattern of expected TF activity was to be seen in the lower dermis, but there was no evidence of TFs normally found very early or very late in the process, then this might indicate that sampling had been started too late for the former, or had been curtailed too early for the latter.

A recent review of TF activity in adipogenesis was used as a starting point for this analysis (White and Stephens, 2010), in which the process is summarised and represented diagrammatically as a sequential series (Figure 3.36). Briefly, during the very early stages of adipogenesis, activation of AP-1, STATs and KLFs receptors takes place. Then the next step is related with up-regulation of C/EBPbeta and C/EBPdelta which trigger over-expression of other KLFs and SREBP-1 factors. Finally, PPARgamma and C/EBPalpha are activated and they control activation of genes in the later stages of adipogenesis (Figure 3.36). These major transcription factor families were analysed in the LD microarray data, and results used to build up a picture of TF activity in the LD based on the original template.

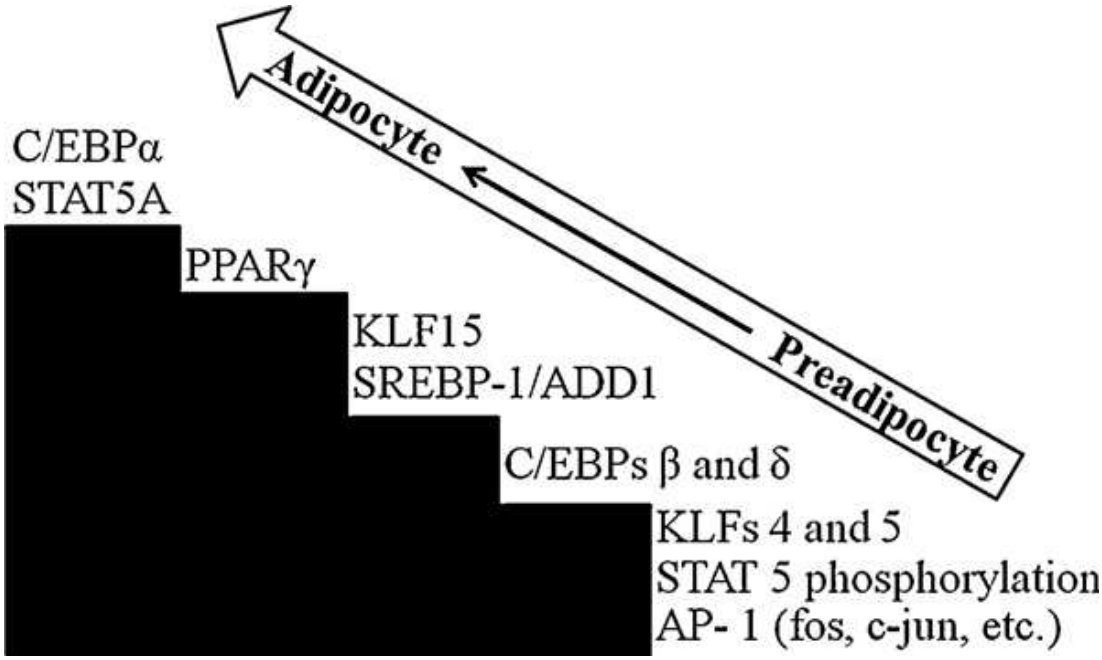


Figure 3.36. A schematic presentation of transcription factors activated during adipogenesis. The figure was taken from White and Stephens, 2010. For the full names of presented factors see figure 3.42.

**The activating protein-1 (AP-1) family of transcription factors.**

Dimeric transcription factors consisting of subnunits c-Jun, Jun-B, Jun-d, c-Fos and Fos-B, Fra-1 and Fra-2 are referred as AP-1 and many of these have been shown to be up-regulated very shortly after activation of adipogenesis (reviewed by White and Stephens, 2010). It is suggested that elements of AP-1 might be crucial for adipose tissue development *in vivo*. In the LD microarray data, only two subunits of AP-1 were up-regulated at significant levels. Both *c-Jun* (*Jun*; jun oncogene) and *Fos* (C-FOS; FBJ osteosarcoma oncogene) had mRNA expression levels highest at the early point of comparison: e18 versus e17 compared with the later e19 to e17 sample time point (Figure 3.37A and B).

**Signal transducer and activator of transcription factors (STAT).**

In 3T3-L1 cells, the growth hormone interacts with growth hormone receptor and activates phosphorylation of Signal Transducer and Activator of Transcription factors (STAT), such as STAT5B and STAT5C which were shown to influence other families of adipogenic transcriptional factors: C/EBPs (C/EBPbeta and C/EBPdelta) and PPARgamma (Kawai *et al*; 2007). In addition, other members of the STAT family including STAT3 and STAT1 have been related to adipogenic differentiation in 3T3-based cell lines (reviewed by White and Stephens, 2010). Interestingly, in the LD microarray data, *Stat1* gene was the only STAT family member showing significant up-regulation during development of the lower dermal cells. It was up-regulated significantly at the later e19 to e17 comparison point (Figure 3.37C).

A)

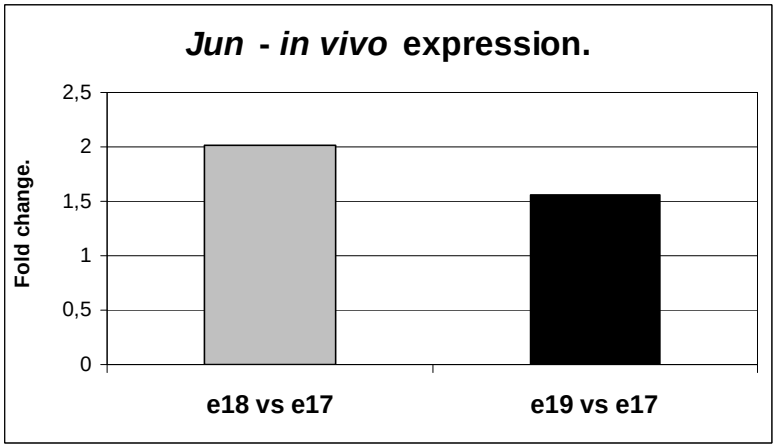


B)

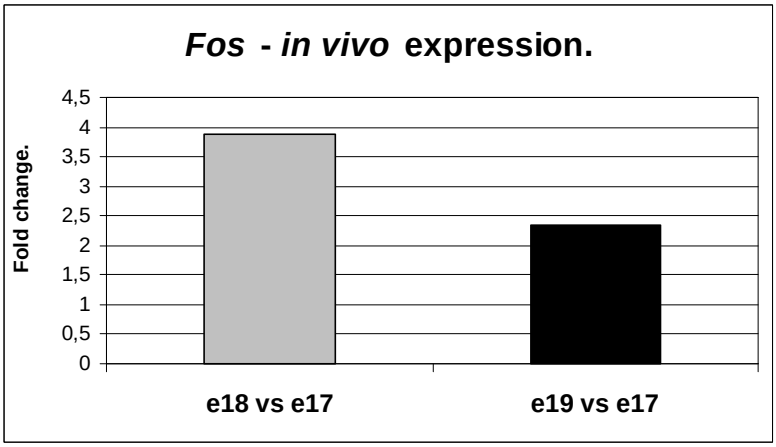


C)

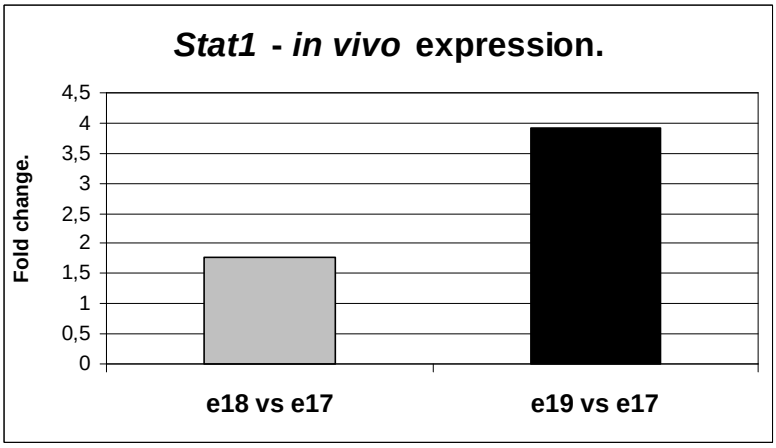


Figure 3.37. The expression profiles of *Jun* (A), *Fos* (B) and *Stat1* (C) genes in the lower dermis from e17 till e19 time points. Grey columns - regulation at e18 versus e17 time points. Black columns - regulation at e19 versus e17 time points. Fold change values are based on the lower dermis (LD) microarray list. *Jun* - Jun oncogene. *Fos* - FBJ osteosarcoma oncogene. *Stat1* - signal transducer and activator of transcription 1.

**Krüppel-like factors (KLFs) and early growth response proteins (Krox).**

Krüppel-like zinc finger transcription factors (KLFs) are another group of transcription factors, directly linked with adipogenesis (reviewed by White and Stephens, 2010; Figure 3.36). Both, KLF4 and KLF5 have been shown to be involved in early stages of adipocyte differentiation (Oishi *et al*, 2005; Birsoy *et al*, 2008). In the *in vivo* LD array data both, *Klf4* and *Klf5* genes were more highly expressed at the earlier (e18 versus e17) than at the later (e19 versus e17) time point (Figure 3.38A). In addition, another family member, Krüppel-like factor 15, thought to play a role later in the adipogenic cascade (Figure 3.36), was strongly up-regulated at the later (e19 versus e17) sample time point (Figure 3.38A). Three additional KLF family members (*Klf3*, *Klf6* and *Klf9*) were also present in lower dermis and these genes were enriched from e17 time point (Figure 3.38A). Krüppel-like factors 3, 6 and 9 have been also associated with regulation of adipogenesis (Li *et al*, 2005; Sue *et al*, 2008; Pei *et al*, 2011).

Early on in adipogenesis, Krüppel-like factor 4 is thought to activate the promoter of C/EBPbeta together with another transcription factor Krox20 (Chen *et al*, 2005; Birsoy *et al*, 2008, see also Figure 3.36). *Krox20* gene, also termed Early growth response 2 (*Egr2*) was not seen in the LD microarray data. However, an *Egr1*/*Krox24* gene was present in this microarray list with the highest up-regulation at the e18 versus e17 time point (Figure 3.38B).

**Sterol regulatory element binding protein (SREBP).**

Sterol regulatory element binding protein (ADD1/SREBP-1) is a basic helix-loop-helix transcription factor recognized in three isoforms: SERBP-1a, SREBP-1c and SREBP-2 (Yokoyama *et al*, 1993; Kim and Spiegelman, 1996). SREBP-1 was shown to take part in promoting adipogenesis in 3T3-based cells (Kim and Spiegelman, 1996).

*Srebp1*/*Srebf1* gene was present in the lower dermis microarray data and this gene was up-regulated significantly in lower dermal cells at the later (e19 versus e17) time point (Figure 3.39).

A)

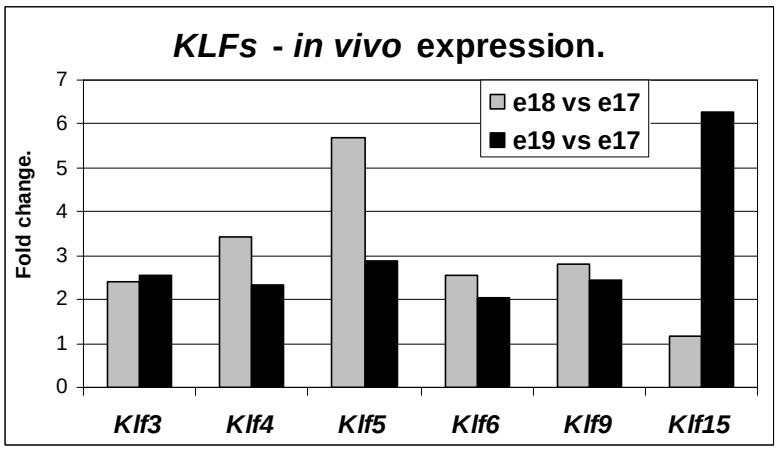


B)

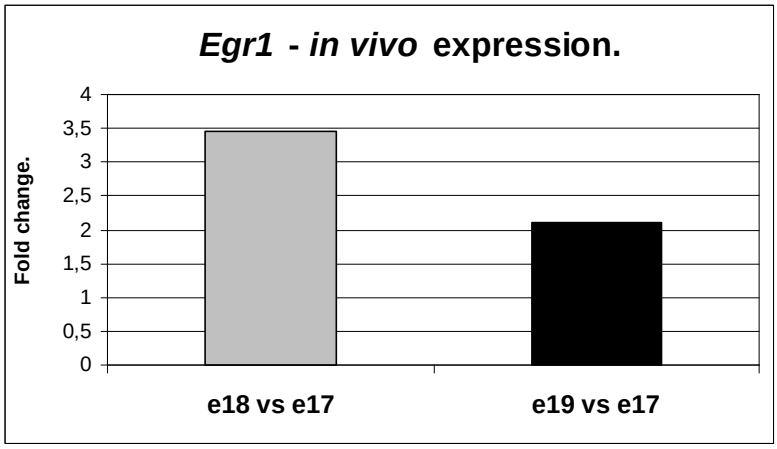


Figure 3.38. The expression profiles of *KLFs* genes (A) and *Egr1* (B) gene in the lower dermis from e17 till e19 time points. Grey columns - regulation at e18 versus e17 time points. Black columns - regulation at e19 versus e17 time points. Fold change values are based on the lower dermis (LD) microarray list. *Klf3* - Krüppel-like factor 3. *Klf4* - Krüppel-like factor 4. *Klf5* - Krüppel-like factor 5. *Klf6* - Krüppel-like factor 6. *Klf9* - Krüppel-like factor 9. *Klf15* - Krüppel-like factor 15. *Egr1* - early growth response 1.

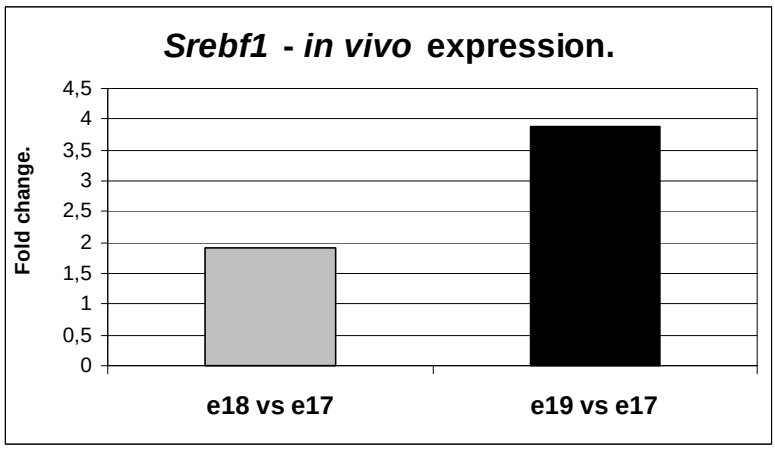


Figure 3.39. The expression profiles of *Srebf1* gene in the lower dermis from e17 till e19 time points. Grey columns - regulation at e18 versus e17 time points. Black columns - regulation at e19 versus e17 time points. Fold change values are based on the lower dermis (LD) microarray list. *Srebf1* - sterol regulatory element binding transcription factor 1.

**CCAAT/enhancer binding proteins (C/EBPs) and peroxisome proliferator-activated receptor gamma (PPARgamma).**

As was discussed previously (Chapter 1, sections 1.3.1.2 and 1.3.3) family of C/EBPs factors and PPARgamma have crucial roles in adipogenic processes and the proper development of adipose tissue.

Analysis of the LD array data showed that *Cebpa* gene expression was significantly and similarly up-regulated through all sample time points (approximately 2.19 fold at e18 versus e17 and 2.66 fold at e19 versus e17, see Figure 3.40A). A higher level of expression was observed for *Pparg* gene, which showed an increase at the later e19 versus e17 time point (Figure 3.40B). The expression of these genes was verified at the mRNA level by qRT-PCR analysis on samples from both upper and lower dermis from all three analysed time points (Figure 3.41). This analysis confirmed up-regulation of these transcriptional factors *in vivo* during development of lower dermal cells. The relative mRNA expression for *Cebpa* and *Pparg* genes increased in lower dermis cells from e17 to e18 time points (Figure 3.41A and B). Both factors were significantly increased in expression at e19 in the lower dermis when compared with the lower dermis of e17 time point, according to a t-test. Expression of these adipogenic factors was also observed in the upper dermis at all analysed time points but the enrichment of these factors in the lower dermis at e19 time point was significant when compared to their expression in the upper dermis at all analysed time points (Figure 3.41).

In relation to other family members, the activation of both C/EBPbeta and C/EBPdelta is reported to occur before expression of C/EBPalpha and PPARgamma (reviewed by Rosen and Spiegelman, 2000; White and Stephens, 2010). No significant expression of either *Cebpb* or *Cebpd* genes was observed in the LD microarray data at any of the time points. However, the LD microarray data revealed up-regulation on the mRNA level of *Cebpg* gene, which also belongs to the C/EBPs family of transcription factors. *Cebpg* was up-regulated from e17 and at similar levels in both e18 and e19 time points (Figure 3.40C). C/EBPgamma was not mentioned in studies on C/EBPs transcriptional factors crucial in the regulation of adipogenesis (Cao *et al*, 1991; reviewed by Gregoire *et al*, 1998).

A)

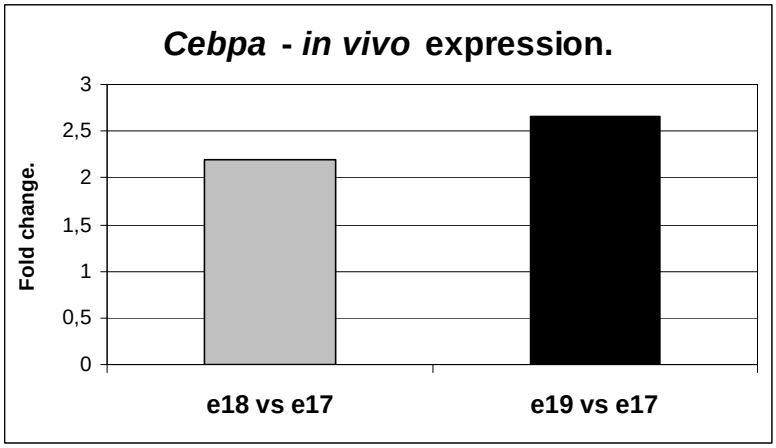


B)

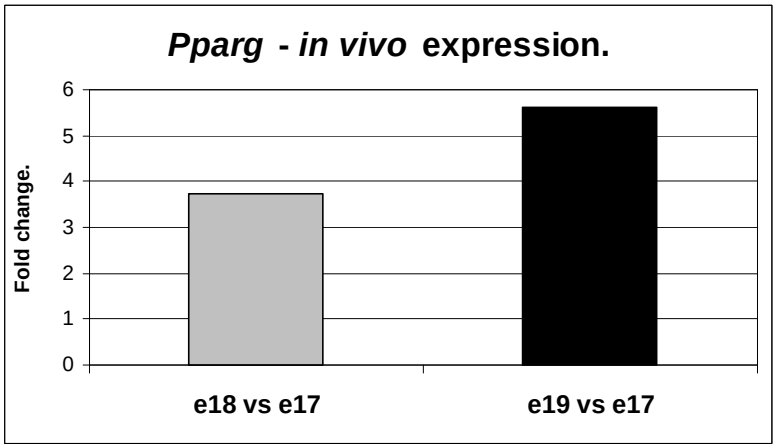


C)

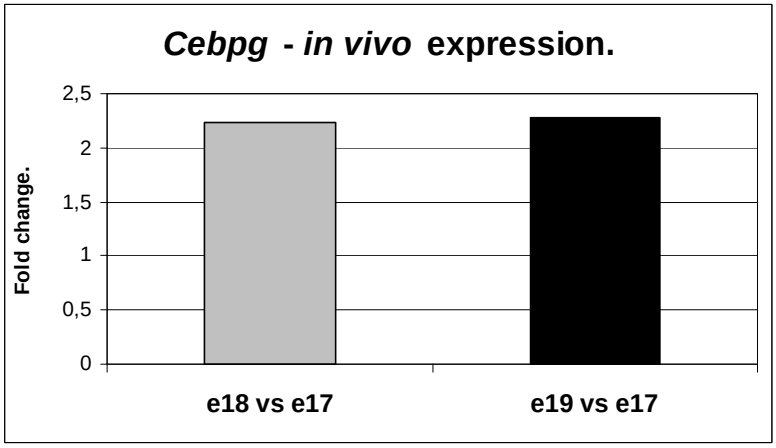


Figure 3.40. The expression profiles of *Cebpa* (A), *Pparg* (B) and *Cebpg* (C) genes in the lower dermis from e17 till e19 time points. Grey columns - regulation at e18 versus e17 time points. Black columns - regulation at e19 versus e17 time points. Fold change values are based on the lower dermis (LD) microarray list. *Cebpa* - CCAAT/enhancer binding protein (C/EBP), alpha. *Pparg* - peroxisome proliferator activated receptor gamma. *Cebpg* - CCAAT/enhancer binding protein (C/EBP), gamma.

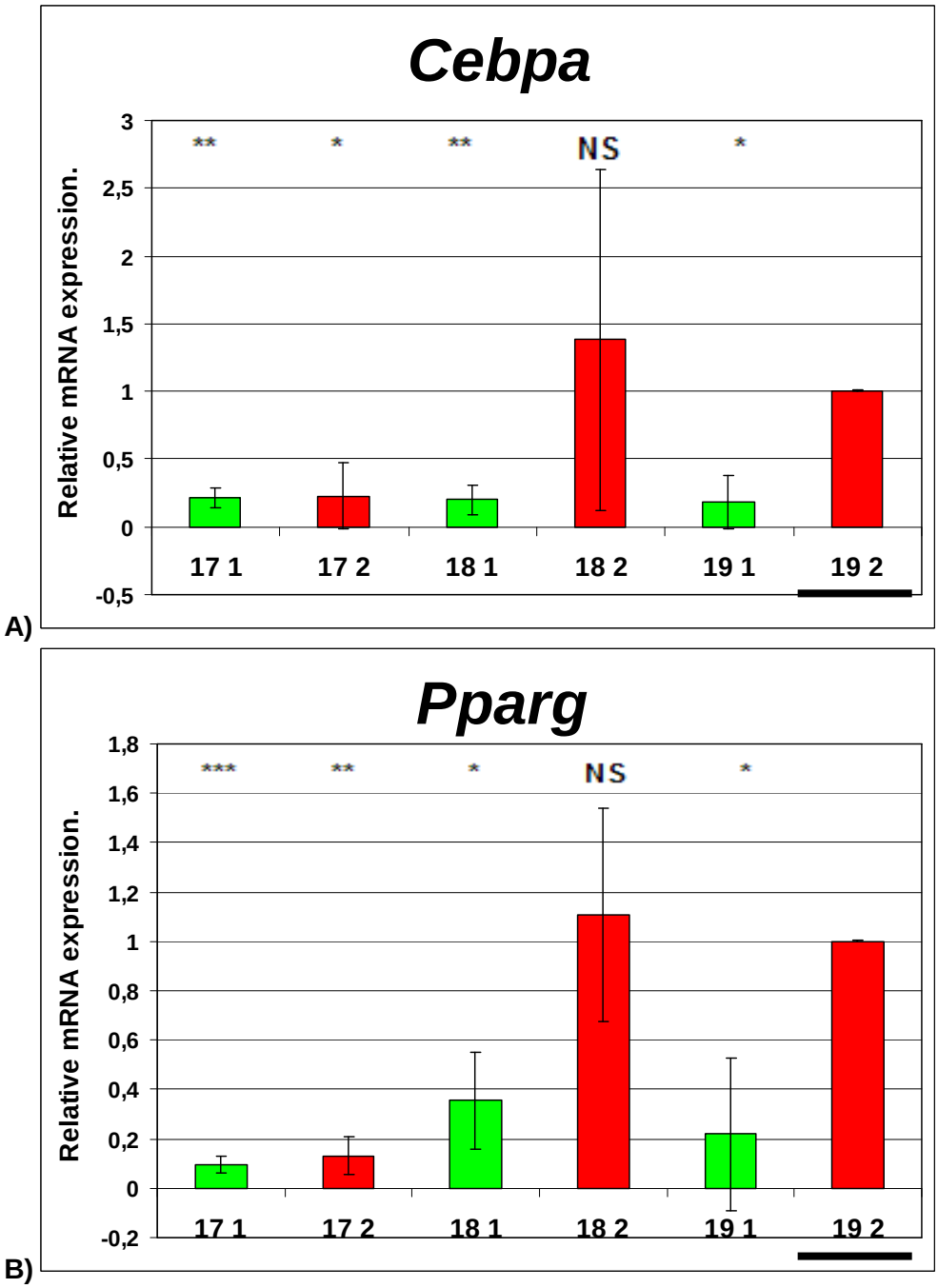


Figure 3.41. Verification of microarray data by qRT-PCR for two genes: *Cebpa* and *Pparg*. The relative mRNA expression for both genes was analysed on samples from dermis at: e17 (17), e18 (18) and e19 (19) time points, from upper (Area "1", green) and lower (Area "2", red) dermis area. Data were obtained from triplicate biological replicates. The baseline (1-fold change) was established for the e19 lower dermis sample (underlined on the figure) and the mRNA levels of the other samples are shown relative to this. Both genes are up-regulated in lower dermis (Area "2") when compared with upper area (Area "1") in e18 and e19 time points. This observation is in agreement with *in vivo* microarray data generated from lower dermal cells. P value refers to the comparison with "19 2" sample (* P <0.05, ** P <0.01, *** P <0.001). The "NS" indicates not significant differences in the mRNA gene expression.

It can be said that several transcription factors, which play an important role in activation and regulation of adipogenesis seen in studies of cell lines, such as 3T3-L1 cells (reviewed by White and Stephens, 2010), are also enriched in lower dermal cells of mouse back skin during late stages of embryonic development (Figure 3.42).

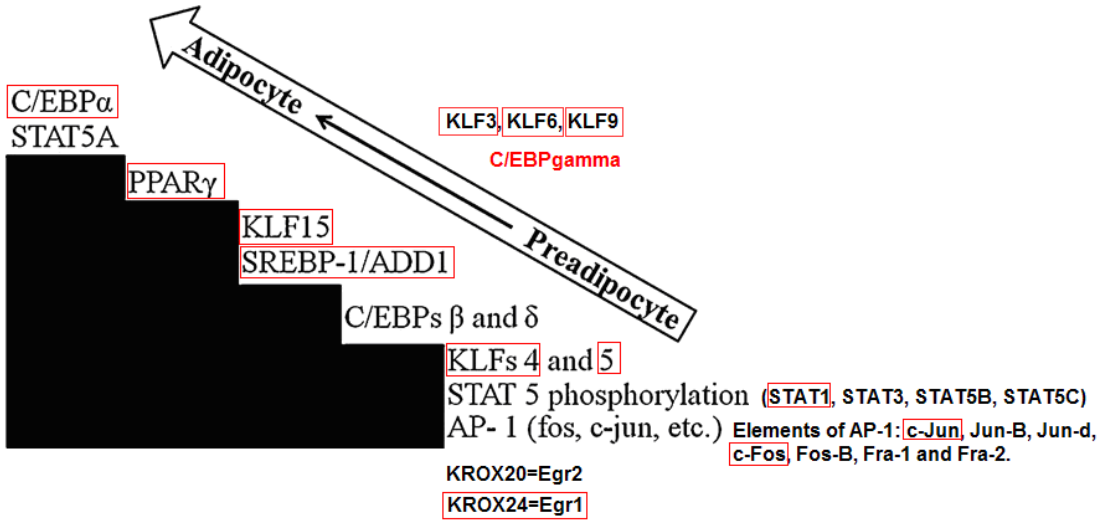


Figure 3.42. Transcription factors activated during adipogenesis. Factors in black are involved in adipogenesis based on available studies mainly on 3T3 cells. Factors marked with red rectangles were regulated in lower dermal cells during mouse embryonic development based on the *in vivo* LD microarray list. The figure was adapted from White and Stephens (2010). Factor written in red (C/EBPgamma) was observed in the *in vivo* LD microarray list, however its involvement in the regulation of adipogenesis has not been considered (see section 3.3.5.1). C/EBPα - CCAAT/enhancer binding protein (C/EBP), alpha. STAT5A - signal transducer and activator of transcription 5A. PPARγ - peroxisome proliferator activated receptor gamma. KLF15 - Krüppel-like factor 15. SREBP-1/ADD1 - *(Srebf1*) sterol regulatory element binding transcription factor 1. C/EBPs β and δ - CCAAT/enhancer binding protein (C/EBP), beta and delta. KLFs 4 and 5 - Krüppel-like factor 4 and 5. STAT1 - signal transducer and activator of transcription 1. STAT3 - signal transducer and activator of transcription 3. STAT5B - signal transducer and activator of transcription 5B. STAT5C - signal transducer and activator of transcription AP-1 - activating protein-1. c-Jun - (*Jun*) Jun oncogene. c-Fos - (*Fos)* FBJ osteosarcoma oncogene. KROX20=Egf2 - early growth response 2. KROX24=Egf1 - early growth response 1.

**Other transcription factors regulated in the lower dermal cells.**

Apart from the transcription factors whose role in adipogenesis has been widely investigated *in vitro* several additional transcriptional factors families were selected from the LD microarray list and examined in relation to available information about their involvement in adipogenesis.

The *Gata2* gene (for the zinc-finger transcription factor: GATA binding protein 2), was down-regulated in lower dermal cells *in vivo* (Figure 3.43A). Previously, expression of this gene was shown to be down-regulated during differentiation *in vitro* of brown adipocytes and it has been suggested that it regulates differentiation of brown fat cell lines and primary cells (Tsai *et al*, 2005).

*Maf* (avian musculoaponeurotic fibrosarcoma (v-maf) AS42 oncogene homolog) and *Mafb* (v-maf musculoaponeurotic fibrosarcoma oncogene family, protein B; avian) genes that encode basic leucine zipper (bZIP) transcription factors were also regulated in lower dermal cells (Figure 3.43B and C). *Maf*, also known as *c-Maf* (based on the genecard website), was down-regulated in dermal arrays from e17 to e19 time points (Figure 3.43B). Previously *c-Maf* gene has been shown to be down-regulated during adipogenesis of mesenchymal fibroblast cells 58 hours after the adipogenic induction by medium in cell culture (Serria *et al*, 2003).

Among other genes involved in regulation of transcription that were identified in the LD microarray data, were *Xbp1* (X-box binding protein 1) and *Smarca5* (SWI/SNF related, matrix associated, actin dependent regulator of chromatin, subfamily a, member 5). Both genes were up-regulated in lower dermal cells *in vivo* (Figure 3.43D and E). *Xbp1* gene has been found previously to undergo a low up-regulation in differentiating 3T3-L1 cells (Hackl *et al*, 2005) whereas no publication was found that would discuss regulation of Smarca5 expression in these cells.

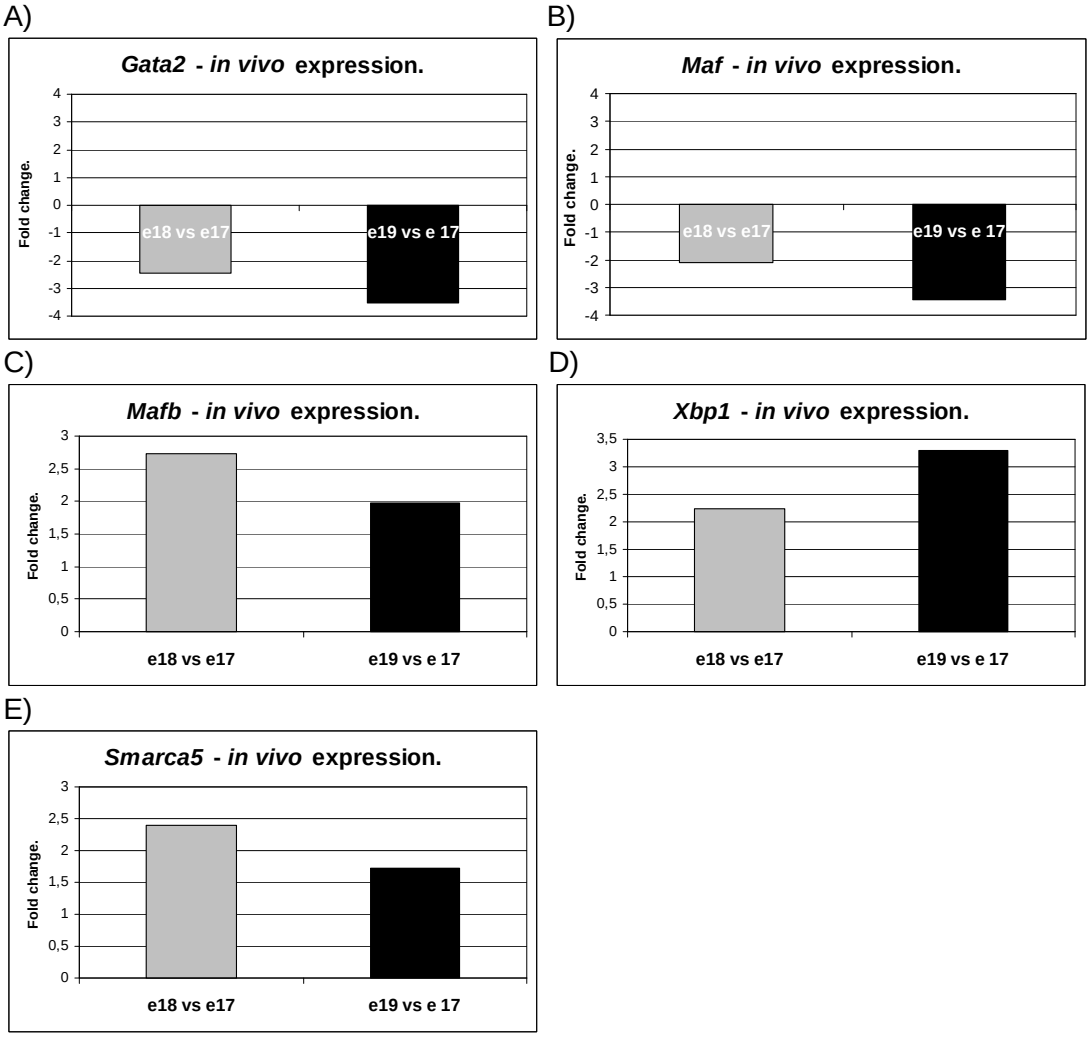


Figure 3.43. The expression profiles of *Gata2* (A), *Maf* (B), *Mafb* (C), *Xbp1* (D) and *Smarca5* (E) genes in the lower dermis from e17 till e19 time points. Grey columns - regulation at e18 versus e17 time points. Black columns - regulation at e19 versus e17 time points. Fold change values are based on the lower dermis (LD) microarray list. *Gata2* - GATA binding protein 2. *Maf* - avian musculoaponeurotic fibrosarcoma (v-maf) AS42 oncogene homolog. *Mafb* - v-maf musculoaponeurotic fibrosarcoma oncogene family, protein B (avian). *Xbp1* - X-box binding protein 1. *Smarca5* - SWI/SNF related, matrix associated, actin dependent regulator of chromatin, subfamily a, member 5.

In order to complete the analysis of transcription factors whose expression changes during adipogenesis, the results of the current work were compared to another study where groups of different transcription factors were either up- or down-regulated during differentiation of 3T3-L1 cells, based on the applied microarray approach (Kim *et al*, 2007). The presence of these genes, regulated during *in vitro* adipogenesis, was checked in the LD microarray list (Table 3.9). Interestingly, among eleven analysed factors from *in vitro* study, only three were present in the *in vivo* LD microarray list, namely *Narg1* (NMDA receptor-regulated gene 1), *Atrx* (alpha thalassemia/mental retardation syndrome X-linked homolog; human) and *Twist1* (twist gene homolog 1; Drosophila). Both *Narg1* and *Atrx* were shown to be up-regulated in 3T3-L1 cells (Kim *et al*, 2007) and accordingly in the dermal arrays both were highly expressed specifically at the e18 time point (Figure 3.44A, B). *Twist1* gene was shown to be down-regulated in differentiating 3T3-L1 cells, and similarly its level decreased from the e17 to e19 time points in the dermal cells *in vivo* (Figure 3.44C).

Another observation was that several representatives of previously discussed transcription factor families were present in the LD microarray list, but their regulation was not discussed by Kim *et al* (2007) in differentiating 3T3-L1 cells. These were *Tsc22d1* (TSC22 domain family, member 1), *Foxp1* (forkhead box P1), *Foxh1* (forkhead box H1), *Foxn3* (forkhead box N3), *Nfix* (nuclear factor I/X), *Fhl1* (four and a half LIM domains 1) and *Twist2* (twist homolog 2; Drosophila) (Table 3.45A - G). These genes were characterised by either down-regulation or up-regulation in lower dermal cells between e17 and e19 time points (Figure 3.45A - G).

Table 3.9. Comparison of transcription factors regulated during *in vitro* (3T3-L1 cells) and *in vivo* (lower dermal cells) adipogenesis. Representatives of several transcription factor families were regulated in differentiating 3T3-L1 cells (microarray study of Kim *et al*, 2007; see left column) and their presence in lower dermal cells (the lower dermis LD microarray data) was analysed (see right column).

| **"*In vitro* up-regulated genes" in 3T3-L1 cells (Kim *et al*, 2007).** | **Presence of "*In vitro* up-regulated genes" (from Kim *et al*, 2007) in lower dermal cells (the LD microarray list).** |
|---|---|
| TSC22 domain family 3 (Tsc22d3) | NP* |
| NMDA receptor-regulated gene 1 (Narg1) | +** |
| Iroquois related homeobox 5 (Drosophila) (Irx5) | NP* |
| Forkhead box B2 (Foxb2) | NP* |
| Alpha thalassemia/mental retardation syndrome X-linked homolog (human) (Atrx) | +** |
| **"*In vitro* down-regulated genes" in 3T3-L1 cells (Kim *et al*, 2007).** | **Presence of "*In vitro* up-regulated genes" (from Kim *et al*, 2007) in lower dermal cells (the LD microarray list).** |
| Activating transcription factor 4 (*Atf4*) | NP* |
| Activating transcription factor 5 (*Atf5*) | NP* |
| Interferon regulatory factor 8 (*Irf8*) | NP* |
| Nuclear factor I/B (*Nfib*) | NP* |
| Twist gene homolog 1 (Drosophila) (*Twist1*) | +** |
| Four and a half LIM domains 2 (*Fhl2*) | NP* |

* gene was not present (NP) in the LD microarray list
** gene was present (+) in the LD microarray list

A)

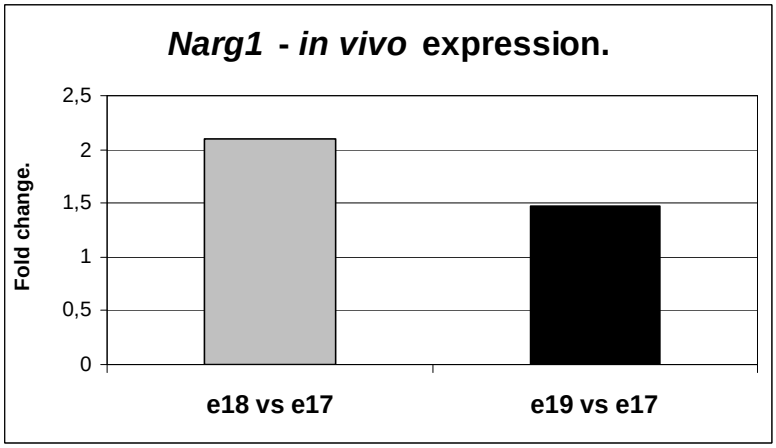


B)

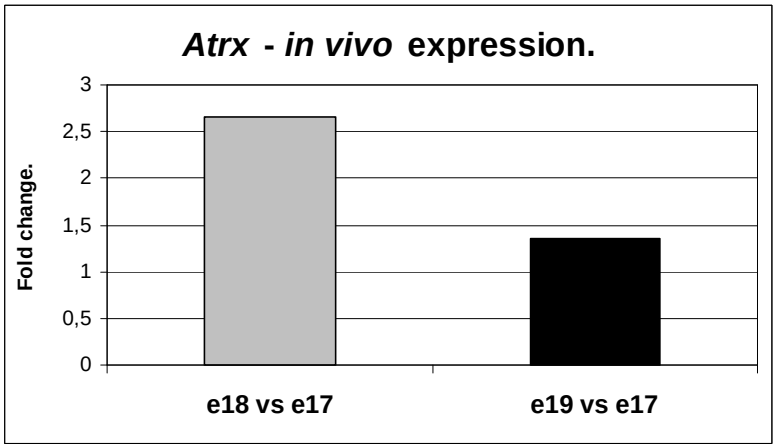


C)


Figure 3.44. The expression profiles of *Narg1* (A), *Atrx* (B) and *Twist1* (C) genes in the lower dermis from e17 till e19 time points. Grey columns - regulation at e18 versus e17 time points. Black columns - regulation at e19 versus e17 time points. Fold change values are based on the lower dermis (LD) microarray list. *Narg1* - NMDA receptor-regulated gene 1. *Atrx* - alpha thalassemia/mental retardation syndrome X-linked homolog (human). *Twist1* - twist gene homolog 1 (Drosophila).

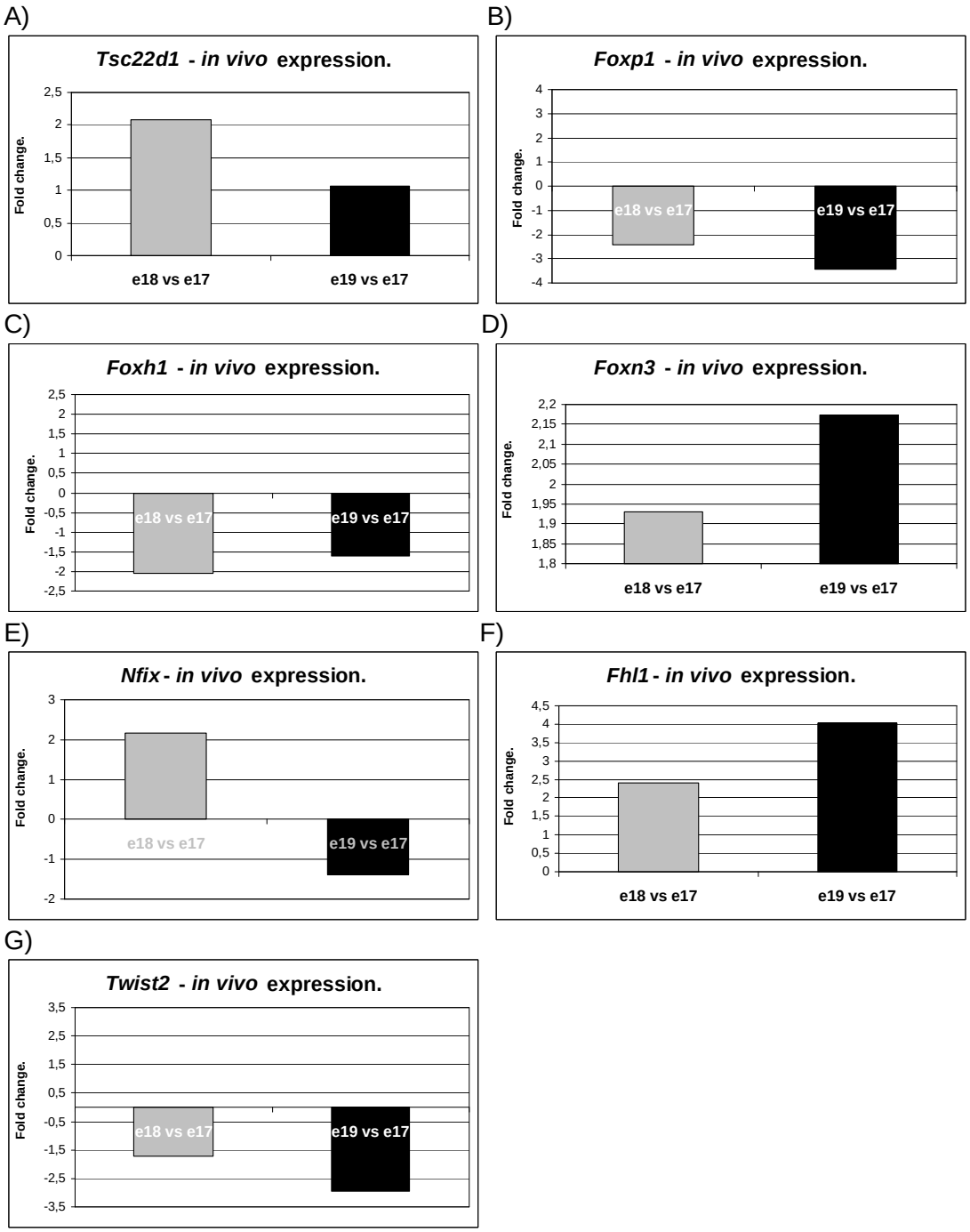


Figure 3.45. The expression profiles of *Tsc22d1* (A), *Foxp1* (B), *Foxh1* (C), *Foxn3* (D), *Nfix* (E), *Fhl1* (F) and *Twist2* (G) genes in the lower dermis from e17 till e19 time points. Grey columns - regulation at e18 versus e17 time points. Black columns - regulation at e19 versus e17 time points. Fold change values are based on the lower dermis (LD) microarray list. *Tsc22d1* - TSC22 domain family, member 1. *Foxp1* - forkhead box P1. *Foxh1* - forkhead box H1. *Foxn3* - forkhead box N3. *Nfix* - nuclear factor I/X. *Fhl1* - four and a half LIM domains 1. *Twist2* - twist homolog 2 (Drosophila).

### 3.3.5.2. Pref-1, growth hormone and growth factors.

The cell line-based studies revealed that different genes are involved in the regulation of adipogenesis activation and are crucial for a proper activation of the whole adipogenic cascade and such factors are discussed in this section. In addition, a presence of such factors in the *in vivo* LD microarray data is analyed in order to establish how similar or different processes observed in embryonic back skin are to differentiation of cells *in vitro* that develop into mature adipocytes.

**Pref-1.**

A preadipocyte marker Pref-1 has been characterised and treated as inhibitor of adipogenesis (Wang *et al*, 2006a; Wang *et al*, 2010). It is a EGF repeat-containing transmembrane protein expressed abundantly by 3T3-L1 preadipocytes and not present in mature fat cells (Smas and Sul, 1993). As lower dermal cells from e17 time point were suggested to represent preadipocytes *in vivo*, it was expected to see dramatic down-regulation of Pref-1 mRNA level from e17 to e19 time points. However gene for Pref-1 was not present in the generated *in vivo* LD microarray data which could suggest lack of its regulation during development of dermal cells *in vivo* between e17 and e19 time points.

**Growth hormone (GH).**

A growth hormone (GH), which regulates transcription of IGF-1, influences adipose tissue and regulates metabolism, was shown to be crucial for differentiation of mouse cell lines 3T3-L1 and 3T3-F442A however no effect of GH was seen on primary cell lines (reviewed by Gregoire *et al*, 1998). GH functions through growth hormone receptor for which up-regulation has been spotted in differentiating 3T3-L1 cells (Hackl *et al*; 2005; Kawai *et al*, 2007; see also Figure 3.46A). The up-regulation of growth hormone receptor (*Ghr*) mRNA was observed *in vivo* in developing lower dermal cells, with a dramatic increase in expression at the e19 time point (Figure 3.46B).

**Growth factors.**

In order to activate adipogenic differentiation, cells are required to obtain appropriate signals from the environment in a form of different growth factors, depending on type of cell line (reviewed by Gregoire *et al*, 1998).

**Insulin-like growth factors.**

The insulin-like growth factors genes: *Igf1* and *Igf2* were present in the lower dermal microarray data. *Igf1* was enriched, whereas *Igf2* was down-regulated from e17 to e19 (Figure 3.46D and F). Previously both *Igf1* and *Igf2* were shown to be highly up-regulated in differentiating 3T3-L1 cells after 24 hours of adipogenic induction (Burton *et al*, 2004; Hack *et al*, 2005; see Figure 3.46C and E). In addition, the up-regulation of the Igf1 receptor (*Igfr1r*) was spotted in lower dermal cells (Figure 3.46K) as well as the increased expression of insulin-like growth factor binding protein genes, such as *Igfbp3*, *Igfbp4* and *Igfbp7* (Figure 3.46I and J). Two previous microarray-based studies from Burton *et al* (2004) and Hack *et al* (2005) on 3T3-L1 cells showed regulation of *Igfbp4*, however they revealed different regulation patterns for this genes (compare Figure 3.46G with H). The IGBFP3 protein was suggested to be an inhibitor of adipogenesis in 3T3-L1 cells (Chan *et al*, 2009).

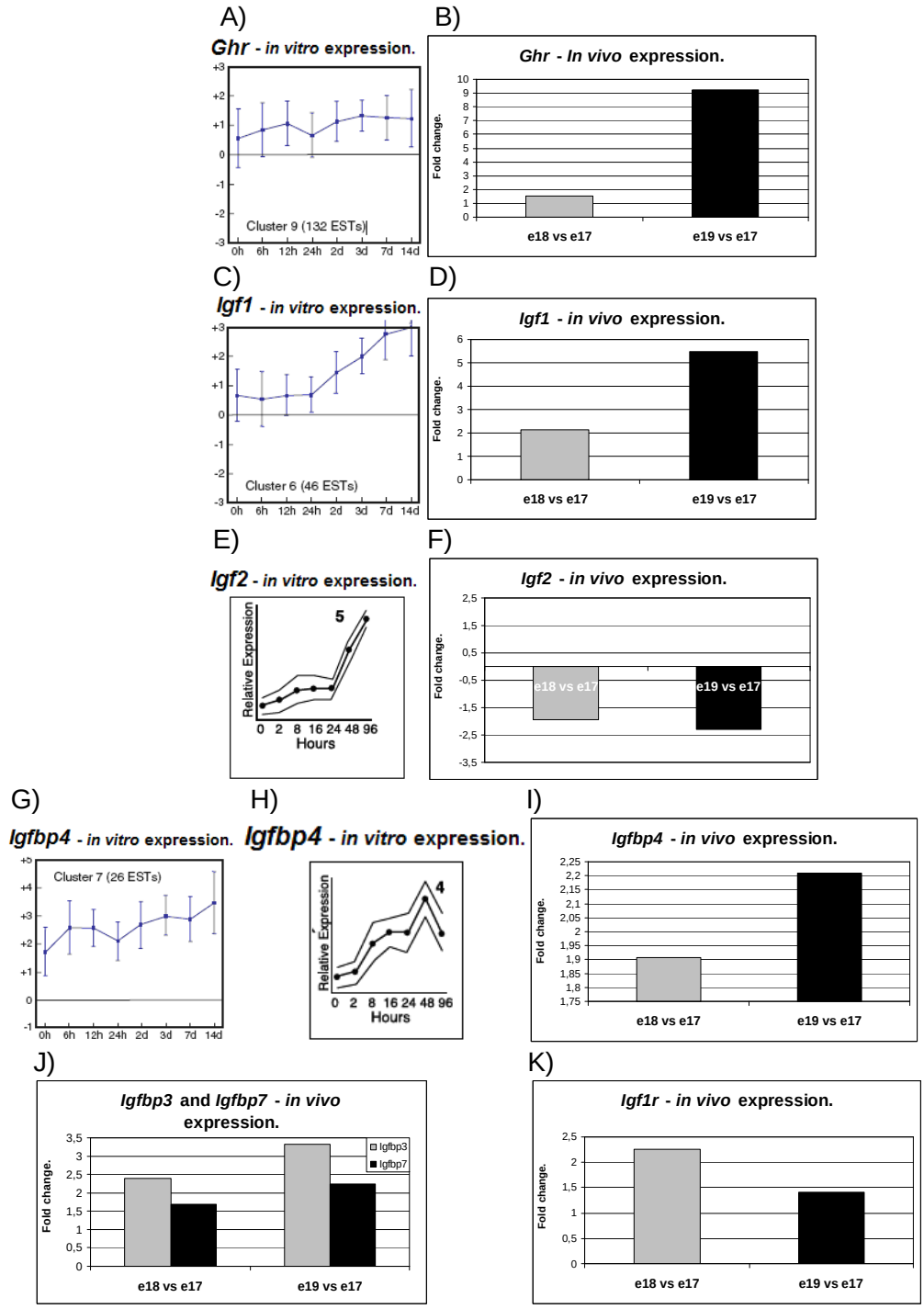


Figure 3.46. The expression profiles of *Ghr* (A, B), *Igf1* (C, D), *Igf2* (E, F), *Igfbp4* (G, H, I), *Igfbp3* (J), *Igfbp7* (J) and *Igf1r* (K) genes. (A, C, E, G, H) The expression profiles of analysed genes during *in vitro* adipogenesis in 3T3-L1 cells (based on Burton *et al*, 2004; Hackl *et al*, 2005). (B, D, F, I, J, K) The expression profiles of selected genes in the lower dermis from e17 till e19 time points. Grey columns - regulation at e18 versus e17 time points. Black columns - regulation at e19 versus e17 time points. Fold change values are based on the lower dermis (LD) microarray list. *Ghr* - growth hormone receptor. *Igf1* - insulin-like growth factor 1. *Igf2* - insulin-like growth factor 2. *Igfbp4* - insulin-like growth factor binding protein 4. *Igfbp3* - insulin-like growth factor binding protein 3. *Igfbp7* - insulin-like growth factor binding protein 7. *Igf1r* - insulin-like growth factor I receptor.

**Other growth factors.**

There are several growth factors suggested to be mainly related with inhibition of adipogenesis (reviewed by Gregoire *et al*, 1998; reviewed by Rosen and Speigelman, 2000). Among these are epidermal growth factor (EGF) or transforming growth factor alpha (TGF-alpha) (reviewed by Gregoire *et al*, 1998). *Tgfa* and *Egf* genes were not seen in the LD microarray data, however specific expression pattern of Egf receptor (*Egfr*) was observed in lower dermal cells (Figure 3.47A). Because of the uncertain role of Egf-Egfr pathway in adipogenesis regulation *in vivo* in relation to back skin adipose tissue, the detailed analysis of this factor in relation to adipocyte differentiation in mouse embryonic back skin dermis was performed and is presented in Chapter 4 of this thesis. Other growth factors, with suggested involvement in regulation of adipogenesis but with no clarified role in this process are basic fibroblast growth factor (bFGF; FGF2) and platelet-derived growth factor (PDGF) (Neubauer *et al*, 2004; reviewed by Rosen and Spiegelman). Genes for these two factors were not present in the LD microarray data. However, genes for fibroblast growth factor receptor 2 (*Fgfr2*) and platelet-derived growth factor receptor, alpha (*Pdgfra*) were found in the LD data with specific gene expression patterns (Figure 3.47B and C). The mRNA expression for all three receptors was highly up-regulated in lower dermal cells at the e18 time point. At the e19 time point the *Pdgfra* mRNA level underwent the most dramatic down-regulation when compared with e17 time point. These observations tallied with other verification work on the protein level by immunofluorescence staining against PDGFRa, which also showed a marked decrease in its expression in the lower dermis at e19 (see Figure 3.22).

To sum up, lower dermal cells are characterised by a dynamic regulation, at mRNA level, growth hormone receptor and several growth factor receptors (Egfr, *Fgfr2*, *Pdgfra*, *Igfr*) together with insulin-like growth factors (*Igf1* and *Igf2*) and insulin growth factor binding proteins (*Igfbp3*, *Igfbp4* and *Igfbp7*) between e17 and e19 time points (Figure 3.48).

A)

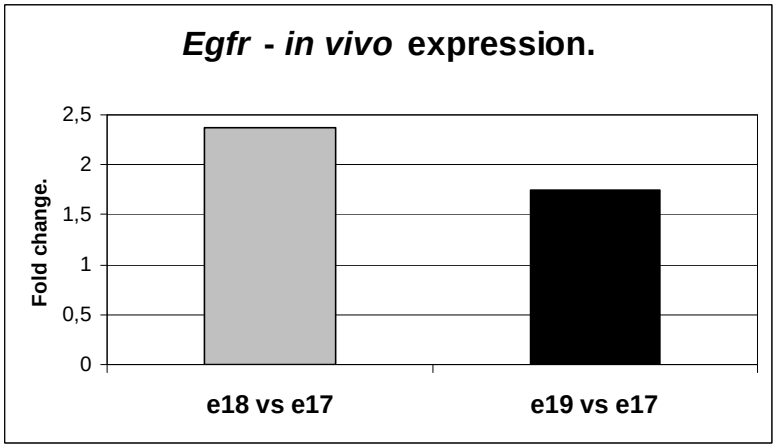


B)

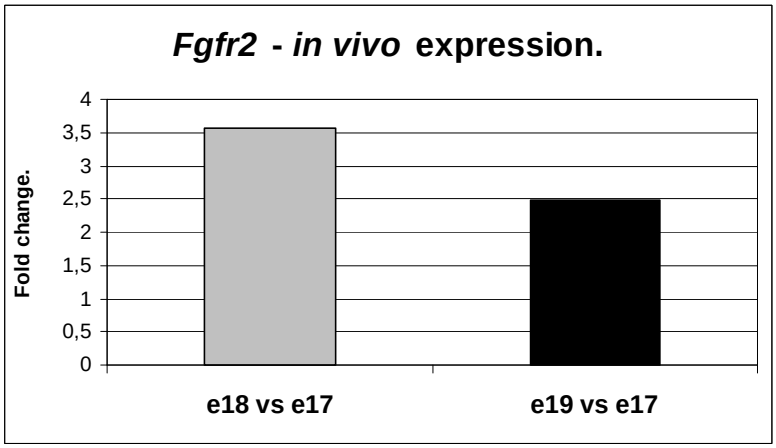


C)

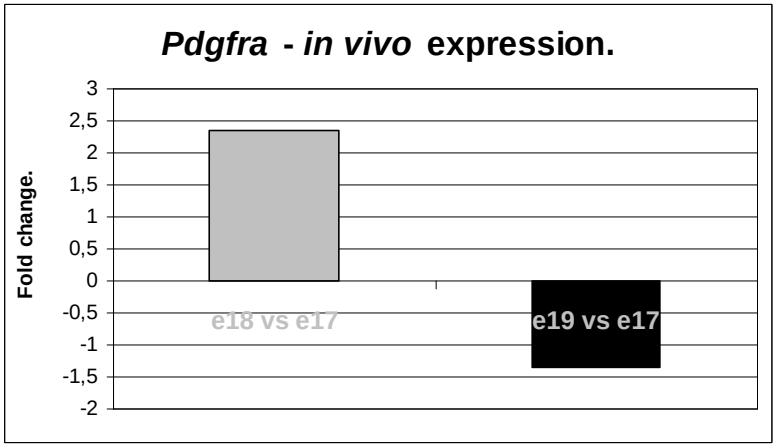


Figure 3.47. The expression profiles of *Egfr* (A), *Fgfr2* (B) and *Pdgfra* (C) genes in the lower dermis from e17 till e19 time points. Grey columns - regulation at e18 versus e17 time points. Black columns - regulation at e19 versus e17 time points. Fold change values are based on the lower dermis (LD) microarray list. *Egfr* - epidermal growth factor receptor. *Fgfr2* - fibroblast growth factor receptor 2. *Pdgfra* - platelet-derived growth factor receptor, alpha polypeptide.

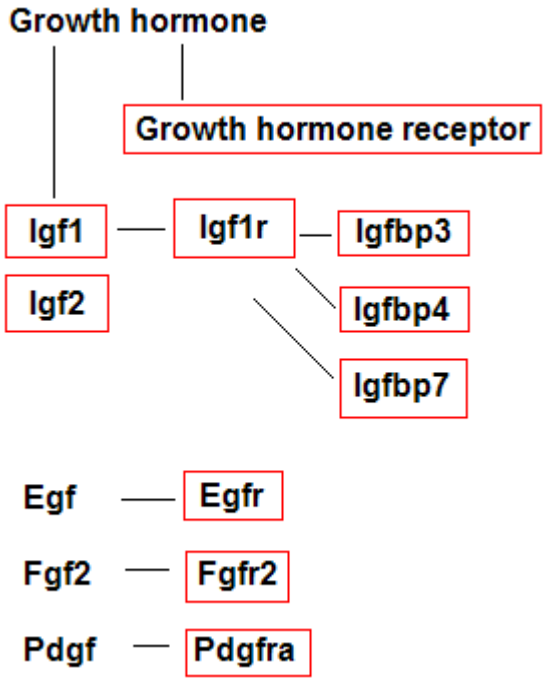


Figure 3.48. The lower dermis (LD) microarray data revealed regulation of growth hormone receptor, several growth factors, growth factor receptors and growth factor binding proteins (marked with red rectangles) in lower dermal cells. For the full names of presented receptors, factors and proteins see section 3.3.5.2 and Figures 3.46 - 3.47.

### 3.3.5.3. Cell cycle processes involved in adipogenesis.

Based on the knowledge about adipogenesis from cell lines (Chapter 1, section 1.3.1.1) growth arrest, together with the occurrence of confluence (or its lack, depending on the cell type), is the first step of the activation of adipogenesis *in vitro* (Rosen and Spiegelman, 2000). This growth arrest is followed by a clonal expansion process and cells require factors which activate/enhance the next steps of differentiation. During the clonal expansion one or two rounds of cell division take place (Ailhaud *et al*, 1989; Rosen and Spiegelman, 2000; see also Chapter 1, section 1.3.2.1). Preadipocytes need the influence of growth factors in order to undergo adipogenic modification, while the expression of so-called adipogenic transcriptional factors takes places in a very specific pattern (see sections 3.3.5.1 and 3.3.5.2).

Genes associated with the cell cycle and observed during 3T3-L1 differentiation have been summarised in a microarray-based study by Hackl *et al* (2005). To perform the comparative study a summary/digest of the 3T3-L1 study is shown in Figure 3.49A, taken from a supplementary data from this paper and adjusted for the analysis presented in this section. Figure 3.49A, represents genes seen by Hackl *et al* (2005) in 3T3-L1 cells (written in green or blue or marked by coloured circles). The presence of genes from this data was cross-checked with the LD microarray data and when genes were found in the dermal array data they were marked by red rectangles (Figure 3.49A). In addition, where *in vitro* associated genes were not present in the LD arrays, but other representatives of their families were found *in vivo*, these were also included (in Figure 3.49A, shown by yellow rectangles). There were also cell cycle genes in non-coloured circles, if they were not seen in both *in vitro* and *in vivo* cells. If a gene in non-coloured circle was additionally marked by a red rectangle, its presence was only seen *in vivo*. In total, for all analysed genes from Figure 3.49A, only 21% were common for both *in vitro* and *in vivo* differentiating cells, 32% were specific for only the lower dermal cells and 37% were found only in the microarray data from 3T3-L1 cells (Figure 3.49B).

In total, 14 genes were common for both *in vitro* and *in vivo* differentiating cells. Of these 14 genes, 9 were highly enriched *in vitro* at 24 hours after adipogenic induction (Figure 3.50A) whereas the other five were up-regulated between 12 and 24 hours after induction (Figure 3.50C). When the expression pattern of these genes was investigated *in vivo*, 13 genes were highly up-regulated at the e18 versus e17 time point (Figure 3.50B and D). Their expression change at e19 versus e17 was

lower when compared with expression change at e18 versus e17 (Figure 3.50B and D). Only one gene, centromere protein A (*Cenpa*) did not share the same expression pattern as it was down regulated from e17 (Figure 3.50B - gene marked by black star).

In order to complete the analysis of cell cycle related genes during adipogenic differentiation, the microarray data on 3T3-L1 cells from Burton *et al* (2002) and Burton *et al* (2004) were also used in this study. During the early stages of *in vitro* adipocyte differentiation, specific activation of growth arrest and DNA damage genes (GADDs) and proteins involved in regulation of the cell cycle (such as GADD153, p18 or p21) have been described (reviewed Gregoire *et al*; 1998, Burton *et al* 2002, Burton *et al*, 2004). In the LD microarray data, changes in mRNA levels for *Gadd153* or p21 (*Cdkn1a*) were not found. However *Gadd45g* mRNA was observed to change in lower skin dermis, with the highest up-regulation at e18 (Table 3.10). *Gadd45* is believed to be under the control of the adipogenic transcriptional factor C/EBPalpha (Constance *et al*, 1996), as is p21 (Timchenko *et al*, 1996). Richon *et al* (1997) shown that in cells before adipogenic treatment (day 0) and then 1, 2 3 or 4 days after adding adipogenic factors, dramatic changes in protein levels can occur with p107, p130 and p107-E2F or p130-E2F complexes (Richon *et al*, 1997). These changes were related to specific activities following the experimental induction of adipogenesis *in vitro,* where a reported growth arrest phase is followed by a clonal expansion step. At the mRNA level, p107 gene (*Rbl1*) was observed to be up-regulated at day 1, and then its level subsequently decreased (Richon *et al*, 1997). This expression pattern was not observed for p107 mRNA in work described in this thesis, and the p107 gene (*Rbl1*) was not present in the generated LD microarray list.

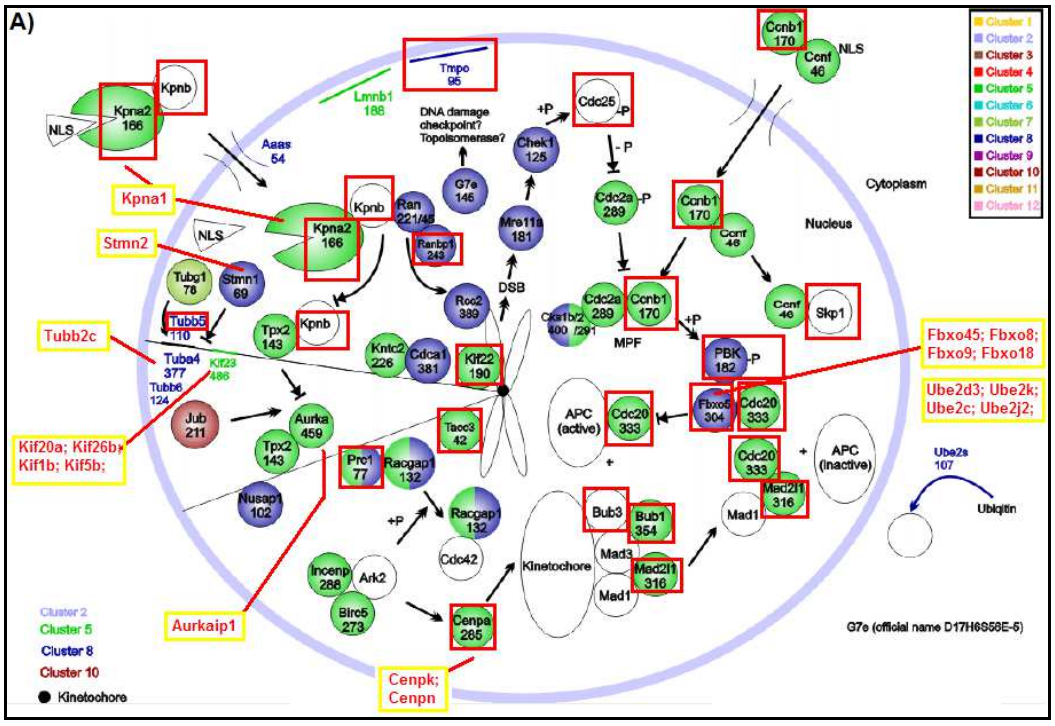


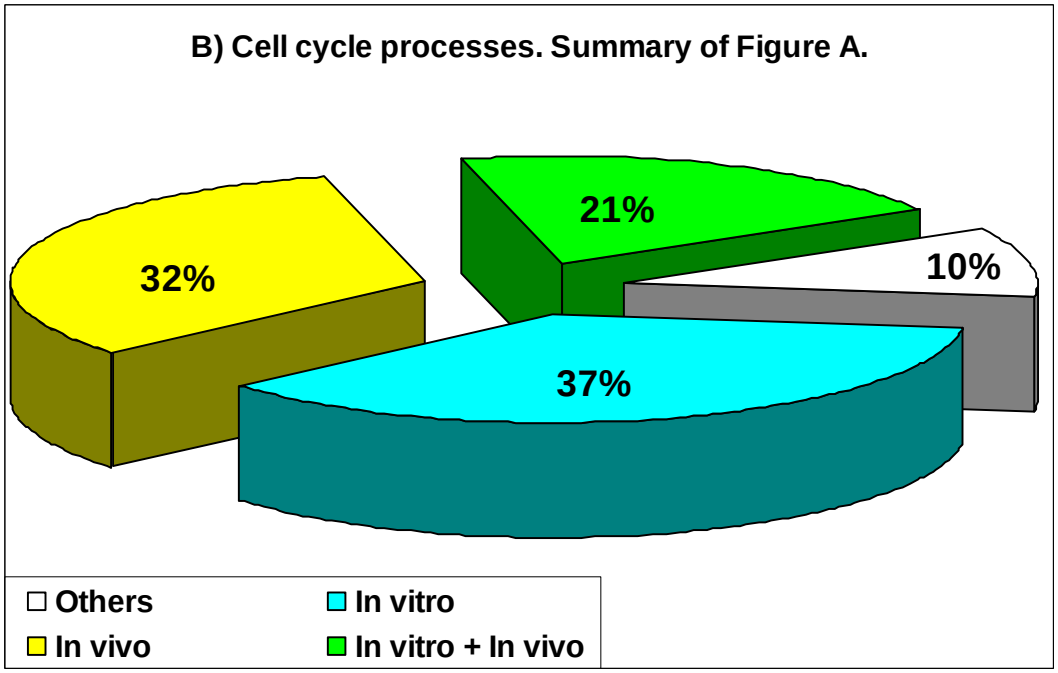


Figure 3.49. Genes associated with cell cycle processes during adipogenic differentiation *in vitro* (3T3-L1 cells) and *in vivo* (cells from lower dermis in mouse embryonic back skin). The analysis is based on microarray approach. (A) Figure A was adapted from Hackl *et al* (2005) and *in vivo* microarray data was compared with *in vitro* data from Hackl *et al*, 2005. Genes regulated *in vitro* are marked with coloured circles or are written in blue or green, whereas genes spotted *in vivo* are marked with red rectangles. In addition, genes spotted only *in vivo* and not observed by Hackl *et al* (2005) are shown by yellow rectangles or marked with both non-coloured circles and red rectangles. (B) The summary of Figure A. Yellow-In vivo: genes seen *in vivo* but not observed in 3T3-L1 cells. Blue-In vitro: genes observed during *in vitro* differentiation but not *in vivo*. Green-In vitro + In vivo: genes seen in both *in vitro* and *in vivo* cells. White-Others: cell cycle genes/components presented on Figure A not observed in both *in vitro* and *in vivo* cells.

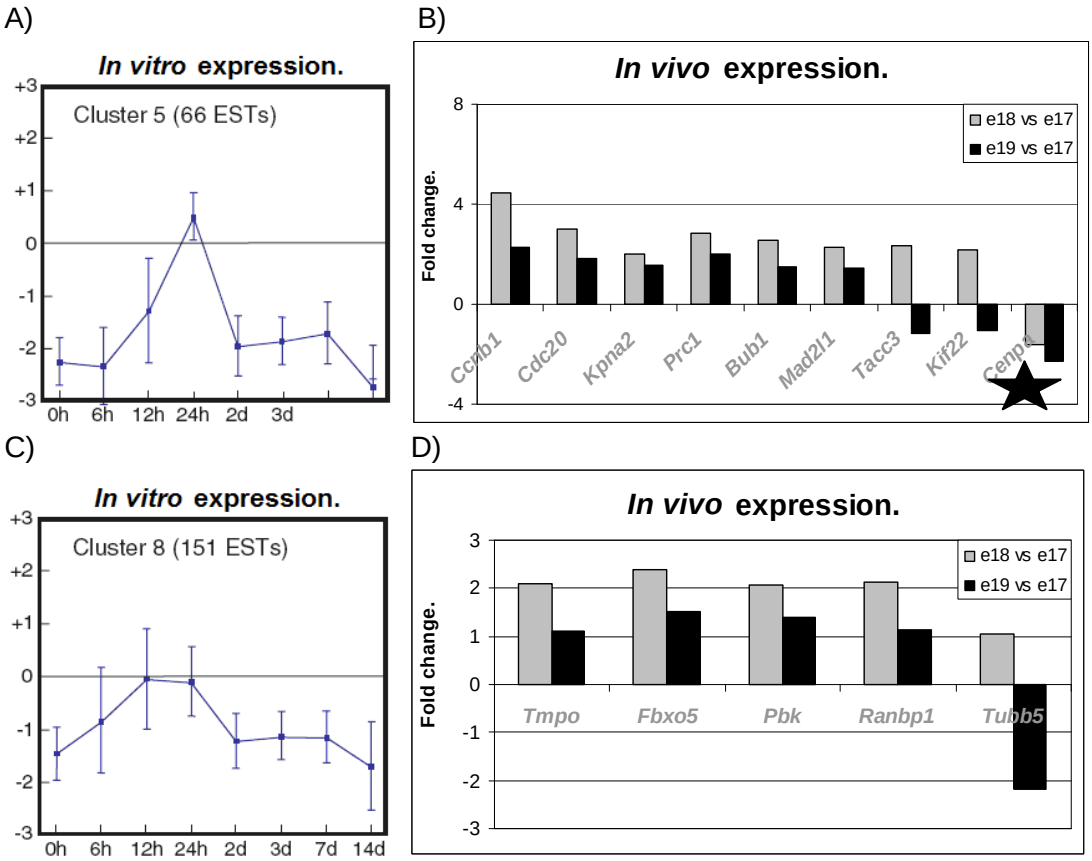


Figure 3.50. The expression profiles of genes related with cell cycle processes. (A, C) The expression profiles of cell cycle genes observed in differentiating 3T3-L1 cells (based on Hackl *et al*, 2005). (B, D) The expression profiles of cell cycle genes in the lower dermis from e17 till e19 time points. Grey columns - regulation at e18 versus e17 time points. Black columns - regulation at e19 versus e17 time points. Fold change values are based on the lower dermis (LD) microarray list. Genes common for *in vivo* and *in vitro* cells (A - D) were classified by Hackl *et al* (2005) into two clusters because of their up-regulation *in vitro* (in 3T3-L1 cells) approximately 12 - 24h following adipogenic induction and then their subsequent progressive down-regulation (see A and C). Majority of these genes spotted in *in vivo* were highly up-regulated from e17 time point (B and D), except for the *Cenpa* gene (B - marked with a star). *Ccnb1* - cyclin B1. *Cdc20* - cell division cycle 20 homolog (S. cerevisiae). *Kpna2* - karyopherin (importin) alpha 2. *Prc1* - protein regulator of cytokinesis 1. *Bub1* - budding uninhibited by benzimidazoles 1 homolog (S. cerevisiae). *Mad2l1* - MAD2 mitotic arrest deficient-like 1 (yeast). *Tacc3* - transforming, acidic coiled-coil containing protein 3. *Kif22* - kinesin family member 22. *Cenpa* - centromere protein A. *Tmpo* - thymopoietin. *Fbxo5* - F-box protein 5. *Pbk* - PDZ binding kinase. *Ranbp1* - RAN binding protein 1. *Tubb5* - tubulin, beta 5.

Table 3.10. Genes related with progression of adipocyte differentiation *in vitro* and their presence or absence in the lower dermis (LD) microarray list (*in vivo* adipogenesis).

| ***In vitro* studies on cell cycle components:** | | **Lower dermis (LD) microarray data (*in vivo* approach):** | |
|---|---|---|---|
| | | **e18 versus e17 (fold change)** | **e19 versus e17 (fold change)** |
| p21/SDI-1 (cyclin-dependent kinase inhibitor 1A: *Cdkn1a*) | Cell cycle component which level (both mRNA and protein) is increased by C/EBPalpha (Timchenko *et al*; 1996). mRNA level slightly decreased 1 day after adipogenic induction* and then its gradual increase from day one was seen (Morrison and Farmer, 1999). | NP** | |
| p27 (cyclin-dependent kinase inhibitor 1B: Cdkn1b) | mRNA level dramatically decreased till day 2 after adipogenic induction*, next a slight increase is seen till day 6 of induction*. (Morrison and Farmer, 1999). | NP** | |
| p18 (cyclin-dependent kinase inhibitor 2C: *Cdkn2c*) | The level of p18 was induced by PPARgamma in NIH-3T3 fibroblasts (Morrison and Farmer, 1999). In 3T3-L1 cells, low p18 mRNA level seen at day 0, disappears at day 1 and 2 of induction*, then an increase of p18 is seen from day 3 of induction*. | + 3.779247*** | + 3.988036*** |
| p107 (retinoblastoma-like 1:*Rbl1*) | mRNA level dramatically increased approximately 24 hours after induction*. Next, its level decreased at day 2, 3 and 4 after adipogenic induction (Richon *et al*, 1997) | NP** | |
| *Gadd153* (DNA-damage-inducible transcript 3: *DDIT3)* | The growth arrest gene mRNA levels presented in cells before adipogenic induction* (day 0) dramatically decreased 2 hours after the adipogenic induction in 3T3 cells (Burton *et al*; 2002). | NP** | |
| *Gadd45* (growth arrest and DNA-damage-inducible, alpha: DDIT1) | Expresssed in differentiated 3T3-L1 cells and regulated by C/EBPalpha (Constance *et al*; 1996). | + 5.532627*** | + 3.565415*** |

* treatment of analysed cells with adipogenic medium which factors activate fat cell differentiation cascade (see Chapter 1, part 1.3.2.2 for more details).
** gene was not present (NP) in the LD microarray list
*** gene was present in the LD microarray list and up-regulated from e17 time point

### 3.3.5.4. The use of GeneCoDis 2.0 (gene annotations co-occurrence discovery) tool for the analysis of cytoskeletal and extracellular matrix genes.

First the lower dermis (LD) data underwent analysis by the GeneCoDis 2.0 tool in order to get a view on such features of these genes as cellular localisation. It is known, from *in vitro* studies, that during very early stages of adipogenic differentiation (after reaching the confluence and during the up-regulation of C/EBPalpha and PPARgamma; Spiegelman and Farmer, 1982; reviewed by Gregoire *et al*, 1998) changes in cytoskeletal proteins and extracellular matix components (EMC) are taking place which are crucial for the development and maintenance a specific architecture/morphology of fat cells (reviewed by Mariman and Wang, 2010). The lower dermis (LD) microarray data was divided into two sub-lists (a sub-list with genes of fold change equal and more than 2 at e19 vs e17 and the sub-list with genes lower than 2 at e19 vs e17) that were next analysed by the GeneCoDis tool. The division was needed because of the limitation in number of genes that can be analysed at the same time by GeneCoDis tool. The GeneCoDis 2.0 tool allowed the investigation of cellular localisation (Gene ontology_Cellular Component; GO_CC) of genes differently expressed in the lower skin dermis. The GeneCoDis is a freely available tool for the analysis of biological features of a given gene group (Carmona-Saez *et al*, 2007; Nogales-Cadenas *et al*, 2009). The microarray data underwent the analysis by GeneCoDis 2.0 tool and groups with the highest number of genes associated with a term for cytoskeletal proteins or a term for extracellular matrix components - EMC ("proteinaceous extracellular matrix") were selected. The term "cytoskeleton" (GO:0005856) was defined as "…any of the various filamentous elements that form the internal framework of cells…" (citation from: http://amigo.geneontology.org/cgibin/amigo/term_details?term=GO:0005856).

Finally, term "proteinaceous extracellular matrix" (GO:0005578), defined as "…A layer consisting mainly of proteins (especially collagen) and glycosaminoglycans (mostly as proteoglycans) that forms a sheet underlying or overlying cells such as endothelial and epithelial cells…" (citation from: http://amigo.geneontology.org/cgi-bin/amigo/term_details?term=GO:0005578) was used for the selection of EMC from the microarray data.

The presence of genes from the *in vivo* LD list, classified into either "cytoskeleton" or "proteinaceous extracellular matrix" term was further analysed in microarray data from *in vitro* differentiating adipocytes (3T3-L1 cells) (microarray studies from Burton *et al*, 2004; Hackl *et al*, 2005; Kim *et al*, 2007). This comparison verified how many "cytoskeleton" or "proteinaceous extracellular matrix" genes are common for both *in vitro* (3T3-L1) and *in vivo* cells (from lower dermis) (see below).

**Cytoskeleton proteins.**

The group of 64 genes associated with "cytoskeleton" term (by GeneCoDis 2.0 tool) from the *in vivo* LD microarray data was compared with several *in vitro* microarray studies (Burton *et al*, 2004; Hackl *et al*, 2005 and Kim *et al*, 2007). Only 25% of *in vivo* "cytoskeleton" genes were found in differentiating 3T3-L1 cells (Figure 3.51) therefore the majority of cytoskeletal genes from the lower dermal cells (75%) were not present on any of the *in vitro* microarray lists.

The analysis of differentiating 3T3-L1 cells revealed important changes in the levels of several cytoskeletal components and Spiegelman and Farmer (1982) showed a dramatic decrease in gene expression of actin (beta and gamma) and tubulin (alpha and beta) during adipogenic differentiation. The microarray work by Hackl *et al* (2005) confirmed the specific changes in these cytoskeleton proteins and showed specifically that between first 6 and 12 hours of adipogenic induction in 3T3-L1 cells there was up-regulation of *Acta1* (alpha actin) and *Actg1* (gamma actin) but then after 12 hours a decrease of these genes took place (Figure 3.52A and C). For the *in vivo* LD data presented in this Chapter, only the *Acta1* gene was specified and its expression profile showed a general up-regulation from e17 to e19 (Figure 3.52B). The Hackl *et al* (2005) study has also revealed specific expression pattern for tubulin alpha (*Tuba4*) and tubulin beta (*Tubb5*) in 3T3-L1 cells (Figure 3.52D and F). Expression of *Tuba4* and *Tubb5* decreased after 24 hours of adipogenic induction. Only tubulin beta (*Tubb5*) was found on the LD cell array list (Figure 3.52E). Moreover, this gene was up-regulated at e18 versus e17 but its down-regulation was observed at e19 versus e18 time points (Figure 3.52E).

Hackl *et al* (2005) showed also that in 3T3-L1 cells other cytoskeleton components are undergoing clear down-regulation after 12 hours (for example: Myosin light chain 2; tropomyosin 1 and 2; fascin homolog 1; transgelin 1 or Calponin 2) or 24 hours (for example transgelin 2) of adipogenic induction therefore they share expression profiles either with *Acta1* and *Actg1* genes (Figure 3.52A and C; Cluster 10) or with *Tuba4* and *Tubb5* genes (Figure 3.52D and F; Cluster 8). The

presence of these seven genes (Myosin light chain 2; tropomyosin 1 and 2; fascin homolog 1; transgelin 1, Calponin 2 and transgelin 2) was checked in the LD microarray list and only three genes (tropomyosin 1; transgelin and transgelin 2) were spotted in lower dermal cells (Figure 3.53A - C). All these three genes were up-regulated from e17 time point (Figure 3.53A - C).

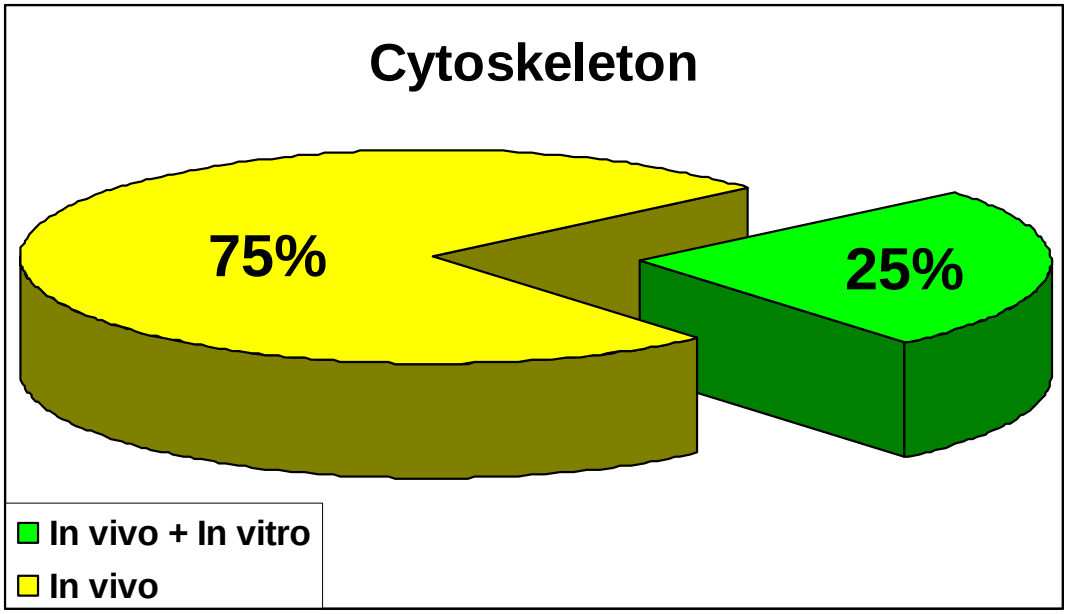


Figure 3.51. Cytoskeleton genes. Genes from the lower dermis (LD) microarray data that were associated with the cytoskeleton term by GeneCoDis 2.0 tool and their presence/absence was analysed in 3T3-L1 cells undergoing adipogenesis (based on *in vitro* microarray data from Burton *et al*, 2004; Hackl *et al*, 2005; Kim *et al*, 2007). Yellow-In vivo: genes seen *in vivo* but not observed in 3T3-L1 cells. Green-In vitro + In vivo: genes seen in both differentiation processes.

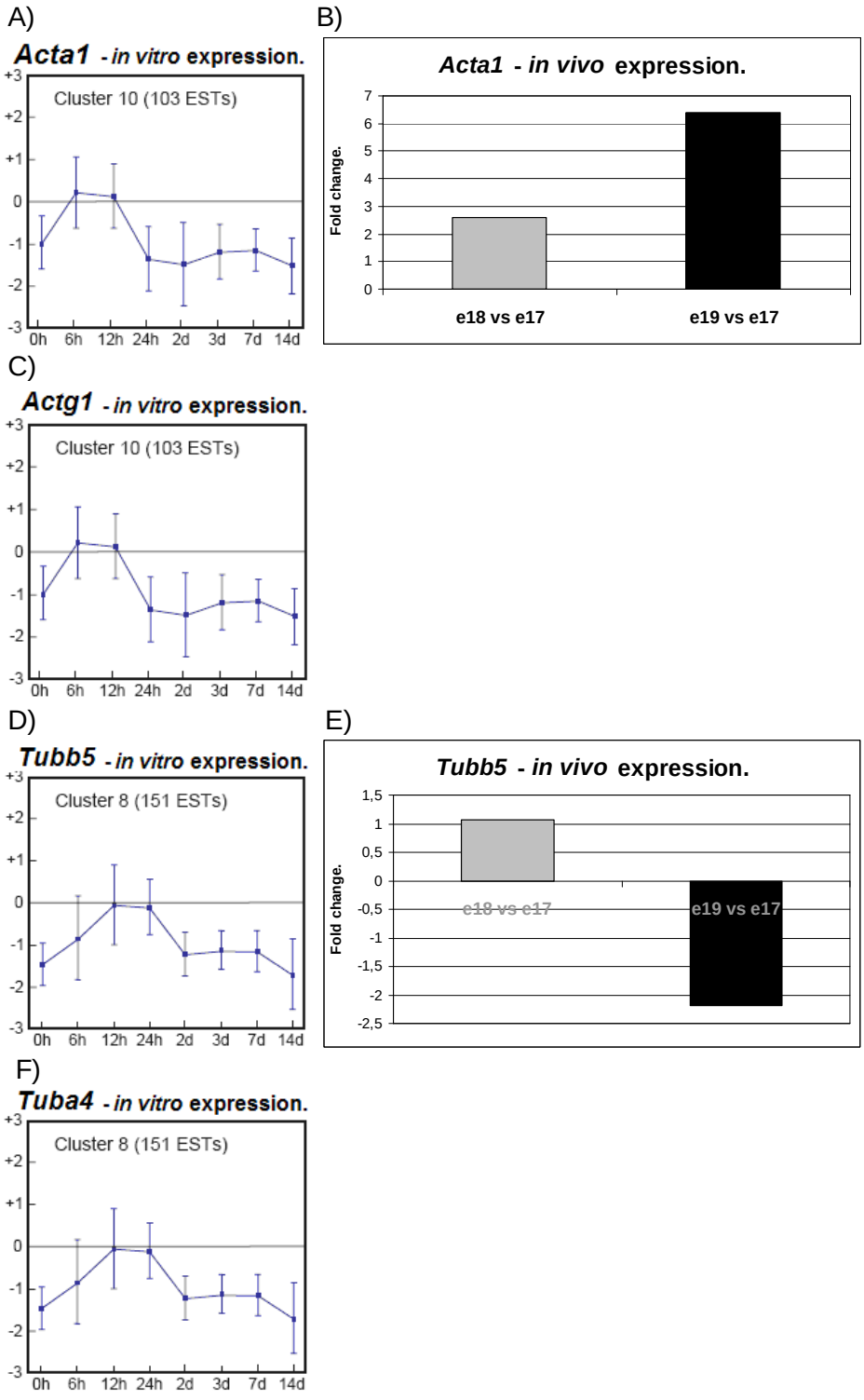


Figure 3.52. The expression profiles of *Acta1* (A, B), *Actg1* (C), *Tubb5* (D, E) and *Tuba4* (F) genes. (A, C, D, F) The expression profiles of analysed genes during *in vitro* adipogenesis in 3T3-L1 cells (based on Hackl *et al*, 2005). (B, E) The expression profiles of selected genes in the lower dermis from e17 till e19 time points. Grey columns - regulation at e18 versus e17 time points. Black columns - regulation at e19 versus e17 time points. Fold change values are based on the lower dermis (LD) microarray list. *Acta1* - actin, alpha 1, skeletal muscle. *Actg1* - actin, gamma 1. *Tubb5* - tubulin, beta 5. *Tuba4* - tubulin alpha 4.

A)

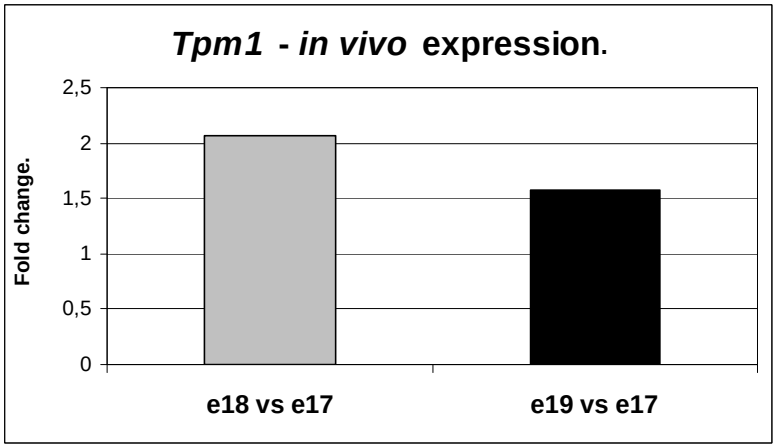


B)

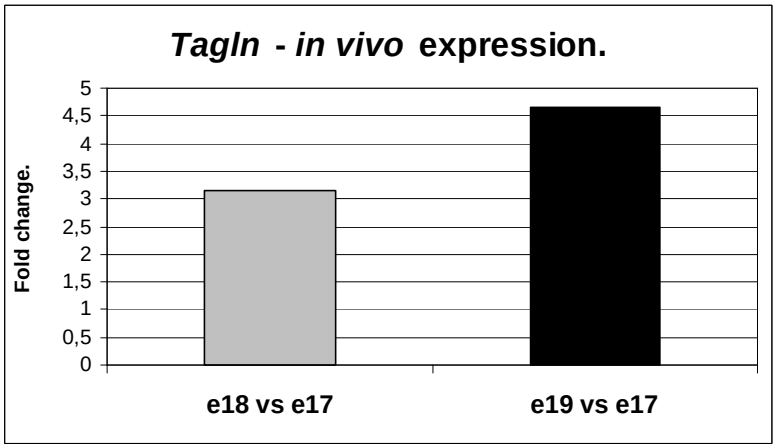


C)

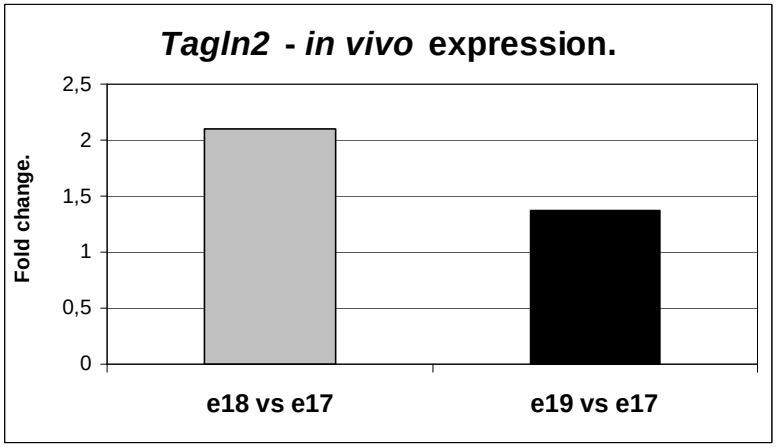


Figure 3.53. The expression profiles of *Tpm1* (A), *Tagln* (B) and *Tagln2* (C) genes in the lower dermis from e17 till e19 time points. Grey columns - regulation at e18 versus e17 time points. Black columns - regulation at e19 versus e17 time points. Fold change values are based on the lower dermis (LD) microarray list. *Tpm1* - tropomyosin 1, alpha. *Tagln* - transgelin. *Tagln2* - transgelin 2.

**The extracellular matrix components (ECM).**

A very broad review on ECM elements was recently published by Mariman and Wang (2010) which summarised knowledge about the ECM of fat cells mainly based on proteomic work. This study pointed to *in vitro* differences in ECM elements between human, mouse and rat fat cells (Table 3.11). The presence of ECM components described by Mariman and Wang (2010) was therefore cross-checked with the *in vivo* lower dermis microarray data and this combined analysis is shown in Table 3.11. Only five ECM elements were common for three cell lines (human visceral/omental adipocytes, 3T3-L1/3T3-F44A mouse cells and rat white adipose tissue primary adipocytes) and *in vivo* cells from the lower skin dermis (Table 3.11). These common elements were two collagens (Collagen a 2(IV) chain and Collagen a 1(XV) chain), Laminin b-1 chain, Laminin c-1 chain and Nidogen 1). Of 33 proteins listed for the mouse-derived 3T3-L1/3T3-F422A cells, 14 of the representative genes were also present in the *in vivo* LD cell array lists (Table 3.11). In addition, there were genes in the *in vivo* LD microarray data common for ECM proteins in human and/or rat cells but not 3T3-based mouse cells (Table 3.11).

The microarray-based work on the dermal adipose layer in mouse back skin is aimed at investigating the steps of adipogenesis *in vivo*. As changes in ECM elements are found to be specific for adipogenic cell lines (reviewed by Mariman and Wang, 2010) the question was what kind of ECM components are regulated during *in vivo* adipogenesis and how many of these are in common with 3T3-L1 cell lines used as the main *in vitro* model for adipogenesis studies (reviewed by Gregoire *et al*, 1998). First a global analysis of ECM elements was performed where the GeneCoDis 2.0 tool associated genes from the LD microarray list with different terms depending on the cellular localisation of each gene. A group of 50 genes, associated with a term “proteinaceous extracellular matrix” (GO:0005578), was selected for further analysis. The presence of these genes was then cross checked in microarray data from differentiating 3T3-L1 cells from three studies - Burton *et al* (2004), Kim *et al* (2007) and Hackl *et al* (2005). In total, 24% of genes selected from the LD list were spotted in differentiating 3T3-L1 cells, whereas 76% of *in vivo* genes were not represented in the *in vitro* microarray studies (Figure 3.54).

Table 3.11. The comparison of ECM elements in fat cells undergoing *in vitro* adipogenesis and *in vivo* adipocytes from lower skin dermis. The table was modified from Mariman and Wang, 2010).

| ECM components: | *In vitro* adipogenic differentiation: | | | *In vivo* lower dermal cells: |
|---|---|---|---|---|
| | Human * | Mouse ** | Rat *** | |
| Agrecan 1 | | | + | |
| Basement membrane-specific heparan sulfate proteoglycan core protein (HSPG) (perlecan) | + | | + | |
| Betaglycan (transforming growth factor beta receptor III) | | + | + | |
| Biglycan BGN | | + | | |
| Calreticulin CALR | + | + | | |
| Cartilage intermediate layer protein CILP1 | | | + | |
| Chitinase-3-like protein 1 CHI3l1 | + | | + | |
| Chondroitin sulfate proteoglycan 4 (NG2 proteoglycan) | | | + | |
| Coiled coil domain containing protein 80 CCDC80 | + | | | + |
| Collagen a 1(I) chain COL1A1 | + | + | | + |
| Collagen a 2(I) chain COL1A2 | + | + | | + |
| Collagen a 1(II) chain COL2A1 | | | + | |
| Collagen a 1(IIII) chain COL3A1 | + | + | | |
| Collagen a 1(IV) chain COL4A1 | | + | + | + |
| Collagen a 2(IV) chain COL4A2 | + | + | + | + |
| Collagen a 3(IV) chain COL4A3 | | | + | |
| Collagen a 5(IV) chain COL4A5 | | + | | |
| Collagen a 1(V) chain COL5A1 | + | + | | |
| Collagen a 2(V) chain COL5A2 | | | + | |
| Collagen a 3(V) chain COL5A3 | | + | + | + |
| Collagen a 1(VI) chain COL6A1 | + | + | | |
| Collagen a 2(VI) chain COL6A2 | + | + | | |
| Collagen a 3(VI) chain COL6A3 | + | + | | |
| Collagen a 1(XI) chain COL11A1 | | | + | + |
| Collagen a 1(XII) chain COL12A1 | + | | + | + |
| Collagen a 1(XIV) chain (undulin) COL14A1 | + | | + | + |
| Collagen a 1(XV) chain COL15A1 | + | + | + | + |
| Collagen a 1(XVIII) chain COL18A1 | + | | + | |
| Collagen a 1(XXIII) chain COL23A1 | | | + | |
| Connective tissue growth factor CTGF | | | + | |
| Decorin (bone proteoglycan II) DCN | + | + | | |
| Dermatopontin (tyrosine-rich acidic matrix protein; early quiescence protein 1) DPT | + | + | + | |
| Dystroglycan 1 DAG1 | | + | | + |
| Extracellular matrix protein 1 ECM1 | | + | | |
| Elastin microfibril interface-located protein 1 EMILIN1 | + | | + | + |
| Fibrillin 1 FBN1 | | | + | + |
| Fibromodulin FMOD | | | + | |
| Fibronectin (FN) (cold-insoluble globulin) FN1 | + | + | | |
| Fibulin-1 FBLN1 | + | | + | + |
| Fibulin-2 FBLN2 | | | + | + |
| Fibulin-3 (EGF-containing fibulin-like extracellular matrix protein 1) FBLN3 | + | | + | |
| Fibulin-4 (EGF-containing fibulin-like extracellular matrix protein 2) EFEMP2 | | + | | |
| Fibulin-5 (developmental arteries and neural crest EGF-like protein FBLN5 | + | | + | |
| Galectin-1 LGALS1 | + | | | + |
| Galectin-3-binding protein (lectin galactoside-binding | + | | | |

| | | | | |
|---|---|---|---|---|
| soluble 3-binding protein) LGALS3BP | | | | |
| Glypican 1 GPC1 | + | | + | |
| Laminin a-2 chain LAMA2 | | | + | + |
| Laminin a-4 chain LAMA4 | + | + | + | |
| Laminin b-1 chain LAMB1 | + | + | + | + |
| Laminin b-2 chain LAMB2 | + | | + | |
| Laminin c-1 chain LAMC1 | + | + | + | + |
| Lumican (keratan sulfate proteoglycan lumican) LUM | + | + | | |
| Matrilin-2 MATN2 | + | | | |
| Microfibril-associated glycoprotein 4 MFAP4 | + | | | |
| Mimecan (osteoglycin) OGN | + | + | | + |
| Nidogen 1 (entactin) NID1 | + | + | + | + |
| Nidogen 2 (osteonidogen) NID2 | + | + | | + |
| Periostin POSTN | + | + | | |
| Proline arginine rich end leucine-rich repeat protein (prolargin) PRELP | | | + | + |
| Proteoglycan 4 PRG4 | + | | | |
| SPARC (osteonectin) SPARC | + | + | + | |
| SPARC-like protein 1 SPARCL1 | | + | | + |
| Spondin-1 (F-spondin) (vascular smooth muscle cell growth-promoting factor) SPON1 | + | | + | + |
| Spondin-2 SPON2 | + | | | |
| Tenascin-C (TN) (hexabrachion) (cytotactin) (neuronectin) (GMEM) TNC | + | | | |
| Tenascin-N TNN | | | + | |
| Tenascin-X TNXB | + | | | + |
| Thrombospondin-1 THBS1 | + | | + | |
| Thrombospondin-2 THBS2 | + | + | | + |
| Transforming growth factor-b-induced protein IG-H3 (bIG-H3) TGFBI | + | | | |
| Versican core protein (large fibroblast proteoglycan) CSPG2 | + | + | | |
| Versican V3 isoform VCAN | | | + | + |

Continuation of Table 3.11.
* Human omental/visceral cells
** 3T3-L1/3T3-F422A mouse cells
*** primary adipocytes

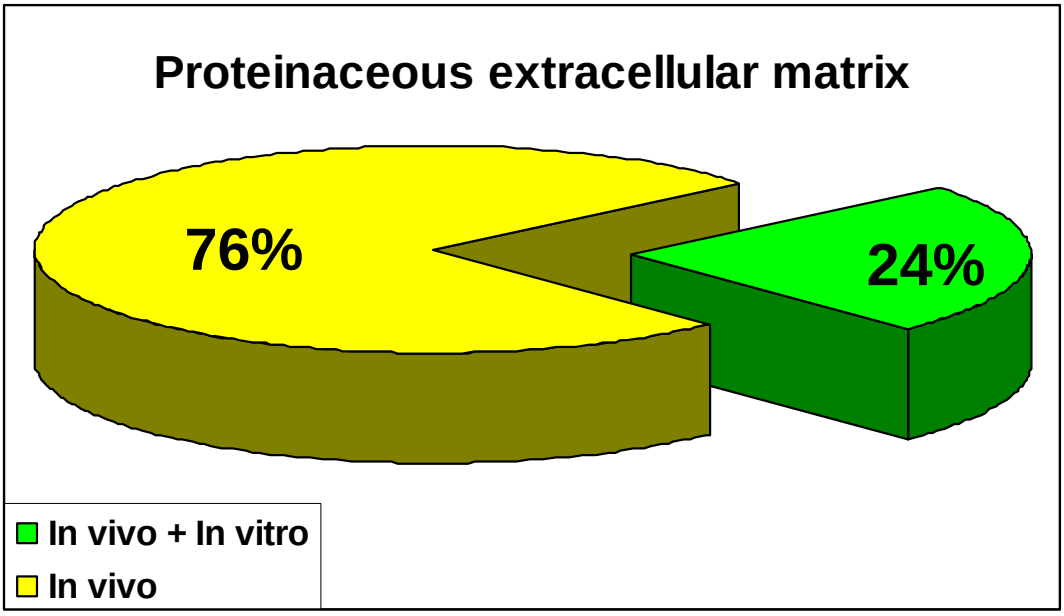


Figure 3.54. Proteinaceous extracellular matrix. Genes from the lower dermis (LD) microarray data that were associated with the proteinaceous extracellular matrix term by GeneCoDis 2.0 tool and their presence/absence was analysed in 3T3-L1 cells undergoing adipogenesis (based on *in vitro* microarray data from Burton *et al*, 2004; Hackl *et al*, 2005; Kim *et al*, 2007). Yellow-In vivo: genes seen *in vivo* but not observed in 3T3-L1 cells. Green-In vitro + In vivo: genes seen in both differentiation processes.

Among the ECM constituents observed in 3T3-L1 adipocytes is nidogen (reviewed by Mariman and Wang, 2010; Hackl *et al*, 2005). Microarray studies presented by Burton *et al* (2004), pointed to the enrichment of the nidogen (nidogen 1) gene between 16 and 24 hours after adipogenic induction, whereas Hackl *et al* (2005) study showed the up-regulation of nidogen 2 during adipogenesis (Figure 3.55A and C). Both genes were present in the *in vivo* LD data and both were up-regulated from e17 to e19 time points (Figure 3.55B and D).

In total, the whole LD microarray data included 14 collagen genes represented by different gene expression profiles (Figure 3.56A). Of these, 7 (namely *Col1a1*, *Col1a2*, *Col4a1*, *Col4a2*, *Col5a3*, *Col11a1* and *Col15a1*) are also undergoing changes in differentiating 3T3-L1 cells based on the Mariman and Wang (2010), Burton *et al* (2004), Hackl *et al* (2005) and Kim *et al* (2007). The microarray study performed by Hackl *et al* (2005), revealed specific expression pattern of three collagen genes, *Col4a1*, *Col4a2* and *Col6a2* (Figure 3.56B, D and F). Both, *Col4a1* and *Col4a2* were up-regulated also in the lower dermal cells of mouse back skin but *Col6a2* gene was not present in this LD microarray data (Figure 3.56C and E). Kim *et al* (2007) observed the down-regulation of *Col1a2* and *Col11a1* genes. However in the lower dermal cells only *Col1a2* underwent down-regulation from e17 to e19 time points, whereas *Col11a1* was up-regulated between e18 and e17 time points (Figure 3.56A). Among regulated *in vivo* (in lower dermal cells) genes but not seen in microarray data from the differentiating *in vitro* 3T3-L1 cells (Burton *et al*, 2004; Hack *et al*, 2005; Kim *et al*, 2007) were *Col16a1*, *Col25a1* and *Col27a1* yet these were associated with a down-regulation during the development of lower dermal cells (Figure 3.56A).

ECM elements undergo modifications under the control of so-called ECM processing enzymes (summarised by Mariman and Wang, 2010). Procollagens are precursors of collagen and they contain of N- and C- terminal peptides that are removed during processing. Among enzymes involved in ECM modifications are a desintegrin and metalloproteinase with thrombospondin type 1 motif 1 (ADAMTS1), a desintegrin and metalloproteinase with thrombospondin type 1 motif 4 (ADAMTS4) and a desintegrin and metalloproteinase with thrombospondin type 1 motif 5 (ADAMTS5), based on the analysis of the secreted proteome in human adipose tissue and rodent adipocytes (reviewed by Mariman and Wang, 2010). Genes for all mentioned above three ADAMTS were present in the LD data together with regulation of *Adamts15* gene (Figure 3.57). All these genes were highly up-

regulated at e18 versus e17 time point. Their expression level at e19 time point versus e17 was lower when compared with expression at e18 versus e17 time point. Interestingly, *Adamts15* gene was characterised by the highest up-regulation at e18 versus e17 time point when comparing with the other three genes. This gene did not appear in microarray work on 3T3-L1 cells from Burton *et al* (2004), Hackl *et al* (2005) and Kim *et al* (2007).

Among other enzymes involved in ECM modifications of adipocytes are matrix metalloproteinases (Mmp) and metalloproteinase inhibitors (Timp) (reviewed by Mariman and Wang, 2010). Hackl *et al* (2005) described the specific expression patterns of matrix metalloproteinase 2 (*Mmp2*) and two Timp family members (*Timp2* and *Timp3* genes) during the differentiation of 3T3-L1 cells (Figure 3.58A, B and D). Interestingly, *Timp2* gene was also found in 3T3-L1 cells by Burton *et al* (2004) but with a different expression profile than in Hackl *et al* (2005) work (compare Figure 3.58B and C). In the *in vivo* LD data, no *Mmp2* gene regulation was seen and only down-regulation of a different matrix metalloproteinase was observed, called *Mmp16* (Figure 3.58E). Among metalloproteinase inhibitors regulated in lower dermal cells were *Timp3* and *Timp4* and both of these genes were up-regulated from e17 to e19 (Figure 3.58F and G). Both *Mmp16* and *Timp4* genes, seen *in vivo*, were not present in any of the analysed *in vitro* microarray studies on 3T3-L1 cells (Burton *et al*, 2004; Hackl *et al*, 2005; Kim *et al*, 2007).

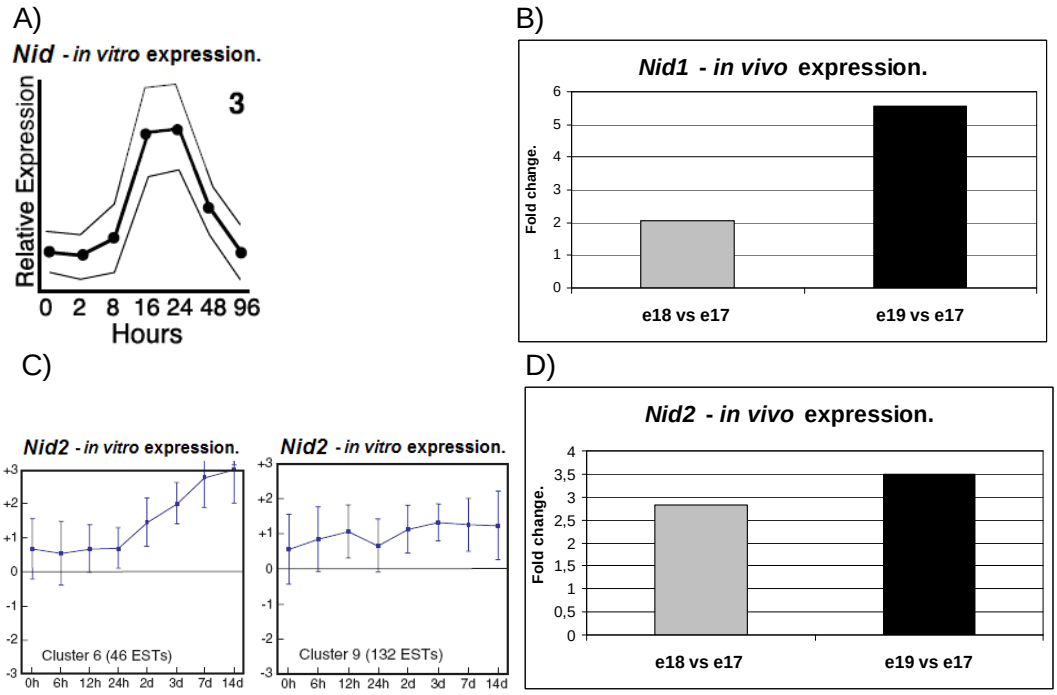


Figure 3.55. The expression profiles of *Nid* (A, B) and *Nid2* (C, D) genes. (A, C) The expression profiles of analysed genes during *in vitro* adipogenesis in 3T3-L1 cells (based on Burton *et al*, 2004; Hackl *et al*, 2005). (B, D) The expression profiles of selected genes in the lower dermis from e17 till e19 time points. Grey columns - regulation at e18 versus e17 time points. Black columns - regulation at e19 versus e17 time points. Fold change values are based on the lower dermis (LD) microarray list. *Nid* - nidogen 1. *Nid2* - nidogen 2.

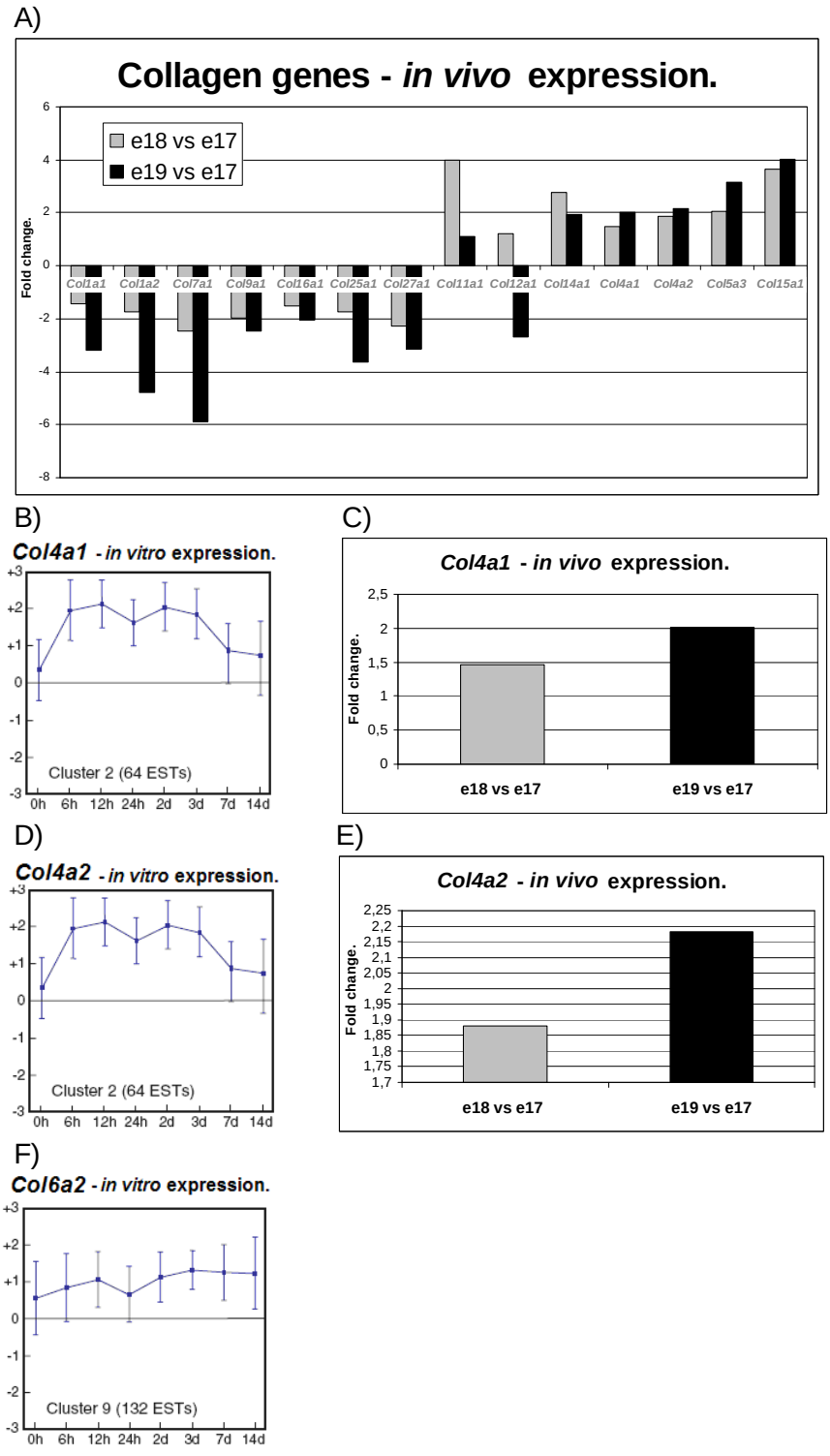


Figure 3.56. The expression profiles of collagen genes. (A, C, E) The expression profiles of selected genes in the lower dermis from e17 till e19 time points. Grey columns - regulation at e18 versus e17 time points. Black columns - regulation at e19 versus e17 time points. Fold change values are based on the lower dermis (LD) microarray list. (B, D, F) The expression profiles of selected genes during *in vitro* adipogenesis in 3T3-L1 cells (based Hackl *et al*, 2005). *Col7a1* - collagen, type VII, alpha 1. *Col9a1* - collagen, type IX, alpha 1. *Col16a1* - collagen, type XVI, alpha 1. *Col25a1* - collagen, type XXV, alpha 1. *Col27a1* - collagen, type XXVII, alpha 1. For the full names of genes: *Col1a1*, *Col1a2*, *Col11a1*, *Col12a1*, *Col14a1*, *Col4a1*, *Col4a2*, *Col5a3* and *Col15a1*, see Table 3.11.

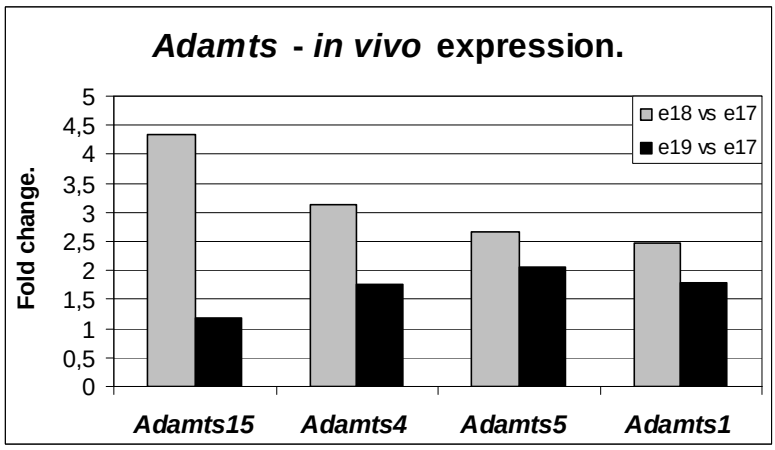


Figure 3.57. The expression profiles of *Adamts* genes in the lower dermis from e17 till e19 time points. Grey columns - regulation at e18 versus e17 time points. Black columns - regulation at e19 versus e17 time points. Fold change values are based on the lower dermis (LD) microarray list. *Adamts15* - a disintegrin-like and metallopeptidase (reprolysin type) with thrombospondin type 1 motif, 15. *Adamts4* - a disintegrin-like and metallopeptidase (reprolysin type) with thrombospondin type 1 motif, 4. *Adamts5* - a disintegrin-like and metallopeptidase (reprolysin type) with thrombospondin type 1 motif, 5 (aggrecanase-2). *Adamts1* - a disintegrin-like and metallopeptidase (reprolysin type) with thrombospondin type 1 motif, 1.

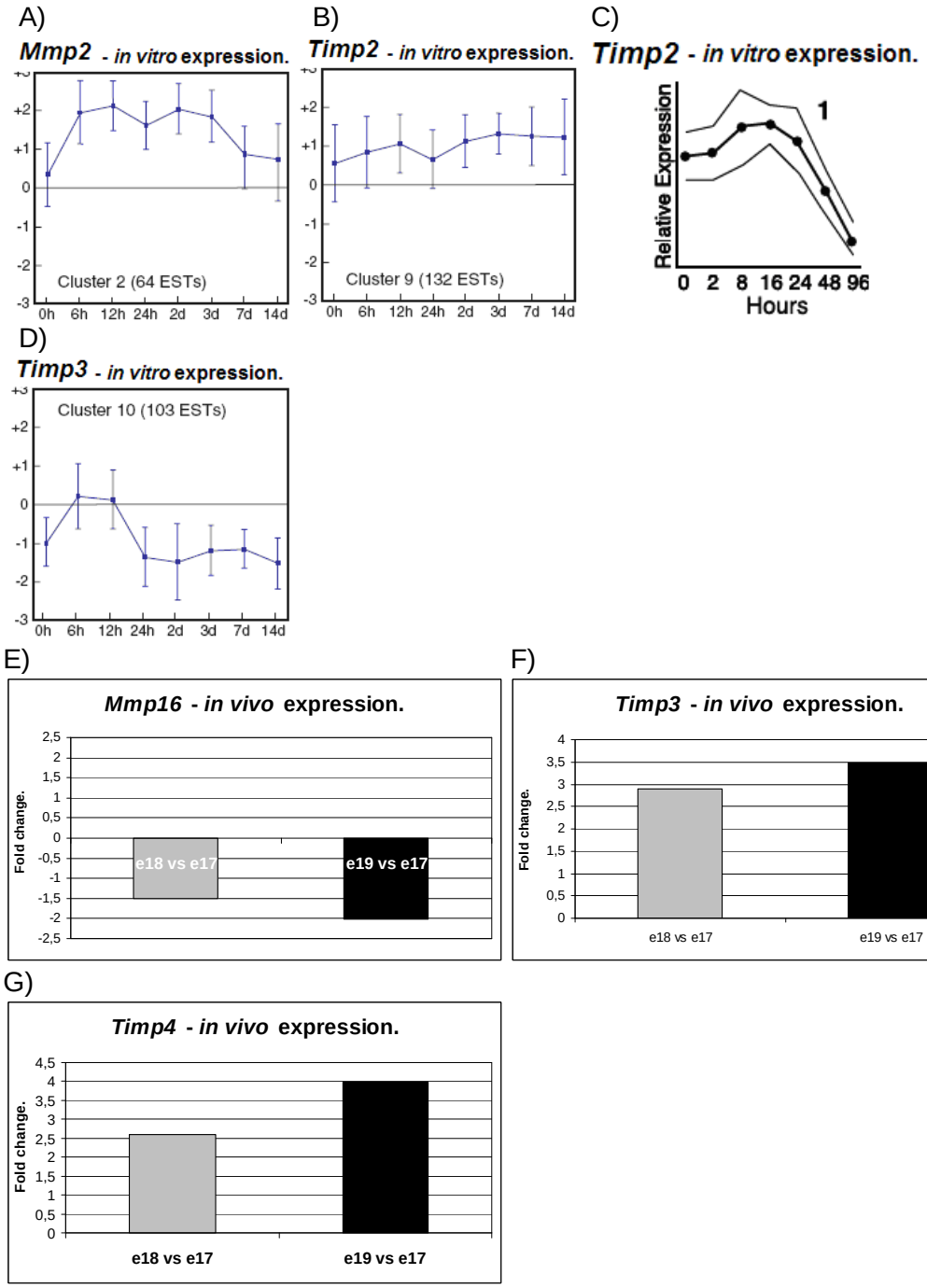


Figure 3.58. The expression profiles of *Mmps* (A, E) and *Timps* (B, C, D, F, G) genes. (A, B, D) The expression profiles of analysed genes during *in vitro* adipogenesis in 3T3-L1 cells, based on Hackl *et al*, 2005. (C) The expression profile of analysed gene during *in vitro* adipogenesis in 3T3-L1 cells, based on Burton *et al*, 2004. (E, F, G) The expression profiles of selected genes in the lower dermis from e17 till e19 time points. Grey columns - regulation at e18 versus e17 time points. Black columns - regulation at e19 versus e17 time points. Fold change values are based on the lower dermis (LD) microarray list. *Mmp2* - matrix metalloproteinase 2. *Mmp16* - matrix metallopeptidase 16. *Timp2* - tissue inhibitor of metalloproteinase 2. *Timp3* - tissue inhibitor of metalloproteinase 3. *Timp4* - tissue inhibitor of metalloproteinase 4.

### 3.3.5.5. Late steps of adipogenic differentiation *in vivo* and *in vitro*.

Based on the *in vitro* adipogenic process, it has been shown that activated adipogenic transcriptional factors control the up-regulation of genes related with metabolism of lipids and production of proteins secreted by mature adipocytes (reviewed by Gregoire *et al*, 1998; Rosen and Spiegelman, 2000).

**Investigation of key enzymes activated during adipogenic differentiation.**

During adipogenesis *in vitro*, gradual activation of pathways associated with metabolism takes place and main pathways together with key enzymes involved in these processes have been summarised by Hackl *et al* (2005) (see Table 3.12 and columns "Metabolic pathway" and "Key enzymes"). This work was used for the comparison study in order to verify if processes activated during *in vitro* adipogenesis in 3T3-L1 cells are also observed *in vivo* in lower dermal cells. The *in vitro/in vivo* comparison is shown in Table 3.12 which lists individual genes from the 3T3-L1 cell work (Hackl *et al*, 2005) that are analysed in the LD data. In total, from 33 genes, presented in Table 3.12, 61% of them were spotted in both *in vitro* and *in vivo* cells, whereas the rest 39% was not present in the LD microarray data (Figure 3.59A). Therefore in contrast to many previous comparisons, in general there was much closer approximation between the data sets at this later stage of adipogenesis/lipogenesis.

In addition, the LD microarray data, represented in total by 2179 Affymetrix IDs, underwent first the analysis on DAVID v6.7 programme for the investigation of KEGG pathways associated with genes from this microarray work (Table 3.13). Interestingly, among KEGG pathway terms generated for the LD data several were associated with metabolism of amino acids: "Valine, leucine and isoleucine degradation", "Cysteine and methionine metabolism", "Selenoamino acid metabolism", "Glycine, serine and threonine metabolism", "beta-Alanine metabolism", "Tryptophan metabolism", "Arginine and proline metabolism" and "Tyrosine metabolism" (Table 3.13 - see underlined terms).

The pathway involved in cholesterol metabolism with two key enzymes (3-hydroxy-3-methylglutaryl-CoA synthase 1 and 3-hydroxy-3-methylglutaryl-CoA reductase) was suggested to be activated during the *in vitro* adipogenesis (Table 3.12, No.3). Among these two enzymes, only expression of 3-hydroxy-3-methylglutaryl-CoA synthase 1 took place in the lower dermal cells. In addition, a term "steroid biosynthesis" was associated with *in vivo* microarray data (Table 3.13 -

see term shown in italic). In general, cholesterol is known to serve as a precursor for the synthesis of different steroids (Hu *et al*, 2010). Several other genes representing enzymes crucial for metabolic processes were regulated *in vivo* in lower dermal cells. These were for example lipoprotein lipase (*Lpl*), involved in the "triglyceride hydrolysis", acetyl-CoA dehydrogenase, medium chain (*Acadm*) and isovaleryl-CoA dehydrogenase (Acad), both associated with "beta-oxidation" or stearoyl-CoA desaturase 1 (*Scd1*) involved in "unsaturated fatty acid biosynthesis" (Table 3.12, No.4, No.5 and No.11).

All 20 genes, present on both the *in vitro* and *in vivo* adipogenic microarray lists (Figure 3.59A), were up-regulated in the lower dermal arrays from e17 time point (Figure 3.59B). Several genes were very dramatically up-regulated at e19 versus e17 time points, for example *Lpl* (lipoprotein lipase; with a 17.98-fold change) or *Scd1* (stearoyl-Coenzyme A desaturase 1; with a 26.44 fold change) (Figure 3.59B). Therefore, lower dermal cells are characterised by the dramatic up-regulation of a high number of metabolic genes at embryonic stages of their development *in vivo*. For example, four genes spotted in the LD microarray list represented enzymes involved in triacylglycerol metabolism (Table 3.14). The highest up-regulation for these genes was at e19 versus e17 time point where the expression of two genes (malic enzyme and fatty acid synthase) was changed around 2 fold, whereas two other enzymes (glycerol-3-phosphate dehydrogenase and acyl-CoA synthetase long-chain family member 1) showed much higher fold changes (compare fold change values in Figure 3.60A, B, C and D).

Glycerol-3-phosphate dehydrogenase (*Gpd1*) was chosen for the verification work by the qRT-PCR technique, as it is the key enzyme involved in the glycerol synthesis and interestingly its enhanced activity was observed in adipose tissue of obese individuals (Swierczynski *et al*, 2003). The *Gpd1* mRNA was detected at three time points, in both upper and lower dermis (Figure 3.61). The up-regulation of *Gpd1* gene in lower dermis versus upper skin was seen in e18 and e19 time points and the increase in its expression in lower dermis occurred between e17 and e19. The enrichment of *Gpd1* in lower dermis at e19 was significant, according to a t-test, when compared with cells from lower dermis at other two time points. The PCR results from this analysis confirmed the expression pattern of *Gpd1* gene at mRNA level (compare Figure 3.60C with Figure 3.61).

Table 3.12. Key metabolic pathways and enzymes regulated in 3T3-L1 cells (Hackl *et al*, 2005) and their presence in lower dermal cells (the LD microarray data).

| No. | 3T3-L1 cells: | | Lower dermal cells. |
|---|---|---|---|
| | **Metabolic pathway:** | **Key enzyme:** | |
| 1. | Urea cycle and arginine-citrulline cycles | Arginine succinate synthase | NP* |
| 2. | Phosphatidylinositol | Phosphatidylinositol 3-kinase, regulatory subunit, polypeptide 1 | +** |
| | | Myoinositol 1-phosphate synthase A1 | NP* |
| 3. | Cholesterol biosynthesis /keto-body synthesis | 3-hydroxy-3-methylglutaryl-CoA synthase 1 | +** |
| | | 3-hydroxy-3-methylglutaryl-CoA reductase | NP* |
| 4. | Triglyceride hydrolysis (fatty acid assimilation) | Lipoprotein lipase (LPL) | +** |
| 5. | beta-oxidation | Acetyl-CoA dehydrogenase, medium chain (Acadm) | +** |
| | | Isovaleryl-CoA dehydrogenase (Acad/Ivd) | +** |
| | | Acyl-CoA dehydrogenase, short/branched chain (Acadsb) | NP* |
| 6. | Triglyceride metabolism | Adipose triglyceride lipase (Pnpla2/Atgl) | +** |
| 7. | CoA biosynthesis | Pantothenate kinase 3 (Pank3) | +** |
| 8. | Anaplerotic processes | Pyruvate carboxylase (Pcx) | +** |
| 9. | Branched chain amino acid metabolism (AKAmetabolism) | Branched chain ketoacid dehydrogenase E1, alpha polypeptide (Bckdha) | +** |
| 10. | Methylation | S-adenosylhomocysteine hydrolase | NP* |
| | | Methionine adenosyltransferase II, alpha (Mat2a) | +** |
| 11. | Unsaturated fatty acid biosynthesis | Stearoyl-CoA desaturase 1 (Scd1) | +** |
| 12. | Nucleotide metabolism | Xanthine dehydrogenase | NP* |
| 13. | Taurin biosynthesis | Cysteine dioxygenase (Cdo1) | +** |
| 14. | NH4 + metabolism/glutamate | Glutamate-ammonia ligase (glutamine synthase)(Glul) | +** |
| 15. | Glycolysis | Pyruvate kinase 3 | NP* |
| 16. | Substrate cycle (glycolysis/gluconeogenesis) | Fructose bisphosphatase 2 | NP* |
| 17. | Nucleotide biosynthesis | Deoxycytidine kinase | NP* |
| | | Ribonucleotide reductase M2 | NP* |
| 18. | Pentose phophate shunt | Hexose-6-phosphate dehydrogenase (AI785303) (H6pd) | +** |
| 19. | NAD(P) biosynthesis | Pre-B-cell colony-enhancing factor (Nampt) | +** |
| 20. | Polyamine biosynthesis | Ornithine decarboxylase, structural (Odc1) | +** |
| 21. | Tetrahydrobiopterin biosynthesis | GTP cyclohydrolase 1 | NP* |
| 22. | Purine biosynthesis | Phosphoribosyl pyrophosphate amidotransferase (Ppat) | +** |
| 23. | Asparagine biosynthesis | Asparagine synthetase (Asns) | +** |
| 24. | Long chain fatty acids | ELOVL family member 6, elongation of long chain fatty AIDS (Elovl6) | +** |
| 25. | Serine biosynthesis | Phosphoserine phosphatase | NP* |
| 26. | Gluconeogenesis | PEPCK 2 (Riken 9130022B02) | NP* |
| 27. | Prostaglandin E biosynthesis | Prostaglandin E synthase (ri\|2410099E23; ri\|9230102G02) (Ptges2) | +** |

* gene was not present (NP) in the LD microarray list
** gene was present (+) in the LD microarray list

A)

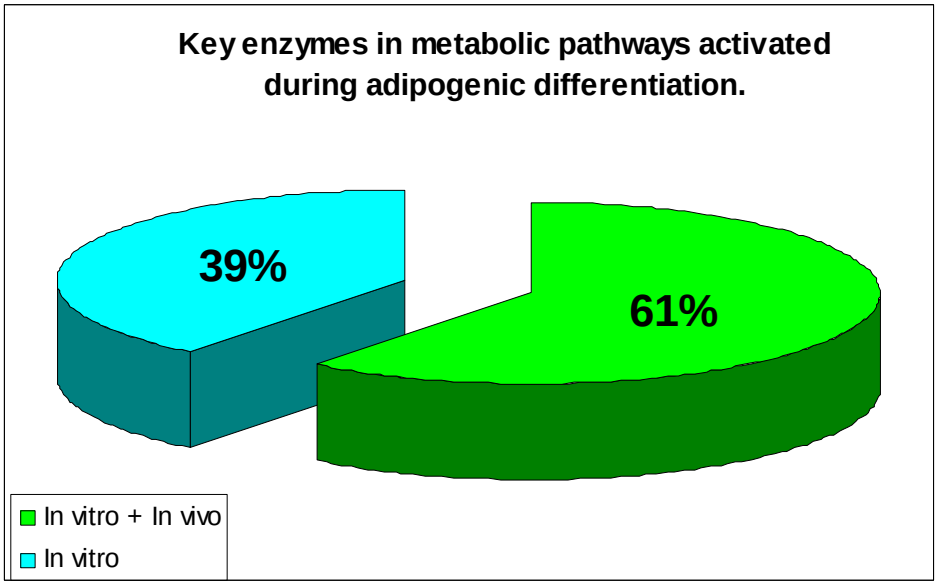


B)

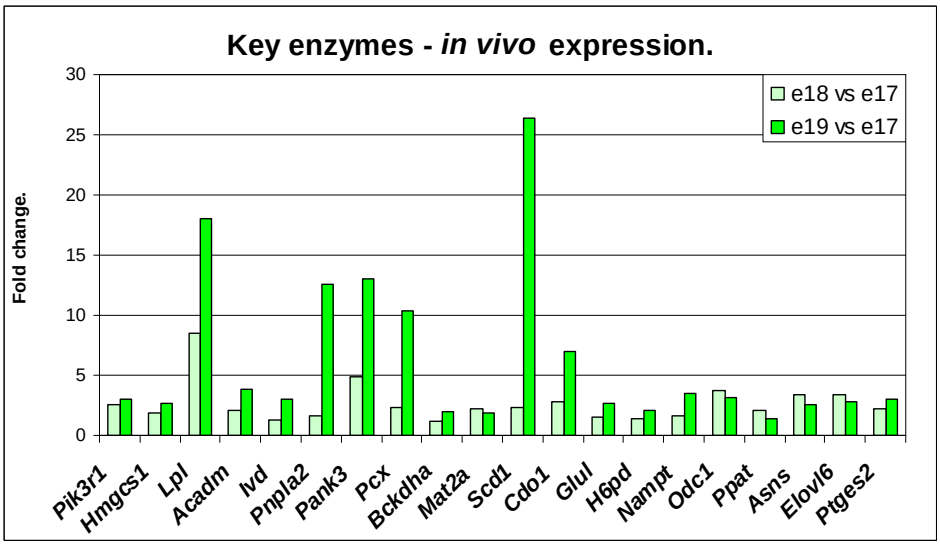


Figure 3.59. Enzymes associated with metabolic pathways during adipogenic differentiation *in vitro* (3T3-L1) and *in vivo* (cells from lower dermis in mouse embryonic back skin). The analysis is based on the microarray approach. (A) The presence of key enzymes, seen in 3T3-L1 cells (based on Hackl *et al*, 2005), was investigated in the lower dermal cells (based on the LD microarray list). Blue-In vitro: genes related only with 3T3-L1 cells. Green-In vitro + In vivo: genes expressed in 3T3-L1 cells and lower dermal cells. (B) *In vivo* expression (based on the LD microarray list) of genes common for *in vitro* and *in vivo* cells.

Table 3.13. KEGG terms associated with genes from the LD microarray data. The analysis was performed by DAVID v6.7 programme.

| **KEGG terms:** | |
|---|---|
| mmu00903:Limonene and pinene degradation | mmu05212:Pancreatic cancer |
| mmu00630:Glyoxylate and dicarboxylate metabolism | mmu00010:Glycolysis / Gluconeogenesis |
| **mmu00410:beta-Alanine metabolism** | mmu04520:Adherens junction |
| ***mmu00100:Steroid biosynthesis*** | mmu05215:Prostate cancer |
| **mmu00450:Selenoamino acid metabolism** | mmu04512:ECM-receptor interaction |
| mmu00910:Nitrogen metabolism | mmu05222:Small cell lung cancer |
| mmu00030:Pentose phosphate pathway | mmu04914:Progesterone-mediated oocyte maturation |
| mmu01040:Biosynthesis of unsaturated fatty acids | mmu00020:Citrate cycle (TCA cycle) |
| **mmu00260:Glycine, serine and threonine metabolism** | mmu03320:PPAR signaling pathway |
| **mmu00350:Tyrosine metabolism** | mmu03050:Proteasome |
| **mmu00270:Cysteine and methionine metabolism** | mmu05210:Colorectal cancer |
| **mmu00380:Tryptophan metabolism** | **mmu00280:Valine, leucine and isoleucine degradation** |
| mmu00561:Glycerolipid metabolism | mmu04114:Oocyte meiosis |
| mmu04150:mTOR signalling pathway | mmu04110:Cell cycle |
| mmu05217:Basal cell carcinoma | mmu04310:Wnt signalling pathway |
| **mmu00330:Arginine and proline metabolism** | mmu00190:Oxidative phosphorylation |
| mmu00640:Propanoate metabolism | mmu05012:Parkinson's disease |
| mmu00620:Pyruvate metabolism | mmu05016:Huntington's disease |
| mmu00071:Fatty acid metabolism | mmu04010:MAPK signalling pathway |
| mmu03018:RNA degradation | mmu05010:Alzheimer's disease |
| mmu05214:Glioma | mmu04510:Focal adhesion |
| mmu04115:p53 signalling pathway | mmu05200:Pathways in cancer |
| mmu05218:Melanoma | |

Table 3.14. Enzymes involved in triacylglycerol metabolism and enriched at late stages of adipogenesis.

| **Enzymes related with triacylglycerol metabolism and up-regulated during late/terminal stages of adipocyte differentiation in 3T3-L1 cells (based on Gregoire *et al*, 1998).** | **Presence of enzymes related with triacylglycerol metabolism in the lower dermal cells (based on the LD microarray data).** |
|---|---|
| malic enzyme (*Me*) | +* |
| fatty acid synthase (*Fasn*) | +* |
| glycerol-3-phosphate dehydrogenase (*Gpd*) | +* |
| acyl-CoA synthetase long-chain family member 1 (*Acsl1*) | +* |

* gene was present (+) in the LD microarray list

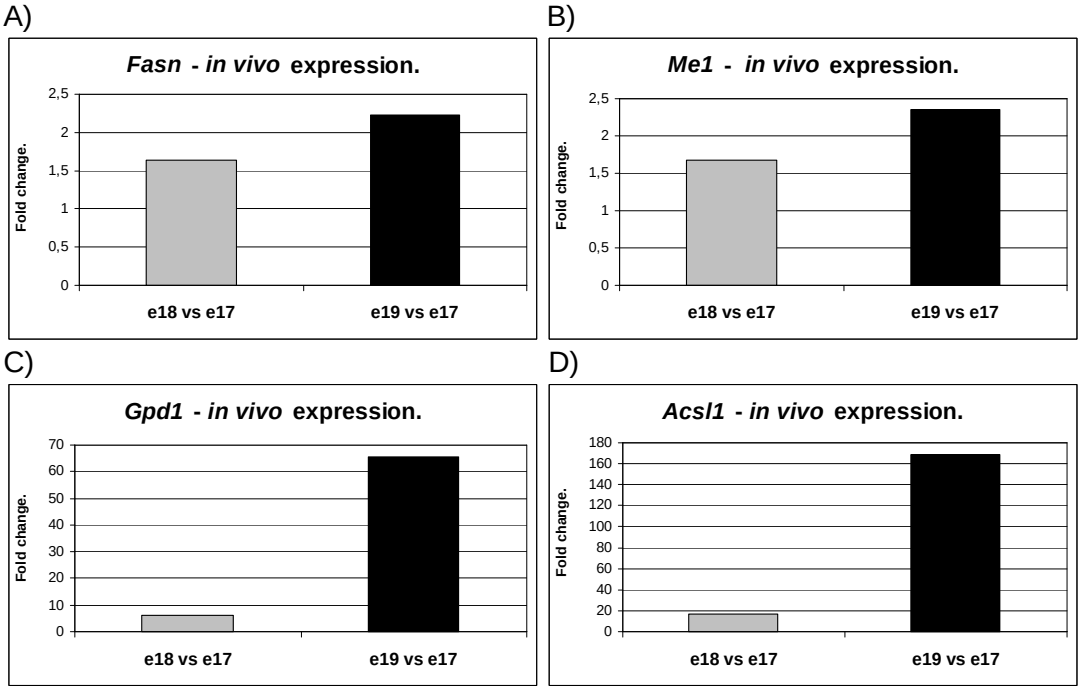


Figure 3.60. The expression profiles of *Fasn* (A), *Me1* (B), *Gpd1* (C) and *Acsl1* (D) genes in the lower dermis from e17 till e19 time points. Grey columns - regulation at e18 versus e17 time points. Black columns - regulation at e19 versus e17 time points. Fold change values are based on the lower dermis (LD) microarray list. *Fasn* - fatty acid synthase. *Me1* - malic enzyme 1, NADP(+)-dependent, cytosolic. *Gpd1* - glycerol-3-phosphate dehydrogenase 1 (soluble). *Acsl1* - acyl-CoA synthetase long-chain family member 1.

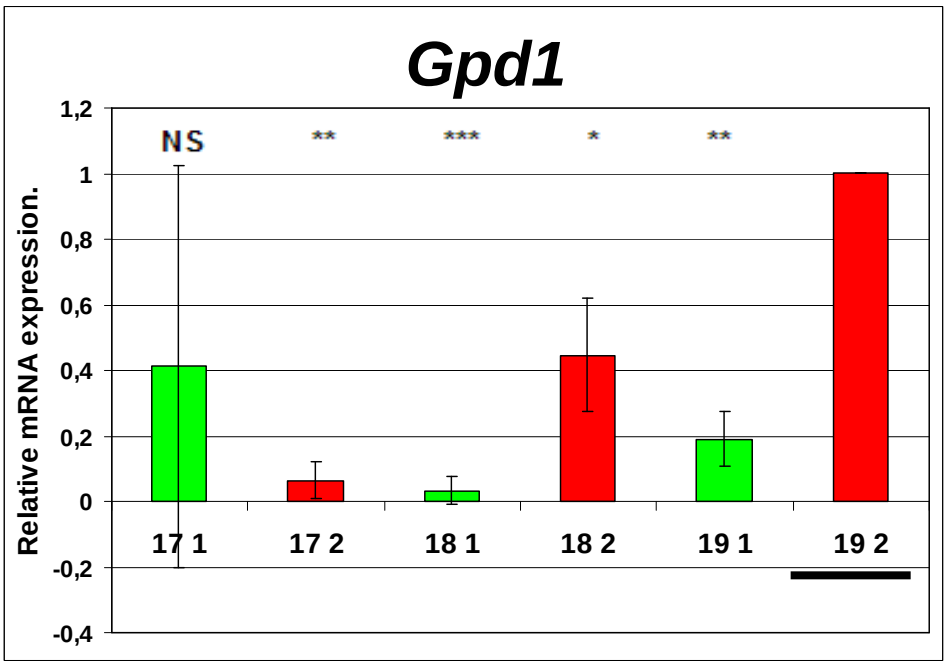


Figure 3.61. Verification of microarray data by qRT-PCR for one gene: *Gpd1*. The relative mRNA expression for gene was analysed on samples from dermis at: e17 (17), e18 (18) and e19 (19) time points, from upper (Area "1", green) and lower (Area "2", red) dermis area. Data were obtained from triplicate biological replicates. The baseline (1-fold change) was established for the e19 lower dermis sample (underlined on the figure) and the mRNA levels of the other samples are shown relative to this. *Gpd1* gene is up-regulated in lower dermis (Area "2") when compared with upper area (Area "1") in e18 and e19 time points. This observation is in agreement with *in vivo* microarray data generated from dermal cells (Table 3.4). P value refers to the comparison with "19 2" sample (* P <0.05, ** P <0.01, *** P <0.001). The "NS" indicates not significant differences in the mRNA gene expression.

**Adipocyte specific products.**

Cell line-based studies on adipocytes revealed a number of proteins produced and/or secreted by these cells (reviewed by Gregoire *et al*, 1998; Rosen and Spiegelman, 2000). Presence of several genes specific for mature fat cells was checked in the lower dermal microarray data (Table 3.15). The reason was that the Oil Red O analysis pointed to the development of fat cells with lipid droplets and an increase in their number in lower skin dermis from e17 till e19 time points (Figure 2.5, Chapter 2).

Among three selected fat-specific products: FABP4, CD36 and perilipin, only expression of perilipin was not seen in the LD microarray data. *Fabp4* gene expression in the lower dermal cells was verified by qRT-PCR and results of this analysis were discussed in section 3.3.2 (see also Figure 3.10B). Based on the microarray data, *Cd36* gene was up-regulated in lower dermis from e17 time point (Table 3.15). The qRT-PCR analysis, confirmed the over-expression of *Cd36* gene in lower dermis during mouse skin development (Figure 3.62A). mRNA for *Cd36* was almost not detected in the upper dermis (Figure 3.62A - green columns), whereas, in the lower dermal cells, higher up-regulation of CD36 mRNA took place in the e18 sample, when compared with younger specimens (e17 time point). A fairly similar level of CD36 was next observed at e18 and e19 (Figure 3.62A - red columns). The t-test confirmed a significant enrichment of this gene at e19 in the lower dermis when compared with lower dermis area at e17 time point and with upper dermis samples at all three analysed time points (Figure 3.62A).

Among proteins known to be produced and secreted by adipocytes are resistin, adipsin, angiotensinogen and adiponectin (reviewed by Gregoire *et al*, 1998; Rosen and Spiegelman, 2000). The array data showed that genes for all four proteins were regulated during development of LD cells *in vivo* (Table 3.15). mRNA levels for these genes increased significantly but relatively modestly between e17 and e18, whereas the enrichment of these genes at e19 was very dramatic. Quantitative RT-PCR confirmed the high up-regulation of these four proteins at mRNA level in lower dermal cells at the latest analysed time point (e19). Results from the qRT-PCR analysis for *Adipoq*, resistin (*Retn*) and adipsin (*Adn*) are shown in section 3.3.2 (Figure 3.13B and Figure 3.17). The angiotensinogen (*Agt*) mRNA levels in dermal cells are shown in Figure 3.62B. *Agt* was expressed at detectable levels in lower dermal cells (Figure 3.62B - red columns). Its expression increased from e17 to e19 time points and the enrichment of this gene at e19 time point was

statistically significant (according to a t-test) when compared with samples from other time points (Figure 3.62B).

Table 3.15. Genes related with late stages of adipogenesis in 3T3 cells, expressed and secreted in mature adipocytes. Their presence or absence was analysed in lower skin dermis during mouse embryonic development.

| ***In vitro* studies (mainly on 3T3 cells).** | **Lower dermis (LD) microarray data: *in vivo* approach.** | | |
|---|---|---|---|
| | **Gene symbol (Affymetrix ID):** | **e18 versus e17 (fold change)** | **e19 versus e17 (fold change)** |
| **Fat cell specific products*** | | | |
| fatty acid binding protein 4 | *Fabp4* (1425809_at) | + 3.800351** | + 8.378724** |
| FAT/CD36 (fatty acid transporter) | Cd36 (1450883_a_at) | + 5,071104** | + 8,146752** |
| Perilipin 1, Perilipin 2 (lipid-droplet associated proteins) | NP*** | | |
| **Secreted (by adipocytes) proteins*** | | | |
| Resistin | *Retn* (1449182_at) | + 1.003697** | + 5.248189** |
| Adipsin | *Adn/Cfd* (1417867_at) | + 1.22378** | + 12.15824** |
| Angiotensinogen | *Agt* (1423396_at) | + 3.769306** | + 10.97713** |
| Acrp30/AdipoQ | *Adipoq* (1422651_at) | + 51.95553** | + 710.0637** |

* based on the review from Gregoire *et al*, 1998.
**gene was present in the LD microarray list and up-regulated from e17 time point
*** gene was not present (NP) in the LD microarray list

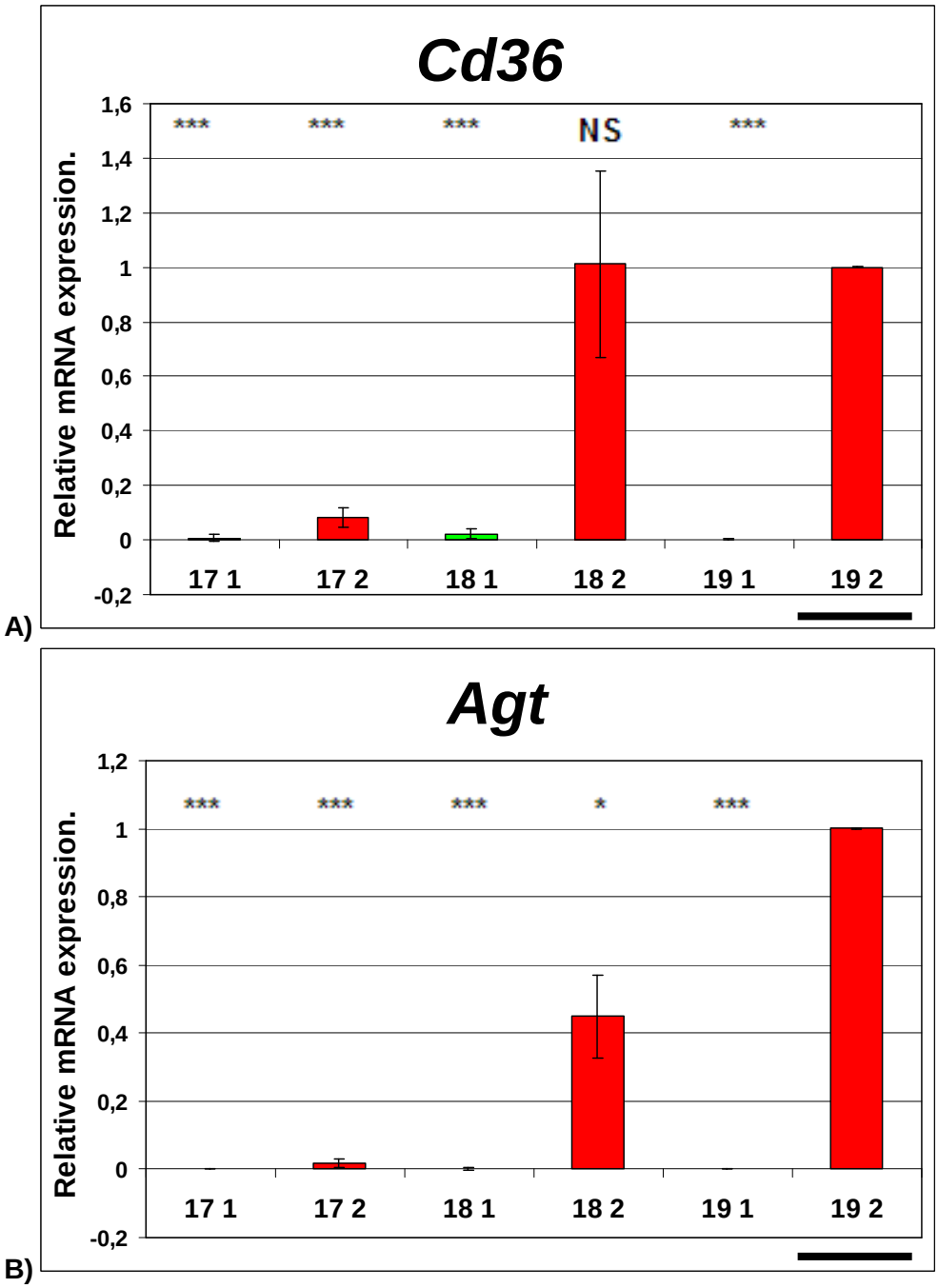


Figure 3.62. Verification of microarray data by qRT-PCR for two genes: *Cd36* and *Agt*. The relative mRNA expression for both genes was analysed on samples from dermis at: e17 (17), e18 (18) and e19 (19) time points, from upper (Area "1", green) and lower (Area "2", red) dermis area. Data were obtained from triplicate biological replicates. The baseline (1-fold change) was established for the e19 lower dermis sample (underlined on the figure) and the mRNA levels of the other samples are shown relative to this. Both genes are up-regulated in lower dermis (Area "2") when compared with upper area (Area "1") in e17, e18 and e19 time points. This observation is in agreement with *in vivo* microarray data generated from dermal cells (Table 3.4). P value refers to the comparison with "19 2" sample (* P <0.05, ** P <0.01, *** P <0.001). The "NS" indicates not significant differences in the mRNA gene expression.

## 3.4. Discussion.

Work presented in Chapter 2 revealed that around e17 and e18 in mice, cells from the lower skin dermis, between and around hair follicle end bulbs, undergo dynamic changes which lead to adipogenic differentiation and development of the dermal adipose tissue layer after birth. The aim of this section of the thesis was to identify changes in gene expression during the processes taking place in such cells, especially since these developmental events have never been analysed at the molecular level *in vivo* to best of my knowledge. The laser capture microdissection (LCM) technique together with the microarray approach proved to be a very suitable tool for such a study.

**Output of the microarray study.**

This study generated a very large amount of data, with 1001, 1309 and 2460 Affymetrix IDs for genes differently expressed in the upper and lower dermal cells at three time points, respectively at e17, e18 and e19. In addition, 2179 Affymetrix IDs characterised genes whose expression changed in lower dermal compartment from e17 till e19 time point (the LD microarray data). Consequently, even with the assistance of bioinformatics tools, complete analysis of the data was unfeasible given the time limits and individual nature of the project. Therefore the aim was to concentrate on key questions relating to general biological features of cells from lower and upper embryonic dermis and to changes taking place at molecular level in lower dermis during embryonic development that give a rise to dermal adipose tissue (based on Chapter 2).

The results have: (a) Provided an overall picture of cellular and molecular changes during *in vivo* adipogenesis. (b) Confirmed differences in cellular and molecular profiles between cells in the lower and upper dermis and provided some indications of what might be happening during embryonic dermis development. (c) Shown clear differences between adipogenesis as represented by the 3T3 model and that seen *in vivo*. (d) Highlighted specific genes, and gene families, not previously associated with the developmental process.

**Limitations/disadvantages of the time points, microdissection technique and microarray technology - technical discussion.**

It is important to discuss the technical aspects of work preformed and presented in this Chapter. Starting from the beginning, the laser capture microdissection (LCM) technique was applied to the isolation of dermal areas only at three time points (e17, e18 and e19). These adjustments were related with a careful isolation of skin specimens, appropriate storage conditions of specimens and preparation of back skin cross-sections for the LCM (see sections 3.2.2 and 3.2.3 for more details). During the microdissection, each single fragment of a collected dermis had to be first carefully marked and then microdissected by a laser. The collected pieces were only visible under the microscope and the successful isolation of such pieces was dependent on the power settings of the laser as well as on the size of marked dermis area. Therefore there is the possibility that some tissue/cells that belonged to the follicle dermis rather than inter-follicular dermis could have been incorporated into the samples. This is especially likely to happen where an obvious follicle structure may not be visible in any given section, but where the cryostat slices might be going into or out of a follicle.

In relation to the generated microarray data, arrays themselves are unlikely to be perfect e.g. because of alternate splicing
(see: http://www.people.vcu.edu/~mreimers/OGMDA/summarize.expression.html).
It has been also reported that in microarray analysis a relatively short data series can lead to greater error. Therefore bigger problems can occur in distinguishing a real process from random ones when the clustering algorithms are applied for the analysis of microarray data (Ernst *et al*, 2005). The fact that the hierarchical clustering analysis here revealed correlations between genes from upper and lower dermis at e17 time point or correlated expression profiles of genes from lower dermis between e18 and e19 time points (section 3.3.1) could be then due to an error in a used clustering algorithm. However, the other explanation of the obtained results could be due to the highly dynamic nature of the changes taking place in the lower and upper dermis.

The next technical issue relates to the cell types collected from the areas and the age of animals used for this work. In Chapter 2, it was observed that between e17 and e19 cells of the lower dermis changed from being all unstained by Oil Red O dye to having a mixture of fat containing and non-fatty cells. Therefore, if the non-fatty cells sampled during the LCM process were not adipogenic this could be

problematic. The initial and important concern with this experimental strategy was that gene expression in cells undergoing adipogenesis in the lower dermis would be masked or distorted by “noise” from non-adipogenic cells in the same region. However, in this context the work of the previous Chapter 2 providing a long term analysis of fat formation in this region until well after birth was highly informative and reassuring, since essentially all the cells in this area (apart from those associated with vasculature) became fat. Since we have found no evidence of large scale cell death following the initiation of adipogenesis in this region (data not shown), this indicates that vast majority of the lower dermis cells harvested for microarray were adipocyte precursors.

The main consideration is therefore the timing of events and the fact that the process of adipogenesis, while starting at a defined point in time, is not synchronous amongst all the lower dermal cells, but a process where adipogenesis is being initiated over a considerable time period.

**Verification.**

Bearing in mind the above considerations, the verification of selected genes from the *in vivo* microarray data, both at the mRNA and the protein level largely confirmed the array results. When conventional RT-PCR was used initially to confirm the presence or absence of genes, there was 95 - 100% confirmation of the array data in terms of basic expression. Genes selected for analysis by qPCR, were shown in the arrays as being enriched in the lower dermis, although some were also chosen from the upper dermis. Among genes, for which primer pairs occurred to be efficient for the qRT-PCR analysis (see Table 3.2), 100% showed the appropriate expression in terms of overall trends and timing, and 100% showed significant differences (between upper and lower dermis) for at least one time point.

At the protein level, 6 out of 7 genes whose expression was investigated and for which a working antibody was found showed expression consistent with the array data. Again this was true of molecules being expressed in the upper as well as the lower dermis. For example TRPS that has been shown to be important in relation to hair follicle development in the upper dermis around e14 (Fantauzzo *et al*, 2008) persists as a marker there in late gestation skin. In one case (AdipoQ) there was evidence of the expression being more concentrated within the hair follicle dermis, than more broadly within the lower dermis.

### 3.4.1. Dynamic changes in two dermal skin compartments during mouse embryonic development.

The microarray data, generated by the GeneSpring software, gave an interesting insight into features of back skin compartments at late stages of mouse embryonic development. The comparison of genes enriched in upper and lower dermis revealed clear differences between these two skin compartments at molecular level.

**General findings.**

The basic, global analysis of microarray data pointed to a presence of enriched genes in both upper and lower dermis areas from e17 to e19 time points (section 3.3.1). In addition, the analysis of numbers of Affymetrix IDs for genes showing significant differences in expression increased over the sampling points from 1001 to 2460 (Figure 3.6) was highly indicative that dynamic events were occurring in this dermal compartment at these time points.

The Venn diagram revealed the presence of genes common for two or all three analysed time points which could suggest that enrichment of such common genes is important for proper *in vivo* developmental processes of dermal skin compartments. In addition, the hierarchical clustering analysis of the gene expression intensity revealed a close correlation between upper and lower dermis at e17 time point. Then expression of genes from lower dermis at e18 was correlated with expression profile of lower dermis genes at e19 time points, whereas samples from upper dermis at e18 and e19 were clustered together because of similarly expressed genes in this skin compartment. Therefore specific changes seemed to take place between e17 and e18 time points in skin dermis that leaded to a gradual development of two distinguishable (at molecular level) dermal compartments: upper and lower dermis.

Because of a correlation between enriched genes from the lower dermis at e18 and e19 time points (hierarchical clustering) and a fact that the first lipid accumulating cells were observed in this lower dermal compartment after e17 and between e18 and e19 (Chapter 2), a question arises about the global features of genes enriched in lower dermal cells between e17 and e19 time points. The majority of genes with the highest up-regulation in lower dermis at e17 and e19 time point (respectively 42% and 60% analysed genes) were related with adipocytes, adipose tissue and/or functions of fat cells (Figure 3.9). Therefore it becomes apparent that

regulation of gene expression in lower dermis between e17 and e19 time points is crucial for the differentiation of fat cells.

**Fat-related processes in lower skin dermis.**

Bioinformatics analysis of gene ontology (GO_BP terms) showed that genes from both dermal compartments were associated with general terms for differentiation and developmental processes (Figure 3.24. Part A). However only genes enriched in lower dermis were associated with terms crucial for the regulation of lipid metabolism (Figure 3.24. Part C).

The KEGG pathway analysis also confirmed differences between upper and lower dermis areas. For example, a high number of genes from lower dermis were associated with lipid metabolism and adipocyte-specific terms, such as the “fatty acid elongation in mitochondria”, the “biosynthesis of unsaturated fatty acids” or the “insulin signalling pathway” (Figure 3.25). These processes are widely known to be crucial for the regulation of adipogenesis or they are taking place in adipose tissue (Pearce, 1983; Guerre-Millo, 2004; Duncan *et al*, 2007; see also section 1.2.2.2.2 in Chapter 1). The occurrence of genes involved in the above mentioned KEGG pathways in lower dermal cells between e17 and e19 time points clearly suggested the gradual development of fat cells taking place in lower dermal compartment in mouse embryonic back skin.

In addition to the general trends and indicators provided in the initial analysis, the array data and the verification process highlighted individual genes. Several genes from the *in vivo* microarray data, whose specific expression profile in skin dermis was confirmed by qRT-PCR reaction and/or immunofluorescence analysis, seemed to be interesting candidates for a future study of their role in relation to dermal cells development and will be discussed further here.

**CD36/FAT**

The “PPAR signalling pathway” that was associated (by DAVID v6.7 programme) with several genes from *in vivo* microarray data (see Figure 3.25) is related with activity of fatty acids transporters. Fatty acids can be transported for example by FAT/CD36 (fatty acid translocase; CD36 antigen) which is a membrane protein (Pohl *et al*, 2005). In addition, CD36/FAT (fatty acid translocase) is involved in metabolism of long-chain fatty acids (Campbel *et al*, 2004). This translocase was seen in 3T3-L1 adipocytes and it plays crucial role in the uptake of fatty acids by these cells (Pohl *et al*, 2005). The expression of CD36 was also linked with preadipocyte differentiation processes in 3T3-F422A (Sfeir *et al*, 1999). In addition, the up-regulation of CD36 was seen in a human preadipocyte cell lines derived from patients with familiar combined hyperlipidemia (FCHL), which is related with higher levels of cholesterol in the blood (dyslipemia) and metabolic syndrome (Meex *et al*, 2005). This specific expression pathway suggested the impact of CD36 on adipocyte differentiation and its up-regulation in patients may be related with a genetic effect (Meex *et al*, 2005). Also, obesity and type 2 diabetes were related with up-regulation of CD36/FAT in subcutaneous adipose depots (Bonen *et al*, 2006).

The *Cd36* gene was selected from microarray data because of its high up-regulation in lower dermis at e 18 and e19 time points (Table 3.4), and its specific expression profile was confirmed by qRT-PCR (Figure 3.62A). The fact that this protein can be found in membranes, gave a possibility to suggest it can be a useful marker of lower dermis cells committed to adipogenesis. Such marker was then tested for the flow cytometry analysis for the collection of CD36 positive cells from mouse embryonic skin dermis. This work, performed by the fluorescence activated cell sorting (FACS) technique has been successfully performed and is presented in details in the Chapter 5.

**FABP4 (aP2)**

In microarray data, presented in this thesis, the up-regulation of fatty acid binging protein 4 (FABP4) was observed in lower dermis (Table 3.4). Fatty acid binding proteins are capable of binding long-chain fatty acids and take part in their transport as well as in lipid metabolism (Makowski and Hotamisligil, 2004). Interestingly, FABP4 has been associated with obesity and type 2 diabetes and its higher level was observed in obese children (Khalyfa *et al*, 2010). FABP4 (also known as adipocyte FABP, A-FABP or aP2) was mainly related with the localisation in mature adipose tissue. However, more recent work indicated a role of FABP4 in the early stages of pig adipocyte differentiation (Samulin *et al*, 2008). The verification work on both mRNA and protein level, confirmed the up-regulation of fatty acid binding protein 4 in lower part of skin dermis, around hair follicles at all analysed time points (Figure 3.10B and Figure 3.11). In general, fatty acid binding protein 4 is highly expressed in adipose tissue (mature adipocytes) and interacts with PPARs, has capability to bind long-chain fatty-acids, is involved in the lipid metabolism or inflammatory response (reviewed by Gregoire *et al*, 1998). In addition, several studies have been recently preformed in order to investigate relation between FABP4 and development of obesity and diabetes. First, studies on chicken showed the correlation between FABP gene polymorphism with ligand-binding capabilities of FABP that resulted in changes in fat accumulation (Wang *et al*, 2009). Mice deficient for fatty acid binding protein 4 had lower risk of the type 2 diabetes development, similarly to humans with specific polymorphism in *Fabp4* gene (Tuncman *et al*, 2006). Next, the increased levels of FABP4 were observed in obese children (Khalyfa *et al*, 2010). However, it is important to mention recent work on "…multiethnic cohort of postmenopausal women…" (50-79 years old) who were a subject of study on the specific polymorphism in *Fabp4* gene (haplotype-tagging single-nucleotide polymorphisms-tSNPs) which seemed not to have significant influence on the risk of diabetes development (Chan *et al*, 2010). In addition, the fatty acid binding protein 4 knockout mouse was characterised by higher weight and accumulation of fat mass but no effect on lipid metabolism was seen (Yang *et al*, 2010a). To sum up, relation between FABP4, obesity and fat-related disorders is not fully understood and has to be elucidated by more detailed study in future. Also, a suggestion was made about the use of FABP4 inhibitors as a drug for treatment of metabolic disorders (Furuhashi *et al*, 2007; Furuhashi and Hotamisligil, 2008).

Taking together mentioned above work on FABP4 with the information from the *in vivo* microarray data, an investigation should be performed for the detailed analysis of upper dermis genes and its potential inhibitory role on FABP4 expression.

Fatty acid binding protein 4 was expressed at very low level in upper dermis with highly up-regulation in lower dermis and this can suggest mechanisms/molecules involved in "keeping" the specific expression profile of FABP4 in this dermis compartment. By the analysis of microarray data from upper dermis, it might be possible to identify novel genes involved in inhibiting fatty acid binding protein 4 expression that can be a potential new drug in diabetes-related disorders. In addition, such work could benefit for the analysis of FABP4 role in mouse back skin during embryonic development. The study on FABP4 promoter expression at embryonic level, based on the use of site-specific Cre recombinase technology and antibodies against FABP4 suggested the presence of this protein at embryonic level in brown tissue but also in other tissues (dorsal root ganglia or vertebrae) (Urs *et al*, 2006). Also, the expression (on protein level) of FABP4 was analysed in neonatal mice skin dermis and observed between hair follicles (Wolnicka-Glubisz *et al*, 2005). The microarray data presented in this thesis could suggest the function of FABP4 in mouse embryonic skin dermis development.

To sum up, the microarray data appears to provide a rich source of information about genes differently regulated during adipogenesis. By designing follow up studies on selected genes it should be possible to either a) further understand the role of such genes in developing dermal cells in rodent embryos or b) use the information to make practical use of the data to search for example for preadipocyte and/or adipocyte markers. Along these lines, further studies were performed on two genes, selected from this data (*Egfr* and *Cd36*) and are presented in Chapter 4 and Chapter 5 respectively.

**The lower versus upper dermis.**

As biological processes specific for adipocytes were associated with lower dermis, a question could be asked why these processes occur only in cells from lower dermis and not in the upper dermal cells? What type or types of cells are creating this skin compartment and what kind of mechanism (if any) controls a fate of these cells?

Maybe cells from lower dermis compartment are different from the upper dermis area and represent cell population committed to adipogenesis from very early stages of embryonic development. On the other hand, whole analysed dermal compartment could consist of the same or very similar cell type, but only cells from lower dermis are obtaining signals to switch them into adipocytes, whereas the upper cells are devoid of such signals. In addition to proposed signalling processes, maybe both upper and lower cells are obtaining signals that lead to two opposite situations: the inhibition of adipogenesis in upper dermis and the activation of fat cell maturation in lower dermis area. Finally, if the signalling processes do exist and control fate of dermal cells, what is the source of such signals? Is it the epidermis layer, hair follicles and/or tissues laying beneath the skin?

In order to investigate signalling pathways that could control differentiation of dermal cells in mouse embryos, the generated microarray data was searched for genes with interesting expression pattern in back skin between e17 and e19 time points (see above).

**Evidence for signalling.**

In relation to signalling that might be occurring in the skin dermis, an obvious approach was to look for genes, previously reported as being important to this process. For example, the DAVID v6.7 programme linked genes enriched in upper dermis at e18 and e19 time points (respectively 8 and 19 genes) with the WNT signalling term (Figure 3.25). Independent from this bioinformatics analysis of microarray sub-lists revealed the presence of other genes specific for the WNT-based pathway (Table 3.8B). In general, there are three Wnt signaling cascades: the canonical pathway, the cell polarity pathway and the Wnt/Ca2+ pathway. Briefly, in the WNT-canonical cascade, the Wnts proteins bind to frizzled receptors and the cytoplasmic mediators of WNT signaling (Dishevelled proteins - Dvl) are activated. Active Dvls inhibit comples of Axin, GSK-3 and APC, that is responsible for the b-catenin degradation. When this complex is inhibited, degradation of b-catenin does not take place. Next, accumulated b-catenin enters nucleus, interacts with TCF/LEF

ranscription factors and specific gene expression takes place (see Figure 1.8 in Chapter 1). Ross *et al* (2000) tested the influence of WNT pathway on adipogenesis in 3T3-L1 cells. The overexpression of Axin in these cells leaded to activation of adipocyte differentiation. The inhibitory effect of this pathway on adipogenesis was also observed in myoblasts (Ross *et al*, 2000). The *in vivo* and *in vitro* studies were performed in order to analyse WNT cascade during adipogenesis (Prestwich and Macdougald, 2007). *Axin2* gene, together with *Gsk3b* gene were up-regulated in upper dermis either in both e18 and e19 (*Axin2*) or only at e19 (*Gsk3b*) time point (Table 3.8A).

In 18 day old embryonic skin dermis the up-regulation of *Wnt4* gene (2-fold change) and *Wif1* (3.71-fold change) was observed in upper dermis (Table 3.8A). Then, at e19 up-regulation of *Wif1* was noticed with high fold change (28-fold change). The Wnt4 was related with non-canonical WNT pathway and its role may be associated with the activation of adipogenesis (Nishizuka *et al*, 2008), whereas the Wnt inhibitory factor 1 (Wif1) binds to Wnt proteins and inhibits their activity. Based on the observation in presented study, the Wif1 activity in upper dermis could be crucial for the inhibition of WNT cascade in order to keep upper dermis in a form of non-fatty layer. However, a comment should be made, that also work is known where Wif1 was suggested to increase adipocyte differentiation (Cho *et al*, 2009). This shows that the "real" function of Wif1 remains under the investigation.

On the other hand it was noticed that a gene, widely known to be crucial for the Wnt pathway has not been seen in the *in vivo* data. The enrichment of of beta-catenin (*Ctnnb*) gene, crucial element of the canonical WNT signalling pathway, was not found in any of the analysed skin area at any on three time points (based on the microarray data). The active beta-catenin together with the WNT pathway are thought to inhibit adipogenesis (Ross *et al*, 2000). The controversial explanation could be that such gene is not enriched in skin dermis as it simply does not have a crucial role for adipogenesis regulation *in vivo* in this tissue at analysed stages of mouse embryonic development. However, this explanation would be against widely accepted and verified fact about beta-catenin's role in the WNT signalling pathway and their involvement in *in vitro* and *in vivo* adipogenesis (reviewed by Prestwich and Macdougald, 2007). Also, maybe changes of this gene were at very low level and therefore not spotted in generated microarray data due to a 2-fold value cut off (only genes enriched with fold equal or higher at least in one of the comapred time points were present in the generated LD data). However on the other hand, if b-catenin regualtion is related with fold change value lower than 2 in all compared time

point (e18 versus e17 and e19 versus e17), it could means that these changes are not very significant in relation to specific expression of this gene.

The next explanation is that the involvement of b-catenin in the regulation of this differentiation process *in vivo* in dermis takes place earlier than the e17 time point, which was chosen as the earliest sample point in the present study.

**Other potential regulatory genes.**

In relation to the idea that there may be inhibitors of adipogenesis in the upper dermis**,** Gremlin 2 (*Grem2*) was found to be up-regulated in the upper skin dermis and selected for further analysis (Table 3.4). The qRT-PCR analysis confirmed its up-regulation in upper dermis at e18 and e19 time points (Figure 3.18). *Grem2* gene is a representative of bone morphogenetic protein (BMP) antagonist family and by binding to BMPs can inhibit the BMP2 and BMP4 (Sun *et al,* 2006). Bone morphogenic protein 4 is involved in the development of different body parts and its inhibition can occur by interactions with such inhibitor molecules as noggin or gremlin. The gremlin can interact with precursor protein of BMP4 and inhibits its development into mature form (Sun *et al*, 2006). Both gremlin and BMP4 were analysed in relation to the development of feather bulb and presence in embryos (Bardot *et al*, 2004).

Bone morphogenetic protein 2 (BMP2) can induce differentiation processes in cell lines (and *in vivo*) that lead to development of chondrocytes and adipocytes (Date *et al*, 2004). In addition, BMP4 takes part in regulating adipogenesis in cell lines (Bowers *et al*, 2006). Interestingly, Plikus *et al,* (2009) suggested the role of BMPs in regulation of a hair follicle growth. Moreover, expression of BMP2 observed in the fat deposits that surround hair follicles was considered as crucial for the interactions between hairs and fat depot (Plikus *et al*, 2009). Finally, the up-regulation of a gene with high identity (88%) to gemlin was observed in 3T3-L1 preadipocytes but not in differentiating preadipocytes or mature adipocytes (Wade *et al*, 2005).

The exact role of gremlin in regulating adipocyte differentiation has not been clearly defined (Wade *et al*, 2005). Thus, the microarray approach presented in this thesis may help to understand its role in adipogenesis, moreover its role in *in vivo* developmental processes in mouse embryonic back skin. Because the dermis microarray data showed the up-regulation of *Grem2* gene in upper dermis, it is possible that enrichment of this genes has a role in the upper dermis as an inhibitor of adipogenic differentiation in this skin compartment.

Another interesting gene expression pattern that could provide a clue as to what controls the difference between the upper and lower dermis is that of adiponectin. *Adipoq* expression in lower skin dermis was verified by the qRT-PCR technique (Figure 3.13B). In addition, investigation of AdipoQ protein expression in back skin sections by immunofluorescence showed an interesting pattern during late stages of embryonic development (Figure 3.14). This analysis showed AdipoQ in cells either adjacent to epidermis or along the lower (basal) layer of epidermis. AdipoQ-positive cells were also present in the dermal sheath.

Adiponectin (AdipoQ) is an adipocyte-derived factor, produced and secreted by mature adipocytes and its level dramatically increases during adipogenesis (Gregoire, 2001). AdipoQ was suggested to have the autocrine function on the adipocyte differentiation in 3T3-L1 cells (Fu *et al*, 2005). The autocrine function of AdipoQ has been pointed in human fat cells (Dietze-Schroeder *et al*, 2005). In addition, the decrease of this adipocytokine was related with some cases of obesity (reviewed by Haluzík *et al*, 2004). The expression profile of adiponectin was investigated during mouse embryogenesis (in brown adipose tissue - BAT and surrounding BAT tissues) (Fujimoto *et al*, 2005). Recently, a study was presented on human foetuses where the expression of adiponectin was observed at both mRNA and protein levels in skin (Corbetta *et al*, 2005). In this work, the expression of AdipoQ was found in the epidermis and underlying dermis of human foetus skin (at mid- and late gestation) and during the progressive growth the signal in skin decreased. A specific expression patterns of AdipoQ during human foetus development lead to a suggestion about the possible involvement of this hormone in the regulation of differentiation/developmental processes at embryonic level. However this hypothesis remains untested.

Analysed, in this Chapter, presence of AdipoQ in embryonic mouse skin and its mRNA up-regulation in lower skin dermis at e18 and e19, may also suggest its potential role in embryonic developmental processes in relation to skin compartments, such as dermal adipose tissue. It will be crucial to analyse the expression pattern of AdipoQ in skin at earlier (than e17) stages of embryonic development and compare this work with findings based on human skin specimens (described above). The potential role of AdipoQ is discussed further in the context of a more global analysis of signalling in Chapter 6 of the thesis.

**MicroRNAs.**

In relation to the question about processes that control adipogenesis, there is an increasing body of literature suggesting that microRNAs might be important for regulation of adipogenesis and indeed specific microRNAs have been identified that stimulate adipogenesis *in vitro* (Xie *et al*, 2009). Although not the subject of this thesis, it must be considered that microRNA regulation could be also important in the control of adipocyte differentiation *in vivo* in lower skin dermis. Therefore, in order to fulfil information about events taking place in embryonic skin dermis, a future experiment could be designed where miRNA microarrays would verify the expression of miRNAs during adipogenesis in lower dermal cells.

**The limitations of bioinformatics analysis.**

The analysis of microarray E17, E18 and E19 sub-lists by DAVID v6.7 programme gave interesting information about processes and general features of cells developing in both dermal compartments. However it seems also important here to point out that it is crucial to combine such computational analysis with a detailed investigation of microarray data where each single selected gene is analysed in relation to a term of interest. This time-consuming, non-computational analysis is related with the investigation of any available literature (for example by the search of the pubmed website) where a selected gene (from the *in vivo* microarray data) has been spotted in adipogenic-based study. As a result of combining the software analysis with the pubmed investigation, a more detailed view can be obtained about processes taking place during dermal cells development. An example of such “double” analysis is the investigation of genes involved for example in the WNT signalling pathway (section 3.3.3) The DAVID v6.7 programme has associated several genes from E18 and E19 sub-lists with the “WNT signalling pathway” term. When the other four sub-lists were analysed by this programme, the “WNT signalling pathway” term was not present for these sub-lists. However, when these fours sub-lists were searched for several crucial genes related with WNT pathway, it occurred obvious that they are present in this data (Table 3.8).

Therefore, despite the usefulness of the computational bioinformatics analysis of microarray data it seemed crucial to combine such work with the literature search that can give a better view on what is exactly happening *in vivo*. A “double” analysis (bioinformatics and non-bioinformatics) was performed for the comparison study of adipogenesis process observed *in vitro* in cell lines with differentiation process *in vivo* of lower dermal cells that are giving rise to mature fat

cells in mouse back skin. This analysis, based on the GeneCoDis2.0 tool and the pubmed search is presented in section 3.4.2.

### 3.4.2. The comparison of *in vitro* adipogenesis with *in vivo* development of fat cells in lower dermis area.

The detailed analysis of generated microarray data in the previous section investigated features of developing dermal cells at molecular level. This work revealed dynamic processes taking place in embryonic skin dermis *in vivo* which leaded to a progressive differentiation of fat cells in lower dermis area.

Due to the fact that the early steps of adipogenic differentiation were widely analysed in cell lines, mainly in 3T3-L1 cells (Green and Kehinde, 1974; reviewed by Gregoire *et al*, 1998) the next step of microarray data analysis was to investigate if changes at mRNA level in *in vivo* fat cells (lower dermal cells) are the same as these observed in differentiating *in vitro* adipocytes (3T3-L1 cells). In addition to this study, a question was asked if it is possible to compare and adjust timing of early adipogenic events in 3T3-L1 cells with the time-schedule of processes seen in lower dermal cells between e17 and e19 time points. This analysis could help to see if (and to what extent) *in vitro* and *in vivo* processes of fat cell maturation differ from each other.

**Advantages and limitations of proposed model for the analysis of adipogenic differentiation *in vivo*.**

Despite a broad knowledge about adipogenesis, obtained mainly from cell lines and verified on mouse models (Chapter 1; section 1.3.1) there is still a need to obtain information about fat cell origin, early steps of fat cell maturation and mechanisms that control fat cell fate (summarised by Gesta *et al,* 2007). In addition, to best of my knowledge, detailed analysis on fat cells developing between hairs in skin dermis has not yet been performed.

In addition, several disadvantages can be pointed in widely used in adipogenic studies 3T3-L1 cell line, such as the two-dimensional environment of growth cells, lack of the contact with other cell types (tissues, organs) and the need to use adipogenic medium in order to “push” 3T3-L1 cells into the fully differentiated state. These problems were avoided in experimental approach presented in this Chapter where the microdissection technique and microarray approach gave possibility to track events in three-dimensional, natural environment of cells undergoing spontaneous adipogenesis during mouse embryonic development.

One of the problems that should be discussed here is the timing of performed study and general features of cells selected for this work. The microarray data was generated only for three time points (e17, e18 and e19) and the lower dermal area was characterised by the heterogeneous nature in relation to the occurrence of first lipid droplets in a form of clusters localised between cells that did not accumulate yet lipids (Figure 2.5; Chapter 2). Therefore, this short-term study was possibly missing some additional information about cells before e17 time point. However, from the Chapter 2 analysis, it is clear that the adipogenic differentiation process in lower skin dermis did not occur in the synchronised way as it can be observed in 3T3-L1 cells. Therefore, as adipogenesis may be initiating after e17 it is hoped that the microarray technique will have "picked up" changes in developing preadipocytes (early stages of adipogenesis) present in lower dermal compartment between e17 and e19 time points.

For analysis several available publications were selected where adipogenesis has been investigated in 3T3-L1 cells using the microarray approach (sections 3.3.4 and 3.3.5). Then, the presence of genes repressed or enriched in differentiating 3T3-L1 cells was analysed in the lower dermis (LD) microarray data.

**Global analysis.**

First, the global analysis based on the Burton *et al* (2004) work showed a gradual increase in the percentage of genes present in both *in vitro* and *in vivo* adipogenic process in later stages of such differentiation. In addition, a majority of present genes that were up-regulated *in vitro* was also undergoing enrichment *in vivo*, whereas more than half of present genes that were repressed *in vitro* were actually up-regulated between e17 and e19 time points *in vivo*. This simple comparison work suggested clear differences between 3T3-L1 cells and lower dermal cells in relation to early changes occurring during adipogenesis.

**Detailed comparisons of adipogenesis differentiation *in vivo* and *in vitro*. Transcription factors.**

Several families of adipogenic transcriptional factors have been pointed to as being crucial for adipogenic differentiation (reviewed by Gregoire *et al*, 1998; White and Stephens, 2010), therefore a presence of these factors was investigated in the *in vivo* microarray data (section 3.3.5.1). It become obvious that several of these transcriptional factors were regulated also *in vivo* in lower dermal cells, such as C/EBPalpha, PPARgamma, KLFs family or SREPBP-1 (Figure 3.42).

Among members of the Krüppel-like factors (KLFs) that were found in the LD microarray list were *Klf3*, *Klf4*, *Klf5*, *Klf6*, *Klf9* and *Klf15* genes (Figure 3.38). These factors have been widely studied in relation to adipogenesis regulation. For example, transgenic animals with knockout for KLF3, were characterised by the decrease in an amount of adipose tissue and 3T3-L1 based studies showed the ability of KLF3 to bind to the promoter of C/EBPalpha (Sue *et al*, 2008). KLF6 was shown to activate adipogenesis for example in 3T3-based cells (Li *et al*, 2005). Finally, KLF9 was shown to interact with C/EBPalpha and activate a promoter of PPARgamma2 (Pei *et al,* 2011). KLF15 was shown to be up-regulated during adipogenic differentiation and its role in regulation of this process has been suggested (Mori *et al*, 2005). The KLF family seemed to be crucial for developmental processes taking place in lower skin dermis at embryonic level that lead to development of dermal adipose tissue in mouse back skin.

On the other hand regulation on mRNA level of such transcriptional factors as *Cebpb*, *Cebpd* or *Stat5* was not seen *in vivo*. The issue about absence of *Cebpb* and *Cebpd* genes in the LD microarray list is widely discussed later in this section.

In general, transcriptional factors are creating a complicated cascade of interactions with each other in order to properly regulate differentiation (Figure 3.42). The lack of some of these elements *in vivo* in mouse back skin, could be related with a fact that some other (maybe unknown yet) factors are replacing these elements as for example the adipogenesis process that takes part in mouse back skin could undergo other regulatory cascade that other fat depots or that all *in vitro* cell-based studies are missing steps that normally takes part in life body *in vivo*. For example, *Smarca5* gene was spotted in this data to be up-regulated *in vivo* (Figure 3.43E), however no information was found that would define its role in adipogenesis.

**Growth factors.**

The analysis of growth factors was also performed on the LD microarray data (Figure 3.48). Expression of growth hormone receptor, *Igf1*, *Igf2*, *Igf1r* or *Igfbps* was seen in lower dermal cells. Insulin-like growth factor-1 (IGF-1) is crucial for the adipogenesis activation in many cell lines, for example in 3T3-L1 cells (reviewed by Gregoire *et al,* 1998). In addition, IFG-1 was shown to be expressed in adipose tissue, for example in rat white adipose tissue - WAT (Peter *et al,* 1993). It is believed that different factors can be secreted by cells undergoing adipogenesis in order to trigger this process in other fat cells through autocrine/paracrine stimulation. Such a suggestion arose for insulin-like growth factor 1 (IGF-I) in mouse

preadipocyte Ob1771 cells (Kamai *et al*, 1996). IGF-1 interacts with insulin growth factor-1 receptor; IGF-1R that was found to be present in 3T3-L1 cells (Huo *et al*, 2003). It was also shown that fat cells can produce and secrete insulin-like growth factor binding proteins (IGFBPs) which may influence the IGF-1 activity (reviewed by Gregoire *et al*, 1998). The up-regulation of *Igf1* and *Igfbp4* genes were found in microarray based studies during differentiation of 3T3-L1 cells (Hackl *et al*, 2005). To the best of my knowledge *Igfbp7*, which was up-regulated in the lower dermal array (Figure 3.46J) seemed not to be related functionally with adipogenesis *in vitro*, and previously only high serum levels of Igfbp7 were observed in adults with type 2 diabetes (reviewed by Ruan and Lai, 2010).

**Early adipogenic processes in relation to cell cycle regulation.**

Cell line-based studies on adipogenesis show specific changes at early steps of adipogensis in relation to cell cycle and re-arrangements of a cell shape with dramatic changes of both cytoskeletal and extracellular matrix proteins levels (reviewed by Gregoire *et al*, 1998; reviewed by Rosen and Spiegelman, 2000). Depending on cell line, either confluence and cell-cell contact or a lack of the confluence are the first signs of changes and the so-called “initial growth arrest” taking place. By influencing cells with adipogenic medium (discussed in section 1.3.2.2 of Chapter 1), cells undergo differentiation, and growth arrest is then followed by one or two rounds of the cell division (the “clonal expansion” step) which is observed in 3T3 cells. Finally, cells enter the “post-mitotic growth arrest” step and then “terminal differentiation” occurs (Morrison and Farmer, 1999). Richon *et al* (1997) performed analysis of 3T3-L1 cell proliferation and DNA synthesis by BrdUrd incorporation into these cells. This analysis showed that before adipogenic induction only a small number of cells show BrdUrd staining due to quiescence. Then, cells at one day after the adipogenic induction were characterised by the high proliferation rate due to the high amount of incorporated BrdUrd, whereas at day three these cells were undergoing a withdrawal from cell cycle. Not all cell lines that have been analysed (primary human preadipocytes) seemed to require the growth arrest step said to be needed for adipogenesis (Entenmann and Hauner, 1996). Therefore a suggestion was made that the additional rounds of mitosis are occurring due to artificial environment in which two-dimensional cells are kept, or such changes occurred in the *in vivo* before cell lines were isolated and cultured (by Rosen and Spiegelman, 2000). The question is whether the array findings in this study can determine whether *in vitro* models genuinely mirror *in vivo* events.

**Growth arrest and clonal expansion.**

A first step in investigating this question was the verification of the presence of cell cycle related genes in lower dermal cells. The global comparison analysis revealed that only 21% of cell cycle genes, summarised in by Hackl *et al* (2005) were common for both 3T3-L1 and lower dermal cells (see Figure 3.49A and B). These common genes in differentiating 3T3-L1 cells were up-regulated during first 12 and/or 24 hours of adipogenic induction, and then their quite dramatic down-regulation took place after one day of adipogenesis (Figure 3.50A and C). These common genes, except one (centromere protein A) were up-regulated also *in vivo* from e17 time point and their over-expression was higher at e18 than e19 time point (Figure 3.50B and D). Therefore it could be said that this small group of common genes is sharing similar expression pattern in differentiating *in vitro* and *in vivo* cells.

What seemed more interesting is the fact that 37% of cell cycle genes pointed out by Hackl *et al* (2005) in differentiating 3T3-L1 cells were not seen to be regulated in the lower dermal cells. In addition, several representatives of cell cycle genes seen in the LD microarray data (32% of analysed genes, Figure 3.49) were not related with 3T3-L1 cells in Hackl *et al* (2005) study. Therefore in global terms there were considerable differences between the present *in vivo* array data and what has been found previously.

The widely described studies on 3T3-L1 cells have revealed specific expression profiles of different cell cycle genes. Richon *et al* (1997) showed that in cells before adipogenic treatment (day 0) and then 1, 2, 3 and 4 days after the addition of adipogenic factors, dramatic changes at the protein levels occurred for p107, p130 and p107-E2F or p130-E2F complexes. At the mRNA level, p107 (*Rbl1* gene) was observed to be up-regulated in 3T3-L1 cells at day 1, and then its level subsequently decreased (Richon *et al*, 1997). This expression pattern was not observed for p107 mRNA in work described in this thesis, and the p107 (Rbl1) gene was not present in the LD microarray data at any of the time points.

Specific changes in expression profile of p21, p27 and p18 were spotted during the differentiation of 3T3-L1 cells. Morrison and Farmer (1999) showed that the p21 gene was up-regulated between day 1 and 3 of adipogenic induction in 3T3-L1 cells. The mRNA level of p27 dramatically decreased between days 1 and 2 of adipogenic induction and then p27 was up-regulated at day 3 in 3T3-L1 cells, whereas the up-regulation of p18 was seen from day 3 of adipogenic induction (Morrison and Farmer; 1999). Both p21 and p27 belong to the kinase inhibitor

protein (KIP) family and the p18 is a member of the inhibitor of cdk4 (INK4) family. These inhibitors of cyclin-dependent kinases (cdks) take part in the regulation of cell cycle progression (Schafer, 1998). Both p27 (cyclin-dependent kinase inhibitor 1B; *Cdkn1b*) and p21 (cyclin-dependent kinase inhibitor 1A; *Cdkn1a*) were not regulated in lower dermal cells between e17 and e19 time points and only p18 gene (cyclin-dependent kinase inhibitor 2C; *Cdkn2c*) was up-regulated in these cells from e17 time point (Table 3.10). Morrison and Farmer (1999) also showed that the addition of adipogenic medium into the confluent 3T3-L1 cells led to the down-regulation of cyclin D1 gene (*Ccnd1*) four days after the adipogenic induction. This gene was also regulated *in vivo* in lower dermal cells (based on the LD microarray data) with about 2-fold change at e18 versus e17 time-point and approximately 1.7-fold change at e19 versus e17 time point.

In addition, the LD microarray data clearly showed over-expression of cyclin-dependent kinase 4 gene (*Cdk4*) with a 2.50-fold change at e18 versus e17 time point and with a 1.38-fold change at e19 versus e17 time point. Maybe the increased expression of *Cdk4* at e18 versus e17 time point is important for the correct regulation of the cell cycle *in vivo*. Then, the over-expression of p18 (*Cdkn2c*) in lower dermal cells could be crucial for the accumulation of this protein in the dermis between e17 and e19 time points, and its interaction with Cdk4. This interaction could be then crucial for inhibition of Cdk4 which could then help to withdraw these cells from the cell cycle and “push” them into the adipogenic differentiation process and development of mature fat cells. The Cdk4 function was investigated in 3T3-L1 cells and its role in the clonal expansion phase as well as in the regulation of terminal steps of adipogenesis and control of mature fat function was suggested by Abella *et al* (2005). Therefore it could be interesting to further investigate the role of Cdk4 in developing lower dermal cells in embryonic/foetal skin.

**Timing of *in vitro* and *in vivo* adipogenesis.**

As was mentioned already in this section, the generated microarray data did not contain either *Cebpb* or *Cebpd* genes, suggesting that these two factors did not undergo significant enrichment in the lower dermis between e17 and e19. However, the up-regulation of these genes could take place in dermal compartment from an earlier time than was the scope of this study (for example e16 time point).

In addition, genes for two major adipogenic transcription factors *Cebpa* and *Pparg*, known to be enriched from day 2 in differentiating 3T3-L1 cells (after the up-regulation of *Cebpb* and *Cebpd*; Morrison and Farmer, 1999), were also enriched in lower dermal cells from e17 till e19 time point (Table 3.4). In addition, the *in vivo* up-regulation of p18 gene (*Cdkn2c*) together with a very robust enrichment of adipsin gene (*Adn*; well known protein secreted by mature adipocytes) at e19 time point (Table 3.10 and Table 3.4) revealed quite similar expression pattern of these two genes in 3T3-L1 cells between days 3 and 5 during adipogenesis (Figure 3.63). This analysis suggests that there is a lower dermal cell population already committed to adipogenesis and undergoing dynamic differentiation processes from e17 till e19 time point. On the other hand the up-regulation of cyclin D1 gene (*Ccnd1*), seen between e17 and e19 time point could suggest the presence of cells in lower dermal cells that are at the very early stages of adipocyte differentiation, due to a fact that enrichment of this gene takes place in 3T3-L1 cells till day 3 (after adipogenic induction) and drops dramatically at day 4 (Figure 3.63). This fact could be explained by a heterogeneous nature of lower dermal cells where adipogenesis in back skin dermis is a non-synchronised process and at specific time points, around fully (or almost fully) differentiated fat cells are still adipocytes that just start to undergo changes related with regulation of cell cycle processes. Therefore the absence of several cell cycle genes (for p107; p21; p27) together with *Cebpb* and *Cebpd* genes in the lower dermal microarray data could be also related with the fact that that actually these genes do not play a significant role in the regulation of fat cell development *in vivo* between e17 and e19 time point in embryonic back skin dermis.

In order to fully characterise and define early steps of adipogenesis *in vivo* in lower dermal cells in relation to cell cycle processes, the analysis of these cells at the mRNA level should be combined with an investigation at the protein level. The reason for this is that some published studies on 3T3-L1 cells showed that not only mRNA levels but also protein levels of cell cycle genes significantly are changing during *in vitro* adipogenesis (Richon *et al*, 1997; Morrison and Farmer, 1999). Moreover some cell cycle related genes, for example p130 in differentiating 3T3-L1 cells, do not change at the mRNA level but actually at the protein level during *in vitro*

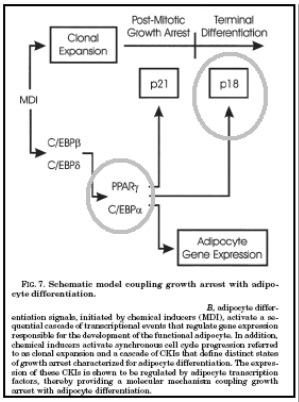


FIG. 7. Schematic model coupling growth arrest with adipocyte differentiation.

*B*, adipocyte differentiation signals, initiated by chemical inducers (MDI), activate a sequential cascade of transcriptional events that regulate gene expression responsible for the development of the functional adipocyte. In addition, chemical inducers activate synchronous cell cycle progression referred to as clonal expansion and a cascade of CKIs that define distinct states of growth arrest characterized for adipocyte differentiation. The expression of these CKIs is shown to be regulated by adipocyte transcription factors, thereby providing a molecular mechanism coupling growth arrest with adipocyte differentiation.

**(Morrison and Farmer, 1999)**

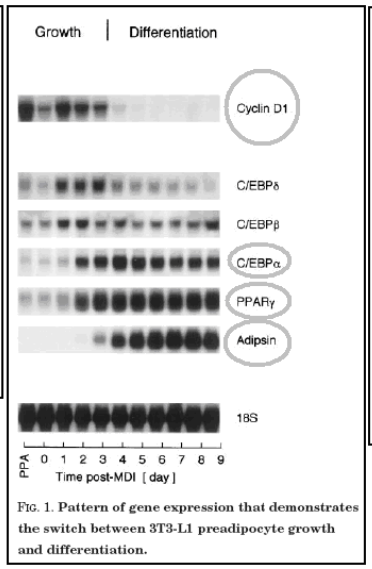


FIG. 1. **Pattern of gene expression that demonstrates the switch between 3T3-L1 preadipocyte growth and differentiation.**

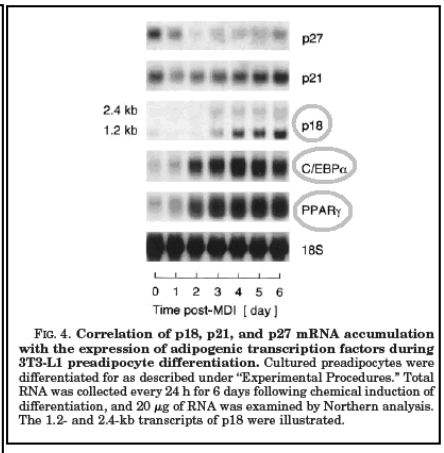


FIG. 4. **Correlation of p18, p21, and p27 mRNA accumulation with the expression of adipogenic transcription factors during 3T3-L1 preadipocyte differentiation.** Cultured preadipocytes were differentiated for as described under "Experimental Procedures." Total RNA was collected every 24 h for 6 days following chemical induction of differentiation, and 20 μg of RNA was examined by Northern analysis. The 1.2- and 2.4-kb transcripts of p18 were illustrated.

Figure 3.63. The suggested model of early steps of adipogenesis and expression pattern of several genes associated differentiating 3T3-L1 cells. The figures were taken from Morrison and Farmer (1999). Genes regulated in the lower dermis cells (based on the microarray data) were circled in grey.

adipogenesis (Richon *et al*; 1997). Finally, in order to verify the state of proliferation of lower dermal cells during mouse back skin development, an experiment could be performed where the incorporation of BrdUrd would be analysed for example in back skin sections from mouse embryos. Finally, all this analysis should be combined with younger than e17 time point skin specimens to obtain a fuller view in processes taking place in lower dermal cells.

**Cytoskeletal and ECM proteins during adipogenesis.**

The cell line based studies showed that changes in cytoskeletal proteins and extracellular matrix components (ECM) are crucial for rearrangements of differentiating cells from the fibroblast-like to a spherical shape where the major cell space is taken by accumulated lipids. The changes in levels of actin, tubulin or different collagen types, have been widely described in both human and rodent-derived cell lines (reviewed by reviewed by Gregoire *et al*, 1998; Mariman and Wang, 2010). In addition, Mariman and Wang (2010) pointed out that the enrichment of collagen in *in vitro* cells could be due to artificial conditions of culturing two-dimensional cells. Therefore it seemed interesting to verify how many of both cytoskeletal and ECM specific genes are up-regulated *in vivo* during dermal cells development.

The GeneCoDis2.0 tool allowed cytoskeletal and extracellular matrix genes regulated in developing lower dermal cells to be identified and compared to microarray data from differentiating 3T3-L1 cells (Burton *et al*, 2004; Hack *et al*, 2005; Kim *et al*, 2007). Striking differences were spotted between *in vitro* and *in vivo* cells as for example only 25% of cytoskeletal genes and 24% of ECM genes regulated in the lower dermal cells were seen in the *in vitro* microarray data (Figure 3.51 and Figure 3.54). Therefore, the *in vivo* developing cells did not share an exact ECM protein profile with any of these cells, suggesting that clearly adipogenic differentiation *in vivo* in mouse back skin has its own, specific features. However in order to develop a better conclusion the future study should be performed where the presence of *in vitro* ECM proteins in the lower dermal cells could be verified on the protein level.

In general, changes in the expression of different types of collagen (such as collagen IV) were observed in differentiating *in vitro* cells (reviewed by Mariman and Wang, 2010). Therefore the LD data was searched for the collagen genes and out of 14 genes, half of them were also seen in *in vitro* cells (for example *Col4a1*, *Col4a2*). Interestingly, half of these *in vivo* collagen genes were down-regulated during development of lower dermal cells from e17 till e19 time points. In addition, the *in*

*vitro* based studies on adipogenesis revealed regulation of many ECM processing enzymes such as ADAMTS, MMP or TIMP and ADAMTS enzymes can be involved in processing of procollagens by cutting off their N- or/and C- ends (reviewed by Mariman and Wang, 2010). *Adamts1*, *Adamts4* and *Adamts5* genes, regulated in lower dermal cells, were shown to be associated with adipocytes (section 3.3.5.4). The *Adamts15* gene, also present in the LD data, was up-regulated during early step of adipogenic differentiation in mouse embryonic fibroblasts (Baudry *et al*, 2006) but it seemed not to be so far functionally defined in relation to *in vivo* development of fat cells. What is interesting, is the fact all four *Adamts* genes had the highest fold change regulation at e18 time point (versus e17) whereas at e19 (versus e17) their expression was at lower level. Therefore the *in vivo* cell development from e18 to e19 time points could be related with a progressive reduction of ECM processing enzymes due to a lack of need to modify ECM components in these developing three-dimensional cells. Also it could be interesting to develop a future study where the role of ADAMTS15 in developing *in vivo* lower dermal cells will be analysed due to the fact that among all four *Adamts* genes this one had the most dramatic down regulation from e18 to e19 time points.

To sum up, huge differences between cytoskeletal and ECM proteins regulated during *in vitro* and *in vivo* adipogenesis clearly suggest that the differentiation process observed in two-dimensional cell lines undergo different regulation at the level of re-arrangement of morphology and shape of cells than in three-dimensional cells in lower dermal area. Probably the artificial environment of the cell culture dish is not a normal situation where cells have to activate cascades and pathways normally not needed in cells developing in the body. Therefore the further investigation of these lower dermal cells could be crucial for the understanding the “real” processes under which cells become mature adipocytes.

**The late stages of adipogenesis: metabolic processes and production of secreted proteins.**

The final comparison study related to the late stages of adipogenesis (lipogenesis) when mature adipocytes are filled with lipid droplets, produce different secreted proteins and are involved in the regulation of metabolism (reviewed by Gregoire *et al*, 1998; Rosen and Spiegelman, 2000). Interestingly, *in vitro* and *in vivo* differentiating cells seemed to share more common genes when undergoing later stages of development. Hackl *et al* (2005) have performed an interesting analysis where the key enzymes and metabolic processes activated in 3T3-L1 cells

were summarised. The presence of these key enzymes was investigated in the lower dermal microarray data and 61% enzymes occurred to be common for both *in vitro* and *in vivo* developing fat cells. All these common genes were up-regulated from e17 time point in lower dermal cells. Moreover, among these 20 common genes only five had lower fold change value at e19 time point (versus e17) when comparing with e18 time point (versus e17) and the rest 15 had the highest over-expression at e19 time point (versus e17) (Figure 3.59B). This analysis showed that key metabolic processes underwent progressive activation in lower dermal back skin at late stages of embryonic development. In addition, *in vitro* and *in vivo* cells seemed to be similar because of the production of secreted proteins that also take place in differentiated fat cells. Among genes of secreted proteins, seen in the LD microarray data were resistin (*Retn*), adipsin (*Adn*), angiotensinogen (*Agt*) or adiponectin (*Adipoq*). All four genes were enriched in lower dermal cells from e17 till e19 time points with a dramatic over-expression at e19 versus e17 time points. This analysis showed that just before an animal birth a very robust expression process in developing fat cells takes place, which could be crucial for the establishment of fully functional mature fat cells that create dermal adipose tissue after the animal birth.

The developmental stages of lower dermal cells, observed here on the molecular level are therefore more likely to be real *in vivo* events due to a fact that they lead to development of a fat cells that shares features (over-expression of mRNA for specific secreted fat proteins, enrichment of genes involved in metabolic processes) with mature fat cells differentiated from cell lines or dissected from fat depots (reviewed by Gregoire *et al*, 1998; Soukas *et al*, 2001).

In addition, the processes related with regulation of transcriptional factors, cell cycle genes, cytoskeletal and extracellular matrix proteins in lower dermal cells between e17 and e19 time points, are also likely to be real. Moreover, occurrence of differences in types of genes regulated at early stages of adipogenesis between lower dermal cells and in 3T3-L1 cells could be simply because the experimental approach used in this thesis allowed to track features of cells *in vivo* and not in artificial environment of the cell culture dish.

To sum up, work presented in Chapter 3 gave a unique insight into *in vivo* molecular processes taking place in embryonic skin dermis between e17 and e19 time points. Moreover, this study revealed gene expression patterns in embryonic lower dermal cells that give rise to dermal adipose tissue postnatally.

# *In vivo* and *in vitro* studies of adipogenesis with particular reference to adipocyte development in rodent skin.

## (Vol. I and Vol. II)

### Volume II of two volumes

by
Kamila Wojciechowicz-Grzadka

**Thesis submitted for the degree of Doctor of Philosophy.**
**School of Biological and Biomedical Sciences**
**Durham University**

2012

This thesis is entirely a result of my work. It has not been accepted for any other degree and is not being submitted for any other degree.

Kamila Wojciechowicz-Grzadka

2012

## Table of contents

**VOLUME II** **page**

## List of Tables

**VOLUME II** **page**

## List of Figures

**VOLUME II** **page**

## List of Appendices

**Volume II** **page**

## Abbreviations

| | |
|---|---|
| ADIP | adipogenic medium |
| BT | bottom part of the back skin |
| C | control medium |
| cDNA | complementary deoxyribonucleic acid |
| d | day |
| DAPI | 4',6-diamidino-2-phenylindole |
| DAT | dermal adipose tissue |
| DEPC | diethylpyrocarbonate |
| DMD | dermis microarray data |
| D-MEM | Dulbecco's Modified Eagle's Medium |
| DNA | deoxyribonucleic acid |
| dNTP | deoxynucleoside triphosphate |
| DP | dermal papilla |
| DS | dermal sheath |
| e | embryo |
| EDTA | ethylenediaminetetraacetic acid |
| EGF | Epidermal Growth Factor |
| EGFR | Epidermal Growth Factor Receptor |
| FBS | foetal bovine serum |
| FLs | fat layers |
| Fu | funigzone |
| Ge | gentamicyn |
| H&E | Haematoxylin and Eosin |
| LCM | laser capture microdissection |
| LD | lower dermis |
| mRNA | messenger ribonucleic acid |
| M | muscle layer |
| MEM | Minimal Essential Medium |
| N | newborn |
| NCBI | National Centre for Biotechnology Information |
| NCS | newborn calf serum |
| PBS | phosphate buffered saline |
| PCR | polymerase chain reaction |
| PF | posterior fat |
| qRT-PCR | quantitative reverse transcription-polymerase chain reaction |
| RNA | ribonucleic acid |
| RT | room temperature |
| SAT | subcutaneous adipose tissue |
| S-d | skin from the dermis site |
| S-e | skin from the epidermis site |
| TP | top part of the back skin |
| 2D | two dimensional |
| 3D | three dimensional |

# Chapter 4:
# Techniques “mimicking” *in vivo* conditions for the analysis of embryonic skin and dermis because of the capability to accumulate lipids.

## 4.1. Introduction.

The aim of this Chapter is to establish an effective *ex vivo* experimental method for the investigation of lipid accumulation in back skin dermis at embryonic level, and to perform a functional study of a gene selected from the microarray data presented in Chapter 3. An outline of the work described in this Chapter is shown in Figure 4.1.

Based on the dermis microarray data, the specific up-regulation of epidermal growth factor receptor (EGFR) expression was observed in lower mouse embryonic skin dermis (see Table 4.4). EGFR is a cell-surface receptor known to play a role in skin and hair development (Richardson *et al*, 2009). EGFR can be activated by an interaction with epidermal growth factor (EGF) and EGF has been suggested to take part in controlling adipogenesis in 3T3-L1 cells (Adachi *et al*, 1994). EGF enhanced differentiation in cells already undergoing adipogenesis, however it inhibited adipocyte conversion when added to preadipocytes (cells not yet undergoing adipogenesis). In addition, the activation or inhibition of adipogenesis by EGF-EGFR pathway (in cell culture) was dependent on concentrations of EGF (Harrington *et al*, 2007).

The pivotal role of the EGFR-EGF signalling pathway and fat development has been observed *in vivo*. In a mouse model where a dominant negative mutant of EGFR was analysed in relation to skin development, 21 day old transgenic animal skin was seen to have necrotic hair follicles. This skin was lacking fat cells between the hair follicles, the adipose cells had been replaced by a granulomatous tissue (Murillas *et al*, 1995). In addition, unexpected results in relation to decrease in fat deposition in skin were observed in postnatal Wa5 mice which had an antimorphic EGFR allele (Sugawara *et al*, 2010).

The hypothesis tested in this Chapter says that the EGF-EGFR signalling pathway can be involved in the regulation of fat cell differentiation in lower dermis at late stages of mouse embryonic development. To best of my knowledge, no *in vivo* experiment has been designed so far to verify this hypothesis. Thus, the analysis of this hypothesis is presented in this Chapter. First, the verification of EGFR expression in back skin dermis was performed by qRT-PCR and immunofluorescent staining. Then, an attempt to develop an effective technique for mimicking the *in vivo*-like environment was performed by growing 3D structures (the hanging-drop versus the substrate organ culture). Finally, the substrate organ culture technique was used for further experiments, where small pieces of embryonic back skin were treated with either an inhibitor (AG1478) or an activator (EGF) of EGFR and the capability of lipid accumulation was investigated by the Oil Red O staining.

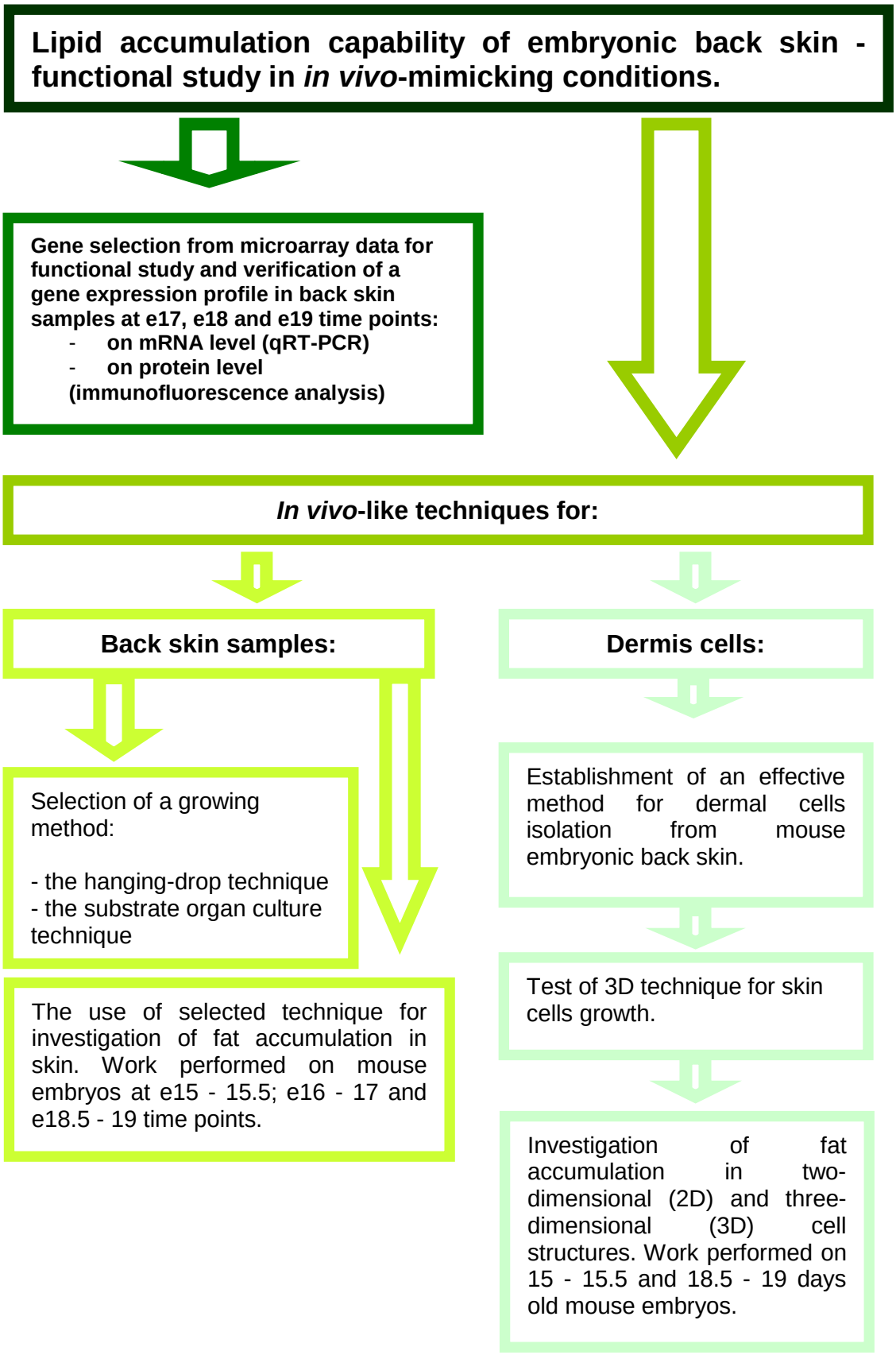


Figure 4.1. Summary of work presented in Chapter 4. The aims were to develop efficient methods for mimicking *in vivo* conditions in relation to the analysis of embryonic back skin, to analyse development of fat cells in lower skin dermis and to perform a functional study for gene from dermis microarray data (from Chapter 3).

In the second part of Chapter 4, features of embryonic skin dermis were analysed in relation to fat accumulation capability. For this study, dermis was used from mouse embryos well before the accumulation of fat (e15 - 15.5) and 18.5 - 19 day old mouse embryos in which the first lipid droplets are easy to detect in close proximity to hair follicle end bulbs (see Chapter 2). The aim was to isolate dermal cells from these samples, grow them either in two-dimensional (2D) conditions or in three-dimensional (3D) spheroid cell culture then analyse their capabilities to accumulate lipids.

In the commonly used 2D monolayer culture method cells attach and grow on the artificial surface of cell culture dishes. This technique is widely used for the cell-based studies, however it is important to note that when cells are “pushed” to recreate an *in vivo* behaviour, such as the onset of adipogenesis on the culture dishes, then the environment is artificial and consequently the observed cell changes may not be a representative of the *in vivo* conditions. Thus, there is a general need for techniques that will better recreate the *in vivo* environment and allow cells to be in three-dimensions as happens in the body. The 3D spheroid cell culture method allows cells to be suspended in small droplets of culture medium. In such an environment, cells gather together and form a sphere. Cells in the sphere are not in contact with plastic culture substrates and are surrounded only by medium. They therefore interact only with other cells in all dimensions. The 3D spheroid cell culture has been successfully applied in hair follicle-related studies by Prof. CAB Jahoda’s research group, where a dermal papilla-like structure was recreated (Higgins *et al*, 2010).

The spheroid cell culture method was used on cells derived from human and rodent skin. The general features of such 3D cultures were compared with 2D cultures by the analysis of both cytoskeletal and nuclear envelope proteins. Nuclear proteins, such as lamins or emerin are important components of the nuclear envelope. They interact with each other (for example lamin A with emerin) and take part in different processes connected with maintaining cell shape, controlling cell function and DNA replication or RNA transcription (Goldman *et al*, 2002; Hutchison, 2002; Lee *et al*, 2001; Vaughan *et al*, 2001).

In summary, this Chapter builds on the microarray data from Chapter 3, an investigation of the gene shown to have differential regulation *in vivo* in mouse dermal cells. It seems possible to use microarray data for the selection of a gene whose role in developing embryonic skin compartment can be further investigated. In addition, several *in vivo*-like techniques have been introduced in Chapter 4, in

order to verify which method would be the most efficient for the growth of skin samples or skin-derived cells and which one would be most suitable for use in the functional study of a gene selected from the microarray data. Such work will lead to a better understating of pathways involved in dermal adipose tissue development.

## 4.2. Methods.

Experiments presented in Chapter 4 were repeated at least two times.

### 4.2.1. Housing, breeding and feeding conditions of rodents.

Detailed description of housing, breeding and feeding conditions used for rodents is presented in Chapter 2, section 2.2.1.

In addition, section 2.2.1 contains the procedure for a determination of the embryos age and methods used to sacrifice animals.

### 4.2.2. EGFR analysis - verification of the dermis microarray work.

#### 4.2.2.1. qRT-PCR analysis of the EGFR mRNA level.

Preparation of mRNA and details of qRT-PCR were described in Chapter 3, section 3.2.6.1.2. Primers used for the verification work were presented in Table 3.2. (Chapter 3, section 3.2.6.1.2).

#### 4.2.2.2. Immunofluorescence analysis of EGFR protein.

The back skin sections from mouse embryos at e17, e18 and e19 time points were prepared and stained with antibodies against EGFR according to a method presented in Chapter 3, section 3.2.6.2.

### 4.2.3. The hanging-drop organ culture technique.

The hanging-drop technique was used previously for the growth of mouse embryonic back skin (Fliniaux *et al*, 2008).

Rectangular pieces of mouse back skin, with a maximum size of approx. 2.5 mm x 3 mm, were cut from 16 - 17 day old mouse embryos (e16 - 17) and specimens were placed in media droplets (approximately 30 μl) on Petri dish lids. Then, lids were inverted and placed on the bases of the Petri dishes which contained sterile water to control humidity. The medium used consisted of D-MEM - Dulbecco's Modified Eagle's Medium (Sigma), 1% FBS - foetal bovine serum (Sigma) and antibiotics (2 μl/ml Fu - fungizone from Sigma and 1 μl/ml Ge - gentamicin from Gibco) as a base (control) medium. In addition, for the experimental medium, either the inhibitor of EGFR, AG1478 (with final concentrations of 50 μM and 200 μM, prepared from the 10 mM stock; Calbiochem) or the EGFR activator, EGF (with the final concentrations of 25 ng/ml and 100 ng/ml, prepared from the 10 μg/ml stock; Sigma) were added. The experiment was run for three days, after which samples were carefully transferred into Tissue Tek, frozen in liquid nitrogen and kept at -80$^{o}$C.

Frozen specimens were cut on a cryostat (LEICA CM 3050S) and sections (7 μm) were attached to SuperFrost®Plus slides (Menzel-Glaser), air dried for up to 90 minutes at room temperature, and then used immediately for lipid detection (see section 4.2.7).

### 4.2.4. The substrate organ culture technique.

The organ culture technique was used previously for the growth of mouse embryonic back skin by Richardson *et al* (2009).

Rectangular pieces of mouse back skin, with a maximum size of approx. 2.5 mm x 3 mm, were cut from 15 - 15.5, 16 - 17 and 18.5 - 19 day old embryos (named as e15 - 15.5; e16 - 17; e18.5 - 19 time points). Specimens were transferred on the Nucleopore membrane filters (Whatman), coated with rat-tail collagen type 1 (Sigma) (Figure 4.2). Samples were placed with the epidermis side up. Filters were then floated on 2 ml of control medium (D-MEM; 1% FBS; antibiotics: 2 μl/ml Fu - fungizone and 1 μl/ml Ge - gentamicin) or experimental media (Table 4.1) in a 35 mm dish. The samples were incubated in 5% $CO_2$ and 37$^{o}$C for 72 hours. Samples were cryopreserved and cryostat sectioned for analysis as described above (see section 4.2.3).

Table 4.1. Types of experimental media used for the substrate organ culture work.

| **Experimental medium:** | **Ingredients:** |
|---|---|
| **"Activation"(A) medium** | D-MEM; 1% FBS; antibiotics (2 μl/ml Fu - fungizone, 1 μl/ml Ge - gentamicin); EGFR activator: EGF (25 ng/ml or 100 ng/ml, Sigma) |
| **"Inhibition" (I) medium** | D-MEM; 1% FBS; antibiotics (Fu, Ge; for concentrations see above); EGFR inhibitor: AG1478 (50 μM or 200 μM Calbiochem) |
| **Adipogenic (ADIP) medium** | D-MEM; antibiotics (Fu, Ge; for concentrations see above); 15% rabbit serum (Sigma); 2.6 - 2.07 μM Insulin (Sigma); 100 nM Dexamethasone (Sigma); 0.45 mM IMBX (Sigma) |

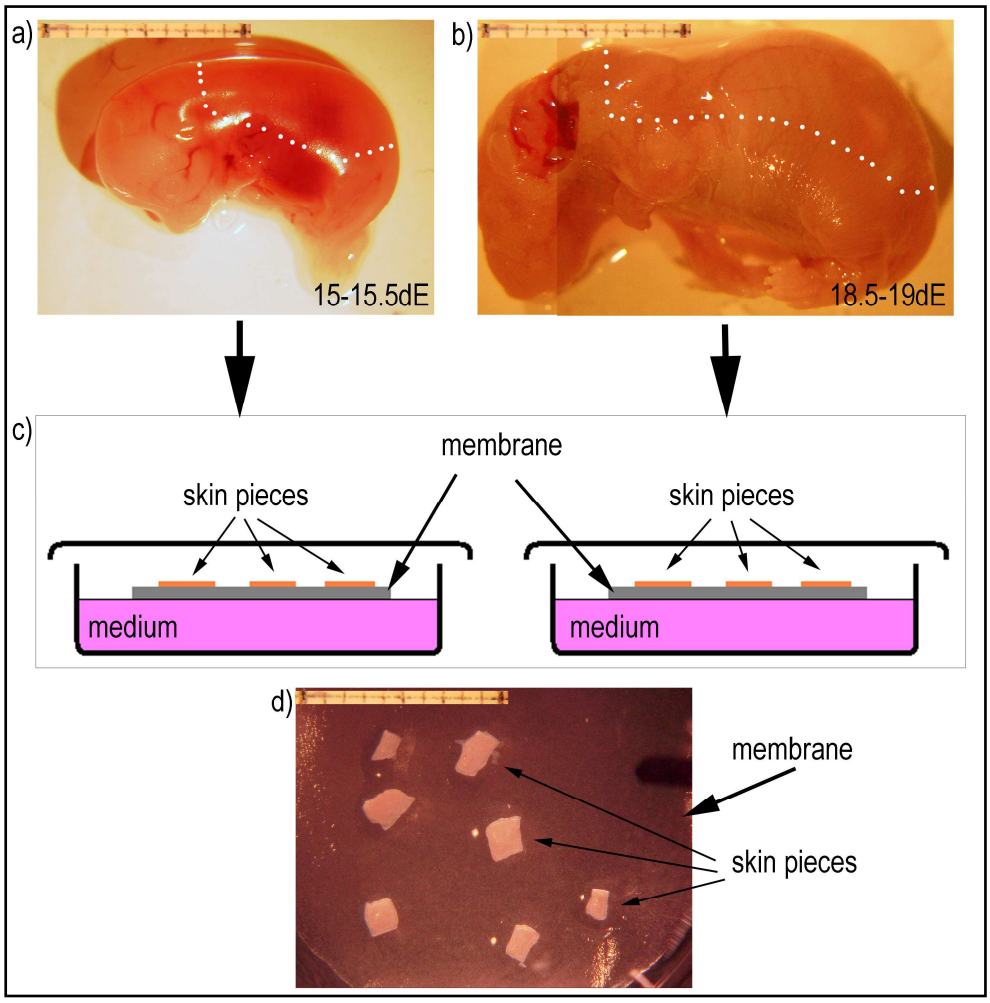


Figure 4.2. Preparation of back skin samples for the substrate organ culture work. Back skin samples from 15 - 15.5 (a) and 18.5 - 19 (b) day old mouse embryos were cut into rectangular pieces and placed on rat-tail collagen-coated membranes (c and d). Samples were incubated in different experimental culture medium. Scale bar = 1 cm. Photo (d) was taken on the Ziess StemiSVII microscope (with the digital camera KY-FI030 JVC and with the KyLink software).

### 4.2.5. The establishment of skin cell lines used for two- (2D) and three- (3D) dimensional cells.

Dermal papilla (DP), dermal sheath (DS) and dermal skin fibroblasts (FI) cell lines were established from rodent (mice - CD1 and rats - PVG) and human skin samples. Animals were obtained from the animal house at Durham University, whereas human skin samples were obtained from the University Hospital of North Durham and the Royal Victoria Infirmary Hospital (Newcastle Upon Tyne). All human skin samples used for research had patient consent and were treated in accordance with the Human Tissue Act 2004. Methods for DP, DS, and FI cell line preparations are presented below with human skin samples as an example.

#### 4.2.5.1. Cell lines from human skin samples.

Skin samples were obtained from different parts of human body (e.g. beard, breast biopsy, etc.) and were recorded and numbered (for example, skin sample no. 2_06 was a second sample given from the hospital in 2006 year). FI, DP and DS cells were established from each skin sample and got the same name as the skin sample, from which they were established. When skin samples were big and contained excess layer of fat tissue, they were cut into smaller pieces and fat layer was removed. Then the samples were stored in MEM - Eagle's Minimum Essential Medium (Sigma) with antibiotics (4 μl/ml Fu - fungizone from Sigma and 2 μl/ml Ge - gentamicin from Gibco) at 4ºC over night. The next day, samples were washed in MEM with antibiotics (4 μl/ml Fu and 2 μl/ml Ge).

##### 4.2.5.1.1. Dermal papilla and dermal sheath cell lines.

Human end bulbs were cut from the skin sample, transferred into drops of MEM and the fat layer was removed from the end bulb. Mouse hair follicles require an additional step to remove the collagen cap that surrounds the hair follicle. Next the bulb was inverted and the dermal papilla was pushed out from the end bulb (Figure 4.3), cleaned from the epithelial matrix, and transferred into 4-well dish (Nunclon) that contained MEM with 20% foetal bovine serum (FBS; from Sigma) and antibiotics (2 μl/ml Fu - fungizone from Sigma and 1 μl/ml Ge - gentamicin from Gibco). Dermal sheath was cleaned and transferred into 4-well dish with MEM, 20% FBS and antibiotics (2 μl/ml Fu and 1 μl/ml Ge). DP and DS were put on the bottom of the dishes and left for 6 - 7 days in the incubator (37$^{o}$C, 5% $CO_2$). After one week, media was changed. When cells reached 80 - 95% confluence, they were carefully transferred into the 35 mm dish (first passage), then into the T25 flask (second

passage). After second passage, cells were grown in MEM with 10% FBS and antibiotics (2 µl/ml Fu and 1 µl/ml Ge). Dissection of DP and DS was performed using the Stemi SV6 microscope (ZIESS).

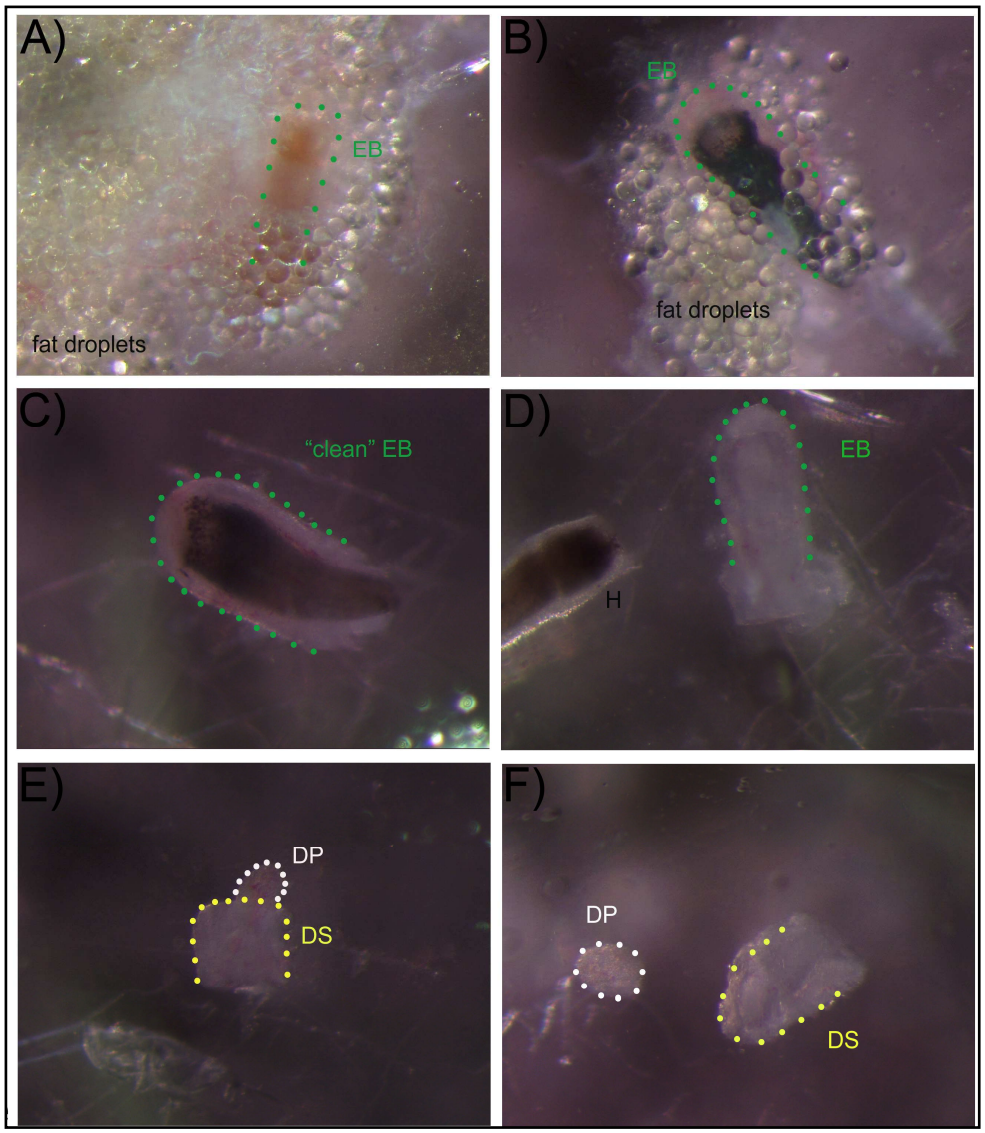


Figure 4.3. Schematic presentation of dermal papilla and dermal sheath microdissection from human hair follicle end bulb (sample number: 41_07). (A, B) end bulb (EB) surrounded by fat droplets. (C) "cleaned" EB. (D) piece of hair (H) pulled put from EB. (E) "inverted" EB; DP- Dermal Papilla; DS- Dermal Sheath. (F) DP cut from DS. Photos were taken on the Ziess StemiSVII microscope (with the digital camera KY-FI030 JVC and with the KyLink software).

#### 4.2.5.1.2. Fibroblasts cell lines.

For the preparation of skin fibroblasts (FI), the fat layer and the dermis part with hair follicle end bulbs were removed from the skin sample. Then, thin skin layer was cut into rectangular pieces (approximately 1 mm x 1 mm). Next pieces of skin were put into the T25 flask (Nunclon) with MEM, 20%FBS and (2 μl/ml Fu - fungizone; 1 μl/ml Ge - gentamicin) and left for a week in the incubator (37$^{o}$C, 5% $CO_2$). After first passage, cells were grown in MEM with 10% FBS and antibiotics (2 μl/ml Fu and 1 μl/ml Ge). All passages were done, when cells reached 80 - 95% confluence.

### 4.2.5.2. Conditions of growing and splitting cells.

All established cell lines were grown in T25 or T75 flasks (Nunclon) in the incubator (37$^{o}$C, 5% $CO_2$). Cells were fed twice a week. A growth medium with MEM, 10% or 20% FBS and antibiotics (2 μl/ml Fu - fungizone; 1 μl/ml Ge - gentamicin) was used for feeding cells. When cells reached 80 - 95% confluence, they were passaged. For this purpose, cells were washed in PBS (prepared from phosphate-buffered saline tablets; Sigma or Oxoid) with 0.5mM EDTA. Then they were incubated with 1 ml of trypsin (0.25%) with EDTA (Gibco) for 2 - 3 min, in 37$^{o}$C after which the reaction was stopped by adding 2.5 ml of growth medium (see above for ingredients). Then, cells were centrifuged (1000 rpm; 5 min; at room temperature). The cell pellet was re-suspended in 1 ml of growth medium and cells were placed in new T25 or T75 flasks containing 5 ml growth media (10% FBS).

For the passage description, the “p” letter and the number of passage were placed in the cell line name. For example, the 21_07 DP p3 cell line, established from dermal papilla from patient number 21 obtained in 2007 year, was at passage 3.

### 4.2.5.3. Two-dimensional (2D) human cell structures.

Cells grown on artificial surfaces of the cell culture dishes (35 mm dish; Nunclon) and on coverslips in 4-well plates (Nunclon) were treated as the two-dimensional cells (the 2D cell structures). When cells grown in T25 or T75 flasks reached 80 - 95% confluence, the medium was changed to D-MEM (Dulbecco's Modified Eagle's Medium from Sigma) with 10% FBS, without antibiotics. After 24 hours cells were trypsinised, counted using a haemocytometer and seeded at the appropriate density for the experiment they were prepared for. For the lipid analysis, 40 000 cells were seeded into 35 mm dishes (Nunclon), whereas for the immunofluorescence analysis, 10 000 cells were seeded into the wells of a 4-well

dish (Nunclon) which had a sterile glass coverslip in the bottom. Cells were kept in normal/growth medium (D-MEM, 10% FBS) or adipogenic medium (D-MEM, 15% rabbit serum, 2.6 μM insulin and 100 nM DEX from Sigma). Cells were incubated in 37$^{o}$C and 5% $CO_2$ and medium was changed mainly every second day. Four days after the incubation cells were used for the immunofluorescence and Oil Red O analysis.

### 4.2.5.4. Three-dimensional (3D) human cell structures - spheroid cell culture.

The 3D culture method allows cells to form a spherical aggregate (Figure 4.4). It was successfully used for the growth of human dermal papilla cells by Higgins *et al* (2010). Cells were placed on the lid of Petri Dishes, in media drops. Each medium drop (D-MEM with 10 %FBS, without antibiotics) was 10 μl and contained 3 000 cells. For each Petri dish, 50 droplets were prepared and positioned about 0.7 - 1 cm apart. The base of Petri dish was filled with sterile PBS (to avoid drying of medium drops). The lid with drops was turned over and put on the base. The Petri dishes were stacked and on the top of the stack, a Petri dish with $H_2O$ was put. Droplets were incubated in 37$^{o}$C, 5% $CO_2$. Once spherical aggregates (spheres) formed after 2 - 4 days of incubation, they were transferred (by 10 μl or 20 μl pipette tips) into fresh droplets of growth medium (D-MEM with 10% FBS no antibiotics) or adipogenic medium (D-MEM, 15% rabbit serum, 2.6 μM insulin and 100 nM DEX from Sigma). The transfer of spheres was done under the Stemi SV6 microscope (ZIESS). Next, 3D structures were incubated for 4 days in 37$^{o}$C, 5% $CO_2$ and then used for the immunofluorescence and Oil Red O analysis. In addition, the Oil Red O analysis was also performed on spheres incubated only 24 hours.

For the immunofluorescence and lipid analysis, spheres were first collected from Petri dishes by 10 μl or 20 μl pipette tips and transferred into Tissue-Tek$^{R}$ O.C.T.$^{TM}$ Compound (Sakura). From ten to twenty spheres were collected into a 7 x 7 mm base mold (VWR) with Tissue-Tek, frozen in liquid nitrogen and stored at -80$^{o}$C. Next 7μm sections were cut on a cryostat (LEICA CM 3050S) and attached to SuperFrost®Plus slides (Menzel-Glaser), these were dried for 90 min at room temperature and used for the further analysis (see sections 4.2.5.5 and 4.2.5.6).

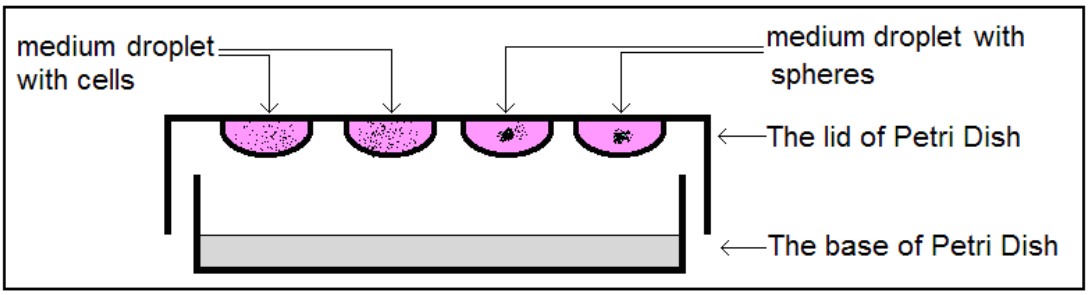


Figure 4.4. The schematic presentation of a spheroid cell culture technique. Cells were suspended in medium droplets, on the Petri Dish lid. The base of each Petri Dish was filled with PBS to avoid drying of medium droplet. During incubation in 5% $CO_2$ and 37$^{o}$C, cells gathered together and formed three dimensional cell structures (spheres).

### 4.2.5.5. Immunofluorescence analysis of human 2D and 3D cell structures.

Two- and three- dimensional cells were used for the investigation of both cytoskeleton and nuclear envelope proteins by the immunofluorescence analysis. Used fixation methods and the staining protocol are described below.

#### 4.2.5.5.1. Fixation techniques.

##### 4.2.5.5.1.1. Acetone/Methanol method.

Acetone/Methanol method was used when cytoskeleton proteins (aSMA, tubulin) were analysed. First, 2D and 3D cell samples (on coverslips or on slides) were washed in PBS (3 x 5 min) and incubated with 95% acetone/5% methanol (10 min, -20$^{o}$C). Then washed in PBS (3 x 5 min) and used for immunofluorescence analysis immediately. Alternatively, they were kept at 4$^{o}$C for no more than two days then washed in PBS (3 x 5 min) and used for immunofluorescence analysis.

##### 4.2.5.5.1.2. Formaldehyde method.

Formaldehyde method was used for the nuclear envelope proteins lamin type A and emerin. First, samples were washed in PBS (3 x 5 min), incubated with 4% formaldehyde (15 min; at room temperature - RT) and 0.5% Triton-X100 (5 min; 4$^{o}$C). Then, samples were washed in PBS (3 x 5 min) and used for immunofluorescence analysis immediately. Alternatively, after incubation with 4% formaldehyde, samples were stored at 4$^{o}$C, then washed in PBS (3 x 5 min), incubated with 0.5% Triton-X100 (5 min; 4$^{o}$C), washed in PBS (3 x 5 min) and used for immunofluorescence analysis.

#### 4.2.5.5.2. Staining procedure.

All samples prepared on coverslips and SuperFrost®Plus slides were washed in PBS (3 x 5 min). Then samples from back skin sections were incubated with 20% goat or donkey serum (Sigma) in PBS for 30 min, whereas the 2D and 3D cultured cells were not washed in serum. Next, samples were incubated with primary antibodies (Table 4.2) overnight at 4$^{o}$C (or 1 hour; at RT). Then samples were washed in PBS (3 x 5 min) and incubated with secondary antibody 1 hour at room temperature (or overnight; at 4$^{o}$C). Normally DAPI (Insight Biotechnology) was added to secondary antibody solutions (Table 4.3), at final dilution of 1:5000. Next, samples were washed in PBS (3 x 5 min) and mounted in anti-fade Immu-mount (Thermo Electron Corporation). All antibodies were diluted in 1% goat (or donkey)

serum/PBS. Immunofluorescence analysis was performed using a Zeiss Axio Imager.M1 microscope with OpenLab software.

Table 4.2. Primary antibodies used for immunofluorescence analysis of 2D and 3D skin cell structures.

| Antibody: | Manufacturer: | Type | Dilutions: |
|---|---|---|---|
| α-SMA | Sigma | Mouse | 1:200 |
| Tubulin | Abcam | Mouse | 1:300 |
| Jol2 (anti-lamins type A) | A gift from Prof C. J. Hutchison's laboratory (Durham University, UK) | Mouse | 1:10 - 1:100 |
| Jol4 (lamin A)* | A gift from Prof C. J. Hutchison's laboratory (Durham University, UK) | Mouse | Undiluted |
| Emerin | Vector Laboratories | Mouse | 1:20 |

*Jol4 antibody was used for the analysis of lamin A in back skin section from 1 day old newborn rat (section 4.3.4.1; Figure 4.13).

Table 4.3. Secondary antibody used used for immunofluorescence analysis of 2D and 3D skin cell structures.

| Secondary antibody: | | Manufacturer: | Dilution: |
|---|---|---|---|
| GantiM (FITC) | AlexaFluor® 488 goat anti-mouse IgG(H+L) 2ml/ml | Invitrogen/Molecular probes | 1:500 |

### 4.2.5.6. Lipid detection in human 2D and 3D cell structures.

Two-dimensional cultures (in 35 mm dishes) and three-dimensional cultures (on coverslips) underwent Oil Red O staining. Briefly, cells were washed in PBS (3 x 5 min) and fixed in calcium formal (see Appendix I) for 1 hour at room temperature. Next cells were incubated for 15 min in 60 % isopropanol and then stained for 15 min with a filtered solution of three parts of Oil Red O (saturated in isopropanol) and two parts of $H_2O$. Then cells were briefly rinsed in 60 % isopropanol and washed few times in $H_2O$.

Next, 2 ml of PBS were placed on the 2D cultures, which were then stored at 4$^{o}$C. Slides with stained 3D structures were mounted with Glycergel or Immunomount mount (Thermo Electron Corporation) and covered with coverslips. The Oil Red O analysis was performed using a Zeiss Axio Imager.M1 microscope with OpenLab software.

### 4.2.6. Mouse dermis work.

#### 4.2.6.1. Dermal-epidermal separation.

Skin separation was performed enzymatically by an established (during this PhD study) method based on both work from Richardson *et al* (2009) and consultations with Professor Colin Jahoda. Mouse embryos were collected in a Petri dish filled with MEM - Minimal Essential Medium (Sigma) with antibiotics (2 μl/ml fungizone from Sigma and 1 μl/ml gentamicin from Gibco) to avoid drying of the skin. Then, each animal was attached to a 5% agar plate (filled with MEM with antibiotics) by needles in order to stretch skin for the ease of skin removal. Fragments of back skin (from the area below the head and above the tail, see Figure 4.2) were carefully removed and cleaned of any muscle tissue. Next, rectangular pieces of skin (2.5 mm x 3 mm) were prepared and collected in a watch-glass filled with MEM and antibiotics over ice. Then, skin samples were washed in sterile DPBS (Gibco) twice and placed in a cold, filtered solution of 5% trypsin (BD)/6% pancreatin (Sigma)/DPBS (1:1:2) and incubated for 40 - 90 minutes (depending on the age and size of skin pieces) at 4$^{o}$C. Then, pieces of dermis were separated from the epidermis using watchmakers' forceps and collected in cold DPBS. Dermal specimens were then transferred to a warm solution of collagenase II/DNase I working solution (see Appendix I) and incubated for 15 min at 37$^{o}$C. Then dermis was disrupted into a single cell suspension by repeated use of an automatic pipette with a 200 μl tip. Once the single cell suspension was obtained, it was centrifuged (3000 rpm, 5 min, at room temperature) and the cell pellet was suspended in 1 ml of a medium that consisted of MEM (Minimal Essential Medium from Sigma), antibiotics (2 μl/ml fungizone from Sigma and 1 μl/ml gentamicin from Gibco) and 10% FBS (Sigma). Cells were counted and used for the 2D and 3D cell cultures.

### 4.2.6.2. Two-dimensional (2D) rodent cell structures.

Dermal cells were placed in 35 mm dishes for the 2D cell structures (up to 200 000 cells per dish) and left in medium (that consisted of MEM; 10% or 20% FBS - foetal bovine serum and antibiotics: 2 μl/ml fungizone from Sigma and 1 μl/ml gentamicin from Gibco) to settle down and attach to the plastic for about 2 - 3 hours (in 5% $CO_2$ and 37$^{o}$C). Then the media was changed for fresh growth media (treated as control media) or adipogenic media (Table 4.1) and the experiment was stopped four days later. Cells were used for the Oil Red O analysis (see section 4.2.7).

### 4.2.6.3. Three-dimensional (3D) rodent cell structures - spheroid cell culture.

The 3D structures were obtained by seeding 3 000 cells in 10 μl growth media droplets (MEM; 10% FBS; 2 μl/ml fungizone from and 1 μl/ml gentamicin). Up to 50 droplets were placed on the lid of each Petri dish and then the lid was carefully transferred on the base of the Petri dish filled with sterile water or PBS (prepared from phosphate-buffered saline tablets; Sigma or Oxoid) to avoid drying of droplets (Figure 4.4). Stacked Petri dishes were incubated (in 5% $CO_2$ and 37$^{o}$C) for about 24 hours to allow cells to settle and make three-dimensional structures. Then 3D cell structures (spheres) were transferred to fresh droplets of growth medium (treated as a control medium) or adipogenic medium (Table 4.1). Spheres were then incubated for another four days and experiments were stopped by placing the 3D structures into tissue tek and freezing in liquid nitrogen. Samples were cryopreserved and cryostat sectioned for analysis as described above (see section 4.2.3).

### 4.2.7. Oil Red O staining and modified H&E staining.

The Oil Red O staining and modified H&E staining were performed on skin sections obtained from hanging drop cultures and substrate organ cultures. Oil Red O staining was used on sections of the 3D cell structures. A detailed description of these methods is presented in Chapter 2, in section 2.2.4.

The 2D cultured cells, grown in 35 mm dishes, underwent a shortened version of the Oil Red O protocol. Briefly, cells were washed in PBS (3 x PBS; few min), fixed in calcium formal solution for 10 min, incubated with 60% isopropanol (approximately 5 min) and incubated in the Oil Red O working solution (see section 2.2.4) for up to 10 min, then washed in 60% isopropanol and PBS. Fixed 2D cells were either kept in sterile PBS at 4$^{o}$C, or mounted with mowiol (see Appendix I), covered carefully by circular coverslips and stored at 4$^{o}$C.

## 4.3. Results.

### 4.3.1. EGFR expression in the lower dermis of mouse embryonic back skin.

One of the genes shown to be up-regulated in the lower dermis in the dermal microarray data (detailed analysis of which has been described in Chapter 3) was epidermal growth factor receptor (EGFR). This is a cell surface receptor involved in skin development, and also in relation to hair follicle development (Richardson *et al*, 2009). In addition, the role of EGF receptor has been investigated in 3T3 cell lines (Harrington *et al*, 2007). In the current study, the up-regulation of this receptor was observed in E18 and E19 microarray sub-lists (Table 4.4A). In 18 day old lower skin dermis, EGFR was up-regulated by 3.8 fold compared to upper dermis, whereas at e19 time point the EGFR mRNA was 2.62 fold more prevalent in lower dermis than upper. In addition, the lower dermal (LD) microarray data showed changes in EGFR expression in lower dermal cells between analysed time points (Table 4.4B). The e18 showed about 2.37 fold increased over the e17 and the e19 a 1.75 fold increase over e17 (Table 4.4B).

For the verification work of microarray data, qRT-PCR analysis was performed on samples from lower and upper dermis areas from e17, e18 and e19 samples. Only e18 time point was successfully analysed by qRT-PCR reaction with all three biological replicates having detectable levels of EGFR mRNA (Figure 4.5A). At this time point, cells from lower dermis were significantly enriched for the EGFR according to performed t-test analysis. Among three biological replicates from e17 time point, only one gave a signal during the qRT-PCR reaction. Moreover, at e19, one biological sample failed to provide an acceptable signal during the qRT-PCR reaction (obtained Ct value was higher than acceptable for this work baseline, for the explanation see section 3.2.6.1.3). The other two samples from e19 time point, were characterised by a big difference in the EGFR mRNA levels between each other. Samples that failed to give signal on the PCR machine were treated as their expression of mRNA is equal zero. Therefore, only e18 samples did not have unacceptably large standard deviation values (Figure 4.5B). This analysis confirmed predictions from microarray data, that EGFR gene seems to be significantly enriched in lower dermal cells, at the e18 time point.

Expression of EGFR was also analysed by the immunofluorescence. The selected antibody against EGFR failed to work couple of times when used. However in several cases this antibody stained epidermis at all analysed time points (Figure 4.6A). In addition, green signal in dermis area occurred to be weaker when compared with epidermal expression of EGFR. In the lower dermis in regions in close proximity to hair follicle end bulbs staining for EGFR was visible from e18 (compare Figure 4.6Ab with Figure 4.6Aa and d). In addition, some areas of the lower dermis seemed not to be stained to the same extend as others in back skin from 18 day old embryos (compare Figure 4.6Ab with Figure 4.6Ac).

Table 4.4. The *Egfr* gene expression profile in embryonic skin dermis between e17 and e19 time points. (A) The E18 and E19 microarray sub-lists revealed the enrichment of *Egfr* at mRNA level in lower dermal cells versus upper dermal cells at e18 and e19 time points. (B) The lower dermal (LD) microarray list showed the up-regulation of *Egfr* gene in lower dermal cells from e17 time point.

A)

| **Whole name; gene symbol; probe set Affymetrix ID.** | **Time points:** | **Fold change value:** |
|---|---|---|
| Epidermal growth factor receptor; *Egfr*; 1435888_at | e18 lower dermis vs* e18 upper dermis | + 3.802172 |
| | e19 lower dermis vs* e19 upper dermis | + 2.621013 |

B)

| **Whole name; gene symbol; probe set Affymetrix ID.** | **Time points:** | **Fold change value:** |
|---|---|---|
| Epidermal growth factor receptor; *Egfr*; 1435888_at | e18 lower dermis vs* e17 lower dermis | + 2.377378 |
| | e19 lower dermis vs* e17 lower dermis | + 1.75338 |

* vs - versus

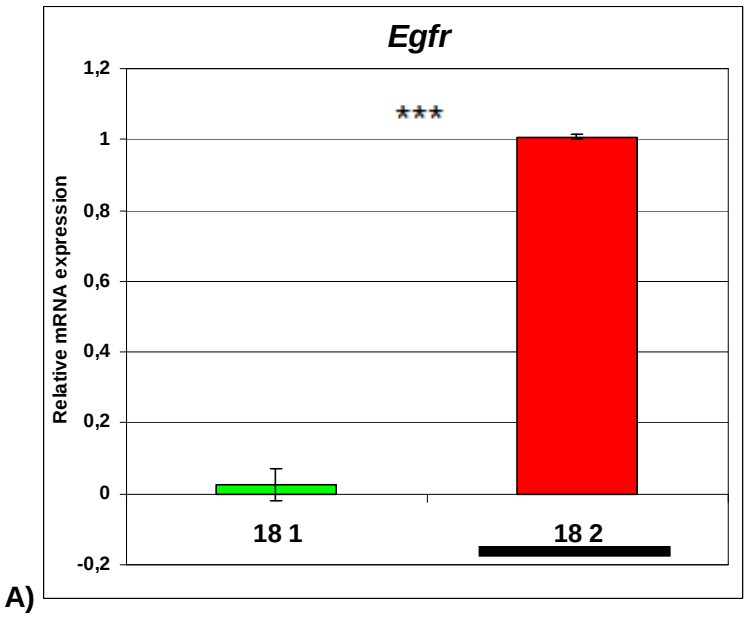


A)

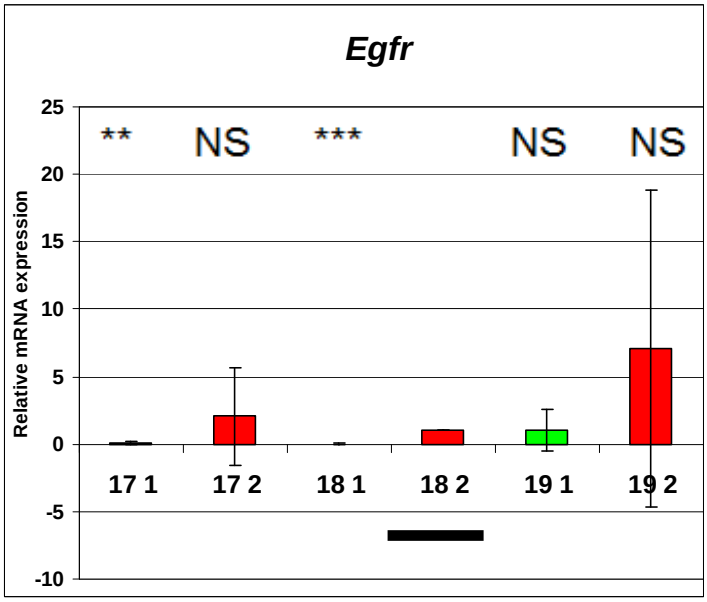


B)

Figure 4.5. Verification of microarray data by qRT-PCR for *Egfr* gene. The relative mRNA expression for gene was analysed on samples from dermis at e17 (17), e18 (18) and e19 (19) time points, from upper (Area "1", green) and lower (Area "2", red) dermis. The analysis was performed on three biological replicates and only "18 1" and "18 2" samples gave signal from all triplicates. (A) There was a significant enrichment of *Egfr* gene in lower dermis versus upper dermis at e18 time point. (B) Samples from other time points were characterised mainly by high standard deviation values. The baseline (1-fold change) was established for the e18 lower dermis sample (underlined on the figure) and the mRNA levels of other samples are shown relative to underlined sample. P value refers to the comparison with "18 2" sample (* P <0.05, ** P <0.01, *** P <0.001). The "NS" indicates not significant differences in the mRNA gene expression between compared samples.

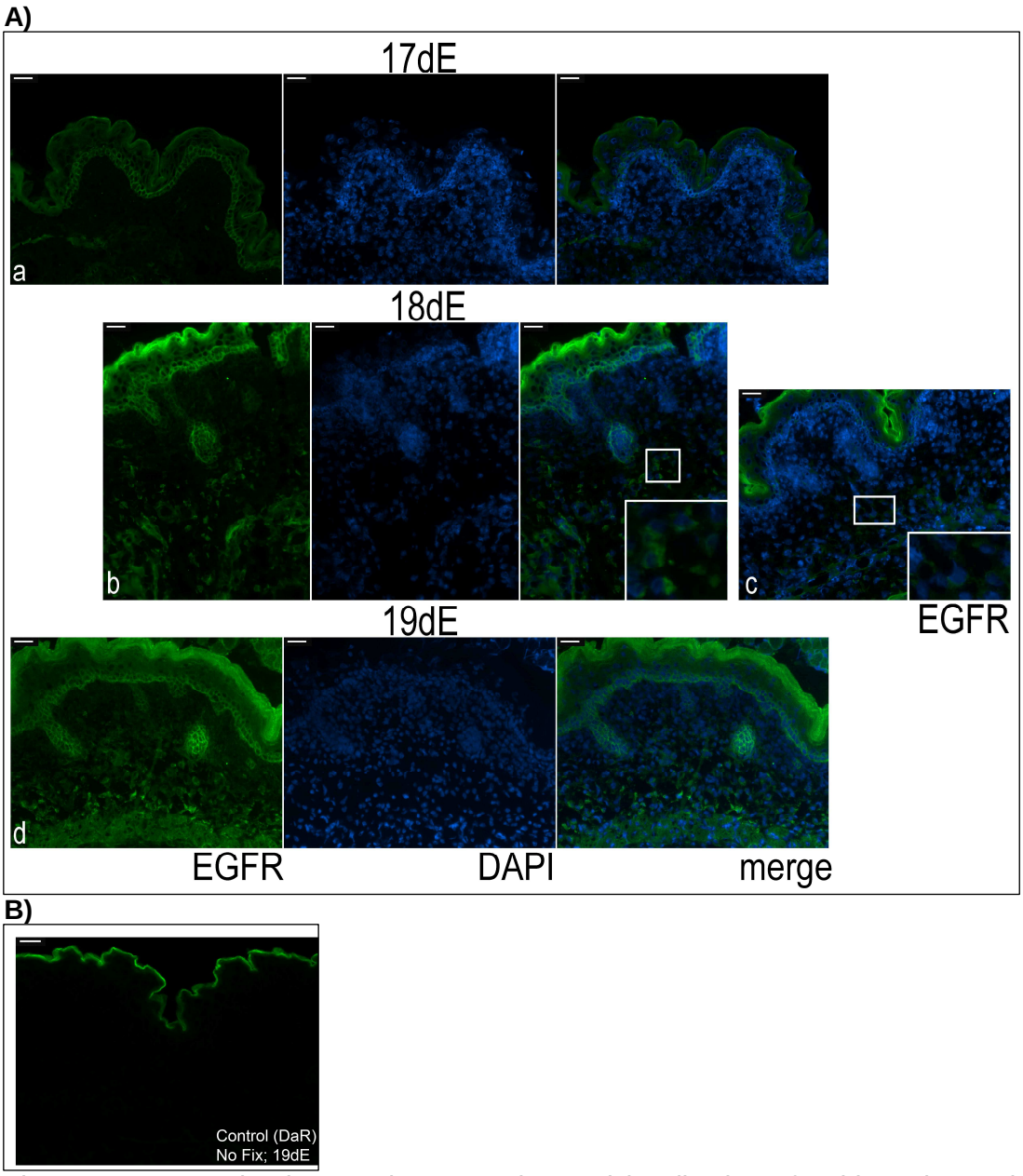


Figure 4.6. Dynamic changes in expression and localisation of epidermal growth factor receptor - EGFR during mouse embryonic skin development. (A) Back skin sections (7 μm) were prepared from embryos at e17 (17dE), e18 (18dE) and e19 (19dE) time points and probed with antibody against EGFR, diluted 1:50 (d) or 1:100 (a, b, c). Green staining is seen along epidermis at all analysed time points. EGFR signal in lower dermis can be seen in some areas of 18 day old back skin samples (b). (B) Control samples, where primary antibody was replaced by 1% serum. DaR - donkey anti-rabbit secondary antibody. Slides with skin samples did not undergo fixation. DNA was counterstained with DAPI. (A, B) Scale bar = 30 μm. Fluorescent images were visualised using a Zeiss Axio Imager M1. microscope.

### 4.3.2. Investigation of the role of EGFR signalling in lipid accumulation in embryonic back skin.

In order to mimic *in vivo*-like conditions for the analysis of back skin samples, two experimental techniques were initially tested: a hanging-drop and a substrate organ culture method. The same small, rectangular pieces of back skin taken from e16 - 17 day mouse embryos were compared for this purpose. Skin samples were either placed on membranes (organ culture technique) or suspended in media droplets (the hanging-drop technique). These samples were then incubated in media that contained activator or inhibitor of EGF receptor (see Table 4.1 for more details).

Skin cultured using the hanging-drop technique did not look healthy. The epidermis was often ripped and separated from dermis. In addition, samples had not stayed flat but their ends had rolled and they had a round shape (Appendix VII). Thus, this method seemed not to be useful for further study of back skin.

Organ culture, performed on e16 - 17 embryonic mouse skin, incubated in the control medium produced healthy-looking samples (Figure 4.7a). When stained with the Oil Red O the distribution of staining was not uniform. In a few sections the red dye was not seen in the dermis, only in subcutaneous glands (Figure 4.7a - top panel). In addition, some samples had small amounts of lipids stained near hair follicles (Figure 4.7b - middle panel). Then, for a number of sections, the Oil Red O staining gave a stain along the whole dermis (Figure 4.7c - bottom panel). Interestingly, many very small red dots were seen around nuclei of dermal cells as well as along the hair follicles (Figure 4.8).

In skin specimens, incubated in medium with the EGFR activator at a concentration of 100 ng/ml (Figure 4.7b), the red dye was observed along the dermis and hair follicles, and was similar to several skin sections incubated in control medium. Finally, the skin was analysed after the incubation with EGFR inhibitor and in these skin sections fat cells were not seen in the lower dermis area and were not present around hair follicles (Figure 4.7c and d). However, skin from the higher concentration of EGFR inhibitor looked less healthy and disruptions (gaps) between epidermis and dermis were seen (Figure 4.7d - top panel). In addition, the red dye was seen in the area suspected to be a fat depot presented beneath the skin (Figure 4.7d - bottom panel). In general, these specimens looked slightly less healthy than from other experiments.

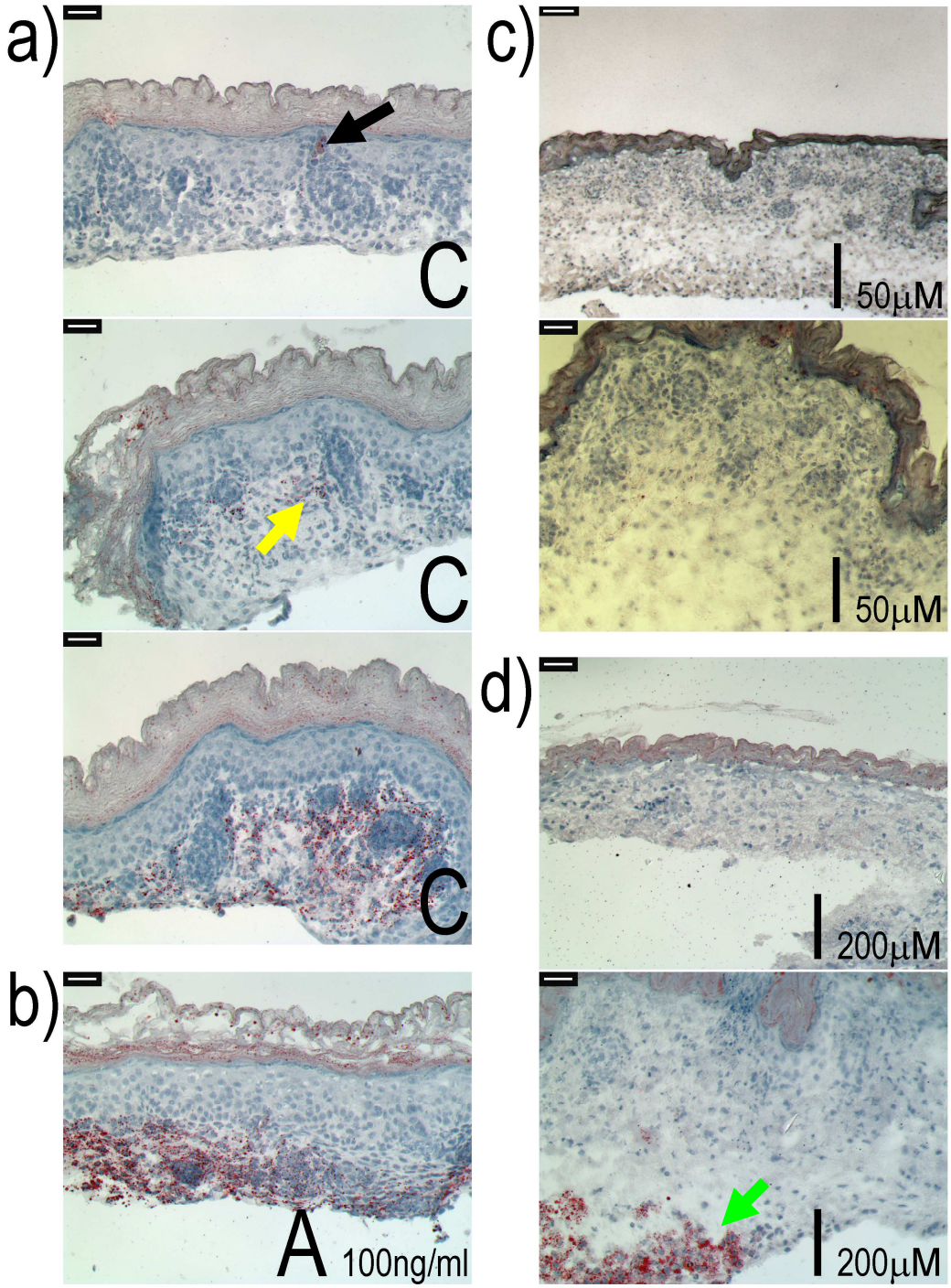


Figure 4.7. Lipid accumulation in mouse embryonic skin at e16 - 17 time point. The substrate organ culture method was applied for the growth of skin pieces. Skin sections were stained with Oil Red O to detect lipids. a) Skin after 72h incubation in control medium (C). b) Skin after 72h incubation in medium with EGFR activator (A). c) Skin after 72h incubation in medium with EGFR inhibitor (I). Red dye in sebaceous gland is shown by a black arrow (a - upper panel), whereas small lipid droplets in lower dermis are pointed by a yellow arrow (a - middle panel). Green arrow identifies an area stained by red dye that might be a fat depot (adipose tissue) beneath the skin (c - lower panel). (a, b, c - lower panel and d) Scale bar = 30 µm. (c - upper panel) Scale bar = 65 µm. Images were captured using a Zeiss Axio Imager.M1. microscope.

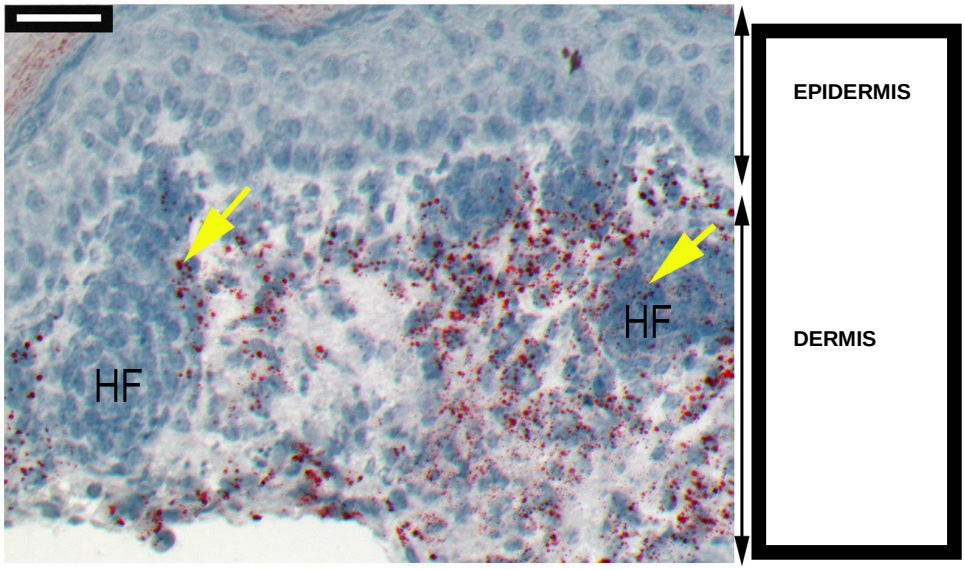


Figure 4.8. Magnification of a skin section obtained from mouse embryonic skin at e16 - 17 time point after the substrate organ culture study. Skin section, after 72h incubation in control medium, was stained with Oil Red O to detect lipids. Lipid accumulation is shown by red dye. Yellow bars show the lipid droplets in hair follicles. HF - hair follicle. Scale bar = 30 μm. Images were captured using a Zeiss Axio Imager.M1. microscope.

### 4.3.3. Younger (e15 - 15.5) and older (e18.5 - 19) mouse back skin organ culture.

After the organ culture experiment on 16 - 17 day old embryonic skin, two other time points were chosen for further study, younger skin from e15 - 15.5 and skin from e18.5 - 19 day old embryonic animals.

As it was shown (Chapter 2) cells from lower dermis start to accumulate easily distinguishable lipid droplets between 18 and 19 day of mouse embryonic development. Therefore, it seemed useful to use the organ culture method for the analysis of lipid accumulation capability and the role of EGF-EGFR signalling pathway in mouse embryonic skin at these times. After 48 hours of incubation the skin samples in the different media conditions were cut on the cryostat for the analysis of lipid accumulation. Back skin from 15 - 15.5 day old mouse embryos did not stain with Oil Red O dye, whereas the older skin was characterised by lipid droplets in lower dermis (compare Figure 4.9a with Figure 4.10a). Skin specimen from e15 - 15.5, when incubated in a control medium, maintained its fat-free feature after 48 hours of incubation (Figure 4.9b). In addition, sections from older specimens, incubated in control medium, had areas full of lipids along the whole dermis (Figure 4.10b - left panel) but also there were sections where lipids were mainly seen in lower dermis rather than in upper dermis (Figure 4.10b - right panel).

In addition, skin samples were incubated for 48 hours in experimental media with EGFR activator (EGF) or EGFR inhibitor (AG1478). Dermis compartment in the younger skin samples did not show Oil Red O staining after the organ culture, with EGF or AG1478 (Figure 4.9c and d). However, the Oil Red O staining was seen in samples from 18.5 - 19 day old mice that were incubated with activator or inhibitor of EGFR (Figure 4.10c and d).

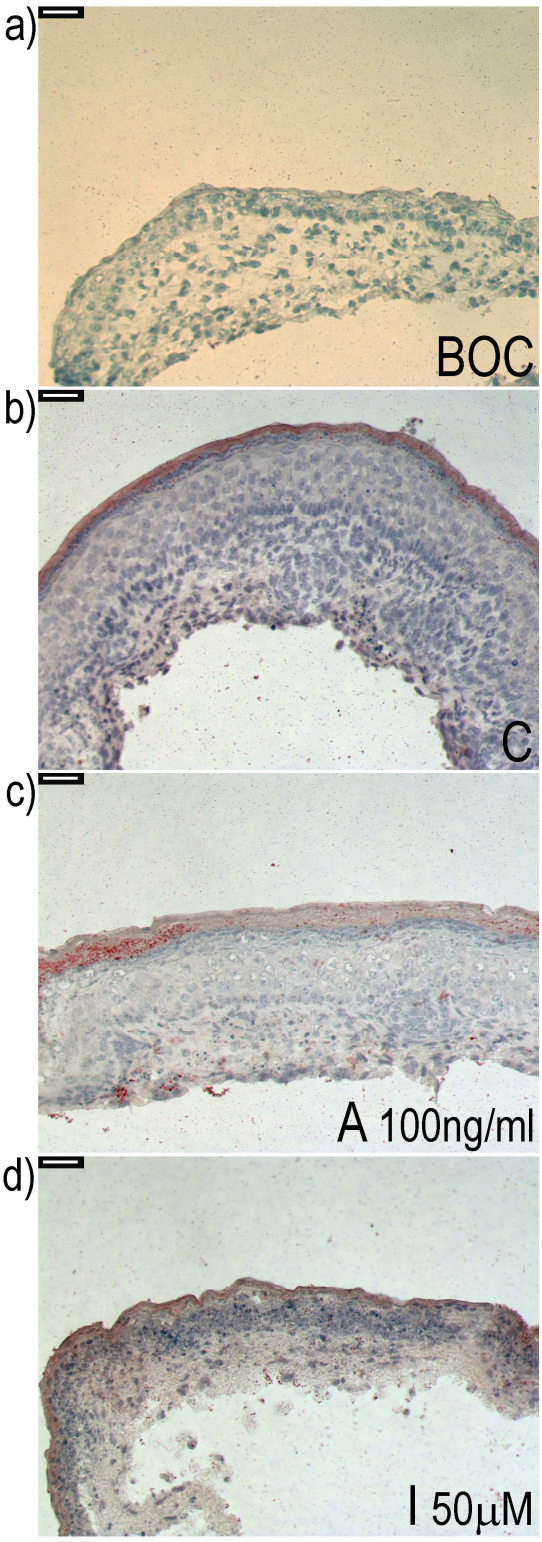


Figure 4.9. Lipid accumulation in mouse embryonic skin at e15 - 15.5 time point. The substrate organ culture method was applied for the growth of skin pieces. Skin sections were stained with Oil Red O to detect lipids. a) Skin before organ culture (BOC). b) Skin after 48h incubation in control medium (C). c) Skin after the incubation (48h) in medium with EGFR activator (A). d) Skin after 48h incubation in medium with EGFR inhibitor (I). (a - d) Scale bar = 30 µm. Images were captured using a Zeiss Axio Imager.M1. microscope.

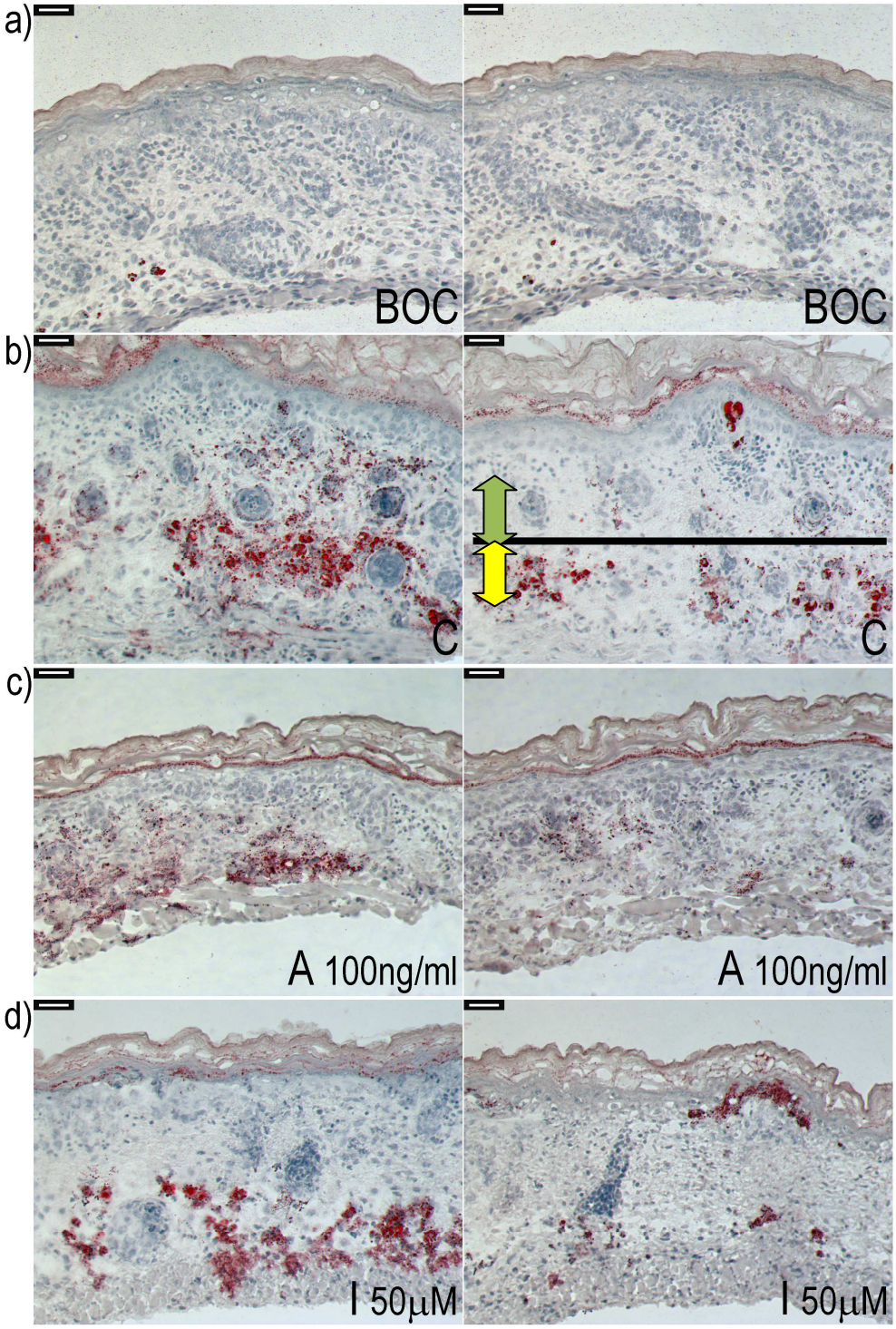


Figure 4.10. Lipid accumulation in mouse embryonic skin at e18.5 - 19 time point. The substrate organ culture method was applied for the growth of skin pieces. Skin sections were stained with Oil Red O to detect lipids. a) Skin before organ culture (BOC). b) Skin after 48h incubation in a control medium (C). c) Skin after 48h incubation in medium with EGFR activator (A). d) Skin after 48h incubation in medium with EGFR inhibitor (I). (b - right panel): the upper area with less red dye when compared with the lower area. (a - d) Scale bar = 30 μm. Images were captured using Zeiss Axio Imager.M1. microscope.

Skin specimens were also analysed after incubation with adipogenic medium in organ culture. As was mentioned in Chapter 1, section 1.3.2.2, adipogenic medium contains of factors that activate signalling cascades needed for the differentiation of cells into mature adipocytes (fat cells that accumulate lipids). Organ culture samples, incubated in such medium in general were characterised by a specific rounded shape (Appendix VIII). It seemed that epidermis “aimed to close” the skin sample in a kind of round-shape structure, thus it was difficult to decide if the red staining seen in the dermis of cross-sections was related to the influence of adipogenic medium on skin as the epidermal growth would limit the contact with media by growing around the whole sample. Thus, reliable analysis of the influence of adipogenic media on organ culture samples seemed not to be possible. Therefore, a decision was made to use a different experimental approach for the analysis of the influence of adipogenic medium on skin cells. A spheroid cell culture method was applied for the analysis of the embryonic skin dermis. Moreover this facilitated study of dermal cells without the epidermal cells causing problems.

### 4.3.4. Investigation of skin cells in two- (2D) and three- (3D) dimensional structures.

Epidermal-dermal interactions are crucial for the hair follicle development (Chapter 1, section 1.1.3.1). The question arose if specific cell-cell interactions are also important for development of fat cells in skin dermis. Because the lipid accumulating cells are localised in the lower and not in the upper dermal compartment, it would be interesting to investigate if cells from these two dermal areas develop from the same progenitor cells, when and what influences their fate during embryonic development. Are there specific epidermal-dermal and/or dermal-dermal processes crucial for the development of dermal adipose tissue?

In order to analyse features of only dermal skin compartment, without the epidermal layer, at two different stages of embryonic development (e15 - 15.5 and e18.5 - 19 time points), an experiment was performed where enzymatic treatment (see section 4.2.6.1 for more details) allowed the dermis to be separated from the epidermis. Next, dermal cells were used for either two-dimensional (2D) or three-dimensional (3D) cell culture and the analysis of their lipid accumulation capabilities.

#### 4.3.4.1. Different human skin compartments and 3D culture as a method for their analysis.

As was mentioned in the introduction to this Chapter, the 3D spheroid cell culture method allows cells to be maintained in a spherical aggregate without contact to the surface of a cell culture dish as would be the case in conventional 2D cell structures.

In order to become familiar with the 3D spheroid technique, first human and mouse skin specimens were used in order to establish cell lines from skin fibroblasts (FI) and hair follicle end bulb structures, such as the dermal papilla (DP) and dermal sheath (DS). A brief summary of the micro-dissection method of human DP and DS is presented in section 4.2.5. These cells were used for the 3D cultures, according to the protocol shown in section 4.2.5.4. Human FI, DP and DS cells gave nice, spherical structures (Figure 4.11). In most cases, the surface of such structures was smooth and they had symmetric rounded shapes.

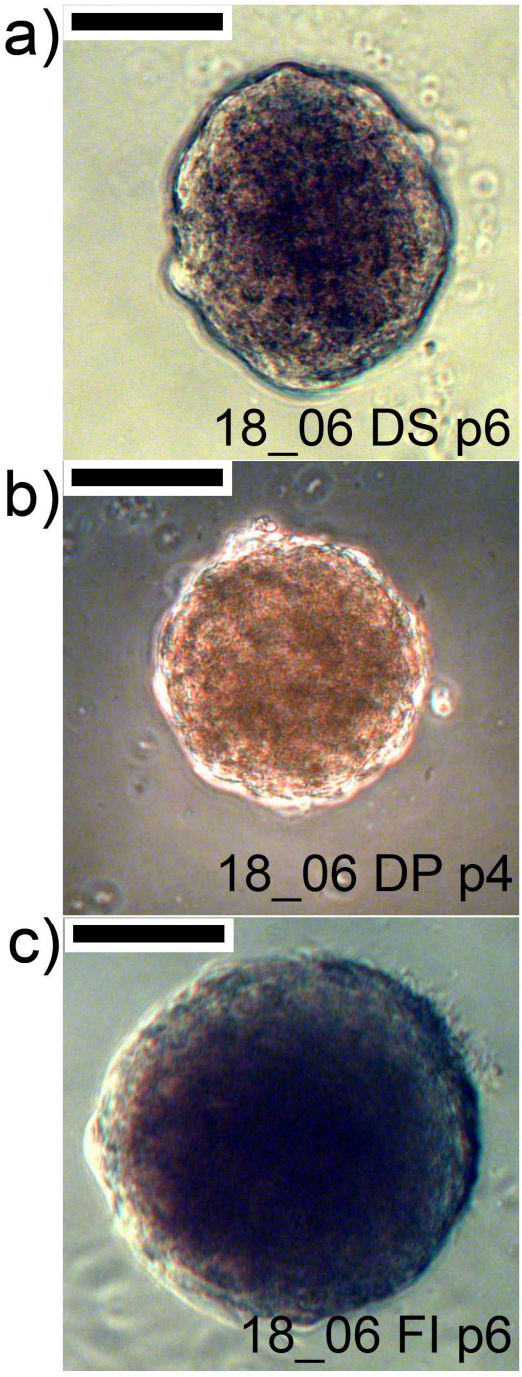


Figure 4.11. Three-dimensional (3D) cell structures obtained from human skin cells. (a) dermal sheath - DS cells. (b) dermal papilla - DP cells. (c) skin fibroblast - FI cells. 3D structures were created from cells at passage 4 or 6. Cells were established from human skin sample number 18_07. (a - c) Scale bar = 100 μm. Images were captured using a Carl Zeiss Axiovert 10 inverted microscope (with accompanying AnalySIS software).

Both 2D and 3D cell cultures, obtained from human dermal papilla (DP) cell lines, were analysed using immunofluorescence to investigate the presence and localisation of either cytoskeletal or nuclear envelope proteins (Figure 4.12). Specific localisation of alpha smooth muscle actin (aSMA) seen in 2D cell cultures was not present in spheres (compare Figure 4.12a with Figure 4.12b). This result was in agreement with work shown by Higgins *et al* (2010), where aSMA signal was lost from DP spheres. Also, tubulin did not have its fibrillar-type of localisation in 3D structures, and the signal from anti-tubulin antibodies seemed to be present only on the outside layer of cells of the sphere (see Figure 4.12c and Figure 4.12d).

In addition, nuclear envelope proteins were analysed in both 2D and 3D cultures. Lamin A and lamin C are representatives of A-type lamins and the Jol2 antibody against these nuclear envelope proteins together with antibody against another nuclear envelope protein: emerin were used for the analysis of 2D and 3D cultured cells. In 2D culture both emerin and A-type lamins displayed round-shape nuclei (Figure 4.12e and Figure 4.12g). However, cells kept in 3D structures were lacking the round and smooth-like shape of nucleus that was seen in two-dimensional cells (Figure 4.12f and Figure 4.12h). The nuclei of cells in spheres seemed to be “squeezed”. Their shapes were reminiscent of those of intact hair follicle end bulb cell nuclei, for example in the dermal papilla (DP), when expression of lamin A (by Jol4 antibody) was analysed previously in back skin samples from one day newborn rats (compare Figure 4.12f and 4.12h with Figure 4.13).

In addition, the generated microarray data from mouse embryonic skin dermis revealed specific regulation of lamin A gene (Table 4.5). The E19 microarray sub-list contained a lamin A gene whose enrichment was related with the upper dermis (Table 4.5A). The lower dermis (LD) microarray data showed the down-regulation of lamin A gene in lower dermal compartment from e17 till e19 time points (Table 4.5B).

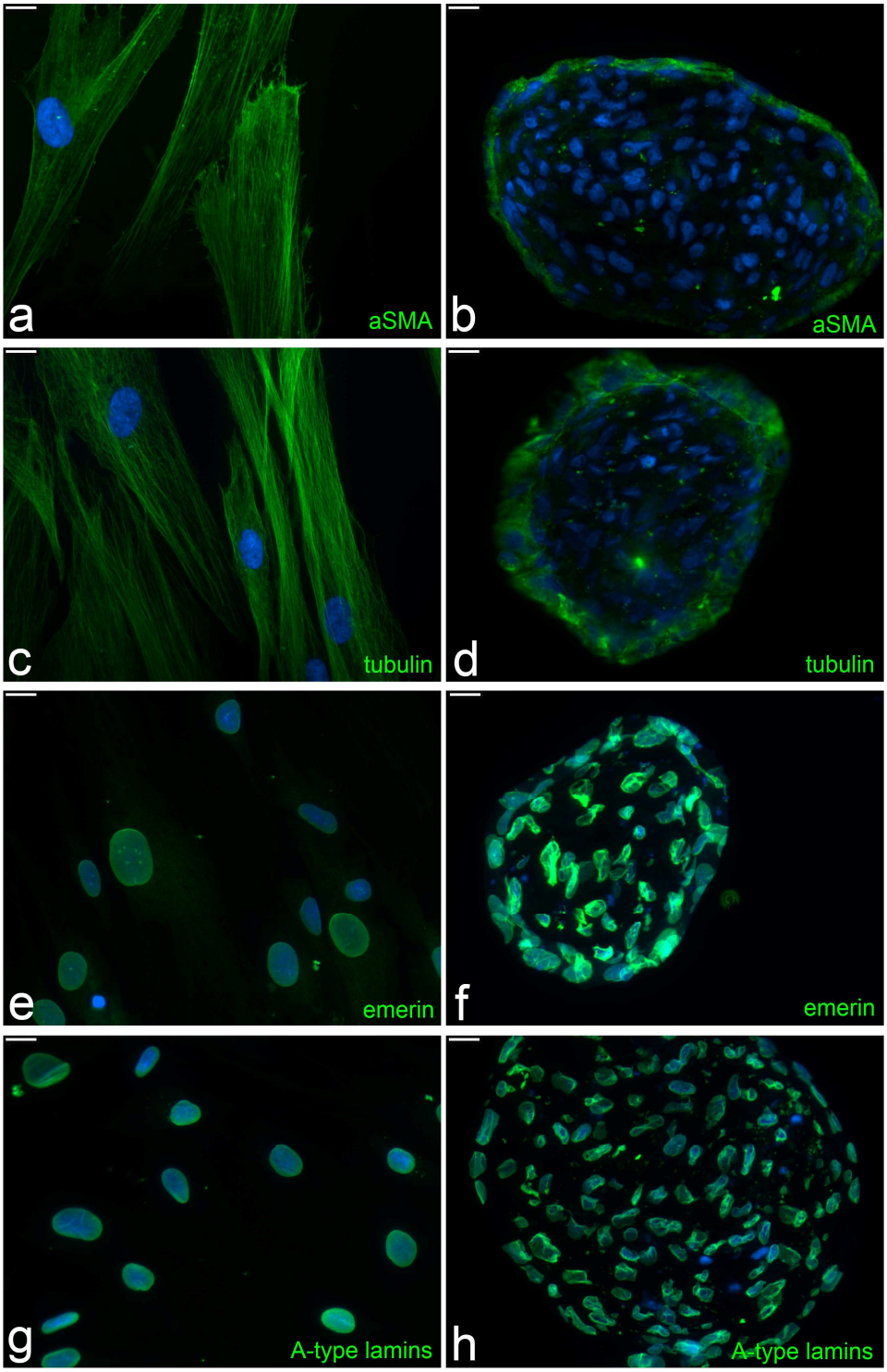


Figure 4.12. Analysis of cytoskeletal and nuclear envelope proteins in two- (2D) and three- (3D) dimensional cell structures. Both structures were established from human dermal papilla (DP) cells, number 5_07, at passage 7. Although characteristic, for 2D structures, the expression pattern observed for alpha smooth muscle actin (aSMA) and tubulin (a and c) was lost in 3D structures (b and d). The rounded morphology of nuclei in 2D structures, based on emerin and A-type lamin localisation (e and g) was not seen in 3D structures where nuclei looked shrunken (f and h). DNA was counterstained with DAPI. Antigens of interest are green: a and b - alpha smooth muscle actin (aSMA); c and d - tubulin; e and f - emerin; g and h - A-type lamins (Jol2 antibody). (a - h) Scale bar = 15 μm. Fluorescent images were visualised using a Zeiss Axio Imager M1. microscope.

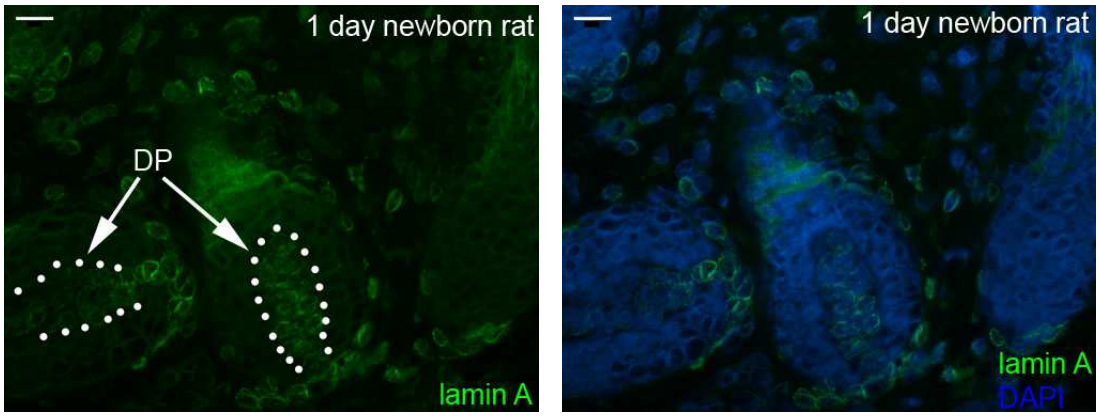


Figure 4.13. Localisation of lamin A in skin sections taken from a 1 day old newborn rat. Expression of lamin A could be seen in dermis cells or hair follicle end bulbs cells. DNA was counterstained with DAPI. Antigen of interest is green: lamin A (Jol4 antibody). DP - Dermal papilla. Scale bar = 15 μm. Fluorescent images were visualised using a Zeiss Axio Imager M1. microscope.

Table 4.5. The lamin A gene (*Lmna*) expression profile in embryonic skin dermis between e17 and e19 time points. (A) E19 microarray lists revealed the decrease in *Lmna* mRNA in lower dermal cells versus upper dermal cells at e19 time point. (B) The lower dermal (LD) microarray list showed the down-regulation of *Lmna* in lower dermal cells from e17 time point.

A)

| **Whole name; gene symbol; probe set Affymetrix ID.** | **Time points:** | **Fold change value:** |
|---|---|---|
| lamin A; *Lmna*; 1457670_s_at | e19 lower dermis vs* e19 upper dermis | - 3.381616 |

B)

| **Whole name; gene symbol; probe set Affymetrix ID.** | **Time points:** | **Fold change value:** |
|---|---|---|
| lamin A; *Lmna*; 1457670_s_at | e18 lower dermis vs* e17 lower dermis | - 1.351853 |
| | e19 lower dermis vs* e17 lower dermis | - 2.934171 |

* vs - versus

Jahoda *et al* (2003) showed that two-dimensional cell cultures obtained from both DP and DS are capable of accumulating lipids in the presence of adipogenic medium (Jahoda *et al*, 2003). The behaviour of human dermal papilla (DP) and human fibroblast (FI) cells in both 2D and 3D environment was investigated. Once formed, structures were incubated either in normal or adipogenic medium for up to 4 days. 2D cultured FI and DP cells, were stained by the Oil Red O dye, only when incubated in adipogenic medium (compare Figure 4.14a and c with Figure 4.14b, d and i). In general, spheres from several human fibroblasts samples were characterised by the presence of red dye along the whole cross-section of the structures in both normal and adipogenic medium (Figure 4.14e - f). Interestingly, in some 3D samples from DP cells, the number of areas positive for red dye seemed to be lower (or even not present) when compared with fibroblast spheres when incubated for 24 hours or 4 days in both normal and adipogenic media (compare Figure 4.14e - f with Figure 4.14g - h; see also Appendix IX).

After the successful use of the 3D cell culture method on human skin cells, this technique was applied for the analysis of mouse-derived skin cells. This study is described in next section (4.3.4.2) of the Chapter 4.

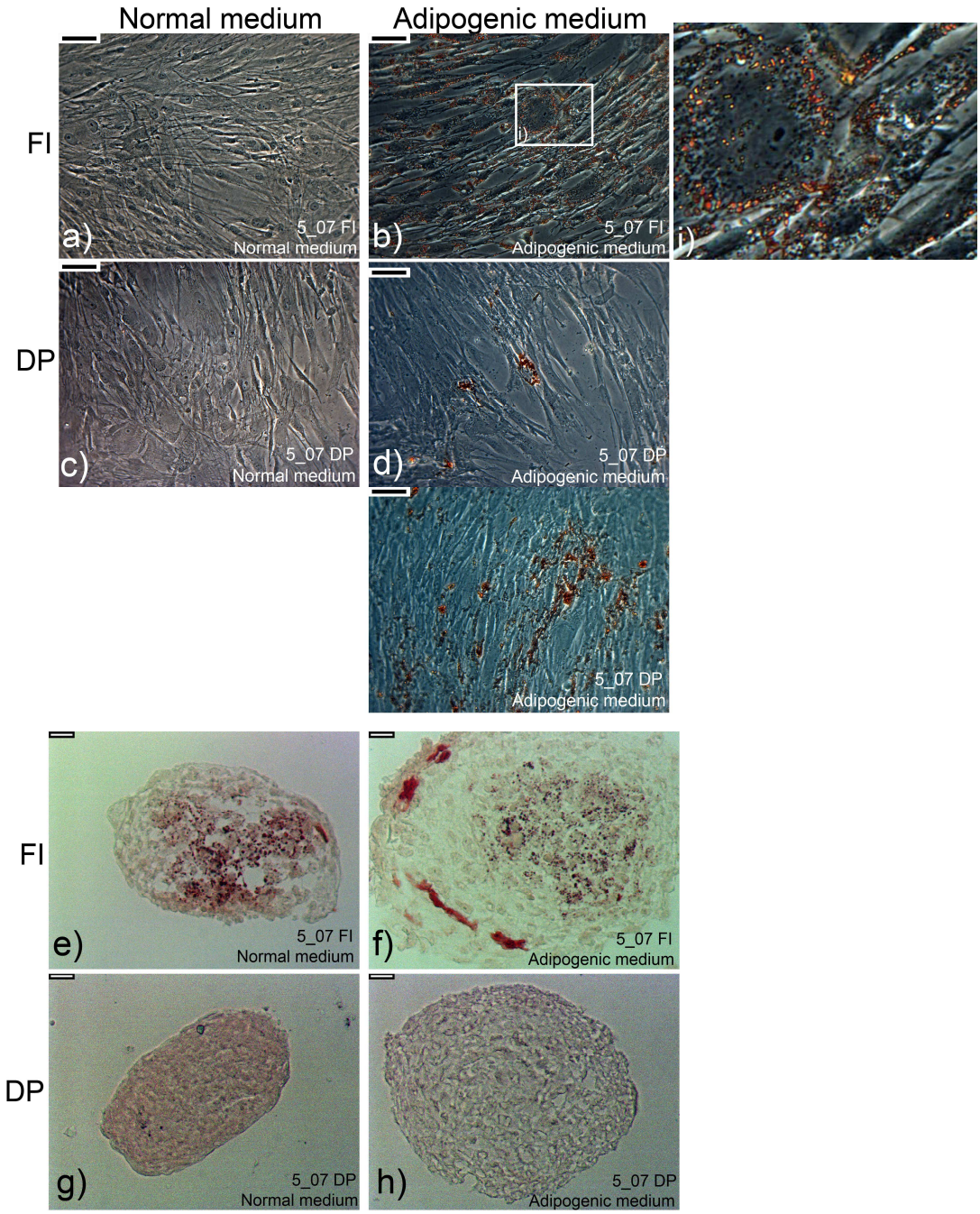


Figure 4.14. The analysis of lipid accumulation in 2D and 3D cell structures obtained from human skin sample number 5_07. Once 2D and 3D structures were formed, they were incubated in normal or adipogenic medium for 4 days. Cell structures were stained with Oil Red O to detect lipids. Fl - fibroblasts. DP - dermal papilla cells. (a - d) Scale bar = 100 μm. (e - h) Scale bar = 15 μm. Images were captured using the inverted microscope Carl Zeiss Axiovert 10 (a - d and i) and Zeiss Axio Imager.M1. microscope (e - h).

### 4.3.4.2. Mouse dermis cells and their fat accumulation in 2D culture.

Dermal cells from back skin samples of 15 - 15.5 and 18.5 - 19 day old mouse embryos were obtained during enzymatic treatment. Skin from e18.5 - 19 time point underwent separation of dermis from epidermis allowing the accumulation of high numbers of clean pieces of dermis. However, some difficulties were encountered with younger skin where the thin epidermis was harder to remove from the dermis. Therefore, there is a possibility of low-level contamination of the dermal cells with epidermal cells.

Dermal cells were seeded into cell culture dishes in order to obtain 2D cell structures (for mode details see section 4.2.6.2). 2D cultures from mouse back skin dermis at both e15 - 15.5 and e18.5 - 19 time points grew well in the control medium. Their growth in adipogenic medium was slightly inhibited (compare Figure 4.15c and e with Figure 4.15d and f; also compare Figure 4.16c and e with Figure 4.16d and f). Perhaps as a result of media cells were more likely to stop proliferating and start their differentiation process.

The dermal cells from young mouse embryos, when kept in control medium, did not accumulate lipids and all cells were small and had the same morphology (Figure 4.15a). However changes in the e15 - 15.5 skin derived dermal cells, kept in adipogenic medium, were noticed. First, after 48 - 72 hours of the incubation in the differentiation medium, small darker “dots” could be observed in cells in the cytoplasm around nuclei, which could be an indication of the presence of first tiny lipid droplets around nucleus (Figure 4.15d - see white arrows). At day four, cells with different morphology could be identified when incubated in adipogenic medium. These cells, assumed a round shape because of the lipid droplets in their cytoplasm (Figure 4.15f). Depending on the selected area with analysed cells, approximately 20% of cells appeared to have started adipogenic differentiaion (see marked rectangular area in Figure 4.15f).

Interestingly, dermal cells from 18.5 - 19 day old mouse embryos were characterised by the presence of round shaped cells with characteristic lipid droplets inside them when kept in normal medium (Figure 4.16a - bottom panel). These cells had features of multilocular cells with several small lipid droplets. The number of fat cells remained almost unchanged in normal medium from 48 to 96 hours (compare Figure 4.16a, c and e). However, the morphology of these fat cells seems to undergo some changes during the incubation period in normal medium, as cells kept

longer in normal medium had a single large lipid drop instead of several smaller ones (compare Figure 4.16a - bottom panel with Figure 4.16e). The incubation of e18.5 - 19 skin derived dermal cells for 48 hours in adipogenic medium lead to the occurrence of unilocular fat cells with one large central fat droplet (Figure 4.16b - lower panel). Therefore, the adipogenic medium seemed to enhance lipid accumulation in fat cells from 18.5 - 19 day old mouse skin dermis.

In addition, for cells from e18.5 - 19 derived skin dermis, in both media conditions and at each time point analysed there were areas where cells did not have fat-like morphology (Figure 4.16a - f).

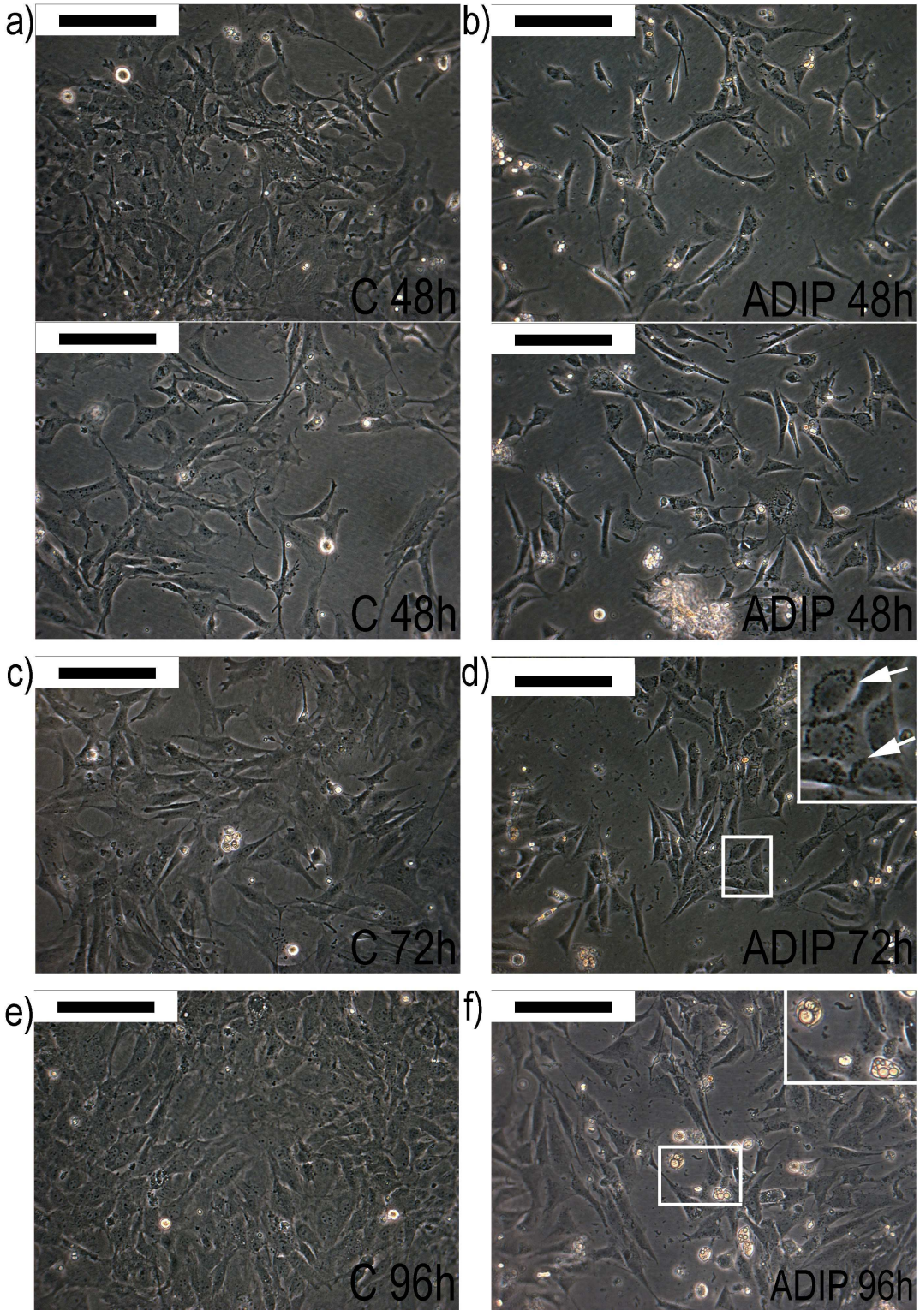


Figure 4.15. The general morphology of young embryonic two-dimensional cell structures incubated (48, 72 or 96 hours) in control (C) or adipogenic (ADIP) medium. Cells were obtained from the dermis of 15 - 15.5 day old mouse embryos (e15 - 15.5 time point). (d) Darker “dots” seen around nuclei of cells incubated in adipogenic medium are shown by white arrows. (a - f) Scale bar = 100 μm. Images were captured on a Carl Zeiss Axiovert 10 inverted microscope.

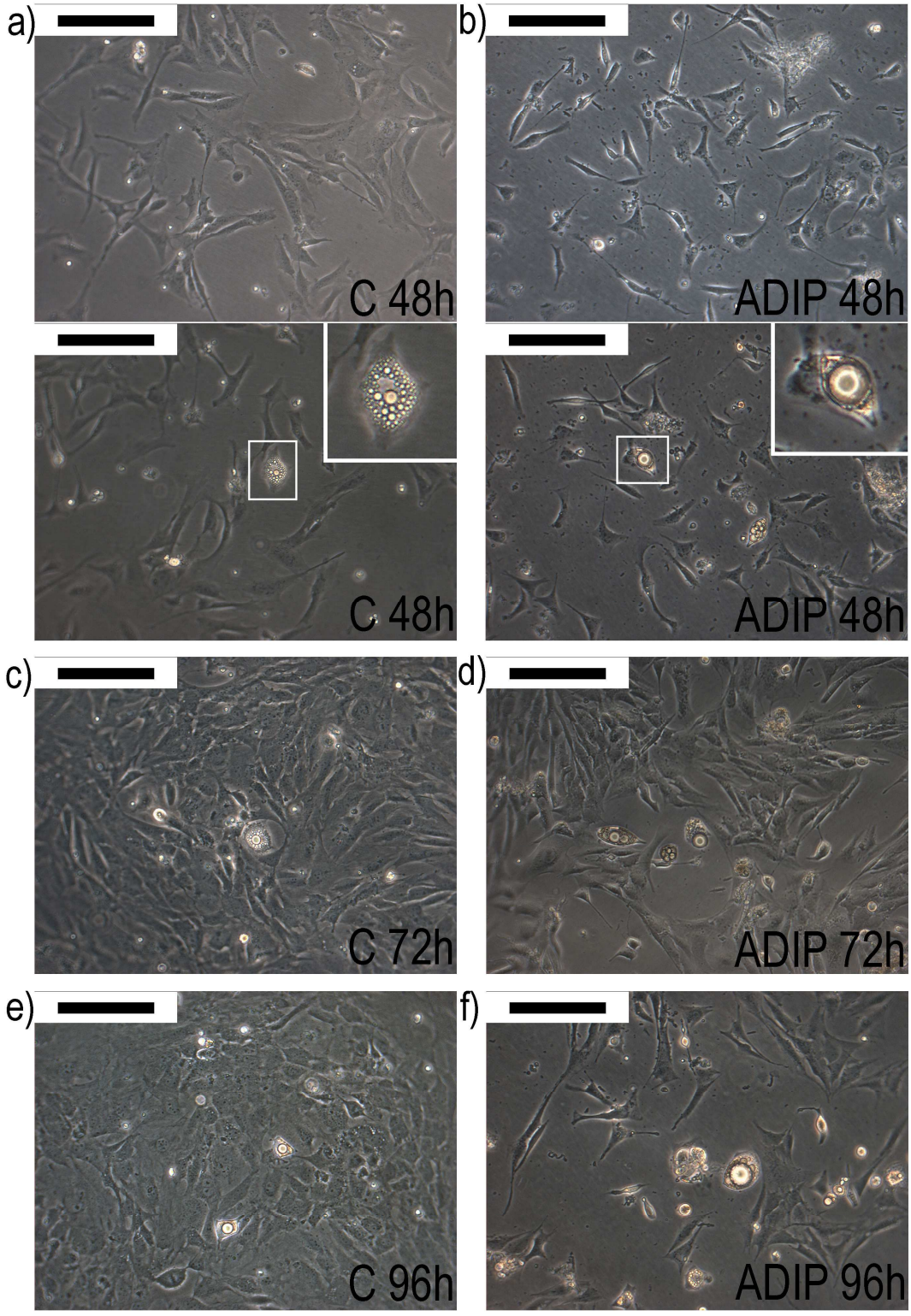


Figure 4.16. The general morphology of old embryonic two-dimensional cell structures incubated (48, 72 or 96 hours) in control (C) or adipogenic (ADIP) medium. Cells were obtained from the dermis of 18.5 - 19 day old mouse embryos (e18.5 - 19 time point). (a - f) Scale bar = 100 μm. Images were captured using a Carl Zeiss Axiovert 10 inverted microscope.

### 4.3.4.3. Comparison of lipid accumulation capabilities of mouse embryonic dermal cells in two- and three- dimensional cell cultures.

The 3D spheroid cell culture method, introduced in section 4.3.4.1, is a useful method for recreating the *in vivo*-like environment of human skin derived cells (Higgins *et al*, 2010). This 3D culture technique was tested on cells from embryonic mouse dermis. It seemed interesting to investigate whether embryonic cells can be grown as spheres. The 3D technique could be a useful for the investigation of processes naturally taking place in the body of an embryo. The question asked here was if the capability to accumulate lipids differs between dermal cells grown on the cell culture dish and suspended in a medium droplet.

Dermal cells, obtained from 15 - 15.5 and 18.5 - 19 day old mouse embryos, were suspended in droplets of normal medium for approximately 24 hours to allow cells to settle down. When three-dimensional structures had formed, they were transferred to either a fresh droplet of normal (control) medium or adipogenic medium for the next four days. Two-dimensional cell cultures were also established and the Oil Red O analysis was performed on both cell cultures.

Two-dimensional cell cultures from 15 - 15.5 day old mouse embryos did not stain with Oil Red O dye, when kept in normal medium, whereas the adipogenic medium leaded to fat cell differentiation and lipid accumulation (compare Figure 4.17a with Figure 4.17b). Cells that accumulated lipids seemed to be equally distributed along the cell culture dish when incubated with adipogenic medium (Figure 4.17b - both panels). Interestingly, when these cells were grown as 3D structures, the red dye stained intensively spheres from both normal and adipogenic medium (compare Figure 4.18a with Figure 4.18b). In addition, areas with red dye in spheres grown in normal medium seemed to be organized in clusters surrounded by areas less intensively or even not stained by the Oil Red O (Figure 4.18a - both panels). Whereas, the whole cross-sections of spheres from adipogenic medium were stained by red dye (Figure 4.18b - both panels). Therefore, the environment created by the 3D technique seems to enhance accumulation of fat droplets in young (e15 - e15.5) dermal cells even in the normal medium.

The Oil Red O staining of two-dimensional e18.5 - 19 derived skin dermis cells, showed the presence of several fat cells in normal medium (Figure 4.17c; white arrows show presence of red dye). Cells in adipogenic medium contained more cells stained by the dye and these had larger lipid droplets than in normal

medium (compare Figure 4.17c with Figure 4.17d). The 3D cultures obtained from 18.5 - 19 day old mouse embryonic skin were characterised by many areas negative for the red dye when grown in normal medium (Figure 4.18c). When cultured in adipogenic medium lipid accumulation capabilities in these spheres were enhanced (compare Figure 4.18c with Figure 4.18d).

The cell culturing techniques, clearly revealed differences in relation to fat droplet accumulation of dermal cells derived from two analysed time points.

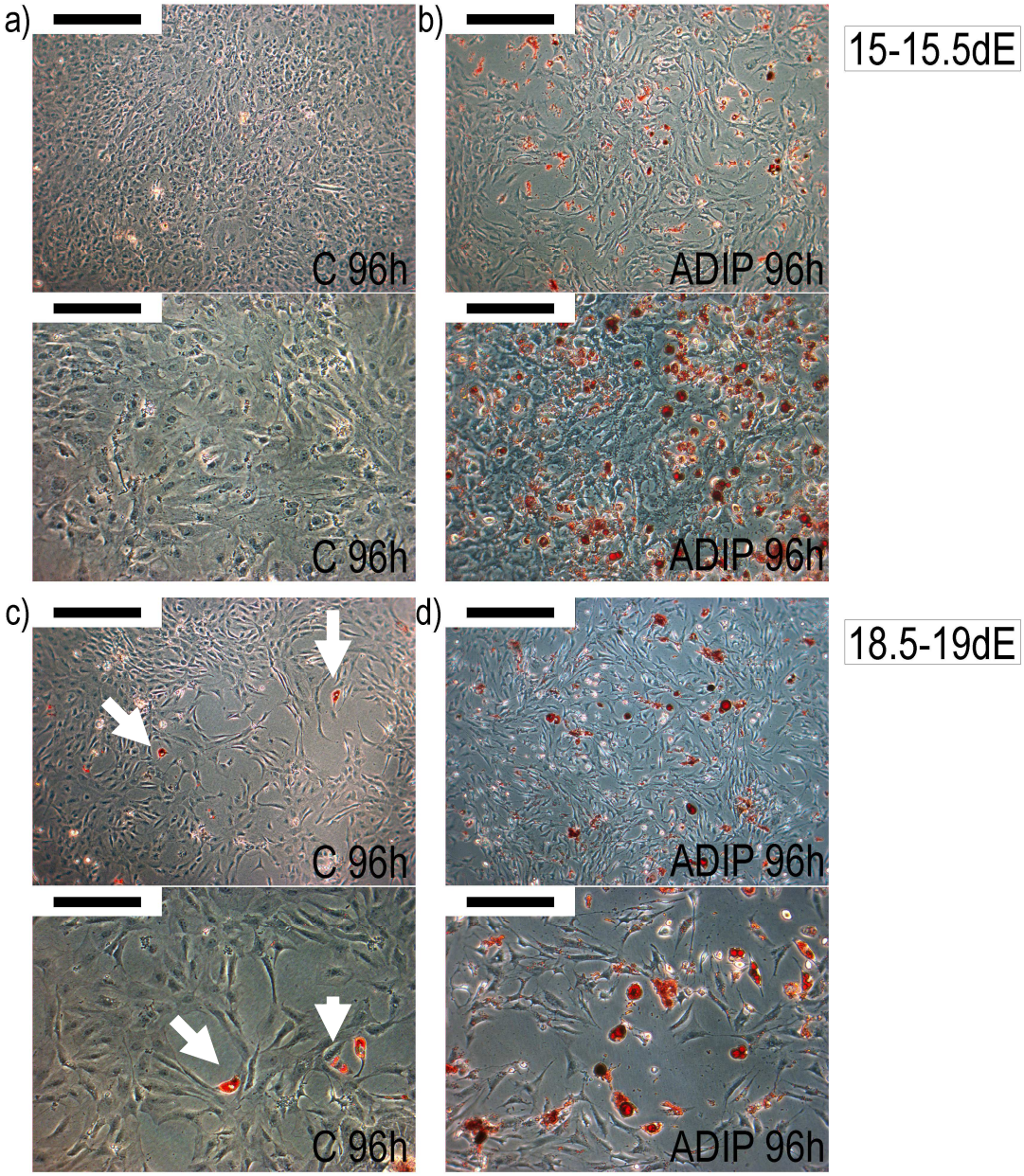


Figure 4.17. Lipid accumulation in two-dimensional cell structures incubated for 96 hours in control (C) and adipogenic (ADIP) medium. Cells were obtained from the dermis of 15 - 15.5 and 18.5 - 19 day old mouse embryos. Structures were stained with Oil Red O to detect lipids. Red dye in cells from 18.5 - 19 day old mouse embryos, kept in control medium, was shown by white arrows (c). (a, b, c, d - top panels) Scale bar = 200 μm. (a, b, c, d - bottom panels) Scale bar = 100 μm. Images were captured on Carl Zeiss Axiovert 10 inverted microscope.

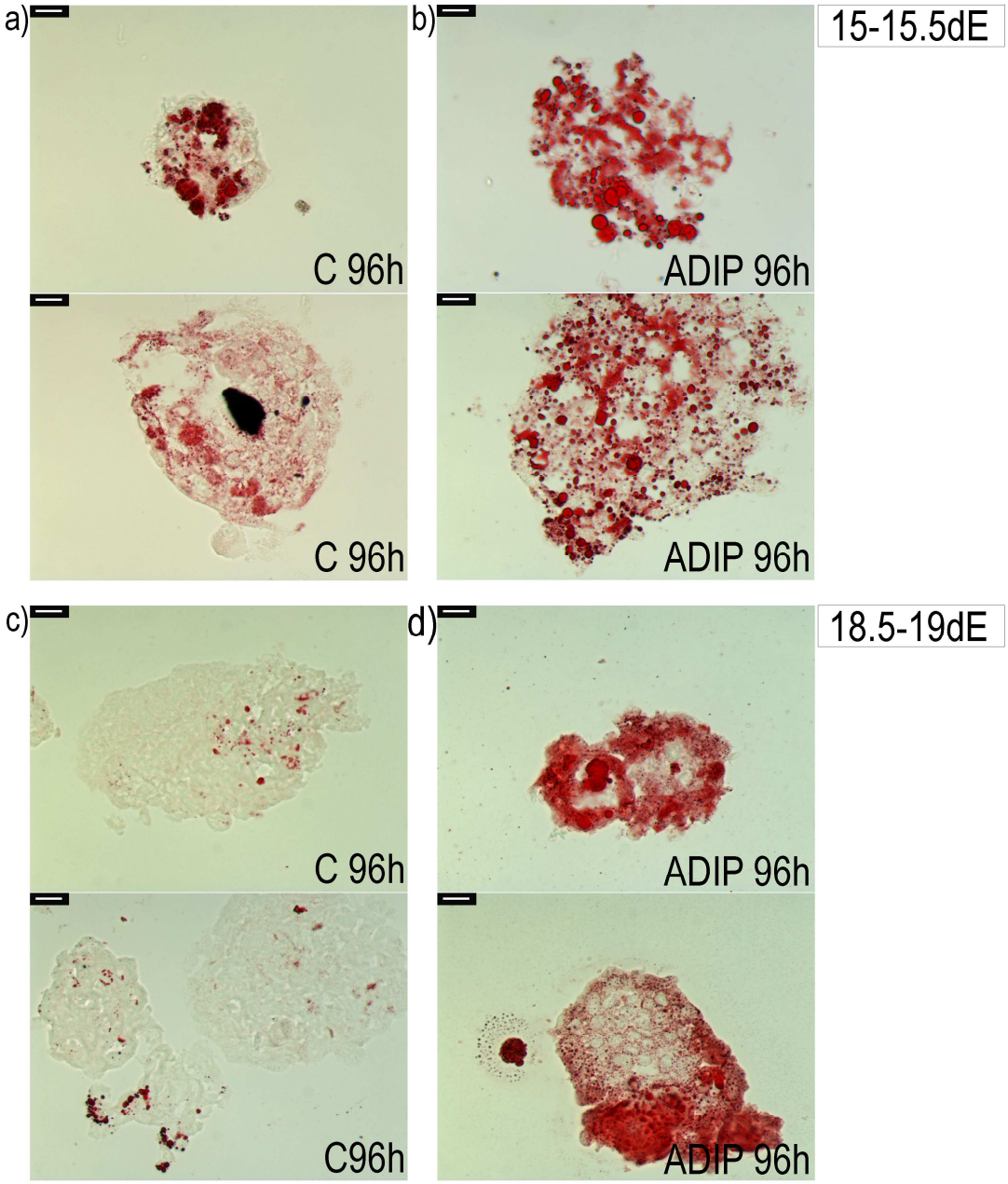


Figure 4.18. Lipid accumulation in three-dimensional cells incubated for 96 hours in control (C) and adipogenic (ADIP) medium. Cells were obtained from the dermis of 15 - 15.5 and 18.5 - 19 day old mouse embryos. Structures were stained with Oil Red O to detect lipids. (a - d) Scale bar = 15 µm. Lipid accumulation was analysed by Oil Red O staining. Images were captured using a Zeiss Axio Imager.M1. microscope.

## 4.4. Discussion.

The microarray work on dermal cells, presented in Chapter 3, allowed investigation of gene expression patterns during the embryonic development of fat cells in the lower dermis of mouse skin. It is important now to use this data in order to be able to better understand the very early steps of fat cell differentiation *in vivo*. Moreover, there is a need for efficient experimental techniques that will successfully mimic the environment of the body. These methods may help in the investigation of fat cell origin and mechanisms involved in the regulation of adipocyte differentiation in skin.

### 4.4.1. The substrate organ culture technique as a potential tool for better understanding fat cell development *in vivo*.

Among two methods tested for the growth of back skin pieces in a three-dimensional environment, only the substrate organ culture technique was useful. The hanging-drop organ culture failed in obtaining healthy skin pieces. The possible reason could be that medium droplets in which pieces were suspended were too small to maintain the skin fragments.

#### 4.4.1.1. The lipid accumulation capabilities of skin pieces are dependent on the age of mouse embryos.

The substrate organ culture technique tested the capacity of embryonic back skin pieces to produce fat in the absence of signals from the different parts of the body.

The youngest tested fragment was obtained from a back skin of 15 - 15.5 day old mouse embryo, where lipid droplets were not present in dermis and this lipid accumulation free feature was maintained in the organ culture experiment (section 4.3.3). In contrast, skin fragments from 18.5 - 19 day old mouse embryos in which back skin had a small number of fat cells in lower dermis surrounded by non-fatty cells, were characterised by an increase in areas that accumulated many small lipid droplets in skin piece when kept in organ culture conditions.

Therefore, the capability to accumulate lipids can be maintained in older embryonic skin fragments when removed from the body and kept in an *in vivo*-like environment. Maybe once committed to adipogenesis, cells that are in skin dermis at e18.5 - 19 time point are irreversibly committed to adipogenisis, moreover they could stimulate other dermal cells to undergo this differentiation process. Or it could

be that cells from other skin compartments within the analysed skin piece are responsible for the activation of lipid accumulation in dermal compartment.

However, it seems also that signals responsible for the controlling exactly which types of cells in embryonic back skin can become adipocytes could be dependent on other body sites. It was shown in Chapter 2 that during the development of dermal adipose tissue, fat droplets occurred in lower dermis and not in hair follicle structures. The size of fat droplets was increased due to progressive accumulation of lipids. In addition, an easy to spot layer of dermis free from lipid bodies and localised beneath the epidermis was observed in all analysed specimens from both mouse embryonic and newborn back skin (Chapter 2). In the organ culture samples from e18.5 - 19 day old mouse embryonic back the Oil Red O dye stained the whole dermis and even the hair follicle structures. In addition, these accumulated lipids were characterised by very tiny diameter droplets. Therefore, it seems possible that the specific signals have to occur from other body parts and together with signals from the skin compartment they control the balance between activation of adipogenesis in lower skin dermis and its inhibition in other skin parts.

#### 4.4.1.2. The role of EGFR signalling in the activation of adipogenesis in back skin dermis during the mouse embryonic development.

One of the important aims of the work presented in the Chapter 4 was to verify if the microarray data, obtained from embryonic dermal skin cells (Chapter 3), could be used for the selection of genes with a potential important role in the *in vivo* development of dermal adipose tissue. The second aim was to find a reliable experimental method that would mimic *in vivo* environment and help to verify a role of microarray-based gene in adipogenic differentiation of lower dermal cells.

The microarray data was searched for a gene with interesting expression profile in lower dermal cells from e17 to e19 time points and whose function in adipogenesis regulation *in vivo* has not been clearly defined. The gene of choice was epidermal growth factor receptor (EGFR) as it was enriched in lower dermal cells at e18 time point, according to microarray data. Its up-regulation in embryonic skin dermis at this time point was confirmed both at mRNA and protein level, by performed qRT-PCR reaction and immunofluorescence analysis (section 4.3.1). The fact that both mRNA and proteins levels of this gene are specific to the same analysed time point could be explain as follows. The up-regulation of EGFR mRNA could take place in animal couple of hours older that e17 time point and then stayed high at e18 time point, when also protein level of EGFR is enriched. However,

because the analysis was performed on time points 24 apart from each other, the exact moment when the EGFR mRNA level is up-regulated between e17 and e18, can not be elucidated in this study, but it can be seen that the expression is significantly related with e18 time point.

According to available literature, the epidermal growth factor receptor is known to be involved in development of skin components such as hair (Richardson *et al*, 2003). In addition, the function of EGF (activator of EGFR) was investigated in adipocyte differentiation of 3T3-L1 (Harrington *et al*, 2007). Moreover, in transgenic mice with a dominant negative mutation of EGFR (in skin epidermis), the replacement of fat layer in skin (by granulomatous tissue) was observed when they were a few weeks old (Murillas *et al*, 1995). In addition, a Waved-5 mouse, characterised by a highly limited EGFR-based signalling pathway, had reduced thickness of fat layer localised in skin between hair follicles at postnatal days 8.5 and 10.5 (Sugawara *et al*, 2010). It is important to mention here that EGFR-related studies with mouse models are mainly focused on the analysis of EGFR role in the hair follicle development, and observations related with fat deposits seemed to be “unexpected” elements of such work (Sugarawa *et al*, 2010).

The substrate organ culture technique was applied in a study where embryonic skin specimens at different time points were used. These were treated with either the inhibitor (AG1478) or activator (EGF) of EGFR in order to verify the role of the epidermal growth factor receptor in the regulation of adipogenesis in lower skin dermis. Interestingly, among three selected time points (e15 - 15.5, e16 - 17 and e18.5 - 19), only skin pieces from 16 - 17 day old mouse back skin were influenced by inhibitor of EGFR as no staining was seen in these pieces when incubated in AG1478, whereas incubation in the normal medium revealed the presence of fat droplets in skin specimens.

Because the inhibitory effect was seen in dermis area, whereas the red dye still stained a fat depot present beneath the dermal layer, a suggestion could be made that dermal adipose tissue and the subcutaneous fat layer (beneath the skin) do not share the same regulatory mechanism which control adipogenic differentiation *in vivo*. In addition, specimens from this particular time point, looked less healthy than samples grown in normal media. A question can be asked if this result is related with a potentially toxic concentration of the inhibitor that “destroyed” whole skin or if it was related with the inhibition effect of AG1478 on used skin. If the second explanation is true, AG1478 either inhibited development of fat cells in lower dermis and the lack of the adipocytes disrupted the proper growth of skin. On the other hand, the inhibitor of EGFR could influence first epidermis and different dermal

cells and as an effect of that, the development of fat cells was inhibited as the crucial cell-cell signals in skin were inhibited by AG1478.

It seemed that the “decision” about right time point in relation to the control of adipocyte differentiation in skin is crucial for such organ culture experiments, The inhibitory effect on lipid accumulation was seen at e16 - 17 time point but not for example in 18.5 - 19 day old embryonic back skin. Probably when skin from younger animals was chosen, the concentration of AG1478 was sufficient to inhibit low levels of EGF receptors in lower dermis and this lead to a final inhibition of fat accumulation. Then, when such experiment was performed on skin from e18.5 - 19 time point (where the up-regulation of EGFR is seen in lower dermis versus upper dermis, based on microarray data and qRT-PCR), the same concentration of AG1478 was not sufficient to inhibit EGFR and then inhibition of fat accumulation could not take place (for example because of too low amount of inhibitor and high up-regulation of EGFR in older skin).

### 4.4.2. The analysis of skin cells by two- and three-dimensional technologies.

As it was discussed in previous section, it is possible to analyse the lipid accumulation in the intact skin pieces by the *in vivo*-like organ culture. The next step of the study was to investigate features of embryonic skin dermal cells from different time points, without the epidermal layer. As the epidermal-dermal interactions are crucial for the development of hair follicles, the removal of epidermis could help to determine if such interactions exist in relation to dermal adipose layer development.

The Oil Red O staining of young embryonic mouse back skin sections (e15 - 15.5 time point) showed no lipid accumulation, and the first lipid droplets in lower dermis were only seen at later stages of embryonic development (e18.5 - 19) (section 4.3.3). Therefore it was interesting to investigate if the removal of epidermal layer could influence the features of dermal cells at e15 - 15.5 and at e18.5 - 19 time points. In addition, as lipid droplets were not seen along the whole dermis at the younger time point, the question arose if all dermal cells at this time point represent the same cell type, and that during the embryonic development different signalling pathways determine the adipogenic differentiation in the lower dermis.

First, an efficient cell culture method was investigated for this study in order to be able to recreate an *in vivo* environment. Cell culture techniques on plastic substrates are the most popular technologies for the analysis of adherent cell activities. Most of the key knowledge on fat cell differentiation was obtained from such two-dimensional cell lines, such as 3T3 cells (for more details see Chapter 1, section 1.3). However, it is also known that the restriction of cells to two-dimensions limits many real interactions with other cells that might normally happen in the body. Therefore, a spheroid cell culture method was introduced in this study. Cells are seeded into suspended media droplets wherein they aggregate into a 3D spherical structure. This method has been successfully applied for the recreating of hair follicle structures (Higgins *et al*, 2010). In work, described in section 4.3.4.1 this 3D technique was initially tested on human skin fibroblasts and hair follicle dermal papilla cells. The analysis of nuclear envelope proteins in both 2D and 3D cell structures showed that cells in spheres had nuclear structures more similar to those in cells from intact hair follicle end bulbs (compare Figure 4.12 with Figure 4.13). Cultured DP cells are capable of differentiation into adipogenic or osteogenic lines and they are considered as an example of adult stem cells (Jahoda *et al*, 2003). Therefore both 2D and 3D cultures from human DP cells were analysed because of their lipid accumulation capabilities. The fact that DP cells in 3D structures were less

prone to lipid accumulation than fibroblast cells suggests that they may be partially recovering or returning to their origin as an intact hair follicle DP. In this context they would be reflecting the more differentiated DP role of controlling hair follicle activities, and might therefore become less sensitive to adipogenic influences. Assuming that this is true and combining it with suggestions from Higgins *et al* (2010) that spheroid cell culture method can help to investigate "real" processes in hair follicle end bulbs (in relation to DP structure), this method could be a very useful *in-vivo* like tool for analysis of skin compartments. Therefore, spheroid cell culture method was applied in this thesis for the analysis of other cells from skin.

After the successful enzymatic removal of the epidermis from skin of 15 - 15.5 and 18.5 - 19 days old mouse embryos, dermal cells were able to grow as both 2D and 3D cultures. It was observed that cells from younger animals lacked lipid accumulation capability when grown as 2D cultures in normal medium, but the 3D structures were intensively stained by Oil Red O. In addition, such high accumulation of the lipids was not seen in 3D cultures obtained from older animals grown in normal (control) media (Figure 4.17 and Figure 4.18). Assuming the spherical cell culture method mimics the *in vivo* environment, dermal cells cultured in three-dimensional structures could behave as *in vivo*, but without an epidermal layer. Then, the high lipid accumulation in 3D structures at the earlier time point could occur due to the fact that these young dermal cells are representatives of undifferentiated cells with a high adipogenic capacity which would ordinarily be inhibited by the epidermal layer. The absence of epidermal layer, leads to uncontrolled differentiation of such cells into adipocytes. The dermal cell population at this earlier time point seemed to be potential progenitor of fat cells, as cross-sections from dermal cell spheres kept in normal medium were stained by the red dye.

Furthermore, the dermal cell population, obtained from 18.5 - 19 day old mouse embryos seemed to be characterised by the presence of two cell types, as in 3D structures from this time point that were kept in normal medium, small lipid droplets were surrounded by many lipid-free areas. Probably at this stage of embryonic development, one population of cells is being committed to adipogenesis (cells in the lower dermis area), the second type of cells (from the upper dermis) are not committed to undergo such adipogenic differentiation. These cells from the later embryonic developmental stage already "know who they are" and are less plastic than younger dermal cells (from e15 - 15.5 time point). Therefore, in the 3D

structure, without the epidermis layer, already committed/differentiated cells can not be influenced by the lack of epidermis in the same extent as younger dermal cells.

In order to further investigate features of dermal cells and their capability to accumulate lipids, the fluorescence activated cell sorting (FACS) was applied to isolate, two distinguishable dermal cell types: those fated to become adipocytes and those which cannot become adipocytes. This study is presented in Chapter 5.

# Chapter 5:

# The fluorescence activated cell sorting (FACS) technique as an efficient tool for the analysis of cell populations from mouse embryonic back skin.

## 5.1. Introduction.

Chapter 5 describes an approach for the isolation of cells from mouse embryonic back skin dermis by a flow cytometry-based technique. Flow cytometry is a widely used method for the analysis of cell features, such as cell size, cytoplasmic complexity or a presence of specific proteins on cell surface (Mandy *et al*, 1995). The fluorescence activated cell sorting (FACS), based on flow cytometry rules, is also a widely used method for the investigation of cell features and provides a method for sorting specific cell types from a heterogeneous mixture of cells (Herzenberg *et al*, 2002). The flow cytometry technique has been applied in studies on mature rat adipocytes (Bernstein *et al*, 1989). FACS technology was used to sort fat cells from a differentiated murine embryonic stem cell line where adipocytes were sorted from heterogeneous cells based on Nile red staining and cell granularity (Schaedlich *et al*, 2010). Nile red is an intensely fluorescent dye that stains lipid droplets. Schaedlich *et al* (2010) showed that sorted cells with increased granularity and high uptake of the Nile Red expressed (at the mRNA level) adipsin, adiponectin and leptin, known products of mature adipocytes.

It has been reported that when working with mature fat cells, the size ranges, presence of fat globules and tendency to aggregate, makes adipocytes quite a demanding material for the flow cytometry analysis (Bernstein *et al*, 1989).

In this thesis a FACS-based approach was developed in order to sort dermal cells that started adipogenesis but were not fully developed fat cells (Figure 5.1). First, a marker for fat cells from lower embryonic skin dermis was investigated that could be applied for the FACS study. The microarray data from embryonic skin dermis, presented in Chapter 3, highlighted two potentially useful surface antigens (CD36 and Fzd4) of which one (CD36) proved to be a reliable marker for FACS work. CD36 is a known membrane protein of adipocytes that binds long fatty acids and its role in regulation of fatty acid metabolism was suggested (Rodrigue-Way *et al*, 2007; Pohl *et al*, 2005). Fzd4 is a member of a family that encodes receptors for Wnt proteins and its expression was shown to be enriched in white adipose tissue (peri-uterine fat pads) isolated from 8 weeks old mice (Gupta *et al*, 2010; Soukas *et al*, 2001). After the successful sort of two dermal cell populations (CD36 positive and negative cells) and the analysis of their gene expression profile (by the qRT-PCR), the spheroid cell culture method was applied to mimic an *in vivo* environment of sorted cells. The spheroid method, introduced in Chapter 4, helped to grow sorted dermal cells in three-dimensional conditions where the presence of fat specific genes and their capability to accumulate lipids was investigated by,

immunofluorescence and Oil Red O staining respectively. The hypothesis tested in this Chapter was that CD36 positive cells, isolated by FACS method from mouse embryonic back skin, represent the lower dermal cell population that is predisposed to undergo adipogenesis and has a capability to accumulate lipids.

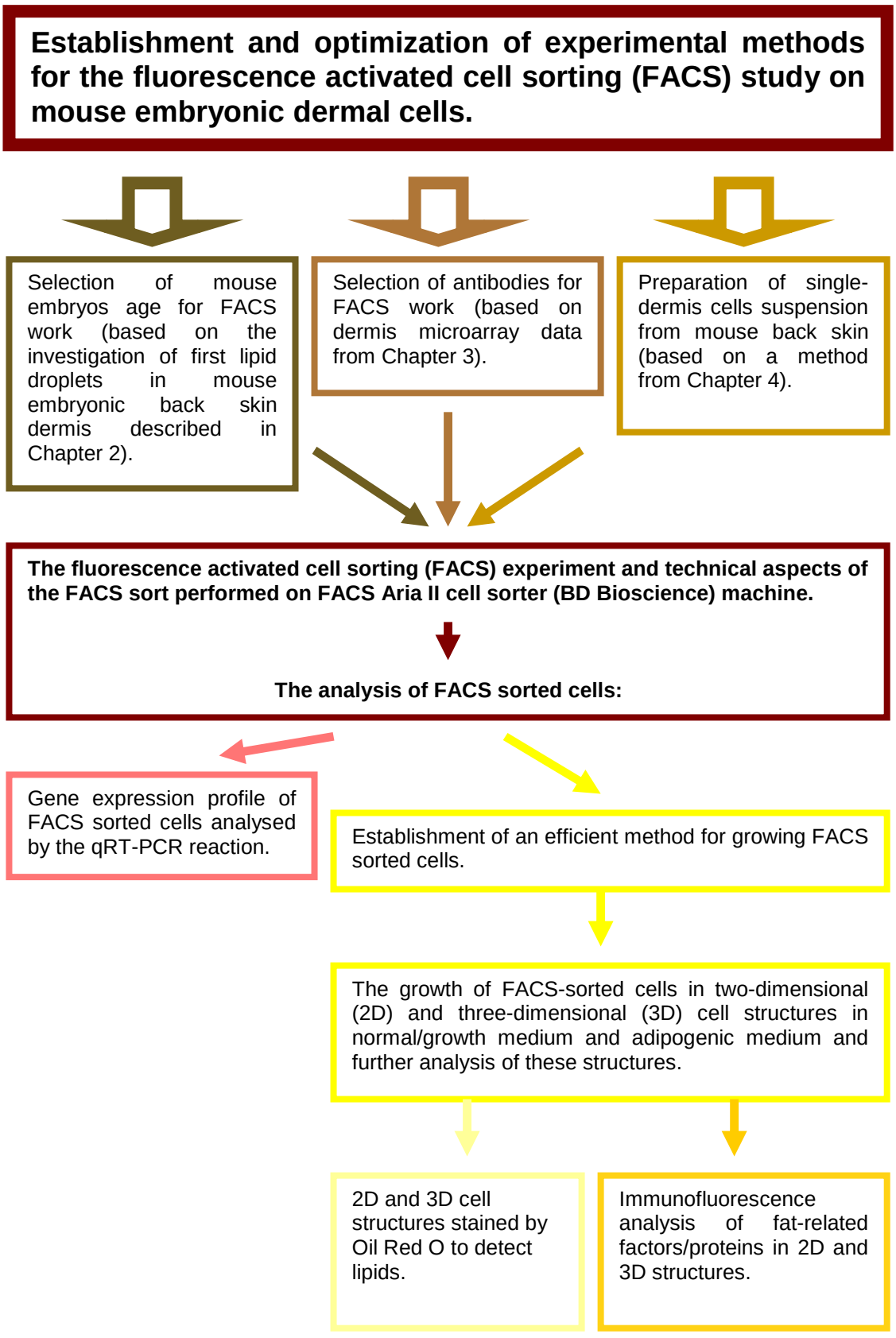


Figure 5.1. Summary of work presented in Chapter 5. Study aimed to develop efficient method for fluorescence activated cell sorting (FACS) experiment on mouse embryonic dermal cells.

## 5.2. Methods.

A schematic representation of the strategy and processes used in this chapter is shown in Figure 5.1.

Briefly, this work could be split into three stages. The first involved optimisation of the methods for obtaining dissociated cells from skin of an appropriate age, and of the ideal antibody concentration. The second stage was to devise an efficient sorting strategy to obtain sufficient viable cells. The final element was directed at validation of the initial sorted populations and then investigations of their adipogenic potential.

The flow cytometry work was performed in the Institute of Human Genetics (Bioscience Centre; International Centre for life) in Newcastle Upon Tyne, by Dr Rebecca Stewart and Mr Ian Dimmick. This work required a journey of 15 - 20 miles between Durham and Newcastle therefore there was a delay between dermal cells dissociation and final sorting as well as sorting process and culturing of these cells. During the journey samples were kept on ice and in the dark.

### 5.2.1. 3T3-F442A cells for the titration work.

3T3-F442A cells (kindly provided by Dr Ewa Markiewicz, Durham University) were grown in T75 flasks in control medium that consisted of D-MEM with GlutaMax™ (Gibco), 10% NCS, 2% penicillin/streptomycin, 1x Glutamine (Invitrogen/Fisher, Sigma) or adipogenic medium (for ingredients see Chapter 4, Table 4.1). Next, cells were prepared for the flow cytometry work. First, cells were washed in cell culture PBS, and approximately 2 - 3 ml of trypsin with EDTA (Gibco) was added for 1 - 2 min. The trypsinisation was stopped by adding 2 ml of MEM-minimum essential medium (Sigma) with 10% FBS-foetal bovine serum (Sigma) with or without antibiotics (for antibiotics details see section 5.2.3) and cells were centrifuged 1000 rpm for 5 min. Then, supernatant was removed and the pellet was washed in sterile DPBS (Gibco) and centrifuged (1000 rpm, 5 min). Next, the pellet was re-suspended in 1 ml of sterile DPBS. In case of cell clumps DNase I was added (see Appendix I). Samples (approximately 1 million cells per sample) were incubated with antibodies (Table 5.1) and analysed on the flow cytometry machine. The minimal working amount of antibodies was 6 µl for the antibody against CD36 and 5 µl for the antibody against Fzd4 (Figure 5.2 in section 5.3.1).

The titration experiment was done on a 3 laser FACSCanto II machine (BD Biosciences) with the BD FACSDiva v6.0 software.

### 5.2.2. Housing, breeding and feeding conditions of rodents used for FACS work.

The detailed information about animals breeding and maintaining conditions are presented in Chapter 2, section 2.2.1.

### 5.2.3. Dermal cells from mouse embryonic back skin.

Skin splitting was performed on 18.5 - 19 day old mouse embryos. Embryos were collected into sterile Petri dishes filled with medium (MEM - minimum essential medium from Sigma; antibiotics: 2 µl/ml Fu - fungizone from Sigma and 1 µl/ml Ge - gentamicin from Gibco). Next, embryos were attached to 5% agar in a Petri dish, and medium (MEM; Fu & Ge antibiotics) was added in order to avoid drying of skin. The back skin was cut off from the animals (for details see Chapter 4, Figure 4.2). Each skin sample was carefully separated from muscle and cut into small (maximum size: 2.5 mm x 3 mm), rectangular pieces. Pieces of back skin were collected into a watch glass filled with 500 µl of MEM with antibiotics and kept on ice. Next, skin samples were washed twice in 1 ml of sterile DPBS and transferred into a new

watch glass with 250 μl of cold, filtered solution of 5% trypsin (BD)/6% pancreatin (Sigma)/DPBS (1:1:2) and incubated for 40 - 60 min in 4$^{o}$C in order to separate dermis from epidermis. Next, the epidermis was carefully removed from each piece of skin using forceps, and the dermis was placed in a watch glass filled with 500 μl of MEM with antibiotics.

All collected dermal pieces were washed (once or twice) in 1 ml of sterile DPBS and transferred into a new watch glass with 1 ml of warm collagenase II with DNaseI (Appendix I) and incubated for approximately 15 min at 37$^{o}$C (in 5% $CO_2$) in order to obtain single cells from dermis. Next, the dissociation was continued mechanically by 200 μl tip pipette. After 5 min of mechanical dissociation, a fresh 200 - 600 μl of collagenase II with DNaseI working solution was added and sample was kept for 5 - 10 min at 37$^{o}$C (in 5% $CO_2$). Finally, the mechanical dissociation was continued till all dermis pieces were separated into single cells. Next, the sample was transferred into 1.5 ml Eppendorf and centrifuged at 3000 - 3300 rpm for 5 min at room temperature (RT). The supernatant was removed and 1 ml of sterile DPBS was added to the pellet. In order to keep single cell suspension and to avoid cell clumping, the DNaseI was added to a final concentration of 50 μg/ml.

In addition, all steps of dermal cells preparation for FACS sort were performed under the hood and with sterilized tools (120$^{o}$C; 60 min) and enzymatic solutions were filtered (0.2 um) to minimize any potential contamination of skin samples.

### 5.2.4. The fluorescence activated cell sorting (FACS) of dermal cells.

In order to perform a FACS sort, isolated dermal cells were incubated with flurochrome-labelled antibodies (Table 5.1). The number of cells used for the sort and the optimal amount of antibodies was established during several experiments as discussed in sections 5.3.2 - 5.3.4. The incubation with antibodies lasted up to 2 hours, on ice and in the dark. Then, cells were washed in DPBS, centrifuged (3000 rpm; 5 min) and suspended in several ml of fresh DBPS. Just before the FACS sort, cells were put through a 30 micron filter (Partec UK) to eliminate any clumps.

First, unstained (control) cells were analysed on the FACS machine to check non-specific signal (auto-fluorescent background) from the dermal cells. Next, experimental cells, stained with antibodies were processed through the machine. Several cell populations were collected: Negative cell population (no signal for used antibodies/markers), CD36+ cells expressing CD36, Fzd4+ cells expressing Fzd4

and dual population of cells expressing both CD36 and Fzd4. Different amounts of cells were collected in different experiments in order to find the optimal number of cells that should be sorted for further analysis (sections 5.3.2 - 5.3.4).

The fluorescence activated cell sorting (FACS) was performed on FACS Aria II cell sorter (BD Bioscience) with 100 micron nozzle at 20PSI and on the BD FACSDiva v6.0 software.

Table 5.1. Details of antibodies used for the FACS sort work.

| **FACS antibodies:** | **Fluorochrome:** | **Type:** | **Concentration:** | **Company:** |
|---|---|---|---|---|
| **CD36** | Allophycocyanin (APC) | Anti-mouse | 0.2 mg/ml | BioLegend |
| **Fzd4** | Phycoerythrin (PE) | Anti-human/mouse | 0.025 mg/ml | R&D Systems |

**The final optimized FACS sort protocol (in relation to section 5.3.4).**

Up to 14 embryos provided the dermal cells that were finally suspended in sterile DPBS. The DNase I was added before the staining (to a final concentration of a 50 μg/ml) and 800 μl of these cells were stained with 36 μl of CD36 antibody. The amount of stained cells used for FACS was about 10 million/ml. These cells were used for the FACS. In more detail, 200 000 cells (for each analysed cell population) were collected into sterile 1.5 ml Eppendorf with 200 μl of medium (MEM; 10%FBS; antibiotics: Fu and Ge), these were immediately placed on ice for transportation. In total four samples, with 200 000 cells per each sample, were collected for the Negative cell population and four for the CD36 positive cells. One sample of each of the collected cell types (one for the negative cells and one of the CD36 positive cells) was used for RNA isolation, the second and third for the establishment of 2D structures and the fourth for the 3D structures.

### 5.2.5. The analysis of FACS sorted cells.

#### 5.2.5.1. DNA/RNA work.

Cells, from the sort, were collected into the 200 µl of warm growth medium (MEM - minimum essential medium from Sigma; 10% FBS - foetal bovine serum from Sigma; antibiotics: 2 µl/ml Fu - fungizone and 1 µl/ml Ge - gentamicin) and kept on ice until centrifuged (2000 rpm; 3 min and if needed for additional 2000 rpm; 1 min). Then, cells were suspended in a total volume of 150 µl of the RLT buffer (Qiagen) with beta-mercaptoethanol (b-ME) and kept in -80$^{o}$C.

##### 5.2.5.1.1. RNA isolation.

The RNeasy® kit with RNeasy MinElute® columns (Qiagen) were used for the RNA isolation from FACS sorted cells. The purification of total RNA from animal cells was performed according to the RNeasy®Micro handbook with a few modifications in order to enhance the efficiency of cleaning process.

Briefly, to the 150 µl of prepared samples, additional RLT buffer with b-ME (mercaptoethanol) was added to the final volume of 350 µl. Next, one volume of 70% ethanol (prepared from Sigma's molecular biological grade ethanol) was added to each sample, mixed and transferred to a RNeasy MinElute® spin column and centrifuged (>=10 000 rpm; 15 sec). The flow-through was placed once again on the column and centrifuged (10 000 rpm; 15 sec). Then, the flow-through was discarded and column was washed with 350 µl of buffer RW1 (>=10 000 rpm, 15 sec). Next, the DNase digestion step was applied, where 10 µl of DNase I stock solution (Qiagen) with Buffer RDD (Qiagen) was placed on the RNeasy MinElute® spin membrane and samples were left for 15 min at RT. Then, 350 µl of Buffer RW1 was added to columns and samples were centrifuged (>=10 000 rpm; 15 sec). The flow-through was discarded, 500 µl of Buffer RPE was added and samples were centrifuged (>=10 000 rpm, 15 sec). The flow-through was discarded. Then, 500 µl of 80% ethanol was added to columns which were then centrifuged (>=10 000 rpm, 2 min) and the flow-through was discarded. Columns were placed in new collection tubes and centrifuged with open lids at full speed for 5 min. Then, columns were placed in new 1.5 ml collection tubes and 14 µl of warm (68$^{o}$C) RNase-free water was added to the centre of the spin columns. Columns with warm water were incubated for 5 min at RT and centrifuged for 1 min at full speed for the RNA elution. The flow-through was placed once again on the column and centrifuged for 1 min at full speed. Finally, the purified RNA was used for the cDNA synthesis.

#### 5.2.5.1.2. First-strand cDNA synthesis.

The concentration of purified RNA from FACS sorted cells was checked on the NanoDrop® Spectophotometer ND-1000 (with ND-1000 v3.5.2. software) and approximately 490 ng of total purified RNA from each sample was used for the cDNA synthesis.

The SuperScript® III RT kit (Invitrogen) was used for this step. Briefly, each sample for cDNA synthesis contained total RNA (490 ng), 1 μl of oligo(dT), 1 μl of 10mM dNTP mix (Bioline) and RNase free water (to a total volume of 13 μl) and was heated to 65$^{o}$C for 5 min and immediately placed on ice for at least 1 min. Then, a 7 μl of master mix was added to each sample (4 μl of 5 X First Strand Buffer; 1 μl of 0.1 M DTT, 1 μl of SuperScript$^{TM}$ III RT and 1 μl of RNase free water per each sample) that was then incubated for 60 min at 50$^{o}$C. The reaction was inactivated by incubation for 15 min at 70$^{o}$C. All incubation steps were performed on a Biometra PCR machine with the lid temperature set up for 99$^{o}$C. The cDNA was stored at -20$^{o}$C.

#### 5.2.5.1.3. The quantitative RT-PCR reactions.

The synthesized cDNA from FACS sorted cells was used for the investigation of mRNA levels by the quantitative RT-PCR technique.

The cDNA was diluted 1 to 6 in RNase free water and used for the qRT-PCR reactions. Briefly, each reaction contained 1 μl of diluted cDNA, 1 μl of 2.5 μM forward and reverse primers mix, 10 μl of Power SYBR Green PCR Master MIX (Applied Biosystems) and 8 μl of sterile miliQ water. For control samples, no cDNA was added. For each set of primers and each cDNA sample, four reactions were prepared as repeats. The reactions were performed on 96-well plates (MicroAmp® Fast Optical 96-Well Reaction Plate with Barcode, 0.1 ml, Applied Biosystems) covered with MicroAmp® Optical Adhesive Film, Applied Biosystems) on the 7500 Fast Real-Time System with compatible 7500 Fast System (SDS version 1.4) software (Applied Biosystems). Conditions for PCR reactions are shown in Chapter 3, Table 3.1. Primers used for this analysis are presented in Chapter 3, Table 3.2.

Once the Ct values were obtained, the three samples with the most similar Ct values were used for further analysis of relative mRNA expression and the Delta-Delta-Ct (ddCT) algorithm was applied for this purpose. The baseline (1-fold

change) was set up for Negative cells and changes in the expression level in CD36 positive cells were checked according to this baseline.

To ensure consistency for each run, dermal cells derived from the embryos of one mother were FACS sorted and used for the qRT-PCR analysis.

### 5.2.5.2. Establishment of two-dimensional (2D) and three-dimensional (3D) cell structures from FACS sorted cells.

Sorted cells were collected into 200 µl of warm MEM with 10% FBS and antibiotics (2 µl/ml Fu 1 µl/ml Ge). Cells were kept on ice until used for both two-dimensional (2D) and three-dimensional (3D) cell structures.

For 2D cell culture, sorted cells were placed either in 35 mm dishes (for the Oil Red O staining: approximately 50 000 cells per 35 mm dish, with 1 ml of growth medium) or on 60 mm dishes with coverslips (for immunoflorescence: approx. 100 000 cells, per dish, with 1 ml of growth medium) and left in the incubator (37$^{o}$C; 5% $CO_2$) for 90 - 160 min to settle down. Next, medium was changed for fresh growth medium and adipogenic medium (Table 5.2), cells were incubated for either 2 or 4 days (37$^{o}$C; 5% $CO_2$) after which lipid and immunofluorescence analysis were performed (sections 5.2.5.3 and 5.2.5.4).

3D cell structures were established according to protocol described in Chapter 4, section 4.2.5.4. Spheres were created after first 24 hours of incubation at 37$^{o}$C with 5% $CO_2$. Once formed, three dimensional cell structures were transferred by 10 microlitre tip (under the microscope) into fresh media drops (prepared from fresh growth medium and adipogenic medium). 3D structures were then incubated for either 2 or 4 days (37$^{o}$C; 5% $CO_2$) and finally transferred into the Tissue Tek, carefully frozen in the liquid nitrogen and kept in -80$^{o}$C. Next, 7 µm sections of 3D structures (cut on the cryostat) were used for the lipid detection and the immnofluorescence analysis (sections 5.2.5.3 and 5.2.5.4).

Table 5.2. Components of the growth and adipogenic medium used for FACS sorted cells.

| Type of medium: | Components of medium: |
|---|---|
| **Growth medium** | MEM - Minimal Essentium Medium<br>Antibiotics: 2μl/ml fungizone; 1 μl/ml gentamycin<br>10% FBS - Foetal Bovine Serum |
| **Adipogenic medium (differentiation medium)** | MEM - Minimal Essentium Medium<br>Antibiotics: 2μl/ml fungizone; 1 μl/ml gentamycin<br>15% Rabbit Serum (Sigma)<br>2.07μM Insulin (Sigma)<br>100nM Dexamethasone – DEX (Sigma)<br>0.45mM 3-isobutyl-1-methylxanthine - IBMX (Sigma) |

### 5.2.5.3. The Oil Red O staining protocol.

The Oil Red O dye was used in order to investigate lipid accumulation in FACS sorted cells that were incubated in growth and adipogenic medium (as 2D and 3D structures) for four days. All steps of the lipid detection were performed at room temperature (RT).

2D cell structures were washed in PBS (3 x PBS; few min), fixed in the calcium formal solution for 10 min, incubated with 60% isopropanol (approximately 5 min) and kept in the Oil Red O working solution for up to 10 min, then washed by 60% isopropanol and PBS (see Appendix I for details of calcium formal solution and section 2.2.4 for the Oil Red O working solution). 2D cells structures were kept in PBS, in 4$^{o}$C.

Sections from spheres, cut on the cryostat and placed on superfrost slides (VWR), were air dried (up to 90 min) and used for the lipid detection. The lipid detection was performed according to protocol used for 2D cells (see above). For better fixation of spheres, an alternative protocol was applied where the incubation in the calcium formal lasted for 1 hour, then samples were incubated in 60% isopropanol for 15 min and in Oil Red O working solution for 15 min. Some sections with 3D cell structures underwent an additional washing step with 60% isopropanol in order to fully remove red dye not attached to lipids (and avoid background/non specific staining). Slides with spheres were then mounted with mowiol (Appendix I) and covered by coverslips.

The analysis of lipid accumulation was performed either on Zeiss Axio Imager.M1 (with the Openlab™ Improvision® software) or on PALM MicroBeam Zeiss Microscope, CryLaS, FTSS 355-50 (with PALM@Robo v3.2 software).

### 5.2.5.4. Immunofluorescence analysis of FACS sorted cells.

The analysis of C/EBPalpha was performed on established 2D and 3D cell structures that were incubated 2 days in growth and adipogenic medium. Detection of FABP4 was performed on structures kept 4 days in both types of media.

The immunofluorescent analysis of stained samples was performed on the Zeiss Axio Imager.M1 (with the Openlab™ Improvision® software).

#### 5.2.5.4.1. Protocol for the C/EBPalpha detection.

Both, 2D and 3D cell structures were first fixed 15 min in 4% paraformaldehyde (Sigma)/PBS at room temperature (RT) and 5 min in 0.5% Triton-X100 (Sigma)/PBS (at 4°C). Then cells were washed in PBS (3 x PBS; 5 min) and blocked in 20% donkey serum/PBS (Sigma) for 30 min, at RT. Fixed cells were incubated (up to 90 min, at RT) with primary antibodies (diluted in 1% donkey serum/PBS) against C/EBPalpha (rabbit antibody, dilution 1:100, Santa Cruz Biotechnology). Next, cells were washed in PBS (3 - 5 x PBS; 1 - 5 min) and incubated (up to 90 min, at RT) with secondary antibody: AlexaFluor® 488 donkey-anti rabbit, FITC conjugated (diluted 1: 500, Table 3.3.B.) and DAPI (diluted 1:5000). Secondary antibody with DAPI was diluted in 1% donkey serum/PBS. Finally, samples were washed in PBS (3 - 5 x PBS; 1 - 5 min), mounted with mowiol (Appendix I) and 2D and 3D cells were covered with coverslips.

#### 5.2.5.4.2. Protocol for the FABP4 detection.

Both, 2D and 3D cells were first fixed 10 min in 100% acetone (Sigma; at -20°C) and 10 min in 100% methanol (Sigma; at -20°C). Then cells were washed in PBS (3 x PBS; 5 min) and blocked in 20% donkey serum/PBS (Sigma) for 30 min, at RT. Fixed cells were incubated (90 min, at RT) with primary antibodies (diluted in 1% donkey serum/PBS) against FABP4 (goat antibody, dilution 1:50, R&D Systems). Next, cells were washed in PBS (3 - 5 x PBS; 1 - 5 min) and incubated (60 min, at RT) with secondary antibody: AlexaFluor® 488 donkey-anti goat, FITC conjugated (diluted 1:500) and DAPI (diluted 1:5000). Secondary antibody with DAPI was diluted in 1% donkey serum/PBS. Finally, samples were washed in PBS (3 - 5 x PBS; 1 - 5 min), mounted with mowiol (Appendix I) and 2D and 3D cells were covered with coverslips.

## 5.3. Results.

### 5.3.1. The investigation of a surface marker for lower dermal cells committed to adipogenesis in mouse embryonic back skin.

The microarray data, presented in Chapter 3, was examined for a gene highly expressed in lower dermal compartment, whose enrichment would take place from e17 to e19 time point and which encoded a membrane protein. The specific localisation and high expression of this gene in lower dermis was required for the selection of cells that, based on the Oil Red O analysis (Chapter 2) were gradually accumulating lipids in embryonic skin dermis and create dermal adipose tissue in lower dermis. In addition, the specific protein localisation on cell surface was crucial for the performance of fluorescence activated cell sorting (FACS) on dermal cells.

Two candidates were found, namely CD36 and Fzd4 (Table 5.3 and Table 5.4). Both genes were enriched in lower dermal cells when compared with upper area of dermis and their expression level increased in the lower skin compartment from e17 till the e19 time point (Table 5.3. and Table 5.4). Based on the fold change values the enrichment of *Cd36* was higher when compared with *Fzd4* gene.

Due to this specific expression pattern of CD36 and Fzd4, two antibodies were chosen with different fluorochromes in order to perform an analysis of both potential markers during the same sort procedure (Table 5.1). An anti-Fzd4 antibody was conjugated with phycoerythrin (PE), whereas an anti-CD36 antibody was characterised by a presence of allophycocyanin (APC).

The final FACS sort protocol was successfully optimized for anti-CD36 antibody (sections 5.3.2 - 5.3.4). For the verification work of the expression profile of *Cd36* gene in embryonic skin dermis, the qRT-PCR reaction with a primer set designed for *Cd36* gene (see Table 3.2 in Chapter 3) confirmed the significant up-regulation of *Cd36* in lower dermal cells from e17 till e19 time points, when compared with cells from upper dermis (see Figure 3.62A in Chapter 3). In addition, an attempt was made to analyse the expression of CD36 protein in embryonic back skin samples between e17 and e19 time points. However, the antibody (goat

polyclonal antibody against CD36; Santa Cruz Biotechnology) used failed to give conclusive results (data not shown).

Table 5.3. The *Cd36* gene expression profile in embryonic skin dermis between e17 and e19 time points. (A) The E17, E18 and E19 microarray sub-lists revealed enrichment of *Cd36* at mRNA level in lower dermal cells versus upper dermal cells at e17, e18 and e19 time points. (B) The lower dermal (LD) microarray list showed the up-regulation of *Cd36* gene in lower dermal cells from e17 time point.

A)

| **Whole name; gene symbol; probe set Affymetrix ID.** | **Time points:** | **Fold change value:** |
|---|---|---|
| CD36 antigen; *Cd36*; 1450883_a_at | e17 lower dermis vs* e17 upper dermis | + 9.251164 |
| | e18 lower dermis vs* e18 upper dermis | + 29.43071 |
| | e19 lower dermis vs* e19 upper dermis | + 52.71146 |

B)

| **Whole name; gene symbol; probe set Affymetrix ID.** | **Time points:** | **Fold change value:** |
|---|---|---|
| CD36 antigen; *Cd36*; 1450883_a_at | e18 lower dermis vs* e17 lower dermis | + 5.071104 |
| | e19 lower dermis vs e17 lower dermis | + 8.146752 |

* vs - versus

Table 5.4. The *Fzd4* gene expression profile in embryonic skin dermis between e17 and e19 time points. (A) The E17, E18 and E19 microarray sub-lists revealed enrichment of *Fzd4* at mRNA level in lower dermal cells versus upper dermal cells at e17, e18 and e19 time points. (B) The lower dermal (LD) microarray list showed the up-regulation of *Fzd4* gene in lower dermal cells from e17 time point.

A)

| **Whole name; gene symbol; probe set Affymetrix ID.** | **Time points:** | **Fold change value:** |
|---|---|---|
| frizzled homolog 4 (Drosophila); *Fzd4*; 1419301_at | e17 lower dermis vs* e17 upper dermis | + 2.65587 |
| | e18 lower dermis vs* e18 upper dermis | + 7.128446 |
| | e19 lower dermis vs* e19 upper dermis | + 9.34063 |

B)

| **Whle name; gene symbol; probe set Affymetrix ID.** | **Time points:** | **Fold change value:** |
|---|---|---|
| frizzled homolog 4 (Drosophila); *Fzd4*; 1419301_at | e18 lower dermis vs* e17 lower dermis | + 1.518623 |
| | e19 lower dermis vs e17 lower dermis | + 2.657529 |

* vs - versus

3T3-F442A cells were chosen for an antibody titration experiment. This cell line has been used for the investigation of adipogenesis (Pairault and Lasnier, 1987). Confluent 3T3-F442A cells accumulated lipids, when incubated in adipogenic medium (compare Figure 5.2Aa, b and c).

3T3-F442A cells from either control or adipogenic medium were used for flow cytometry analysis (Figure 5.2Ba - d). Unstained cells were used to verify background staining (Figure 5.2Ba and Figure 5.2Bc). Then, samples stained with antibodies against CD36 and Fzd4 were analysed (for minimal working volume of antibodies and their concentrations see section 5.2.1 and Table 5.1). A signal was difficult to obtain from cells kept in adipogenic medium (Figure 5.2Bd). Fortunately, cells from control medium revealed the presence of cells positive for either CD36 or Fzd4 antigen and a small population of cells stained by both antibodies was also observed (compare Figure 5.2Ba with Figure 5.2Bb).

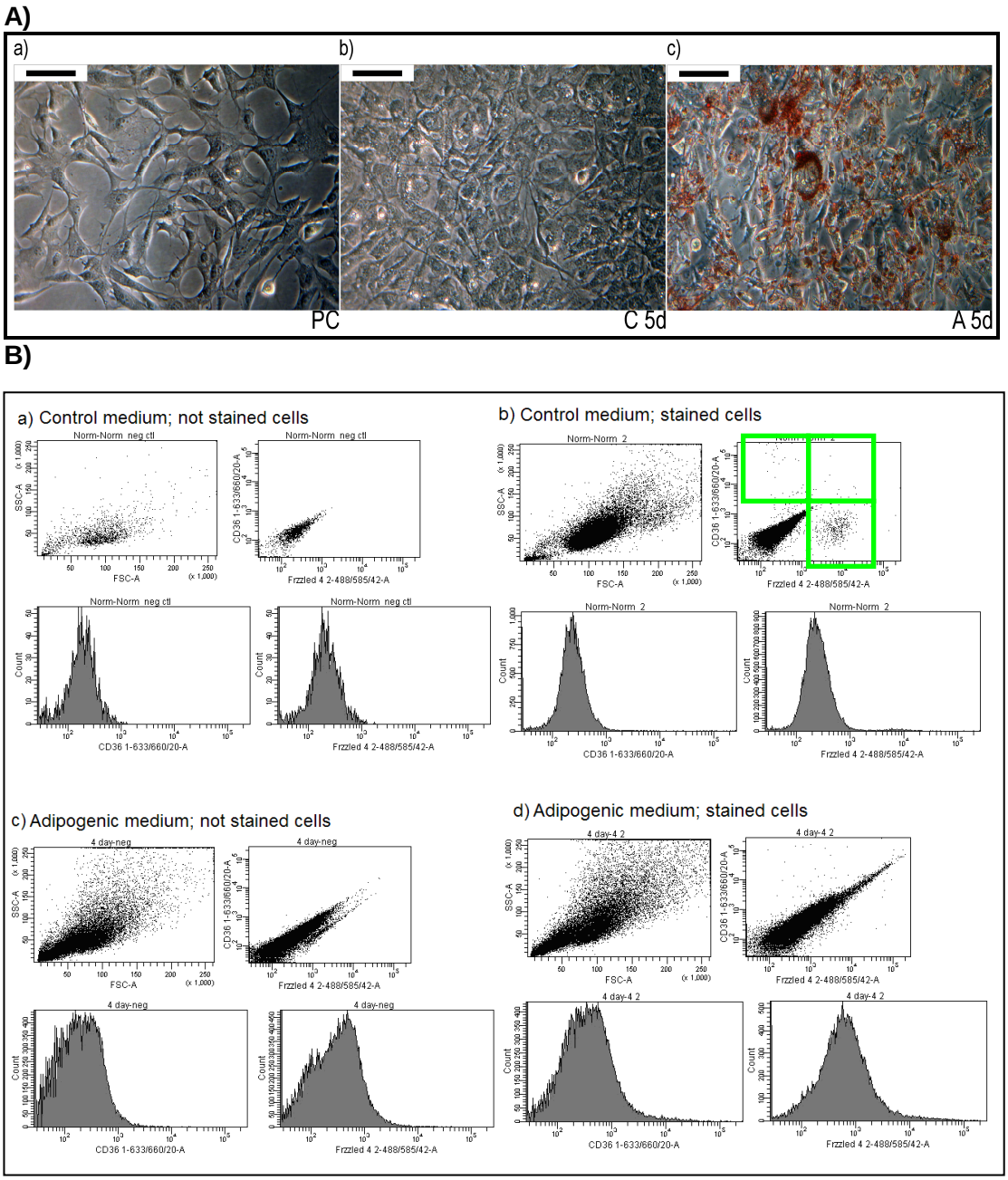


Figure 5.2. Characterisation of adipocyte differentiation in 3T3-F442A cells.
(A) 3T3-F442A cells stained with Oil Red O to detect lipids. (a) preconfluent cells - PC. (b) confluent cells kept 5 days in control medium - C 5d. (c) confluent kept 5 days in adipogenic medium (A 5d). (a - c) Scale bar = 100 µm. (a - c) Images were captured using a Carl Zeiss Axiovert 10 inverted microscope with accompanying AnalySIS software.
(B) An antibody titration experiment on 3T3-F442A cells. Confluent cells incubated 4 days in control (a and b) and adipogenic medium (c and d) underwent the flow cytometry analysis as cells not stained (a and c) and stained with antibodies against CD36 and Fzd4 (b and d). (a - d: top left panels): Two-parameter histograms: FSC-forward scatter (size of cells), SSC-side scatter (cell-complexity or number of internal compartments). (a - d: top right panels): Two-parameter histograms: antibody against CD36 with APC-fluorochrome/1-638/67/14-A; antibody against Fzd4 with PE-fluorochrome/4-488/585/42-A. (a - d: bottom panels): Intensity of staining with specific antibodies. Cells positive for CD36 and/or Fzd4 are marked by green squares.

### 5.3.2. Initial FACS sort on dermal cells.

The aim of this Chapter was to isolate cells committed to adipogenesis in lower skin dermis before they become mature adipocytes. The Oil Red O detection combined with the immunofluorescence analysis of C/EBPalpha occurrence in lower dermal cells, presented in Chapter 2, suggested that embryonic skin from lower dermis area older than e17 time point is filled with preadipocytes that express adipogenic tranciptional factor (C/EBPalpha) and start to accumulate first small lipid droplets between e18 and e19 time point. Therefore, a decision was made to perform FACS work on embryonic dermis between 18.5 and 19 day old.

Dermal cells were obtained according to the method described in Chapter 4 where two steps of enzymatic treatment (based on the use of trypsin, pancreatin and collagenase II) allowed a separation of epidermis from dermis layer and a dissociation of dermal layer into a single cell suspension.

One pregnant mouse was the donor of embryos for a single FACS experiment. During initial FACS experiments, approximately 1 500 000 dermal cells were obtained from six embryos. First, unstained cells underwent analysis in order to check auto-fluorescence/background, whereas an experimental sample was incubated with antibodies against CD36 and Fzd4 (Figure 5.3). It was possible to collect cells with high levels of either only CD36 or Fzd4 as well as cells positive for both CD36 and Fzd4 markers (compare Figure 5.3Ac with Figure 5.3Bc). The highest population of collected cells was negative cells (cells devoid of CD36 and Fzd4). Among cells expressing antigens of interest, the highest number of cells was obtained for CD36 positive cells (CD36+ cells), whereas Fzd4 positive cells (Fzd4+ cells) and dual positive cell population (dual cell population: CD36+ and Fzd4+ cells) had lower numbers of cells (Figure 5.3Bc and f).

**A) Control sample:**

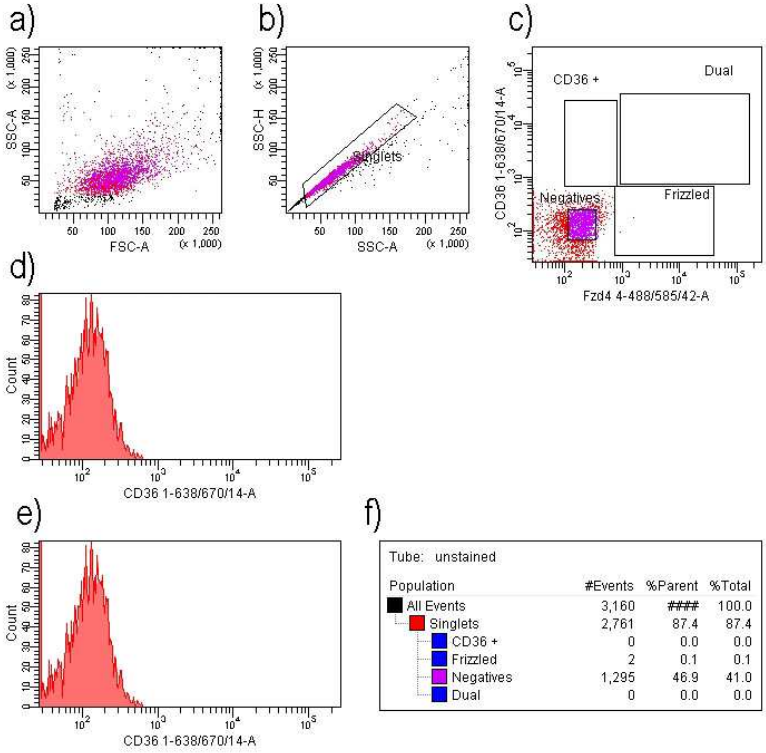


**B) Experimental sample:**

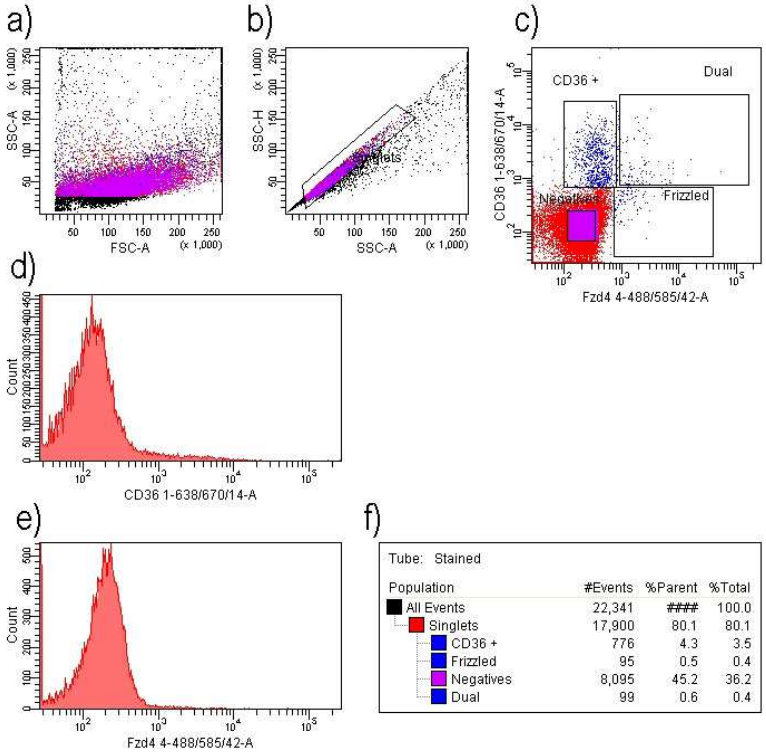


Figure 5.3. Initial FACS experiment. (A) non-stained cells used as control sample. (B) cells stained with antibodies against CD36 (APC-fluorochrome: 1-638/67/14-A) and Fzd4 (PE-fluorochrome: 4-488/585/42-A). (a, b, c) Two-parameter histograms. (d, e) One-parameter histograms. (a) FSC-forward scatter (size of cells), SSC-side scatter (cell-complexity or number of internal compartments). (b, c) Gating of singlets and collected cells. (d, e) Intensity of staining with specific antibodies. (f) % of events during sort reaction.

### 5.3.3. Selection of dermal cell populations sorted by FACS technology and their viability.

It was important to establish optimal conditions for maintaining the viability of sorted cells. First, a capability to grow sorted cells as two-dimensional (2D) structures was tested. When sorted cells were collected into Eppendorf tubes with 200 µl of growth medium (MEM with 10% or 20% FBS and antibiotics: Fu and Ge) and placed in a 4-well dish (or 35 mm dish) with growth medium, they were able to attach to a surface of culture dish (Figure 5.4). In addition, keeping cells on ice (in Eppendorf) straight after the sort and before the incubation on cell culture dishes seemed to improve the viability of cells.

**Fzd4 positive (Fzd4+) cells and dual positive (CD36+ and Fzd4+) cell population.**

As was mentioned in the previous section, the Fzd4 positive (Fzd4+) cell population was characterised by a low number of collected cells when compared with CD36 positive (CD36+) cells. This population had a low viability and low percentage of cell survival when seeded onto cell culture dishes (compare Figure 5.4c with Figure 5.4a, b and d). Therefore this cell population was eliminated from further analysis.

In addition, the number of cells positive for both markers (dual cell population: CD36+ and Fzd4+ cells) was lower than the CD36+ cells (Figure 5.3Bc). This resulted in longer time needed for the FACS in order to obtain sufficient amount of cells positive for both antigens. It was crucial to shorten time of the sort to increase cell survival, therefore a decision was made to eliminate also dual cell population and focus on the collection of cells displaying high levels of CD36 antigen.

**CD36 positive (CD36+) cells and Negative (CD36- and Fzd4-) cell population.**

It was relatively easy to collect sufficient amount of Negative and CD36+ cells that were able to grow when kept as 2D cell structures for up to 7 days (Figure 5.5a and b). In addition, CD36+ cells had a specific adipocyte-like morphology, as they contained of round-shaped droplets that were hypothesised to be accumulated lipids (Figure 5.5b). Because of this it seemed that CD36+ cells were likely to be cells from the lower skin dermis committed to adipogenesis.

In addition, to enhance the number of CD36+ sorted cells, the amount of antibody used was increased six times in next FACS experiments (36 µl of anti-

CD36 antibody and 30 μl of anti-Fzd4 antibody per FACS sort experiments; for antibody stock concentrations see Table 5.1).

**Two populations of CD36+ positive cells.**

One of the next steps for FACS-based study was related with modification of the gate for CD36 positive cells. The originally established gate for the sort of CD36 positive population consisted of cells with the relative fluorescence intensity (for APC-antibody against CD36) equal and higher than 1 000 (see Figure 5.3Bc). CD36 positive cells close to the bottom line of this gate might represent a population of cells with auto-fluorescence and not cells positive for CD36 antigen. Therefore an experiment was designed where two gates for CD36+ cells were set up: “top” gate for cells with the relative fluorescence signal higher than approximately 10 000 and “bottom” gate for cells with relative fluorescence signal between about 1 000 and 10 000 (Figure 5.6). Two collected populations of CD36 positive cells were analysed for their capabilities to accumulate lipids (Figure 5.7). The Oil Red O staining showed that two-dimensional cell cultures from both sorted cell populations (“top” and “bottom”) were capable of lipid accumulation when kept in growth medium for up to 8 days (compare Figure 5.7a with b and c). Therefore, the original (bigger) gate for CD36+ positive cells, with the relative fluorescence signal equal and higher than 1 000, was treated as a sufficient for the collection of dermis cells expressing CD36 antigen and undergoing adipogenesis.

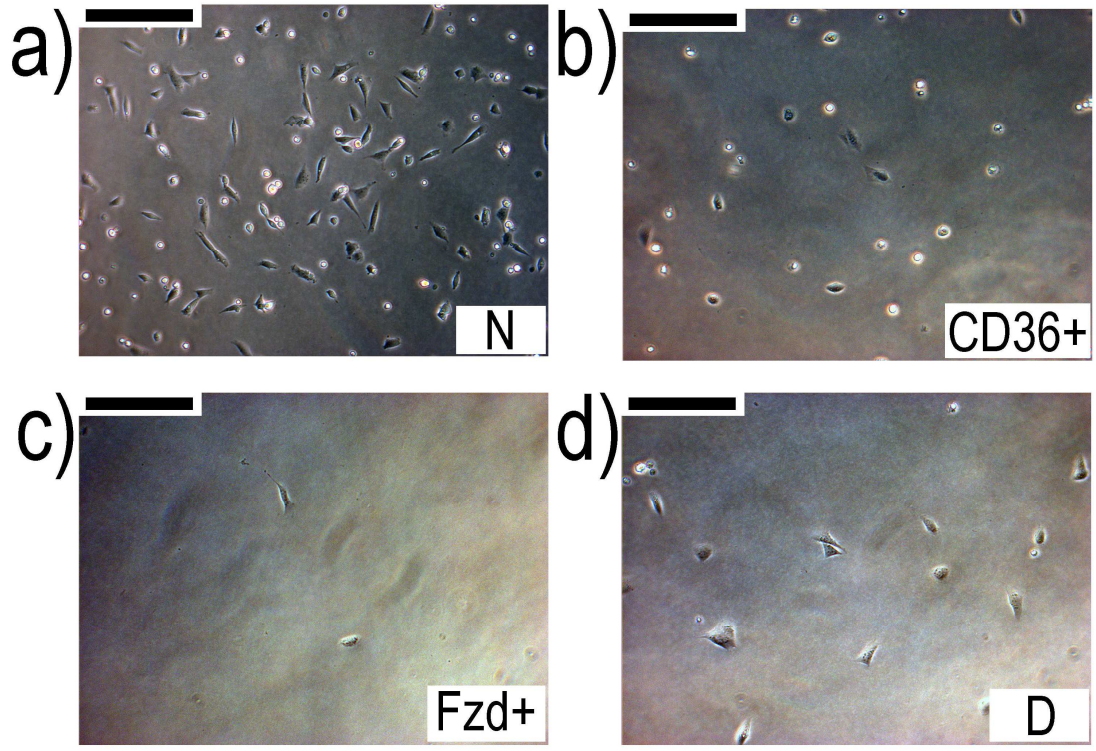


Figure 5.4. FACS sorted cells placed on the 4-well dish in growth medium. Photos were taken approximately 24 hours after placement in the culture dish. N: Negative cells (CD36- and Fzd4- cells). CD36+: cells sorted as positive for antibody against CD36. Fzd+: cells sorted as positive for antibody against Fzd4. D: dual cells (cells positive for CD26 and Fzd4). (c) Fzd4+ cells that attached to cell culture dish are shown by white arrows. (a - d) Scale bar = 100 µm. Photos were taken on the inverted microscope Carl Zeiss Axiovert 10 with accompanying AnalySIS software.

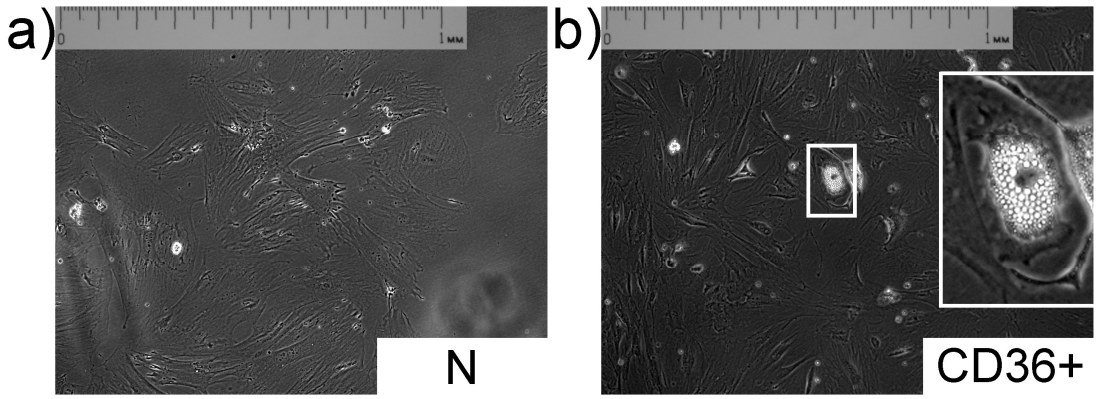


Figure 5.5. FACS sorted cells kept in the growth medium for several days. N: Negative cells. CD36+: cells sorted as positive for antibody against CD36. (a - b) Scale bar = 1 mm. Photos were taken using an inverted microscope Zeiss Axiovert 200M microscope with accompanying AxioVision Rel.4.8 Imaging System software.

**A) Control sample:**

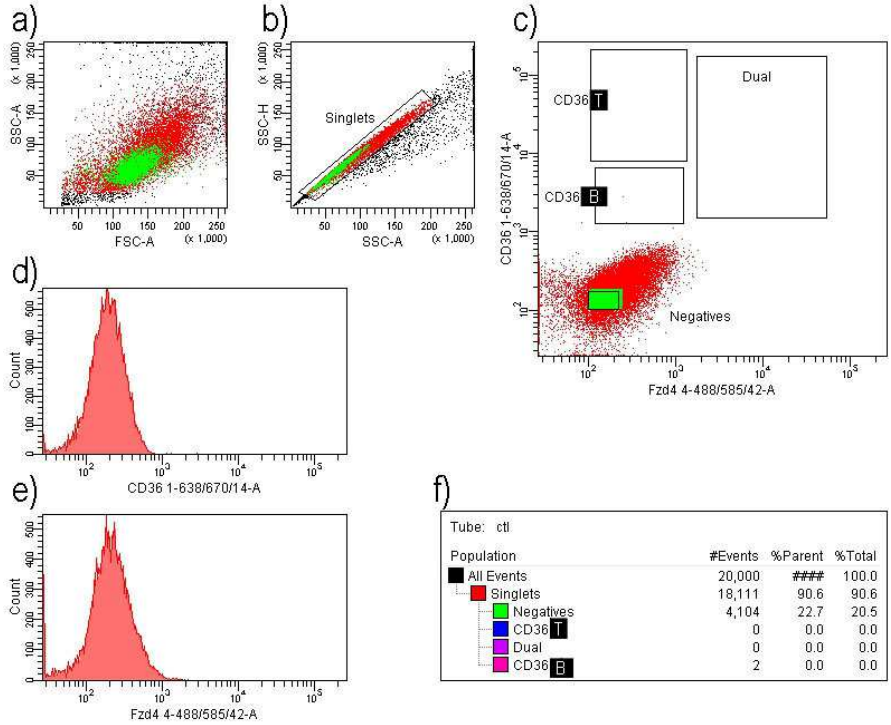


**B) Experimental sample:**

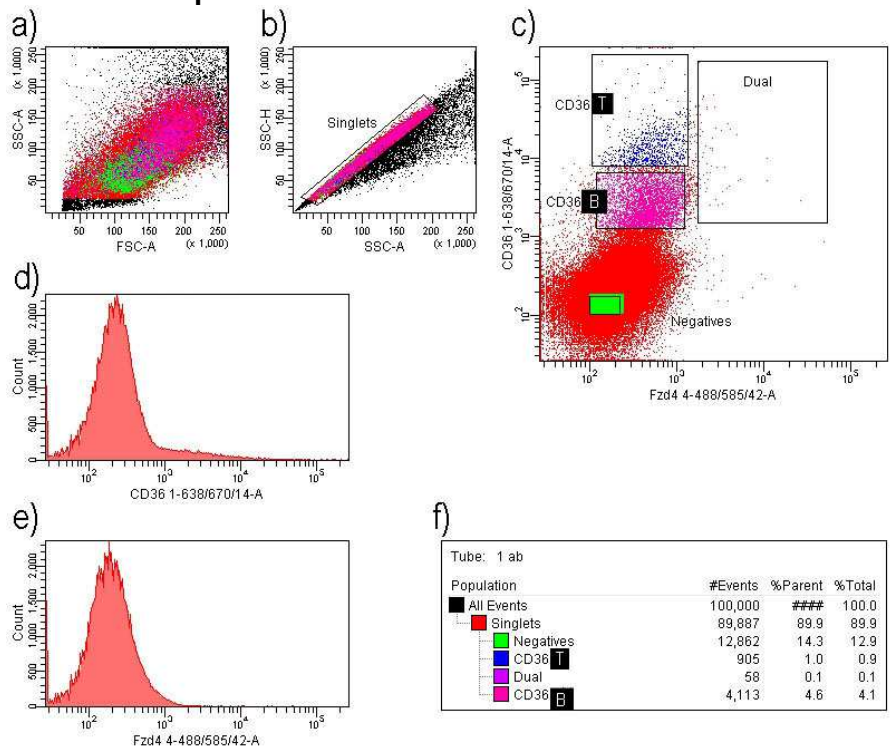


Figure 5.6. The FACS sort experiment with modified gates for cells. (A) non-stained cells used as control sample. (B) cells stained with antibodies against CD36 (APC-fluorochrome: 1-638/67/14-A) and Fzd4 (PE-fluorochrome: 4-488/585/42-A). (a, b, c) Two-parameter histograms. (d, e) One-parameter histograms. (a) FSC-forward scatter (size of cells), SSC-side scatter (cell-complexity or number of internal compartments. (b, c) Gating of singlets and collected cells. (d, e) Intensity of staining with specific antibodies. (f) % of events during sort reaction. “T” – Top gate for CD36 positive cells. “B” – Bottom gate for CD36 positive cells.

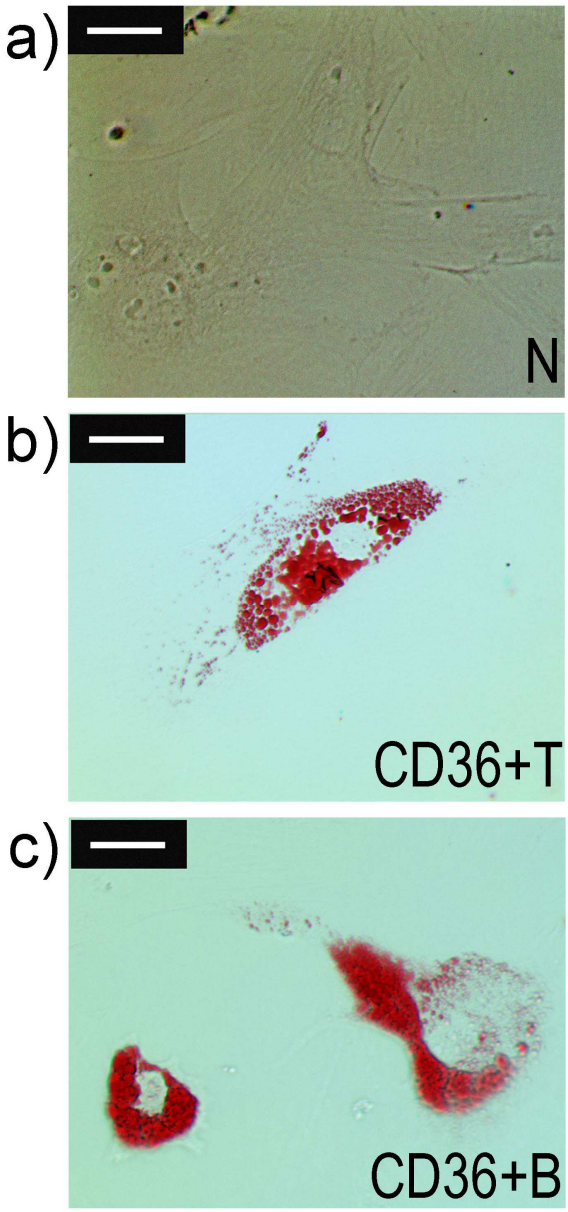


Figure 5.7. Analysis of two-dimensional (2D) structures derived from FACS sorted cells. Oil Red O staining was performed after 8 days of incubation in growth medium. a) N - Negative cells. b) CD36+ T - CD36 positive cells collected from the "top" gate. c) CD36+ B - CD36 positive cells collected from the "bottom" gate. (a - c) Scale bar = 30 μm. Photos were taken using a Zeiss Axio Imager.M1. microscope.

### 5.3.4 Detailed analysis of CD36 positive (CD36+) and Negative FACS sorted cells.

The final, optimized FACS (see section 5.2.4 for protocol) resulted in the collection of sufficient amount of CD36+ cells, together with Negative cells (Figure 5.8). These cells were used for the analysis of mRNA expression profile and to set up two-dimensional and three-dimensional cell cultures.

**The mRNA expression of fat-related genes in FACS-sorted cells.**

In order to obtain a gene expression profile of sorted cells, several genes were chosen (Figure 5.9) based on microarray data generated from mouse embryonic skin dermis (Chapter 3). The qRT-PCR reaction with primers for *Cd36* gene confirmed its high mRNA level in CD36+ sorted cells (Figure 5.9a).

Interestingly, a very high up-regulation of *Fabp4* gene was observed in CD36+ cells (Figure 5.9b). This fatty acid binding protein 4, was highly enriched in mouse embryonic lower dermal cells between e17 and e19 time points on both gene and protein levels (microarray data in Chapter 3; see Table 3.4, Figures 3.10B and 3.11). In addition, several other adipocyte-related genes, such as adiponectin (AdipoQ), GO/G1 switch gene, carbonic anhydrase (CarbAnhyd), haptoglobin, retinol binding protein 4 (Rbp4) and Major urinary proteins (MUPs) were highly enriched in lower dermal skin compartment according to microarray data (Chapter 3). All these genes were also enriched in CD36+ cell population (Figure 5.9b, c and Figure 5.9f - j). Genes for two crucial adipogenic transcriptional factors, C/EBPalpha and PPARgamma, were also up-regulated in CD36+ cells (Figure 5.9d and e).

In addition, two other genes (Gremlin2 and Trps) were also analysed in FACS-sorted cells, because of their up-regulation in upper dermis, where no lipid accumulation was seen (Chapter 3). Both these genes had higher mRNA levels in negative sorted cells when compared with CD36+ cells (Figure 5.8k and Figure 5.8l).

This preliminary work showed that CD36+ cells are characterised by an enrichment of fat-related genes when compared with CD36 negative sorted cells and they seemed to represent cells from lower dermal area of mouse back skin.

**A) Control sample:**

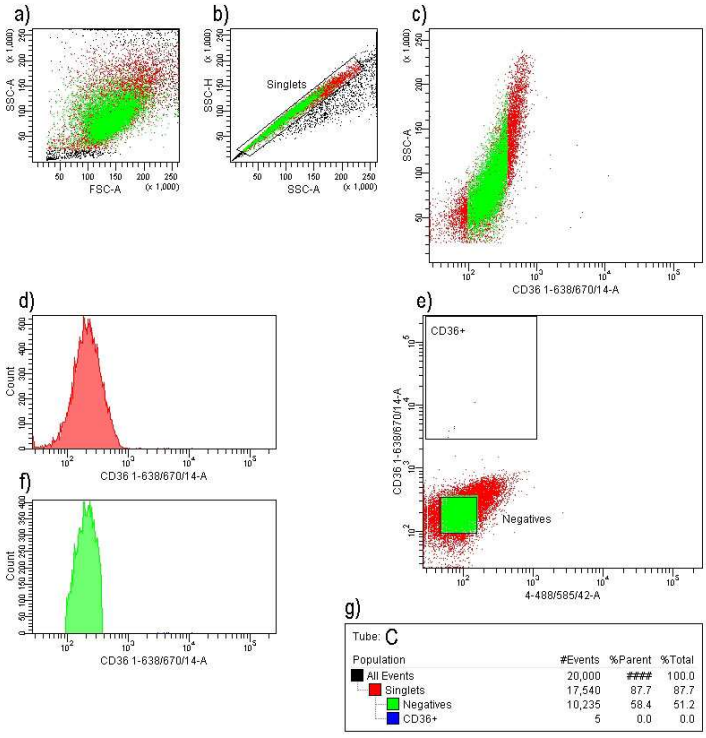


**B) Experimental sample:**

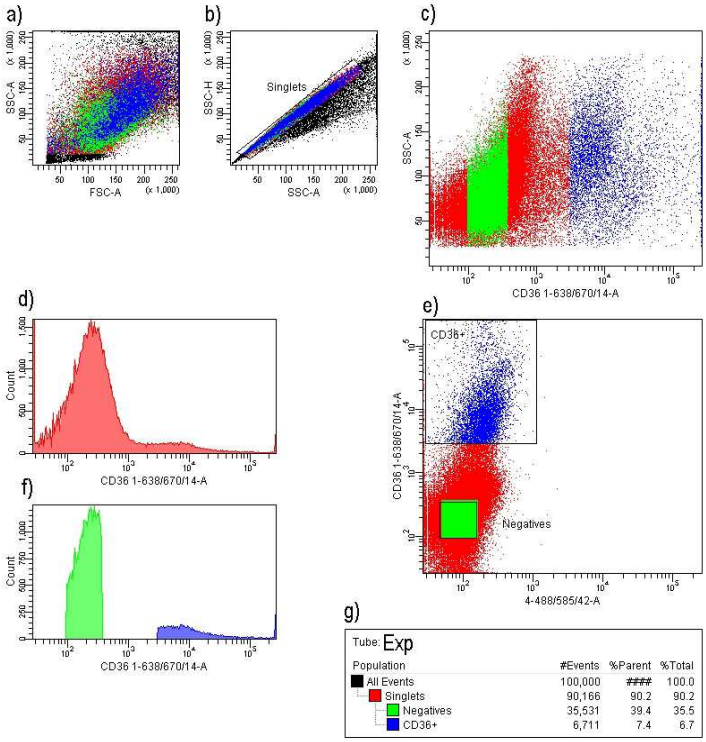


Figure 5.8. The final FACS sort experiment. (A) non-stained cells used as control sample. (B) cells stained with antibodies against CD36 (APC-fluorochrome: 1-638/67/14-A). (a, b, c and e) Two-parameter histograms. (d, f) One-parameter histograms. (a) FSC-forward scatter (size of cells), SSC-side scatter (cell-complexity or number of internal compartments). (b, e) Gating of singlets and collected cells. (d, f) Intensity of staining with specific antibodies. (g) % of events during sort reaction.

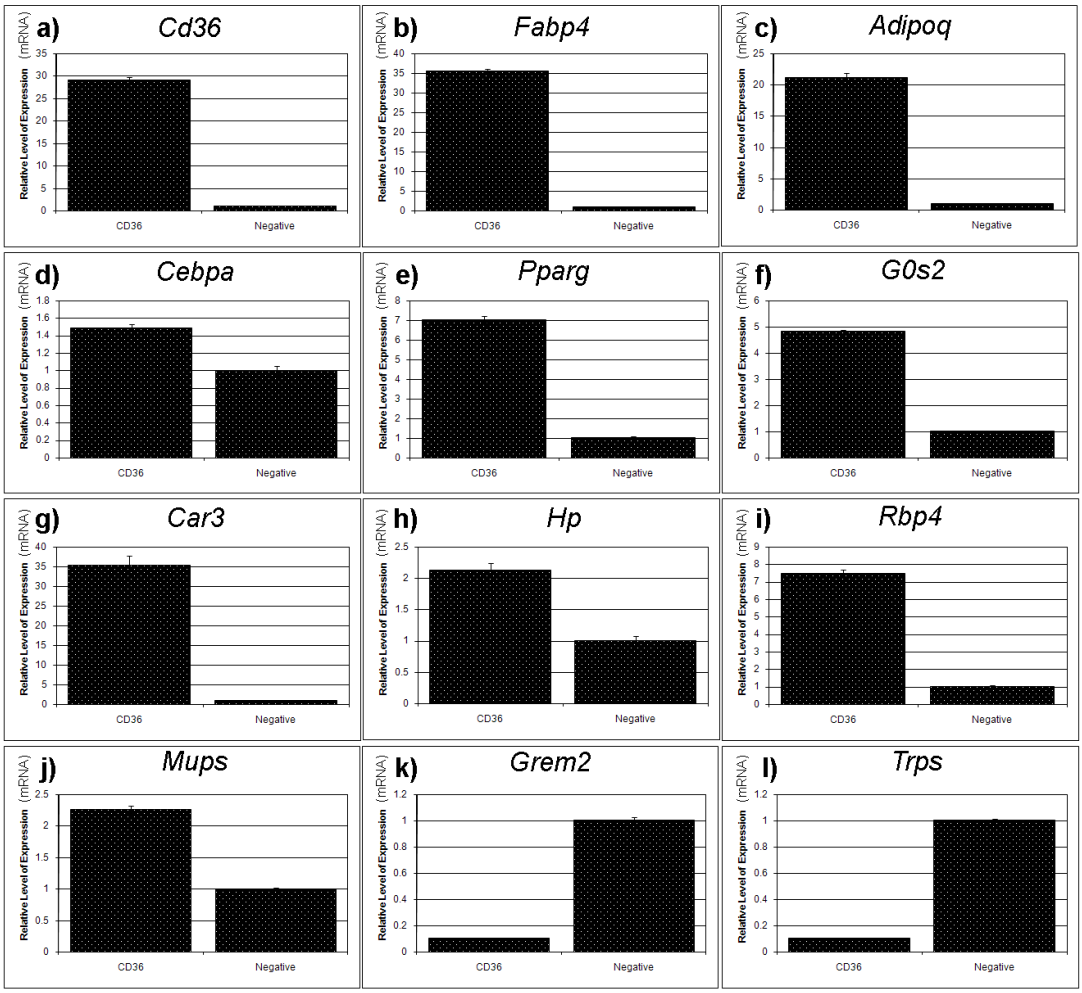


Figure 5.9. The analysis of relative mRNA expression of selected genes in two populations of FACS sorted cells. The relative expression was analysed in CD36 positive cells and negative cells. The baseline (1-fold change) was established for samples prepared from Negative cells. *Fabp4* - fatty acid binding protein 4; *Adipoq* - aiponectin; *Cebpa* - CCAAT/enhancer binding protein, alpha; *Pparg* - Peroxisome proliferator activated receptor gamma; *G0s2* - G0/G1 switch gene 2; *Car3* - carbonic anhydrase 3; *Hp* - haptoglobin; *Rbp4* - retinol binding protein 4; *Mups* - major urinary proteins; *Grem2* - gremlin 2; *Trps* - trichorhinophalangeal syndrome I. The analysis was performed on FACS sorted cells that were prepared from embryos of the same mother and treated as one biological sample. For each analysed gene, Ct values from three PCR reactions were used to count standard deviations.

**Lipid accumulation capabilities 2D and 3D cell structures established from FACS sorted cells.**

It was discussed in Chapter 4 that three dimensional techniques for growing cells might have the potential to mimic the *in vivo* environment for skin-derived cells. The spheroid cell culture method revealed differences in lipid accumulation capabilities of embryonic cells obtained from the whole dermal compartment when compared with cells grown in two-dimensional (2D) cell structures (section 4.3.4.3 in Chapter 4). Therefore it seemed interesting to investigate if FACS sorted dermal cells, both CD36 positive (CD36+) cells and Negative (CD36-) cells, would also be influenced by the growing method in relation to their lipid accumulation features. Therefore, the influence of adipogenic medium was analysed in such 2D and 3D cell cultures established from FACS sorted populations.

Cells used for this work were derived from the final, optimized FACS sort (Figure 5.8). Both, CD36+ and Negative population attached easily to culture dish surface when 2D cell structures were established (Figure 5.10). CD36+ cells contained rounded structures in their cytoplasm in close proximity to nuclei in growth and adipogenic medium (Figure 5.10a and b). The Oil Red O staining confirmed presence of lipids in these cell structures in growth medium (Figure 5.11a). Moreover the number and size of droplets filled with red were greater in cells incubated in adipogenic medium (compare Figure 5.11a with Figure 5.11b).

Negative FACS sorted 2D cells in the growth medium had different morphology from CD36+ cells, as no lipid-droplets were observed in their cytoplasm and 99% of analysed cells were not stained by red dye (Figure 5.10c and Figure 5.11c). These negative cells kept 3 days in adipogenic medium contained tiny dots around nuclei that were easily stained by red dye at day 4 of adipogenic incubation (Figure 5.10d and Figure 5.11d).

Both FACS sorted cell populations also created spheres when grown in medium droplets (Figure 5.12). Despite the fact that similar amount of cells was used for the spheres establishment, CD36+ cells gave bigger spheres. On the surface of some of these 3D cell structures round inclusions could be spotted that might represent lipids accumulated on spheres. Interestingly, the Oil Red O staining, performed on 3D sections from CD36+ cells, revealed the presence of lipids among spheres from both growth and adipogenic medium (Figure 5.13a and b). As such robust lipid accumulation was not seen in 2D cell cultures from CD36+ sorted cells

when kept in growth medium, it seemed that the spheroid cell culture method might enhance the capability to accumulate lipids in CD36+ positive cells, independent of the presence of external factors, such as adipogenic medium (compare Figure 5.11a and b with Figure 5.13a and b). Moreover such enhancement for lipid accumulation, seen in CD36+ spheres did not take place in spheres from the Negative cell population (compare Figure 5.13a with Figure 5.13c).

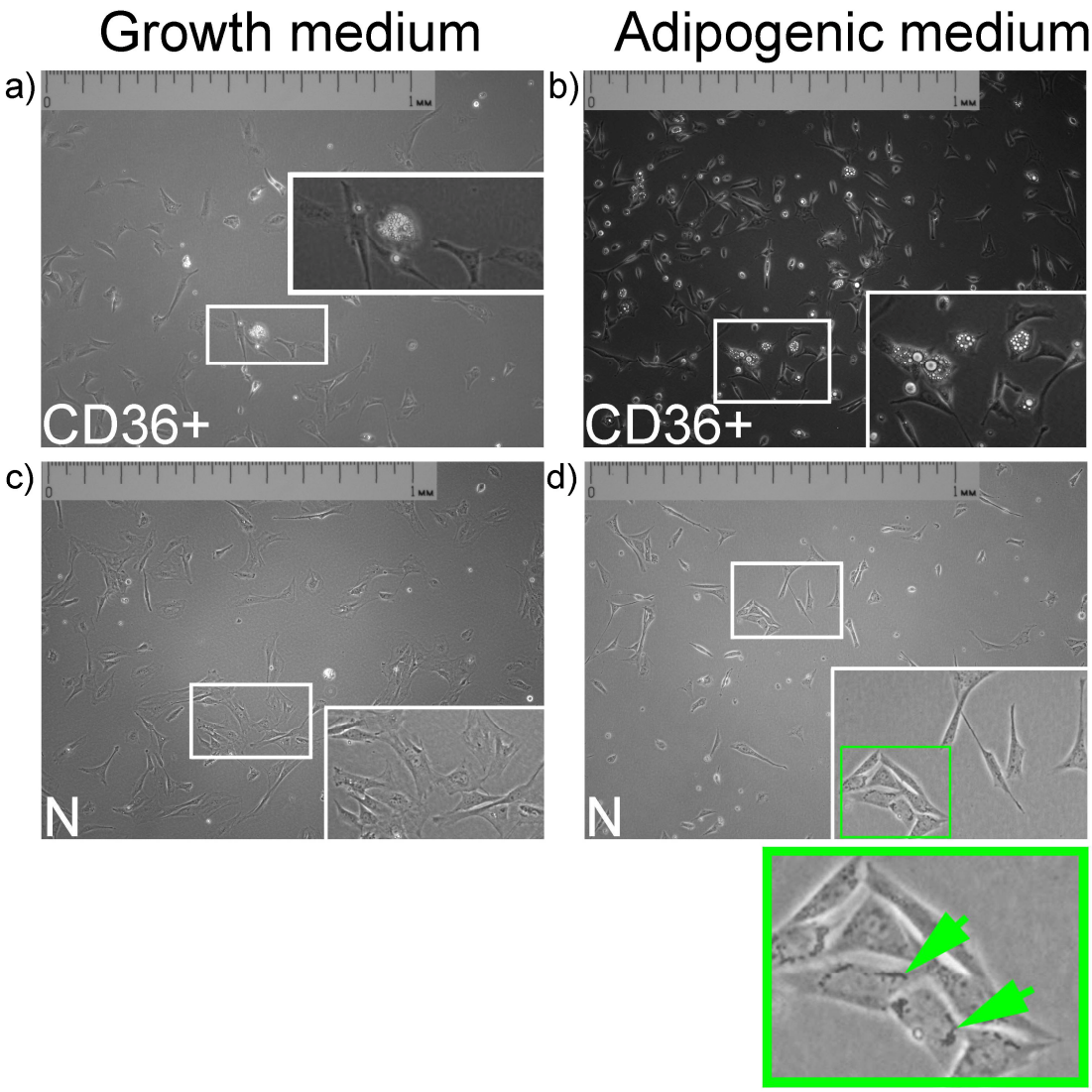


Figure 5.10. The morphology of FACS sorted two-dimensional (2D) cells. N: Negative cells. CD36+: cells sorted as positive for antibody against CD36. Sorted cells were kept in growth (a, c) or adipogenic (b, d) medium for three days. Darker areas seen in Negative cells incubated in adipogenic medium are shown by green arrows. Scale bar = 1 mm. Photos were taken using an inverted Zeiss Axiovert 200M microscope (with accompanying AxioVision Rel.4.8 Imaging System software).

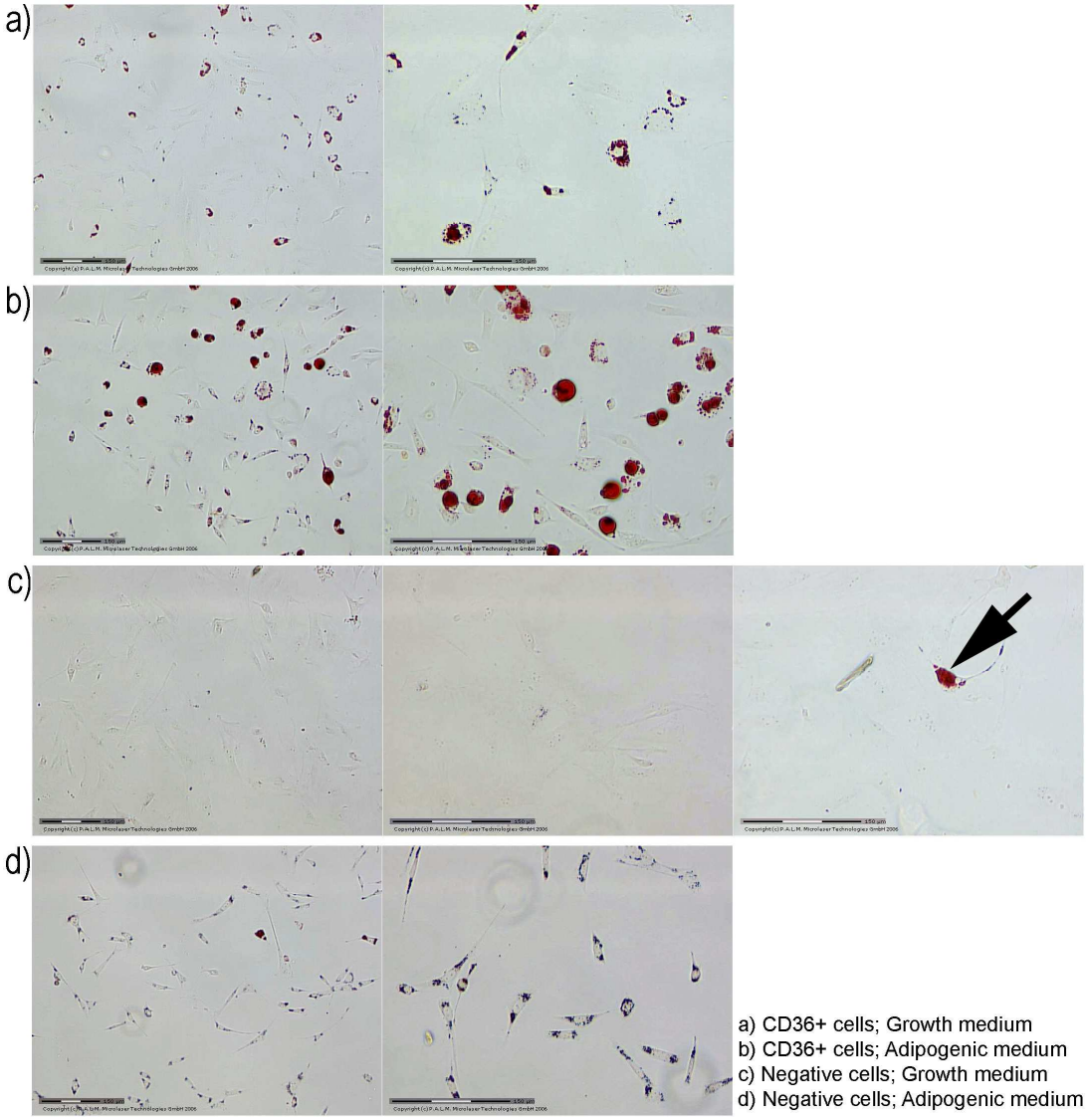


Figure 5.11. Oil Red O analysis of lipid accumulation in FACS sorted cells grown as 2D cell structures in normal (growth) and adipogenic medium for four days. (c) Negative cell stained with red dye and kept in growth medium is shown by the black arrow. (a - d) Scale bar = 150 μm. Photos were taken using a Laser Capture Microdissection (LCM) microscope (PALM MicroBeam Zeiss Microscope).

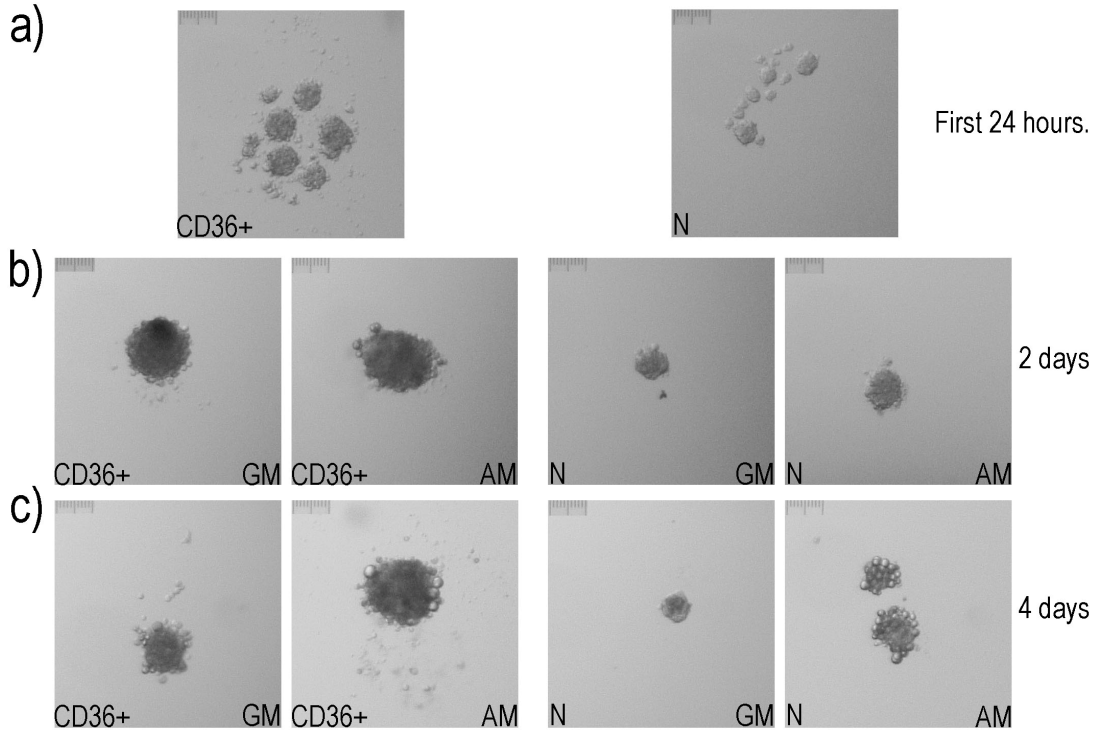


Figure 5.12. Three-dimensional (3D) cell structures created from FACS sorted cells. (a) Sorted cells gathered together during the first 24 hours of incubation. (b) 3D cell structures incubated 2 days in normal growth medium (GM) or adipogenic medium (AM) (c) 3D cell structures incubated 4 days in normal growth and adipogenic medium. N: Negative cells. CD36+: cells sorted as positive for antibody against CD36. (a - c) Scale bar = 100 μm. Photos were taken using a Ziess StemiSVII microscope with a KY-FI030 JVC digital camera and accompanying KyLink software.

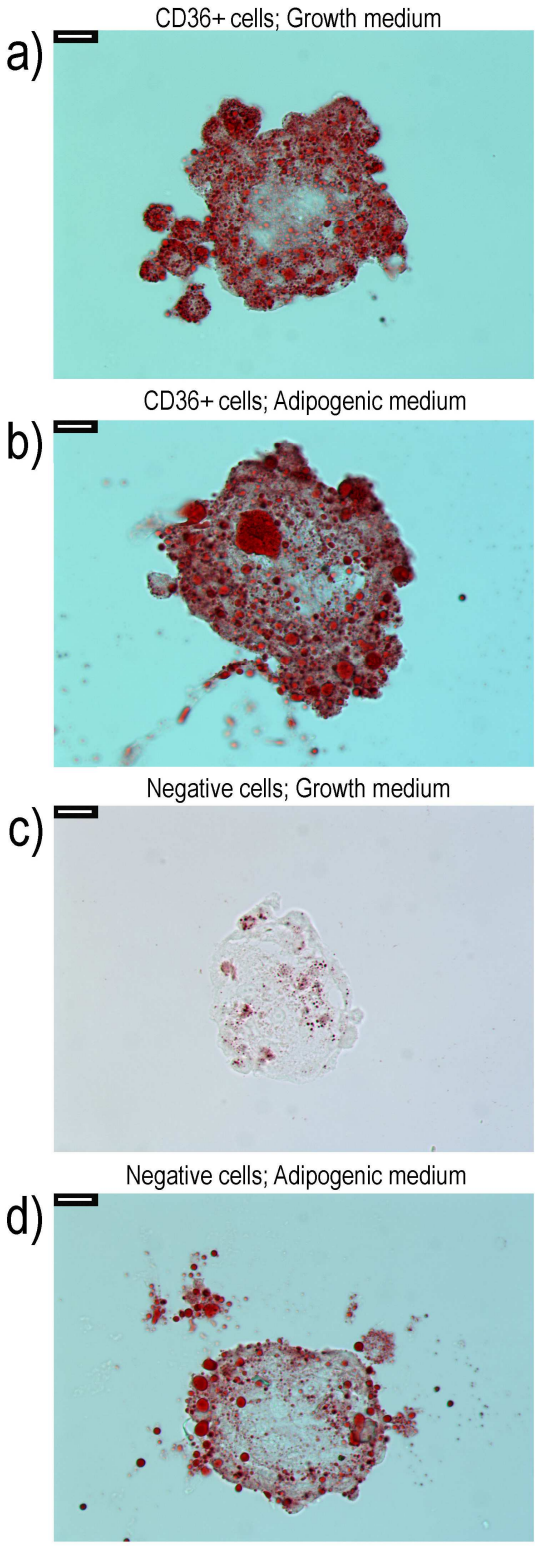


Figure 5.13. Oil red O analysis of lipid accumulation in FACS sorted cells grown as 3D cell structures in normal growth and adipogenic medium for four days. (a - d) Scale bar = 15 μm. Photos were taken on the Zeiss Axio Imager.M1. microscope.

**Protein expression profile in 2D and 3D cell structures from FACS sorted cells.**

CD36+ and Negative cells, grown as 2D and 3D cell cultures underwent immunofluorescence analysis where expression pattern of fat-related proteins was investigated.

The majority of the CD36+ cells, grown as 2D cell cultures in growth medium for two days, displayed a strong nuclear signal for the adipogenic transcriptional factor C/EBPalpha in comparison to Negative 2D cultures in growth medium (compare Figure 5.14a and Figure 5.14c). In addition, 2D cultures from CD36+ and Negative cells seemed to have lost the nuclear localization of C/EBPalpha when kept in adipogenic medium (see Figure 5.14b and d). Surprisingly, three-dimensional cell cultures from both CD36+ and Negative cells had clear nuclear C/EBPalpha staining when cultured in growth media (compare Figure 5.15a and Figure 5.15c). In addition, spheres obtained from both FACS sorted cell populations (CD36+ and negative cells) and kept in adipogenic medium had green staining detected mainly at the periphery of 3D structures and it did not have a nuclear localisation (see Figure 5.15b and d).

Expression of fatty acid binding protein 4 (FABP4) was analysed in FACS sorted cells (Figure 5.16 and Figure 5.17). FABP4 was found in adipocytes, and is known to be involved in binding fatty acids and was related with obesity (Khalyfa *et al*, 2010). Cytoplasmic labelling for FABP4 was observed in CD36+ cells kept as 2D cultures in growth medium, and a slightly stronger staining was seen in adipogenic medium (Figure 5.16a and b). In contrast, 2D structures from Negative cell cultures were without staining for FABP4 in growth medium although a very weak FABP4 signal was seen among very few cells in adipogenic medium (Figure 5.16c and d). When an antibody against FABP4 was used on 3D cultures, a strong fluorescent labelling was observed in spheres from both sorted cell types and in both growth and adipogenic media (Figure 5.17a - d). The control staining (no primary antibody) revealed much lower signal from secondary antibody when compared with experimental samples (compare Figure 5.17a - d with Figure 5.18). Therefore the intensive staining seen for antibody against FABP4 in experimental samples could be due to a high accumulation of this protein in spheres, especially in peripheral cells.

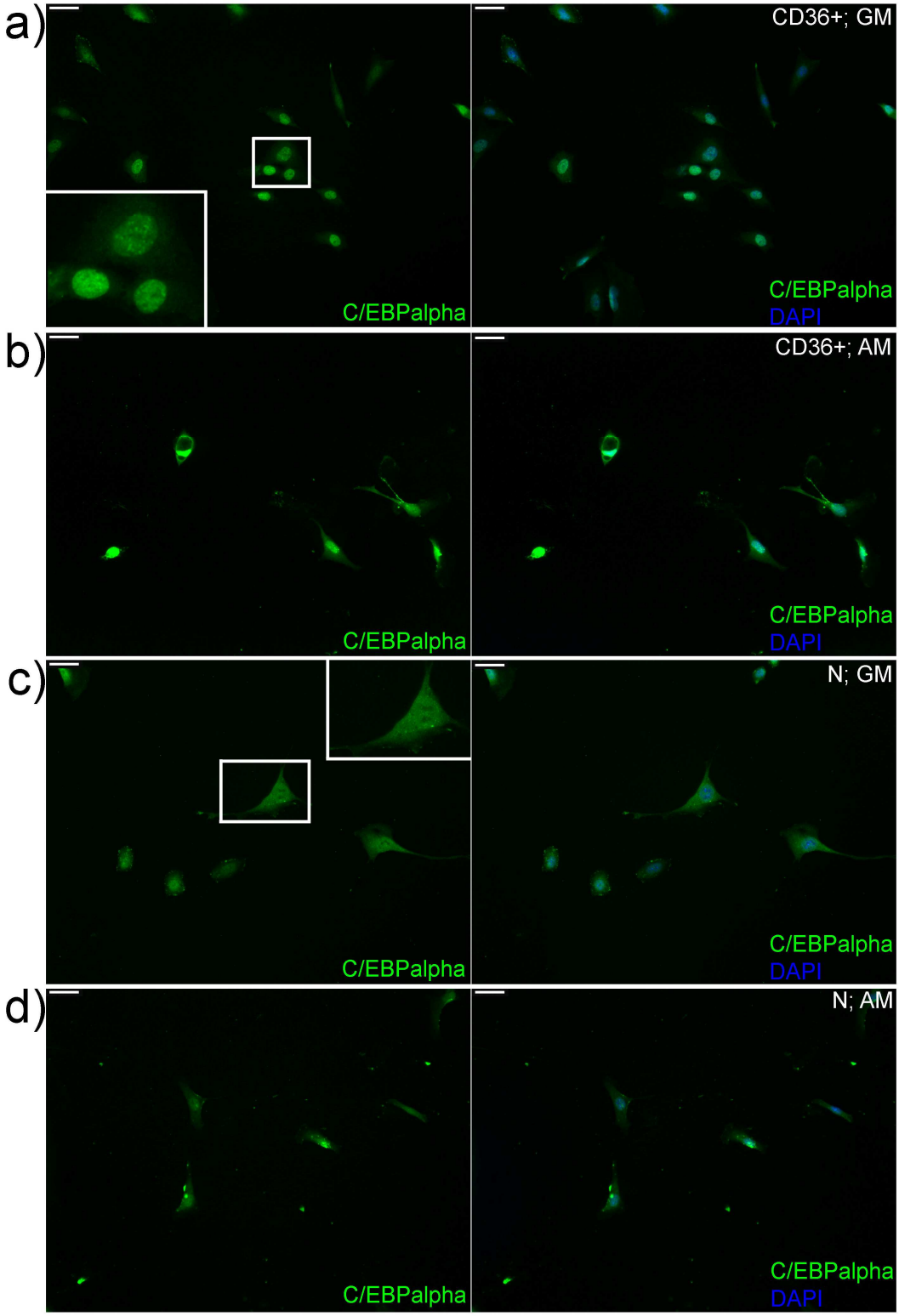


Figure 5.14. Expression and localisation of adipogenic transcriptional factor C/EBPalpha in FACS sorted cells grown as 2D cell cultures. 2D structures were prepared from CD36 positive cells (CD36+) and Negative cells (N) and incubated in normal growth medium (GM) and adipogenic medium (AM) for 2 days. (a) CD36 positive cells in normal growth medium. (b) CD36 positive cells in adipogenic medium. (c) Negative cells in normal growth medium. (d) Negative cells in adipogenic medium. (a - d) Scale bar = 30 µm. DNA was counterstained with DAPI. Fluorescent images were visualised using a Zeiss Axio Imager M1. microscope.

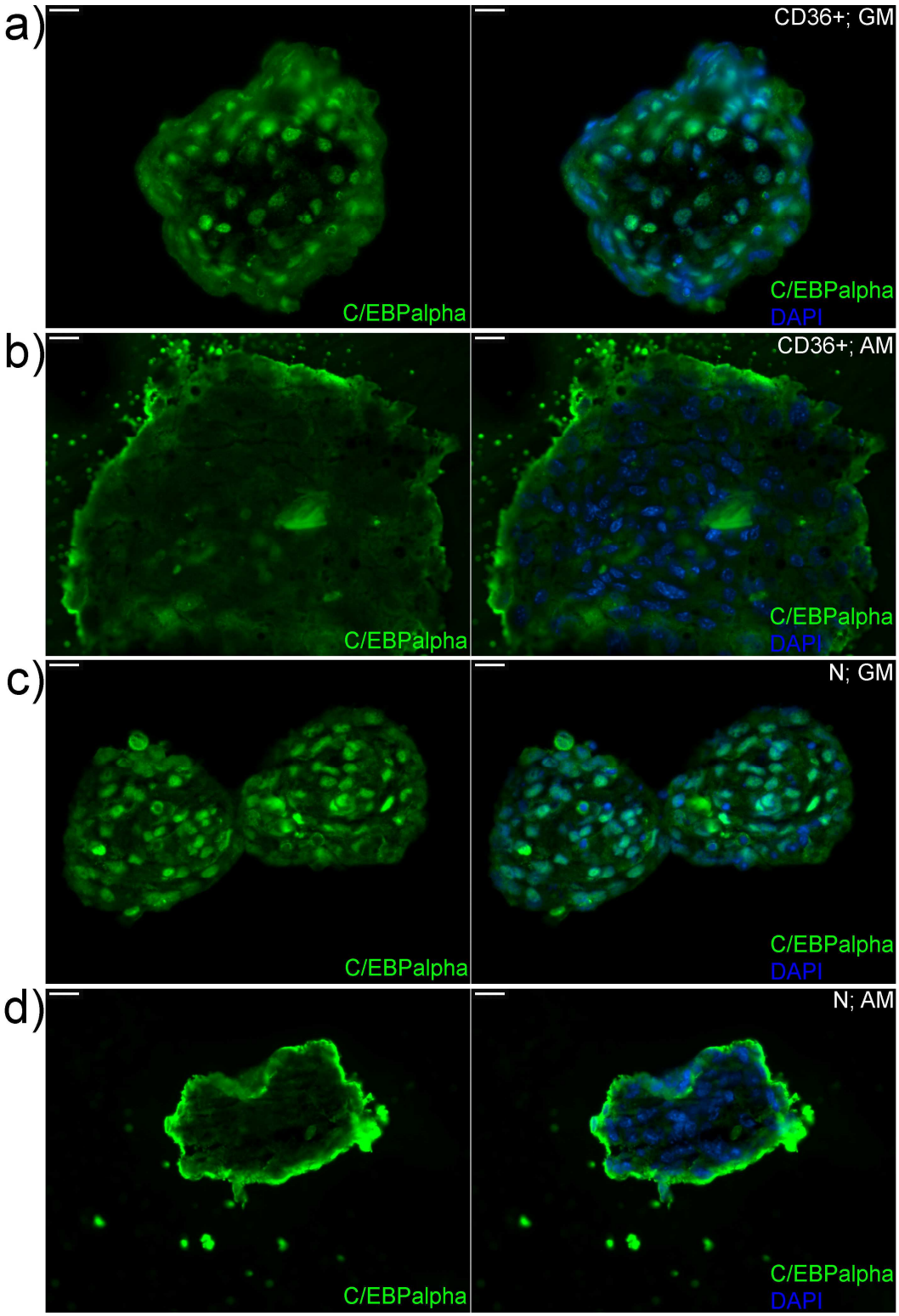


Figure 5.15. Expression and localisation of adipogenic transcriptional factor C/EBPalpha in FACS sorted cells kept as 3D cell structures. 3D structures were prepared from CD36 positive cells (CD36+) and Negative cells (N) and incubated in normal growth medium (GM) and adipogenic medium (AM) for 2 days. (a) CD36 positive cells in normal growth medium. (b) CD36 positive cells in adipogenic medium. (c) Negative cells in normal growth medium. (d) Negative cells in adipogenic medium. (a - d) Scale bar = 15 μm. DNA was counterstained with DAPI. Fluorescent images were visualised using a Zeiss Axio Imager M1. microscope.

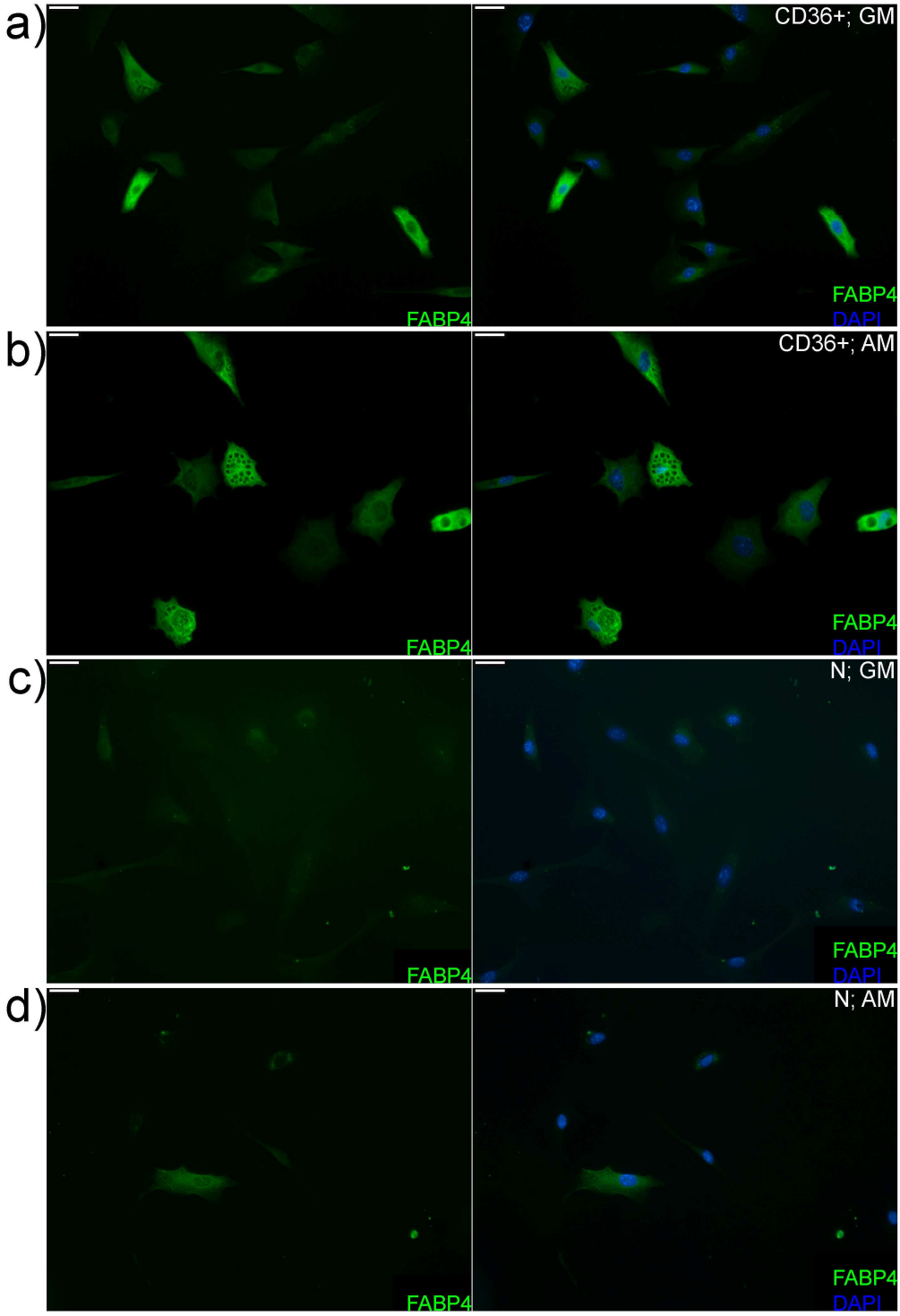


Figure 5.16. Expression and localisation of fatty acid binding protein 4 (FABP4) in FACS sorted cells grown as 2D cell structures. 2D structures were prepared from CD36 positive cells (CD36+) and Negative cells (N) and incubated in normal growth medium (GM) and adipogenic medium (AM) for 4 days. (a) CD36 positive cells in the growth medium. (b) CD36 positive cells in the adipogenic medium. (c) Negative cells in normal growth medium. (d) Negative cells in adipogenic medium. (a - d) Scale bar = 30 μm. DNA was counterstained with DAPI. Fluorescent images were visualised using a Zeiss Axio Imager M1. microscope.

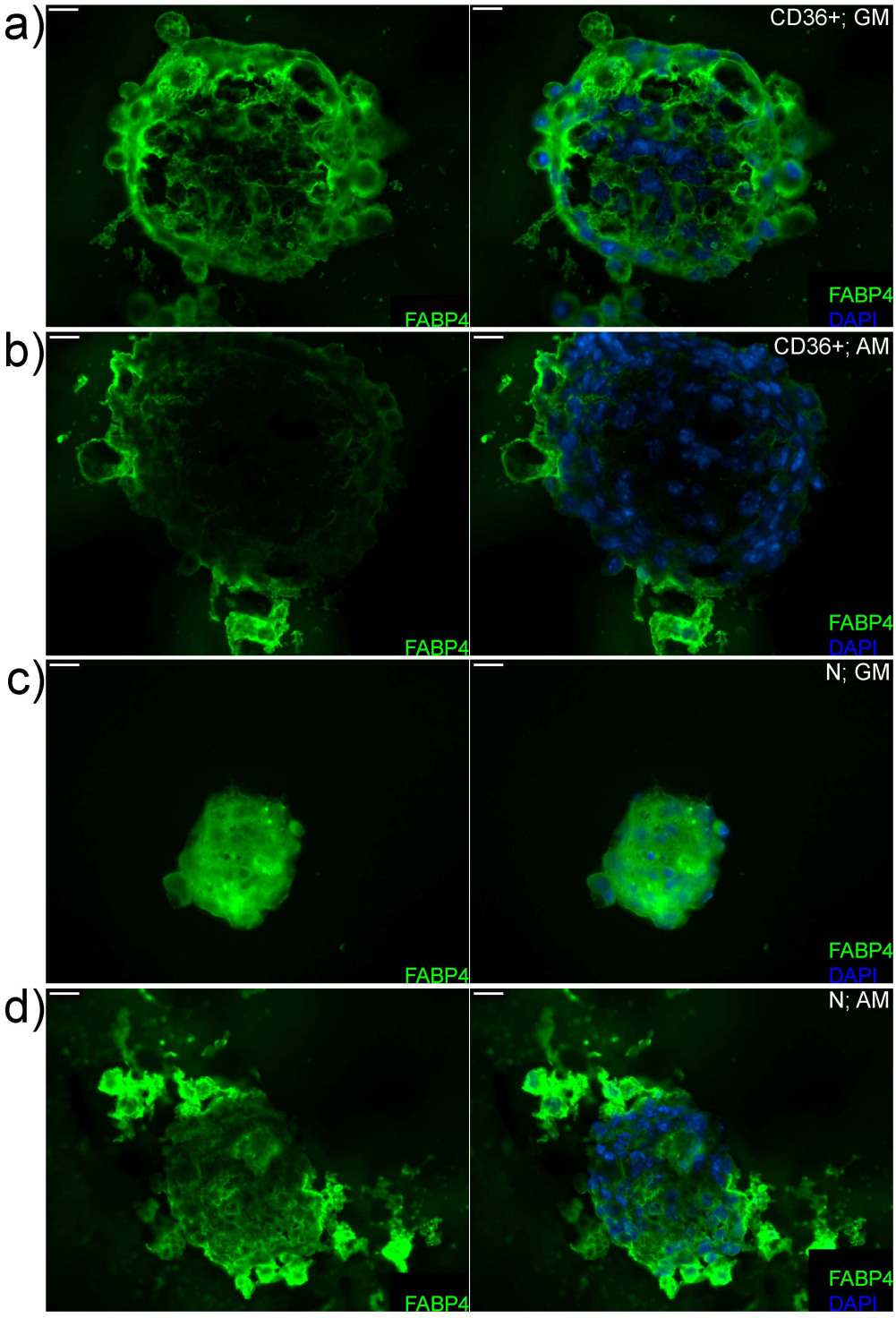


Figure 5.17. Expression and localisation of fatty acid binding protein 4 (FABP4) in FACS sorted cells grown as 3D cell structures. 3D structures were prepared from CD36 positive cells (CD36+) and Negative cells (N) and incubated in growth medium (GM) and adipogenic medium (AM) for 4 days. (a) CD36 positive cells in normal growth medium. (b) CD36 positive cells in adipogenic medium. (c) Negative cells in normal growth medium. (d) Negative cells in normal growth medium. (a - d) Scale bar = 15 μm. DNA was counterstained with DAPI. Fluorescent images were visualised using a Zeiss Axio Imager M1. microscope.

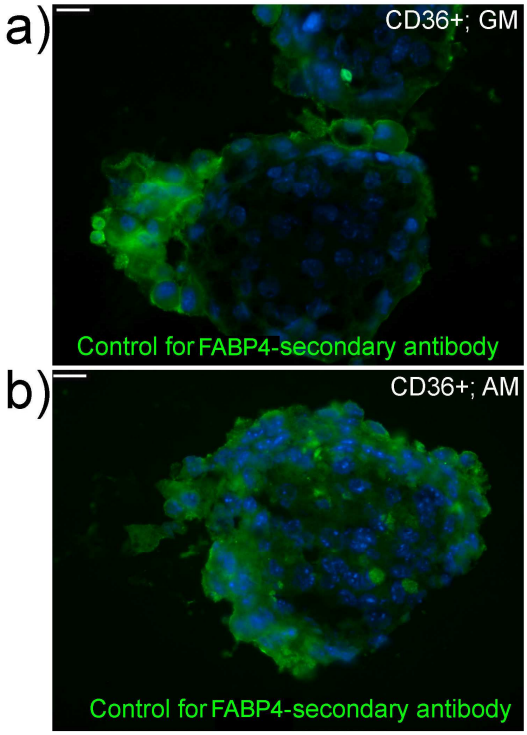


Figure 5.18. Immunofluorescence analysis of secondary antibody (donkey anti-goat) efficiency. Cross-sections with 3D structures obtained from CD36+ sorted cells and cultured in growth (GM) and adipogenic medium (AM) for 4 days were incubated with 1% donkey serum/PBS instead of an antibody against FABP4 followed by the secondary antibody: donkey-anti goat. (a - b) Scale bar = 15 μm. DNA was counterstained with DAPI. Fluorescent images were visualised using a Zeiss Axio Imager M1. microscope.

## 5.4. Discussion.

The aim of this Chapter was to isolate and purify a dermal cell population from mouse embryonic skin dermis representing cells committed to adipogenesis, at the early stages of their differentiation process.

The microarray data, generated from mouse embryonic skin dermis, in Chapter 3, provided information about genes specifically regulated in lower dermal cells which undergo adipogenesis. This identified a membrane protein, named CD36 that was highly enriched in lower dermal cells between e17 and e19 time point. In addition, enrichment of Fzd4 gene took place in lower dermal cells between analysed time points.

First interesting observation from the flow cytometry work was obtained during the tritation process performed on 3T3-F442A cells. It was difficult to get specific fluorescence for tested antibodies (CD36 and Fzd4) from confluent cells grown in adipogenic medium and the signal for tested antibodies was obtained from these cells grown in normal medium. Components of the differentiation medium or processes that occurred in differentiating cells could influence the preparation process of dermal cell suspension, antibody staining and (or) further analysis of cells. Thus, presented in this Chapter an attempt to use embryonic dermis cells which would normally undergoing adipogenesis during skin development aimed to simplify the analysis of fat cells (both adipocytes and preadipocytes) with flow cytometry technology.

A comprehensive optimisation strategy was used to devise the flow cytrometry method. This gave sufficient yield to analyse a CD36+ population. The optimised protocol for FACS-based cell isolation gave viable cells that were successfully cultured in both two- and three- dimensional structures (section 5.3.4). The up-regulation (on the mRNA level) of two well known adipogenic transcriptional factors: C/EBPalpha and PPARgamma in CD36+ (FACS-sorted) cells (Figure 5.9c and d) suggested that this FACS-sorted cell population consists of preadipocytes undergoing early stages of adipogenic differentiation in embryonic back skin. In addition, the enrichment of several other fat-related genes was observed in CD36+ cells (when compared with the Negative cell population), for example Fabp4 (Figure 5.9b) that has been shown to be exclusively expressed in lower dermal compartment of embryonic skin dermis between e17 and e19 time points (Chapter 3; Figure 3.10B and Figure 3.11). In Chapter 2, it was shown that cells from this

lower dermal compartment are undergoing adipogenesis and they create so-called dermal adipose tissue. Therefore, the qRT-PCR analysis of fat-related genes in FACS-sorted cells showed that cells with high level of CD36 surface marker are representative of cells with a gene expression profile similar to cells from lower dermal skin area from which dermal adipose tissue develops. Therefore it became possible to isolate a population of lower dermal cells predisposed to being mature fat cells *in vivo*. In addition, CD36+ cells kept their "fatty-like" feature when grown on cell culture dishes (two-dimensional structures), since the Oil Red O staining revealed a presence of lipid droplets in these cells (Figure 5.11a).

In addition, the Negative cells (CD36-) were characterised by a high up-regulation of *TRPS* gene (Figure 5.9l). Since, the expression of TRPS in the upper dermis of embryonic back skin was verified on both protein and mRNA level (Chapter 3, Figure 3.19 and Figure 3.20), the Negative cell population seemed to represent dermal cells not predisposed to adipogenesis that create a fatty-free layer of demis just below the epidermis. Indeed, the majority (99%) of analysed cells were not stained by a lipid specific dye when kept in two-dimensional structures (Figure 5.11c).

In order to verify further features of sorted cells, a spheroid cell culture method was applied for the growth of these cells. As it was shown in Chapter 4, the spheroid cell culture method would be a useful tool for recreating *in vivo*-like environment for the study of skin cells. Both 2D and 3D cell cultures were obtained from CD36+ and Negative cells in order to compare lipid accumulation capabilities in cells growth in different conditions. The very first observation was that 3D structures obtained from CD36+ cells had bigger diameter when compared with spheres from Negative cells (Figure 5.12). The detailed studies on adipogenesis in cell lines suggested that at the very early steps of fat cell differentiation, cells undergoing approximately two additional rounds of cell division (so-called clonal expansion step; reviewed by Gregoire *et al*, 1998). Therefore, spheres from CD36+ cells that were shown to be enriched with fat-related genes (see paragraph above) could increase their diameter due to the enhanced process of cell division needed for the fat cell differentiation.

In addition, the Oil Red O staining, revealed highly increased lipid accumulation in spheres from CD36+ cells kept in both growth and adipogenic medium, when compared with 3D structures from Negative cells (Figure 5.13). Therefore, the spheroid cell culture method enhanced lipid accumulation in CD36+ cells. The CD36+ spheres seemed to represent structures that contained of either

more cells filled with fat droplets or cells that accumulated more and bigger lipid droplets when compared with spheres from Negative cells.

The 3D technique seemed to have also specific influence on the Negative (FACS-sorted) cell population. This conclusion was given after the analysis of staining for the adipogenic transcription factor: C/EBPalpha in 2D and 3D FACS-sorted cells. Basically, 2D structures from CD36+ cells had a nuclear staining for C/EBPalpha when kept in growth medium, whereas such staining pattern was not seen in 2D structures from Negative cells (Figure 5.14). This clearly suggested that CD36+ are representative of fat cells undergoing adipogensis and indeed the red dye stained some of these two dimensional CD36+ cells but not Negative cells (Figure 5.11). However, the nuclear localisation of C/EBPalpha was seen in these two cell populations when kept as spheres in growth medium (Figure 5.15). Therefore, the 3D spheres seemed to create an environment that not only enhanced adipogenesis in already predisposed to this process CD36+ cells (from lower dermis; see Figure 5.13a), but also crate favorable conditions for an activation of gene crucial for early stages of adipogenesis in “non-fatty” cells and an accumulation of lipids in small population of these Negative cells grown as spheres (Figure 5.13c). These areas, positive for red dye in 3D Negative cells are still surrounded by cells that are not accumulating lipids (lack of the red dye), so they are still “resistant” to adipogenesis, maybe due to a high up-regulation of “inhibitory” genes that could be crucial to keep a “non-fatty” feature of these skin dermis cells.

Clearly the spheroid cell culture method might create conditions when the specific cell-cell interactions occurring (not seen in two dimensional structures) that influence dermal cells in relation to their capability to accumulate lipids. In addition, it is possible that FACS sorted cells when grown as spheres are lacking the company of other dermal cell types and/or contact with other skin/body/blood components that are crucial for the control of adipogenesis activation and lipid accumulation. Spheroid cell culture seems to mimic *in vivo* environment when cells can grow in all dimensions as happens in a whole organism, but a lack of regulatory signals from other skin cells could allow these cells to undergo uncontrolled (enhanced) adipocyte differentiation.

**Future plans**

Using the microarray data (presented in Chapter 3) to provide candidate genes combined with the FACS technique (discussed in Chapter 5) could further enhance our understanding of adipogenesis *in vivo* in embryonic back skin. For example, the microarray data from embryonic back skin dermis could be searched for genes highly enriched in upper dermis, where lipid accumulation does not occur. Then, the influence of such factors on FACS sorted cells from dermis could be verified by the addition of these proteins to growth media during 3D culture and investigation of their effect on lipid accumulation. Similarly, the influence of proteins whose mRNA expression level (based again on microarray work from Chapter 3) was enriched in lower dermis could be analysed on both CD36+ and Negative cell populations kept as spheres.

It seems interesting to design an experiment which will combine the FACS-based experimental method from Chapter 5 with a study from Chapter 4, where it was suggested that the EGF-EGFR signalling may take part in the regulation of adipogenesis in mouse embryonic lower dermis between e17 and e19 time points. The FACS sorted cells (CD36+ and Negative populations), once grown as 2D and 3D structures could be incubated in activator (EGF) and/or inhibitor (AG1478) of EGFR and then the lipid accumulation capabilities would be analysed in these structures. The experiment on FACS-sorted spheres could help to further verify the hypothesis about EGFR role in *in vivo* adipogenesis and expand the study on signalling pathways crucial for the regulation of fat cell fate and differentiation of preadipocytes into mature fat cells.

Work presented in Chapter 5 could be also combined with studies from Sugihara and his colleagues (Misago *et al*, 1998; Shimazu *et al*, 2001; Sugihara *et al*, 2001; Aoki *et al*, 2004; Toda *et al*, 2009) where an influence of adipocytes on different cell types (for example hair follicles, interfollicular keratinocytes or renal epithelial cell line) has been investigated by the interesting culture model. Such model was based on a three-dimensional collagen gel matrix culture, where different types of isolated cells were growth in a collagen gel with or without fat cells. Misago *et al* (1998) performed an experiment on rat (newborn) skin cells and showed that the co-culture of organoid hair follicle cells (HFs) in close proximity to (subcutaneous) fat cells revealed an inhibitory influence of adipocytes on proliferation of both HFs and fibroblasts, however the differentiation of HFs seemed to be speeded up in this experiment. By the use of the collagen gel matrix system on cells isolated from rat newborns, Sugihara *et al* (2001) pointed an activating role of

fat cells on both proliferation and differentiation of keratinocytes and an inhibitory role of adipocytes on dermal fibroblasts proliferation. In addition, the so-called “adipose tissue-organotypic culture system” was established for the three-dimensional growth (in collagen gel) of isolated and minced fragments of rat subcutaneous and visceral adipose tissue depots (Toda *et al*, 2009).

The co-culture methods presented by Sugihara and his colleagues (see above) could be used for the analysis of FACS-sorted cell populations from mouse back skin dermis. For example, sorted cells could be placed in a collagen gel matrix and co-cultured in a presence and absence of other embryonic skin cells. Such work might enhance knowledge on the cell-cell interactions in skin and on function of preadipocytes during embryonic skin development. Moreover the co-culture method from Sugihara et al (2001) could be used for the analysis of modified FACS-sorted cells. For example, FACS-sorted cells could be isolated from animals with a knockout of a gene highly expressed in lower skin dermis (based on microarray data from Chapter 3). Such experiment might help to reveal a function of the gene of choice in the development of skin compartments at embryonic level.

To sum up, the cell sorting technique on embryonic skin samples, presented in Chapter 5, can be a useful method for the isolation of fat cells at early stages of their development. Moreover, the spheroid cell culture method and experimental models from Sugihara and his colleagues (see above) could help to investigate features of such cells outside the body and increase knowledge about features of cells undergoing adipogenic differentiation.

# Chapter 6:
# Final discussion
# and
# future work.

## 6.1. Different mouse fat depots: their localisation, terminology and development in relation to mouse embryonic back skin.

As was mentioned in Chapter 1, section 1.2, fat cells (adipocytes), create white and brown adipose tissues (respectively WAT and BAT), and they can either create easy to distinguish fat depots around internal organs (visceral adipose tissue) or just beneath the skin surface (subcutaneous adipose depot). They can also be an element of other tissues and organs (along the bone marrow or in the intramuscular area) (Gesta *et al*, 2007). In addition, fat cells have been spotted to "infiltrate" skin (Cinti, 2001). Based on the Hausman and Mersmann studies, developing adipocytes were observed in lower dermis of rat and pig skin, around hair follicles (Mersmann *et al*, 1975, Hausman *et al*, 1981a; Hausman *et al*, 1981b; Hausman and Martin, 1982). These fat cells were treated as a representative of the outer layer of subcutaneous adipose tissue, divided by a connective tissue from other fat layers (Poulos *et al*, 2010).

**Subcutaneous adipose tissue (SAT) versus dermal adipose tissue (DAT).**

It was suggested that adipocytes localised in close proximity to hair follicle end bulbs (for example in rats and pigs) represent a different developmental pattern from other subcutaneous cells (Hausman *et al*, 1981a; Hausman *et al*, 1981b). However, to best of my knowledge, this suggestion seemed not to be developed in more detailed work that would investigate for example molecular features of these cells. Also, the word "infiltrate" was used in literature to describe adipocytes localisation along different tissues and organs, for example in skin which may suggests that these fat cells (for example seen in skin) are not creating a compartment big enough to be treated as something significant (for example for the function of organ in which fat cells are observed to be present).

The study presented in this thesis aimed to obtain information on fat cells from skin dermis by a use of mouse skin model. The study performed in Chapter 2, allowed the onset of the first lipid droplets in the lower dermis of mouse back skin, close to developing hair follicles, to be exactly targeted (Figure 2.5). The Oil Red O staining was applied to whole back skin sections together with fat depots localised beneath the skin (anterior white and brown adipose tissue; prosterior white fat layer; named as subcutaneous adipose tissue).

An interesting initial observation was made while the back skin was removed from mice. The fat depots beneath the skin, surrounded by very thin (muscle) layers, were loosely connected with skin and it was difficult to lift them in intact form

together with skin. Moreover, after the whole back skin sectioning and the Oil Red O staining, a difference was observed between fat cells in the skin dermis and fat cell beneath skin. Between e18 and e19 time points, when the first lipids were seen in the lower dermis, the subcutaneous adipose tissue beneath the skin seemed to be quite-well developed and filled densely with lipids (the red staining was observed along the whole organ depots, Appendix III). The occurrence of first lipids in lower dermis, just before animal birth, was characterised by the heterogeneity (dermis areas free from lipids surrounded by areas with lipid droplets). During the further development of animal, this heterogeneity was disappearing as more cells in lower dermis were filled with lipids and the size of lipid droplets increased. Finally, after the animal birth, in skin older than 1 day the easy to distinguish fat layer was seen along the whole lower back skin dermis (Figure 2.6). Interestingly from day 1 to about day 10 - 12, a gradual thickening of skin was observed while anagen hairs were growing inside the skin dermis and it seemed to be related also with the increase of fat layer thickness (Figure 2.6). Then, the gradual thickening of skin occurred, when hairs moved to catagen and telogen phase, which also influenced fat layer that become very thin. This confirmed that correlation between that hair follicle cycle and the dermal fat cell layer takes place not only in adult mice (Borodach and Montagna, 1956), but is related with the very first hair cycle after birth. Interestingly, when the changes in thickens of dermal adipose tissue were observed during the mouse development after the birth, no drastic or significant changes were observed for example in relation to localisation or the size of the subcutaneous adipose tissue beneath the skin. This shows not only the developmental differences between dermal adipose tissue and the subcutaneous adipose tissue but also suggest that these two fat depots in the mouse body may be (are likely to be) independently regulated.

Also, the dermal adipose tissue in lower dermis seemed not to merge with the adipose organ, due to a presence of a non-fatty skin layer (panniculus carnosus) that was localised under the dermal adipose tissue. Only a thin lipid filled layer (1 - 3 cells thick) could be observed along the panniculus carnosus either close to dermal adipose tissue or to fat organs beneath the skin. Therefore the question arises as to whether these additional thin layers of fat cells have any significant influences on the general features of subcutaneous fat depots in mice? Moreover, in the upper dermis no lipid droplets were seen and this feature was observed at all analysed time points (Figure 2.6). Therefore, development of dermal adipose tissue was clearly restricted to the lower area of skin dermis.

To sum up, because of the very loose connection between skin that contained dermal adipose tissue in lower dermis and the subcutaneous adipose tissue localised beneath the skin, the difference in timing of these two fat depots, the presence of the panniculus carnosus) and finally the lack of lipid droplets in the upper dermis area, the suggestion made in this thesis, is that fat cells in skin dermis do not only “infiltrate” (Cinti, 2001) skin, but are creating a distinctive fat layer. In addition, this layer seemed not to be only an outside layer of subcutaneous fat depot (as it is widely suggested; Poulos *et al*, 2010), but develops and functions as an fat depot independent from the rest of the subcutaneous fat.

**Fat depot terminology.**

As was discussed in previous paragraphs, the fat cells localised between hair follicles in lower skin dermis create a fat depot with very distinguishable features when compared with fat depots localised below the mouse skin and named as the subcutaneous adipose tissue. The microarray approach presented in Chapter 3 showed that dynamic processes take place in both upper and lower dermal compartments at embryonic level which are crucial for the creation of a fat layer in lower dermis and a non-fatty area in upper dermis below the epidermis. The term “dermal adipose tissue” has been used by Cinti (2007) and was incorporated in the study presented in this thesis for the description of fat cells localised in lower dermis and between hair follicles. Cinti (2007) mentioned that rodent dermal adipose tissue is being separated from subcutaneous depots by a muscle layer. The study from Chapter 2 has clearly shown that dermal adipose tissue depot does not merge with subcutaneous depots at any of the analysed time points. Therefore is seems reasonable to use a “dermal adipose tissue” term while working on a mouse fat cell layer localised in close proximity to hair follicles in order to point a difference between this adipose layer and a subcutaneous fat.

Interestingly, several recent papers on the subject of skin, hair follicles and fat cells surrounding hair follicles in mouse models do not use the name “dermal adipose tissue” (Plikus *et al*, 2008; Plikus *et al*, 2009; Sugawara *et al* 2010). They seemed to treat adipocytes from lower skin dermis as an integral part of a subcutaneous adipose tissue and not as a distinguishable fat layer in mouse. For example, the study presented by Plikus *et al* (2008 and 2009) has discussed the role of the BMP pathway in the regulation of hair follicle cycle. This work has suggested that adipocytes which surround hairs are involved in the regulation of the hair cycle (see section 6.2 of Chapter 6 for more details about this study). Plikus *et al* (2008 and 2009) used such terms as “subcutaneous adipocytes”, “subcutaneous

adipose tissue" or "subcutaneous fat" to describe these adipocytes localised in close proximity to hairs. Similarly Sugawara *et al* (2010) described changes in a fat layer between hair follicles of a mouse model with highly reduced expression of EGFR gene and the analysed fat cells were names as "subcutaneous adipocytes" whereas the layer created by these adipocytes was termed "subcutaneous adipose tissue" or "subcutis".

Studies described briefly above, clearly show that a form of misunderstanding exists when fat cells around hair follicles are investigated. Therefore, the establishment of a proper terminology for fat depots could be based on such work as a study presented in this thesis or a very recent work from Festa *et al* (2011). Festa *et al* (2011) investigated a role of adipocytes from dermis in the regulation of skin stem cell activity (this work is also discussed in section 6.2 of Chapter 6). In this work such terms were incorporated as "intradermal adipocyte lineage cells", "intradermal adipocyte" or "intradermal adipose tissue" and "intradermal adipocyte layer" in order to describe fat cells/fat layer from skin dermis (which are named in this thesis as dermal adipose tissue). Moreover the term "subcutaneous" was incorporated for the description of a fat depot "below the skin" (Festa *et al*, 2011).

To sum up, the modification of a terminology for fat tissue depots in mouse should be made to distinguish between subcutaneous adipose tissue - SAT (adipose organ below the skin and divided from the lower skin dermis by a panniculus carnosus layer) and dermal adipose tissue - DAT (localised in lower dermis, between hair follicles).

**Differences between visceral (VAT) and subcutaneous (SAT) and potentially between VAT, SAT and dermal adipose tissue (DAT) depot.**

The differences between visceral and subcutaneous depots have been recently investigated in relation to their influence on metabolism. It is known that high amounts of subcutaneous fat depots, which lead to so-called pear-shaped obesity, are related to a lower risk of the onset of diabetes (reviewed by Gesta el at, 2007). The apple-shaped obesity (high amount of visceral fat depots) is observed in patients with diabetes and metabolic syndrome. The growing number of obese people and enhanced epidemic of fat-related disorders (see section 1.2.7 in Chapter 1) lead to the development of surgical procedures for the removal or transplantation of fat depots. These attempts aim to improve life of obese patients and help to investigate the influence on metabolism of such procedures in both humans and rodents.

Such work has reached important conclusions in relation to differences between subcutaneous and visceral fat depots. It was noticed that removal of subcutaneous fat from humans (liposuction procedure) does not benefit them in relation to metabolic abnormalities which develop in obese individuals (Klein *et al*, 2004). When, omentectomy was applied in order to remove visceral adipose tissue (VAT) in humans, levels of both insulin and glucose decreased (Thörne *et al*, 2002). This effect was observed when removal of VAT was combined with adjustable gastric banding.

Finally, studies on the transplantation of preadipocytes, mature adipocytes (3T3-L1 or 3T3-F442A cells which are discussed in section 1.3) and different adipose depots in rodents aimed to enhance knowledge about biology of adipose tissue and metabolic effects of transplantation in host animal (reviewed by Tran and Kahn, 2010). Tran *et al* (2008) performed an experiment on mice, where visceral (epididymal) fat (from donor animal) was transplanted into either the subcutaneous (SC) or visceral (VIS) fat areas in host animal. In addition, the subcutaneous (flank) fat (from donor animal) was transplanted into the SC or VIS fat areas in host animal. The visceral area in the host animal was the intra-abdominal cavity (between epididymal layers, next to the mesenteric fat, below the liver), whereas the SC area was localised below the skin of the back of the recipient. Next, host animals were analysed based on their body weight and levels of both glucose and insulin. Animals with subcutaneous fat depots transplanted into VIS fat areas had decreased body weight and levels of insulin or glucose and they were also characterised by improved insulin sensitivity. Features (as above) of animals with subcutaneous depot transplanted into SC fat area also improved but less efficiently. Finally, mice

with VIS fat transplanted into visceral areas were lacking such effects (Tran *et al*, 2008).

To sum up, it is highly possible that the subcutaneous adipose tissue (SAT) has a beneficial effect on the body metabolism, can be considered as a protective fat depot and transplantation of such depot could help to treat obesity and metabolic disorders (Porter *et al*, 2009; Tran and Kahn, 2010). Since, the dermal adipose tissue (DAT) depot has been suggested in this thesis to be a third distinguishable fat depot, it might be possible that DAT differs from SAT and VAT depots because of the influence on the body metabolism. The microarray work on lower dermal cells has revealed a dramatic up-regulation of several genes whose levels undergo changes in obese and/or diabetic individuals (for example MUPs, Rbp4 or Car3; see sections 3.3 and 3.4 in Chapter 3 for more details). Maybe the expression of such genes in dermal adipose tissue is crucial for both the proper development of this fat depot (at embryonic level) but maybe also is related with an involvement of DAT in regulation of some metabolic processes after the animal birth. This hypothesis should be tested in order to understand better suggested differences between different fat depots on the body metabolism. For example, a method could be tested for the isolation of dermal adipose tissue from the lower dermal skin compartment. Then this depot (isolated from back skin of young healthy mice) could be transplanted into SAT and/or VAT depots in normal (control) and obese (experimental) mice. An effect on the metabolism could be analysed by the measure of blood glucose and insulin levels together with the analysis of the weight of both control and experimental animals kept on normal and/or high fat diet.

**Questions about white and brown fat cells in dermal adipose tissue (DAT), the thickness of DAT and about the hair follicle cycle.**

As was mentioned (Chapter 2), dermal adipose tissue undergoes changes in its thickness during the first couple of days after the mouse birth which seemed to be related with the hair follicle cycle. Such correlation was also suggested to take place in adult mice (Borodach and Montagna, 1956).

It may be interesting to perform an experiment on dermal adipose tissue layer from newborn mouse where the amount of accumulated lipids in lower dermis could be estimated at different stages of the hair follicle cycle. Such work could be based on the quantification analysis of the Oil Red O staining from back skin-cross sections. In more details, the red dye that bounds to lipid droplets can be extracted from cells and the amount of such eluted solution can be analysed on the spectrophotometer. Such technique was successfully used for the analysis of differentiating 3T3-L1 cells by the elution of Oil Red O with 100% isopropanol and the measurement of an eluted solution at 500 nm (Campbell *et al*, 2011). This analysis might reveal the association between changes in DAT thickening and changes in the lipid volume of this fat depot.

This quantitative study could be also combined with an investigation into the type of fat cells (brown or white adipocytes) occurring in the dermal adipose tissue during the hair follicle cycle. Due to specific morphological changes of differentiating cells from lower dermis (multilocular cells with many tiny lipid droplets become unilocular-like cells with mainly one big fat droplet inside the cell; see Chapter 2) it could be suggested that dermal adipose tissue consists of (mainly) white adipocytes which are responsible for the storage of energy. It is know that white fat cells express S-100 protein (calcium binding protein) and leptin (section 1.2.2.2.2.3. in Chapter 1 for more details on leptin), whereas brown adipocytes are expressing the uncoupling protein 1 (UCP-1), which is crucial for the release of energy in a form of heat and serves as a marker for brown fat cells (Cinti, 2001; Cinti, 2007). The microarray data obtained from mouse embryonic back skin (Chapter 3) revealed the up-regulation of several representatives of S100 protein family in lower dermal cells (see Appendix X) as well as the up-regulation of a leptin gene at e19 versus e17 time point in lower dermis where dermal adipose tissue develops (see Appendix XI.A). The UCP-1 was not found in microarray data from embryonic back skin dermis. This observation suggests that between e17 and e19 time points, adipogenic differentiation occurs that lead to development of mature white-like fat cells. One of the future experiments could analyse the expression (on protein level)

of leptin and S-100 proteins in embryonic skin dermis between e17 and e19 time points.

As was mentioned in section 1.2.2.3 (Chapter 1), fat cells seem to undergo reversible transdifferentiation where white adipocytes are capable of becoming brown fat cells (Cinti, 2007). A study by Cousin *et al* (1992) has revealed the presence of UCP-1 in cells that belong to white adipose depot in rats. In addition, cold exposure led to an increase in a number of brown adipocytes (Cousin *et al*, 1992). The question asked here is whether a process of transfdifferentiation occurs along the dermal adipose tissue? After birth, the thickening of skin dermis during hair follicle development could lead to a progressive white fat cell development and increased accumulation of lipids in these adipocytes (Chapter 2; Figure 2.6). Then, in animals older than 12 days, skin “shrinks” while hair follicles stop growing and clearly the thickness of the dermal adipose depot in lower dermis decreases (Figure 2.6). Maybe this specific change in dermal adipose tissue is due to a transdifferentiation process where white adipocytes become brown adipocytes that start expressing UCP-1 and releasing the energy from accumulated lipid droplets and this will lead to decrease in amount of accumulated lipids in lower skin dermis. The alternative explanation of the dermal adipose layer thinning during the hair follicle catagen/telogen could be that some apoptotic processes occur in lower dermis 12 days after the birth, which are crucial for the decrease in the skin thickness. The suggested hypotheses could be tested by the analysis of UCP-1, leptin and S100 proteins expression (for example by immunofluorescence analysis) and the cell death (for example by the TUNEL approach - terminal deoxynucleotidyl transferase-mediated deoxyuridine triphosphate nick end-labeling) along the back skin dermis from newborn mice (between 0.5 and 19 days old). These two suggested processes (transdifferentiation and apoptosis) could be regulated by specific cell-cell interactions along the skin and for example could be controlled by hair follicle cycle.

The potential correlation between hair follicles and fat cells surrounding hairs has become recently the major topic of several studies where the regulation of hair follicle cycle is being investigated (Plikus *et al*, 2008; Plikus *et al*, 2009; Festa *et al*, 2011). Such work seems to open a new direction in understanding correlations between different compartments of skin and is being discussed in more details in section 6.2 of this Chapter.

## 6.2. The experimental techniques mimicking *in vivo* environment for skin and potential signalling pathways in back skin crucial for dermal adipose tissue development - interactions between different skin compartments.

As was shown in Chapter 4, the “selection” of relevant genes from the microarray data seems to be crucial for further exploiting the work presented in this thesis.

The specific enrichment of epidermal growth factor receptor (EGFR) was found in the lower dermal cells at e18 time point (section 4.3.1 in Chapter 4). The EGFR - EGF signalling pathway was suggested previously to be related with adipogenesis in 3T3 cells (Adachi *et al*, 1994). When the EGFR-EGF signalling pathway was disrupted (mouse model work) in relation to the hair follicle cycle, changes in subcutaneous layers were notices, however this correlation has not been analysed in more detail (Sugawara *et al*, 2010). In this PhD study, the substrate organ culture technique has suggested that EGFR signalling pathway influencing skin development at embryonic level, and EGF receptor might be crucial for proper adipocyte differentiation of cells from lower dermal area (Chapter 4).

The growth of cells on cell culture dishes is a widely used technology for the analysis of cell features but its main disadvantage is that such cells are lacking the third dimension and do not interact with other cells in all directions as it happens in the live body. Therefore, in Chapter 4, the spheroid cell culture technique was used, where dermal cells (separated from epidermis) were grown in 3 dimensions, did not touch the culture dish surface and were surrounded only by other cells. This work aimed to analyse the lipid accumulation capabilities of young (e15 - 15.5) and old (e18.5 - 19) dermal cells. The fact that the young cells on cell surface dishes (2D cells) did not accumulate lipids was understandable in relation to the lack of lipid formation in skin from such young animals, however the situation changed dramatically when young cells were kept in 3D structures and lipids in the form of red dye staining was present through the 3D structures. In addition, 3D cell structures from older embryonic skin had lipids, but organized in clusters, and free-from lipids areas were seen. The main difference between the *in vivo* and *in vitro* 3D environments was the lack of epidermal cells. Thus the possibility is that the epidermis layer “normally” influences younger skin and “keeps” it in a kind of un-

differentiated stage (in relation to adipogenesis) at e15 - 15.5. When this layer is not present and cells are kept in 3D structure (so in *in vivo*-like, “normal” conditions but lacking the epidermis layer), then the lack of inhibition signal makes all young dermis cells capable of undergoing adipogenesis. Perhaps dermal cells at e15 - 15.5 resemble more closely mesenchymal stem cells, that are very plastic and if not properly controlled by other cell types (for example epidermis layer) can very easily (in a proper environmental conditions - 3D structure) undergo adipogenesis.

Next, as progressive development of the embryo takes place (from e15 - 15.5 to e18.5 - 19), which is also related with gradual development of hairs, the “rearrangement“ in skin dermis takes place. Perhaps the epidermis influences dermal cells that are in close proximity to the epidermal layer, and tries to maintain the non-fatty profile of these dermal cells, for example by signals that “switch on” inhibitory processes against adipogenesis in these dermal cells (as microarray data showed that, see Chapter 3). Then because of the gradual development of dermis and hairs, the hair follicle end bulbs may influence the lower dermal cells that surround end bulbs and this “activates” adipogenesis in precursor cells. This leads to progressive development of preadipocytes from precursor cells (between e17 and late e18) and leads to accumulation of lipids at e19 in cells close to hair follicle end bulbs. If this is true, then dermal cells from the 18.5 - 19 day old animal, kept in a 3D environment are characterised by much less plasticity and they may already be committed to very particular dermis cell types. Therefore, in these 3D structures, the lack of epidermis does not have the same influence as it does on much younger cells, and around cells committed to be adipocytes (filled with lipids), non-fatty cells are presented that kept their profile because of all inhibitory processes already activated in them.

The process described here is named the epidermal-dermal-skin appendage interaction theory. It seems to make sense especially since the interactions between epidermal and dermal cells leads to development of hairs (Chapter 1, section 1.1.3.1). Then, such interactions could be crucial for further maturation of back skin. In addition, the correlation between developing hairs and fat cells has been already suggested (Hausman *et al*; 1981) and was shown in mouse back skin specimens in work presented in this thesis (Chapter 2). Nowadays, attempts are being made to understand the regulatory mechanisms of the hair follicle cycle in relation to skin stem cell niches and the involvement of fat cells in the regulation of the hair growth (Plikus *et al*, 2008; Plikus *et al*, 2009; Festa *et al*, 2011). Plikus *et al* (2008, 2009

and 2011) investigated the hair follicle cycling (in mouse models after the plucking of hairs) and discussed the importance of a skin (inter-follicular) macro-environment for the function of hair follicle stem cells and further proper regulation of the hair follicle cycle. This work was focused on the analysis of the expression patterns of BMP proteins (for example BMP2), suggested to be involved in the regulation of hair development. Interestingly, Plikus and his colleagues found changes in the level of BMP2 protein along fat dermal cells that surrounded hair follicles. The BMP2 expression was not detected in the early stages of anagen and it gradually appeared at the latest anagen stages and in the first stage of telogen phase (so-called refractory phase) whereas it faded at late telogen (so-called competent phase) and again re-appeared in skin dermis of anagen hairs. In addition, the antagonist of BMPs, called noggin, was observed to oscillate from dermal sheath to dermal papilla (DP) during the progression of anagen and it faded in DP at the end of anagen but was not observed in adipocytes between hairs. The over-expression of the BMP antagonist (noggin) led to a decrease in the telogen (refractory) phase. The mouse model was created were noggin was over-expressed in skin under the keratin 14 promoter (keratin 14 is expressed in the interfollicular epidermis and along the outer root sheath of hairs). This allowed for the down-regulation of BMP signaling pathway at early telogen which led to a dramatic reduction of the telogen phase length and quicker entry to anagen. Plikus *et al* (2008, 2009) suggested that there are two niches crucial for the proper functioning of skin stem cells and further normal hair cycle occurrence, one related with the bulge region of the hair (micro-environment) and the second region related with fat cells around hairs (macro-environment) (see Figure 6.1b). The BMP-based signalling along the micro-environment is crucial for the proper occurrence of hair follicle cycle.

The microarray work in Chapter 3 has revealed the up-regulation of another BMP antagonist, gremlin 2 in the upper dermis of mouse embryonic back skin at e18 and e19 time points (Figure 3.18). Gremlin 2 has been linked to the inhibition of adipogenesis however its exact role remains elucidated (Wade *et al*, 2005; see alse section 3.4.1 in Chapter 3). It will be interesting in future work to test the hypothesis that the proper regulation of BMP signalling is crucial for the regulation of dermal skin compartment development (at embryonic level: non-fatty upper dermis verus adipocytes in lower skin dermis) and for controlling the hair follicle cycle after birth.

Work by Festa *et al* (2011) has also focused on the role of fat cells from lower dermis in the regulation of the hair follicle cycle. In this study, the presence of adipocyte precursor cells in the fat layer localised between hair follicles (named as

the intradermal fat layer) was revealed by the FACS approach and showed that such FACS-isolated cells from skin dermis can accumulate lipids when cultured for 3 days. Festa *et al* (2010) suggested that the size of the intradermal fat layer increases probably due to the activation of this adipocyte precursor cell population and the further development of mature fat cells. In addition, the proliferation process of adipocyte precursors can give higher number of these precursors and the proliferation is activated at the catagen stage of the hair cycle. This work has also suggested that the presence of adipocyte precursors in dermis is crucial for the proper activity of stem cells in skin and the normal presence of the hair cycle. Two mouse models have been applied for thus study. The Ebf-/- mice (with a mutation in the early B cell factor 1 gene) were characterised by a decrease of fat layer in lower skin dermis and the Azip mouse ("fatless" mouse with a dominant-negative C/EBP under the fatty acid binding protein-4 promotor) was lacking white mature adipocytes in different fat depots including the skin dermis. Both mice had delayed occurrence of hair coat development but this feature disappeared after time point p15. However the Ebf-/- mice had defects in hair follicle cycle progression (telogen and catagen morphology was seen from time point p21 till p56), whereas the analysis of hairs at p21 in the Azip mice revealed the anagen induction similar to a wild type mouse. The FACS-based analysis of skin adipocyte precursors showed that Ebf-/- mice were lacking such population of cells. The transplantation of FACS-sorted wild type adipocyte skin precursors into the Ebf-/- mouse skin (at time point p21) allow for the induction of hair follicle regeneration. Therefore, the general conclusion was that adipocyte precursor cell in the intradermal fat depot are needed for the proper activation of hair follicle development by probably proper regulation of stem cell activity in hairs (bulge stem cells) (Festa *et al*, 2011). Finally, this work has suggested the PDGF (plateled-derived growth factor) as a possible molecule responsible for proper skin stem cell activity, since the high up-regulation of this factor was observed in adipocyte precursors from skin dermis.

In work presented in Chapter 3, the up-regulation of the PDGFR (plateled-derived growth factor receptor), on mRNA and protein levels, was observed in the upper dermis of embryonic back skin dermis (Figure 3.22). Based on the data presented by Festa *et al*, 2011, PDGFR expression was observed in the follicle dermal papilla but was not observed in the upper interfollicular dermis in adult mice. It could be interesting to further investigate expression of PDGF and PDGFR along the embryonic skin dermis in mouse models used by Festa *et al* (2011) to reveal the "real" and "exact" functional role of the PDGF-PDGFR signaling pathway in relation

to the development of dermal compartments (at embryonic level) and further regulation of hair follicle cycle after birth.

The above work by Plikus *et al* (2008 and 2009) and Festa *et al* (2010) tries to answer questions about regulatory mechanisms crucial for the hair follicle cycle. Additional aspect of this work should be included where not only involvement of adipocytes in the hair follicle cycle takes place but also where the hair follicles are crucial for the proper development and maintenance of the dermal adipose tissue layer. Specific interactions between hair follicle end bulb cells and lower dermal cells could occur that activate fat cell differentiation in the lower dermal compartment. If such interactions are occurring, the question should be asked about the type of signals between skin cells that are crucial for development of different skin compartments. The follicle end bulb incorporates the dermal papilla (DP) and dermal sheath (DS) which are crucial for the controlling of hair growth and cycle (Chapter 1, section 1.1.3). In addition, the cultured cells from DP and DS are capable to differentiate into for example adipocytes (Jahoda *et al*, 2003). Maybe cells from hair follicle end bulbs are capable of "sending" signals to cells in lower dermis area, and controlling the "fatty" features of these lower dermis cells. The microarray data from dermal cells (presented in Chapter 3), together with information about proteins for example enriched and secreted by hair follicles could help to reveal a potential signalling pathways important for dermal adipose tissue development.

**Leptin - leptin receptor interactions between hair follicles end bulb and cells from lower dermis.**

Leptin is expressed abundantly by mature adipocytes and changes in its levels were correlated with obesity (Chapter 1, section 1.2.7). Leptin interacts through leptin receptors and was suggested to work in an autocrine way on animal adipocytes, however its influence was not observed on human adipocytes (from subcutaneous depots) (Aprath-Hausman *et al*; 2001). In the dermis microarray data, presented in this thesis, expression of leptin receptor and leptin increases in lower dermis cells during mouse embryonic development (see Appendix XI). In addition, the leptin and leptin receptor were analysed in 14.5 day old murine fetus and their presence was observed in developing hair follicles (Hoggard *et al*; 1997). The presence of leptin (in the hair matrix and inner root sheath of the hair bulb) and leptin receptor in human hairs (papilla cells) was also reported (Iguchi *et al*; 2001). In addition, leptin and leptin receptor are also seen in the human epidermis (Poeggeler *et al*; 2010). Because of the localisation of leptin along the skin, a role of

leptin in hair development was suggested (Poeggeler *et al*; 2010). Based on the above mentioned literature and the presence of both leptin and leptin receptor genes in the microarray data, a suggestion can be made that leptin produced by the hair compartment may be influencing the cells from lower dermis (trough leptin receptors seen in these dermal cells) and take part in controlling adipogenesis *in vivo* in skin. Perhaps this occurs first (at embryonic level), where the leptin produced in hair structures influences the hair follicle development. Then, when skin is getting older, developed hairs (dermal papilla for example) secrete leptin to adjacent dermis cells which, as was shown by the microarray data, have up-regulation of the leptin receptor. Finally, as an effect of that interaction between e17 and e19, leptin from hair follicles influences adipogenesis in the lower dermis.

**Adiponectin and its localisation along the back skin.**

An interesting observation in this thesis was related to adiponectin expression in back skin samples. Based on the microarray study and the qRT-PCR verification work, *Adipoq* mRNA expression was up-regulated in lower dermis versus upper dermis and increased in lower dermis during mouse back skin development (Chapter 3, Table 3.4 and Figure 3.13B). When antibodies against AdipoQ were used, interestingly the expression of this protein was seen along the hair follicles in the very outer layer of hairs and in the upper as well as the lower dermis. This “confusing result” could be attributed to unspecific binding of the antibodies used. On the other hand there may be an explanation for such a protein expression pattern for adiponectin. Adiponectin, similarly to leptin is produced and secreted by mature adipocytes, and its level changes during obesity/diabetes and it can have an autocrine influence on fat cells (Dietze-Schroeder *et al*; 2005). In relation to skin, perhaps the adiponectin can be abundantly expressed by different compartments of the skin such as hair follicles (as with leptin, see above). The hairs will produce adiponectin and gradually secrete it to the adjacent dermal cells and this secretion takes part at least between e17 ad e19 (based on the staining presented in Chapter 3, Figure 3.14). The dermis microarray data (DMD) showed that adiponectin receptors are up-regulated in lower dermis versus upper dermis in all analysed time points (Chapter 3, Table 3.7). Thus, maybe secreted AdipoQ from the outer layers of hairs interacts with adiponectin receptors present in lower dermal cells. This interaction (together with many other processes that control adipogenesis *in vivo*), activates preadipocytes to gradual differentiation and as a result of that, the dramatic increase of AdipoQ on mRNA level takes place in 18 and 19 day old embryonic lower skin dermis.

Therefore there are at least two potential signalling pathways, leptin and AdipoQ, that might fit with the idea about signalling in back skin between hair follicle end bulbs and lower dermal cells and control of dermal adipose tissue development. The verification of such hypothesis could be carried for example in three dimensional spheres established from dermal cells at different embryonic developmental stages. These spheres could be treated with factors abundantly expressed by hair follicle end bulbs, for example adiponectin or/and leptin. In addition, the silencing (RNAi) of receptors in lower dermal cells that are specific for proteins secreted by end bulbs (adiponectin, leptin) could be performed before the treatment of these cells with a factor of interest. Then, the lipid accumulation capability of such spheres would be analysed.

## 6.3. Tracking the preadipocytes and adipocytes *in vivo* - why such analysis is important?

The basic knowledge about fat cell differentiation (adipogenesis) comes mainly from *in vitro* studies where many cell lines have been established and usefully used in order to track adipogenesis (for detailed description see Chapter 1, section 1.3). Despite these studies there is still a gap related with understanding the very early stages of adipogenesis *in vivo*. Especially now, when a suggestion was made that different fat depots may have different developmental origin and metabolic functions (Gesta *et al*, 2007).

3T3 cells, have been used widely to track adipocyte differentiation from so called preadipocyte state (cells committed to be mature fat cells, but not accumulating lipids yet) to the development of adipocytes (mature fat cells with accumulated lipid droplets). However, several disadvantages can be pointed here in relation to the use of such cells. First of all, these cells developed from a Swiss cell line that was established by mincing whole mouse embryos between age 17 and 19 (Green and Kehinde, 1974; Green and Meuth, 1974; Green and Kehinde, 1975; Green and Kehinde, 1976). Originally, these cells did not accumulate lipids and after some time in cell culture conditions, they gradually start to accumulate fat in a form of clusters, and from these cells 3T3-fat cells were derived. In general, 3T3-L1 and 3T3-F422A are widely known cell lines that undergo adipogenesis. As, these cells have not been derived from a particular fat depot, thus it seemed impossible to use this model for tracking differences in adipocyte differentiation processes that lead to a development of different fat depots. Next, these cells, although committed to adipogenesis, have to be “pushed” by adipogenic medium that activate whole cascade of changes in these cells and lead to the development of mature fat cells. Thus, it can not be said that all steps specifically occurring during adipogenesis *in vitro*, in these cells, represent exactly and truly the “real” processes that take part in live body. Finally, by keeping cells on artificial surfaces of culture dishes, these two-dimensional cells are lacking the third dimension. That is not a case in the life body, where cells develop in all dimensions, have contact with other fat cells, and create three-dimensional fat organs. Also, during developmental processes in the body, a particular type of cell, tissue or organ is in close proximity to other type of cells, tissues and organs. The cell-cell interaction between different organs could be crucial for proper cell differentiation and development. For example, the epidermal-dermal interactions lead to hairs development (Chapter 1, section 1.1.3.1).

In addition, the adipose organ is known to have an endocrine function that influences other organs however the autocrine functions of several fat-secreted

proteins have been observed (reviewed by Kim and Moustaid-Moussa, 2000). This clearly suggests that for the proper development of adipocytes, signals from other fat cells (an maybe other type of cells) can be important during fat depot development. This suggestion could be difficult to verify by using for example, 3T3-L1 or 3T3-F442A cell lines.

All the above mentioned disadvantages of 3T3 cell lines show the need for developing *in vivo* approaches for the analysis of fat depots. Thus many mouse models have been set up, where for example crucial for early steps of adipogenesis genes have been silenced (Valet *et al*, 2002). Mouse models helped to track functions of particular genes in relation to for example abnormalities in fat depots occurrence or development of metabolic disorders. Interestingly for some of mouse knockouts (for example C/EBPs or PPARgamma) as well as changes in fat depots, a quick death (at birth, death *in utero*) occurs, which clearly shows that many crucial adipogenic processes take place at embryonic level and influences the whole body. However due to an early death of such mouse models, it is difficult to carry studies on very early stages of adipogenesis *in vivo*. In addition, the generation of a transgenic model seems to be a time consuming process and not always occupied by a quick and successful outcome.

Thus, in this thesis an *in vivo* approach was developed to track not only adipocytes cells that are able to accumulate lipid but also preadipocytes during mouse back skin development. When the first signs of lipids were tracked in back skin (discussed in section 6.1), the investigation of a reliable *in vivo* marker for preadipocytes was performed (Chapter 2). As such a marker seemed not to be available for *in vivo* work so far, several *in vitro* adipogenic markers were tested, such as PPARgamma , Pref-1 and C/EBPalpha, widely associated with early stages of adipocyte differentiation (see Chapter 1, section 1.3). Only the antibody against C/EBPalpha allowed preadipocytes and adipocytes to be tracked in mouse embryonic skin, whereas other antibodies gave questionable results (Figures 2.12 – 2.14). This could be a result of the antibodies not being appropriate for immunofluorescence technique used on skin sections, or an occurrence of differences between adipogenesis *in vivo* in skin dermis and adipocyte differentiation process observed *in vitro* in cell lines.

## 6.4. The microarray approach and gene expression profiles during mouse embryonic dermis development *in vivo*.

**Dermal adipocytes and dermal non-fatty cells.**

The microdissection technique together with the microarray approach permitted a detailed *in vivo* study (Chapter 3). Microarray data obtained from lower and upper dermal cells between e17 and e19 time points showed that during the late stages of embryonic development, the dermal cells differentiate into at least two-very specific cell populations, adipocytes and non-fatty cells. Therefore, dermis divided into two layers in adults (papillary localised below epidermis and lower reticular layer; see also section 1.1.2 in Chapter 1) undergoes also an earlier subdivision at embryonic level. Interestingly, these two cell types (adipocytes and non-fatty cells) with totally opposite features are developing in the same skin compartment and co-exist with each other. This observation seemed to be very important in relation to the analysis of mechanisms that control adipogenesis, fate of cells and "decide" how and when particular type of cell develops into a fat organ.

***In vivo* versus *in vitro* adipogenesis.**

The comparison analysis of microarray data from developing lower dermal cells (*in vivo* adipocytes) with microarray-based studies on differentiating 3T3-L1 cells (*in vitro* adipocytes), presented in sections 3.3.4 and 3.3.5 of Chapter 3, revealed a clear difference in a number and type of genes regulated at early stages of these *in vivo* and *in vitro* adipogenic differentiation processes. This difference can be due the fact that some of the processes so widely analysed in cell lines that undergo adipogenesis (3T3-L1 cells, reviewed by Gregoire *et al*, 1998) are effects of a treatment with adipogenic medium of two-dimensional cells that are removed from their normal environment (life body). Whereas the gene expression patterns observed in lower dermal cells from mouse embryonic back are real changes that take place in three dimensional cells present in their natural environment (life body). On the other hand, the *in vivo* analysis should, in future, be supplemented by similar microarray work on samples from 15 or 16 day old embryos that would verify the presence or absence of some genes not seen in the 17 to 19 day old mouse embryos.

**Dermal fat cell origin.**

As was mentioned in Chapter 1, it is still not clear about the origin of fat cells (Chapter 1, section 1.2.3). It is generally suggested that fat cells develops from

mesenchymal stem cells (MSCs), similar to muscles and bone (Billon *et al*; 2008, Gesta *et al*; 2007). Based on the work presented in this thesis, a suggestion can be made that adipocytes in lower dermis “share” developmental origin with dorsal mouse dermis. The dorsal dermis develops from so-called somites which are segmental units of the paraxial mesoderm (Olivera-Martinez *et al*; 2004). Therefore, it might be suggested that dermal adipose tissue, fully created after birth, originates from paraxial mesoderm.

## 6.5. Future study in relation to the dermis microarray data.

The work presented in this thesis has opened a new direction in the analysis of skin compartments and interactions between all skin compartments that lead to development of the dermal fat layer. To the best of my knowledge such work that is giving insight into molecular processes in the embryonic dermis has never been presented before. Thus, it is important to think about future directions of this study that will produce increased knowledge about very early stages of adipogenesis *in vivo* and might help in better understanding mechanisms that control adipocyte differentiation in life body.

**Additional time points.**

Due to a fact that microarray data, generated during this PhD study, was obtained only from three time points (e17, e18 and e19), it could be crucial to perform and experiment, where dermal samples from other time points would be collected and used for the microarray analysis. By analyzing younger skin (e14, e15, e16), it might be possible to analyse the features of precursor cells that develop into preadipocytes and obtain information about very early stages of *in vivo* adipogenesis.

**Selection of genes from generated microarray data.**

As was shown in Chapter 4, functional studies on selected genes (eg EGFR) from the dermal microarray data are crucial to verify the function of genes in early processes of adipogenesis *in vivo.* It was shown that the organ technique helps to maintain *in vivo*-like environment for skin and permits the influence of particular factors on the whole three-dimensional skin structure to be analysed. This environment is crucial for the function of skin and interactions between its compartments. Future work should try to analyse more genes selected from the microarray data. This work could be especially related to genes from the top/upper dermis that is characterised by the presence of genes involved in inhibition of adipogenesis. It could help to find a useful inhibitor of fat cell differentiation that either could prevent or help to treat the abnormalities related with excess accumulation of lipids. The organ culture work with fragments of back skin might be a good model for a preliminary verification of the influence of such genes (their products) on skin cell development and their capability to accumulate lipids.

One future direction could be based on early FABP4 expression and its specific localisation in mouse back skin. The work presented in Chapter 3, showed

that FABP4 on both mRNA and protein level is highly up-regulated in lower skin dermis between e17 and e19 time points (Figure 3.10B and Figure 3.11). This fatty acid binding protein 4 binds and transports fatty acids and since its involvement in the development if insulin resistance has been suggested, and attempts are being made to find an efficient inhibitor of FABP4 (Suhre *et al*, 2011). The function of FABP4 in relation to the development of dermal adipose tissue can be analysed by the use of one of such suggested FABP4 inhibitors. For example, the influence of a selected FABP4 inhibitor (for example the small-molecule FABP4 inhibitor BMS309403 discussed by Suhre *et al*, 2011) could be analysed in relation to lipid accumulation on intact pieces of embryonic back skin (organ culture method from Chapter 4) or FACS-sorted CD36+ cells kept in 3D structures (that are highly expressing FABP4 and are suggested to represent lower dermal cells undergoing adipogenesis; see work presented in Chapter 5).

As a further example of future experiments, the presence of FABP4 could be used for the analysis of function of other genes selected from a microarray data (Chapter 3). A transgenic animal could be obtained with a specific over-expression of a gene with high up-regulation in lower dermis (based microarray data; for example retinol binding protein 4; see Figure 3.10A in Chapter 3) under the FABP4 promoter. In addition, this promoter could be used to drive over-expression in the lower dermis of a gene known to be highly up-regulated in upper dermis (also based on microarray data; for example gremlin 2; see Figure 3.18 in Chapter 3). This could allow for the expression of a selected gene in the lower dermis of embryonic skin and permit analysis of the role of the chosen gene in the inhibition/activation of adipogenesis in mouse embryonic dermal compartments.

**The further analysis of FACS-sorted dermis cells.**

In Chapter 5, the establishment of a fluorescence activated cell sorting (FACS) protocol to provide detailed analysis of dermal cell populations was described. This work showed that selected membrane protein could be an efficient marker for cells that undergo adipocyte differentiation in skin dermis. CD36+ positive cells were capable of accumulating lipids in normal medium. Then, the qRT-PCR analysis showed the up-regulation of fat-related genes in this cell population in comparison with negative (for CD36) sorted cells.

It seems that the FACS tool may be useful in the further analysis of different embryonic dermal cell populations that are crucial for the proper development of skin compartments. This may give the possibility of analysing processes within these cells that are responsible for adipogenesis inhibition or activation. The FACS

allows cells to be collected that are committed to adipogenesis and by keeping them in 3D structures and incubating (or performing a silencing experiment with iRNA or overexpression work) using factors “picked” from the microarray data (for example highly up-regulated genes known to be related with obese and/or diabetic patients), it is possible to investigate what exactly controls adipogenesis in skin. This knowledge can then perhaps be used for the development of pharmaceuticals for treatment of fat-related disorders.

### 6.6. To sum up.

To sum up, the work presented in this thesis may be a new beginning for the investigation of fat cell origin and development. It may help to understand mechanisms that inhibit and activate adipocyte differentiation *in vivo* in skin and in the long term may benefit with the treatments of disorders that are result of abnormal fat accumulation in the body.

# Chapter 7:
# Bibliography.

Abella A, Dubus P, Malumbres M, Rane SG, Kiyokawa H, Sicard A, Vignon F, Langin D, Barbacid M, Fajas L (2005) Cdk4 promotes adipogenesis through PPARgamma activation. Cell Metab. 2(4):239-49.

Adachi H, Kurachi H, Homma H, Adachi K, Imai T, Morishige K, Matsuzawa Y, Miyake A (1994) Epidermal growth factor promotes adipogenesis of 3T3-L1 cell in vitro. Endocrinology. 135(5):1824-30.

Ahima RS (2008) Revisiting leptin's role in obesity and weight loss. J Clin Invest. 118(7):2380-3.

Ailhaud G, Dani C, Amri EZ, Djian P, Vannier C, Doglio A, Forest C, Gaillard D, Négrel R, Grimaldi P (1989) Coupling growth arrest and adipocyte differentiation. Environ Health Perspect. 80:17-23.

Almind K, Kahn CR (2004) Genetic determinants of energy expenditure and insulin resistance in diet-induced obesity in mice. Diabetes. 53(12):3274-85.

Ansel JC, Armstrong CA, Song I, Quinlan KL, Olerud JE, Caughman SW, Bunnett NW (1997) Interactions of the skin and nervous system. J Investig Dermatol Symp Proc. 2(1):23-6.

Aoki S, Toda S, Ando T, Sugihara H (2004) Bone marrow stromal cells, preadipocytes, and dermal fibroblasts promote epidermal regeneration in their distinctive fashions. Mol Biol Cell. 15(10):4647-57. Epub 2004 Aug 3.

Aprath-Husmann I, Röhrig K, Gottschling-Zeller H, Skurk T, Scriba D, Birgel M, Hauner H (2001) Effects of leptin on the differentiation and metabolism of human adipocytes. Int J Obes Relat Metab Disord. 25(10):1465-70.

Avram AS, Avram MM, James WD (2005) Subcutaneous fat in normal and diseased states: 2. Anatomy and physiology of white and brown adipose tissue. J Am Acad Dermatol. 53(4):671-83.

Bain G, Kitchens D, Yao M, Huettner JE, Gottlieb DI (1995) Embryonic stem cells express neuronal properties in vitro. Dev Biol. 1995 Apr;168(2):342-57.

Barak Y, Nelson MC, Ong ES, Jones YZ, Ruiz-Lozano P, Chien KR, Koder A, Evans RM (1999) PPAR gamma is required for placental, cardiac, and adipose tissue development. Mol Cell. 4(4):585-95.

Bardot B, Lecoin L, Fliniaux I, Huillard E, Marx M, Viallet JP (2004) Drm/Gremlin, a BMP antagonist, defines the interbud region during feather development. Int J Dev Biol. 48(2-3):149-56.

Baudry A, Yang ZZ, Hemmings BA (2006) PKBalpha is required for adipose differentiation of mouse embryonic fibroblasts. J Cell Sci. 119(Pt 5):889-97. Epub 2006 Feb 14.

Benito M, Porras A, Nebreda AR, Santos E (1991) Differentiation of 3T3-L1 fibroblasts to adipocytes induced by transfection of ras oncogenes. Science. 253(5019):565-8.

Bennett CN, Ross SE, Longo KA, Bajnok L, Hemati N, Johnson KW, Harrison SD, MacDougald OA (2002) Regulation of Wnt signaling during adipogenesis. J Biol Chem. 277(34):30998-1004. Epub 2002 Jun 7.

Bernstein RL, Hyun WC, Davis JH, Fulwyler MJ, Pershadsingh HA (1989) Flow cytometric analysis of mature adipocytes. Cytometry. 10(4):469-74.

Billon N, Iannarelli P, Monteiro MC, Glavieux-Pardanaud C, Richardson WD, Kessaris N, Dani C, Dupin E (2007) The generation of adipocytes by the neural crest. Development. 134(12):2283-92. Epub 2007 May 16.

Billon N, Monteiro MC, Dani C (2008) Developmental origin of adipocytes: new insights into a pending question. Biol Cell. 100(10):563-75.

Birsoy K, Chen Z, Friedman J (2008) Transcriptional regulation of adipogenesis by KLF4. Cell Metab. 7(4):339-47.

Boeuf S, Klingenspor M, Van Hal NL, Schneider T, Keijer J, Klaus S (2001) Differential gene expression in white and brown preadipocytes. Physiol Genomics. 7(1):15-25.

Bonen A, Tandon NN, Glatz JF, Luiken JJ, Heigenhauser GJ (2006) The fatty acid transporter FAT/CD36 is upregulated in subcutaneous and visceral adipose tissues in human obesity and type 2 diabetes. Int J Obes (Lond). 30(6):877-83.

Boney CM, Fiedorek FT Jr, Paul SR, Gruppuso PA (1996) Regulation of preadipocyte factor-1 gene expression during 3T3-L1 cell differentiation. Endocrinology. 137(7):2923-8.

Borodach GN, Montagna W (1956) Fat in skin of the mouse during cycles of hair growth. J Invest Dermatol. 26(3):229-32.

Bowers RR, Kim JW, Otto TC, Lane MD (2006) Stable stem cell commitment to the adipocyte lineage by inhibition of DNA methylation: role of the BMP-4 gene. Proc Natl Acad Sci U S A. 103(35):13022-7. Epub 2006 Aug 17.

Braissant O, Wahli W (1998) Differential expression of peroxisome proliferator-activated receptor-alpha, -beta, and -gamma during rat embryonic development. Endocrinology. 139(6):2748-54.

Braverman IM, Keh-Yen A (1981) Ultrastructure of the human dermal microcirculation. III. The vessels in the mid- and lower dermis and subcutaneous fat. J Invest Dermatol. 77(3):297-304.

Burton GR, Guan Y, Nagarajan R, McGehee RE Jr (2002) Microarray analysis of gene expression during early adipocyte differentiation. Gene. 293(1-2):21-31.

Burton GR, Nagarajan R, Peterson CA, McGehee RE Jr (2004) Microarray analysis of differentiation-specific gene expression during 3T3-L1 adipogenesis. Gene. 329:167-85.

Butler AA, Cone RD (2001) Knockout models resulting in the development of obesity. Trends Genet. 17(10):S50-4.

Byrne SN, Limón-Flores AY, Ullrich SE (2008) Mast cell migration from the skin to the draining lymph nodes upon ultraviolet irradiation represents a key step in the induction of immune suppression. J Immunol. 180(7):4648-55.

Campbell JE, Peckett AJ, D'souza AM, Hawke TJ, Riddell MC (2011) Adipogenic and lipolytic effects of chronic glucocorticoid exposure. Am J Physiol Cell Physiol. 300(1):C198-209. Epub 2010 Oct 13.

Cao Z, Umek RM, McKnight SL (1991) Regulated expression of three C/EBP isoforms during adipose conversion of 3T3-L1 cells. Genes Dev. 5(9):1538-52.

Carmona-Saez P, Chagoyen M, Tirado F, Carazo JM, Pascual-Montano A (2007) GENECODIS: a web-based tool for finding significant concurrent annotations in gene lists. Genome Biol. 8(1):R3.

Celi FS (2009) Brown adipose tissue--when it pays to be inefficient. N Engl J Med. 360(15):1553-6.

Chan SS, Schedlich LJ, Twigg SM, Baxter RC (2009) Inhibition of adipocyte differentiation by insulin-like growth factor-binding protein-3. Am J Physiol Endocrinol Metab. 296(4):E654-63. Epub 2009 Jan 13.

Chan KH, Song Y, Hsu YH, You NC, F Tinker L, Liu S (2010) Common genetic variants in fatty acid-binding protein-4 (FABP4) and clinical diabetes risk in the women's health initiative observational study. Obesity (Silver Spring). 18(9):1812-20. Epub 2010 Jan 28.

Chen HW, Tzeng CR (2006) Applications of microarray in reproductive medicine. Chang Gung Med J. 29(1):15-24.

Chiellini C, Bertacca A, Novelli SE, Görgün CZ, Ciccarone A, Giordano A, Xu H, Soukas A, Costa M, Gandini D, Dimitri R, Bottone P, Cecchetti P, Pardini E, Perego L, Navalesi R, Folli F, Benzi L, Cinti S, Friedman JM, Hotamisligil GS, Maffei M (2002) Obesity modulates the expression of haptoglobin in the white adipose tissue via TNFalpha. J Cell Physiol. 190(2):251-8.

Cho SW, Yang JY, Sun HJ, Jung JY, Her SJ, Cho HY, Choi HJ, Kim SW, Kim SY, Shin CS (2009) Wnt inhibitory factor (WIF)-1 inhibits osteoblastic differentiation in mouse embryonic mesenchymal cells. Bone. 44(6):1069-77. Epub 2009 Feb 27.

Cinti S (2001) Morphology of the Adipose Tissue. In: Klaus S (Ed.) Adipose Tissues, pp. 11-26. © Landes Bioscience. Austin, TX. ISBN: 978-1-58706-040-3

Cinti S (2007) In: Fantuzzi G and Mazzone T (Eds.) *Nutrition and Health: Adipose Tissue and Adipokines in Health and Disease*, pp. 3-19. © Humana Press Inc., Totowa, NJ. ISBN: 978-1-58829-721-1

Coleman DL (1982) Diabetes-obesity syndromes in mice. Diabetes. 31 (Suppl 1 Pt 2):1-6.

Constance CM, Morgan JI 4th, Umek RM (1996) C/EBPalpha regulation of the growth-arrest-associated gene gadd45. Mol Cell Biol. 16(7):3878-83.

Corbetta S, Bulfamante G, Cortelazzi D, Barresi V, Cetin I, Mantovani G, Bondioni S, Beck-Peccoz P, Spada A (2005) Adiponectin expression in human fetal tissues

during mid- and late gestation. J Clin Endocrinol Metab. 90(4):2397-402. Epub 2004 Dec 28.

Cousin B, Cinti S, Morroni M, Raimbault S, Ricquier D, Pénicaud L, Casteilla L (1992) Occurrence of brown adipocytes in rat white adipose tissue: molecular and morphological characterization. J Cell Sci. 103 ( Pt 4):931-42.

Cypess AM, Lehman S, Williams G, Tal I, Rodman D, Goldfine AB, Kuo FC, Palmer EL, Tseng YH, Doria A, Kolodny GM, Kahn CR (2009) Identification and importance of brown adipose tissue in adult humans. N Engl J Med. 360(15):1509-17.

Dale TC (1998) Signal transduction by the Wnt family of ligands. Biochem J. 329 ( Pt 2):209-23.

Dani C, Smith AG, Dessolin S, Leroy P, Staccini L, Villageois P, Darimont C, Ailhaud G (1997) Differentiation of embryonic stem cells into adipocytes in vitro. J Cell Sci. 110 ( Pt 11):1279-85.

Date T, Doiguchi Y, Nobuta M, Shindo H (2004) Bone morphogenetic protein-2 induces differentiation of multipotent C3H10T1/2 cells into osteoblasts, chondrocytes, and adipocytes in vivo and in vitro. J Orthop Sci. 9(5):503-8.

De Meyts P (2004) Insulin and its receptor: structure, function and evolution. Bioessays. 26(12):1351-62.

de Paula FJ, Horowitz MC, Rosen CJ (2010) Novel insights into the relationship between diabetes and osteoporosis. Diabetes Metab Res Rev. 2010 Oct 11. [Epub ahead of print]

Deslex S, Negrel R, Ailhaud G (1987) Development of a chemically defined serum-free medium for differentiation of rat adipose precursor cells. Exp Cell Res. 168(1):15-30.

Dietze-Schroeder D, Sell H, Uhlig M, Koenen M, Eckel J (2005) Autocrine action of adiponectin on human fat cells prevents the release of insulin resistance-inducing factors. Diabetes. 54(7):2003-11.

DiGirolamo M, Fine JB, Tagra K, Rossmanith R (1998) Qualitative regional differences in adipose tissue growth and cellularity in male Wistar rats fed ad libitum. Am J Physiol. 1998 May; 274(5 Pt 2):R1460-7.

Doi H, Masaki N, Takahashi H, Komatsu H, Fujimori K, Satomi S (2005) A new preadipocyte cell line, AP-18, established from adult mouse adipose tissue. Tohoku J Exp Med. 207(3):209-16.

Drel VR, Mashtalir N, Ilnytska O, Shin J, Li F, Lyzogubov VV, Obrosova IG (2006) The leptin-deficient (ob/ob) mouse: a new animal model of peripheral neuropathy of type 2 diabetes and obesity. Diabetes. 55(12):3335-43.

Duncan RE, Ahmadian M, Jaworski K, Sarkadi-Nagy E, Sul HS (2007) Regulation of lipolysis in adipocytes. Annu Rev Nutr. 27:79-101.

Eberhart CG, Argani P (2001) Wnt signaling in human development: beta-catenin nuclear translocation in fetal lung, kidney, placenta, capillaries, adrenal, and cartilage. Pediatr Dev Pathol. 4(4):351-7.

Elias PM, Feingold KR (1992) Lipids and the epidermal water barrier: metabolism, regulation, and pathophysiology. Semin Dermatol. 11(2):176-82.

Entenmann G, Hauner H (1996) Relationship between replication and differentiation in cultured human adipocyte precursor cells. Am J Physiol. 270(4 Pt 1):C1011-6.

Ernst J, Nau GJ, Bar-Joseph Z (2005) Clustering short time series gene expression data. Bioinformatics. 21 Suppl 1:i159-68.

Fantauzzo KA, Bazzi H, Jahoda CA, Christiano AM (2008) Dynamic expression of the zinc-finger transcription factor Trps1 during hair follicle morphogenesis and cycling. Gene Expr Patterns. 8(2):51-7. Epub 2007 Oct 25.

Febbraio M, Abumrad NA, Hajjar DP, Sharma K, Cheng W, Pearce SF, Silverstein RL (1999) A null mutation in murine CD36 reveals an important role in fatty acid and lipoprotein metabolism. J Biol Chem. 274(27):19055-62.

Fernandes KJ, McKenzie IA, Mill P, Smith KM, Akhavan M, Barnabé-Heider F, Biernaskie J, Junek A, Kobayashi NR, Toma JG, Kaplan DR, Labosky PA, Rafuse V, Hui CC, Miller FD (2004) A dermal niche for multipotent adult skin-derived precursor cells. Nat Cell Biol. 6(11):1082-93.

Festa E, Fretz J, Berry R, Schmidt B, Rodeheffer M, Horowitz M, Horsley V (2011) Adipocyte lineage cells contribute to the skin stem cell niche to drive hair cycling. Cell. 146(5):761-71.

Flemming JF (1871) On the formation and regression of fat cells in connective tissue with comment on the structure of the latter. Arch. R. Mikr. Anat. 7:32.

Fliniaux I, Mikkola ML, Lefebvre S, Thesleff I (2008) Identification of dkk4 as a target of Eda-A1/Edar pathway reveals an unexpected role of ectodysplasin as inhibitor of Wnt signalling in ectodermal placodes. Dev Biol. 320(1):60-71. Epub 2008 Apr 26.

Fu Y, Luo N, Klein RL, Garvey WT (2005) Adiponectin promotes adipocyte differentiation, insulin sensitivity, and lipid accumulation. J Lipid Res. 46(7):1369-79. Epub 2005 Apr 16.

Fujimoto N, Matsuo N, Sumiyoshi H, Yamaguchi K, Saikawa T, Yoshimatsu H, Yoshioka H (2005) Adiponectin is expressed in the brown adipose tissue and surrounding immature tissues in mouse embryos. Biochim Biophys Acta. 1731(1):1-12. Epub 2005 Aug 22.

Furuhashi M, Hotamisligil GS (2008) Fatty acid-binding proteins: role in metabolic diseases and potential as drug targets. Nat Rev Drug Discov. 7(6):489-503.

Furuhashi M, Tuncman G, Görgün CZ, Makowski L, Atsumi G, Vaillancourt E, Kono K, Babaev VR, Fazio S, Linton MF, Sulsky R, Robl JA, Parker RA, Hotamisligil GS (2007) Treatment of diabetes and atherosclerosis by inhibiting fatty-acid-binding protein aP2. Nature. 447(7147):959-65. Epub 2007 Jun 6.

Gesta S, Tseng YH, Kahn CR (2007) Developmental origin of fat: tracking obesity to its source. Cell. 131(2):242-56.

Goldman RD, Gruenbaum Y, Moir RD, Shumaker DK, Spann TP (2002) Nuclear lamins: building blocks of nuclear architecture. Genes Dev. 16(5):533-47.

Green H, Kehinde O (1974) Sublines of mouse 3T3 cells that accumulate lipid. Cell. 1 (3):113-116.

Green H, Meuth M (1974) An established pre-adipose cell line and its differentiation in culture. Cell. 3(2):127-33.

Green H, Kehinde O (1975) An established preadipose cell line and its differentiation in culture. II. Factors affecting the adipose conversion. Cell. 5(1):19-27.

Green H, Kehinde O (1976) Spontaneous heritable changes leading to increased adipose conversion in 3T3 cells. Cell. 7(1):105-13.

Gregoire FM (2001) Adipocyte differentiation: from fibroblast to endocrine cell. Exp Biol Med (Maywood). 226(11):997-1002.

Gregoire FM, Smas CM, Sul HS (1998) Understanding adipocyte differentiation. Physiol Rev. 78(3):783-809.

Grimaldi P, Djian P, Negrel R, Ailhaud G (1982) Differentiation of Ob17 preadipocytes to adipocytes: requirement of adipose conversion factor(s) for fat cell cluster formation. EMBO J. 1(6):687-92.

Grimbaldeston MA, Pearce AL, Robertson BO, Coventry BJ, Marshman G, Finlay-Jones JJ, Hart PH (2004) Association between melanoma and dermal mast cell prevalence in sun-unexposed skin. Br J Dermatol. 150(5):895-903.

Grujic D, Susulic VS, Harper ME, Himms-Hagen J, Cunningham BA, Corkey BE, Lowell BB (1997) Beta3-adrenergic receptors on white and brown adipocytes mediate beta3-selective agonist-induced effects on energy expenditure, insulin secretion, and food intake. A study using transgenic and gene knockout mice. J Biol Chem. 272(28):17686-93.

Guerre-Millo M (2004) Adipose tissue and adipokines: for better or worse. Diabetes Metab. 30(1):13-9.

Guo X, Liao K (2000) Analysis of gene expression profile during 3T3-L1 preadipocyte differentiation. Gene. 251(1):45-53.

Gupta S, Iljin K, Sara H, Mpindi JP, Mirtti T, Vainio P, Rantala J, Alanen K, Nees M, Kallioniemi O (2010) FZD4 as a mediator of ERG oncogene-induced WNT signalling and epithelial-to-mesenchymal transition in human prostate cancer cells. Cancer Res. 70(17):6735-45. Epub 2010 Aug 16.

Hackl H, Burkard TR, Sturn A, Rubio R, Schleiffer A, Tian S, Quackenbush J, Eisenhaber F, Trajanoski Z (2005) Molecular processes during fat cell development revealed by gene expression profiling and functional annotation. Genome Biol. 6(13):R108. Epub 2005 Dec 19.

Haimoto H, Kato K, Suzuki F, Nagura H (1985) The ultrastructural changes of S-100 protein localization during lipolysis in adipocytes. An immunoelectron-microscopic study. Am J Pathol. 121(2):185-91.

Hajer GR, van Haeften TW, Visseren FL (2008) Adipose tissue dysfunction in obesity, diabetes, and vascular diseases. Eur Heart J. 29(24):2959-71. Epub 2008 Sep 5.

Haluzík M, Parízková J, Haluzík MM (2004) Adiponectin and its role in the obesity-induced insulin resistance and related complications. Physiol Res. 53(2):123-9.

Hardy MH (1992) The secret life of the hair follicle. Trends Genet. 8(2):55-61.

Harrington M, Pond-Tor S, Boney CM (2007) Role of epidermal growth factor and ErbB2 receptors in 3T3-L1 adipogenesis. Obesity (Silver Spring). 15(3):563-71.

Hatey F, Tosser-Klopp G, Clouscard-Martinato C, Mulsant P, Gasser F (1998) Expressed sequence tags for genes: a review. Genet Sel Evol. 30(6): 521–541.

Hausman GJ (1978). Cellular and histological aspects of developing adipose tissue. Proc. Recip. Meat. Conf. 31:35

Hausman GJ (1985) Cellular and enzyme-histochemical aspects of adipose tissue development in obese (Ossabaw) and lean (crossbred) pig fetuses: an ontogeny study. J Anim Sci. 60(6):1539-52.

Hausman GJ, Martin RJ (1982) The development of adipocytes located around hair follicles in the fetal pig. J Anim Sci. 54(6):1286-96.

Hausman GJ, Kauffman RG (1986) The histology of developing porcine adipose tissue. J Anim Sci. 63(2):642-58.

Hausman GJ, Richardson RL (1998) Newly recruited and pre-existing preadipocytes in cultures of porcine stromal-vascular cells: morphology, expression of extracellular matrix components, and lipid accretion. J Anim Sci. 76(1):48-60.

Hausman GJ, Campion DR, Richardson RL, Martin RJ (1981a) Adipocyte development in the rat hypodermis. Am J Anat. 161(1):85-100.

Hausman GJ, Campion DR, McNamara JP, Richardson RL, Martin RJ (1981b) Adipose tissue development in the fetal pig after decapitation. J Anim Sci. 53(6):1634-44.

Hebert LF Jr, Daniels MC, Zhou J, Crook ED, Turner RL, Simmons ST, Neidigh JL, Zhu JS, Baron AD, McClain DA (1996) Overexpression of glutamine:fructose-6-phosphate amidotransferase in transgenic mice leads to insulin resistance. J Clin Invest. 98(4):930-6.

Heller MJ (2002) DNA microarray technology: devices, systems, and applications. Annu Rev Biomed Eng. 4:129-53. Epub 2002 Mar 22.

Herzenberg LA, Parks D, Sahaf B, Perez O, Roederer M, Herzenberg LA (2002) The history and future of the fluorescence activated cell sorter and flow cytometry: a view from Stanford. Clin Chem. 48(10):1819-27.

Higgins CA, Richardson GD, Ferdinando D, Westgate GE, Jahoda CA (2010) Modelling the hair follicle dermal papilla using spheroid cell cultures. Exp Dermatol. 19(6):546-8. Epub 2010 Apr 20.

Hoggard N, Hunter L, Duncan JS, Williams LM, Trayhurn P, Mercer JG (1997) Leptin and leptin receptor mRNA and protein expression in the murine fetus and placenta. Proc Natl Acad Sci U S A. 94(20):11073-8.

Holm C (2003) Molecular mechanisms regulating hormone-sensitive lipase and lipolysis. Biochem Soc Trans. 31(Pt 6):1120-4.

Huo H, Guo X, Hong S, Jiang M, Liu X, Liao K (2003) Lipid rafts/caveolae are essential for insulin-like growth factor-1 receptor signaling during 3T3-L1 preadipocyte differentiation induction. J Biol Chem. 278(13):11561-9. Epub 2003 Jan 21.

Hugo ER, Brandebourg TD, Comstock CE, Gersin KS, Sussman JJ, Ben-Jonathan N (2006) LS14: a novel human adipocyte cell line that produces prolactin. Endocrinology. 147(1):306-13. Epub 2005 Sep 29.

Hui X, Zhu W, Wang Y, Lam KS, Zhang J, Wu D, Kraegen EW, Li Y, Xu A (2009) Major urinary protein-1 increases energy expenditure and improves glucose intolerance through enhancing mitochondrial function in skeletal muscle of diabetic mice. J Biol Chem. 284(21):14050-7. Epub 2009 Mar 31.

Hurst HC (1994) Transcription factors. 1: bZIP proteins. Protein Profile. 1(2):123-68.

Hutchison CJ (2002) Lamins: building blocks or regulators of gene expression? Nat Rev Mol Cell Biol. 3(11):848-58.

Huttunen P, Hirvonen J, Kinnula V (1981) The occurrence of brown adipose tissue in outdoor workers. Eur J Appl Physiol Occup Physiol. 46(4):339-45.

Iguchi M, Aiba S, Yoshino Y, Tagami H (2001) Human follicular papilla cells carry out nonadipose tissue production of leptin. J Invest Dermatol. 117(6):1349-56.

Ingalls AM, Dickie MM, Snell GD (1950) Obese, a new mutation in the house mouse. J Hered. 41(12):317-8.

Jahoda CA, Reynolds AJ (2001) Hair follicle dermal sheath cells: unsung participants in wound healing. Lancet. 358(9291):1445-8.

Jahoda CA, Whitehouse J, Reynolds AJ, Hole N (2003) Hair follicle dermal cells differentiate into adipogenic and osteogenic lineages. Exp Dermatol. 12(6):849-59.

Janke J, Engeli S, Boschmann M, Adams F, Böhnke J, Luft FC, Sharma AM, Jordan J (2006) Retinol-binding protein 4 in human obesity. Diabetes. 55(10):2805-10.

Janssen I, Katzmarzyk PT, Boyce WF, Vereecken C, Mulvihill C, Roberts C, Currie C, Pickett W (2005) Comparison of overweight and obesity prevalence in school-aged youth from 34 countries and their relationships with physical activity and dietary patterns. Obes Rev. 6(2):123-32.

Kamai Y, Mikawa S, Endo K, Sakai H, Komano T (1996) Regulation of insulin-like growth factor-I expression in mouse preadipocyte Ob1771 cells. J Biol Chem. 271(17):9883-6.

Kampf JP, Kleinfeld AM (2007) Is membrane transport of FFA mediated by lipid, protein, or both? An unknown protein mediates free fatty acid transport across the adipocyte plasma membrane. Physiology (Bethesda). 22:7-14.

Kamstrup M, Faurschou A, Gniadecki R, Wulf HC (2008) Epidermal stem cells - role in normal, wounded and pathological psoriatic and cancer skin. Curr Stem Cell Res Ther. 3(2):146-50.

Katoh Y, Katoh M (2005) Identification and characterization of rat Wnt1 and Wnt10b genes in silico. Int J Oncol. 26(3):841-5.

Kawai M, Namba N, Mushiake S, Etani Y, Nishimura R, Makishima M, Ozono K (2007) Growth hormone stimulates adipogenesis of 3T3-L1 cells through activation of the Stat5A/5B-PPARgamma pathway. J Mol Endocrinol. 38(1-2):19-34.

Keating GM (2010) Vildagliptin: a review of its use in type 2 diabetes mellitus. Drugs. 70(16):2089-112.

Kennell JA, MacDougald OA (2005) Wnt signaling inhibits adipogenesis through beta-catenin-dependent and -independent mechanisms. J Biol Chem. 280(25):24004-10. Epub 2005 Apr 22.

Khalyfa A, Bhushan B, Hegazi M, Kim J, Kheirandish-Gozal L, Bhattacharjee R, Capdevila OS, Gozal D (2010) Fatty-acid binding protein 4 gene variants and childhood obesity: potential implications for insulin sensitivity and CRP levels. Lipids Health Dis. 9:18.

Kim JB, Spiegelman BM (1996) ADD1/SREBP1 promotes adipocyte differentiation and gene expression linked to fatty acid metabolism. Genes Dev. 10(9):1096-107.

Kim S, Moustaid-Moussa N (2000) Secretory, endocrine and autocrine/paracrine function of the adipocyte. J Nutr. 130(12):3110S-3115S.

Kim SJ, Lee KH, Lee YS, Mun EG, Kwon DY, Cha YS (2007) Transcriptome analysis and promoter sequence studies on early adipogenesis in 3T3-L1 cells. Nutr Res Pract. 1(1):19-28. Epub 2007 Mar 31.

Klein S, Fontana L, Young VL, Coggan AR, Kilo C, Patterson BW, Mohammed BS (2004) Absence of an effect of liposuction on insulin action and risk factors for coronary heart disease. N Engl J Med. 350(25):2549-57.

Kopecky J, Clarke G, Enerbäck S, Spiegelman B, Kozak LP (1995) Expression of the mitochondrial uncoupling protein gene from the aP2 gene promoter prevents genetic obesity. J Clin Invest. 96(6):2914-23.

Kuri-Harcuch W, Marsch-Moreno M (1983) DNA synthesis and cell division related to adipose differentiation of 3T3 cells. J Cell Physiol. 114(1):39-44.

Kuri-Harcuch W, Argüello C, Marsch-Moreno M (1984) Extracellular matrix production by mouse 3T3-F442A cells during adipose differentiation in culture. Differentiation. 28: 173–178.

Lako M, Armstrong L, Cairns PM, Harris S, Hole N, Jahoda CA (2002) Hair follicle dermal cells repopulate the mouse haematopoietic system. J Cell Sci. 115(Pt 20):3967-74.

Landschulz WH, Johnson PF, Adashi EY, Graves BJ, McKnight SL (1988) Isolation of a recombinant copy of the gene encoding C/EBP. Genes Dev. 2(7):786-800.

Large V, Peroni O, Letexier D, Ray H, Beylot M (2004) Metabolism of lipids in human white adipocyte. Diabetes Metab. 30(4):294-309.

Lee KK, Haraguchi T, Lee RS, Koujin T, Hiraoka Y, Wilson KL (2001) Distinct functional domains in emerin bind lamin A and DNA-bridging protein BAF. J Cell Sci. 114(Pt 24):4567-73.

Lee CH, Olson P, Evans RM (2003) Minireview: lipid metabolism, metabolic diseases, and peroxisome proliferator-activated receptors. Endocrinology. 144(6):2201-7.

Lee YH, Nair S, Rousseau E, Allison DB, Page GP, Tataranni PA, Bogardus C, Permana PA (2005) Microarray profiling of isolated abdominal subcutaneous adipocytes from obese vs non-obese Pima Indians: increased expression of inflammation-related genes. Diabetologia. 48(9):1776-83. Epub 2005 Jul 30

Lehmann JM, Moore LB, Smith-Oliver TA, Wilkison WO, Willson TM, Kliewer SA (1995) An antidiabetic thiazolidinedione is a high affinity ligand for peroxisome proliferator-activated receptor gamma (PPAR gamma). J Biol Chem. 270(22):12953-6.

Li D, Yea S, Li S, Chen Z, Narla G, Banck M, Laborda J, Tan S, Friedman JM, Friedman SL, Walsh MJ (2005) Krüppel-like factor-6 promotes preadipocyte differentiation through histone deacetylase 3-dependent repression of DLK1. J Biol Chem. 280(29):26941-52. Epub 2005 May 25.

Linhart HG, Ishimura-Oka K, DeMayo F, Kibe T, Repka D, Poindexter B, Bick RJ, Darlington GJ (2001) C/EBPalpha is required for differentiation of white, but not brown, adipose tissue. Proc Natl Acad Sci U S A. 98(22):12532-7. Epub 2001 Oct 16.

Litthauer D, Serrero G (1992) The primary culture of mouse adipocyte precursor cells in defined medium. Comp Biochem Physiol A Comp Physiol. 101(1):59-64.

Lu HL, Wang HW, Wen Y, Zhang MX, Lin HH (2006) Roles of adipocyte derived hormone adiponectin and resistin in insulin resistance of type 2 diabetes. World J Gastroenterol. 12(11):1747-51.

Lucarz A, Brand G (2007) Current considerations about Merkel cells. Eur J Cell Biol. 86(5):243-51. Epub 2007 Mar 6.

Lynch CJ, Brennan WA Jr, Vary TC, Carter N, Dodgson SJ (1993a) Carbonic anhydrase III in obese Zucker rats. Am J Physiol. 264(4 Pt 1):E621-30.

Lynch CJ, Hazen SA, Horetsky RL, Carter ND, Dodgson SJ (1993b) Differentiation-dependent expression of carbonic anhydrase II and III in 3T3 adipocytes. Am J Physiol. 265(1 Pt 1):C234-43.

Maffei M, Halaas J, Ravussin E, Pratley RE, Lee GH, Zhang Y, Fei H, Kim S, Lallone R, Ranganathan S, et al. (1995) Leptin levels in human and rodent: measurement of plasma leptin and ob RNA in obese and weight-reduced subjects. Nat Med. 1(11):1155-61.

Magun R, Burgering BM, Coffer PJ, Pardasani D, Lin Y, Chabot J, Sorisky A (1996) Expression of a constitutively activated form of protein kinase B (c-Akt) in 3T3-L1 preadipose cells causes spontaneous differentiation. Endocrinology. 137(8):3590-3.

Makowski L, Hotamisligil GS (2004) Fatty acid binding proteins--the evolutionary crossroads of inflammatory and metabolic responses. J Nutr. 134(9):2464S-2468S.

Mandy FF, Bergeron M, Minkus T (1995) Principles of flow cytometry. Transfus Sci. 16(4):303-14.

Margetic S, Gazzola C, Pegg GG, Hill RA (2002) Leptin: a review of its peripheral actions and interactions. Int J Obes Relat Metab Disord. 2002 Nov;26(11):1407-33.

Mariman EC, Wang P (2010) Adipocyte extracellular matrix composition, dynamics and role in obesity. Cell Mol Life Sci. 67(8):1277-92. Epub 2010 Jan 27.

Martinez-Botas J, Anderson JB, Tessier D, Lapillonne A, Chang BH, Quast MJ, Gorenstein D, Chen KH, Chan L (2000) Absence of perilipin results in leanness and reverses obesity in Lepr (db/db) mice. Nat Genet. 26(4):474-9.

Massiera F, Seydoux J, Geloen A, Quignard-Boulange A, Turban S, Saint-Marc P, Fukamizu A, Negrel R, Ailhaud G, Teboul M (2001) Angiotensinogen-deficient mice exhibit impairment of diet-induced weight gain with alteration in adipose tissue development and increased locomotor activity. Endocrinology. 142(12):5220-5.

McGrath, J. A., Eady, R. A. J. and Pope, F. M. (2008) Anatomy and Organization of Human Skin, in Rook's Textbook of Dermatology, Seventh Edition (eds T. Burns, S. Breathnach, N. Cox and C. Griffiths), Blackwell Publishing, Inc., Malden, Massachusetts, USA. doi: 10.1002/9780470750520.ch3

Meex SJ, van der Kallen CJ, van Greevenbroek MM, Eurlings PM, El Hasnaoui M, Evelo CT, Lindsey PJ, Luiken JJ, Glatz JF, de Bruin TW (2005) Up-regulation of CD36/FAT in preadipocytes in familial combined hyperlipidemia. FASEB J. 19(14):2063-5. Epub 2005 Oct 11.

Mei B, Zhao L, Chen L, Sul HS (2002) Only the large soluble form of preadipocyte factor-1 (Pref-1), but not the small soluble and membrane forms, inhibits adipocyte differentiation: role of alternative splicing. Biochem J. 364(Pt 1):137-44.

Merad M, Ginhoux F, Collin M (2008) Origin, homeostasis and function of Langerhans cells and other langerin-expressing dendritic cells. Nat Rev Immunol. 8(12):935-47.

Mersmann HJ, Goodman JR, Brown LJ (1975) Development of swine adipose tissue: morphology and chemical composition. J Lipid Res. 16(4):269-79.

Millar SE (2002) Molecular mechanisms regulating hair follicle development. J Invest Dermatol. 118(2):216-25.

Misago N, Toda S, Sugihara H, Kohda H, Narisawa Y (1998) Proliferation and differentiation of organoid hair follicle cells co-cultured with fat cells in collagen gel matrix culture. Br J Dermatol. 139(1):40-8.

Moldes M, Zuo Y, Morrison RF, Silva D, Park BH, Liu J, Farmer SR (2003) Peroxisome-proliferator-activated receptor gamma suppresses Wnt/beta-catenin signalling during adipogenesis. Biochem J. 376(Pt 3):607-13.

Mori T, Sakaue H, Iguchi H, Gomi H, Okada Y, Takashima Y, Nakamura K, Nakamura T, Yamauchi T, Kubota N, Kadowaki T, Matsuki Y, Ogawa W, Hiramatsu R, Kasuga M (2005) Role of Krüppel-like factor 15 (KLF15) in transcriptional regulation of adipogenesis. J Biol Chem. 280(13):12867-75. Epub 2005 Jan 20.

Morrison RF, Farmer SR (1999) Role of PPARgamma in regulating a cascade expression of cyclin-dependent kinase inhibitors, p18 (INK4c) and p21(Waf1/Cip1), during adipogenesis. J Biol Chem. 274(24):17088-97.

Moustaïd N, Hainque B, Quignard-Boulangé A (1988) Dexamethasone regulation of terminal differentiation in 3T3-F442A preadipocyte cell line. Cytotechnology. 1(4): 285-293.

Münzberg H, Myers MG Jr (2005) Molecular and anatomical determinants of central leptin resistance. Nat Neurosci. 8(5):566-70.

Murillas R, Larcher F, Conti CJ, Santos M, Ullrich A, Jorcano JL (1995) Expression of a dominant negative mutant of epidermal growth factor receptor in the epidermis of transgenic mice elicits striking alterations in hair follicle development and skin structure. EMBO J. 14(21):5216-23.

Nakamura T, Shiojima S, Hirai Y, Iwama T, Tsuruzoe N, Hirasawa A, Katsuma S, Tsujimoto G (2003) Temporal gene expression changes during adipogenesis in human mesenchymal stem cells. Biochem Biophys Res Commun. 303(1):306-12.

Neely KA, Quillen DA, Schachat AP, Gardner TW, Blankenship GW (1998) Diabetic retinopathy. Med Clin North Am. 82(4):847-76.

Négrel R, Grimaldi P, Ailhaud G (1978) Establishment of preadipocyte clonal line from epididymal fat pad of ob/ob mouse that responds to insulin and to lipolytic hormones. Proc Natl Acad Sci U S A. 75(12):6054-8.

Nishizuka M, Koyanagi A, Osada S, Imagawa M (2008) Wnt4 and Wnt5a promote adipocyte differentiation. FEBS Lett. 582(21-22):3201-5. Epub 2008 Aug 15.

Nogales-Cadenas R, Carmona-Saez P, Vazquez M, Vicente C, Yang X, Tirado F, Carazo JM, Pascual-Montano A (2009) GeneCodis: interpreting gene lists through enrichment analysis and integration of diverse biological information. Nucleic Acids Res. 37(Web Server issue):W317-22. Epub 2009 May 22.

Nosjean O, Boutin JA (2002) Natural ligands of PPARgamma: are prostaglandin J(2) derivatives really playing the part? Cell Signal. 14(7):573-83.

Oishi Y, Manabe I, Tobe K, Tsushima K, Shindo T, Fujiu K, Nishimura G, Maemura K, Yamauchi T, Kubota N, Suzuki R, Kitamura T, Akira S, Kadowaki T, Nagai R (2005) Krüppel-like transcription factor KLF5 is a key regulator of adipocyte differentiation. Cell Metab. 1(1):27-39.

Olivera-Martinez I, Thélu J, Dhouailly D (2004) Molecular mechanisms controlling dorsal dermis generation from the somitic dermomyotome. Int J Dev Biol. 48(2-3):93-101.

Osada S, Yamamoto H, Nishihara T, Imagawa M (1996) DNA binding specificity of the CCAAT/enhancer-binding protein transcription factor family. J Biol Chem. 271(7):3891-6.

Öst A, Örtegren U, Gustavsson J, Nystrom FH, Strålfors P (2005) Triacylglycerol is synthesized in a specific subclass of caveolae in primary adipocytes. J Biol Chem. 280(1):5-8. Epub 2004 Nov 9.

Pairault J, Lasnier F (1987) Control of the adipogenic differentiation of 3T3-F442A cells by retinoic acid, dexamethasone, and insulin: a topographic analysis. J Cell Physiol. 132(2):279-86.

Pearce J (1983) Fatty acid synthesis in liver and adipose tissue. Proc Nutr Soc. 42(2):263-71.

Pei H, Yao Y, Yang Y, Liao K, Wu JR (2011) Krüppel-like factor KLF9 regulates PPARγ transactivation at the middle stage of adipogenesis. Cell Death Differ. 18(2):315-27. Epub 2010 Aug 20.

Peter MA, Winterhalter KH, Böni-Schnetzler M, Froesch ER, Zapf J (1993) Regulation of insulin-like growth factor-I (IGF-I) and IGF-binding proteins by growth hormone in rat white adipose tissue. Endocrinology. 133(6):2624-31.

Picardo M, Ottaviani M, Camera E, Mastrofrancesco A (2009) Sebaceous gland lipids. Dermatoendocrinol. 1(2):68-71.

Plikus MV, Mayer JA, de la Cruz D, Baker RE, Maini PK, Maxson R, Chuong CM (2008) Cyclic dermal BMP signalling regulates stem cell activation during hair regeneration. Nature. 451(7176):340-4.

Plikus MV, Widelitz RB, Maxson R, Chuong CM (2009) Analyses of regenerative wave patterns in adult hair follicle populations reveal macro-environmental regulation of stem cell activity. Int J Dev Biol. 53(5-6):857-68.

Plikus MV, Baker RE, Chen CC, Fare C, de la Cruz D, Andl T, Maini PK, Millar SE, Widelitz R, Chuong CM (2011) Self-organizing and stochastic behaviors during the regeneration of hair stem cells. Science. 332(6029):586-9.

Poeggeler B, Schulz C, Pappolla MA, Bodó E, Tiede S, Lehnert H, Paus R (2010) Leptin and the skin: a new frontier. Exp Dermatol. 19(1):12-8. Epub 2009 Jul 8.

Pohl J, Ring A, Korkmaz U, Ehehalt R, Stremmel W (2005) FAT/CD36-mediated long-chain fatty acid uptake in adipocytes requires plasma membrane rafts. Mol Biol Cell. 16(1):24-31. Epub 2004 Oct 20.

Poissonnet CM, Burdi AR, Garn SM (1984) The chronology of adipose tissue appearance and distribution in the human fetus. Early Hum Dev. 10(1-2):1-11.

Porter SA, Massaro JM, Hoffmann U, Vasan RS, O'Donnel CJ, Fox CS (2009) Abdominal subcutaneous adipose tissue: a protective fat depot? Diabetes Care. 32(6):1068-75. Epub 2009 Feb 24.

Poulos SP, Hausman DB, Hausman GJ (2010) The development and endocrine functions of adipose tissue. Mol Cell Endocrinol. 323(1):20-34. Epub 2009 Dec 16.

Prestwich TC, Macdougald OA (2007) Wnt/beta-catenin signaling in adipogenesis and metabolism. Curr Opin Cell Biol. 19(6):612-7. Epub 2007 Nov 9.

Puhl RM, Heuer CA (2009) The stigma of obesity: a review and update. Obesity (Silver Spring). 17(5):941-64. Epub 2009 Jan 22.

Qiu J, Ogus S, Lu R, Chehab FF (2001) Transgenic mice overexpressing leptin accumulate adipose mass at an older, but not younger, age. Endocrinology. 142(1):348-58.

Ramis JM, Franssen-van Hal NL, Kramer E, Llado I, Bouillaud F, Palou A, Keijer J (2002) Carboxypeptidase E and thrombospondin-1 are differently expressed in subcutaneous and visceral fat of obese subjects. Cell Mol Life Sci. 59(11):1960-71.

Ramji DP, Foka P (2002) CCAAT/enhancer-binding proteins: structure, function and regulation. Biochem J. 365(Pt 3):561-75.

Raslova K (2010) An update on the treatment of type 1 and type 2 diabetes mellitus: focus on insulin detemir, a long-acting human insulin analog. Vasc Health Risk Manag. 6:399-410.

Reaven G, Abbasi F, McLaughlin T (2004) Obesity, insulin resistance, and cardiovascular disease. Recent Prog Horm Res. 2004;59:207-23.

Richardson GD, Arnott EC, Whitehouse CJ, Lawrence CM, Hole N, Jahoda CA (2005) Cultured cells from the adult human hair follicle dermis can be directed toward adipogenic and osteogenic differentiation. J Invest Dermatol. 124(5):1090-1.

Richardson GD, Bazzi H, Fantauzzo KA, Waters JM, Crawford H, Hynd P, Christiano AM, Jahoda CA (2009) KGF and EGF signalling block hair follicle induction and promote interfollicular epidermal fate in developing mouse skin. Development. 136(13):2153-64. Epub 2009 May 27.

Richon VM, Lyle RE, McGehee RE Jr (1997) Regulation and expression of retinoblastoma proteins p107 and p130 during 3T3-L1 adipocyte differentiation. J Biol Chem. 272(15):10117-24.

Rodrigue-Way A, Demers A, Ong H, Tremblay A (2007) A growth hormone-releasing peptide promotes mitochondrial biogenesis and a fat burning-like phenotype through scavenger receptor CD36 in white adipocytes. Endocrinology. 148(3):1009-18. Epub 2006 Nov 30.

Rosen ED (2003) Energy balance: a new role for PPARa. Curr. Biol. 13: 961-963.

Rosen ED (2005) The transcriptional basis of adipocyte development. Prostaglandins Leukot Essent Fatty Acids. 73(1):31-4.

Rosen ED, Spiegelman BM (2000) Molecular regulation of adipogenesis. Annu Rev Cell Dev Biol. 16:145-71.

Rosen ED, Hsu CH, Wang X, Sakai S, Freeman MW, Gonzalez FJ, Spiegelman BM (2002) C/EBPalpha induces adipogenesis through PPARgamma: a unified pathway. Genes Dev. 2002 Jan 1;16(1):22-6.

Ross AS, Tsang R, Shewmake K, McGehee RE Jr (2008) Expression of p107 and p130 during human adipose-derived stem cell adipogenesis. Biochem Biophys Res Commun. 366(4):927-31. Epub 2007 Dec 18.

Ross SE, Hemati N, Longo KA, Bennett CN, Lucas PC, Erickson RL, MacDougald OA (2000) Inhibition of adipogenesis by Wnt signaling. Science. 289(5481):950-3.

Ross SE, Erickson RL, Gerin I, DeRose PM, Bajnok L, Longo KA, Misek DE, Kuick R, Hanash SM, Atkins KB, Andresen SM, Nebb HI, Madsen L, Kristiansen K, MacDougald OA (2002) Microarray analyses during adipogenesis: understanding the effects of Wnt signaling on adipogenesis and the roles of liver X receptor alpha in adipocyte metabolism. Mol Cell Biol. 22(16):5989-99.

Ruan W, Lai M (2010) Insulin-like growth factor binding protein: a possible marker for the metabolic syndrome? Acta Diabetol. 47(1):5-14. Epub 2009 Sep 22.

Samulin J, Berget I, Lien S, Sundvold H (2008) Differential gene expression of fatty acid binding proteins during porcine adipogenesis. Comp Biochem Physiol B Biochem Mol Biol. 151(2):147-52. Epub 2008 Jun 22.

Schaedlich K, Knelangen JM, Santos AN, Fischer B, Santos AN (2010) A simple method to sort ESC-derived adipocytes. Cytometry A. [Epub ahead of print]

Schafer KA (1998) The cell cycle: a review. Vet Pathol. 35(6):461-78.

Schmidt-Ullrich R, Paus R (2005) Molecular principles of hair follicle induction and morphogenesis. Bioessays. 27(3):247-61.

Schneider MR, Schmidt-Ullrich R, Paus R (2009) The hair follicle as a dynamic miniorgan. Curr Biol. 19(3):R132-42.

Schoonjans K, Staels B, Auwerx J (1996) The peroxisome proliferator activated receptors (PPARS) and their effects on lipid metabolism and adipocyte differentiation. Biochim Biophys Acta. 1302(2):93-109.

Schröder JM (2010) The role of keratinocytes in defense against infection. Curr Opin Infect Dis. 23(2):106-10.

Seale P, Lazar MA (2009) Brown fat in humans: turning up the heat on obesity. Diabetes. 58(7):1482-4.

Seger R, Krebs EG (1995) The MAPK signaling cascade. FASEB J. 9(9):726-35.

Serria MS, Ikeda H, Omoteyama K, Hirokawa J, Nishi S, Sakai M (2003) Regulation and differential expression of the c-maf gene in differentiating cultured cells. Biochem Biophys Res Commun. 310(2):318-26.

Sfeir Z, Ibrahimi A, Amri E, Grimaldi P, Abumrad N (1999) CD36 antisense expression in 3T3-F442A preadipocytes. Mol Cell Biochem. 192(1-2):3-8.

Shepherd PR, Gnudi L, Tozzo E, Yang H, Leach F, Kahn BB (1993) Adipose cell hyperplasia and enhanced glucose disposal in transgenic mice overexpressing GLUT4 selectively in adipose tissue. J Biol Chem. 268(30):22243-6.

Shergill IS, Shergill NK, Arya M, Patel HR (2004) Tissue microarrays: a current medical research tool. Curr Med Res Opin. 20(5):707-12.

Shimazu K, Toda S, Miyazono M, Sakemi T, Sugihara H (2001) Morphogenesis of MDCK cells in a collagen gel matrix culture under stromal adipocyte-epithelial cell interaction. Kidney Int. 60(2):568-78.

Ship JA (2003) Diabetes and oral health: an overview. J Am Dent Assoc. 134 Spec No:4S-10S.

Simpson MA, LiCata VJ, Ribarik Coe N, Bernlohr DA (1999) Biochemical and biophysical analysis of the intracellular lipid binding proteins of adipocytes. Mol Cell Biochem. 192(1-2):33-40.

Smalley MJ, Dale TC (1999) Wnt signalling in mammalian development and cancer. Cancer Metastasis Rev. 18(2):215-30.

Smas CM, Sul HS (1993) Pref-1, a protein containing EGF-like repeats, inhibits adipocyte differentiation. Cell. 73(4):725-34.

Smith PJ, Wise LS, Berkowitz R, Wan C, Rubin CS (1988) Insulin-like growth factor-I is an essential regulator of the differentiation of 3T3-L1 adipocytes. J Biol Chem. 263(19):9402-8.

Sorrell JM, Caplan AI (2004) Fibroblast heterogeneity: more than skin deep. J Cell Sci. 117(Pt 5):667-75.

Soukas A, Socci ND, Saatkamp BD, Novelli S, Friedman JM (2001) Distinct transcriptional profiles of adipogenesis in vivo and in vitro. J Biol Chem. 276(36):34167-74. Epub 2001 Jul 9.

Spiegelman BM, Farmer SR (1982) Decreases in tubulin and actin gene expression prior to morphological differentiation of 3T3 adipocytes. Cell. 1982 May;29(1):53-60.

Sue N, Jack BH, Eaton SA, Pearson RC, Funnell AP, Turner J, Czolij R, Denyer G, Bao S, Molero-Navajas JC, Perkins A, Fujiwara Y, Orkin SH, Bell-Anderson K, Crossley M (2008) Targeted disruption of the basic Krüppel-like factor gene (Klf3) reveals a role in adipogenesis. Mol Cell Biol. 28(12):3967-78. Epub 2008 Apr 7.

Sugawara K, Schneider MR, Dahlhoff M, Kloepper JE, Paus R (2010) Cutaneous consequences of inhibiting EGF receptor signaling in vivo: normal hair follicle development, but retarded hair cycle induction and inhibition of adipocyte growth in Egfr(Wa5) mice. J Dermatol Sci. 57(3):155-61. Epub 2010 Jan 8.

Sugihara H, Toda S, Yonemitsu N, Watanabe K (2001) Effects of fat cells on keratinocytes and fibroblasts in a reconstructed rat skin model using collagen gel matrix culture. Br J Dermatol. 2001 Feb;144(2):244-53.

Suhre K, Römisch-Margl W, de Angelis MH, Adamski J, Luippold G, Augustin R (2011) Identification of a potential biomarker for FABP4 inhibition: the power of lipidomics in preclinical drug testing. J Biomol Screen. 16(5):467-75. Epub 2011 May 4.

Sun J, Zhuang FF, Mullersman JE, Chen H, Robertson EJ, Warburton D, Liu YH, Shi W (2006) BMP4 activation and secretion are negatively regulated by an intracellular gremlin-BMP4 interaction. J Biol Chem. 281(39):29349-56. Epub 2006 Jul 31.

Swierczynski J, Zabrocka L, Goyke E, Raczynska S, Adamonis W, Sledzinski Z (2003) Enhanced glycerol 3-phosphate dehydrogenase activity in adipose tissue of obese humans. Mol Cell Biochem. 254(1-2):55-9.

Sydow K, Mondon CE, Cooke JP (2005) Insulin resistance: potential role of the endogenous nitric oxide synthase inhibitor ADMA. Vasc Med. 10 Suppl 1:S35-43.

Tansey JT, Sztalryd C, Gruia-Gray J, Roush DL, Zee JV, Gavrilova O, Reitman ML, Deng CX, Li C, Kimmel AR, Londos C (2001) Perilipin ablation results in a lean mouse with aberrant adipocyte lipolysis, enhanced leptin production, and resistance to diet-induced obesity. Proc Natl Acad Sci U S A. 98(11):6494-9.

Taylor G, Lehrer MS, Jensen PJ, Sun TT, Lavker RM (2000) Involvement of follicular stem cells in forming not only the follicle but also the epidermis. Cell. 102(4):451-61.

Thörne A, Lönnqvist F, Apelman J, Hellers G, Arner P (2002) A pilot study of long-term effects of a novel obesity treatment: omentectomy in connection with adjustable gastric banding. Int J Obes Relat Metab Disord. 26(2):193-9.

Timchenko NA, Wilde M, Nakanishi M, Smith JR, Darlington GJ (1996) CCAAT/enhancer-binding protein alpha (C/EBP alpha) inhibits cell proliferation through the p21 (WAF-1/CIP-1/SDI-1) protein. Genes Dev. 10(7):804-15.

Toda S, Uchihashi K, Aoki S, Sonoda E, Yamasaki F, Piao M, Ootani A, Yonemitsu N, Sugihara H (2009) Adipose tissue-organotypic culture system as a promising model for studying adipose tissue biology and regeneration. Organogenesis. 5(2):50-6.

Todaro GJ, Green H (1963) Quantitative studies of the growth of mouse embryo cells in culture and their development into established lines. J Cell Biol. 17:299-313.

Toma JG, Akhavan M, Fernandes KJ, Barnabé-Heider F, Sadikot A, Kaplan DR, Miller FD (2001) Isolation of multipotent adult stem cells from the dermis of mammalian skin. Nat Cell Biol. 3(9):778-84.

Tontonoz P, Hu E, Spiegelman BM (1994) Stimulation of adipogenesis in fibroblasts by PPAR gamma 2, a lipid-activated transcription factor. Cell. 79(7):1147-56.

Tran TT, Kahn CR (2010) Transplantation of adipose tissue and stem cells: role in metabolism and disease. Nat Rev Endocrinol. 6(4):195-213. Epub 2010 Mar 2.

Tran TT, Yamamoto Y, Gesta S, Kahn CR (2008) Beneficial effects of subcutaneous fat transplantation on metabolism. Cell Metab. 7(5):410-20.

Tsai J, Tong Q, Tan G, Chang AN, Orkin SH, Hotamisligil GS (2005) The transcription factor GATA2 regulates differentiation of brown adipocytes. EMBO Rep. 6(9):879-84.

Tsatmali M, Ancans J, Thody AJ (2002) Melanocyte function and its control by melanocortin peptides. J Histochem Cytochem. 50(2):125-33.

Tsoi E, Shaikh H, Robinson S, Teoh TG (2010) Obesity in pregnancy: a major healthcare issue. Postgrad Med J. 86(1020):617-23.

Tuncman G, Erbay E, Hom X, De Vivo I, Campos H, Rimm EB, Hotamisligil GS (2006) A genetic variant at the fatty acid-binding protein aP2 locus reduces the risk for hypertriglyceridemia, type 2 diabetes, and cardiovascular disease. Proc Natl Acad Sci U S A. 103(18):6970-5. Epub 2006 Apr 25.

Uppenberg J, Svensson C, Jaki M, Bertilsson G, Jendeberg L, Berkenstam A (1998) Crystal structure of the ligand binding domain of the human nuclear receptor PPARgamma. J Biol Chem. 273(47):31108-12.

Urs S, Smith C, Campbell B, Saxton AM, Taylor J, Zhang B, Snoddy J, Jones Voy B, Moustaid-Moussa N (2004) Gene expression profiling in human preadipocytes and adipocytes by microarray analysis. J Nutr. 134(4):762-70.

Urs S, Harrington A, Liaw L, Small D (2006) Selective expression of an aP2/Fatty Acid Binding Protein 4-Cre transgene in non-adipogenic tissues during embryonic development. Transgenic Res. 15(5):647-53. Epub 2006 Sep 2.

Valet P, Tavernier G, Castan-Laurell I, Saulnier-Blache JS, Langin D (2002) Understanding adipose tissue development from transgenic animal models. J Lipid Res. 43(6):835-60.

Vaughan A, Alvarez-Reyes M, Bridger JM, Broers JL, Ramaekers FC, Wehnert M, Morris GE, Whitfield WGF, Hutchison CJ (2001) Both emerin and lamin C depend on lamin A for localization at the nuclear envelope. J Cell Sci. 114(Pt 14):2577-90.

Vuorisalo S, Venermo M, Lepäntalo M (2009) Treatment of diabetic foot ulcers. J Cardiovasc Surg (Torino). 50(3):275-91.

Wade FM, Wakade C, Mahesh VB, Brann DW (2005) Differential expression of the peripheral benzodiazepine receptor and gremlin during adipogenesis. Obes Res. 13(5):818-22.

Wagers AJ, Weissman IL (2004) Plasticity of adult stem cells. Cell. 116(5):639-48.

Wajchenberg BL (2000) Subcutaneous and visceral adipose tissue: their relation to the metabolic syndrome. Endocr Rev. 21(6):697-738.

Wajchenberg BL, Feitosa AC, Rassi N, Lerário AC, Betti RT (2008) Glycemia and cardiovascular disease in type 1 diabetes mellitus. Endocr Pract. 14(7):912-23.

Wallenius V, Wallenius K, Ahrén B, Rudling M, Carlsten H, Dickson SL, Ohlsson C, Jansson JO (2002) Interleukin-6-deficient mice develop mature-onset obesity. Nat Med. 8(1):75-9.

Wang ND, Finegold MJ, Bradley A, Ou CN, Abdelsayed SV, Wilde MD, Taylor LR, Wilson DR, Darlington GJ (1995) Impaired energy homeostasis in C/EBP alpha knockout mice. Science. 269(5227):1108-12.

Wang Y, Kim KA, Kim JH, Sul HS (2006a) Pref-1, a preadipocyte secreted factor that inhibits adipogenesis. J Nutr. 136(12):2953-6.

Wang H, Li H, Wang Q, Wang Y, Han H, Shi H (2006b) Microarray analysis of adipose tissue gene expression profiles between two chicken breeds. J Biosci. 31(5):565-73.

Wang Q, Guan T, Li H, Bernlohr DA (2009) A novel polymorphism in the chicken adipocyte fatty acid-binding protein gene (FABP4) that alters ligand-binding and correlates with fatness. Comp Biochem Physiol B Biochem Mol Biol. 154(3):298-302. Epub 2009 Jul 10.

Wang Y, Hudak C, Sul HS (2010) Role of preadipocyte factor 1 in adipocyte differentiation. Clin Lipidol. 5(1):109-115.

White UA, Stephens JM (2010) Transcriptional factors that promote formation of white adipose tissue. Mol Cell Endocrinol. 318(1-2):10-4. Epub 2009 Sep 4.

Whitelaw AG (1976) Influence of maternal obesity on subcutaneous fat in the newborn. Br Med J. 1(6016):985-6.

Wojciechowicz K, Markiewicz E, Jahoda CA (2008) C/EBPalpha identifies differentiating preadipocytes around hair follicles in foetal and neonatal rat and mouse skin. Exp Dermatol. 2008 Aug;17(8):675-80. Epub 2008 Mar 4.

Wolnicka-Glubisz A, King W, Noonan FP (2005) SCA-1+ cells with an adipocyte phenotype in neonatal mouse skin. J Invest Dermatol. 125(2):383-5.

Wu Z, Rosen ED, Brun R, Hauser S, Adelmant G, Troy AE, McKeon C, Darlington GJ, Spiegelman BM (1999) Cross-regulation of C/EBP alpha and PPAR gamma controls the transcriptional pathway of adipogenesis and insulin sensitivity. Mol Cell. 3(2):151-8.

Xie H, Lim B, Lodish HF (2009) MicroRNAs induced during adipogenesis that accelerate fat cell development are downregulated in obesity. Diabetes. 58(5):1050-7. Epub 2009 Feb 2.

Xiong C, Xie CQ, Zhang L, Zhang J, Xu K, Fu M, Thompson WE, Yang LJ, Chen YE (2005) Derivation of adipocytes from human embryonic stem cells. Stem Cells Dev. 2005 Dec;14(6):671-5.

Yang R, Castriota G, Chen Y, Cleary MA, Ellsworth K, Shin MK, Tran JL, Vogt TF, Wu M, Xu S, Yang X, Zhang BB, Berger JP, Qureshi SA (2010a) RNAi-mediated germline knockdown of FABP4 increases body weight but does not improve the deranged nutrient metabolism of diet-induced obese mice. Int J Obes (Lond). [Epub ahead of print]

Yang X, Lu X, Lombès M, Rha GB, Chi YI, Guerin TM, Smart EJ, Liu J (2010b) The G(0)/G(1) switch gene 2 regulates adipose lipolysis through association with adipose triglyceride lipase. Cell Metab. 11(3):194-205.

Yarwood SJ, Anderson NG, Kilgour E (1995) Cyclic AMP modulates adipogenesis in 3T3-F442A cells. Biochem Soc Trans. 23(2):175S.

Yokoyama C, Wang X, Briggs MR, Admon A, Wu J, Hua X, Goldstein JL, Brown MS (1993) SREBP-1, a basic-helix-loop-helix-leucine zipper protein that controls transcription of the low density lipoprotein receptor gene. Cell. 75(1):187-97.

Yuan JS, Reed A, Chen F, Stewart CN Jr (2006) Statistical analysis of real-time PCR data. BMC Bioinformatics. Feb 22;7:85.

Zandbergen F, Mandard S, Escher P, Tan NS, Patsouris D, Jatkoe T, Rojas-Caro S, Madore S, Wahli W, Tafuri S, Müller M, Kersten S (2005) The G0/G1 switch gene 2 is a novel PPAR target gene. Biochem J. 392(Pt 2):313-24.

Zhang Y, Proenca R, Maffei M, Barone M, Leopold L, Friedman JM (1994) Positional cloning of the mouse obese gene and its human homologue. Nature. 372(6505):425-32.

Zhu Y, Qi C, Korenberg JR, Chen XN, Noya D, Rao MS, Reddy JK (1995) Structural organization of mouse peroxisome proliferator-activated receptor gamma (mPPAR gamma) gene: alternative promoter use and different splicing yield two mPPAR gamma isoforms. Proc Natl Acad Sci U S A. 92(17):7921-5.

## Appendix I

## Reagents and working solutions. Part A.

Immunofluorescence staining and the Oil Red O staining (reagents in alphabetical order):

| | |
|---|---|
| Calcium formal solution (100 ml)<br>(4% formaldehyde. 1% calcium chloride): | Prepare 100 ml of 4% formaldehyde (from 37% formaldehyde solution; Sigma) in $H_2O$*.<br>Add calcium chloride (granular anhydrous; Sigma) to 4% formaldehyde to a final volume of 1%. |
| Mowiol (Stock): | 6 g glycerol<br>2.4 g mowiol (mowiol 4-88)<br>6 ml $H_2O$*<br>12 ml 0.2 M Tris (pH 6.8)<br>Leave stirring over-night at 37$^{o}$C then leave for 10 min at 50$^{o}$C. Centrifuge and add to a supernatant DABCO (1.4-diazobicylo-(2.2.2)-octane) to final concentration of 2.5%. Aliquots (500 µl) kept in -20$^{o}$C. |
| 4 % paraformaldehyde (100 ml): | Add slowly 4 g of paraformaldehyde (Sigma) to PBS (up to 100 ml) and warm it up (50 - 60$^{o}$C) till it dissolves and is transparent. |
| PBS - Phosphate buffered saline (5 liters): | 40.00 g NaCl<br>9.03 g $Na_2HPO_4$ $2H_2O$ or 7.2 g $Na_2HPO_4$<br>1.45 g $KH_2PO_4$<br>1.00 g KCl<br>Adjust pH to 7.4<br>Up to 5 liters of $H_2O$* |
| 1.0 M Tris buffer; pH 6.8 (1 liter): | 121.14 g Tris base<br>Adjust pH to 6.8<br>Up to 1 liter of $H_2O$* |
| 0.2 M Tris buffer; pH 6.8 (100 ml): | 20 ml 1.0 M Tris (pH 6.8)<br>80 ml $H_2O$* |
| 10X TBS (Stock; 1 liter): | 24.23 g Trizma HCl<br>80.06 g NaCl<br>Adjust pH to 7.6<br>Up to 1 liter of.$H_2O$* |
| 0.5% TritonX-100 (100 ml): | 0.5 ml TritonX-100 (Sigma)<br>up to 100 ml PBS |

## Appendix I

## Reagents and working solutions. Part B.

RNA and DNA work (reagents in alphabetical order):

| | |
|---|---|
| DEPC water: | Add appropriate amount of DEPC (diethylpyrocarbonate; Sigma) to miliQ water or $H_2O$* in order to obtain conc. 0.1%. Incubate overnight at room temperature and autoclave. |
| DNA ladder (100 µl): | 5 µl the stock ladder (1 Kb Plus DNA Ladder; conc. 1µg/µl; Invitrogen Life Technologies)<br>20 µl loading buffer<br>75 µl $H_2O$* |
| 0.5 M EDTA (500 ml): | 93.05 g EDTA sodium salt<br>up to 500 ml of $H_2O$*<br>pH 8.0 |
| Loading Buffer: | 15% Ficoll<br>5 mM EDTA pH 8.0<br>Bromophenol blue<br>Made up in $H_2O$*<br><br>Or<br><br>0.25% bromophenol blue<br>0.25% xylene cyanol FF<br>30% glycerol in $H_2O$* |
| 50 x TAE buffer - Stock buffer (1 liter): | 242 g Tris base<br>57.1 ml glacial acid acid<br>100 ml 0.5 M EDTA (pH 8.0)<br>up to 1 liter of $H_2O$* |

## Appendix I

## Reagents and working solutions. Part C.

| Reagents (in alphabetical order) for dermis splitting work: | |
|---|---|
| Collagenase II / DNase I working solution: | Add approx. 3900 units of collagenase II (Worthington) and 100 µl of 1mg/ml DNase I into 15 ml of MEM-minimal essential medium (Sigma) with antibiotics: 2 µl/ml fungizone (Sigma) and 1 µl/ml gentamicyn (Gibco). |
| 1 mg/ml DNase I (Stock): | 0.01 g DNase I (Roche)<br>10 ml DPBS (Gibco)<br>Mix slowly. |
| 6% pancreatin (100 ml): | Add 6 g of pancreatin (Sigma) to DPBS (Gibco, up to 100 ml DPBS).<br>Leave stirring over-night at 4°C.<br>Centrifuge and collect supernatant.<br>Aliquots (500 µl) kept in -20°C.<br>Filter (0.2 µm syringe filter) before the use. |
| 5% trypsin (100 ml): | 5 g trypsin (BD)<br>up to 100 ml DPBS (Gibco)<br>Aliquots (500 µl) kept in -20°C.<br>Filter (0.2 µm syringe filter) before the use. |

## Appendix I

## Reagents and working solutions. Part D.

| Reagents for adipogenic medium (in alphabetical order): | |
|---|---|
| 100 nM DEX (dexamethasone): | Prepared from 50 μM DEX (Sigma) and used for adipogenic medium. |
| 1 M IBMX (3-isobutyl-1-methylxanthine) (Stock no. 1): | Dissolve 250 mg of IBMX (Sigma) in 1.125 ml of DMSO (dimethyl sulfoxide; Sigma) (needs warming up). Aliquots (50 μl) kept in -20°C. Filter (0.2 μm syringe filter) before the use. |
| 0.1 M IBMX (3-isobutyl-1-methylxanthine) (Stock no. 2; 500 μl): | 50 μl of 1 M IBMX Stock no. 1<br>450 μl of DMSO<br>Stock no. 2 used for the 0.45 mM IBMX for adipogenic medium. |
| 5 mg/ml Insulin (Stock no. 1): | Dissolve 50 mg of Insulin (Sigma) in 10 ml sterile water* (pH 2-3). Aliquots (50 μl) kept in -20°C. Filter (0.2 μm syringe filter) before the use. |
| 207 μM Insulin (Stock no. 2; 1 ml): | 237.2 μl 5 mg/ml Insulin Stock no. 1<br>762.8 μl of MEM (with or without antib)<br>Stock no. 2 used for the 2.07 μM Insulin for adipogenic medium. |

*Used water: distilled or double-distilled water

## Appendix II

The mathematical calculation of the average diameter of lipid droplets.

Lipid droplets were analysed in mouse skin dermis sections that were prepared from back skin specimens at different time-points (Figure 2.9). The diameter of lipid droplets was calculated according to length of the scale bar (30 μm = 93 pixels).

| Length: / Time-point: | Pixels | μM |
|---|---|---|
| 0.5 day | 27 | 8.709677 |
| | 18 | 5.806452 |
| | 4 | 1.290323 |
| 1 day | 20 | 6.451613 |
| | 57 | 18.3871 |
| | 122 | 39.35484 |
| 8 day | 100 | 32.25806 |
| | 99 | 31.93548 |

**Appendix III**

Lipid accumulation in subcutaneous adipose tissue (SAT) and dermal adipose tissue (DAT) associated with back skin from 18.5 - 19 day old mouse embryo.

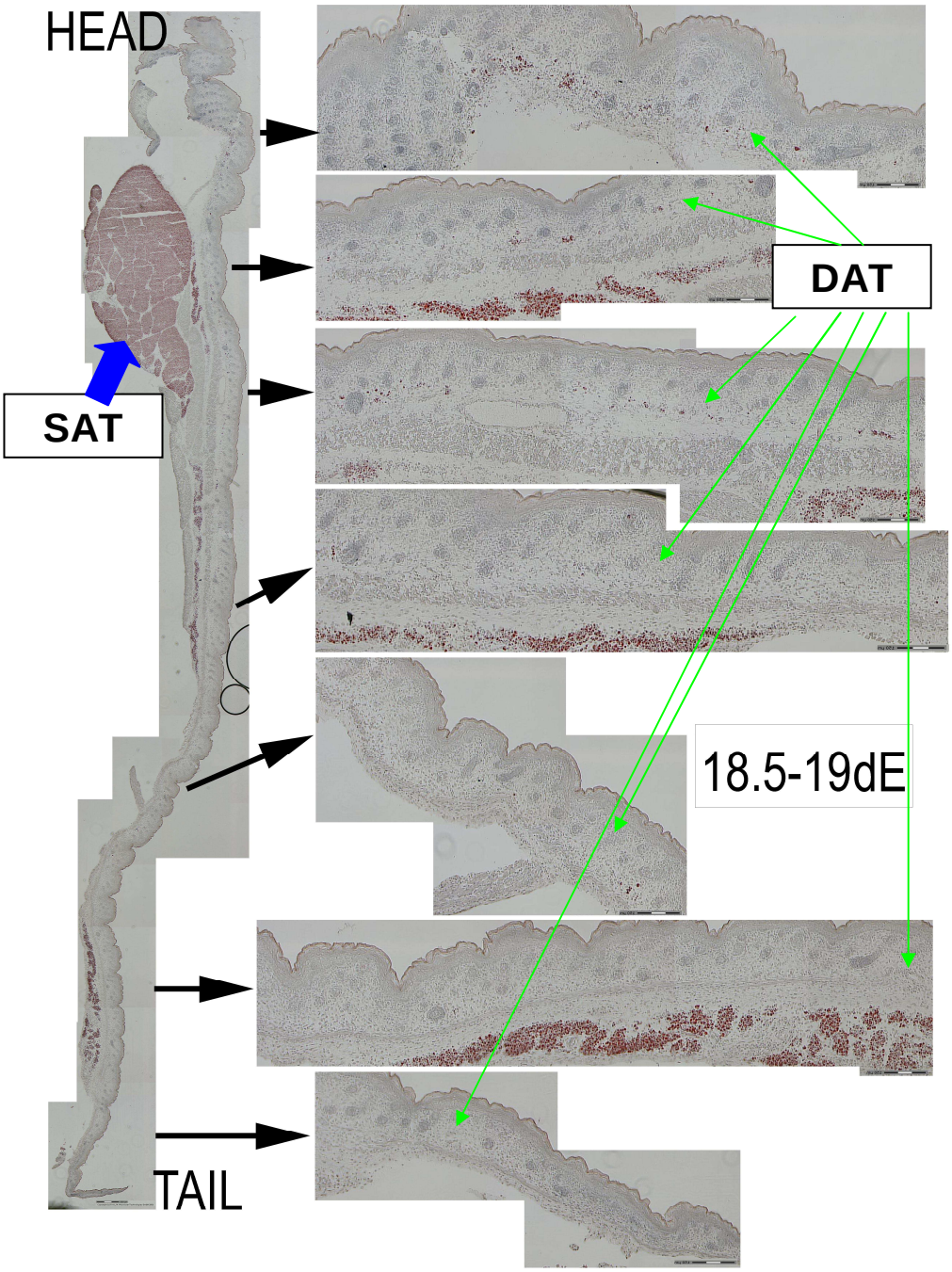


Lipid accumulation in back skin section and fat depots beneath the skin from 18.5 - 19 day old mouse embryo (18.5 - 19dE) was analysed by Oil Red O dye. Subcutaneous adipose tissue (SAT) is shown by blue arrow. Dermal adipose tissue (DAT) is shown by green arrows. Left panel: Scale bar = 300 μm. Right panels: Scale bar = 150 μm. Images were captured by Laser Capture Microdissection Microscope (PALM MicroBeam Zeiss Microscope).

**Appendix IV**

Lipid accumulation in subcutaneous adipose tissue (SAT) and dermal adipose tissue (DAT) associated with back skin from half a day old newborn mouse.

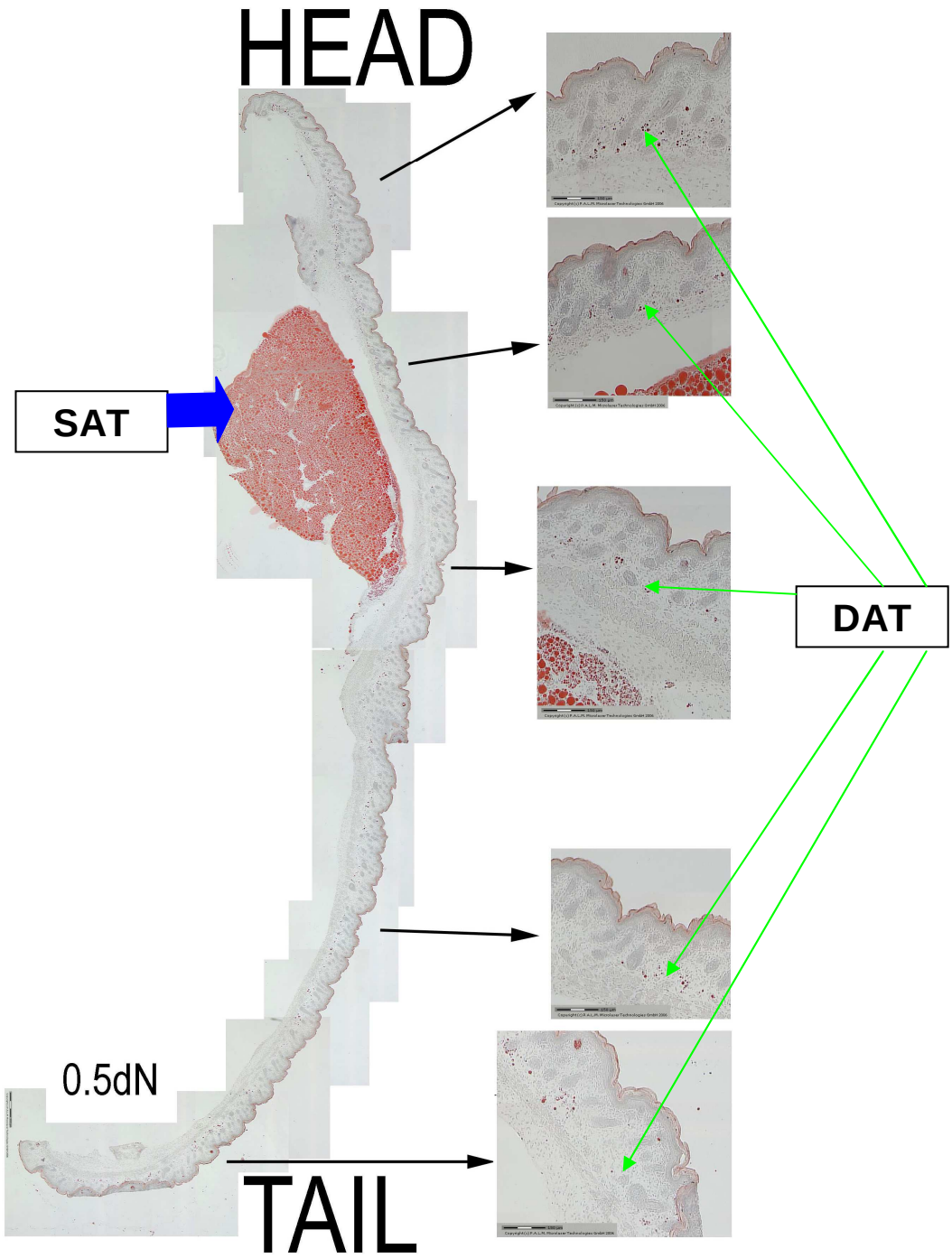


Lipid accumulation in back skin section with fat depots beneath the skin from 0.5 day old newborn mouse (0.5dN) was analysed by Oil Red O dye. Subcutaneous adipose tissue (SAT) is shown by blue arrow. Dermal adipose tissue (DAT) is shown by green arrows. Left panel: Scale bar = 300 μm. Right panels: Scale bar = 150 μm. Images were captured by Laser Capture Microdissection Microscope (PALM MicroBeam Zeiss Microscope).

## Appendix V

Genes from microarray data associated with the Wnt signalling pathway by DAVID v6.7 programme.

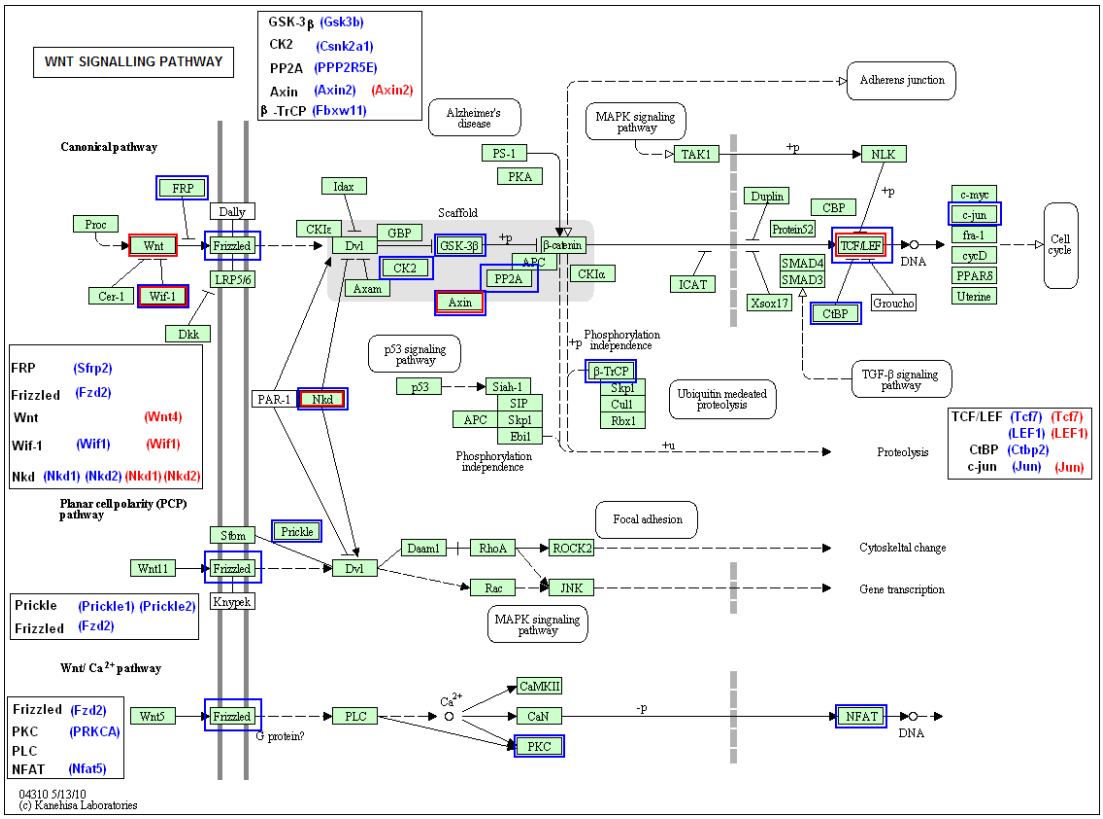


The WNT signalling pathway generated by KEGG database with underlined steps where genes from microarray sub-lists were present. The analysis was performed by DAVID v6.7 programme. Steps underlined in red - genes from E18 UPPER sub-list; in blue - genes from E19 UPPER sub-list. The WNT signalling pathway was addapted from KEGG pathway website.

## Appendix VI

The full names of genes presented in Figures 3.27 - 3.55. For more details see section 3.3.4 in Chapter 3.

| Figure number: | Gene symbol: | Whole name: |
|---|---|---|
| **3.27** | *Rhob* | ras homolog gene family, member B |
| | *Thbd* | thrombomodulin |
| | *Tsc22d1* | TSC22 domain family, member 1 |
| **3.28** | *Hspd1* | heat shock protein 1 (chaperonin) |
| | *Mafb* | v-maf musculoaponeurotic fibrosarcoma oncogene family, protein B (avian) |
| | *Mknk2* | MAP kinase-interacting serine/threonine kinase 2 |
| | *Sphk1* | sphingosine kinase 1 |
| | *Sdc1* | syndecan 1 |
| | *Ank3* | ankyrin 3, epithelial |
| | *Bcat1* | branched chain aminotransferase 1, cytosolic |
| **3.29** | *Aqp1* | aquaporin 1 |
| | *Cdc45l* | cell division cycle 45 homolog (S. cerevisiae)-like |
| | *Ccnb1* | cyclin B1 |
| | *Ccne2* | cyclin E2 |
| | *Hells* | helicase, lymphoid specific |
| | *Kpna2* | karyopherin (importin) alpha 2 |
| | *Lmo4* | LIM domain only 4 |
| | *Mcm5* | minichromosome maintenance deficient 5, cell division cycle 46 (S. cerevisiae) |
| | *Mcm7* | minichromosome maintenance deficient 7 (S. cerevisiae) |
| | *Mcm2* | minichromosome maintenance deficient 2 mitotin (S. cerevisiae) |
| | *Osmr* | oncostatin M receptor |
| | *Pnp1 /// Pnp2* | purine-nucleoside phosphorylase 1 /// purine-nucleoside phosphorylase 2 |
| | *Kif20a* | kinesin family member 20A |
| | *Slbp* | stem-loop binding protein |
| **3.30** | *Glul* | glutamate-ammonia ligase (glutamine synthetase) |
| | *Igfbp4* | insulin-like growth factor binding protein 4 |
| | *Gart* | phosphoribosylglycinamide formyltransferase |
| **3.31** | *Pex13* | peroxisomal biogenesis factor 13 |
| | *Pparg* | peroxisome proliferator activated receptor gamma |
| | *Phb* | prohibitin |
| | *Pcx* | pyruvate carboxylase |
| | *Nrip1* | nuclear receptor interacting protein 1 |
| | *Scd1* | stearoyl-Coenzyme A desaturase 1 |
| | *Timm23* | translocase of inner mitochondrial membrane 23 homolog (yeast) |
| | *Tob1* | transducer of ErbB-2.1 |
| | *Taldo1* | transaldolase 1 |
| **3.32** | *Tank* | TRAF family member-associated Nf-kappa B activator |
| | *Slc19a1* | solute carrier family 19 (sodium/hydrogen exchanger), member 1 |
| | *Fasn* | fatty acid synthase |
| | *Ldhb* | lactate dehydrogenase B |
| | *Me1* | malic enzyme 1, NADP(+)-dependent, cytosolic |
| | *Qk* | quaking |
| | *Apoc1* | apolipoprotein C-I |
| | *Ddt* | D-dopachrome tautomerase |
| | *Fah* | fumarylacetoacetate hydrolase |
| | *Cbr3* | carbonyl reductase 3 |
| | *Alad* | aminolevulinate, delta-, dehydratase |
| | *Rab3d* | RAB3D, member RAS oncogene family |
| | *Scarb1* | scavenger receptor class B, member 1 |
| | *Itga6* | integrin alpha 6 |
| | *Hadh* | hydroxyacyl-Coenzyme A dehydrogenase |

| | | |
|---|---|---|
| | *S3-12* | plasma membrane associated protein, S3-12 |
| | *Rnf11* | ring finger protein 11 |
| | *Bckdhb* | branched chain ketoacid dehydrogenase E1, beta polypeptide |
| | *Cdkn2c* | cyclin-dependent kinase inhibitor 2C (p18, inhibits CDK4) |
| | *Hsd11b1* | hydroxysteroid 11-beta dehydrogenase 1 |
| | *Hipk2* | homeodomain interacting protein kinase 2 |
| | *Cd1d1* | CD1d1 antigen |
| | *Dld* | dihydrolipoamide dehydrogenase |
| | *Arl4a* | ADP-ribosylation factor-like 4A |
| | *Scp2* | sterol carrier protein 2, liver |
| | *Nnmt* | nicotinamide N-methyltransferase |
| | *Aoc2 /// Aoc3* | amine oxidase, copper containing 2 (retina-specific) /// amine oxidase, copper containing 3 |
| | *Cfd* | complement factor D (adipsin) |
| | *Bnip3* | BCL2/adenovirus E1B interacting protein 3 |
| | *Thrsp* | thyroid hormone responsive SPOT14 homolog (Rattus) |
| | *Lpl* | lipoprotein lipase |
| | *Scd1* | stearoyl-Coenzyme A desaturase 1 |
| | *Dgat2* | diacylglycerol O-acyltransferase 2 |
| | *Hp* | haptoglobin |
| | *Adipoq* | adiponectin, C1Q and collagen domain containing |
| **3.33** | *Dnm3* | dynamin 3 |
| | *Fbn1* | fibrillin 1 |
| | *Fbln2* | fibulin 2 |
| | *Il6st* | interleukin 6 signal transducer |
| | *Ly6c1 /// Ly6c2* | lymphocyte antigen 6 complex, locus C1 /// lymphocyte antigen 6 complex, locus C2 |
| **3.34** | *Emp3* | epithelial membrane protein 3 |
| | *Ogn* | osteoglycin |
| | *Pdpn* | podoplanin |
| | *Pltp* | phospholipid transfer protein |
| | *Twist2* | twist homolog 2 (Drosophila) |
| | *Vcl* | vinculin |
| | *Tspan6* | tetraspanin 6 |
| | *Timp3* | tissue inhibitor of metalloproteinase 3 |
| **3.35** | *Dnm3* | dynamin 3 |
| | *Cxcl1* | chemokine (C-X-C motif) ligand 1 |
| | *H2-T10 /// H2-T17 /// H2-T22 /// H2-T9* | histocompatibility 2, T region locus 10 /// histocompatibility 2, T region locus 17 /// histocompatibility 2, T region locus 22 /// histocompatibility 2, T region locus 9 |
| | *Thbs2* | thrombospondin 2 |
| | *Vcam1* | vascular cell adhesion molecule 1 |
| | *Cdkn2b* | cyclin-dependent kinase inhibitor 2B (p15, inhibits CDK4) |
| | *Egr1* | early growth response 1 |
| | *Fos* | FBJ osteosarcoma oncogene |
| | *Gtpbp4* | GTP binding protein 4 |
| | *Klf4* | Kruppel-like factor 4 (gut) |
| | *Anxa1* | annexin A1 |
| | *Acot10 /// Acot9* | acyl-CoA thioesterase 10 /// acyl-CoA thioesterase 9 |

**Continuation of Appendix VI prom previous page.**

**Appendix VII**

Lipid detection in back skin specimens from 16 - 17 day old mouse embryos used for the hanging-drop organ culture experiment.

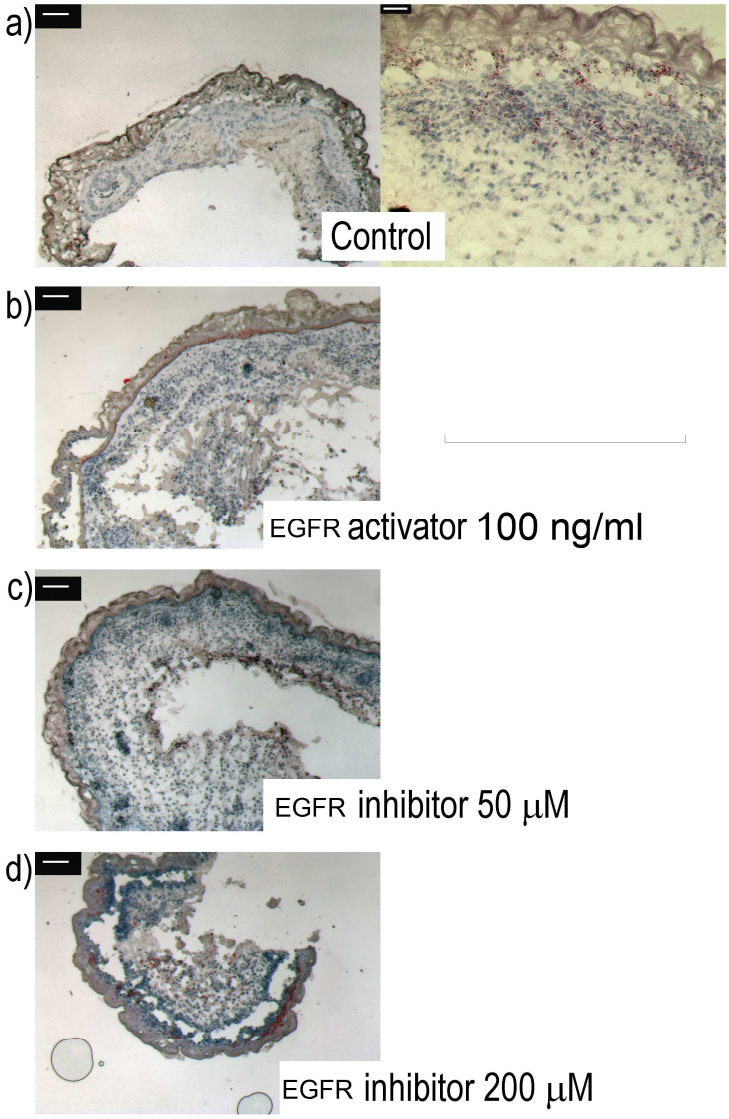


a) Skin sample kept in control (normal growth) medium. b) Skin sample kept in medium with EGFR activator (EGF). c) and d) Skin samples kept in medium with EGFR inhibitor (AG1478). Incubation lasted 72 hours and skin sections were analysed by Oil Red O dye to detect lipids. (a - left panel, b - d) Scale bar = 65 μm (a - right panel) Scale bar = 30 μm. Images were captured using Zeiss Axio Imager.M1. microscope.

## Appendix VIII

Lipid detection in skin specimens from 15 - 15.5 and 18.5 - 19 day old mouse embryos used for the substrate organ culture experiment.

**a)**

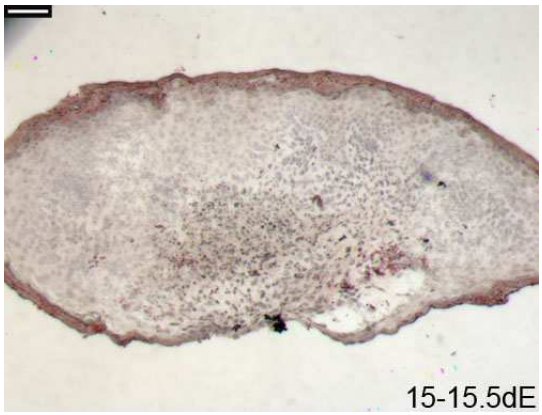


**b)**

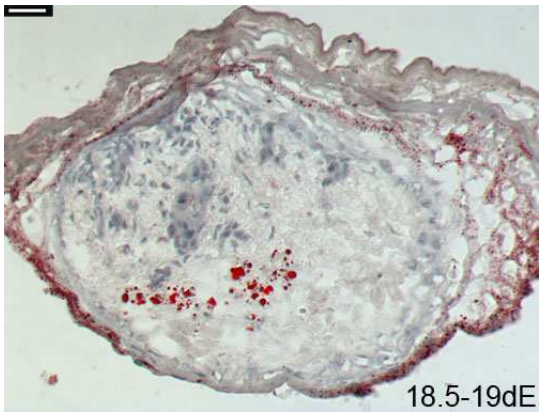


a) Skin sample from 15 - 15.5 day old mouse embryonic back skin kept in adipogenic medium. b) Skin sample from 18.5 - 19 day old mouse embryonic back skin kept in adipogenic medium. Incubation lasted 48 hours and skin sections were analysed by Oil Red O dye to detect lipids. (a) Scale bar = 65 μm. (b) Scale bar = 30 μm. Images were captured using Zeiss Axio Imager.M1. microscope.

**Appendix IX**

The analysis of lipid accumulation in 3D cell structures, obtained from human skin sample number 18_06.

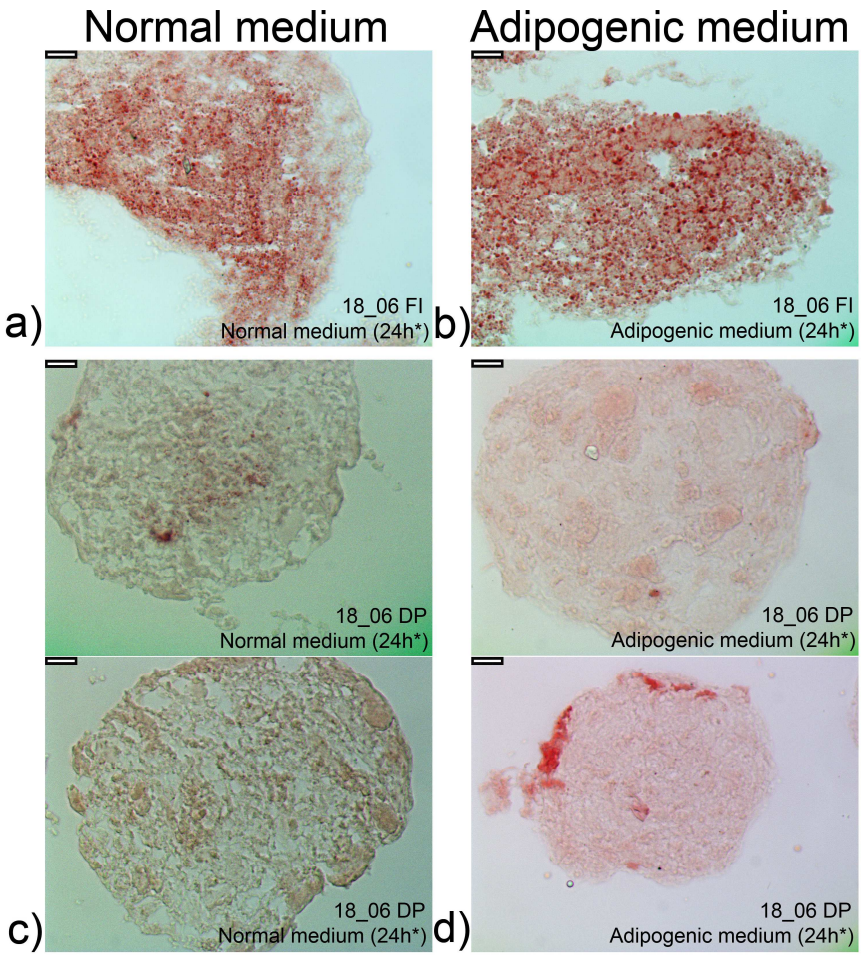


(*) Once spheres were established in a medium droplet, they were incubated in normal or adipogenic medium for 24 hours. Cell structures were stained with Oil Red O to detect lipids. FI - fibroblasts. DP - dermal papilla cells. Scale bar = 15 μm Images were captured using Zeiss Axio Imager.M1. microscope.

## Appendix X

Expression profiles of genes encoding calcium binding proteins in embryonic skin dermis, based on microarray data. For more details see section: **Questions about white and brown fat cells in dermal adipose tissue (DAT), the thickness of DAT and about the hair follicle cycle.** in Chapter 6.

Table presented in Appendix X contains calcium binding proteins expression profiles in embryonic skin dermis between e17 and e19 time points. (A, B, C) The E17, E18 or E19 microarray sub-lists revealed the enrichment of analysed genes at mRNA level in lower dermal cells versus upper dermal cells at e17, e18 or e19 time points. (D) The lower dermal (LD) microarray list showed the up-regulation of analysed gene in lower dermal cells from e17 time point.

A)

| **Whole name; gene symbol; probe set Affymetrix ID.** | **Time points:** | **Fold change value:** |
|---|---|---|
| S100 calcium binding protein A16; S100a16; 1447676_x_at | e17 lower dermis vs* e17 upper dermis | **+** 4.363894 |
| | e18 lower dermis vs* e18 upper dermis | + 4. 817356 |
| | e19 lower dermis vs* e19 upper dermis | + 6.481481 |

B)

| **Whole name; gene symbol; probe set Affymetrix ID.** | **Time points:** | **Fold change value:** |
|---|---|---|
| S100 calcium binding protein A14; S100a14; 1449166_at | e17 lower dermis vs* e17 upper dermis | NP** |
| | e18 lower dermis vs* e18 upper dermis | + 3.270873 |
| | e19 lower dermis vs* e19 upper dermis | NP** |

C)

| **Whole name; gene symbol; probe set Affymetrix ID.** | **Time points:** | **Fold change value:** |
|---|---|---|
| S100 calcium binding protein A10 (calpactin); S100a10; 1416762_at | e17 lower dermis vs* e17 upper dermis | NP** |
| | e18 lower dermis vs* e18 upper dermis | + 2.170815 |
| | e19 lower dermis vs* e19 upper dermis | NP** |

D)

| **Whole name; gene symbol; probe set Affymetrix ID.** | **Time points:** | **Fold change value:** |
|---|---|---|
| S100 calcium binding protein A10 (calpactin); S100a10; 1416762_at | e18 lower dermis vs* e17 lower dermis | + 2.632241 |
| | e19 lower dermis vs* e17 lower dermis | + 1. 699655 |

* vs - versus

** NP - gene not present in microarray list

## Appendix XI

Expression profiles of genes encoding leptin and leptin receptor in embryonic skin dermis, based on microarray data. For more details see section: **Leptin - leptin receptor interactions between hair follicles end bulb and cells from lower dermis.** in Chapter 6.

Table presented in Appendix XI contains leptin (A) and leptin receptor (B) expression profiles in embryonic lower skin dermis between e17 and e19 time points. The fold change values are based on the lower dermis (LD) microarray data.

A)

| **Whole name; gene symbol; probe set Affymetrix ID.** | **Time points:** | **Fold change value:** |
|---|---|---|
| Leptin; *Lep*; 1422582_at | e18 lower dermis vs* e17 lower dermis | - 1.087906 |
| | e19 lower dermis vs e17 lower dermis | + 3.644211 |

B)

| **Whole name; gene symbol; probe set Affymetrix ID.** | **Time points:** | **Fold change value:** |
|---|---|---|
| leptin receptor; *Lepr*; 1425644_at | e18 lower dermis vs* e17 lower dermis | + 6.40568 |
| | e19 lower dermis vs e17 lower dermis | + 2.512982 |

* vs - versus